AGARD-CP-548

AGARD-CP-548

AGARD

ADVISORY GROUP FOR AEROSPACE RESEARCH & DEVELOPMENT
7 RUE ANCELLE 92200 NEUILLY SUR SEINE FRANCE

AGARD CONFERENCE PROCEEDINGS 548

Technologies for Highly Manoeuvrable Aircraft

(Les Technologies pour
les Aéronefs à Haute Manoeuvrabilité)

Copies of papers presented at the Flight Mechanics Panel Symposium, held in Annapolis, Maryland, United States, from 18th–21st October 1993.

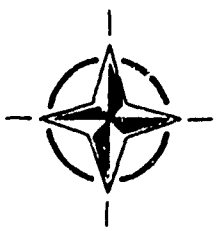

NORTH ATLANTIC TREATY ORGANIZATION

Published March 1994

Distribution and Availability on Back Cover

AGARD
ADVISORY GROUP FOR AEROSPACE RESEARCH & DEVELOPMENT
7 RUE ANCELLE 92200 NEUILLY SUR SEINE FRANCE

AGARD CONFERENCE PROCEEDINGS 548

Technologies for Highly Manoeuvrable Aircraft

(Les Technologies pour
les Aéronefs à Haute Manoeuvrabilité)

Copies of papers presented at the Flight Mechanics Panel Symposium, held in Annapolis, Maryland, United States, from 18th–21st October 1993.

North Atlantic Treaty Organization
Organisation du Traité de l'Atlantique Nord

The Mission of AGARD

According to its Charter, the mission of AGARD is to bring together the leading personalities of the NATO nations in the fields of science and technology relating to aerospace for the following purposes:

- Recommending effective ways for the member nations to use their research and development capabilities for the common benefit of the NATO community;
- Providing scientific and technical advice and assistance to the Military Committee in the field of aerospace research and development (with particular regard to its military application);
- Continuously stimulating advances in the aerospace sciences relevant to strengthening the common defence posture;
- Improving the co-operation among member nations in aerospace research and development;
- Exchange of scientific and technical information;
- Providing assistance to member nations for the purpose of increasing their scientific and technical potential;
- Rendering scientific and technical assistance, as requested, to other NATO bodies and to member nations in connection with research and development problems in the aerospace field.

The highest authority within AGARD is the National Delegates Board consisting of officially appointed senior representatives from each member nation. The mission of AGARD is carried out through the Panels which are composed of experts appointed by the National Delegates, the Consultant and Exchange Programme and the Aerospace Applications Studies Programme. The results of AGARD work are reported to the member nations and the NATO Authorities through the AGARD series of publications of which this is one.

Participation in AGARD activities is by invitation only and is normally limited to citizens of the NATO nations.

Published March 1994

ISBN 92-835-0740-1

Printed by Specialised Printing Services Limited
40 Chigwell Lane, Loughton, Essex IG10 3TZ

Preface

The new generation of combat aircraft, currently at demonstrator or development stage, incorporate significant advances in manoeuvre capability, especially in such areas as post-stall control and sustained supersonic manoeuvre. These technologies expand the operational capabilities, and are essential for survival in a sophisticated threat scenario, and also to obtain favourable exchange ratios against an opponent using the current generation of fighters. The aim of this Symposium was to review the various technologies, which combine to give this increased operational capability, and the techniques which are available or being developed, to overcome the design problems associated with the attainment of these goals.

The Symposium was divided into six sessions covering propulsion and integrated flight control, aerodynamics and control at high angles of attack, post-stall flight and control, flying qualities-applied criteria, agility and simulation. Examples of results from current demonstrator programmes were covered in appropriate sessions.

Two keynote papers presented an overview from an operational and acquisition viewpoint of the contribution of manoeuvrability to combat success.

For the first time in a Flight Mechanics Panel Symposium, the programme included a paper by a Russian author.

A Technical Evaluation Report on the Symposium is also included in this Conference Proceedings document.

Préface

La nouvelle génération d'avions de combat, qui est actuellement au stade des essais de développement, voire avion de démonstration, intègre des progrès importants en ce qui concerne la manoeuvrabilité, en particulier dans des domaines comme le contrôle en post-décrochage et la manoeuvre supersonique continue. Il s'agit de technologies qui permettent d'augmenter les capacités opérationnelles et qui sont indispensables à la survie dans un scénario sophistiqué de menace. Elles permettent aussi d'obtenir des rapports de potentiels favorables contre un adversaire qui dispose d'avions de combat de la génération actuelle.

Le symposium a eu pour objet de faire le point des différentes technologies qui, combinées, concourent à l'obtention de cet accroissement des capacités opérationnelles, ainsi que des techniques, disponibles ou en développement, qui permettent de résoudre les problèmes de conception associés à la réalisation de ces objectifs.

Le symposium a été structuré en six sessions, couvrant la commande de vol intégrée, l'aérodynamique et le contrôle aux grands angles d'attaque, le vol en post-décrochage et le contrôle, les critères appliqués aux qualités de vol, la manoeuvrabilité et la simulation. Des exemples des résultats obtenus des programmes de démonstration en cours ont été donnés lors des sessions appropriées.

Un aperçu de la contribution de la manoeuvrabilité dans l'efficacité des combats, tant du point de vue opérationnel que de l'acquisition d'objectifs, a été donné par deux communications d'ouverture de séance.

Pour la première fois lors d'un symposium du Panel de la Mécanique de Vol, le programme comprenait une communication présentée par un auteur russe.

Le compte-rendu conférence comprend un rapport d'évaluation technique.

Flight Mechanics Panel

Chairman: Professor L.M.B. da Costa Campos
Instituto Superior Tecnico
Pavilhao de Maquinas
1096 Lisboa Codex
Portugal

Deputy Chairman: Dipl.-Ing. H. Wünnenberg
Head of Flight Mechanics
Dornier Luftfahrt
D-88039 Friedrichshafen
Germany

TECHNICAL PROGRAMME COMMITTEE

Professor L.M B. da Costa Campos
Instituto Superior Tecnico
Pavilhao de Maquinas
1096 Lisboa Codex
Portugal

Mr R. Hildebrand
Technical Director
Air Force Flight Test Center
AFFTC/CA
1, South Rosamond Blvd
Edwards AFB, CA 93524-1031
United States

Mr K. McKay
Assistant Manager EFA Aerodynamics
Aerodynamics Department (W310P)
British Aerospace Defence Ltd
Military Aircraft Division
Warton Aerodrome
Preston, Lancs. PR4 1AX
United Kingdom

HOST NATION COORDINATOR

Mr R.A. Russell
Technical Director (FW02)
Force Warfare Test Directorate (FW02)
Naval Air Warfare Center
Aircraft Division
Patuxent River, MD 20670-5304
United States

PANEL EXECUTIVE

Mr M.K. Foster

Mail from Europe:
AGARD—OTAN
Attn. FMP Executive
7, rue Ancelle
92200 Neuilly-sur-Seine
France

Mail from USA and Canada:
AGARD—NATO
Attn: FMP Executive
Unit 21551
APO AE 09777

Tel: 33(1)47 38 57 70
Telex: 610176 (France)
Telefax: 33 (1) 47 38 57 99

Acknowledgements

The Flight Mechanics Panel wishes to express its thanks to the National Authorities of the United States for the invitation to hold this meeting in Annapolis, Maryland, and for the facilities and personnel which made the meeting possible.

The Flight Mechanics Panel also wishes to express its thanks to the Propulsion and Energetics Panel and to the Fluid Dynamics Panel for their assistance in proposing authors for some of the papers presented at this Symposium.

La Commission du Mécanique du Vol tient à remercier les Autorités Nationales des Etats Unis pour leur invitation à tenir cette réunion à Annapolis, Maryland, ainsi que des installations et du personnel mis à sa disposition.

La Commission du Mécanique du Vol remercie également la Commission du Dynamique des Fluides ainsi que la Commission de Propulsion et Energetiques pour leur assistance en proposant les auteurs de certains papiers présentés lors de ce Symposium.

Contents

Technical Evaluation Report

by
Richard A. Borowski
5027 Desert Shadow Place
Las Cruces, New Mexico 88011
USA

BACKGROUND

The historic city of Annapolis was an appropriate setting for the AGARD Flight Mechanics Panel symposium "Technologies for Highly Manoeuvrable Aircraft." During the conference, historic diplomatic, military, technical, and budgetary issues faced NATO and AGARD.

After the dissolution of the Warsaw Pact, eastern European nations and Russia petitioned for membership in NATO. During the symposium, the US proposed NATO "partnerships" for the nations of the former Warsaw Pact and other European nonmembers. Through AGARD's Outreach program, Professor Petrov from Russia was one of the participants in the conference. Over four years earlier, at the Paris Air Show, a Russian Su-27 startled the aeronautics establishment by performing a Cobra manoeuvre, a dynamic pitch up to over a 90-degree pitch angle from near-level flight during an aerial demonstration. The manoeuvre became a staple of Russian participation in air shows worldwide and served as a wake-up call to the NATO technical establishment.

NATO military issues at the time of the symposium included enforcing a no-fly zone and airlifting supplies to besieged populations of Bosnia-Herzegovina. In this situation, air-to-air rules of engagement may require that a potential adversary demonstrate hostile intent before allowing armed response. Manoeuvrability would be essential. Although manoeuvrability is often considered an air-to-air fighter attribute, the siege of Sarajevo presented a potentially difficult and complex air-to-ground environment. Besieged and attacking forces were in proximity and lodged in mountainous terrain. Close air support would place extreme manoeuvre demands on the aircraft. During the year of the symposium, Sarajevo had been supported by airlift. Increased manoeuvrability could reduce the susceptibility of those aircraft. Even transport aircraft air-dropping cargo could benefit from increased manoeuvrability resulting in more precise flight path control and in reduced exposure about centre-of-gravity-imposed control limits.

Technology was also at a historic juncture. Fly-by-wire flight controls allowed multiple inputs and outputs with complex algorithms. Computational Fluid Dynamics allowed analysis and visualization of fluid-flow phenomena with fidelity and detail not previously possible. The result was improved aerodynamic designs of new aircraft such as the European Fighter Aircraft (EFA) and the French Rafale. The US/Lockheed F-22 incorporates a two-dimensional, thrust-vectoring engine nozzle for manoeuvrability. At Edwards AFB, two thrust-vectoring systems were in flight test: an axisymmetric thrust-vectoring nozzle and thrust vectoring achieved through paddles in the engine exhaust stream. The potential for operational benefit from such improved manoeuvrability was to emerge as an element of controversy as the symposium continued.

Finally, the end of the cold war resulted in reduced military research and procurement budgets. The budget reductions mandated not only affordable systems but also affordable research to develop those systems.

OPENING

Rear Admiral Boecker of the US Navy opened the conference. He welcomed attendees to Annapolis and reminded us of the proud history of the city. He commented knowledgeably on the importance of agility and manoeuvrability to modern fighter aircraft.

KEYNOTES

The keynote speakers were General Berret of the French Air Force and General Mantiles of the US Air Force. Both speakers had past operational experience and current responsibility for fighter aircraft procurement, including the Rafale and the F-22. General Berret cited fly-by-wire as an example of technology providing the means to increase many aspects of performance. He predicted advancements in fly-by-wire technology would allow the pilot to focus his attention on higher level functions. He spoke of the importance of properly balancing aircraft capabilities with those of the weapons it carries. Acknowledging the benefits and necessities of collaboration, General Berret recognized the Flight Mechanics Panel as a remarkable forum for technical progress and a potential

Technical Evaluation Report on Flight Mechanics Panel Symposium on Technologies for Highly Manoeuvrable Aircraft
October 1995

source of collaborative programs. Referring to reductions in defense expenditures, he spoke of the necessity to maintain intact design teams, perhaps through development of a series of prototypes.

General Muellner spoke of the proper balance of various aircraft attributes including weapons capability and radar signature. While not strongly endorsing exceptional manoeuvrability as a primary design requirement, General Muellner and General Brevot both considered manoeuvrability and agility valuable design options. General Muellner did support the need to restore manoeuvrability lost in the initial search for stealth. He also referred to the high cost of aircraft lost to problems at high angles of attack. Like General Brevot, General Muellner highlighted the need to balance weapons capability and various aircraft capabilities to maximize system payoff.

SESSION 1: PROPULSION AND INTEGRATED FLIGHT CONTROL

The first three papers in the session concentrated on integration of the engine in the classical sense of matching engine airflow and airframe propulsive requirements. The best way to consider these three papers is in reverse order. The third paper, "Engine Characteristics for Agile Aircraft," started with aircraft requirements. It demonstrated the decomposition of those requirements into propulsion system requirements and identified specific engine technologies to address the requirements. Specific requirements were shown to have primary connections with specific technologies. This link from propulsion technology to aircraft requirements will allow technology managers to make decisions based on operational needs as well as on technical opportunities.

In this author's experience, the link from operational requirements to propulsion system technology is not always fully understood by either technology planners or by propulsion technologists. Long lead times for propulsion system development compound the problem because propulsion systems often enter development *before definition of aircraft requirements*. Propulsion system technologists will be better able to forecast requirements using the approach outlined in this paper.

The second paper of the session "Progress and Purpose of the IHPTET Program," described a large-scale US industry and government program to advance turbine engine technology. The paper describes a process starting with top-level engine performance requirements and proceeding to identification of component technologies and development of strategies for advancing those technologies. Technologies provide not only capabilities but also alternatives. Individual technologies can, simultaneously, be both synergistic and competitive, depending on the specific requirement. IHPTET addresses a set of requirements with a set of programs run by individual, independent players. Common interest seems, for the moment, to have overcome the competitive instinct. Government participation with substantial funding available may have been the key to this cooperation. As government research funding declines in the US, it will be a *challenge to the multiple managers to maintain the* progress and cooperation of the IHPTET initiative.

The first paper "Aerodynamic and Propulsion Ground Test and Evaluation Techniques for Highly Manoeuvrable Aircraft - Capabilities and Challenges," describes innovative methods to ground test engines designed to meet manoeuvrability-related requirements. The capabilities described include test of thrust-vectoring systems and testing under closely controlled and accurately emulated inlet distortion. This assures system-level requirements are met on the propulsion subsystem level. This paper also illustrates using highly controlled tests under other-than-operational conditions to validate analysis (for propulsion systems this means ground testing rather than flight testing). Analysis validates a model available for system evaluation and operation. Perhaps the most remarkable aspect of the test capability documented in this paper is that it was in place in time to test the first prototype systems that needed it. Anticipating new requirements and making the resources available to address those requirements in time is a rare achievement.

The fourth through sixth papers of the first session concentrated on the potential benefits of integration of control systems of the aircraft and the engine. The fourth paper, "Design of Integrated Flight and Power Plant Control Systems," provides an excellent tutorial on the progression from independent control systems for aircraft and engine to a fully integrated system. This paper focuses on benefits of flight and propulsion control integration for VSTOL. Perhaps most dramatic was the evolution from the Harrier system of three control inceptors to using only a single inceptor for all the same functions. (The author's perceptions may be influenced by prior experience as a Harrier pilot). Further progress along this path will address General Brevot's vision of allowing pilots to concentrate on strategy and tactics.

The next two papers report on similar implementations of thrust vectoring for control, but again, are best considered in reverse order. Paper six, "Results from the STOL and Maneuver Technology Demonstrator" reports on functional integration of flight and propulsion control. It documents manoeuvrability, performance and flying qualities benefits of such integration. It also describes using engine thrust to provide pitching moment and braking. Multimode controls are used to

optimize aircraft response for various tasks including air-to-air tracking and accurate landings. Like Paper four, it discusses innovative control inceptor design. Flight test results mostly validated design objectives, but one unexpected result was documented -- a pitch oscillation after touchdown while in reverse thrust. Considered with Viggen and Tornado experiences in the same thrust-reversing environment, this illuminates the difficulties of control in conditions of complex flow and powerful forces. Although recent experience in developing Level I flying qualities in new aircraft has been excellent, this oscillation serves as a reminder of the potential for problems resulting from complex mechanizations, unexpected dynamics, and multiple control modes. (Readers should be aware that this author was program manager of the F-15 STOL for three years and executive program manager for the last year of the program).

While the F-15 STOL and Maneuver Technology Demonstrator did not address increased angles of attack, manoeuvres at high angles of attack were a primary goal of the YF-22 thrust-vectoring implementation discussed in Paper five, "Thrust Vector Aided Manoeuvring of the YF-22 Advanced Tactical Fighter Prototype." This paper documents substantial improvements in usable high-angle-of-attack capability while emphasizing the importance of superb aerodynamics. Thrust vectoring can make high angles of attack available and speed angle-of-attack reduction when the tactical situation dictates. To avoid absolute reliance on the propulsion system, the YF-22 retains a capability for aerodynamic recovery.

Paper five also addresses tactical requirements for high manoeuvrability and agility. The author states that the design objective blended substantial requirements for manoeuvrability and agility with requirements for low observables. The paper justifies manoeuvrability and agility to cope with future low-observable fighters, highly manoeuvrable fighters planned or already in production and expected reliance on infrared-guided weapons in the air-to-air battles of the future. This part of the presentation is best understood considering the specification to which the US Air Force procured the YF-22 and YF-23. Program officials specified capability against a mission requirement, rather than aircraft performance numbers. A later paper describes Working Group 19 conclusions on specification of operational agility. In the broadest sense, the YF-22 program office used the approach the Working Group would recommend -- the aircraft was designed to respond with agility to a wide range of threats, including a numerically superior foe.

By the conclusion of Session I, the tone of the conference was set. One aspect of technology for highly manoeuvrable aircraft had been thoroughly explored. Participants in the symposium had reported on rapid progress in performance and control capability. Papers had described methods of breaking down objectives to specifications and to functional implementations. Papers also discussed technical and programmatic approaches to advancing technology and testing.

SESSION II: AERODYNAMICS AND CONTROL AT HIGH ANGLE OF ATTACK

Paper seven, "Numerical Study of High Incidence Flow Over the Rafale A," documents analysis of Rafale aerodynamics using a three-dimensional Euler code to determine the lift coefficient contributions of the fuselage, wings, and canard. The presentation focuses on high angles of attack. With controls fixed at full-nose down, the wing contribution to lift decreases while the fuselage and canard contributions increased with increasing angles of attack. Similar analyses are presented for pitch-moment coefficient contributions. Analysis predicts reduced directional stability at high angles of attack. The approach combines numerical techniques with engineering judgment and models vortical flow without extreme sensitivity to calculated vortex origins and other difficult-to-predict phenomena. The results of these tests provide qualitative and quantitative data for validation of numerical results as well as valuable and accurate design data for Rafale development.

Paper eight, "Dynamic Tests to Demonstrated Lateral Control Using Forebody Suction On Large Scale Models in the DRA 24 Foot Wind Tunnel," demonstrates that various means of forebody vortex control can provide strong yaw moments at high angles of attack. Other documented methods include blowing through nozzles or slots and using small strakes. Focusing on a method not frequently reported, this paper constitutes a welcome addition to the literature.

The paper describes two wind-tunnel experiments using active control of suction through small holes near the apex of a model nose. In the first experiment, the model was free to yaw and the only active control mechanism was nose suction. In the second experiment, the model was free to pitch, roll, and yaw with aerodynamic control surfaces and nose suction active. The experiments demonstrated that nose suction could effectively generate lateral forces and could be effectively integrated into a flight control system.

One significant element of the research presented is the discussion of lags in response to suction. The paper documents the existence of such lags and some parameters affecting the lag. A full understanding of these effects at various flight conditions will be necessary to forecast whether suction devices will meet

flying qualities requirements and to properly design control systems implementing this technique. Ultimately, full-scale wind-tunnel and flight testing must follow to validate this implementation and to generate the parameters necessary for control system integration.

In response to questions, the presenter discussed various suction port positions. The most effective position for the port was as close to the apex as possible. Control was most effective using a long, fine nose rather than a short, blunt nose section.

For scheduling considerations, Paper 11, "Control of Leading-Edge Separation on a Cambered Delta Wing," was switched with Paper 9. Paper 11 addresses the need for a versatile design responding to several design requirements. In this case, the requirements addressed are for efficient supersonic flight as well as high-angle-of-attack manoeuvrability at subsonic speeds. The approach selected was a highly swept wing for supersonic performance and a special mechanism for control of leading-edge flow separation at subsonic, high-angle-of-attack flight conditions. The mechanism discussed uses thin wires positioned within the attached turbulent boundary layer. It will be interesting to track the development of this technology, especially high-angle-of-attack characteristics at full scale with normal production deviations in dimension. This author was reminded of asymmetric deployment of the aerodynamically actuated leading-edge flaps on the Douglas A-4 Skyhawk during moderate angle-of-attack manoeuvres.

Paper 10, "Yaw Control by Tangential Forebody Blowing," is best considered together with Paper 8. Rather than using suction as a side-force generator and control mechanism, Paper ten examines using blowing through slots further aft. A critical advantage postulated for this approach is that the installation is insensitive to the location of the vortex. Paper ten also addresses modification of attached flow as well as modification of vortices as an important mechanism for control.

It is not clear to this author whether repeatable vortex positions exist for several examples of a given design. If it is not possible to determine vortex positions generically for a given design, the robustness of an implementation to inaccurately determined vortex location is important. Future research in vortex manipulation for control should address whether control effectiveness changes with tiny variations in forebody dimensions.

A comparative study of various mechanizations and a comparison of test results would be helpful. Wind-tunnel tests underway on an F-18 at the NASA Ames Research Center may provide such data. Flight tests performed on the X-29 during 1992 provide important information. As illustrated by the X-29 vortex flow experiment, it may not be necessary to collect and collate a complete body of data to begin successful flight testing. However, without the data, the possibility remains that a slightly different approach may have been more successful. It would have been beneficial to report on the F-18 and the X-29 investigations during this symposium.

Paper nine, "Techniques for Aerodynamic characterization and Performance Evaluation at High Angle of Attack," was presented next. This paper pulls together wind-tunnel testing, sophisticated modeling, and data reduction, advanced methods for measuring dynamic response, and model tests in the vertical tunnel and free flight.

The sequence proposed in this paper is to first use experimental testing to bound a problem and select parameters for evaluation. The next step is to perform analysis at sufficient depth to obtain predictions. Finally, the predictions should be validated. Large-scale wind-tunnel tests, flight testing,, and sophisticated numerical analysis may be appropriate methods of validation, depending on the subject, the budget, and the objective.

In future research, this author proposes using the approach of Paper nine to address the broad technical area of forebody flow control. The current state of research concerning highly leveraged control techniques at the forebody of a fighter aircraft is concentrated in experimental testing. Several approaches have been examined, but in varying depth and in different ranges of various parameters. Predictions are being made. Predictions have been validated in several large-scale wind-tunnel tests and in the X-29 flight test. Continuation of the investigations along all these fronts is likely to continue, but more discipline as proposed by this paper will enhance productivity. AGARD may provide the forum for the difficult task of compromise and cooperation leading to more productive interagency investment.

SESSION III: POST-STALL FLIGHT AND CONTROL

Attendees eagerly anticipated Session III. Paper 12, "Aerodynamic Design of Supermanoeuvrable Aircraft," was presented by Professor A. Petrov, TsAGI, Russia. Papers 13, 14, and 15 discuss the latest results of X-31A flight. Controversy about the utility of post-stall flight was set aside for the moment. The uniqueness and audacity of the two subjects captivated the audience.

Paper 12 was a configuration study of supermanoeuvrable aircraft. It quickly became apparent that beyond the discussion of two versus three surface

configurations, span-wise blowing, and the contribution of a Leading Edge Extension (LEX) lay the theoretical basis of the Cobra manoeuvre. First, the audience needed to adjust its perspective of lift and drag. Professor Petrov spoke of lift as being generated by thrust and of drag along the aircraft's z-body axis when the aircraft is momentarily at angles of attack nearing 90 degrees. We know lift is perpendicular to the relative wind, but a lift vector so far from the z axis is just as counter-intuitive for this author as was flying an airplane with the velocity vector far displaced from the view out the front window.

With this author and perhaps others in the audience having overcome intuition, the discussion moved on to the center of lift and the center of pressure. Up to about a 40-degree angle of attack, lift increases in a near-linear fashion. Beyond a 40-degree angle of attack, normal force stabilizes, but the center of pressure for an aircraft of appropriate configuration moves aft. If the center of gravity is between the original center of lift and the center of pressure at a high angle of attack, a restoring pitch-down moment results.

This insight into the Cobra manoeuvre led to several questions. Responses indicated that the Cobra is a difficult manoeuvre requiring a skilled pilot and that uncommanded moments occur during the manoeuvre. The description of the manoeuvre as dynamic indicates that the pilot's approach is to pass quickly through unfavorable regions. Answers to questions indicated current efforts were to increase the speed at which the manoeuvre could be performed and to move the manoeuvre into the horizontal plane. The current speed range was 200 to 300 kilometers per hour. In answer to further questions, Professor Petrov said that roll and yaw control at high angles of attack was important, but that it was not the subject of the presentation. Professor Petrov expressed interest in using reaction controls for increased authority at low speed and high angle of attack. In a discussion hampered by language difficulties, he seemed to indicate the angle-of-attack rate during the manoeuvre was about 25 degrees per second.

In any discussion of the X-31A, it is important to acknowledge the contributions of the late Dr. Wolfgang Herbst. Dr. Herbst conceived, mathematically described, and convinced technologists and operators of the importance of high-angle-of-attack control and manoeuvre. Without his contributions, it is unlikely this symposium would have occurred or that much of the research would have been pursued. He was certainly present in spirit and would have contributed much to the presentations and discussions.

For the record, this author must disclose involvement in the early days of the X-31A program. I urged against substantial US Air Force participation, but gave the program an audience with Air Force leadership. My reasons were personal judgments regarding tactics and resource utilization. I will try not to let these judgments color the discussion that follows.

Paper 15, "X-31A Tactical Military Utility Results," was presented next. The introduction discusses program goals, including minimizing program costs through innovative design and manufacturing. A significant aspect of the X-31A program is the number of participants. Keeping a large team committed for years is a challenge for any program.

The aircraft and programmatic descriptions in this paper are valuable because few research (as opposed to prototype or technology demonstration) aircraft have been designed and flown in recent years. An X-31A program history would be extremely valuable. X-29 experience in writing such a history has shown that data can very quickly be lost.

In manoeuvring at high angles of attack, the X-31A uses stability axis rolls. Discussion of the pilot acceptability of this approach was useful. More research into high-angle-of-attack roll/yaw control and response would represent a welcome addition to the flying qualities body of knowledge.

Several changes were made to the aircraft to solve problems and improve test results. The program was structured to allow such changes quickly and without unnecessary approval. Robustness of the original design, including strong aerodynamic control power, improved the opportunity to make such changes.

One item of interest was the difference between the two aircraft. Early in the flight program, pilots found one aircraft more susceptible to side-force "lurches" than the other. Program engineers were unable to find a cause for the difference. In the discussion that followed, one attendee mentioned the example of a large-scale wind-tunnel test on a forebody carefully polished to eliminate side force. In that test, thumbprints were sufficient to cause side forces one way or the other. Strips of "grit" were used to reduce the difference between the two X-31A aircraft. For future production aircraft, similar solutions or closed-loop control may be required to reduce differences among aircraft. Flight testers and designers must develop techniques to assure that the absence of undesired response in high-angle-of-attack flight tests of one aircraft means an absence of undesired response throughout the fleet.

The X-31A relied heavily on simulation, validated by flight test, to address tactical utility. This was necessary because the experimental aircraft were not equipped

with avionics or weapons systems. The value of post-stall manoeuvring as an air-to-air tactic remained a matter of controversy. Resolution may require the latest generation of combat aircraft to be tested in battle, using post-stall manoeuvres. On the other hand, using aerodynamic and thrust-vectoring- control power to protect against departure from controlled flight will eliminate envelope and asymmetric store restrictions.

The next paper, "X-31A Control Law Design," discusses control system design, including issues associated with thrust vectoring. Multiple control modes are used to control various phases of flight. In the portions of the flight envelope where high angle of attack is available, longitudinal input commands angle of attack. At higher speeds, longitudinal input commands g. Unless the aircraft is in the angle-of-attack command mode and other parameters are met, the post-stall mode is inhibited.

The control law that blends out the rudder as angle of attack increases is of interest. As rudder effectiveness diminishes, thrust vectoring takes over directional control. This is one (and perhaps the most simple) example using multiple control effectors in a given axis and presages a possible next step of the X-31A program, elimination of the vertical tail.

In operation, the pilot must elect to use post-stall flight. He must overcome a stick detent and satisfy several other conditions. Thrust vectoring operates whether or not post-stall manoeuvring is engaged. The presenter indicated that side slip is limited to prevent departure as angles of attack increase.

Given the radical expansion of the flight envelope pioneered by the X-31A, the achievement of Level 1 flying qualities on the first try is remarkable. The F-15 STOL and Maneuver Demonstrator and the F-22 had the same success, indicating that current flying qualities specifications and simulations work well. All three aircraft have experienced unanticipated responses, indicating that general good flying qualities are not in themselves proof of a fully worked-out control implementation.

Paper 14, "X-31A System Identification Applied to Post-Stall Flight - Aerodynamics and Thrust Vectoring," presents progress in parameter identification. Parameter identification has become more difficult as redundant control effectors have proliferated. In the post-stall flight regime, dynamic and non-linear effects cause more difficulty.

A primary objective of the work presented in this paper was identification of thrust-vectoring effectiveness. Possible causes of inaccurate prediction include errors in thrust modeling, aerodynamic effects that modify thrust-vector angles, entrainment of air flow causing unpredicted aerodynamic forces on the aft body, and structural deflections from thrust and aerodynamic forces.

The paper discusses difficulties introduced by instabilities of the basic X-31A airframe and by process noise introduced by stochastically shed vortices. The paper also notes that data analyzed so far were developed from small, slow manoeuvres about the trim point. The effects of aerodynamic and propulsive nonlinearities were largely avoided. Plans for future extraction of unsteady effects were presented.

The paper expresses a desire for single-effector excitation to allow separation of effects such as longitudinal vectoring, canard deflection, and stabilator deflection. Difficulties in parameter identification without such provisions suggest program officials should decide early whether these techniques will be used. Often program authorities are motivated to bet on success -- to assume that these techniques will not be required. A definitive evaluation of the utility of parameter identification for modern aircraft with expanded flight envelopes would be a valuable outcome for the X-31A program.

SESSION IV: FLYING QUALITIES - APPLIED CRITERIA

At the time of the symposium, the EFA was nearing first flight. The first paper of the session, Paper 16, "EFA Flying Qualities Specification and Its Utilization," presented simulation and analytical approaches for EFA control-system performance specification and verification before first flight. Although the paper was primarily based on results from the DASA simulator at IABG, simulation was also conducted at other simulators in Germany and the UK. It remains to be seen whether these complimentary efforts speed development and improve results. In today's environment where multiple participants are the rule rather than the exception, a good strategy for division of responsibilities is critical.

The usual approach of pilot familiarization, classical flying qualities manoeuvres, and tracking manoeuvres was supplemented by targets programmed to "jump," driving pilot gain levels up to uncover flying qualities problems, particularly pilot-induced oscillations. Pilots had the opportunity to provide extensive comments as well as numerical ratings.

Besides piloted simulation, analytical evaluations helped scan the flight envelope for regions in which time and frequency-domain criteria for successful flying qualities were violated. In this process, phase relationships were

found to be highly influenced by the fidelity of the mathematical models selected. Numerous models were used and correlation with piloted simulation was part of the evaluation process. We all look forward to correlation of flying qualities projections with flight-test results.

Paper 17, "Application of Current Departure Resistance Criteria to the Post-Stall Manoeuvring Envelope," is based on X-31A derived data and recognizes the need for new criteria for expanded flight envelopes. The paper recognizes the aerodynamic and the control-system capabilities and complexities in new fighter aircraft. An important conclusion is that while it is necessary to determine the stability of the aircraft as a nonlinear system, this is usually done by making the necessary assumptions to develop a linear model. Stability predictions are, therefore, related to selected points in the flight envelope and care must be taken not to make unwarranted extrapolations.

The paper documents several approaches to stability determination and highlights the need to expand existing criteria. It refers to the fact that the X-31A becomes departure susceptible if coupling is considered and as little as 5 degrees of sideslip is allowed. Advancement in nonlinear and unsteady aerodynamics and controls is clearly called for to address these limitations. Fundamental concepts, new formulations, and ambitious application of engineering design as addressed in this paper must become the standard.

The expansion in the flight envelope exceeds the data base used in contemporary standards such as MIL-STD-1797A. Recognizing that flight envelopes are expanding rapidly, Paper 18, "Flying Qualities Evaluation Manoeuvres," addresses one aspect of keeping flying qualities specifications up to date. A fundamental difference between the manoeuvres examined in this paper and those used previously is the necessity to unite flying qualities and closed-loop system performance, a theme that would occur again in the following paper.

In viewing video animations of some evaluated manoeuvres and recalling some X-31A flight test information, it was apparent that a manoeuvre looking precisely like a spin is within the capability of the new generation of highly manoeuvrable aircraft. Other unconventional manoeuvres remain to be developed and discovered. These manoeuvres should not be discovered during operational use. Allowing this new generation of fighters into the field without thoroughly developing the new manoeuvres could recall the bad old days of pitch-ups and roll-coupled departures.

The paper goes on to describe selection of manoeuvres, their tactical relevance, and hopes for expanding the data base for these manoeuvres by flying them in the multi-axis vectoring F-16, the X-31A, F-22, and the F-18 HARV. All the manoeuvres have evident tactical relationships and the correlation of the manoeuvres with aircraft performance parameters is particularly instructive. The similarity of these manoeuvres to manoeuvres often proposed as sources of agility metrics clearly indicates to this author that flight-mechanics-oriented aspects of agility are entering the mainstream of specification and evaluation of aircraft.

In this author's research and development experience with flying qualities, manoeuvrability, and agility, perhaps the most significant single event was his exposure to the rotary wing view of agility at the first meeting of the *AGARD FMP Working Group 19*. The idea of unifying precision, manoeuvring performance, and flying qualities through objective data was elegant. Paper 19, "Study Findings on the Influence of Manoeuvrability and Agility on Helicopter Handling Qualities," illustrated the effectiveness and maturity of that approach.

The paper presents methodology and results for three experiments. It is interesting to note that results suggest flying qualities criteria could be relaxed from ADS-33C, the US Army Design Standard. It is also of interest that using simulation enabled enough test runs and subject pilots that statistical confidence could be computed for Cooper-Harper ratings. A similar approach could insert *a higher degree of integrity into flight test where* conclusions of a small group of elite pilots can mask problems.

In remarks after the presentation, one conference attendee remarked that the flying qualities specification for the RAH-66 helicopter had been changed because of the findings reported in this paper. He noted that the change was made based on simulation only, without confirming flight test. While the Ames vertical motion simulator provides exceptional capability to duplicate rotorcraft flight, this is still a significant step.

This paper concluded the session. The complexity and high capability of modern aircraft and control systems *offer remarkable capability, but also demand* mathematical and physical understanding. The opportunity to make startling advances in mission performance is balanced by the danger of incomplete or erroneous design execution leading to subtle hazards that may not manifest themselves until certain unique circumstances occur.

Pilot preferences when flying such aircraft are not fully documented and issues of high-angle-of-attack flying under operational conditions are poorly understood.

Achieving full operational benefits of highly manoeuvrable aircraft will likely not occur until flying qualities criteria are established. The necessary structured research programs will require a research aircraft similar to the NT-33, but vastly more capable in flight envelope or, alternatively, a large body of operationally derived flying qualities results. The problem with operationally derived flying qualities results is that such data tends to be inordinately expensive, costing money, aircraft, and even pilot lives.

Today the US has a successor to the NT-33, the F-16 based VISTA. In spite of strong commitments and best intentions, the VISTA is not capable of the necessary research without enhancement as might be achieved with a more capable version of the thrust-vectoring nozzle now installed on the aircraft.

At this point, the author must insert another personal note. As Director of Flight Dynamics at Wright Laboratory, budget shortfalls prevented me from bringing VISTA to a satisfactory state of completion. Although not engaged in aircraft programs, I am employed by Lockheed Corporation and, with the acquisition of the Lockheed Fort Worth Division (formerly General Dynamics - Fort Worth), Lockheed has an interest in further investment in VISTA.

SESSION V: AGILITY

Paper 20 was titled "Operational Agility - An Overview of AGARD Working Group 19." This author was a member of this working group and fully supports the conclusions of the paper. The paper was presented by the chairman, who first approached me about writing this technical evaluation.

The working group met for the first time in 1991, with most members prepared to spend two years immersed in flight mechanics. Flight mechanics was a primary subject, but the focus of the working group was significantly broader, including avionics, weapons interface, and the pilot/vehicle interface. In considering these subjects, the working group came to the same conclusion expressed by the symposium's keynote speakers -- balance must be the prime consideration in application of technology for agility.

The paper and the planned Working Group report provide a set of definitions that should ease future work in the area. The paper outlined the structure of the report and a methodology for specifying and assessing agility of weapons systems.

Twelve conclusions are presented, the last of which is "The study of Operational Agility is still immature." Eight recommendations include a list of additional studies, concluding with a recommendation in support of concurrent engineering. The paper includes a self-assessment of the degree to which the working group accomplished eight assigned objectives. Of these, seven were reasonably well accomplished. The objective "To collate the results of lessons learned from experiments on agility" was only partially achieved because many of the experiments are still underway and data are only sporadically available. This objective is important enough that it should be continued in the appropriate AGARD forum.

Paper 21 is an "Operational Agility Assessment with the AM-X Aircraft." One of the co-authors was a member of Working Group 19 so this paper was written with knowledge of working group deliberations. The AM-X is a relatively mature aircraft and was designed with attention to agility, but without the benefit of substantial research over the past several years. Looking back at the aircraft from today's perspective illustrates the extent to which "agility" is an eternal truth in aircraft design. Today's point of view also illustrates the improvement in appreciation and understanding of agility as a result of recent investigations and considerations. Unfortunately, none of the authors were able to attend and the paper was presented by one of the session chairmen.

Significant aspects of the AM-X investigation include the extensive use of simulation and the application of concepts emerging from Working Group 19. The approach of performance-oriented evaluations rather than subjective flying qualities is notable

Results are presented for four manoeuvres The methodology for collecting, correlating, and presenting agility data in terms of time to accomplish a specified manoeuvre is in keeping with several of the presentations preceding this one Consistent with other results already presented at this symposium, this paper validates the applicability of agility metrics, the use of simulation, and the concept of evaluating a complete pilot-in-the-loop system.

TECHNICAL TOUR - NAVAL AIR WARFARE CENTER, PATUXENT RIVER, MARYLAND

At this point, the symposium was interrupted for a tour of the Naval Air Warfare Center, NAS Patuxent River, Maryland. This author was assigned there as a test pilot from 1980 to 1983. The technical tour included an opportunity to witness a land-based steam catapult launch of an F/A-18 and inspection of the land-based arresting gear. Both the catapult and the arresting gear are similar to those installed on US aircraft carriers. Other tour stops included the Chesapeake Test Range and the adjacent data acquisition system. These two systems have long set the standard for generic, flight-test ground terminals.

The power of the US Navy's plan to consolidate aeronautical research, procurement, and testing at one location was evident in the simulation facility. This operation is well beyond that normally found at a research or a test establishment. The adjacent, connected anechoic chamber for test of full-scale aircraft provides an important capability and a strong argument for concentration of resources. The tour also visited the US Navy Test Pilot School and static display of school aircraft. As interesting as the display was, the USAF NT-33 and the CALSPAN Learjet, both equipped for variable stability flight, soon became a center of attention. The presence of these two aircraft and the impromptu explanations of their role in the Test Pilot School served the objectives of the tour well.

SESSION V: AGILITY (continued)

Assuring that technology discussed during the symposium can be made available to the pilot is addressed in Paper 22, "Expanding the Pilot's Envelope." This author is a strong supporter of the point of view presented, a point of view I developed as a combat pilot and presented as one author of the Pilot/Vehicle Interface Chapter of the Working Group 19 report.

The most significant contribution of the paper may be its presentation of human capability as an envelope to be expanded by careful, insightful design. The human envelope is multidimensional, with the interplay of several stresses operating over time to affect capability. In particular, the discussion of fatigue as not a condition in itself, but as a result of conditions was insightful. Understanding fatigue is difficult because it cannot be directly measured until a sudden drop-off in pilot performance is noted. The paper also discusses the contribution of training as a means to expand pilot capability, the importance of a properly designed informational interface and the structure of a successful control strategy.

The discussion of display menus is particularly insightful. This author would add the observation that display menu sequences are often set up in consideration of a "design mission" that the pilot almost never flies. While leading the pilot to the next "right" decision, designers must avoid confining the pilot to a predetermined sequence of events

Paper 23, "The Influence of Flying Qualities on Operational Agility," illuminates two important concepts. In a variation on the idea that good flying qualities lead to good pilot/aircraft system performance, this paper proposes measuring the agility factor as the ratio of performance achieved by the pilot to the maximum theoretical performance. The second concept links flying qualities, as measured on the Cooper-Harper rating scale, to safety and mission accomplishment.

The objective in using the agility factor is to achieve a value of one, meaning the pilot achieves the maximum performance available from the system. His inputs might consist of a step input to full control deflection and an abrupt full opposite deflection to complete the manoeuvre, all occurring without overshoot, undershoot, bobble, or oscillation. This author suggests that the approach is meaningful only in the context of high-performance manoeuvres by high-performance aircraft. A 30-degree roll by an airliner, performed at an electronically limited rate, would achieve a high rating but would not, in this author's opinion, be evidence of agility.

To link flying qualities and safety, the paper's author considers Cooper-Harper pilot ratings as Gaussian distributions. For a given aircraft and a given task, there is a finite possibility that the pilot rating for a specific occurrence will be worse than 6, meaning the mission is compromised and another possibility that the pilot rating will be 10, meaning loss of control occurs. There are numerous caveats on this approach, including the assumption that pilot ratings are Gaussian and that the rating scale is linear. Fully developed, the approach would make it possible to determine cost/benefit ratios for flying qualities improvement.

Paper 24, "An Agility Metric Classification Scheme for Operational Agility," reflects the proceedings of Working Group 19 and the Working Group report. The contribution of this paper and the corresponding part of the report is a structure for agility specifications for program officials. The resulting system specification can be constructed entirely at the mission level or it can extend to the flight mechanics level. Once the top-level specification is in place, the structure presented in this paper provides a means to decompose toward flight mechanics and eventually to detail design. One thread that runs through all metrics considered is time, both as an independent variable and as a measure of merit. Considering this paper with the previous two, the reader can integrate the human performance dimension and the probability of mission success with other considerations. This integration, if successful, can guide system design from earliest concept to evaluation of alternate technological approaches.

A further conclusion from Paper 24 is that the available data are incomplete. In today's marketplace, where the value of addressing issues "up-front and early" is understood, but is expensive, availability of the individual metrics and the overall structure presented in the paper will pay off.

Paper 25, "Application of Centrifuge Based Dynamic Flight Simulation to Enhanced Manoeuvrability RDT&E," builds on the demonstrated value of

simulation and shows one more approach to increasing simulation fidelity. Use of centrifuge-based simulation is well accepted for some applications, particularly those associated with measuring and improving g tolerance. The question addressed by this paper, however, is flying qualities research using motion-based simulation. Six-degree-of-freedom motion is used in many simulators but, because of limited ranges of motion, can only provide onset cues. A centrifuge can provide continuous, substantial accelerations, but only within tightly linked relationships limited by the fact that the gondola must remain affixed to the end of the centrifuge arm. Human perception plays an important role in development of rules for selecting which accelerations to duplicate and which to compromise.

The core issue, not addressed in the paper, is selecting the niche for centrifuge-based simulation. This author would suggest that the centrifuge-based simulator's role in flying qualities research will remain limited by unintended artifacts. One example of such an artifact was cited in the paper. This was the need to operate around an elevated g level to simulate one g, to be able to simulate less than one g. To be competitive in flying qualities research, centrifuge-based simulation must offer an advantage over other forms of motion-based simulation.

Paper 26 was not presented. As a historical note and a lesson learned, the Russian presenter could not attend because of lack of a passport. Within the month preceding the symposium, an attempted coupe d'état in Russia may have disrupted the functioning of governmental agencies. AGARD was not able to solve the problem.

Paper 27, "Optimal Manoeuvring in Air-to-Air Combat - A Differential Game Methodology," could have been a dry, mathematical presentation. Instead, this paper became the focus of controversy. The author's stated intention is to provide a means to link simulation and analysis for quick development and evaluation of air-to-air tactics and technology. The purpose is to evaluate tactics with new technology before the aircraft is designed rather than after. If successful, this will avoid expenditure on technology that has little tactical value and identify alternative technology with high payoff.

One critical element of the paper's approach is a recognition that in the air-to-air environment, pilots fight weapons envelopes, not just aircraft. Flying one's own aircraft in a manner that enlarges the opponent's envelope confers an advantage on the opponent. In the context of "fighting the envelope," post-stall manoeuvring usually increases the opponent's envelope and increases susceptibility to the opponent's missile. On the other hand, the advantage of post-stall manoeuvring can be a quick kill. Therein lies the controversy.

The paper presents results of an innovative low-cost simulation running on a work station to compare technologies for effectiveness in selected scenarios. Differential gaming guided the experiment and evaluated results. One technology set evaluated was supermanoeuvre to point the nose plus a missile capable of launch at high angle of attack. To quote the paper, "...the pilots thought it would be unbeatable. However, the technology in this test offered little advantage ..." The author includes the note, "Perhaps there is more advantage to this technology in real (within visual range) air-combat...", but to no avail. Individual members of the audience vociferously rejected or defended the results. Protests by the author that the study and the paper offered a methodology rather than a conclusion did little to defuse the tension.

In this episode, the controversy obscured the issue. The cost of research is so high that every available means must be used to understand potential benefits. One serious difficulty continues to be the lack of understanding between the technical and operational communities. Fly-by-wire, totally accepted today, presents an excellent illustration. The developers of the technology knew very well that the benefits would be design freedom and improved flying qualities. The operational community did not perceive that design freedom would lead to stealth aircraft or that improved flying qualities could eliminate many fatal accidents while improving system performance. So, how to sell fly by wire? It was sold based on the concerns of the operational community at the time -- weight reduction and the ability to survive battle damage. Experience tells us that our customer works in the present. Our choices are to present our technology in terms of present issues or to provide our customer with the means to see the future. Developing a view of the future is the intent of the technology of Paper 27. It is most important that the controversy not obscure the real issue -- can differential game methodology effectively screen tactics and technology sets? Can it help the customer select among alternative futures?

At the end of the conference, this author was given an opportunity to make remarks. With a perspective developed in just over a year spent mostly in pursuits other than aeronautics and military aircraft, it is clear that rapid progress has continued. Information technologies from the civil sector are a significant contributor to this progress. In the period of reduced military spending to come, adapting other technology developed outside the military sector will be an important key to effectiveness and cost control.

CONCLUSIONS AND RECOMMENDATIONS

Selected conclusions and recommendation follow. Others may be found in the text of this report.

Conclusion: Simulation and analysis can provide the basis for accurate predictions of high-angle-of-attack characteristics and flying qualities. Used in conjunction with on-line simulations, an accurate preflight data base can speed flight test and envelope expansion.
Recommendation. Programs study examples like YF-22 envelope expansion to develop techniques to minimize time and expense in flight test.

Conclusion: A comparative study of forebody flow control and forebody vortex control would benefit the aeronautics community. Such a study should include various mechanisms, port/slot locations, nose shapes, and correlation of analytical, simulation, and flight-test results.
Recommendation: AGARD consider establishing such a study, perhaps starting with a forebody control workshop.

Conclusion: High-angle-of-attack flying qualities research lags aeronautical development.
Recommendation: AGARD schedule a workshop or symposium to address the subject.

Conclusion: Parameter identification may provide an important approach to addressing expansion of the flight envelope into non-linear regimes. Fast-moving flight-test programs do not encourage use of the technique.
Recommendation: Advocates of the technique consider how to better fit into accelerated flight test.

Conclusion: Poor communication between technologist and user of the value of exceptional manoeuvrability inhibits both communities.
Recommendation: AGARD establish a forum with carefully selected membership from both communities to further explore applications of manoeuvrability.

Conclusion: The X-31A program advanced high-angle-of-attack flight test instrumentation and testing techniques.
Recommendation. With the EFA and the F-22 program pending, it may be beneficial to all participants to develop a forum, perhaps within AGARD, for sharing problems and solutions. Rafale lessons may also be valuable.

Conclusion: Advancements in information technology are significantly affecting aircraft development, design, and tactical utilization.
Recommendation: AGARD should consider sponsoring a forum to better understand the impact of this technology and to position the flight mechanics community to achieve full benefit from these advances.

SUMMARY

The symposium was highly successful in presenting a wide-ranging review of recent advances in fighter aircraft manoeuvrability. The Rafale, YF-22, and EFA represented the current generation with significant advances over earlier technology. The F-15 STOL and X-31A programs represented recent and current research activities. The various sessions covered aerodynamic and propulsive aspects of enlarging the flight envelope.

Flying qualities and agility sessions addressed implementation and application of manoeuvrability technology. The simulation session and analytical discussions embedded in other sessions documented using these techniques for charting new directions, evaluating technology options, and advancing selected technology.

Missing from the symposium were X-29 vortex flow control flight test results, F-18 High Angle of Attack Research Vehicle (HARV) tests and results from NASA Ames full-scale F-18 wind-tunnel tests. Other advanced programs outside the US and beyond the author's familiarity might have made similar contributions. The absence of these programs highlighted the necessity for a comprehensive review of forebody flow and vortex control research, simulation, and testing.

Controversy about the application of high-angle-of-attack capability illuminated the difficulty of communication between technologists and operators. The keynote speakers, both operationally oriented and technically literate, highlighted the need to balance technology with cost and mission needs. Nonetheless, during the course of the conference, controversy about the value of high-angle-of-attack manoeuvrability surfaced. The broad approach taken by AGARD Working Group 19, as reported during the symposium, illuminated several technology needs and recommended approaches to satisfying those needs. The report of Working Group 19 may provide a framework for addressing issues associated with post-stall manoeuvre.

The author thanks AGARD and all symposium attendees for a stimulating opportunity. As NATO's role changes, the personal contacts afforded by AGARD participation may provide glue to help keep the alliance successful.

NOTE DOMINANTE DE LA CONFERENCE – 1

par

Le Général de Brigade Aérienne J-G. Brévot
Sous Chef Programmes Matériels
E.M.A.
24, Boulevard Victor
00460 Armées
France

Laissez moi tout d'abord vous dire le plaisir qui est le mien de prononcer l'intervention d'ouverture de ce symposium consacré aux technologies pour les aéronefs à haute manoeuvrabilité.

Je suis en effet en quelque sorte un ancien du Flight Mechanics Panel de l'AGARD puisque, plusieurs fois au cours de ma carrière aéronautique, j'ai eu l'occasion d'apporter mon expérience lors de symposiums précédents ou pour des travaux d'Aerospace Application Studies.

Je suis d'ailleurs particulièrement heureux de retrouver aujourd'hui des personnalités qui ont longtemps oeuvré pour la qualité des travaux du Panel, et je tiens tout spécialement à saluer Mr J-M DUC, co-chairman de la 1er session de ce symposium, dont les compétences aéronautiques sont remarquables et qui me fit connaître l'AGARD il y a maintenant bien des années.

* *
*

Comme à l'accoutumée, je pense que les travaux de ce symposium seront de grande qualité et que les progrès et les perspectives de la technique dans le domaine de la haute manoeuvrabilité seront brillamment évoqués.

Il convient donc, avant de laisser place aux exposés et aux débats sur les possibilités offertes par cette technique de pointe, de vous faire part des réflexions de l'opérationnel que j'étais et du responsable de l'équipement de l'Armée de l'air française que je suis maintenant.

Et pour commencer je vous parlerai des commandes de vol électriques dont l'arrivée dans le courant des années 70 a véritablement révolutionné le monde de l'aviation de combat.

Vous en appréciez certainement les qualités remarquables en matière de stabilité, de rapidité de réponse, de manoeuvrabilité ou de sécurité.

Je voudrais ajouter un point qui est trop souvent oublié face à ces remarquables apports techniques. En effet l'apport peut-être le plus étonnant de ces dispositifs de commandes de vol électriques est que, pour la première fois, on a cessé de constamment charger l'esprit du pilote par des tâches de second ordre. Pour la première fois on a cherché à utiliser son intelligence pour des tâches productives.

Presented at an AGARD Meeting on 'Technologies for Highly Manoeuvrable Aircraft', October 1993.

Je m'explique.

L'avion étant devenu redoutablement facile à manoeuvrer, l'esprit du pilote est devenu beaucoup plus disponible pour se consacrer au système d'armes, à la maîtrise de la situation, à la tactique, bref pour assurer les fonctions de haut niveau qui assurent la victoire dans le combat aérien moderne. Il s'agit là probablement de l'apport le plus remarquable, bien que souvent mal perçu parce qu'indirect, des commandes de vol électriques sur l'efficacité globale des avions de combat.

Cet exemple illustre d'ailleurs fort bien l'interaction constante qui existe entre les qualités manoeuvrières d'un avion et les fonctions de son système d'armes, que cette interaction soit techniquement directe ou tactiquement indirecte.

Je pense que c'est une considération que vous ne devrez jamais oublier au cours des débats de ce symposium.

* *
*

Un autre sujet d'intérêt pour l'opérationnel est de savoir bien cerner les domaines dans lesquels nous devons appliquer les progrès fulgurants de la technologie. Accessoirement, le financier désire savoir quels sont les axes technologiques dans lesquels il doit investir les francs, les écus ou les dollars... devenus de plus en plus rares.

Le sujet est d'importance car l'expérience des conflits récents au premier rang desquels la guerre du Golfe, montre qu'il est totalement vain d'espérer une victoire aérienne complète dans un théâtre d'opérations moderne si on ne dispose pas de la technologie la plus évoluée.

Mais dans quelles technologies faut-il investir ?

Dans le domaine de la haute manoeuvrabilité qui est celui de ce symposium, je vous pose en particulier la question suivante : pour être efficace en combat aérien, vaut-il mieux développer la manoeuvrabilité de l'avion ou au contraire celle de l'armement et en particulier des missiles?

Il semble en effet économiquement plus rentable de rendre extêmement manoeuvrant les missiles, au détriment éventuel des capacités manoeuvrières de l'avion porteur ; surtout si ce dernier dispose d'un système d'armes évolué avec des dispositifs de tir rapide et fortement dépointé comme les viseurs de casques ou les senseurs infra-rouge.

Seulement, que se passe-t-il alors s'il n'y a plus de missiles à bord de l'avion et s'il faut tirer au canon ?... canon que les opérationnels, conscients des coûts très élevés des missiles modernes, appellent "l'arme du troisième jour". Et puis la haute manoeuvrabilité présente d'autres avantages : aptitude à se positionner très rapidement donc à percevoir et à dominer la situation, maîtrise permanente de l'appareil, retombées sur les capacités STOL...

La réalité est qu'à enveloppe budgétaire constante il faut trouver un juste milieu. J'ose espérer que certains éléments permettant d'apprécier ce juste milieu sortiront de ce symposium.

* *
*

Vous avez bien senti à mes propos que je suis particulièrement attaché à la question des coûts. Et c'est bien normal quand on est le responsable de la programmation et de l'équipement d'une Armée de l'air.

Au départ de mon travail il y a d'ailleurs l'expression du besoin, laquelle est particulièrement difficile dans le domaine de la haute manoeuvrabilité, surtout si on se heurte au problème évoqué précédemment de la frontière entre l'avion et le missile. Comment en effet spécifier la manoeuvrabilité ? de façon rigide par des chiffres, ou de façon ouverte par des résultats dans des scénarios donnés ?

D'où l'importance particulièrement grande que nous attachons aux simulations d'étude et de conception. J'espère que ce domaine sera évoqué au cours de ce symposium.

Mais revenons-en aux coûts.

Nous ne faisons pas de la technique pour la technique, nous faisons de la technique dans un but d'efficacité militaire sous contrainte budgétaire.

Je ne pourrai donc que vous inciter au cours de nos présentations et débats à garder constamment présent à l'esprit le souci de la justification opérationnelle face au budget, et du rapport coût/efficacité. En effet il ne sert à rien d'étudier des dispositifs fabuleux d'hyper-manoeuvrabilité si on est dans l'incapacité totale de se les payer. Il faut savoir s'arrêter, car l'avion est un tout qui a d'autres besoins d'investissement.

C'est bien là le plus difficile.

* *
*

Et puisque nous évoquons le problème des coûts, parlons alors des réalités industrielles.

Le domaine de la haute manoeuvrabilité est particulièrement fourni en dispositifs coûteux destinés à maîtriser le vol aux très grandes incidences, le post-décrochage, la poussée vectorielle et bien d'autres sujets encore... De nombreux et très certainement brillants exposés sur ces dispositifs sont prévus au cours de ce symposium.

Puisque ces réalisations sont coûteuses, il va certainement falloir s'allier et se regrouper entre industriels et entre Nations. Et c'est un des grands bénéfices de ce type de manifestation de réunir les meilleurs spécialistes des applications concernées, de présenter mutuellement les compétences et d'être peut-être le générateur de coopérations et d'alliances industrielles futures.

C'est en tout cas ce que je souhaite, désireux que je suis de voir l'industrie apte à offrir dans l'avenir aux forces armées les réalisations techniques de qualité dont elles ont besoin.

Je ne peux terminer sans vous faire part de mes soucis pour l'avenir.

Chaque nouveau programme d'avion de combat représente environ 10 ans de charge de travail pour les bureaux d'étude concernés. Or les coûts particulièrement élevés de ces nouveaux programmes entraînent les responsables de programmation à vouloir rentabiliser les investissements du développement et donc à conserver les avions pendant 25 à 30 ans, quitte à planifier un "Mid life update" pour le système d'armes.

Comme par ailleurs les avions sont devenus polyvalents, il n'y a plus l'alternance des programmes air-air et air-sol. La conséquence est claire : la charge de travail devient insuffisante pour les bureaux d'études et ceux-ci ont tendance à se démanteler, perdant ainsi définitivement la compétence.

Par ailleurs on assiste à un mouvement généralisé de regroupements industriels pour des raisons évidentes de coûts de production et d'effets de série.

Face à ces regroupements, le client militaire que je suis s'inquiète de voir disparaître petit à petit la concurrence et par conséquent l'incitation à la qualité de conception.

Le tableau est donc plutôt noir : pertes de compétence, baisse de qualité de conception.

Oserai-je avancer une solution à cette situation critique : le maintien d'un nombre suffisant de sociétés de bureaux d'études, accompagné d'une programmation budgétaire propre à maintenir un travail permanent de conception, pouvant aller jusqu'au prototype, avec incitation financière en cas de choix du produit pour la production dans les grandes filières regroupées et éventuellement uniques.

* *
*

Je terminerai en vous remerciant encore de m'avoir invité à m'exprimer devant vous.

L'AGARD, et plus particulièrement le Flight Mechanics Panel, constituent un forum remarquable du progrès technologique.

Je ne peux que vous féliciter par avance pour la qualité des travaux que j'entrevois pour ce symposium.

J'en suis heureux car cette qualité est le gage de la vitalité du monde de l'aéronautique et donc de l'efficacité future de nos Armées de l'air.

KEYNOTE ADDRESS -- 2

MANEUVERABILITY -- ONE KEY TO COMBAT EFFECTIVENESS

by

Brigadier General George K. Muellner
Director of Requirements
Headquarters Air Combat Command
HQ ACC/DR
204 Dodd Blvd, Ste 226
Langley AFB, Virginia 23665-2777
United States

Good Morning, Ladies and Gentlemen. It is an honor and a pleasure to be able to make some opening remarks to help initiate this symposium. The agenda over the next several days promises to provide us a great review of the state of the technology to support highly maneuverable aircraft. As expected from a symposium sponsored by the Flight Mechanics Panel, the agenda will focus on the Aerodynamic and Flying Qualities aspects of the subject. (CHART F-1)

I believe we will see that significant advances have been made in both better understanding and better being able to exploit aircraft maneuverability as a design variable contributing to the effectiveness of a weapon system. It is this broader issue of weapon system effectiveness that I wish to focus my comments on this morning.

As the Director of Fighter, C2 and Weapons Programs for the Secretary of the Air Force my responsibility is to oversee the fielding of weapon systems for the U.S. Air Force's Combat Air Forces. I am happy to report to you today that despite the austere budget environment and force structure drawdowns, the U.S. Air Force will continue to modernize our forces. In fact, as our force structure reduces it is increasingly important that each weapon system contribute the maximum combat effectiveness to the overall force.

Over the past several years the Air Force has performed hundreds of trade studies and thousands of hours of modelling and simulation to determine the proper balance of design variables to optimize the effectiveness of both our next generation Air Superiority fighter (CHART F-2). All of this analysis has reaffirmed that the effectiveness of the weapon system is strongly dependent on not only the performance characteristics of the aircraft but also on the characteristics of the weapons and supporting avionics employed by the aircraft and the command and control environment in which the aircraft will operate. It is from this broader systems perspective that we have attempted to define and optimize our weapon system requirements.

The Air Force's next generation Air Superiority aircraft is the F-22 which is the outgrowth of the Advanced Tactical Fighter program. (CHART F-3)

This design emphasizes a balance (CHART F-4) toward achieving "First Look, First Shot and First Kill". This balanced approach was chosen to provide air superiority in a very hostile air-to-air and ground-to-air environment. The F-22 will need to operate within an Integrated Air Defense System (IADS) which will include very capable fighters equipped with long range RF missiles and with short range IR weapons capable of being employed in a very dynamic close-in battle. Additionally, the IADS will include both RF and IR surface-to-air missiles which must be dealt with to preserve freedom of maneuver.

The F-22 design emphasizes stealth and integration of on and offboard sensor information to gain the "first look". To gain "first shot" an integrated avionics architecture is combined with The AIM-120, Advanced Medium Range Air-to-Air Missile. Balanced signature reduction and the AIM-9X provide the shorter range capability with a 20MM gun and an all aspect gunsight completing the armament suite.for the close battle. Affordability from both the acquisition and cost of ownership aspects has been a key design consideration.

The extensive analysis performed by the Air Force and numerous contractors identified the leveraging characteristics (CHART F-5) for the F-22. For each of these key performance parameters, thresholds, or minimum acceptable, values were established which were necessary to achieve the desired level of combat effectiveness and to insure " First look, first shot and first kill". These threshold values have been the focus of several years worth of deliberation and tradeoff analysis. They of course represent the "live or die" performance of the system in operational test.

Presented at an AGARD Meeting on 'Technologies for Highly Manoeuvrable Aircraft', October 1993.

Maneuverability was identified as one of the key performance characteristics. (CHART F-6) The minimum acceptable maneuver capability allowed effective exploitation of the tactical surprise provided by stealth and minimized the time spent within an enemies effective sensor or weapons envelope. In the close battle our simulation analysis showed that maneuver advantage alone would not guarantee superiority against an adversary equipped with an all-aspect IR weapon that exploited wide field-of-view cueing (CHART F-7)

Superiority against this threat required not only agility, but also good acceleration, reduced signature and a similar weapons capabilities. The key to favorable exchange ratios was to minimize time spent within this very hostile arena - especially if the scenario involved multiple adversary aircraft. System configurations, lacking a balanced design, generally achieved only equivalency in exchange ratio in the close-in battle - clearly unacceptable !

As a result of this analysis the F-22's maneuver requirements are only slightly greater than those of the F-15 or F-16. The key is that these maneuver characteristics must be achieved by a design that also emphasizes signature reduction, superior acceleration, supercruise and significant range. This balanced design introduced many new challenges since our previous stealth design had not stressed maneuverability. The challenges of achieving this balanced design requires technologies matured in the programs you will hear about over the next several days.

The F-22 (CHART F-8) program will exploit an integrated flight and powerplant control, a blended wing/body design exploiting effective vortex control and superior high angle of attack flying qualities which allow effective and safe operation at angles of attack up to 60 degrees. The application of digital simulation has allowed us to work the optimization and trade-off within the design variable with mission effectiveness as the governing criteria. Thus, for the F-22 maneuverability remains an important design requirement. However, this is maneuverability achieved within a balanced design.

Recently, the Air Force completed a Multi-Role Force analysis to identify the leveraging characteristics of the replacement for the F-16. This aircraft has a primary air-to-ground role with a secondary air-to-air capability. As with the F-22, maneuverability proved to be a key characteristic (CHART F-9) but only within a balanced design emphasizing some stealth, excellent reliability and supportability and reduced cost. Once again the required maneuverability for our next generation multi-role fighter was only slightly better than the F-16 exhibits today, but it must be achieved in a platform that is more heavily influenced by air-to-ground weapons delivery requirements and affordability. Given these two fighter programs drive our operational requirements, let me summarize the maneuverability requirements we see for these 21st generation aircraft (CHART F- 10).

First, we must maintain or slightly improve maneuverability while decreasing observables and increasing range. Second, we must refine control technologies and flying qualities to permit high agility and safe transition of the high angle of attack arena. While we do not see long sustained engagements at high angle of attack, we will certainly need to exploit this arena in the close-in battle. Third, we must reduce the development and life cycle costs of the advanced control systems required for our balanced design to keep these aircraft affordable. Given austere budgets and the need to replace a large number of F-16s in the early 21st century, our replacement aircraft must be affordable to develop and have low life-cycle operating costs.

The three challenges i have described are significant but as you will hear so is the progress we are making through our technology programs. (CHART F-11) Clearly, the introduction of stealth and the advances in weapons technology have not obviated the need for maneuverability. Rather, it places more burden on you as technologists to harmonize your developments into a balanced design.

As a warfighter I remain optimistic that our expectations will be met and that the F-22 will provide air superiority and that the combat effectiveness of our force will continue to increase.

Thank you for your attention. I will be glad to entertain your questions.

MANEUVERABILITY
ONE KEY TO COMBAT EFFECTIVENESS

B/GEN GEORGE MUELLNER

ASSISTANT SECRETARY OF THE AIR FORCE (ACQUISITION)
DIRECTOR OF FIGHTER, C2, AND WEAPONS PROGRAMS

FIGURE 1

REQUIREMENTS BACKGROUND

F22

TRADE STUDIES AND SIMULATIONS INDICATE THAT A BALANCE OF PERFORMANCE, SURVIVABILITY, AND RM&S CHARACTERISTICS OFFERS THE HIGHEST PAYOFF FOR AIR SUPERIORITY FIGHTERS

TRADE STUDIES REFINED DESIGN REQUIREMENTS

- APPROXIMATELY 18,150 MAN-IN-THE-LOOP ENGAGEMENT SIMULATIONS (1V1, 2V6, 4V12)
- OVER 32,140 TAC BRAWLER / ESAMS SIMULATIONS

BALANCED BY TECHNOLOGY, AFFORDABILITY AND DESIGN MATURATION

- OVER 26,000 HOURS OF WIND TUNNEL TESTING
- OVER 2,436 HOURS OF FULL SCALE RCS TESTING

FIGURE 2

A BALANCED DESIGN

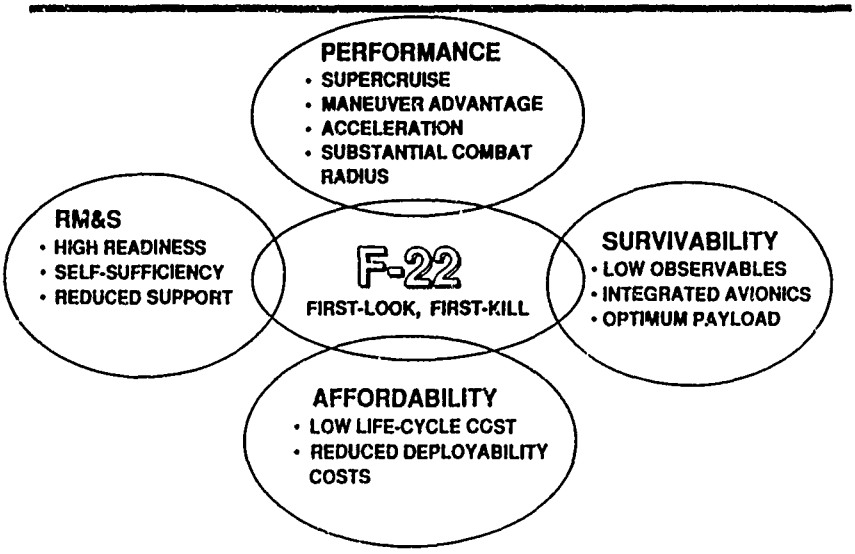

FIGURE 3

KEY PERFORMANCE PARAMETERS

KEY PERFORMANCE PARAMETERS IN ACQUISITION PROGRAM BASELINE

- RADAR CROSS SECTION
- SUPERCRUISE
- ACCELERATION
- MANEUVERABILITY
- PAYLOAD
- COMBAT RADIUS
- RADAR DETECTION RANGE
- INDEPENDENT AIRLIFT
- SORTIE GENERATION RATE
- MEAN TIME BETWEEN MX

FIGURE 4

MANEUVERABILITY

ONE OF A NUMBER OF KEY FACTORS CONTRIBUTING TO COMBAT EFFECTIVENESS

SORD REQUIREMENT: F-22 AERODYNAMIC MANEUVERING PERFORMANCE CAPABILITIES MUST EXCEED BOTH CURRENT AND PROJECTED THREAT AIRCRAFT

SUPERIOR ACCELERATION AND AGILITY ENHANCE BOTH OFFENSIVE POTENTIAL AND SURVIVABILITY

- LEVERAGES LOW OBSERVABILITY CHARACTERISTICS
- COMPLEMENTS HIGH ANGLE OFF-BORESIGHT SRM CAPABILITY
- PRESERVES THE OPTION OF RAPIDLY SEPARATING FROM A MERGE
- DENIES WEAPONS PARAMETERS TO ATTACKING AIRCRAFT AND DEFEATS ORDNANCE IN TERMINAL FLIGHT
- ENABLES PILOTS TO SAFELY TRANSIT THE HIGH AOA REGIME

FIGURE 5

WEAPONS ENVELOPES

MANEUVERABILITY ALONE IS INSUFFICIENT TO ENSURE SURVIVABILITY

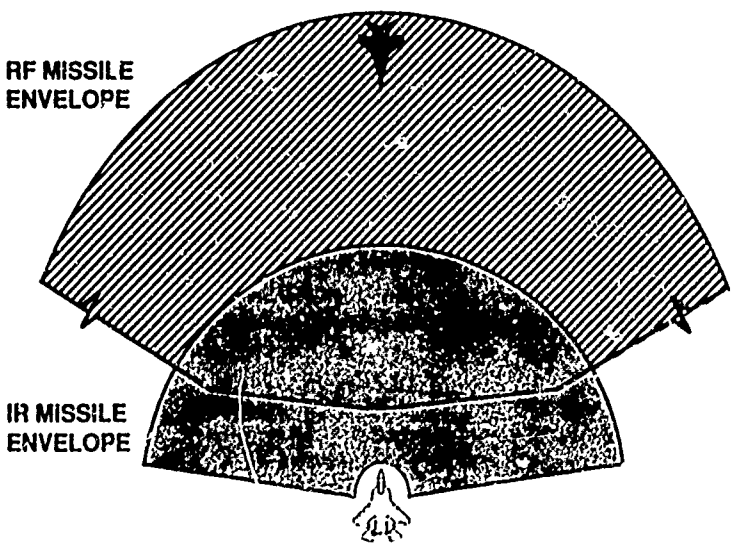

FIGURE 6

F-22 DESIGN FEATURES

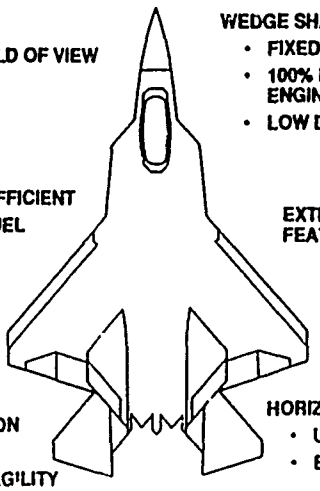

BUBBLE CANOPY
- EXCELLENT FIELD OF VIEW

WEDGE SHAPED INLET DESIGN
- FIXED RAMP
- 100% LINE-OF-SIGHT BLOCKAGE TO ENGINE FACE
- LOW DISTORTION/HIGH RECOVERY

BLENDED WING/BODY
- STRUCTURALLY EFFICIENT
- HIGH INTERNAL FUEL

EXTERNAL SHAPING DESIGN FEATURES FOR LOW RCS

INTEGRATED AERO PROPULSION
- SUPERCRUISE
- TRUST VECTORING FOR AGILITY

HORIZONTAL/VERTICAL TAIL DESIGN
- UNRESTRICTED MANEUVERING
- BATTLE DAMAGE REDUNDANCY

FIGURE 7

MRF LEVERAGING CHARACTERISTICS

1. DEPLOYABILITY	- CUT DEPLOYMENT PACKAGE IN HALF (8 OR FEWER C-141B LOADS)
2. RM&S	- IMPROVE SORTIE GENERATION BY INCREASING MTBCF BY A FACTOR OF 3 TO 4
3. RANGE	- INCREASE UNREFUELED RANGE BY 50%, PREFERABLY WITH INTERNAL FUEL ONLY
4. PAYLOAD	- DOUBLE THE WEAPONS PAYLOAD - EXPAND PRECISION WEAPON CAPABILITY
5. AVIONICS AND SENSORS	- BETTER CAPABILITY FOR NIGHT, ADVERSE WEATHER, AND MEDIUM ALTITUDE - MULTIPLE WEAPONS LAUNCH PER PASS
6. EQUIVALENT SIGNATURE	- REDUCE (DATA CLASSIFIED)
7. MANEUVERABILITY	- EQUIVALENT TO F-16

FIGURE 8

SUMMARY REQUIREMENTS

MANEUVERABILITY WITHIN A BALANCED DESIGN

SAFE AND EFFECTIVE OPERATIONS AT HIGH AOA

REDUCED DEVELOPMENT AND LIFE-CYCLE COSTS

FIGURE 9

CONCLUSION

MANEUVERABILITY REMAINS A MAJOR CONTRIBUTOR TO OVERALL COMBAT EFFECTIVENESS

A BLEND OF CRITICAL SYSTEM CHARACTERISTICS IS REQUIRED TO OPTIMIZE COMBAT PERFORMANCE

THE BALANCED DESIGN OF THE F-22 ENABLES IT TO ACHIEVE THE NUMBER ONE PRIORITY OF EVERY MILITARY CAMPAIGN: CONTROL OF THE AIR

FIGURE 10

USAF/AEDC AERODYNAMIC AND PROPULSION GROUND TEST AND EVALUATION TECHNIQUES FOR HIGHLY MANEUVERABLE AIRCRAFT -- CAPABILITIES AND CHALLENGES

by

Edward M. Kraft, Ph.D
Calspan Corporation/
AEDC Operations

Glen R. Lazalier
Sverdrup Technology Inc.,
AEDC Group

M.L. Laster, Ph.D
USAF/AEDC

Arnold Engineering Development Center
877 Avenue E
Arnold Air Force Base, Tennessee 37389-5051
United States

SUMMARY

The simulation of highly agile aircraft during the development phase presents a significant challenge to aerodynamic and propulsion ground test and evaluation methodologies. The primary simulation challenges are caused by the inherent unsteady, separated nature of the flow phenomena associated with maneuvering aircraft that cause dynamic effects on the airframe and engine. In general, ground test techniques are quasi-steady and transient effects are represented by linearized superposition of steady-state data and unsteady small disturbances. Current trends in the design of tactical fighter aircraft require close coupling between the airframe, avionics, and propulsion systems. In addition, the extreme attitudes and high angular rate motions of this new breed of vehicle causes a strong nonlinear coupling between components. In the current paper, several aerodynamic and propulsion ground test and evaluation methodologies applicable to maneuvering aircraft are summarized, challenges associated with current techniques are identified, and an emerging integrated test and evaluation concept that can significantly impact the quality, time, and cost of developing a new flight vehicle is introduced.

1. INTRODUCTION

Ground test facilities such as wind tunnels and engine altitude test chambers have traditionally been used to develop flight vehicles. New trends in tactical military aircraft design are pushing the limits of the flight envelope and are consequently placing greater demands on the capabilities of ground test facilities. The traditional approach to simulating the dynamic motion of maneuvering vehicles has relied on the linearized superposition of steady-state data and unsteady small disturbances. Newer test techniques to simulate the high amplitude motion of maneuvering vehicles are being developed, but are not fully realized. Even with such short-comings, the aerodynamic input into the design of highly agile aircraft will continue to come from ground test facilities.

On the other hand, the computational modeling of flight vehicles is progressing rapidly. Unfortunately, the dynamic flows around agile aircraft cannot be numerically predicted from first principles in an adequate fashion using present day capabilities in computational fluid dynamics (CFD). However, integrated test and evaluation methodologies are emerging which combine ground testing, flight motion modeling, and CFD. As the newer integrated methodologies evolve, more of the simulation issues of maneuvering aircraft will be resolved. In this paper, we will present several test and evaluation techniques developed over recent years that can provide a new foundation for the development of highly agile flight vehicles.

2. AERODYNAMIC GROUND TEST AND EVALUATION TECHNIQUE

Wind tunnel tests for dynamic stability, including dynamic and rotary balance methodologies, are well understood and documented (e.g., Ref. 1). Traditional aerodynamic ground test methods have proven to be accurate in low angle-of-attack flight where the aircraft aerodynamics are linear and cross-coupling and acceleration derivatives are small. As angle of attack increases and associated nonlinear flow resulting from separation and asymmetric vortex shedding occurs, secondary cross-coupling and acceleration derivatives become large. Studies have been made[2] of the relative importance of various dynamic derivatives in modeling aircraft motion and the need to include good approximations to these derivatives in the simulation of maneuvering aircraft. In this sec-

---

*The research reported herein was performed by the Arnold Engineering Development Center (AEDC), Air Force Materiel Command. Work and analysis for this research were done by personnel of Calspan Corporation,, technical services contractor for the AEDC flight dynamics facilities; by personnel of Sverdrup Technology, Inc., AEDC Group, technical services contractor for the AEDC propulsion test facilities; and by personnel of the Air Force. Further reproduction is authorized to satisfy needs of the U. S. Government.

Approved for public release.

Presented at an AGARD Meeting on 'Technologies for Highly Manoeuvrable Aircraft', October 1993.

tion we will introduce some nontraditional ground test and evaluation approaches to the aerodynamic simulation of maneuvering vehicles, including the separation of weapons from the aircraft.

2.1 Simulated Aircraft Motion

The traditional approach to the aerodynamic development of a flight vehicle generally consists of the acquisition of a comprehensive static aerodynamic coefficient database over the flight envelope of the vehicle. Using such a static aerodynamic coefficient database in a flight simulator to predict the performance of a maneuvering aircraft in the approach-to-stall/stall/post-stall region will usually not model important nonlinear and hysteresis effects on the aircraft aerodynamics.

A technique for simulating aircraft maneuvers in a wind tunnel without the need of a conventional complex and costly static database has been developed.[3] Captive testing of a flight vehicle during a maneuver is accomplished using a closed-loop system consisting of the model with remotely actuated control surfaces, a wind tunnel, and digital computers as illustrated in Fig. 1. A key element of the process is the remotely controlled actuators. A unique aileron drive system developed at AEDC for obtaining remote aileron control on small models with thin wings is illustrated in Fig. 2. The system is designed around a rhombus with a screw jack actuation.

The captive aircraft testing methodology has been demonstrated for a 1/40-scale F-15 aircraft model.

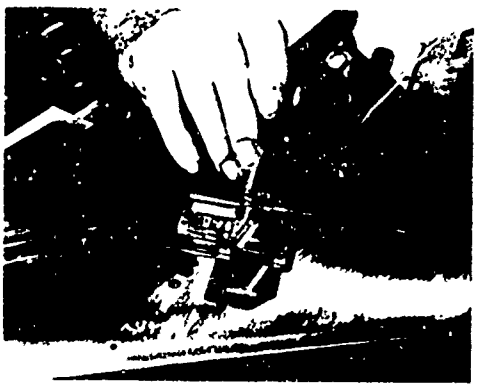

Fig. 2. Aileron drive mechanism developed for captive model.

The wind tunnel model was installed on a six-component internal strain-gage balance which provided the static forces and moments. The wind tunnel acts as an analog forcing function to the model. The model is positioned in the wind tunnel at some trimmed angle of attack and sideslip for a specific condition. Upon initiation of the maneuver, appropriate model control surfaces are deflected and static forces and moments are measured. The static aerodynamic measurements are input to an online digital computer where corrections for the aircraft flexibility, tunnel flow angularity, etc., are applied. The static aerodynamics are then combined with additional external forces (dynamic and thrust characteristics) and a simulated control system and used in solving the Euler Six-Degree-of-Freedom (6-DOF) equations of motion. The computed solutions to the 6-DOF equations are used to control the orientation of the model through a point prediction technique which uses the last two successive measured values of each static aerodynamic coefficient to predict the magnitude of the coefficient over the next prediction interval. The predicted coefficients are then used to calculate the new model angle of attack and sideslip by integrating the equations of motion over very small time steps over the prediction interval. The model positioning system is then commanded to move the model to the new angles, where the static aerodynamic forces and moments are remeasured. The above process is repeated until a complete maneuver is generated.

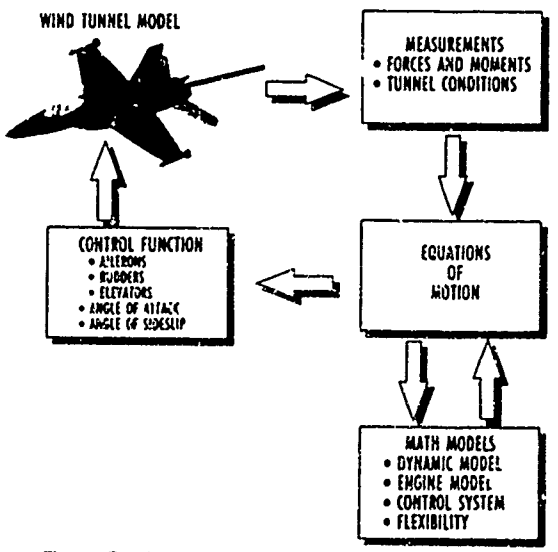

Fig. 1. Captive closed loop data acquisition system.

The aircraft Mach number is also calculated at each prediction interval, and the wind tunnel Mach number is adjusted to the new value. Thus, the aerodynamic coefficients are measured at the correct Mach number throughout the maneuver. Also, the aircraft thrust is calculated and modified with each prediction interval by mathematically modeling the simulated aircraft engine/inlet installed thrust as a function of Mach number, altitude, angle of attack, and angle of sideslip. For a dual-engine aircraft, each engine is modeled separately to account for differences in the inlet attitude during the maneuver.

Specific maneuvers are programmed through the aircraft flight control system. Normally, longitudinal and lateral stick position and rudder pedal position as a function of time are the inputs used in simulating maneuvers. As an option, the control surface deflections may be programmed directly.

Complex longitudinal and lateral/directional high-angle-of-attack maneuvers have been simulated with this technique and compared with flight data from Ref. 4. As an example, an abrupt 1-g wing level stall was simulated for an F-15 aircraft and is illustrated in Fig. 3. As observed in Fig. 3, an uncommanded lateral/directional motion (wing rock) commences at about 20 deg angle of attack while both the lateral stick and rudder pedal are fixed. The oscillatory motion is caused from separated and asymmetric flow over the aircraft resulting in nonlinear and hysteresis effects in the aircraft aerodynamics. Comparison with flight data is excellent. Although this maneuver is considered simple in the flight test program, it is difficult to simulate using a static aerodynamic database in a simulator.

Similar excellent comparisons with flight data are presented in Ref. 3 for simple full lateral stick roll, full rudder pedal roll, and a wind-up turn to stall maneuver for the F-15. A hidden attribute in captive testing of maneuvering aircraft which often plays a significant part in accurate motion simulation is the inherent modeling of control surface interactions (rudder, horizontal stabilizer, etc.). For control surfaces in close proximity which

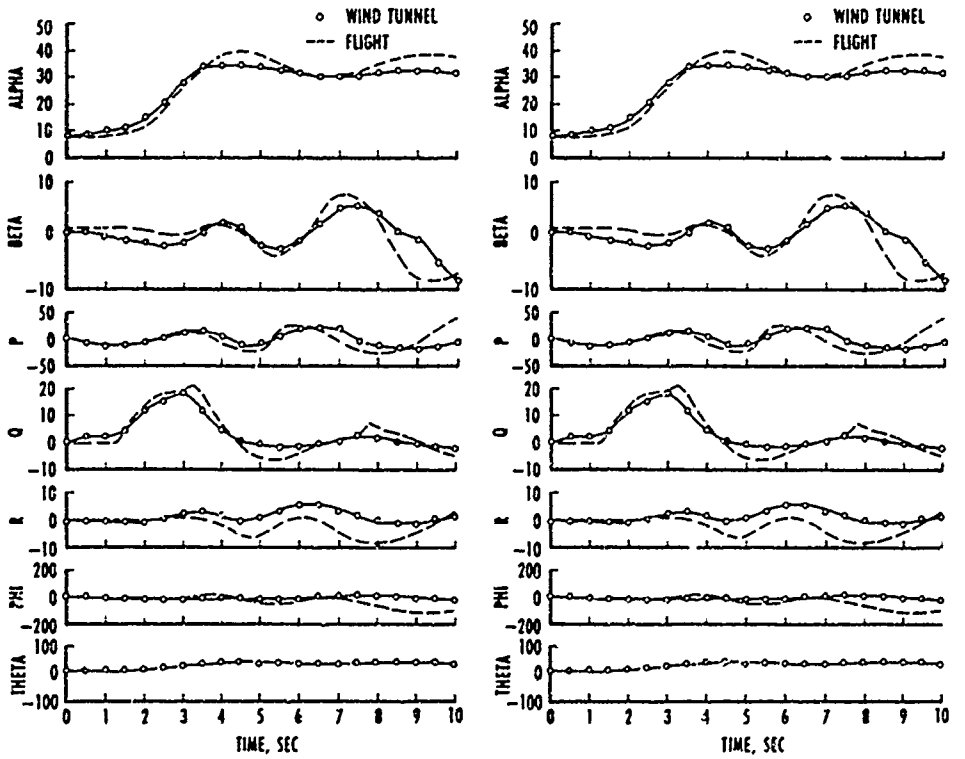

Fig. 3. 1-g wing level stall simulation for F.15.[3]

experience large deflections, interactions often become significant and thereby affect vehicle aerodynamics. Conventional motion simulation cannot sufficiently account for such interactions because of the requirements for unrealistically large data matrices to include all the potential surface deflections.

2.2 Weapon Separation

The new breed of agile fighter aircraft is also expected to perform as a weapon separation platform at extreme attitudes such as a high-angle-of-attack rolling maneuver. Such a condition presents a new challenge to weapon separation simulation because both the aircraft and separated weapon are in accelerated motion. All current wind tunnel test techniques for store separation use a fixed parent aircraft and simulate the weapon motion by either a quasi-steady captive trajectory or a dynamically scaled free drop in the wind tunnel. Consequently, the relative motions of a maneuvering vehicle and separated weapon are not simulated by current wind tunnel test techniques.

In principle, an aircraft model could be placed on one support system and "flown" in the wind tunnel as discussed in the section above while a weapon of interest is "flown" independently on a separate support mechanism. The trajectory equations for the weapon could be solved simultaneously with the Euler equations for the parent aircraft to locate the weapon and aircraft in relative position at each time increment during the maneuver using their independent support systems. No dual, independently controlled support systems exist, and such a testing technique would be time consuming and expensive. In addition, the blockage of such a dual-support mechanism may prohibit smooth operation of a transonic wind tunnel and impact the flow quality. Also, the relative motion of two vehicles would be constrained by the cross-sectional area of the wind tunnel.

Fig. 4. CFD prediction of Mach number contours on a complex fighter aircraft.

motion and predict the store trajectory. The key to the successful use of CFD in such a complex problem is to rely on the CFD model for increments from a well-established baseline. A comparison of an experimentally determined trajectory with one predicted from the CFD model is illustrated in Fig. 5 for the F-15E. For flight conditions where the accelerations of the parent aircraft are not significant, these combined CFD and experimental methods have become very robust and are routinely applied.

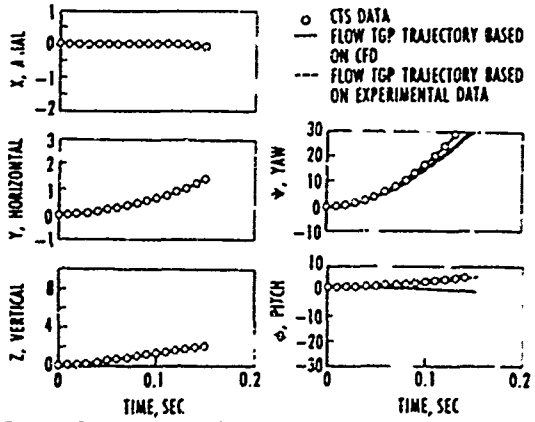

Fig. 5. Corelation of CFD and wind tunnel separation trajectory.[5]

An emerging capability for simulating weapon separation during a maneuver with high angular rates combines computational and experimental methods. Significant advances in computational modeling of complex aircraft with stores have been made in the past few years.[5-7] A representative flow-field solution for the F-15E with stores is illustrated in Fig. 4. Combining the CFD solution with selected wind tunnel data can enable one to use engineering methods to solve the equations of

More recently, the steady-state CFD methods used for store separation have been extended to model the true unsteady motion of the weapon.[8-10] A key element of the advances in modeling the unsteady motion is the use of overset grids (the Chimera scheme,[11]) to model components of the aircraft and weapons. In the overset grid scheme, geometrically complex domains are decomposed into a number of much simpler overlapping grids. Any or all of the grid components can move indepen-

dently with six degrees of freedom. Hence for a moving body, relative motion between body components can be accommodated without stretching or regridding the components during the calculation.

The Armament Directory of the Air Force Wright Laboratory and AEDC have sponsored a set of CFD code validation experiments for store carriage and separation. The test configuration is a clipped delta wing with a pylon and finned store. A representation of the time variation of the surface pressure on the store during the trajectory motion is shown in Fig. 6. The time-accurate CFD solutions were coupled with a 6-DOF trajectory prediction capability to locate the store during the simulated motion. Currently, similar CFD work is underway at AEDC and is being extended to include the relative motion of a maneuvering aircraft and the store. By combining these two capabilities, it is possible to model store separation during a transient maneuver to determine the nonlinear effects of the time-dependent behavior of the flow over the store and the inertial effects on the motion of the weapon. Results from such a computation could also be used to validate or refine approximations used to account for inertial and flow-field effects in current quasi-steady wind tunnel trajectory simulation techniques.

3. PROPULSION GROUND TEST AND EVALUATION TECHNIQUES

Three major propulsion areas are directly influenced by the high maneuverability characteristics of aircraft. These are discussed in the following with the understanding that a great deal of other testing is needed for other aspects of development.

3.1 Compression System

Probably the single most important effect of high maneuverability is evidenced on compression system stability. Many requirements are placed on the inlet system of a highly maneuverable aircraft. These requirements often result in conflicting design characteristics such as blunt leading edges for angle-of-attack capability versus sharp leading edges for efficient supersonic operation. Also, assessing the impact of aircraft maneuverability on compression system stability begins early in the component development phase. Preliminary estimates of inlet flow delivery characteristics are used to provide parametric levels of distortion for surge margin evaluation. In the United States, engine developers generally follow the recommendations of the SAE ARP 1420 for total pressure,[12]

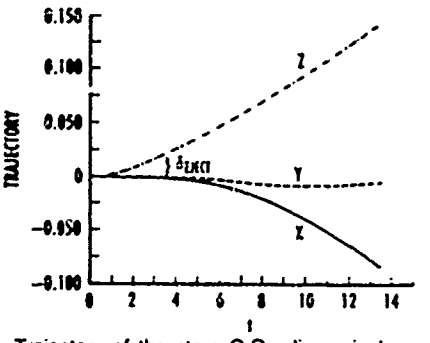

a. Trajectory of the store C.G., dimensionless x, y, z versus dimensionless time ($t = t\ C_o/d_l$). δ_{eject} = 0.0132 ejector piston stoke-length

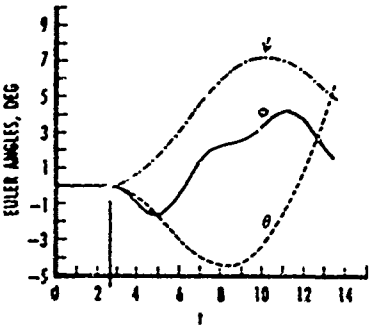

b. Euler angles (degrees) versus dimensionless time (ψ = yaw, θ = pitch, and φ = roll)

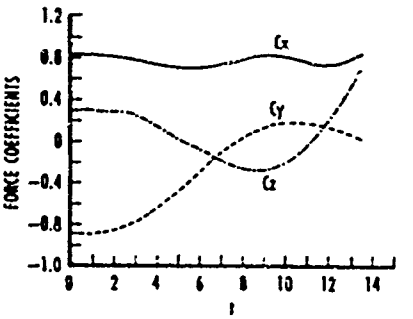

c. Aerodynamic force coefficients versus dimensionless time.

Fig. 6. Time accurate CFD simulation of a store trajectory.[10]

and SAE ARD 50015 for total temperature[13] to provide the framework for a comprehensive database.

While current methodologies are, in general, addressed toward the absolute attitude effects, as aircraft maneuverability rates increase, the effects of the rates of change of attitude may require investigation. For example, consider the capability

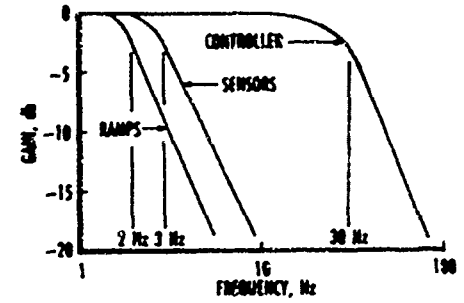

a. Typical response rates

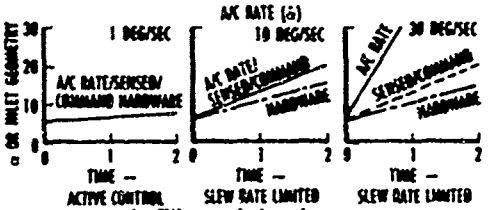

b. Effects of aircraft rate

Fig. 7. Typical inlet system component responses.

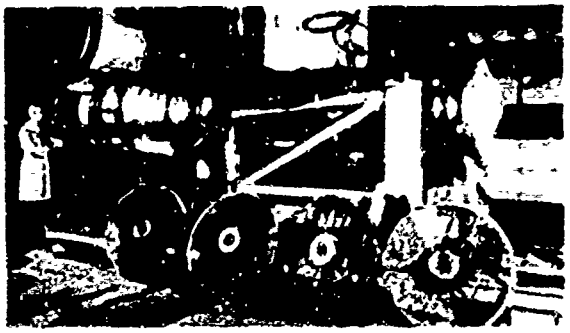

Fig. 8. Conventional distortion screens used in engine tests.

of the aircraft to alter inlet geometry during an attitude transient. Typical inlet geometry rates are shown in Fig. 7. As the aircraft attitude rate increases, the ability of the control system to optimally position the inlet geometry is exceeded, as shown in Fig. 7. While many current aircraft simply preposition the inlet geometry prior to an attitude change, the capability to more nearly match inlet geometry to actual attitude requirements will be more necessary for future highly maneuverable aircraft.

A basic assumption for total pressure effects, supported by a number of experimental studies (e.g., Ref. 14), is that a pattern which persists for a specified length of time may be treated as a steady-state pattern. Typically, the time of persistence is assumed to be that required for the compression component to complete a half or full revolution, although it may be better physically related to axial throughput rates and relaxation times of airflow around airfoils.

Total pressure inlet spatial distortion is most often produced in ground test facilities using the well-known and time-honored mechanism of screens (Fig. 8) with variable porosities down to zero (flat plates). Alternatively, controlled distribution counterflowing airjets have also been used to provide total pressure (and total temperature) distortion. A typical system is shown in Fig. 9. References 15 and 16 describe two such devices.

Engine sensitivities to inlet buzz and other discrete frequency pressure phenomena can be evaluated using a siren-type pressure fluctuation generator. A typical example of such a system is described in Ref. 17.

Current practices for total temperature distortion effects are described in Ref. 13. Both spatial distortion and temporal distortion are treated. The overall effect of spatial distortion is shown to be equivalent to a lowering of the compressor surge line while a temporal distortion moves the operating point. Simple linear superpositioning is recommended for combined spatial and temporal temperature distortions.

A second significant maneuverability effect on compression systems involves structural aspects. Inlet distortion can produce catastrophic reductions of compressor blading due to periodic excitations. An early example of structural effects is described in Ref. 18.

Assessment of the impact of inlet distortion on compressor structural integrity requires very fast analysis capabilities. Typically, the stresses developed in compressor structures are described by use of a Campbell's diagram as shown in Fig. 10. Real-time assessment and evaluation capability is provided by dedicated online computers specifically configured to generate stress data displays with no data gaps. The AEDC has been in the forefront of this effort and has developed a Computer Assisted Dynamic Data Monitoring and Analysis System (CADDMAS), which is shown schematically in Fig. 11. A detailed description of the system may be found in Refs. 19-21.

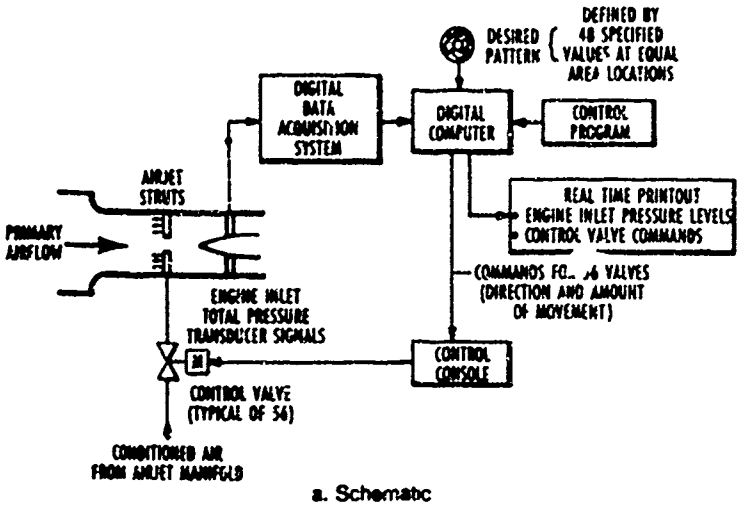

a. Schematic

Fig. 9. Airjet distortion generator.

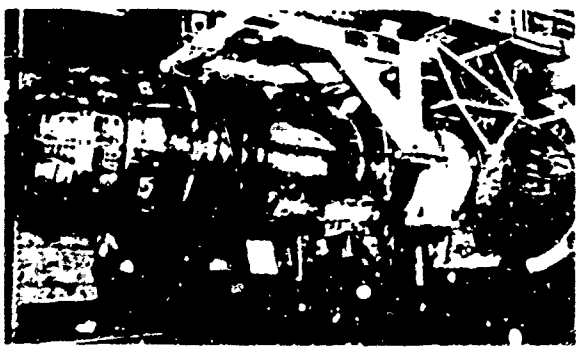

b. Installed in altitute test cell

Fig. 9. Concluded.

3.2 Exhaust Nozzles

Providing adequate forces and moments to a highly maneuverable aircraft may not be possible using only conventional (or even unconventional) aerodynamic surfaces. Use of the high level of energy in the propulsion system exhaust stream to effect attitude changes or to maintain a particular attitude is possible and has been demonstrated in recent flight experiments (e.g., the United States' Short Take-Off and Landing/Maneuverability Technology Demonstrator and the multi-national X-31 aircraft). In

As an aircraft maneuvers at high attitude rates, significant forces are induced on the rotor shaft supporting the compressor(s). Consequent deflections can alter the operating characteristics of the concompressor if tip rubs are experienced, resulting in increased tip clearances. Tip clearances are also directly influenced by the rate of change of temperature of rotating (blades/disk) and fixed (case) components. Testing is typically done with controlled tip clearances set by careful selection and matching of components. The primary influence of tip clearance variations is felt in compressor surge margin, although significant performance changes are also possible.

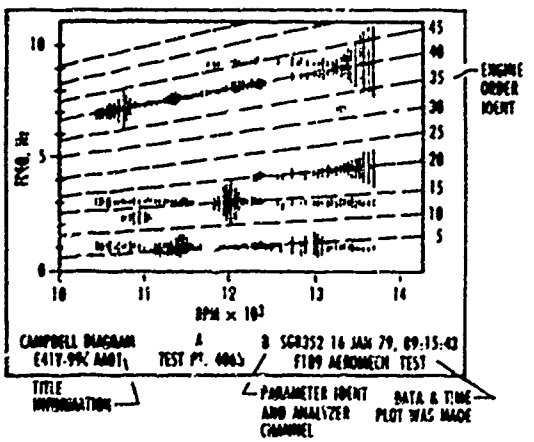

Fig. 10. Campbell diagram.

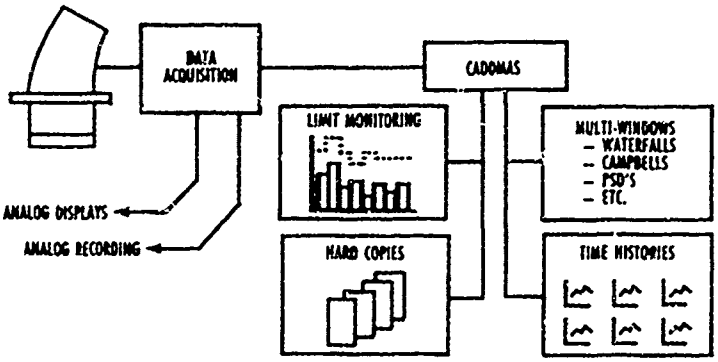

Fig. 11. Computed assisted dynamic data monitoring and analysis system.

order to successfully employ the exhaust gas energy, some means of directing the resultant vector is required. Several vectored thrust concepts are being developed, ranging from two-dimensional pitch or yaw only nozzles to adaptations of existing axisymmetric nozzles which can vector in both pitch and yaw to all-new yaw and pitch axisymmetric nozzles to externally inserted paddles which deflect the engine exhaust.

Testing of nozzles capable of providing non-axial vectored forces is required in three major areas:

1. Performance (force vector definition)
2. Operability (controllability, stability, rate limits)
3. Durability (effects of internal flow fields)

Some of the required performance testing can be accomplished in cold flow, scale model facilities. Further, much of the vector definition task can be accomplished in a sea-level test stand. Performance can then be compared to suitable models to verify the models' fidelity. The models can then be used to predict effects at other flight conditions. However, detailed performance assessments of the full-scale, hot-flow nozzle are also required at altitude conditions. Further, demonstration of the capability of the integrated propulsion system to react the axial and non-axial forces without adverse effects on the other system components (e.g., rotors, blade tip clearances, etc.) must be provided on the full-scale hardware.

Operability assessments are made using a combination of sea-level and altitude test facility capabilities. In particular, the capability of the propulsion system to control the nozzle components at altitude conditions requires the use of an altitude test facility. The interactions of the nozzle with the rest of the propulsion system operability must be demonstrated over the full flight envelope.

Most durability assessment is accomplished in sea-level stands. However, a hybrid form of test facility is used to augment Accelerated Mission Testing in sea-level stands. In this form of testing, conditioned inlet air at elevated pressures and temperatures is provided to the propulsion system with exhaust region pressures near sea-level values. Nozzle durability assessments are made as a part of this testing. Limited durability data on technical matters such as cooling, etc., are obtained during the normal altitude testing.

Testing of a generic vectoring nozzle in a sea-level or an altitude test facility requires provisions for measuring forces in six degrees of freedom. Many configurations can be used to make the required measurements. The configuration used at the AEDC is shown in Fig. 12. As currently used, the AEDC multicomponent force stand yields only five degrees of freedom, but can be easily modified to produce the sixth degree of freedom (yaw moment) by adding two load cells in the flexured lines of action parallel to and on either side of the engine centerline. Care must be taken in bringing engine service lines on board the metric part of the stand. In particular, "stiff" lines which must traverse the metric break should be introduced orthogonally to all desired lines of force measurement.

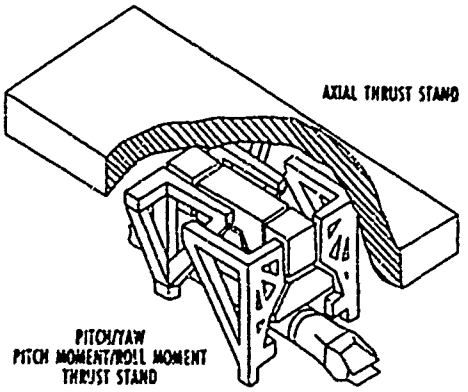

a. Concept

Fig. 12. Multi-component thrust stand.

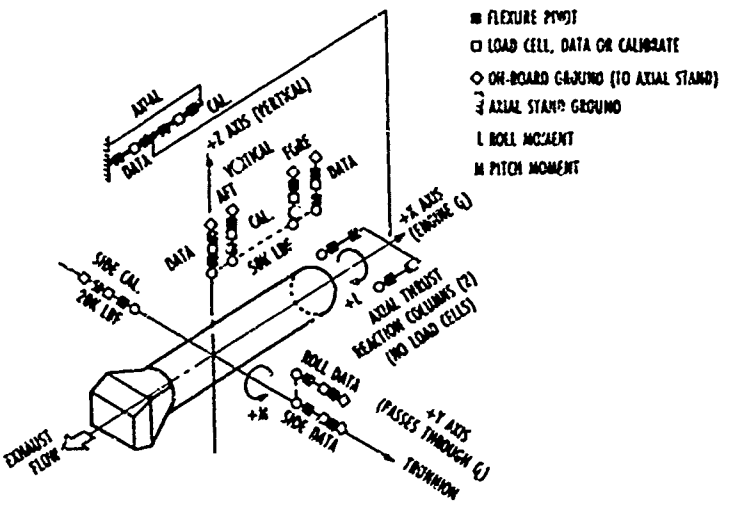

b. Schematic

Fig. 12. Concluded.

In order to accomplish this, there are two "ground planes." The first ground plane is relative to absolute ground and applies to axial thrust only. All other force measurements are then grounded to the metric part of the axial force measurement system. The use of this "floating ground" then provides a path for othogonal crossing of all metric breaks.

Collection of exhaust gases from a vectoring nozzle poses a challenge for both sea-level and altitude stands. Most sea-level stands have existing noise limitations requiring the use of acoustic silencers. In general, the silencers must be somewhat larger than axial flow collectors and have adequate protection from exhaust gas impingement. Similarly, altitude test facilities must also collect the exhaust gases, usually with more stringent space requirements. AEDC uses a non-pressure recovery, very large collector concept with positionable doors to eliminate undesirable recirculation of gases into the test cell as shown in Fig. 13. The particular system shown is also capable of accommodating reverse flow from a two-dimensional nozzle.

a. Photograph

Fig. 13. Exhaust gas management system for vectored thrust systems.

Integrated Propulsion System

The above testing is focused on evaluation of critical components within the propulsion system and, indeed, within the engine. Integration of such component work has been achieved in past developments by a combination of analytical and empirical techniques. However, the demanding requirements of highly maneuverable aircraft are resulting in a more integrated form of testing. Two specific areas which are currently within the testing state of the art are engine mechanical loading resulting from maneuvers and full-scale inlet-engine compatibility assessments.

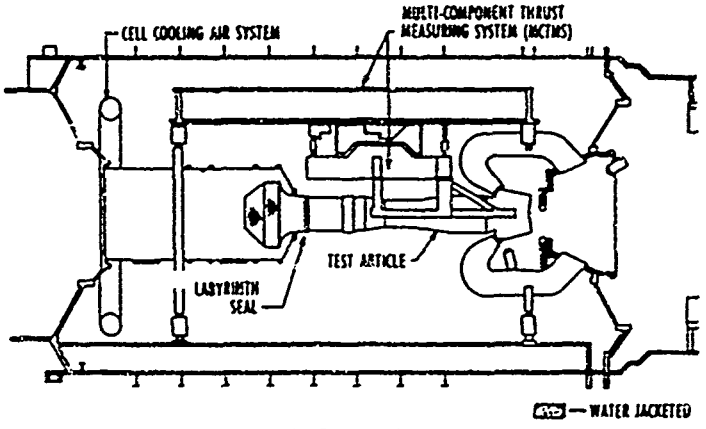

b. Schematic
Fig. 13. Concluded.

Mechanical loads are imposed on engines by both the sustained g-loads encountered during maneuvers and by gyroscopic moments resulting from maneuvers. A pivoting test bed capable of inducing gyroscopic load exists at the Center d' Essais des Propulseurs in France. A centrifuge-mounted engine test facility exists at the U. S. Navy's Lakehurst Facility. Although both of these facilities are available for test, systematic use of these facilities for highly maneuverable aircraft propulsion testing is not currently made.

Inlet-engine compatibility of the near-final configuration aircraft is required. Ground test capabilities for these types of tests fall into two areas: propulsion wind tunnels and freejet facilities. A comparison of the relative characteristics of the two techniques is shown in Fig. 14, and typical installations are shown in Figs. 15 and 16. The two techniques are complementary, as shown in Fig. 14. The flow quality of the propulsion wind tunnel is generally superior to that of the freejet. However, for instances when the flow field at the engine face for an aircraft is dominated by internal viscous effects such as shock-boundary layer interactions, the use of a freejet may be more effective for evaluation of extreme attitude operation. This is the result of the inherent limitations of attitude for full-scale test vehicles in existing wind tunnels. For operation at lower altitudes, the superior flow quality of the propulsion wind tunnel may make the use of the wind tunnel more effective.

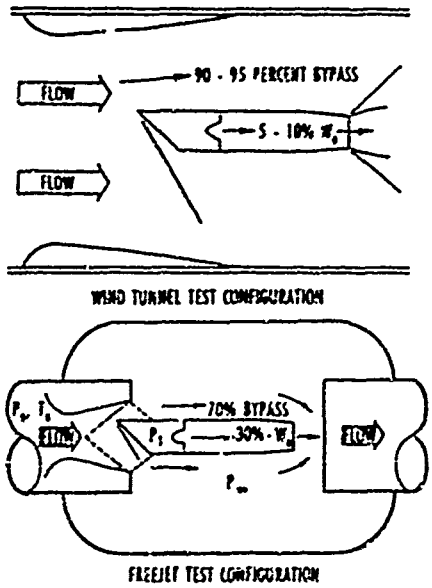

KEY PARAMETER	PROPULSION WIND TUNNEL	FREEJET
M_0	DUPLICATED HI-QUAL	DUPLICATED LO-QUAL
V_0	GENERALLY NON-STD	DUPLICATED LO-QUAL
P_0, P_1	DUPLICATED	DUPLICATED
T_0	GENERALLY NON-STD	DUPLICATED
α, β	LIMITED TO LOW VALUES	HIGH VALUES POSSIBLE
P_∞	DUPLICATED	DUPLICATED INLET ONLY
dM/dt	NOT AVAILABLE	REPRESENTATIVE
$dALT/dt$	NOT AVAILABLE	REPRESENTATIVE
$dPOWER/dt$	DUPLICATED	REPRESENTATIVE
FOREBODY CONFIG	LIMITED REPLICA	VERY LIMITED
INLET CONFIG	FULL-SCALE	FULL-SCALE
ENGINE CONFIG	FULL-SCALE	FULL-SCALE

Fig. 14. Comparison of propulsion wind tunnel and freejet test facilities.

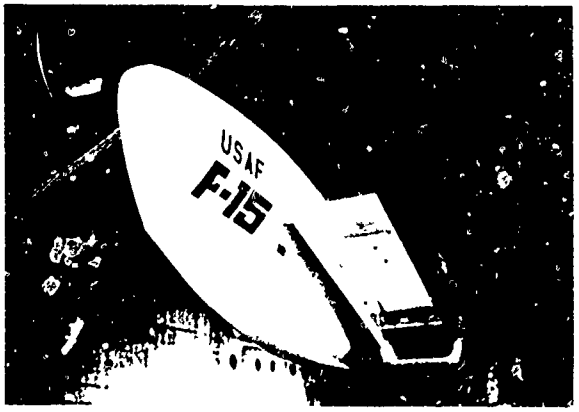

Fig. 15 Full-scale inlet/engine configuration in the AEDC 16ft transonic wind tunnel

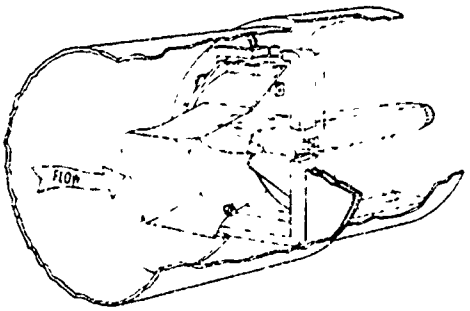

Fig. 16 Freeject

4. AN EMERGING INTEGRATED TEST AND EVALUATION METHODOLOGY

Traditionally, the development of the airframe and propulsion system are done independently and sequentially as suggested in Fig 17 Wind tunnel tests are performed to determine aerodynamic forces and moments and inlet nozzle performance characteristics The inlet distortion information is passed on to the engine test facility and the engine is operated with a prescribed distortion pattern Some time later, the engine performance over a range of operating parameters is included in the so called "engine deck," which is a semi empirical model of the engine Still later, the engine model is incorporated with the aerodynamics and avionics in a simulator to establish the performance of the aircraft Literally years are required to determine the integrated aircraft/engine/avionics performance and then it is difficult to modify the vehicle to try to gain more performance With the trend toward more closely coupled subsystems, such a sequential engineering process is lengthy, expensive and could produce a suboptimum system

Recognizing recent advances in dynamic data reduction and analysis techniques and the utility of CFD as a diagnostic tool, an integrated engine/airframe/avionics simulation has been pro

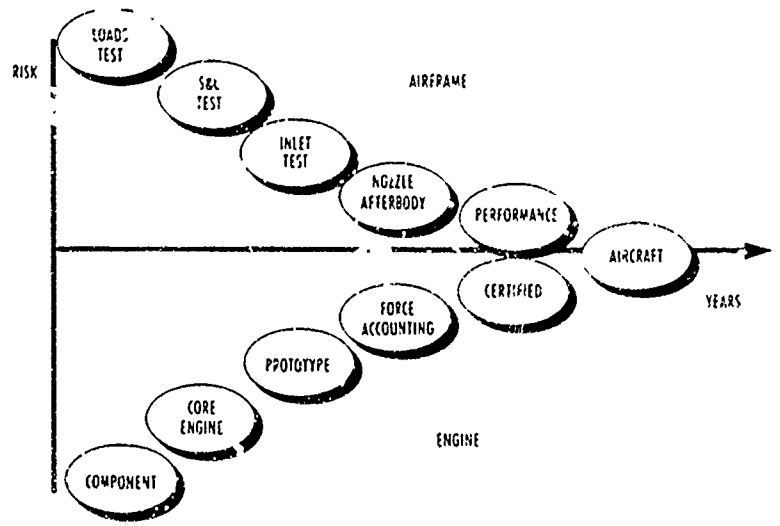

Fig 17 Airframe/propulsion integration

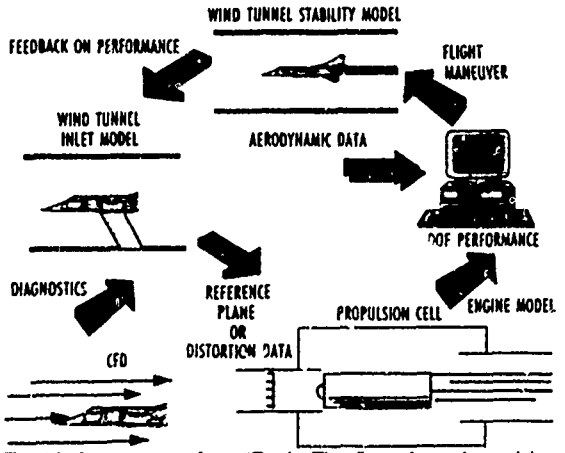

Fig. 18. A concept for "Real Time" airframe/propulsion system optimization.

posed.[22] A schematic of the proposed concept is shown in Fig. 13. Suppose that a model with remotely actuated control surfaces suitable for captive motion simulation is in one wind tunnel and an instrumented inlet model of the vehicle is in another wind tunnel (not necessarily in the same test complex) while the engine is in an altitude test cell. Inlet distortion data measured in the wind tunnel can be reduced and analyzed in minutes and transmitted to the engine facility, where an inlet distortion generator can simulate the desired distortion pattern. Within minutes, the integrated engine performance can be determined and included in a 6-DOF flight performance model including the control system. The combined aerodynamic/avionics/propulsion model can then be used with the other wind tunnel model to "fly" maneuvers in the wind tunnel using the captive motion technique described in Section 2.

With such an integrated test and analysis approach, one can obtain in near-real time (real time here may be measured in days) feedback on the integrated performance. If, for example, the inlet distortion degraded the engine response such that the desired aircraft performance was not met, one could then use CFD as a diagnostic tool by simulating the flow over the forebody and through the inlet to the engine face. By analyzing the streamlines in reverse, one could determine the origin of the distortion. Subsequently, the aircraft model could be modified and the process repeated until the desired performance is obtained. Hence, optimum integrated performance could be obtained in months with this systems approach as compared to years with the traditional sequential method.

Although the proposed scheme appears very complex, each of the individual technologies required exists and has been used independently. New high-speed data acquisition and reduction systems make it possible to obtain the dynamic data at the engine face in a simulated inlet and define the distortion within a minute. Air jet distortion generators, as shown in Fig. 9, or mechanical distortion devices as developed at the Central Institute of Aviation Motors in Russia are capable of reproducing a desired distortion pattern within minutes after the pattern is identified in the wind tunnel. The ability to include the installed engine performance with the aerodynamics to simulate a maneuver in the wind tunnel was demonstrated earlier in this paper.

In addition, major advances in CFD have been made for simulating complete aircraft at high angles of attack. An example from Ref. 23, showing the flow solutions for the F-18 at high angles of attack is shown in Fig. 19. The flow was

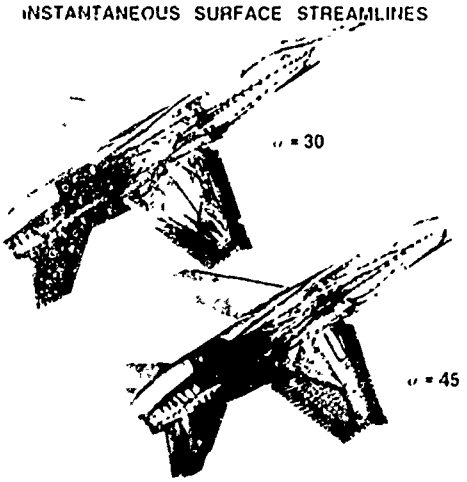

Fig. 19. Instantaneous surface flow paterns on the F-18 at 30 and 45 deg angle of attack.[23]

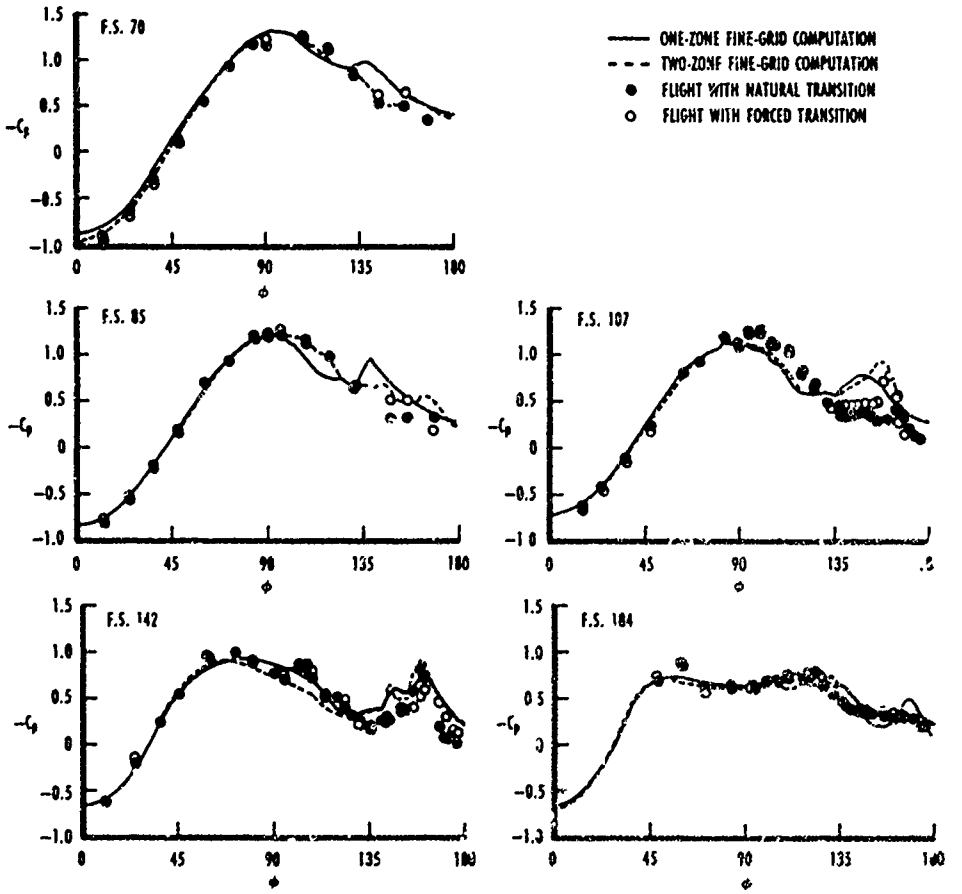

Fig. 20. Forebody pressure distribution on the F-18 at 45 deg angle of attack.[25]

modeled with the thin-layer Naver-Stokes equations. Comparisons of the calculated forebody surface pressure distributions with those measured in flight are presented in Fig. 20. Flow separation and LEX vortex breakdown phenomena are captured in the solutions.

Similarly, a Naver-Stokes solution of supersonic flow over the forebody of an F-18 aircraft is discussed in Ref. 24. The solution successfully modeled the mass flow rates through the bleed zone of the inlet, the operating mass flow ratio, the total pressure recovery at the aerodynamics interface plane (AIP), and the inlet distortion parameters at the AIP. A comparison of the predicted total pressure recovery at the AIP with wind tunnel measurements is presented in Fig. 21. Included in Fig. 21 is a table of recovery and distortion indicators at the AIP. Clearly, such a CFD computation would provide an excellent diagnostic tool to assist in improving the integrated performance of a vehicle during development.

Currently, AEDC is undergoing a developmental simulation of this integrated concept by using existing data measured in traditional sequential tests. Although such an integrated approach using multiple test facilities simultaneously could be difficult to schedule and expensive to perform, such an approach could literally reduce the overall development time for the aircraft by years while providing a more optimum integrated vehicle.

5. CONCLUDING REMARKS

Development testing of highly maneuverable aircraft in ground test facilities, wind tunnels, and propulsion test cells presents added complexities and challenges over and above more conventional aircraft.

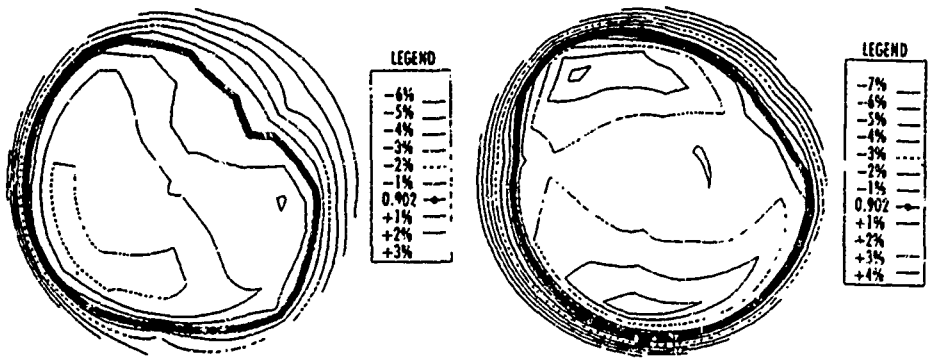

	AVERAGE RECOVERY	IDC		IDR	
		HUB	TIP	HUB	TIP
TEST	0.902	0.038	0.042	−0.020	0 048
GCNSFv	0.0902	0.015	0.028	−0 017	0 067
GCNSFv*	0.902	0 030	0.052	−0.018	0 046

Fig. 21. Comparison of predicted and measured total pressure distributions at the aerodynamic interface place.[26]

There are many available tools to bring to bear upon the problem. The baseline for most of these tools is embodied from their use in development testing of the more conventional fighter-type aircraft such as the F-15 and F-16. Until now, airframe and propulsion systems development generally has been done independently on parallel paths but accounting for the influence of external aerodynamics on the propulsion system and jet effects on the external aerodynamics. High maneuverability requires aircraft to be subjected to large acceleration loads and dynamic flow phenomena which may not be adequately captured in conventional steady-state testing techniques. There are, however, some promising avenues of testing which can be undertaken to accelerate the aircraft development process while at the same time dealing with a more complex development testing process.

Simulated Aircraft Motion

By using a technique of small time increments, experimental evidence suggests that aircraft motion can be well simulated in the wind tunnel as long as model scale and tunnel effects are secondary and the cross coupling and acceleration derivatives are small.

Weapons Separation

Current wind tunnel test techniques do not simulate both the accelerations of the parent aircraft and the weapon on separation. Only the separation of an accelerating weapon is currently simulated. A suggested approach is to combine a CFD solution with appropriate wind tunnel data to solve the equations of motion and predict the weapons separation trajectory.

Aeropropulsion

The effects of attitude of the incoming flow upon the compression system stability is currently investigated routinely. Real-time rate of change of attitude generally is not simulated, and these effects require investigation along with techniques for accomplishment. The capability for testing of engines with vectoring nozzles currently exists in the AEDC ASTF. Also, a new capability exists to a test full-scale combined inlet and engine at subsonic flight Mach numbers.

Integrated Test and Evaluation

Currently, the development of the airframe and propulsion system are done independently and sequentially. This process literally takes years to develop a new aircraft system. It is entirely conceivable to think in terms of simultaneously and interactively performing airframe and inlet testing in the wind tunnel along with the engine test in the propulsion test cell. A perfected process along these lines is envisioned to cut months to years off the aircraft system development time and, consequently, the development cost, and reduce retrofit problems post development.

REFERENCES

1. Orlik-Rückemann, K. J. (Course Director). "Special Course on Aircraft Dynamics at High Angles of Attack: Experiments and Modeling." AGARD-R-776, April 1991.

2. Langham, T. F. "Aircraft Motion Sensitivity to Dynamic Stability Derivatives." AEDC-TR-79-11 (ADA079421), January 1980.

3. Butler, R. W. and Christopher, J. P. "Captive Aircraft Testing at High Angles-of-Attack." AEDC-TR-80-60 (ADA103108), August 1981.

4. Wilson, D. B. and Winters, C. P., "F-15A Approach-To-Stall/Stall/Post-Stall Measurements." AFFTC-TR-85-64, April 1986.

5. Donegan, T. L. and Fox, J. H. "Analysis of Store Trajectories from Tactical Fighter Aircraft." AIAA-91-0183, January 1991.

6. Keen, K. S. "New Approaches to Computational Aircraft/Stores Weapons Integration." AIAA-90-0274, January 1990.

7. Fox, J. H., Donegan, T. L., Jacocks, J. L., and Nichols, R. H. "Computed Euler Flowfields for Transonic Aircraft with Stores." AIAA Journal of Aircraft, Vol. 28, No. 6, pp. 389-396, June 1991.

8. Lijewski, L., and Suhs, N. "Chimera-Eagle Store Separation." AIAA 92-4569, August 1992.

9. Jordan, J. K. "Computational Investigation of Predicted Store Loads in Mutual Interference Flowfields." AIAA-92-4570, August 1992.

10. Meakin, R. L. "Computations of the Unsteady Flow About a Generic Wing/Pylon/Finned-Store Configuration." AIAA-92-4568, August 1992.

11. Benek, J. A., Steger, J. L., Dougherty, F. C., and Buning, P. G. "Chimera: A Grid Embedding Technique." AEDC-TR-85-64 (ADA167466), April 1986.

12. "Gas Turbine Engine Inlet Flow Distortion Guidelines." Society of Automotive Engineers Aerospace Recommended Practice, ARP1420, March 1978.

13. "A Current Assessment of the Inlet/Engine Temperature Distortion Problem." Society of Automotive Engineers Aerospace Research Document, ARD 50015, January 1991.

14. Plourde, G. A., and Brimelow, B. "Pressure Fluctuations Cause Compressor Instability." AFAPL-TR-69-103.

15. Overall, B. W., and Harper, R. E. "The Airjet Distortion Generator System - A New Tool for Aircraft Turbine Engine Testing." AIAA-77-993, July 1997.

16. Braithwaite, W. M., Dicus, J. H., and Moss, Jr., J. E. "Evaluation with a Turbofan Engine of Airjets as a Steady State Inlet Flow Distortion Device." NASA TMX-1955, January 1970.

17. Peacock, R. E., and Des, D. K. "Performance Analysis of a Family of Planar Pulse Generators." AIAA 81-1590, July 1981.

18. Armstrong, E. K., and Williams, D. D. "Some Intake Flow Maldistribution Effects on Compressor Rotor Blade Vibration." Journal of Sound and Vibration, pp. 216-225, May 1966.

19. Hite, S. W., III "Real Time Vibration Health Monitoring for Transiently Operating High-Speed Turbo Machinery." 47th Meeting of the Mechanical Failures Prevention Group, April 1993.

20. Cromer, T. W., Nichol, K. L., and Schroeder, J. S. "New Capabilities for Aeromechanical Testing and Evaluation of Aircraft Turbine Engines." AIAA 91-2498, June 1991.

21. Abbott, B, et al, "Experiences Using Model-Based Techniques for the Development of a Large Parallel Instrumentation System." Int. Conference on DSP Applications and Technology, Cambridge, MA, 1992.

22. Kraft, E. M. "Integrating Computations, Ground Tests, and Flight Tests - Opportunities and Challenges." 12th AIAA Aerospace Ground Test Conference, Nashville, TN, July 1992.

23. Murman, S. M., Schiff, L. B., and Risk, Y. M. "Numerical Simulation of the Flow About an F-18 Aircraft in the High-Alpha Regime." AIAA-92-3405, August 1993.

24. Dwyer, W. P. and Math, J. A. "A Three-Dimensional Supersonic Navier-Stokes Solution Over an F-18D Forebody with Inlet Bleed." AIAA 93-3490, August 1993.

Progress and Purpose of IHPTET Program

Richard J. Hill
Chief of Technology, Turbine Engine Division
Aero Propulsion and Power Directorate, Wright Laboratory
1950 Fifth Street, Wright-Patterson AFB, Ohio 45433-7251, USA

1. SUMMARY

IHPTET is the *Integrated High Performance Turbine Engine Technology* initiative. This paper discusses the purpose (background, goals and applications) and the progress of IHPTET. IHPTET is 30% complete and achieving significant success in advancing turbine engine technology levels. The future of IHPTET is bright. IHPTET developed technologies are being applied to both military and commercial turbine engines -- both new engines and fleet modernization's. IHPTET is the technology base for all future military systems and the springboard for many new commercial engines.

2. IHPTET PURPOSE

2.1 Background

IHPTET is a coordinated, three-phase, Government and Industry visionary initiative. Formally initiated in 1987, IHPTET includes virtually all government and industry sponsored propulsion Research and Development (R&D) activities devoted to advancing technology for military turbine engines. The goal of IHPTET is to develop and demonstrate technologies by the turn-of-the-century that, when applied, will double a 1985 level of turbopropulsion capability. The technologies of IHPTET offer significant payoff when applied to any propulsion system.

Under IHPTET there exists one IHPTET government plan and seven individual industry plans, coordinated among the Department of Defense (DoD) Military Services -- Army, Navy, Air Force; the Advanced Research Projects Agency (ARPA); and the National Aeronautics and Space Administration (NASA). The structure of the IHPTET program is shown in Figure 1.

Figure 1

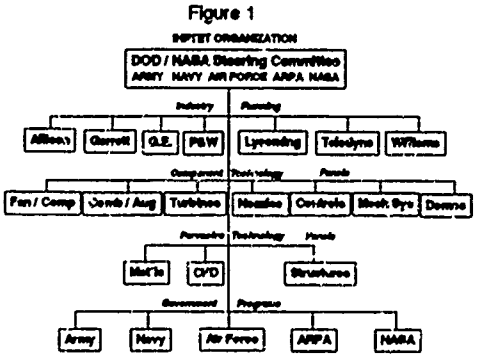

A DoD chaired Steering Committee provides overall IHPTET guidance. The seven US turbine engine companies participating in IHPTET are Allied Signal Propulsion Engines (Garrett); Allison Gas Turbine; General Electric; Pratt and Whitney; Teledyne, CAE; Textron Lycoming; and Williams International. These companies form an Industry Panel that advises the Steering Committee on specific issues. In addition, there are seven Component Panels (compressors, combustors, turbines, nozzles, controls, mechanical systems and technology demonstrators) and three Pervasive Technology Panels (materials, Computational Fluid Dynamics (CFD) and engine structures) that oversee the technology planning and development in each area. Every panel has membership from each of the services and is chaired by one service individual. Each IHPTET technology is developed individually or jointly to the agreed upon plan by one or more of the five IHPTET government organizations. Biannual reviews are held by the Steering Committee where the progress and problems of each technology area are reviewed. Through this process, IHPTET is successfully meeting the technological challenges of Phase I and working on the critical path technologies of Phase II.

2.2 Goals

Payoffs from IHPTET come from increasing propulsion system performance and affordability with no compromises in system life, reliability and maintainability. To focus the initiative on these payoffs, IHPTET management established specific goals as a function of time for each of the three aircraft turbine engine classes -- turbofan/turbojet, turboshaft/turboprop, and expendable. Shown in Figure 2 are the time phases of IHPTET. These goals were chosen as having the highest effect in maximizing payoff to military systems. The three IHPTET phases shown in Figure 2 were created to provide milestones against which to assess progress, and, most importantly, to provide opportunity for transition to current, upgrade, derivative and new engines.

The IHPTET goals for each of the three phases are shown in Table I and are based on a 1985 technology level. They are "typical" technology goals for each class of engine *(do not interpret them as a specific "engine cycle" description)*. Through the achievement of these goals, IHPTET will provide technology for propulsion systems that are lower cost, lighter weight and easier to maintain than today's systems, yet can fly faster, higher, and with increased ...aneuverability.

Through the development and validation of IHPTET technologies, major payoffs to military systems will occur. These modernized high performance military

Presented at an AGARD Meeting on 'Technologies for Highly Manoeuvrable Aircraft', October 1993.

aircraft will supply the affordable battle field advantage -- low fuel burn allowing longer missions; high thrust-to-weight allowing larger pay loads; low maintenance and support in the field yielding higher sortie rates; and excess specific power during critical flight maneuvers -- the air superiority advantage!

It should be noted that the IHPTET goals are not considered to be achieved until the enabling technologies have been assembled and tested under actual engine conditions in an engine demonstrator (core or full engine configuration) -- commonly called a "Tech Demo." The progression of test validation of IHPTET technologies is shown in Figure 3. Under IHPTET sponsorship, technologies mature at a component level until ready for evaluation in dedicated rig testing. The primary IHPTET compressor test facility is the Air Force's Compressor Research Facility (CRF). The newest IHPTET test facility, the Advanced Turbine Aerothermal Research Rig (ATARR), is dedicated to turbine research and also belongs to the Air Force. The best and most promising technologies that successfully complete testing in rigs like CRF and ATARR are further assembled into Tech Demos and evaluated for synergistic problems. All Tech Demo testing is done with significant amounts of instrumentation. Typically over 1000 pieces of instrumentation are used on a single Tech Demo test with the majority of the testing done at sea level conditions. The major workhorse demonstrators for turbofan/jet engines are the Advanced Turbine Engine Gas Generator (ATEGG) core and Joint Technology Demonstrator Engine (JTDE). For turboshaft/prop engines, the demonstrators are the Joint Turbine Advanced Gas Generator (JTAGG) cores. Missile engine technology is demonstrated in the Joint Expendable Turbine Engine Concept (JETEC) engines. Upon successful completion of Tech Demo evaluation, technologies are typically

IHPTET Time Phases
Figure 2

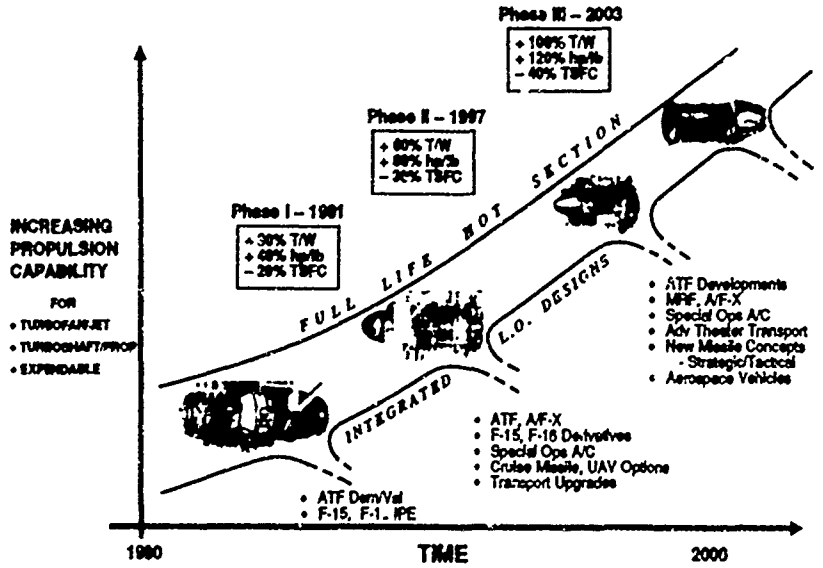

IHPTET Progression of Test Validation
Figure 3

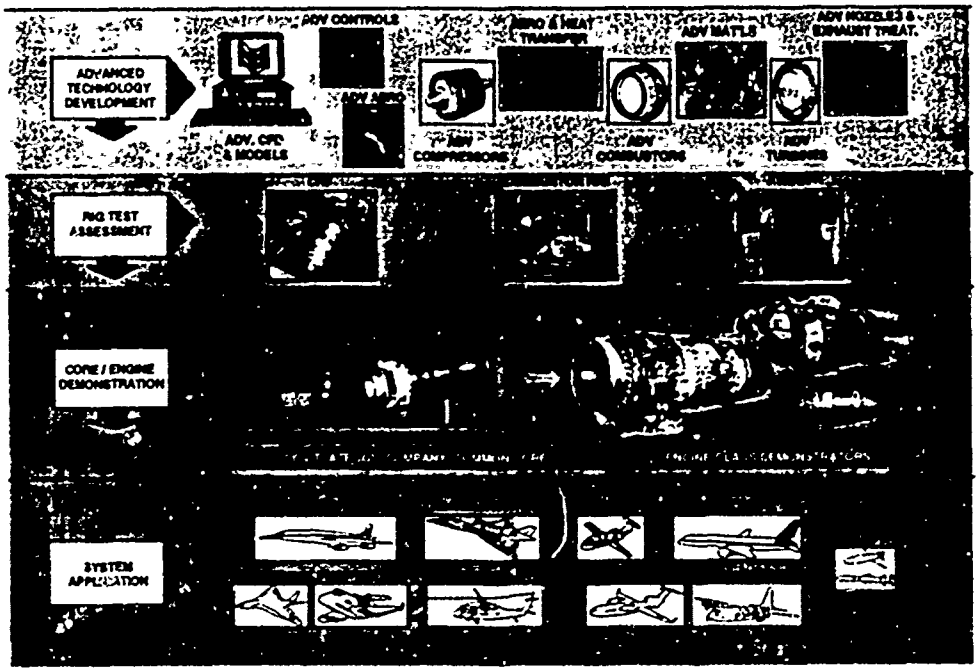

Schematic of Turbine Engine Technology Development Focus
Figure 8

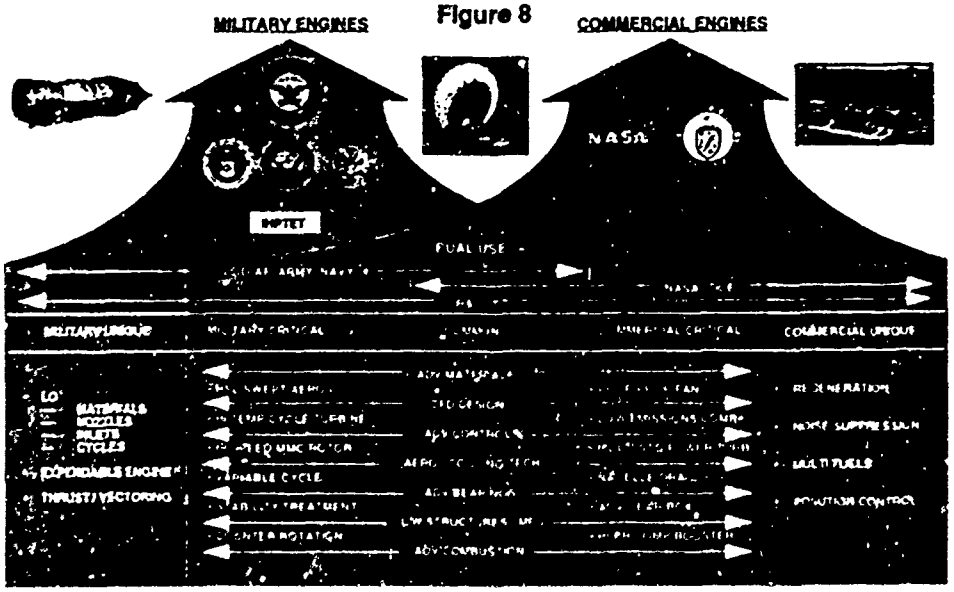

IHPTET Goals by Phase
Table I

	PHASE I	PHASE II	PHASE III
TURBOFAN / TURBOJET			
THRUST / WEIGHT	+30%	+60%	+100%
COMBUSTOR INLET TEMP	+100°F	+200°F	+400°F
MAX. TEMP (TYPICAL)	+300°F	+600°F	+900°F
TURBOSHAFT / TURBOPROP			
SFC	-20%	-30%	-40%
POWER / WEIGHT	+40%	+80%	+120%
MAX. TEMP (TYPICAL)	+300°F	+600°F	+1000°F
EXPENDABLE			
SFC (STRATEGIC)	-20%	-30%	-40%
THRUST / AIRFLOW	+35%	+70%	+100%
COST (TACTICAL)	-30%	-45%	-60%
COMBUSTOR INLET TEMP (TYPICAL)	1100°F	1200°F	1400°F
MAX. TEMP (TYPICAL)	+500°F	+900°F	+1400°F

matured to the level necessary for system transition. Many times, technologies that are tested in the Tech Demo are found to be lacking the qualities necessary to continue further development and are returned to a component rig for further evaluation and correction. Thus the progression of testing can be cyclic in nature between rig evaluation and Tech Demo testing.

2.3 Applications

The IHPTET program was established during the middle 1980's to be the "technology springboard" for the next century's high performance military turbine engines. The main thrust of IHPTET was focused during this time period on a wide spectrum of new systems, and success in IHPTET would assure continued US air superiority over any new aggressor system. A second thrust of IHPTET was the systematic spin-off of technology advancements for modernizing the current fleet of aircraft engines. This opportunity occurs primarily at the end of each Tech Demo test.

The major areas of focus for technology application under IHPTET started as and continues to be the achievement of affordable thrust-to-weight and power-to-weight growth, lower fuel consumption, decreased (low observable) engine signature, increased repairability, operability and maintainability and decreased acquisition, operation and support costs. In the man-rated turbofan/turbojet arena for example, the payoff gained by the achievement of the IHPTET goals is providing the technologies for upgrade and growth F-15 and F-16 aircraft engines (F100 and F110 engine families), as well as provide the technology base for the new F-22 Advanced Tactical Fighter (ATF) engine (F119).

The dismantling of the Warsaw Pact created the need to rethink many of the US military Science and Technology (S&T) plans, including IHPTET. What is seen now by top command officials is a diminishing need to develop new high performance aircraft to overcome new aggressor advancements and an increasing need to modernize the fleet of current systems. The focus of S&T is now changing to be more evenly split between creating new systems and upgrading existing systems. The new systems, when needed, will be developed in minimum numbers and be replacements for near-obsolete aircraft. They will be based on the best, affordable technology available at key points in the development process. The second focus, that of modernizing the current fleets, will also use the best, affordable technology but will be directed at specific engine components combined to form "upgrade kits." The new US military force structure will rely on a combination of these high quality, technologically advanced systems to cope with regional threats. The major objective of this new trend is to continue a high quality, high readiness force to perform regional operations like Desert Storm at a minimum cost. The Gulf War proved that air superiority is a result of superior training and technologically advanced weapons. Both of which are essential for minimizing casualties and length of conflict. For the new S&T plans, IHPTET remains the answer for all turbine engines. This is due to the original broad application (non system specific) focus of IHPTET technology planning with many spin-off opportunities to a wide spectrum of aircraft, rotorcraft and missile uses.

The technologies being developed under IHPTET fit naturally this redefined S&T role in meeting the wider DoD objectives. The IHPTET program is providing the foundation for retaining the affordable air superiority advantage sought in the new Air Force strategy of Global Reach - Global Power. The IHPTET plan is to continue to provide enabling technology for affordable upgrades of the existing

engines and the technology base for all new engines of the future. The result of this long-term view is that IHPTET will produce the technology to equip the next century peace keeping force with affordable, superior systems. As defense draw-down continues and weapon system acquisition starts to be based on selective upgrades and new engine low-rate production with a continual insertion of advanced technology, the application for IHPTET technology will increase proportionately.

3. IHPTET PROGRESS

3.1 Status of Goal Achievement

IHPTET is over 30% complete and has achieved major success! Figure 4 shows the extent of Phase I goal accomplishment for each engine class.

IHPTET Phase I Status
Figure 4

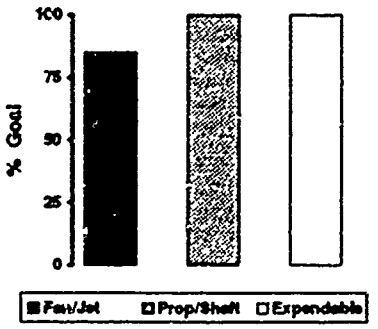

As seen in Figure 4, the goals are achieved for expendable engine and turboprop/turboshaft engine classes; but for the turbofan/turbojet, more work is needed. The technology that slowed the achievement of the turbofan/turbojet goal centers on material maturity for the high temperature rotating structure at the discharge end of the compressor. What is lacking is final development of a full life, low density material system capable of enduring the high combustor inlet temperature (T_3) goal conditions. Significant progress is being made on the class of materials that will meet this need and once the material is fully characterized, the turbofan/turbojet goals will be achieved. The goals of Phase I for turbofan/turbojet will be met in the next engine test. Wisely, IHPTET management did not wait until all of Phase I to be completed prior to initiating the long-lead critical path technologies of Phase II. As a result, the Phase II technologies are becoming well established and on schedule for demonstration by 1997.

3.2 Removing Barriers to Acceptance of IHPTET

The three main elements of IHPTET are (1) development and application of advanced aerodynamic and thermodynamic models and theories, (2) creation of innovative structural designs, and (3) development and application of advanced high strength, low density materials. The best combination (different for each company) of these three elements focused on the goals of Table I is the IHPTET initiative. The major problem now being faced is keeping industry centered on early acceptance and application of these newer IHPTET advancements in an affordability driven market economy. The difficulty stems from the Government's need to keep an industrial defense base alive over a long period of declining budgets and low levels of production and yet capable of short notice, full-scale production on IHPTET materials and innovative designs. The benefits of several new IHPTET innovations can be seen in Figures 5a, b, c and d. As shown in Figure 5a, the application of innovative designs and advanced high strength, low density material is key to IHPTET long-term success. These advancements offer, for example, the potential to reduce a compressor rotor's weight 70%. This is accomplished through the application of advanced materials to advanced designs including Integral Blade/Disk Rotors (IBR or BLISK), hollow airfoils and composite spacers (Figure 5c) and ring rotors (Figure 5d). The final Phase III compressor is envisioned to be made entirely of advanced Metal Matrix Composite (MMC) materials and be only composed of ring type structure. The primary need for these new materials and innovative designs is centered on the compressor's need for high rotational speeds to take full advantage of the advancements in IHPTET aerodynamics in the blade rows. If the rotor had to be constructed of conventional materials, the design would require full webs and bores on each rotor stage. This would result in a heavy and lengthy rotor. For comparison, a conventional rotor was designed to meet the rotational speed requirements of an IHPTET configuration, but constructed from conventional nickel-based alloys. The result of this design effort is shown in Figure 5b as the Baseline 1985 Technology Compressor. Using this base design, the major IHPTET compressor technologies were added to the design with the results as shown in Figure 5a

Figure 5a
Benefits of Innovative Design and Advanced Materials to a Compressor Rotor

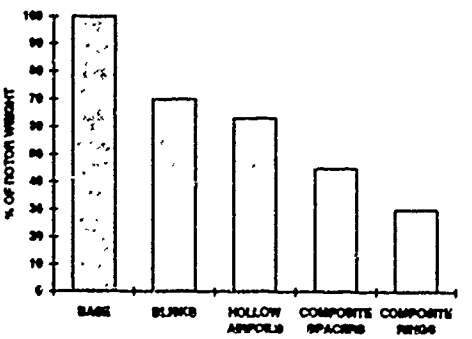

The technologies shown in Figure 5a can be used independently or bundled together to increase the performance attributes of a chosen design application -- new or upgrade component or engine.

Figure 5b
Baseline 1983 - All Nickel Compressor

Figure 5c
Addition of Composite Spacers and Blades

Figure 5d
Addition of MMC Rings to the Rotors

Figure 6
Advanced MMC Reinforced Ring Rotor

Each of the technologies in Figure 5c has been tested successfully in a Tech Demo. In addition, Figure 6 shows an IHPTET ring rotor that was tested successfully in a recent core engine Tech Demo.

3.2 Affordability -- A Reduced Cost Approach

A perceived problem with several IHPTET technologies centers on "affordability." Metal matrix composite material is a prime example. The problem with the MMC class of materials is that they are process sensitive and currently expensive to manufacture, inspect and repair. At best, only a "lean production" of these classes of material will be available for a data base if they remain only applicable to advanced military systems. A solution to this problem is the broadening of the production base for MMC and Ceramic Matrix Composite (CMC) class materials by broadening the non military market application. The Organic Matrix Composite (OMC) industry is a prime example of how to lower the cost and increase the knowledge base on a new material. This industry created a need for the material system by applying the technology to sports equipment, automotive equipment and home products. With this broadened base for production and broadened demand for the material, the price came down and the quality went up. IHPTET management is trying to encourage the same success gained by the OMC industry by broadening the need for MMC and CMC material systems. Thus far, some limited success is being achieved with application to racing car components and golf clubs with more commercial applications anticipated in the near future.

IHPTET management is also trying to increase affordability of technologies more globally through the encouragement of teaming and the formation of industry consortia. The intent of these actions is to minimize the cost and maximize the production knowledge of technology through data sharing. The action taken thus far has been the formation of jointly sponsored research consortia and funding teamed contractor Tech Demo testing efforts.

Figure 7
Model of an IHPTET Consortium

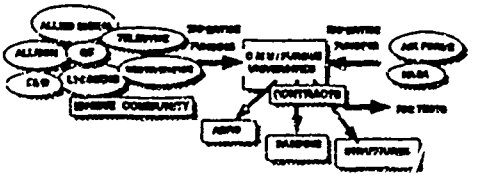

FORCED RESPONSE CONSORTIUM STRUCTURE

The current IHPTET consortia are focused on (1) forced response prediction methods and (2) fiber development for advanced MMC and CMC material. The consortium idea is shown in Figure 7 using the Forced Response Consortium as an example.

IHPTET consortium are structured with an organization (in this case, Carnegie Mellon and Purdue Universities) as the integrating subcontractor. Each member of the consortium contributes resources at varying levels (funds, facilities or data) and technical expertise to help meet the consortium goals. In addition, the Government contributes funds, expertise and in some cases, rig testing to the consortium. Contracts are then let to chosen organizations to actually conduct the research and report the findings. The Forced Response Consortium shown in Figure 7 is focused on the establishment of standard industry assessment methods of structural damping and understanding structural response to engine/inlet induced aerodynamic forcing functions. The Materials Consortium, like the Forced Response Consortium, is a jointly funded effort by all the seven engine companies, DoD, ARPA, and NASA. The objective is to develop affordable high temperature fibers for use as reinforcement in both CMC and MMC material. These will be developed as "industry fibers" -- well understood, documented and ready for production use by each of the participants. As shown in Figure 7, the consortium is unique and acts as an impetus for industry to work together on other common IHPTET technology problems resulting in cost benefits and market opportunity to all.

In the area of contractor-teamed Tech Demo testing, significant progress has been achieved. Currently, General Electric and Allied Signal Propulsion Engines are teamed in JTAGG to develop and share in the technology payoff of the small to medium class of turboprop/shaft engines. This takes the form of testing each company's technologies in several builds of a common JTAGG Tech Demo.

Considerable synergistic benefit and technology innovation have resulted from this union. A second team of General Electric, Pratt & Whitney and Allison is working on a joint structural Tech Demo focused on advanced intermetallic titanium aluminum compressor blade development, innovative turbine cooling designs and reduced engine weight concepts. This program is called the Component and Engine Structural Assessment Research (CAESAR). It is becoming a successful program as well as business concept. The first test of CAESAR will be in 1995 and will help reduce the risk of these technologies.

3.4 Technology Readiness -- Risk Reduction Through IHPTET Tech Demo Testing

Historically, risk, viewed in terms of level of "readiness," is the reason given for the non use of advanced technology. In choosing technologies for systems, "better" technology has always been, and remains the enemy of "good enough" technology when budgets are tight. This is due to the manager's dilemma of always having to trade part of the desired capability to meet schedule and budget constraints. Historically, the newer and better technology has always had a lower readiness value and higher risk. The same is true for current IHPTET technologies.

Technology readiness is difficult to quantify and understand. However, in IHPTET, a joint industry/government task is underway to both define criteria for assessing readiness of technology and put in place effort to increase the readiness when a low value is determined. The considerations being used to determining the readiness of IHPTET technology centers on the extent of design and test experience with the new technology; the amount of extension beyond known values for manufacturing and production; and the degree of similarity to known design methods, materials processing and manufacturing. Readiness assessment is judgmental and varies from company to company for the same class of material or application of similar technology advancements. Effort to increase readiness has taken different forms in IHPTET. One such form in the Air Force is the formulation of additional Tech Demo tests for specific technology items. This new effort is termed Advanced Technology Transition Demonstrations (ATTDs). These IHPTET programs are short duration, low cost and directed at removing the last remaining risk barriers on a technology -- the ones preventing immediate transition of the technology to a product application. Currently, IHPTET is sponsoring ATTDs for the Air Force's F100, F110 and F119 fighter engines. The completion of these ATTDs will result in significant performance improvements while producing major life cycle cost savings.

4. THE FUTURE OF IHPTET

4.1 IHPTET "Dual-Use"

Today, the American Aerospace industry is facing monetary issues of major proportion. Significant profit losses, undelivered products and declining sales have forced a major restructuring of the aerospace industry. The total US engine production value is down by nearly 1/3 since 1991. Since the IHPTET initiative represents a major investment by industry (nearly 53% of all money from 1988 through 2003 will come from industry), this problem becomes a significant concern to IHPTET management. The National level approach to this situation is the expansion of "Dual-Use" thinking when technology is being developed. Under this idea, technology is developed in such a way that commercial and military application becomes of relative equal importance. Thus, every dollar spent on technology development will energize the commercial economy -- hopefully increasing productivity and availability of new jobs. Such an idea is presented in the Aeronautical Technology Consortium Act of 1993 (Aerotech). IHPTET

management will do anything it can do -- without straying from its basic purpose of pursuing high-payoff military goals in aeronautical technology -- to support initiatives like Aerotech.

IHPTET management recognized early that technology modernization and application are key to increased productivity in the aerospace industry. In IHPTET, Dual-Use has become a significant outlet of the many technologies developed. Numerous IHPTET developed technologies have transitioned into commercial engines so far, and over 100 technologies now being developed under IHPTET have potential future Dual-Use application. In total, nearly 80% of IHPTET has commercial spin-off potential.

4.2 IHPTET and the New NASA Initiatives

The concept of Dual-Use is but one aspect of the new national policy relating to defense reinvestment, diversification, and conversion. This new Congressional policy has inspired new initiatives in the areas of advanced subsonic propulsion and High Speed Research (HSR) for civil air transportation by NASA. IHPTET will be a major springboard for the new NASA initiatives; and together NASA and DoD will work advanced technologies for both military critical and commercial critical applications as depicted in Figure 8. Even though Figure 8 is only a schematic of the development directions of US turbine engine technology, it gives a perspective on how the military and commercial interaction will occur through the nineties. IHPTET will continue with technology development through the nineties focusing on the high-payoff military goals, but will do so in concert with all new national technology development and application initiatives. For example, IHPTET will work on the military unique technologies of stealth, expendable engines, and concepts of thrust vectoring for STOVL applications. NASA will, on the other hand, work on commercial unique technologies -- ideas for pollution control, noise suppression, universal fuels and novel regenerative cycles. Together IHPTET and NASA will work the more common "Dual-Use" technologies such as advanced materials, CFD design codes, advance engine controls and logic, advanced turbine cooling concepts, bearings and structures. Technology success in this common area will be applied to military critical needs and commercial critical needs as necessary. For example, success in advanced turbine blade cooling technology may be applied in military engines to increase the allowable gas temperature at constant turbine blade life and thereby increase the engine specific thrust. In a commercial application, the technology may be applied to lower the turbine blade bulk temperature at constant gas temperature (constant thrust) and increase the life of the component -- same technology but spent differently.

As America approaches the next century and beyond, the programs of IHPTET and NASA, working together, will provide a strong national technology base. Through the NASA efforts the American civil aviation industry will continue its dominance of the global aviation market. Through IHPTET the military will continue to achieve affordable national defense -- global reach and global power.

ENGINE CHARACTERISTICS FOR AGILE AIRCRAFT

K R Garwood
G S Hodges
H E Rogers

Rolls-Royce plc
P O Box 3
Filton
Bristol
BS12 7QE
England

SUMMARY

A number of different factors drive and constrain the development of future technology. This paper looks at the current perspective on the development of agile aircraft systems and more specifically, the engine characteristics these demand.

Having identified the desirable engine characteristics, the key technologies required to enable them are discussed.

It is proposed that the optimum agile aircraft system will be achieved given these technologies by considering the best way in which the engine should be 'rated' to fulfill the operational requirements envisaged.

INTRODUCTION

This paper briefly examines the factors driving and constraining the development of agile aircraft systems, to put the requirements for engine development in the correct perspective, considering an entry into service of around 2010.

As a consequence to the above, the desirable engine characteristics and the key technologies appropriate to achieve these are considered.

Assuming availability of the required technologies the specific applications are then discussed in terms of cycle and rating structure to optimise the engine design for an agile aircraft system.

REQUIREMENTS

The Gulf War proved that in certain theatres of war (where the terrain is compatible), air power is paramount to military success and the achievement of air superiority, air supremacy, needs a highly agile aircraft with high performance radar and missiles.

However, with defence budgets shrinking, the importance of dual or even multirole capability in the design of future fighters is becoming increasingly necessary, with at least greater range potential than traditionally attributed to agile combat aircraft.

Certain scenarios can be envisaged where either a long range penetrator with good available agility, or an agile combat aircraft with greater combat endurance than previously seen, will be key operational requirements.

Historically, we have seen an increase in thrust to weight ratio of combat aircraft (Fig 1). In fact, over the past 40 years it has doubled.

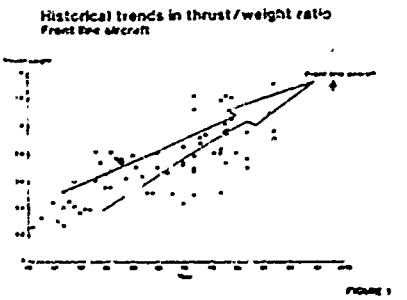

Taking a look at the powerplant fraction of three engines that cover the above range (Fig.2), it can be seen that the development of systems as a whole has led to a reduction in the powerplant relative weight fraction from slightly more than half to below half of the aircraft take-off weight.

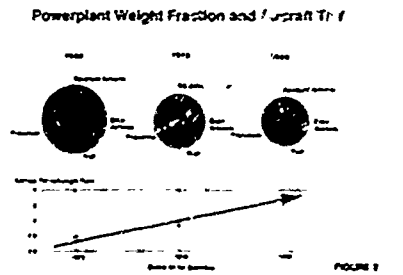

Future developments will be required to maintain current levels of aircraft take-off weight for significant increases in aircraft agility and range by

Presented at an AGARD Meeting on 'Technologies for Highly Manoeuvrable Aircraft', October 1993.

optimisation and integration of both aircraft and engine technology advancement (Fig.3).

Agile Aircraft
Influence of engine technology

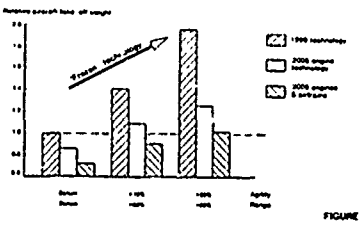

FIGURE 3

DRIVING FACTORS

The four considerations driving any future agile combat aircraft system will be effectiveness and survivability, flexibility and affordability (Fig.4).

The first two of these considerations, the traditional need for effectiveness and survivability, are still a major requirement. These depend upon the systems overall ability to out manoeuvre the opposition, its potential for extended range of operation and time 'in combat' capability and its ability to get home without refuel back-up. Stealth is another factor affecting survivability and effectiveness - this will affect how close to a 'target' the aircraft can get before detection and also how difficult it is for enemy fire to stay locked on' to it.

System flexibility can be interpreted in two ways - the application of a system to more than one role ie. multirole capability, and also the potential use of thrust vectoring for STOL/STOVL and/or increased agility.

The multirole element of a systems flexibility will also contribute to its "affordability" given that if it will perform more than a single role the reduction in first cost may not be as overriding when balanced against the cost of purchasing two different systems. Whether the system is to be single or multirole is unlikely to affect the life cycle cost requirment however.

Engine Development for Future Agile Aircraft

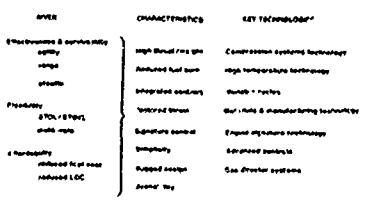

FIGURE 4

CHARACTERISTICS

To achieve the requirements outlined above, there are eight 'desirable' engine characteristics:-

1) Thrust:Weight

As the historical trend has implied (Fig.1), increased thrust:weight ratio has played a major part in development of agile combat aircraft. Developments of engine thrust:weight increases of up to the order of 100% are envisaged for next generation systems.

2) Reduced fuel burn

Improved specific fuel consumption and hence reduced fuel burn for a 'mission profile' will be the major contributor to increased range and should also benefit life cycle costs. However, any improvements in fuel burn will have to be balanced over mission type to give a nett benefit.

3) Integrated Controls

In order that the engine and aircraft performance can be optimised throughout operations, advanced integrated controls will be required not only to maintain best engine matching by control of variables, thrust vectoring and adjustments for deterioration. etc, but also to provide an active aircraft:engine interface. These performance seeking controls will require development of closed loop systems. Despite the potential increase in complexity of the control system, to enable enhanced pilot interaction, the system must be simple to operate and understand, robust and above all reliable.

4) Vectored thrust

A feature first operationally demonstrated by the Rolls-Royce Pegasus engine, vectored thrust can be used to increase agility as well as provide STOL/STOVL capability.

5) Signature control

Measures to control engine signatures in the visual and electromagnetic spectra are necessary as a part of the overall stealth considerations for future aircraft systems. Developments in this field will lead to improvements in a systems effectiveness and survivability.

6) Simplicity

Simplicity of design and operation can be facilitated by materials and manufacture developments. Combined with designed in reliability this will contribute to enhanced reliability and maintainability, as well as giving potential savings in weight and cost.

7) Rugged design

Robust or rugged designs are a necessary characteristic for better survival in the

battle field, not only in terms of damage tolerance but [illegible] terms of 'in the field' operation [illegible] the engine will be exposed to a [illegible] e environment, such as battle damage, sand/dust ingestion, extremes of temperature, non-clean maintenance sites, non-standard fuels, electromagnetic fields.

8) Availability

Time at readiness and conversely 'down time' are heavily influenced by the systems simplicity and ruggedness. Reduction of both scheduled and unscheduled inspections and removals will increase availability and hence operability.

KEY TECHNOLOGIES

In order that the desirable engine characteristics outlined can be realised, various key technologies need to be put in place.

These technologies can be naturally divided into a number of categories, as shown in Fig.4. Each of these is examined here

1. Compression systems technology

The drive in compression system development has been increased stage pressure ratio combined with increased efficiency at a loading level. Figure 5 shows the historical progression of fan and compressor pressure ratios and a projection into the next century. This trend has influenced the length of compression systems keeping them relatively lower for the increases in overall pressure ratio.

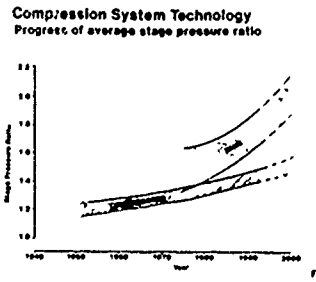

FIGURE 5

The development to these higher pressure ratios while at least maintaining or improving efficiency, increasingly requires the use of variable vanes. Inevitably, as the levels of efficiency tend towards the maximum realisable, the effect required to achieve each step becomes greater. One area of development offering efficiency returns is that of active control of running lines, thus allowing reduced surge margin operation. With reference to Fig.6, although efficiency is seen to reduce with increased loading, it has been shown that some efficiency can be regained by reducing the operating surge margin.

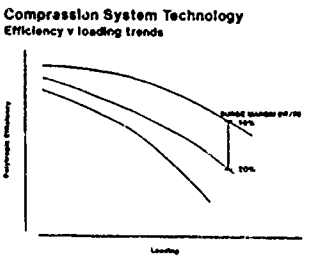

FIGURE 6

A further development in compression technology is that of hybrid compressors where the first stage of the high pressure compressor is a T-stage acting in a similar way to the last stage of the fan, feeding both the HPC (core) and the bypass duct. This style of compressor is particularly applicable to the variable cycle engine concept, presenting a challenge not only in terms of aerodynamic design of the rotors but also in terms of variable vane technology.

A fan plus hybrid compressor configuration also offers the benefit of a reduced demand on the LP Turbine system.

2. High temperature technology

As overall compression ratio is driven higher so too are the gas temperatures seen by the other components of the engine. Of particular concern are the combustion chamber, turbines and nozzles, as combustion temperatures approach stoichiometric levels and higher HPC delivery temperatures are seen. Given the traditional HP turbine cooling air source has been from the HPC, these make the cooling task ever more demanding.

Developments in turbine blade materials and cooling design efficiencies increase the cooling effectiveness achievable, which can be 'cashed' in terms of increased life or peak operating temperature.

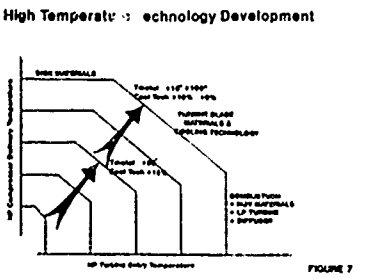

FIGURE 7

Figure 7 shows the path of advancing technology with boundaries on HP compressor delivery set by disk and rear stage blade material capabilities, and turbine entry temperature boundaries set by combustion and LP turbine cooling considerations. Turbine technology development moves forward with improved

cooling designs and materials and could also exploit the use of cooled cooling air. The benefits of the latter are easily identified, potential operation at higher compressor delivery and/or turbine entry temperatures, reduced cooling flows or increased life. Conversely, the disadvantages of added mass and complexity, etc, need to be minimised for any true benefit to be realised.

3. Variable cycles

The potential offered by variable cycle engines, to operate in both the medium and high specific thrust modes has obvious advantage when looking towards any future combat aircraft where the agility requirement is likely to be combined with that for range/durability.

The technologies required for these engines will be common in many cases with conventional engines - increased use of compression system variables, variable mixers, variable 2 parameters con-di rear nozzles, advanced integrated control systems.

However, the degree of compression system variability, for example, will be much more demanding than that of a conventional engine. Furthermore the potential complexity of a control system is also likely to be greater. More specifically, use of valve arrangements will require development of light, reliable, responsive valve and actuator systems, combined with understanding and 'control' of the aerodynamic problems these can present.

These technologies will need to be optimised for the advantages offered by variable cycle engines to be realised.

4. Materials and manufacturing technology

The development of materials and manufacturing technology will be the key to the development of many other technologies - as mentioned earlier, it is the availability of adequate materials that to some extent constrains the advances in high temperature technology.

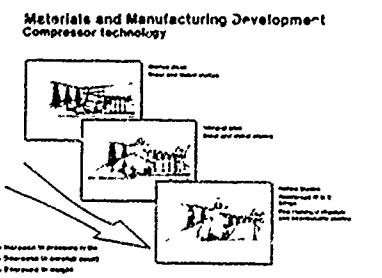

FIGURE 8

Let us consider the compressor, by way of an example. With reference to figure 8, materials and manufacturing technology has enabled the progression from bladed discs, where steel and nickel have been the dominant materials in the static members, to advanced designs utilising hollow blade technology, blisks and blings and fire resistant titanium and intermetallic statics. These developments have enabled a 40% increase in pressure ratio to be achieved with a 30% decrease in aerofoil count and a 65% decrease in weight.

In addition, the move to hollow blades and blings offers the further advantage in terms of reduced inertia components - of particular value in an agile aircraft system where the systems agility is to some extent a function of its own inertia.

5. Engine signature control

Figure 9 shows the technologies for engine signature control, roughly split into front and rear of engine.

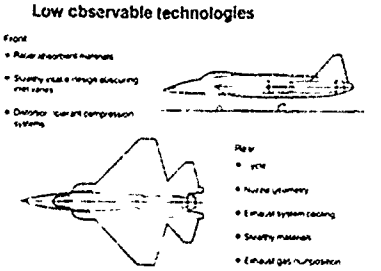

FIGURE 9

The front of the engine would benefit from the use of radar absorbent materials for the intake duct and/or possibly engine face and guide vanes.

Careful inlet design can enable the engine face to be obscured and need not cause undue inlet disturbance, and conversely may offer flow settling for an integral inlet: compressor design. However, it can be envisaged that non-optimal solutions could unduly disturb inlet flow hence requiring a more distortion tolerant compression system.

The choice of engine cycle will involve some trade-off between infra-red and radar signatures. The smallest hottest engine possible offers a better solution with respect to radar cross-section of the aircraft but would be bad for infra-red. On the other hand, a high bypass-ratio, low specific thrust engine, although better for IR could be worse for aircraft radar cross section.

Nozzle geometry is not only an engine design challenge, but also one for the engine:aircraft interface. 2D nozzles blended to the vehicle shape have the potential to not only reduce radar signature, but also may be easier to vector - although paying the penalty of greater weight relative to a 'conventional' nozzle. Careful design of a conventional nozzle could enable a reduced forward radar signature to be achieved such that coupled with its lower weight penalty it is an attractive option for an agile combat aircraft where forward signature is most important.

Temperature control of the external surface of the nozzle petals offers the potential to reduce IR signature. Similarly 'perfect' control of mixing of core exhaust where a cooling effect from the cold stream persists to the nozzle exit plane from which point it is totally mixed with the core flow.

Further measures to reduce back of engine signature would be use of radar absorbing materials where practicable and nozzle design such as to obsure and stop/or reduce reflections from the turbine.

Exhaust gas composition particularly affects the engine's visual signature - advanced combustors will reduce the emissions of smoke and NOx and investigations have also been made into the chemical suppression of vapour trails.

Finally, the use of entrainment offers the potential for signature reduction in terms of exhaust plume cooling and improved exhaust mixing.

6. Advanced controls

The control systems requirement for current and projected agile aircraft is primarily influenced by the increased demand for engine and aircraft integration and the use of variable geometry. A consequence of this is the employ of a greater number of closed-loop controls and inevitably the requirement for a system in which two or more loops operate simultaneously. In some cases there will exist interactions between the several input and output pairs - this will require multivariable control system design.

The primary advantage of multivariable controls is realised in the form of engine performance and/or handling improvements, attainable through the bility to control fan and compressor working points more accurately - for example, the freedom to set any desired fan working point at any time means that surge margin, normaly fixed by the variable geometry schedules, can be reduced to take advantage of low intake distortion estimate to reduce sfc, or can be increased to allow rapid handling during extreme aircraft manoeuvres.

A further advantage is the potential for enhanced engine signature management - other applications can be envisaged.

The field of integrated controls technology is of considerable importance in the dovelopment of future agile combat aircraft and is a subject in itself.

7. Gas director systems

The use of vectored thrust, by means of gas director systems, to increase aircraft agility is an accepted principle. A further role of gas director systems is the provision of STOL/STOVL capability cf. Pegasus in Harrier.

When considering the use of vectored thrust for enhanced agility, the trade-off relative to other aircraft deployed controls has to be examined.

With reference to Figure 10, some of the considerations associated with both thrust vector and aerodynamic control, to obtain enhanced agility, are given.

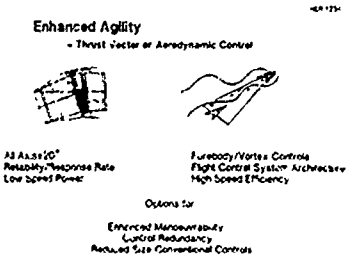

FIGURE 10

Generally thrust vectoring will give good low speed power and aerodynamic control good high speed efficiency. Major concerns with thrust vectoring are the reliability of the system - being dependent on engine reliability, which is inferior to that of aerodynamic controls - and the speed of response to demand, which is dependent on engine system inertia. With aerodynamic controls, the architecture of the flight control system will be of critical importance. Rather than considering the potential for enhanced agility as an either/or situation, there could be a strong case for the use of both thrust vectoring and aerodynamic control to effect enhanced manoeuvrability, with a possible consequent control redundancy and reduced size of conventional controls.

This presents an area of work where close collaboration between airframe and propulsion systems technologists will enable the development of the optimum overall solution.

Assuming the case for vectored thrust is positive enough, or indeed to assess its feasibility, various technologies and considerations need to be developed. Of primary importance are the cost and weight of the system.

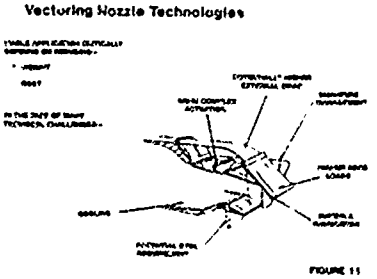

FIGURE 11

Signature management of the system will be more demanding than conventional given the increased number of moving parts or at least increased angles through which they will move. Reduction of signature from these will require careful design as will the need to minimise external drag they potentially could impose.

The aerodynamic loads that would be experienced by a vectoring nozzle will be of considerable concern and designs need to account for these in conjunction with development of the actuation system, which is likely to be more complex and would also be required to be more powerful than required with conventional nozzle actuators where some degree of aerodynamic 'balancing' can be employed.

The fabrication of the structure will need to enable the weight and cost reductions required to allow such a system to be an affordable solution and also to facilitate the difficult task of cooling such an articulated structure.

The requirement for STOL/STOVL potential as well as enhanced agility will significantly influence the design of the system and the demand on the various technologies - for most of these, inclusion of STOL/STOVL capability will increase the demand on the systems capability.

APPLICATION

It is in the application of the key technologies required for the specified engine characteristics that the optimisation of a system can be achieved.

In turn, the mission types affect the optimum balance of the various engine characteristics available as defined by the chosen engine rating and matching.

Given that the mission: rating/matching 'mixes' possible are numerous, considering one typical aircraft study as an example can illustrate the above point most simply.

Consider a possible fighter aircraft design (Fig.12) - a twin engined fighter of 17 tonnes clean take-off weight, with a clean wing loading of 274 kg/m² and a 40% fuel fraction (sizing missions require some range/endurance capability).

RR A/c Studies - Typical Fighter A/c Design

High Fuel Fraction
Advanced Twin Engined Fighter

Clean TOW	17 tonnes	37500 lb
Clean Wing Loading	274 kg/sq m	56.2 lb/sq ft
Fuel Fraction	40%	
Engine Mass Flow	65 kg/sec	143 lb/sec
Thrust/Weight Ratio (Static)	1.1	

FIGURE 12

With engines of 65 kg/s flow each, the aircraft has a static thrust to take-off weight ratio of 1.1 to 1.0.

As most engine rating structures are defined as a function of T1, point performance requirements can be plotted in terms of installed corrected thrust per engine against T1 and the aircraft's 'characteristics' for a given rating system plotted against these - this plot is more traditionally seen against Mach Number and known as a Husk plot.

Figure 13 shows the sea level and tropopause characteristics for the study aircraft, with conventional engines as the dot-dashed lines.

Fighter A/c Combat Thrust Requirements

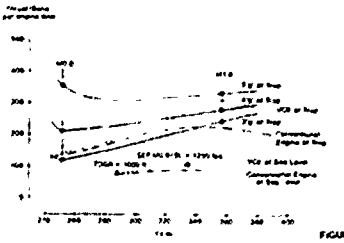

FIGURE 13

Different 'g' level requirements at the tropopause are spotted on the plot and lines of constant 'g' given.

It can be seen from these point performance indicators that a greater thrust delta is required for an increase in 'g' capability at low Mach number (low T1) than at high Mach number (high T1).

The rating of the study aircraft's engines accomodates a sizing point of a 1000ft take-off ground run and gives around 3'g' performance at both sea level and the tropopause.

Typical Agile Aircraft Engine Rating Structure

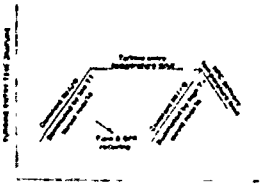

FIGURE 14

The engines have been rated in a similar manner to current agile aircraft, as shown in figure 14. At lower T1s the engine runs up a constant aerodynamic fan speed line, which is effectively a constant corrected air flow. The air flow is eventually pulled back as T1 increases once the engine has reached the HP turbine inlet temperature limit. As T1 increases further the engine will be pulled back on HP turbine inlet temperature as the HP compressor delivery temperature limit is invoked. The point at which peak HP turbine inlet temperature and peak HP compressor delivery temperature coincide is generally the mechanical design point of

the engine. The aerodynamic design point is generally at lower T1's where the corrected fan flow is at a maximum. The rating chosen for the study aircraft's engines gives reasonable low and high mach number performance, having a rating schedule with a range of T1 on the HP turbine inlet temperature limit.

Improved high Mach number performance would have been possible if the fan aerodynamic speed line, HP turbine inlet temperature limit intersect had tended to the right, ie. towards the HP compressor delivery temperature limit line, such that maximum corrected airflow and temperatures are all achieved at high T1 (high Mach numbers).

However, this type of rating would have compromised any low T1, low mach number cases where the turbine would have been operating far below maximum capability and the only way to achieve the thrust levels required would be to increase engine flow i.e. engine size, which in turn will have detrimental effects an aircraft weight and drag. Bias to the high T1 cases will also compromise any cruise/loiter performance that may be required for extended range of operation, as high T1 designs tend towards a low bypass ratio solution which has poorer fuel efficiency at lower thrust settings than a higher bypass engine of equivalent technology.

Had the engines been rated to give better low T1 performance, i.e, trending towards the left hand side of the rating diagram, they would have also had better loiter/cruise performance. However, high T1 thrust would have been compromised as the airflow would have been pulled back from maximum, making the engine reliant on high temperatures to attain the thrust levels, with consequent compromise of engine life.

If we examine the possible performance categories expected for an agile combat aircraft and the rating and matching requirements for each, we can identify the areas which are compatible and those which will require compromise. With reference to figure 15, the combat and supercruise requirements all require high specific thrust and operation in reheat or maximum dry power. These conditions cover the full range of T1 and ideally should have maximum corrected fan flow and HP turbine inlet temperature, rating at high aerodynamic fan speed. Already we can see a diversion of requirements, for a conventional engine maximum corrected fan flow can not be held at maximum HP turbine inlet temperature over a range of T1.

Furthermore, any requirement for cruise/loiter performance requires low specific thrust to give best sfc, this being a throttled dry case that would be better rated at low corrected fan flows exhibiting good low speed turbomachinery efficiencies.

Engine Rating and Matching Requirements

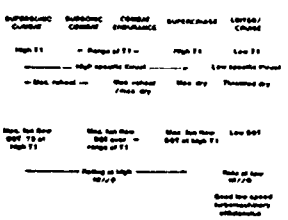

FIGURE 15

An alternative solution to the compromised rating of a conventional engine could be the employ of variable cycle engines. Their use offers the potential for operation in both high and medium specific thrust, thus enabling rating and matching to better satisfy a range of T1 and thrust requirements. Figure 16 shows typical thrust:sfc loops of a high and medium specific thrust engine. As the drive for higher specific thrust engines continues, to achieve combat performance, the loiter/cruise case will be moving further back along the sfc loops, thus increasing the difficulty of the task to obtain good all round performance.

Typical Thrust:sfc Loops

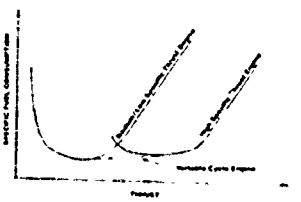

FIGURE 16

A variable cycle engine can offer the potential to combine the good high thrust performance levels of an high specific thrust engine and the better low thrust performance of a medium specific thrust engine, as shown by the dashed line in figure 16. This is achieved by enabling maximum corrected fan flow to be maintained at maximum HP turbine entry temperatures over a range of T1. This characteristic allows variable cycle engines to be smaller than conventional for the same thrust levels.

An additional benefit of the fixed corrected fan flow is the reduced spill and base drag this engine induces relative to conventional engines.

With reference back to figure 13, the dashed line shows the characteristics of the study aircraft with variable cycle engines of the same mass flow as the conventional engines. This shows approximately the same level of lower T1 performance as the conventional engined

aircraft but improved high T1, high mach number performance, with an improvement of 1.8 Tropopause performance from approximately 3'g' to 4½'g'.

As mentioned previously, a variable cycle engine may currently compromise the overall operability of an agile aircraft system given its level of maturity of required technologies. This needs to be compared against the easily identified, but just as technically challenging component requirements of advanced conventional engines. This and other factors need to be judged against the advantages such engines can offer with respect to rating and matching for a range of requirements.

CONCLUSIONS

Future agile aircraft systems will not only have to have greater agility and range than current systems, but are also likely to exhibit some degree of multirole capability.

The desirable engine characteristics required to fulfill the needs of these systems will require the development of a number of key technologies. The emphasis of technology development is dependant on the operational requirements and as such the engine matching and rating will need to be considered with close cooperation between the engine, airframe and operational requirements organisations, to ensure the optimum agile aircraft systems are realised for the perceived roles.

The view expressed are those of the authors and do not reflect any commitment by the Company. The authors would like to thank their colleagues for their support in preparation of this paper.

DESIGN OF INTEGRATED FLIGHT AND POWERPLANT CONTROL SYSTEMS

C.Fielding
Group Leader - FCS Design
Aerodynamics Department
British Aerospace Defence Limited
Military Aircraft Division
Warton, Lancashire PR4 1AX, UK

SUMMARY

During the past decade, British Aerospace has been an active participant in two major UK research programmes involving flight control of vectored thrust combat aircraft:

VAAC - 'Vectored thrust Aircraft Advanced flight Control', which is a UK Ministry of Defence programme in which a Harrier aircraft has been fitted with an experimental digital flight control system.

IFPCS - 'Integrated Flight and Powerplant Control Systems', which is complementary to the VAAC programme and is sponsored jointly by the UK Ministry of Defence, British Aerospace and Rolls-Royce.

This paper describes the work being undertaken by British Aerospace on both of these projects, as a continuation of the flight control and technology demonstration research successfully completed on earlier projects such as the Jaguar Fly-By-Wire and the Experimental Aircraft Programme (EAP).

1. INTRODUCTION

The requirement for enhanced combat aircraft performance has led to the design of aerodynamically unstable airframes, the stabilisation and control of which is made possible by the availability of full authority fly-by-wire flight control systems. These systems have revolutionised combat aircraft by providing significant operational benefits such as reduced pilot workload, carefree manoeuvring, increased flight envelope and excellent handling qualities.

At British Aerospace the evolution of the technology for advanced flight control systems is at a mature state and has been successfully applied to a range of combat aircraft such as Tornado, Jaguar Fly-By-Wire and the EAP aircraft. The experience gained is being fully utilised in the design and development of the Eurofighter 2000.

The technology development process is continuing in order to provide advanced flight control systems for future project aircraft and advanced developments to existing aircraft such as the Harrier. An important aspect under consideration is the integration of the traditionally separate flight and powerplant control systems: individual design and optimisation of each system may include making 'worst case' assumptions for the other system, thereby compromising the achievable design. Studies in the US (Reference 1) have already demonstrated some of the operational benefits of having a fully integrated system: increased engine performance, reduced fuel consumption, improved manoeuvrability, and improved safety and reliability. The latter is the result of having shared information between systems and the 'self-repairing' possibilities associated with control redundancy; e.g. 'propulsion only' control, to cover for total failure of aerodynamic controls.

This paper makes a short review of British Aerospace's previous fly-by-wire combat aircraft project experience, before describing some of the current and future project work being undertaken at BAe, in relation to the design of integrated flight and powerplant control systems.

2. FLY-BY-WIRE AIRCRAFT EXPERIENCE

2.1 Tornado

Tornado is a multi-role combat aircraft incorporating variable wing sweep and which is capable of carrying a diverse range of stores. It has been in operational service with the UK, German and Italian Air Forces since the late 70s and has more recently been acquired by the Royal Saudi Air Force. The aircraft has an aerodynamically stable airframe and is available as air defence and ground attack variants (Figure 1).

Figure 1. Tornado Aircraft

The FCS comprises a triplex analogue Fly-By-Wire system with a mechanical back-up. The baseline Command and Stability Augmentation System (CSAS) is interfaced with the duplex analogue Spin Prevention and Incidence Limiting System (SPILS, Reference 2) and the duplex digital Autopilot and Flight Director System (AFDS).

The aircraft is powered by two Rolls-Royce RB199 engines, each of which is controlled by a duo-duplex Digital Engine Control Unit (DECU). An autothrottle which drives the pilot's throttle levers is available via pilot-selectable autopilot modes.

2.2 Jaguar Fly-by-wire

Over the period 1977 - 1984 British Aerospace undertook a Ministry of Defence funded development programme leading to technology demonstration of a full time digital fly-by-wire flight control system. The Jaguar Fly-By-Wire Programme (Reference 3), although utilising the analogue FCS design experience gained from the Tornado aircraft, involved revolutionary system design and clearance procedures to cover the digital aspects of the FCS. Many features of the system design were based on experience from Concorde's air intake system, which was the world's first safety-critical airborne digital control system. The prime objective of the programme was to identify and demonstrate the design methodology and airworthiness criteria necessary for flight certification, and hence throughout the programme the control system was treated as though intended for production.

Presented at an AGARD Meeting on 'Technologies for Highly Manoeuvrable Aircraft', October 1993.

Using a Jaguar aircraft (Figure 2), a quadruplex digital control system was designed, no electrical or mechanical back-up FCS was provided, making the system the world's most advanced digital fly-by-wire system at that time. The programme successfully flight demonstrated a stall departure and spin prevention system and the ability to control an airframe which was significantly unstable in pitch and yaw. The aircraft was powered by two Rolls-Royce/Turbomeca Adour engines, each controlled by a Mechanical Engine control unit. The aircraft did not include any autothrottle modes as this was not a demonstration requirement.

Figure 2. Jaguar Fly-By-Wire Aircraft

Having successfully demonstrated the safe and practical engineering of a full time digital fly-by-wire system, British Aerospace approached their next combat aircraft design with confidence.

2.3 Experimental Aircraft Programme (EAP)

The purpose of the Experimental Aircraft Programme (EAP) was the flight demonstration of technologies for a future European Combat Aircraft (now called Eurofighter 2000). The programme, which was funded jointly by MoD and industry began in 1983 and spanned the following 7 years. The first flight was achieved in August 1986 some 3 years after initial drawing issue.

The performance requirements for the EAP aircraft resulted in a closely coupled canard-delta configuration (Figure 3) with high levels of longitudinal instability and aircraft performance. The practicality of this type of configuration is made possible by the availability of fly-by-wire system technology, the controllability of the vehicle is dependent upon the FCS. The FCS comprised a full-time full authority fly-by-wire quadruplex digital system based on the Jaguar fly-by-wire system but with higher performance FCS hardware in order to control the increased levels of basic airframe instability; i.e. faster digital computing, higher bandwidth actuation systems and reduced levels of feedback signal noise filtering (for structural vibration and digital aliasing effects).

Figure 3. EAP Aircraft

Specific features demonstrated by the EAP aircraft were high angle of attack at moderate speeds, a departure prevention system at high angles of attack and an automatic g-limiting system. The aircraft was powered by two Rolls-Royce RB199 engines, each of which was controlled by a duo-duplex DECU. The aircraft did not incorporate an autothrottle since this was not required as part of the technology demonstration.

The technologies demonstrated on the EAP aircraft were modern cockpit displays, avionics systems integration, advanced aerodynamics, advanced material construction and active control (References 4,5). The success of the programme provided a solid foundation for the design of the Eurofighter 2000.

2.4 Eurofighter 2000

The Eurofighter 2000 aircraft design and development (Reference 6) is taking full advantage of the technologies developed and lessons learned from the EAP and will provide an advanced high performance agile combat aircraft for the Air Forces of the UK, Germany, Italy and Spain.

The canard-delta configuration (Figure 4) is similar to that of the EAP aircraft but has been optimised to meet the requirements of the four partner nations. The airframe is aerodynamically unstable in pitch and yaw and therefore relies on a full-time fly-by-wire flight control system for stabilisation. The instability levels exceed those of the EAP and hence further advances in FCS hardware technology have had to be made in order to stabilise and control the aircraft.

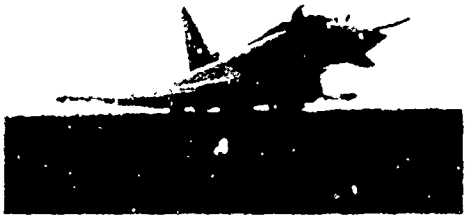

Figure 4. Eurofighter 2000 Aircraft

The digital flight control system is quadruplex with no mechanical or analogue back-up. The control laws have been designed to provide excellent handling qualities, carefree manoeuvring, automatic fuel/store state g-limiting and autopilot/ autothrottle integrated modes.

The first two prototypes for Eurofighter 2000 are to be powered by two Rolls-Royce RB199 engines each with duo-duplex DECUs, these engines are to be replaced within two years by Eurojet EJ200 engines. The other five prototypes and the production aircraft are to be powered by Eurojet EJ200 engines. The aircraft has pilot-selectable autopilot modes which issue autothrottle commands from the FCS to the DECU via the FCS databus; the pilot's throttle levers 'follow-up' the throttle commands (it is noted that all throttle commands are transmitted to the PCS via the FCS databus).

2.5 Integration of Flight and Powerplant Controls

The above sections outline BAe's significant experience in the design of fly-by-wire flight control systems for military aircraft, both analogue and digital. For each aircraft described, any command integration between the FCS and PCS, such as may not be required during flight re-fueling or landing approach is generally performed by the pilot. The autothrottle modes available on Tornado and Eurofighter 2000 provide a form of integration and an associated reduction in pilot workload. The term 'integration' can be interpreted in many ways and covers different types of system, as identified in Figure 5.

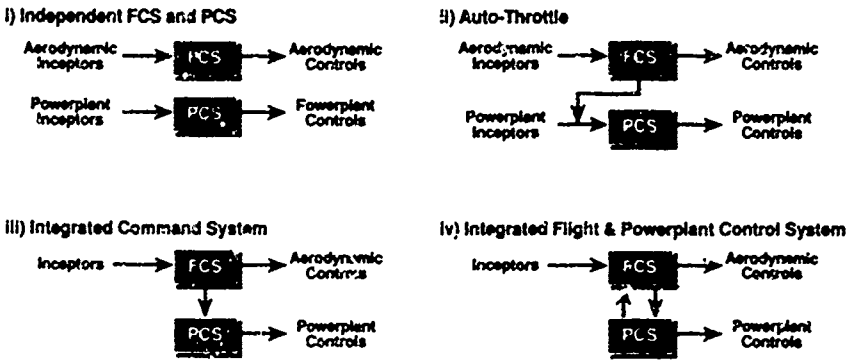

Figure 5. Integration of Flight and Powerplant Controls

i) INDEPENDENT FCS AND PCS - integration is performed manually, with the pilot using his inceptors for flight and powerplant controls in a co-ordinated manner; the pilot uses skill and anticipation to achieve the required response.

ii) AUTO-THROTTLE - the FCS commands the throttle opening with associated driving or follow-up of the throttle lever in the cockpit. It is an optional mode, usually of lower integrity than the baseline system and it is not safety-critical, since the system can be disengaged and the aircraft flown manually.

iii) INTEGRATED COMMAND SYSTEM - the commands from the pilot's inceptors are distributed between the flight and powerplant controls. If FCS does not utilise any feedback from the PCS. The powerplant operation becomes safety-critical if it is essential for flight control; i.e. it is configuration dependent.

iv) IFPCS - Similar to iii) except the information exchange is two-way and the systems are interdependent; the FCS utilises feedback information from the PCS to modify its internal state (for example, to prevent integrator wind-up when powerplant saturation occurs) to achieve a co-ordinated response. Similarly, the PCS might modify its internal state based on the FCS commands; for example, to reduce the engine stall margin in order to increase the powerplant performance. For an IFPCS, the powerplant operation is safety-critical, since it is essential for flight control. Some configurations require an IFPCS for controllability.

This progression of technology results in increasing system complexity but provides improved aircraft performance and reduced pilot workload in terms of aircraft handling, enabling the pilot to concentrate on his other operational tasks.

The remainder of this paper concentrates on some of BAe's current and future research and development activities in the field of integrated flight and powerplant control systems design. The aim of this work is to extend the well-established FCS technology to cover extensive integration with the powerplant to provide reduced pilot workload and improved aircraft performance, relative to an aircraft with independent systems.

Figure 6 shows the natural progressive development of FCS technology from Tornado through to Eurofighter 2000 and in parallel, some other fly-by-wire FCS design activities, notably the VAAC Harrier and IFPCS research programmes which are described below.

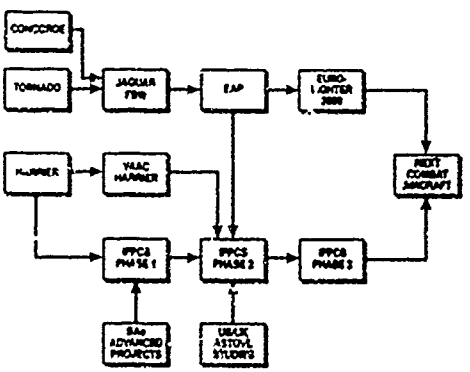

Figure 6. Relationship Between Programmes

3. VECTORED THRUST AIRCRAFT ADVANCED FLIGHT CONTROL (VAAC) RESEARCH

3.1 Background

VAAC is a UK Ministry of Defence programme with the objectives of flight demonstration of advanced VSTOL flight control and handling qualities assessment techniques

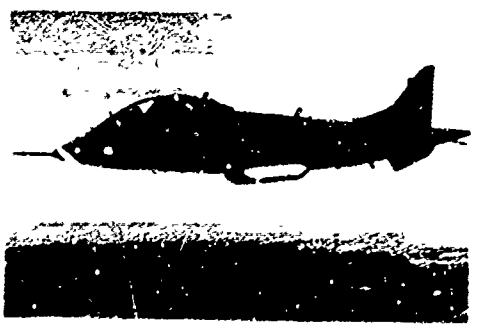

Figure 7 VAAC Harrier
(Photo Courtesy of Defence Research Agency)

(Reference 7). Studies are taken through piloted ground-based simulation, to flight demonstration in the Defence Research Agency's (DRA) project aircraft (Figure 7). The aircraft is a Harrier T4 two-seat trainer which has been fitted with an experimental digital flight control system, designed to permit a wide range of experimental control laws to be flown safely.

As part of the VAAC programme, BAe have designed a 'two inceptor' pitch flight control law for the experimental FCS. This control law provides commands, as outputs from the aircraft's flight control computer, to tailplane, flap, nozzle and throttle, and therefore provides a form of integration with the powerplant control system. This arrangement in terms of Figure 5 is described as an 'Integrated Command System', but is not regarded as a fully integrated flight and powerplant control system since the commands for thrust are made through the hydro-mechanical engine control system.

3.2 BAe 2-Inceptor Pitch Control Law

The pitch control law is based on a two inceptor control strategy ('Hands On Throttle And Stick') which combines the benefits of a modern pitch rate demand response type in wing-borne flight, with a highly automated STOVL system capability, enabling flight down to the hover. This philosophy is aimed at pilots of conventional combat aircraft, who should adapt quickly to flying the Harrier aircraft with this control strategy which provides major pilot workload reduction. A visible and logically arranged control law structure and simple well-proven control law functions have been used to expedite the practical issues of implementation and verification. Known physical effects are separated out within the control law to simplify the subsequent design of gain schedules.

The key features of the control law are:

- Two inceptor control strategy
- Proportional, Integral and Derivative (PID) controllers
- Pitch rate demand in wing-borne flight
- Height rate demand in jet-borne flight
- Continuous blending of modes via airspeed schedules
- 'Control-hierarchy' to determine thrust vector priorities
- 'Decoupled control' in inertial axes for jet-borne flight
- Outputs for tailplane, throttle, nozzles and flaps

3.3 Simulation Results

Figure 8 shows the simulated response of the aircraft with the control law for a vertical take-off, followed by a maximum accelerating transition to wing-borne flight. The nonlinear nature of the system is evident from the responses, which show well-controlled behaviour throughout the rapid transition to wing-borne flight (hover to 200 knots takes approximately 20 seconds). The aircraft begins to climb at 140 knots, as the height rate controller is phased out and the aircraft's lift increases with speed. The pilot would from this point onwards, fly the aircraft like a conventional aircraft via the control law's pitch rate demand.

Similar well-controlled nonlinear time histories are obtained for simulation of the aircraft with the control law for rapid decelerating transitions from wing-borne flight through to jet-borne flight (200 knots to the hover is achieved in approximately 28 seconds).

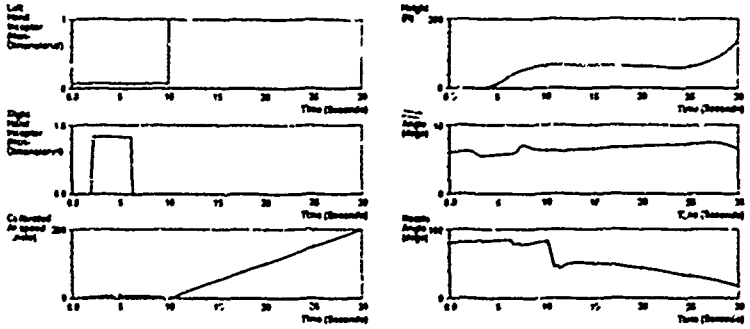

Figure 8 VAAC Harrier with BAe 2-inceptor Pitch Control Law - Simulated Vertical Take-off and Accelerating Transition

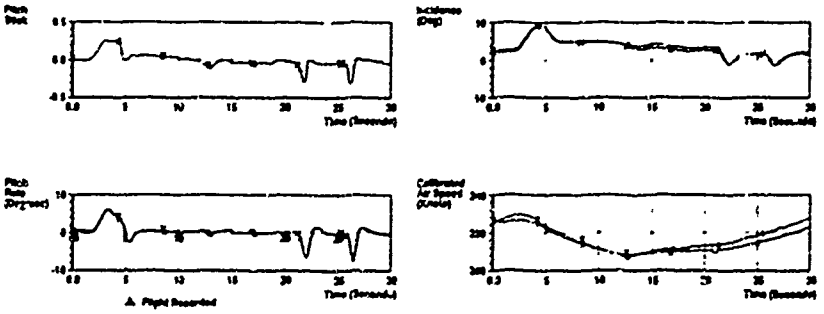

Figure 9 VAAC Harrier - Flight and Simulation Results Compared

3.4 Manned Simulation and Flight Test Results

A substantial amount of piloted simulation work has been performed at both BAe and DRA, during the development of the control law. During the simulation trials, the pilots were provided with realistic operational tasks and asked to give Cooper-Harper Ratings for the tasks. The piloted simulation results were considered to be very satisfactory with the system exhibiting average Cooper-Harper Ratings better than 3.5 for most cases. The simulation trials showed that although the system was found to be easy to fly by non-VSTOL pilots, Harrier pilots found it necessary to re-adjust their technique, relative to their current Harrier piloting experience.

To date, the VAAC Harrier aircraft has made several successful flights with the BAe control law, covering decelerating transitions from wing-borne flight at 250 knots down to jet-borne flight in the hover. Figure 9 shows an excellent match between the flight test and simulated results for a 30 second extract from the flight recording at 220 knots.

The two inceptor control strategy and response type are considered to be appropriate to future STOVL configurations as well as updates of the production Harrier. Similar strategies have already been applied to other BAe STOVL project aircraft (simulation phase only) and a similar strategy is being applied to a RULS (Remote Unaugmented Lift System) aircraft as part of the Integrated Flight and Powerplant Control Systems programme, as described below.

4. INTEGRATED FLIGHT AND POWERPLANT CONTROL SYSTEMS DEMONSTRATION PROGRAMME

4.1 Background

IFPCS is complementary to the VAAC programme and is sponsored jointly by the UK Ministry of Defence, British Aerospace and Rolls-Royce (Reference 8). The main objective of IFPCS is cost-effective rig demonstration of the key control system technologies required for the next generation of combat aircraft, irrespective of the aircraft configuration. The programme currently involves British Aerospace Defence Limited and Rolls-Royce PLC and is divided into 'Systems Activities' which are mainly hardware-oriented (e.g. equipment specification and procurement) and 'Control Activities' which are mainly software-oriented (e.g. control laws design and specification).

The IFPCS programme consists of three phases.

- Phase 1, comprised high-level configuration studies covering feasibility and design concepts for an IFPCS and the system requirements for several aircraft/engine combinations. Advanced Vectored Thrust, Remotely Augmented Lift System (RALS) and Tilting Nacelles ('P103', Figure 10 and Reference 9) configurations were studied.

- Phase 2, utilised the results from the US/UK ASTOVL four concept studies to focus and extend the work previously completed. This phase encompassed design of the IFPCS control laws and established the overall system design, including preliminary specifications for the IFPCS equipment and the demonstration rig.

- Phase 3, is the system development phase and will include 'pilot-in-the-loop' simulation assessments of the IFPCS control laws and demonstration of IFPCS technologies on a ground rig.

The reason for choosing to demonstrate the IFPCS on a ground rig is cost-effectiveness; most of the risk reduction can be achieved, at a fraction of the cost of a flying demonstrator and without needing commitment to any particular aircraft configuration. Once the next combat aircraft is defined, IFPCS technologies will be available for incorporation into a flying technology demonstrator.

The approach to integrated control considered in the IFPCS programme has been to consider functionally integrated, but physically separate control systems. Functional integration is achieved by sharing data between flight and powerplant computers in order to modify the FCS commands and the resulting PCS responses. The engine-mounted Powerplant Control Computers and airframe mounted Flight Control Computers are to be linked by the

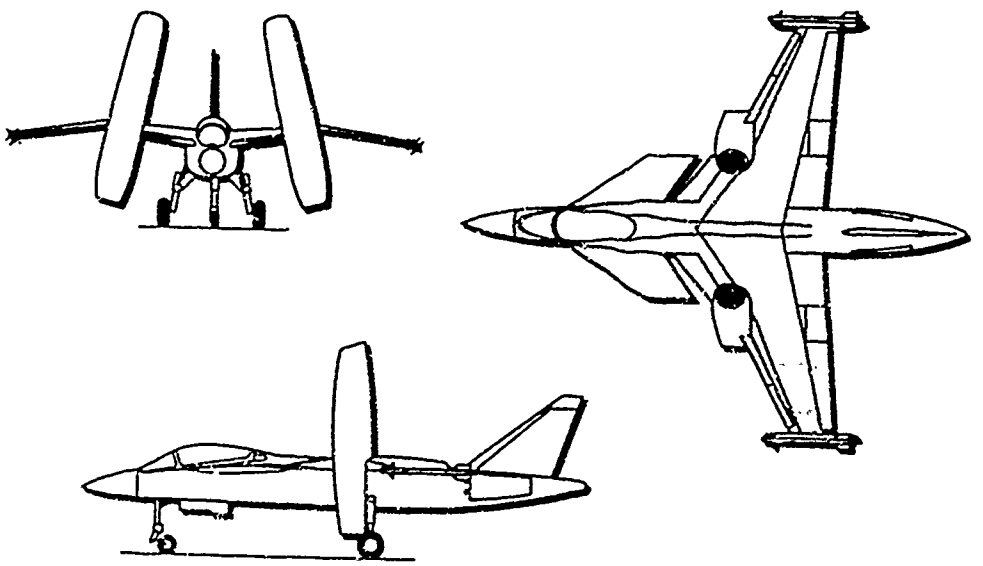

Figure 10. P103 Project Aircraft (IFPCS Phase 1)

safety-critical FCS databus enabling two-way data flow between the separate computers. This offers all the benefits of integration whilst permitting development of airframe and engine to be largely independent.

The Control Activities work has concentrated on the airframe aspects of an IFPCS such as configuration definition and modelling, control laws design and specification, and simulation. The emphasis in this paper is on the Control Activities work, however the Systems Activities are summarised in Section 4.6.

4.2 Aircraft Configurations Studied

Phase 1 of the IFPCS programme preceded the US/UK ASTOVL aircraft studies and considered a variety of configurations in terms of high-level concepts. Although the IFPCS programme is aimed to be generic in terms of its application to future configurations, it was necessary to provide a realistic focus for the Control Activities in Phase 2 of the programme. Two potential future aircraft configurations based on the P112 airframe (Figure 11) were selected for more detailed studies, including the design of integrated flight control laws:

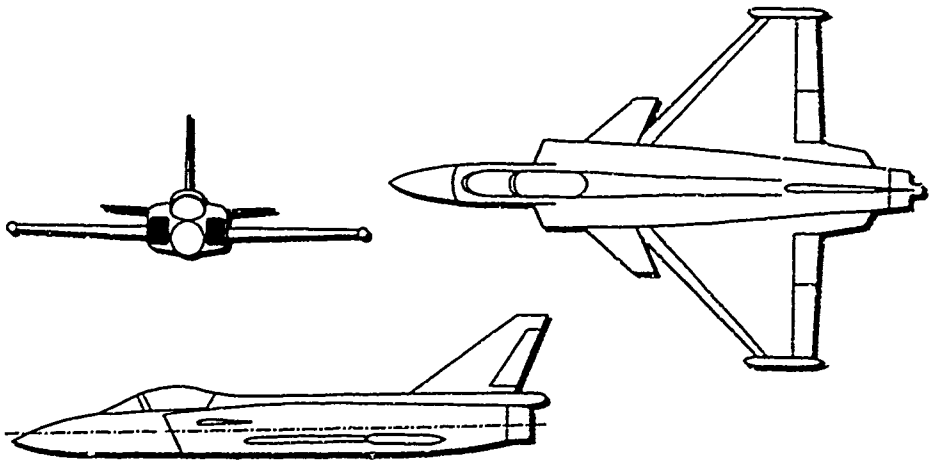

Figure 11. P112 Project Aircraft (IFPCS Phases 1-3)

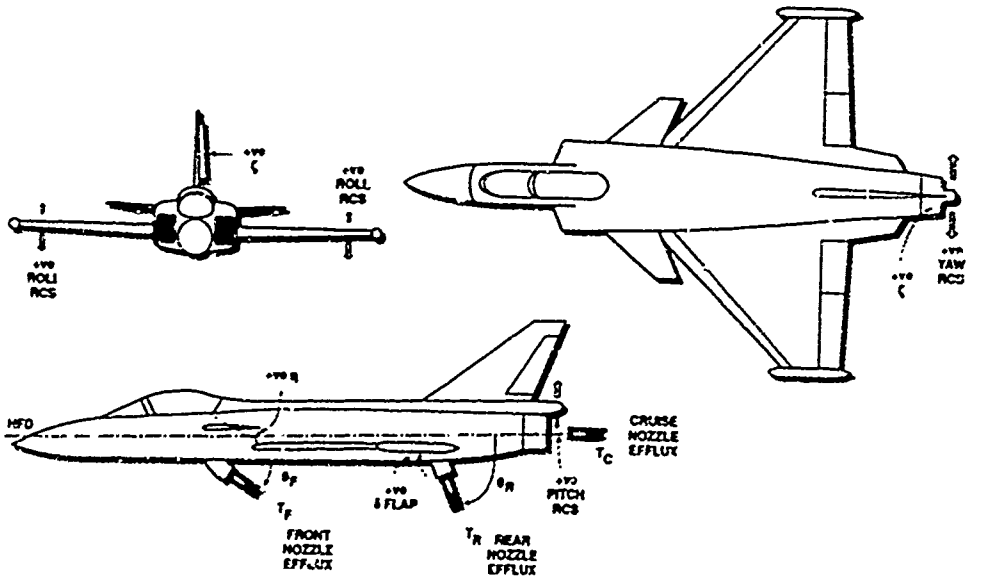

Figure 12. IFPCS Study Vehicle - Configuration 1 Showing Primary Controls

CONFIGURATION 1, is a STOVL multi-role fighter design (Figure 12), which provides a particularly demanding application of an IFPCS. The configuration incorporates an engine which can generate either direct lift through a three poster arrangement with a remotely unaugmented lift system, or axial thrust through a single non-vectoring rear cruise nozzle, for conventional wing-borne flight. At low airspeed a reaction control system supplements the pitch, roll and yaw control power available from conventional control surfaces. The aircraft's reaction control valves are located at the rear fuselage and wing tips.

The baseline engine for Configuration 1 is a Rolls-Royce concept, the general configuration of which is shown in Figure 13. The engine operates in two modes.

- FLIGHT mode with core and bypass flow passing out of the rear nozzle, with reheat available
- LIFT mode with core flow passing out of the rear vectoring lift nozzles and bypass flow leaving the forward vectoring nozzle.

The engine mode change is to be made by pilot selection.

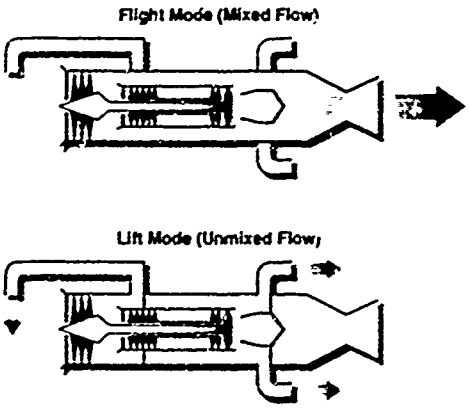

Figure 13 Schematic Arrangement of IFPCS Powerplant (Configuration 1)

resulting in internal valves within the engine performing the transition from one mode to the other, the flight control moding changes simultaneously in an integrated manner, to maintain aircraft control. In the lift mode, forward and rear nozzle vectoring can be performed independently, and it will be possible to vary the differential thrust between forward and rear nozzles. This will enable the aircraft to trim at different attitudes and cover a range of centre of gravity states.

CONFIGURATION 2 is a CTOL agile combat aircraft (Figure 14) has a single vectoring rear cruise nozzle which can be vectored in pitch and yaw. The nozzle can be used to compensate for diminishing aerodynamic control with increasing aircraft incidence, enabling post-stall manoeuvring. The powerplant for this configuration is based on a conventional turbofan. At low airspeeds or high incidence a reaction control system is available to supplement the roll and yaw control power from the aerodynamic controls. The aircraft's reaction control valves are located at the rear fuselage and wing tips.

4.3 Modelling Activities

To allow IFPCS design and assessment an aerodynamic description of the two configurations has been created, covering fundamental aerodynamics, jet/airframe interaction, nozzle vectoring, ground effects, intake momentum and hot gas reingestion.

The aerodynamic data was compiled from theoretical prediction methods and existing, representative wind tunnel test data, extrapolated by use of available high incidence data. The jet-induced aerodynamic data was compiled by blending the most relevant experimental data from a variety of sources, augmented with predictions and extrapolations.

Two powerplant models for the IFPCS activities were provided by Rolls-Royce:-

- A Simple Powerplant Model which includes major dynamic characteristics and is suitable for control strategy and initial control law studies.
- A Detailed Powerplant Model which includes thermodynamic relationships and gas dynamics and is aimed at more detailed investigations of control system performanc

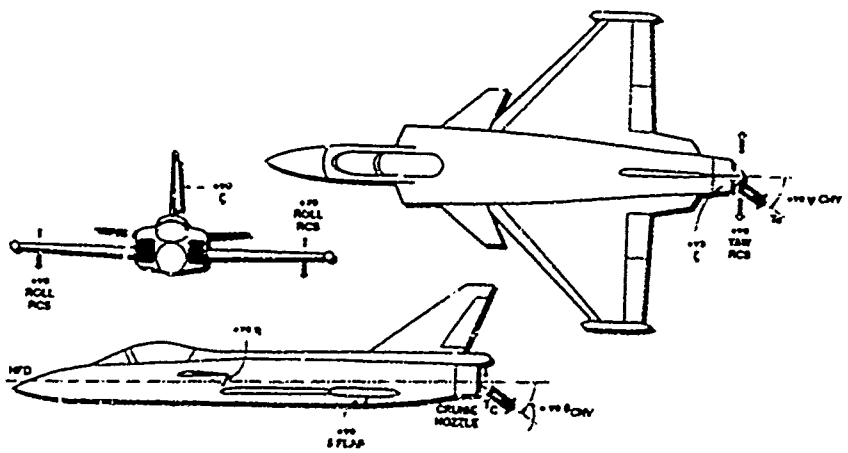

Figure 14 IFPCS Study Vehicle - Configuration 2 Showing Primary Controls

The FCS hardware models assumed in the design studies are based on state-of-the-art technology and cover nonlinear actuation systems (including authority, rate and acceleration limits), air data and inertial sensors, digital computing delays and an allowance for structural mode and anti-aliasing filtering

The components of the model are combined to produce unaugmented 'total aircraft models' (Figure 15), for Configurations 1 and 2, which form the basis for IFPCS control laws design and non-linear simulation. The models are modular, portable and coded in FORTRAN to allow ease of transfer to the manned simulator and other facilities, such as the real-time demonstrator rig proposed for Phase 3 of the IFPCS activities.

4.4 Control Laws Design

4.4.1 Configuration 1

IFPCS Configuration 1 is a representative vehicle for study of the control problems likely to be encountered on advanced STOVL designs. The control laws design task for this aircraft is very complex and involves the control of the aircraft by a combination of thrust magnitude, front/rear thrust split (and hence, powerplant pitching moment), front and rear nozzle angles, reaction controls and aerodynamic surfaces, the vehicle cannot be practically controlled directly by the pilot and an IFPCS is therefore considered to be necessary in order to manage the motivators in an efficient and co-ordinated manner. The system must cater for

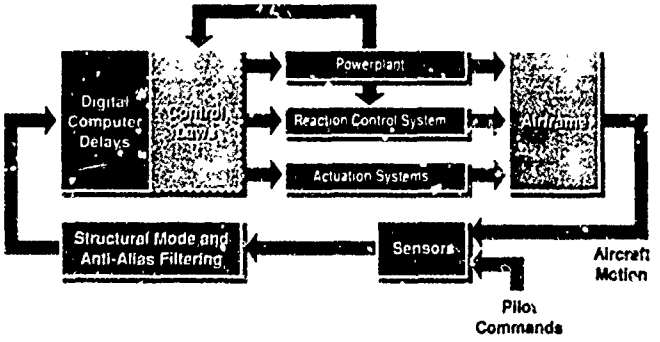

Figure 15 IFPCS Total Aircraft Model Arrangement

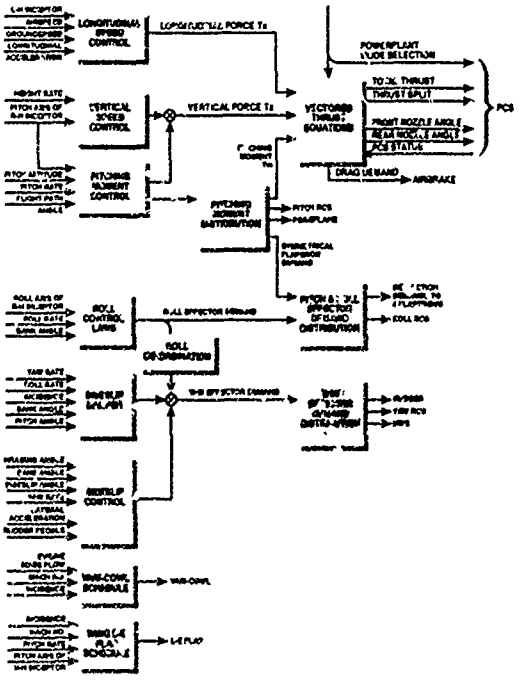

Figure 16 IFPCS Schematic Control Law Arrangement (Configuration 1)

the range of possible saturation states which will naturally arise as control boundaries are encountered; this entails the feedback of powerplant sensor data into the FCS, in order to take appropriate action.

A 'Hands on Throttle and Stick' (HOTAS) philosophy has again been adopted so that flying is a two-handed task. The resulting two inceptor system contains many of the design concepts of the BAe VAAC control law described above and provides a reduction in pilot workload compared with a three inceptor arrangement.

The high-level arrangement of the control laws for Configuration 1 is shown in Figure 16, the key features being:

- Two inceptor control strategy
- Proportional and integral (PI) controllers
- Pitching moment distribution functions
- Vectored thrust equations
- 'Control-hierarchy' to determine thrust vector priorities
- Nonlinear 'Decoupled control'
- Outputs for foreplane, flaps, rudder, reaction controls, nozzles total thrust and differential thrust.

The inceptor functions are scheduled with speed (Figure 17) to provide continuous control of the aircraft in a natural and transient-free manner, thereby maintaining consistent aircraft handling qualities throughout the transition region. At low speed, the left hand inceptor is s[illegible] to a throttle lever (Figure 18) and controls axial accele[illegible]n. The right hand inceptor is a conventional centre stic[illegible]id controls height rate and bank angle. At high speed the inceptors control thrust, pitch rate and roll rate, as on a conventional aircraft. The rudder pedals are used to control yaw rate at low speed and sideslip at high speed.

4.4.2 Configuration 2

The control laws for Configuration 2 are based on the EAP aircraft's laws in the region of the flight envelope where adequate pitch control power is available from the flaps and foreplanes. The EAP laws have been extended into the post-stall regime by 'blending in' cruise nozzle vectoring in pitch and yaw, and maintaining control as the aerodynamic control power effectiveness decreases, i.e. the flight envelope is extended to beyond that available with aerodynamic controls alone. The PCS is required to provide an estimate of current thrust in order for the FCS to establish the vectored thrust control power and therefore determine the vectored thrust command gains within the control laws.

The functionality of the Configuration 2 inceptors is essentially the same as for conventional aircraft with the pitch

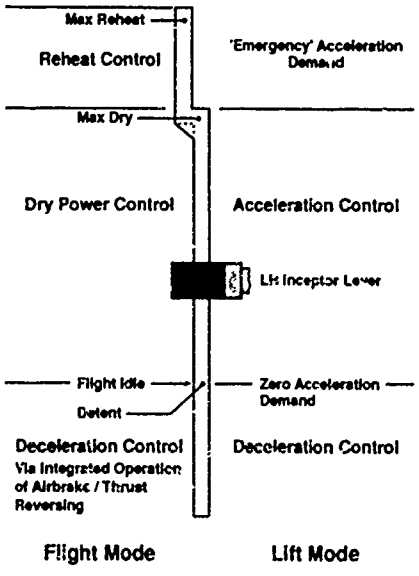

Figure 18 IFPCS Left Hand Inceptor (Configuration 1)

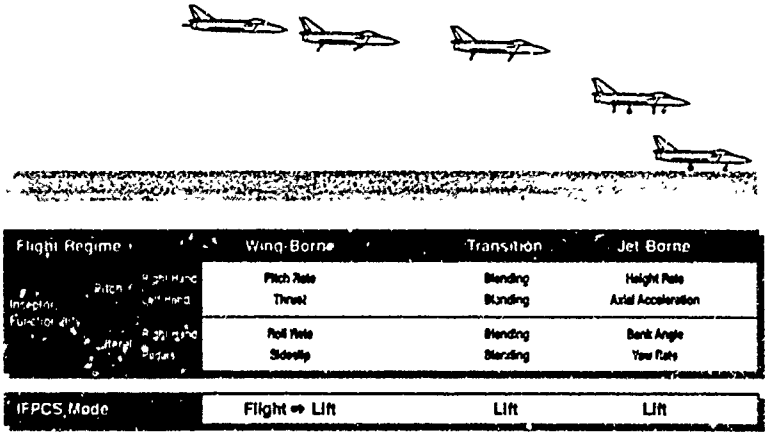

Figure 17. IFPCS Control Law Moding (Configuration 1)

stick commanding pitch rate at low incidence, blending into incidence demand at moderate to high incidence. The lateral stick commands wind-axis roll rate and the rudder pedals control sideslip via a sideslip suppression system. The high-level arrangement of the control laws for Configuration 2 is similar to that shown in Figure 16 but without the vertical speed controller and vectored thrust equations.

4.5 Simulation Results

The results presented in Figure 19 show the responses for Configuration 1, to a 1 Metre/Second height rate demand from the right hand inceptor at the hover condition. The height rate response is clearly well-controlled and deadbeat and is essentially achieved by simultaneously increasing front and rear thrust magnitudes. The change in pitching moment is corrected by transient use of the reaction control system to provide attitude hold.

The results presented in Figure 20 show the responses for Configuration 1, to a 0.1 g longitudinal acceleration demand from the left hand inceptor, at the hover condition. The acceleration response is also well-controlled and deadbeat and is essentially the result of rear nozzle deflection. Pitch interaction is minimised by the control laws.

The results presented in Figure 21 show the responses for Configuration 1 to a commanded change in pitch attitude via the system's attitude trim facility (optional secondary inceptor). The attitude response is again well-controlled and deadbeat, and interaction with height rate control is negligible.

It is noted that in all the above examples the re-trimming of the vehicle is achieved by re-balancing the thrust vector and the reaction control valve is closed in the steady-state, as required for efficiency.

4.6 Systems Activities

In parallel with the Control Activities, the Systems Activities part of IFPCS has addressed the implementation aspects of an IFPCS and has covered system requirements, architecture, preliminary equipment specifications and qualification requirements. This work has defined a triplex IFPCS architecture for the system (Figure 22) with the following features:

- Functional integration of flight control and powerplant control
- Common integrated inertial sensors for flight control and navigation
- Safety-critical direct links to fuel and stores management systems

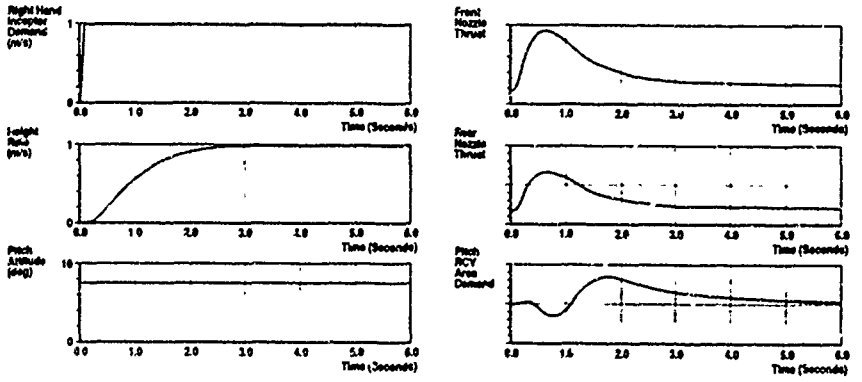

Figure 19. IFPCS Configuration 1 - Height Rate Demand in the Hover

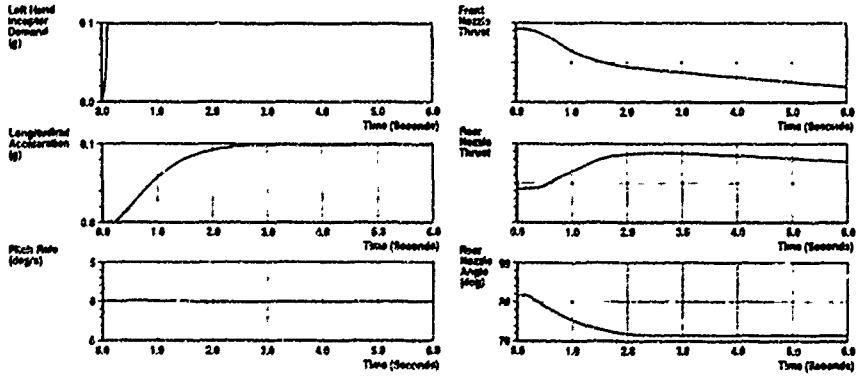

Figure 20. IFPCS Configuration 1 - Accaleration Demand in the Hover

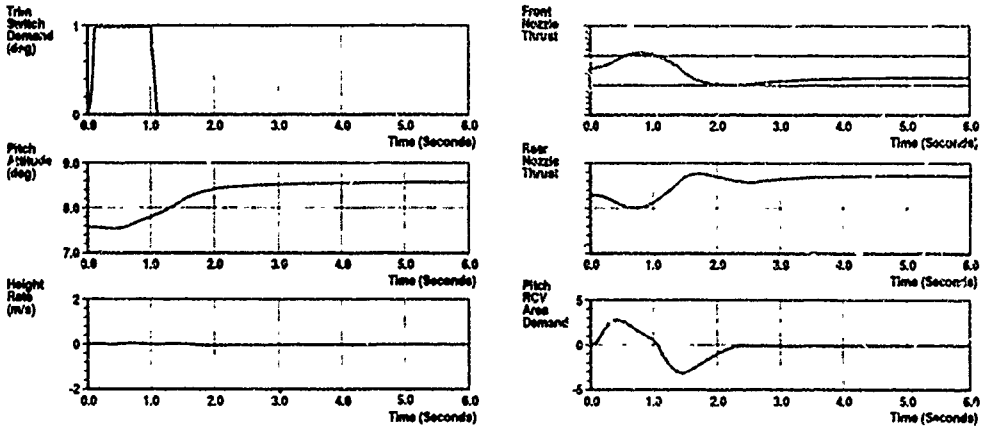

Figure 21. IFPCS Configuration 1 - Pitch Attitude Change in the Hover

- Modular avionics packaging, where applicable
- Safety-critical displays
- Fibre optic databus (DoD-STD-1773)
- Direct drive primary and secondary actuators
- Advanced leading edge system
- Reaction control valves directly controlled
- High performance vectoring nozzles

The System Activities have not been configuration specific and the technologies considered are applicable to a wide range of combat aircraft.

4.7 IFPCS Future Work

Phase 2 of the programme was completed in August 1992, having developed control law designs and established an overall system design. Phase 3, which will commence during 1993, is essentially a systems development phase and will include:

- 'pilot-in-the-loop' simulation assessment of the control laws
- Finalisation of rig equipment specifications
- Tendering and supplier selection
- Equipment design and manufacture
- Equipment acceptance testing
- Integration testing
- Full system rig testing and demonstration

In other words, all the activities necessary, prior to the installation of a system in a flight demonstrator aircraft.

5. CONCLUDING REMARKS

Building on the Fly-By-Wire FCS design experience gained on the successful Tornado, Jaguar Fly-by-wire and Experimental Aircraft Programme, and their application to Eurofighter 2000, further design studies have been undertaken by BAe as part of a co-ordinated FCS design strategy, with particular empnasis on the benefits of integrating the traditionally separate flight and powerplant control systems.

The studies performed on the VAAC Harrier project have covered the design, piloted simulation and flight demonstration of two inceptor pitch control laws for an existing VSTOL aircraft and have shown a reduction in pilot workload, relative to a three inceptor arrangement. It is hoped to further develop the control laws as part of the on-going VAAC programme, to consider 'outer-loop' modes such as auto-approach.

The IFPCS activities have led to the design of control laws for future STOVL and agile CTOL aircraft; these are to be further developed by piloted simulation during the next phase of the IFPCS programme which will contribute towards the demonstration of an IFPCS using real equipment on a ground rig, in preparation for the UK's next combat aircraft. For safety critical systems the demonstration of real equipment provides the only mechanism for rigorously testing, and hence proving, new technologies. The IFPCS programme will enable UK industry to maintain its position as a world leader in the field of aircraft control system design.

It is considered that much of the work described in this paper is applicable to the design of advanced flight control systems for future project aircraft and for advanced developments of existing aircraft such as Harrier.

ACKNOWLEDGEMENT

This work has been carried out with the support of the Ministry of Defence (Procurement Executive), the Defence Research Agency and Rolls-Royce PLC.

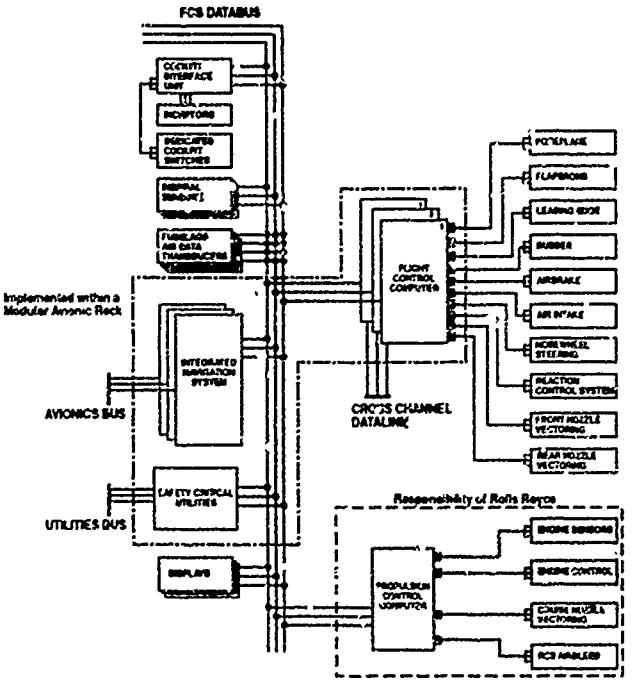

Figure 22. IFPCS Triplex System Architecture

REFERENCES

1. STEWART J F, BURCHAM F.W. and GATLIN D H, 'Flight-Determined Benefits of Integrated Flight-Propulsion Control Systems', NASA Technical Memorandum 4393, 1992.

2. BUTCHER P.S. and McKAY K., 'The Flight Test of an Automatic Spin Prevention System', AGARD Conference Proceedings 373, Paper 2, 1984.

3. NELSON J.R. and SMITH T D., 'Improved Combat Performance Using Relaxed Static Stability and a Spin Prevention System (FBW Jaguar)', AGARD Conference Proceedings 409, Paper 31, 1986.

4 KAUL H J., SELLA F. and WALKER M.J., 'The Flight Control System for the Experimental Aircraft Programme (EAP) Demonstrator Aircraft', AGARD Conference Proceedings 384, Paper 24, 1984

5. GIBSON J.C. and McCluen A M., 'EAP An In-Flight Simulator for EFA', DL Conference Proceedings DGLR-91-05, Paper 20, 1991

6. BARRIE D. 'Fighting for Air', Flight International, 16-22 June 1993, Pages 83-92.

7. SHANKS G.T., 'The VAAC Harrier In-Flight Simulation Facility', DLR Conference Proceedings DGLR-91-05, Paper 4, 1991.

8 ALLEN D.A and SLEEMAN J.R., 'The Integrated Flight and Powerplant Control System Programme RAeS/IMechE Conference on Engine Airframe Integration', Paper 9, 1992.

9 BOOT R., 'From Spitfire to Eurofighter - 45 Years of Combat Aircraft Design', Airlife Publishing, 1990

Thrust Vector Aided Maneuvering of the YF-22 Advanced Tactical Fighter Prototype

Robert W. Barham
Staff Engineer, Flight Test Branch
Lockheed Advanced Development Company
1011 Lockheed Way
Palmdale, California 93599 USA

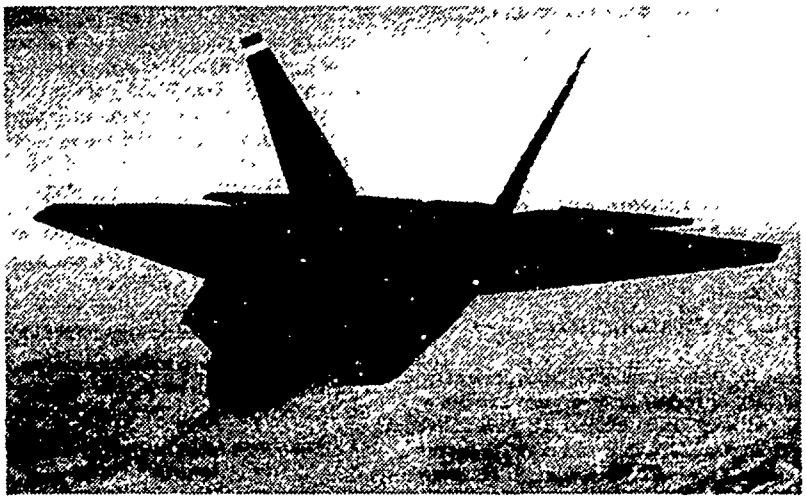

1. SUMMARY

In the mid 1980s design work began on the U. S. Air Force's next generation air superiority fighter. The F-22 team, consisting of Lockheed, Boeing, and General Dynamics, embraced a design philosophy in which low observable technology, maneuverability, and supersonic performance were given equal consideration. Even with low observable features and long range weapon employment capabilities, the team believed that the probabilities of brief, short range air combat engagements, based on historical precedents and postulated future scenarios, demanded a highly agile design. Thrust vectoring emerged as a key feature for obtaining the desired agility without adversely impacting the aircraft's low observable signature. Thrust vectoring technology was incorporated and flown in the YF-22 Advanced Tactical Fighter prototype to investigate and validate the concept for the production F-22. The airframe, flight control system, and propulsion system were fully integrated. Thrust vectoring commands were generated by the aircraft's flight control computers and sent to each engine controller. Each engine controller independently performed the computations and issued the commands necessary to position the nozzle actuators to the correct vector angle while maintaining commanded thrust levels and engine stall margin. Flight tests showed that thrust vectoring provided major improvements in low speed maneuverability, enhanced handling qualities during tracking, and increased supersonic sustained turn performance as compared to current front line fighters.

Presented at an AGARD Meeting on 'Technologies for Highly Manoeuvrable Aircraft', October 1993.

2. LIST OF SYMBOLS AND ABBREVIATIONS

AI	airborne intercept
AOA	angle of attack
CG	center of gravity
C_{Lmax}	maximum coefficient of lift
Deg	degrees
ft	feet
g	gravitational acceleration
hr	hour
IFPC	Integrated Flight/Propulsion Control
INS	inertial navigation system
IR	infrared
IRST	infrared search and track
KCAS	knots calibrated airspeed
kg	kilogram
KIAS	knots indicated airspeed
km	kilometer
LO	low observable
m	meter
MAX	maximum afterburning power setting
MIL	maximum dry power setting
RCS	radar cross section
sec	second
VHF	very high frequency

3. INTRODUCTION

Contracts for the Demonstration/Validation phase of the Advanced Tactical Fighter Program were awarded to Lockheed and Northrop on October 31, 1986. Both Northrop and Lockheed teamed with other contractors to build and flight test two prototype aircraft that incorporated advanced systems and design concepts for the purpose of technology risk reduction. The Lockheed lead team included Boeing and the Fort Worth division of General Dynamics.

As the design concept for the F-22 began to evolve, it was concluded by the team that a highly agile fighter design was required to counter the anticipated threats of the 21st century. The design objective was to achieve a balanced blend of low observable technology, maneuverability and supersonic performance in a reliable and affordable air superiority fighter aircraft. Since low observables dictated that the aircraft carry all weapons and fuel internally, the airframe was driven to an F-15 size aircraft. The challenge was to get F-16 responsiveness and maneuverability into an F-15 size aircraft. It was quickly recognized that thrust vectoring, along with integrated flight/propulsion controls, was an innovative technology that could provide the desired agility while maintaining the low observable characteristics of the aircraft.

This paper will discuss the thrust vectoring technology, incorporated into the YF-22 Advanced Tactical Fighter prototype, that was used to demonstrate "supermaneuverability" well away from the traditional "corner speeds." A brief description of the YF-22 design evolution with respect to agility, a description of the YF-22, and a description of its thrust vectoring system implementation will be presented. A comparison of the demonstrated YF-22 maneuvering performance with respect to current front line fighters will be made to show how thrust vectoring dramatically improved agility.

4. TEXT

4.1 The Historical Case for Agility

Despite the predictions made for the last three decades, the era when the air superiority mission would consist of launching long range missiles at an adversary beyond visual range (BVR) has repeatedly failed to materialize. In every conflict from World War I to the present, the overwhelming majority of air-to-air engagements have occurred within visual range and have involved maneuvering to a position suitable for employment short range weapons. The team's simulation studies had shown and continue to show that close-in combat engagements requiring short-range weapons were highly probable given restrictive rules of engagement, long range air-to-air missile kill probabilities and electronic warfare effects.[1] In the visual arena, aircraft agility and pilot skills have consistently determined the winners and losers.

Postulated future air combat scenarios involving low observable fighter adversaries also appeared to support the decision to balance low observables with agility.

4.2 Low Observable Technology Influence on Future Air Combat

Employment of low observable technology in fighter aircraft design has shown that it can deny long range detection by radar or infrared means. The F-117, a first generation LO design has already proven the inherent advantages of low observable technology in actual combat. Current technology is capable of much better performance.

Generally speaking, the air-to-air combat problem against an aircraft incorporating LO technology boiled down to two fundamental problems. The first problem was initial detection. Radar cross section (RCS) reduction techniques have been proven effective against the airborne intercept (AI) radars used in fighter aircraft. Detection ranges are generally near or within the visual arena. Ground based radars operating in the VHF band may be able to detect LO aircraft at much longer ranges but so far they have demonstrated no capability to guide weapons to within a lethal radius.

Once initial detection has occurred, either by radar or visually, the second fundamental problem appears:

achieving a weapons firing solution. Radar is generally used to measure range, range rate, azimuth and elevation to the target to provide data for the fire control computer. Against a low RCS aircraft the data provided by the radar is likely to be noisy even at short range. An acceptable "lockon" may not be achievable outside the minimum range of the weapon.

Weapons which require stable, accurate radar information in order to launch and/or guide could be significantly degraded against a low observable aircraft, even if the target is well within visual range. Employment of an infrared search and track system (IRST) in conjunction with infrared guided air-to-air missiles may provide only marginally better results from the front aspect. Infrared signature reduction techniques have been able to dramatically lower the detection and tracking ranges.

Against low observable adversaries, it will be increasingly important to maneuver to the adversary's rear quarter where the exhaust plume and engine hot parts dominate the IR signature and where it is the most difficult to shield or alter the IR signature. In the rear quarter, the importance of accurate ranging information from either a radar or laser range/tracking device is minimized since range rates and angle rates are typically less dynamic than in front or beam aspects.

As fighter aircraft incorporating low observable technology begin to enter the inventory of adversaries, the more likely that an LO fighter versus LO fighter engagement will occur and the more likely that the engagement will of necessity be a close range engagement using IR missiles or very short range gun attacks. To be sure there will be advances in missile and AI radar technology that may improve the longer range engagement capabilities. But for the foreseeable future it appears that short range engagements requiring maneuver to the adversary's rear quarter will be the rule rather than the exception for LO fighter versus LO fighter air combat.

The team concluded that the probabilities of brief, short range air combat engagements, based on historical precedents and postulated future scenarios, demanded a highly agile design balanced with low observable technology.

4.3 YF-22A Prototype Design Evolution

General John M. Loh succinctly summed up the team's concept of balanced design when speaking of the Gulf War and the tense hours F-15 pilots spent flying barrier combat air patrols in enemy territory far from friendly forces. He said "Stealth would have reduced that vulnerability. But stealth alone doesn't negate all threats. The things that make a fighter a fighter – agility, speed, the combination of weapons, and capabilities that let us sweep our adversaries from the sky – are still the sine qua non of air superiority."[2]

The Lockheed, Boeing, General Dynamics team adopted a philosophy consistent with other successful air superiority fighters in that it advocated achieving the highest possible first shot, first kill probability. The first shot, first kill problem was addressed in terms of both the long range air-to-air engagement and the short range maneuvering engagement.

At long ranges achieving the highest possible first shot, first kill probability was accomplished by utilizing low observable technology and long range weapons in the design. Low observable technology coupled with weapons system design was used to prevent detection by an adversary until the adversary was well within lethal range of the F-22's weapons. The low observable requirements were derived from known weapons employment envelopes and the best estimates of projected future air and ground threats. However, the team recognized that stealth in and of itself was not the complete answer.

The team, firmly convinced that the era of short range air engagements was far from over, believed that the superior agility was the key for achieving the first shot, first kill in the visual arena. Therefore the team embraced the design concept that "balanced" low observable technology with inherent airframe maneuverability to insure that the F-22 would always have the first shot opportunity whether beyond visual range or within visual range.

For the F-22 to be an effective fighter aircraft well past the turn of the century, maneuvering performance decisively superior to modern air superiority fighters such as the Su-27, Mig-29, F-15 and F-16 aircraft was required. Incorporation of the required low observable technology into a design the equal of these fighters would have been a worthy achievement by itself. However, the team set design goals for instantaneous and sustained turn performance, acceleration, and deceleration that surpassed current fighter capabilities and any postulated future threats. Superior supersonic turn performance was also emphasized since the YF-22 was designed to "supercruise" – i.e. cruise at supersonic speeds without use of afterburning. With a supercruise capability, it was expected that many air-to-air engagements would be entered from supersonic speeds. Hence supersonic turn performance became an area of emphasis.

In addition to the obvious performance implications of a highly agile design, the handling qualities of the aircraft were especially important with respect to agility since the aircraft was designed to routinely operate and maneuver in both the post-stall and supersonic flight regimes. One of the best descriptions was stated by Jon Beesley, Lockheed Fort Worth Company test pilot. "It

is simply the ability to put the airplane any place that I'd like to, whenever I'd like to, and have the aircraft never do anything I didn't ask it to."[3]

Compromises and tradeoffs were made to an achieve acceptable low observable signature based on postulated threats and weapons envelopes while retaining the desired the agility, supersonic performance and handling qualities. The challenge was formidable since low observable designs and techniques did not generally lend themselves to the aerodynamic and excess thrust design demands of a highly agile fighter aircraft. The design evolved into a blending of old and new technology in unique implementation schemes that were flown in the YF-22 Advanced Tactical Fighter prototype aircraft. Thrust vectoring emerged as the design feature critical to achieving unequaled agility throughout the normal flight envelope and into the flight realm well above the angle of attack for maximum lift.

4.4 YF-22A Prototype Description

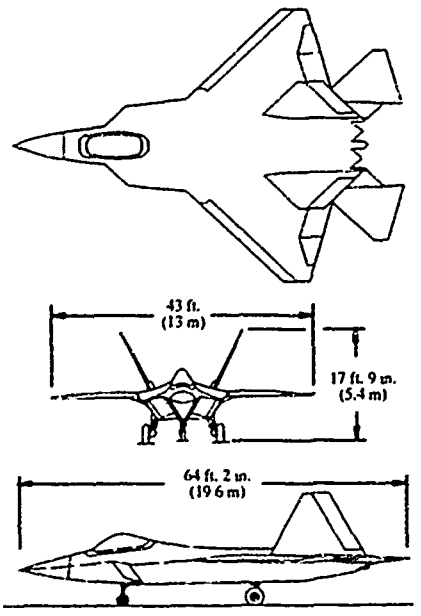

Figure 1. YF-22 External Three View

The YF-22 that rolled out in August of 1990 was a twin engine, F-15 size aircraft that incorporated low observable technology into a highly maneuverable airframe. The aircraft used a fly-by-wire flight control system to stabilize the aircraft since the basic airframe was statically unstable at most subsonic flight conditions. The flight control system was quad redundant for inputs and computation and triple redundant for electrical commands that controlled actuation of the hydraulic servos. The flight controls were scheduled as g-command system above 275 KCAS and blended to a pitch rate command system below 225 KCAS.[4]

Pitch control was provided by symmetric movement of the horizontal tails and engine nozzles when the thrust vectoring mode was active. The horizontal tails were sized to insure adequate nose-down pitching moment to push out of a deep stall at high angles of attack in the case of a thrust vectoring system failure or dual engine flameout and were capable of producing pitching moments sufficient to permit trimmed flight at extreme angles of attack.

The full span leading edge flaps were used to optimize the wing camber for better cruise and maneuvering performance and to improve handling qualities. The leading edge flaps moved symmetrically in a range from 5 degrees deflection up to 30 degrees deflection down.

Roll control was provided by ailerons, flaperons and, differential horizontal stabilator. The vertical tails and rudder were were sized to provide yaw control for coordinated rolls at 25 degrees AOA[4]. The rudder provided directional control and was used to coordinate rolls at low angles of attack. However, rudder effectiveness as a roll coordinating device decreased rapidly as angle of attack increased above 25 degrees. With thrust vectoring available to provide much of the trim pitching moment requirement, the aircraft's unique aerodynamics allowed differential horizontal tail to be used for both rolling and roll coordination at mid and high angles of attack. Aileron and flaperon effectiveness also decreased with increasing AOA and contributed little to the rolling moment at high angles of attack.

Control surface roll authority was limited to prevent pitch divergence due to kinematic coupling between angle of attack and sideslip. At all conditions pitch commands to the horizontal tail were given priority.

The two test aircraft were capable of using either the Pratt & Whitney YF119-PW-100 or the General Electric YF120-GE-100 prototype advanced tactical fighter engines. The engines were advanced designs that produced extraordinarily high thrust at MILITARY power settings thus enabling supercruise.

The YF-22 incorporated an Integrated Flight/Propulsion Control (IFPC) system. Coupled with the air data system, the propulsion system and flight controls functioned and were treated as a single system. The aircraft flight conditions, engine thrust requests, and thrust vectoring commands were passed to the engine controllers via the IFPC digital busses. The engine responded to

signed to provide pitch only vectoring. The exhaust gas stream was mechanically deflected by independently positioning the upper and lower divergent nozzle flaps. The nozzle flap actuators were also used by the engine to control the exhaust exit area. The nozzle flaps were capable of providing continuous vectoring angles of ± 20 degrees at a designed maximum rate of 40 degrees per second. Pitch commands were supplied to the engine electronic controllers by the flight control computers. However, the engine's control computers physically controlled the nozzle flap actuator position to obtain the desired thrust vectoring angle and exhaust exit area simultaneously. This gave the engines direct responsibility for a primary flight control function. While both of the engine controllers received the same pitch commands from the flight control computers, each engine processed the pitch commands and positioned the nozzle flaps to the proper angle independent of the other engine.

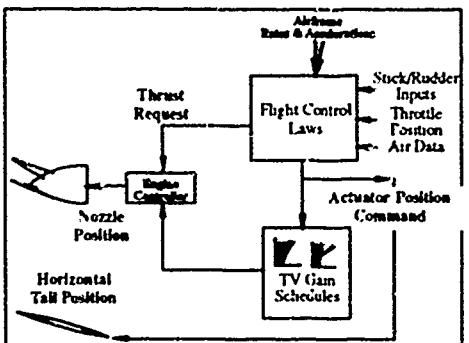

Figure 3. Simplified Pitch Command Schematic with Thrust Vectoring On

A blending between the horizontal stabilizer and the thrust vectoring nozzles was accomplished on the actuator command signals when thrust vectoring was active. Since the pitching moment provided by the engine nozzles was a function of engine power setting, the thrust vectoring commands were also scheduled as a function of average throttle angle. This gave the pilot the appearance of pitch control that was independent of the engine power setting.

The pilot was provided the ability to activate or deactivate thrust vectoring. With thrust vectoring selected OFF by the pilot, the flight control computer still was capable of commanding vectoring under certain predetermined conditions in order to prevent inadvertent departures or deep stalls. When the pilot selected thrust vectoring to ON, vectoring was enabled as a function of angle of attack, airspeed and/or flight condition.

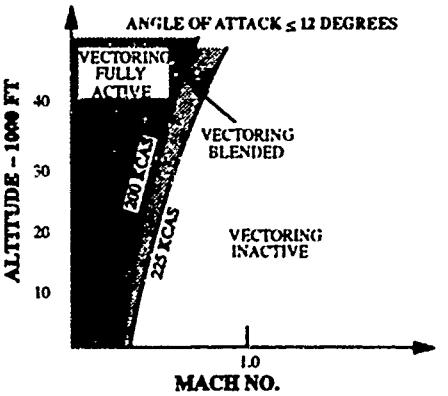

Figure 4. Thrust Vectoring System Operation Below 12 Degrees Angle of Attack

When the angle of attack was 12 degrees or less the thrust vectoring nozzles were fully enabled below 200 KCAS (Figure 4). As airspeed increased, thrust vectoring commands to the nozzle were linearly blended out until vectoring was completely disabled above 225 KCAS.

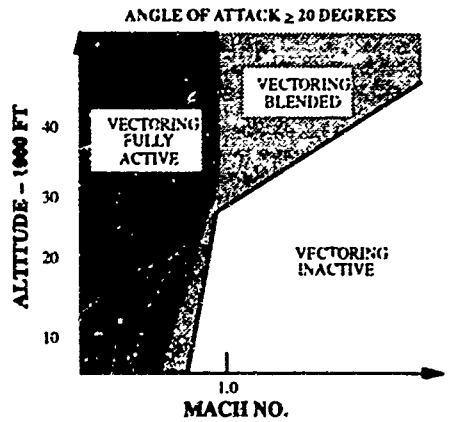

Figure 5. Thrust Vectoring System Operation Above 20 Degrees Angle of Attack

Above 20 degrees angle of attack, vectoring was scheduled as a function of Mach number and altitude (Figure 5). This schedule provided vectoring pitch authority for

thrust requests, positioned the nozzles to the appropriate vector angle and reported actions back the the flight control computers. The flight control computers then evaluated the engine reports, adjusted the engine inlet air controls and made subsequent commands to the propulsion system. The thrust vectoring nozzles, though controlled by the engine, were considered a flight control "surface" in every respect.

The pilot made pitch and roll commands via a side stick and yaw command via rudder pedals. The throttles were not mechanically connected to the engine. Electrical signals were generated by throttle position which the flight control computers then translated into a thrust request signal that was sent to the engine electronic control units via the IFPC bus. The flight control computers scheduled the throttle position input and thrust request output such that the engine thrust was essentially linear with throttle position for any given flight condition. Throttle position gradients were adjusted to accommodate the power settings typical of air refueling and landing such that the thrust response to small throttle movements was optimized for these tasks.

In order to take advantage of the maneuvering capabilities made possible by thrust vectoring, an air data system was required that could provide accurate inputs to the flight control system at extremely low speed, high angle of attack flight conditions up through the supersonic speed regime. The YF-22 air data system design proved to be quite robust and fully up to the task. The system featured a fully integrated design that provided pneumatic and inertial navigation system (INS) derived air data inputs to the flight control computers where data validity was checked and inputs blended in a manner such that accurate air data was available at all flight conditions and angles of attack.

Two dogleg probes on either side of the nose provided static and total pressure to air data transducers where angle of attack, airspeed, altitude, and Mach number information were calculated. Four flush mounted static ports, upper and lower on either side of the nose, were used to calculate sideslip angle. Each probe and flush static port had its own air data transducer for redundancy and data comparison purposes. The six transducers corrected the measured pressures for local flow effects and converted the inputs into electrical signals to the flight control computers.

Wind information was derived from INS and pneumatic air data when the probe and flush static port data were judged valid by the flight control computers. When the pneumatic data was judged to be invalid, air data information was derived from INS measured velocities corrected with the stored wind information.

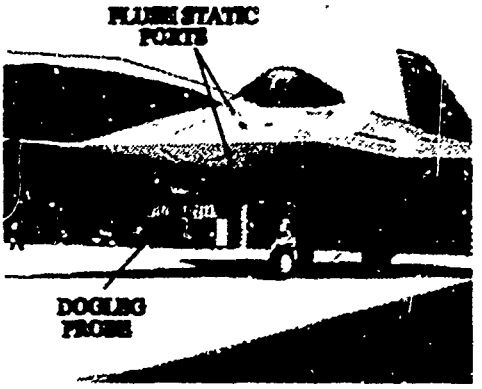

Figure 2. Air Data Sensor Locations

Below 30 degrees angle of attack, pneumatically derived angle of attack data and total pressure where used. Between 30 and 33 degrees angle of attack, pneumatically derived angle of attack data and total pressure were blended with INS derived data. Above 33 degrees angle of attack, INS derived angle of attack and total pressure were used for the flight control computations. The dogleg probes and flush static ports provided pneumatic static pressure up to 60 degrees angle of attack. Irrespective of angle of attack, when airspeed dropped below 75 KCAS (139 km/hr), air data calculations reverted to INS based data.

4.5 Thrust Vectoring Implementation in the YF-22A Prototype

The key element in providing the YF-22 with unprecedented maneuvering capability was the incorporation of pitch axis thrust vectoring. Tradeoff studies showed that thrust vectoring was the most efficient and effective method of achieving the desired pitching moments without the drag and weight penalties associated with aerodynamic control. Additionally, elimination of the aerodynamic surfaces that would have been required to achieve the desired pitching moments capabilities aided in meeting the low observable design criteria. With thrust vectoring, the horizontal tails were sized for more normal flight conditions while the aircraft retained pitch authority that was essentially independent of airspeed. Engineering estimated that each horizontal tail would have required an additional 20 ft^2 (1.86 m^2) of area at a weight penalty of approximately 400 pounds (181 kg) in order to meet the same maneuverability goals.[1]

Both the Pratt & Whitney YF119 and General Electric YF120 were equipped with functionally equivalent two dimensional, thrust vectoring nozzles capable of vectoring the engine exhaust stream at all power settings from idle to maximum augmentation. The nozzles were de-

low speed, high angle of attack conditions and increased the high angle of attack maneuvering capabilities at supersonic conditions where decreased aerodynamic effectiveness of the horizontal tails was limiting.

Between 12 and 20 degrees angle of attack, thrust vectoring was a linearly blended function of both schedules (below 12 AOA schedule and above 20 AOA schedule).

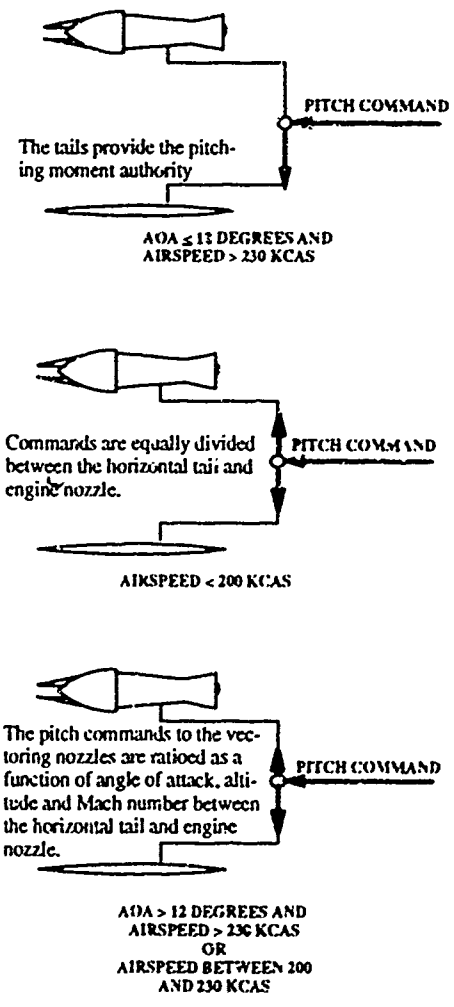

Figure 6. Notional Diagram of Thrust Vectoring Schedule Effects on Pitch Command Division

4.6 YF-22A Thrust Vectoring Flight Test Results

Agility was considered to be a critical design goal and demonstration of the maneuvering performance and handling qualities made possible by thrust vectoring received emphasis during the Demonstration/Validation flight testing.[5] In order to validate the engineering design and demonstrate the contributions of thrust vectoring to agility, both prototypes conducted numerous stability, control and flying qualities tests with thrust vectoring on and off at angles of attack up to 20 degrees at speeds as low as 135 KIAS (250 km/hr). Additionally, a high angle of attack demonstration program was flown. For the purposes of this demonstration program high angle of attack was defined as angles of attack above 20 degrees.

The high angle of attack program was conducted with aircraft number 1 which was equipped with the General Electric YF120 engines. As with all high angle of attack programs, a build up approach was used.[5] Testing occurred at 2 degree increments in angle of attack up to 40 degrees angle of attack. Above 40 degrees angle of attack the increments were expanded to 4 degrees since there was very little change in the aircraft's flight characteristic as angle of attack was increased.

Throttle transients were performed at angles of attack up to 40 degrees with no indication of stall or combustor blowout. No engine or nozzle vectoring operation problems were observed up to the maximum angle of attack demonstrated. Trimmed flight and flight control doublets were performed to evaluate basic control authority and aircraft response. Military power pushovers with thrust vectoring on and idle power pushovers with thrust vectoring off were accomplished to determine the pitching moment authority of the horizontal tail and thrust vectoring contribution to total pitch authority at high angle of attack. Following the pushovers, the angle of attack was reduced about four degrees and a series of full stick, feet on the floor rolls were performed to evaluate the aircraft's maneuvering capabilities. These data were later used to verify and validate the simulator predictions.

On December 17, 1990 after only nine flights and 14.9 flight hours the aircraft attained it's benchmark angle of attack. The aircraft demonstrated trimmed flight at 60 degrees angle of attack at 82 KCAS (152 km/hr) and showed that it was controllable when performing full stick rolling maneuvers. Although the aircraft had no flight control angle of attack limitation, 60 degrees angle of attack was chosen an appropriate stopping point for the Demonstration/Validation phase of the pro-

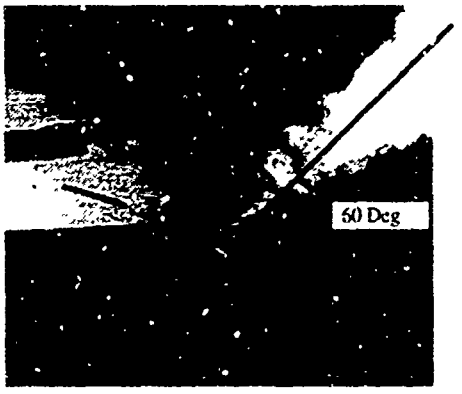

Figure 7 Trimmed Flight at 60 Degrees Angle of Attack

gram since it proved the capability of the YF-22 to achieve trimmed flight and controlled maneuvering at angles of attack substantially above the angle of attack for maximum lift.

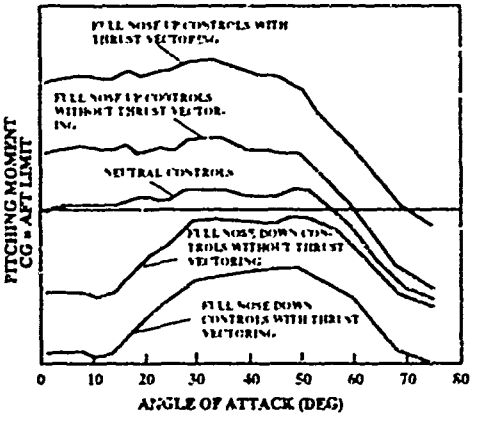

Figure 8. Pitching Moment vs. Angle of Attack

Figure 8 shows the pitching moment characteristics of the YF-22 with thrust vectoring.[4] It was evident that thrust vectoring provided a major increase in the pitching moment authority. Thrust vectoring approximately doubled the effective pitching moment available when compared to aerodynamic controls only. The figure also shows that the aircraft was capable of trimmed flight at angles of attack up to about 70 degrees. Above 70 degrees angle of attack the aircraft exhibited a stabilizing pitching moment slope.

Thrust vectoring provided a powerful nose down pitching moment if required. The aircraft was shown to be capable of high angle of attack recovery with aerodynamic controls only. This indicated that transient maneuvers well above the maximum trim angle of attack were possible. Flight simulation showed that the aircraft was quite capable of performing the "cobra maneuver" first introduced by the Russians at the Paris Air Show and consideration was given to demonstrating the maneuver during the Demonstration/Validation program. However, with only three weeks remaining in the flight test program other testing to support the contractor downselect decision received priority.

At 60 degrees angle of attack the aircraft was capable of generating peak nose down pitch rates of about 18 degrees per second with the engines at MIL power. Even at idle thrust, the aircraft could produce nose down pitch rates of about 15 degrees per second. At higher engine power settings the thrust effects quickly began to dominate the pitching moment capabilities of the aircraft.

	Idle power	MIL power
Time from 20 degrees to 10 degrees	3 sec	1.5 sec
Time from 60 degrees to 10 degrees	7 sec	3.5 sec
Maximum Pitch rate	15 deg/sec	18 deg/sec

Figure 9 Recovery Times from High Angle of Attack

The aircraft displayed rather docile handling qualities and displayed positive control at all high angles of attack conditions tested. Pitch attitude and angle of attack could be held to within 1/2 degree with thrust vectoring on up to 60 degrees angle of attack. When thrust vectoring was turned off control was less precise due to control law changes and the loss in pitch authority from thrust vectoring. Bank angle control was also smooth with no evidence of wing rock and the pilots were able to hold wings level for long periods of time with no perceptible roll off tendency. Roll control was reported to have become slightly more sensitive at 40 to 44 degrees angle of attack and a roll oscillation of $\pm$ 5 degrees could be induced with small lateral stick inputs. These oscilla-

tions quickly damped out if the stick was frozen and the pilots quickly learned that more careful inputs prevented its reoccurrence. Airframe buffet was light, increasing as 24 degrees angle of attack was approached and remained constant thereafter. Overall, the pilots described the aircraft's high angle of attack handling qualities as "just outstanding."[7]

Since the aircraft rolled essentially about the velocity vector (stability axis), the pilots' perceptions of roll angle, roll rate and heading changed as the angle of attack at which the roll maneuver was performed increased. The pilots' perception of rolling maneuvers between about 20 to 40 degrees angle of attack were of a barrel roll. Above 40 degrees angle of attack, the pilots' perceptions were dominated by heading change and yaw rate. Because of the extreme angle of the velocity vector, a bank angle change of approximately 30 degrees resulted in heading changes of about 90 degrees and rolls became essentially heading changes.

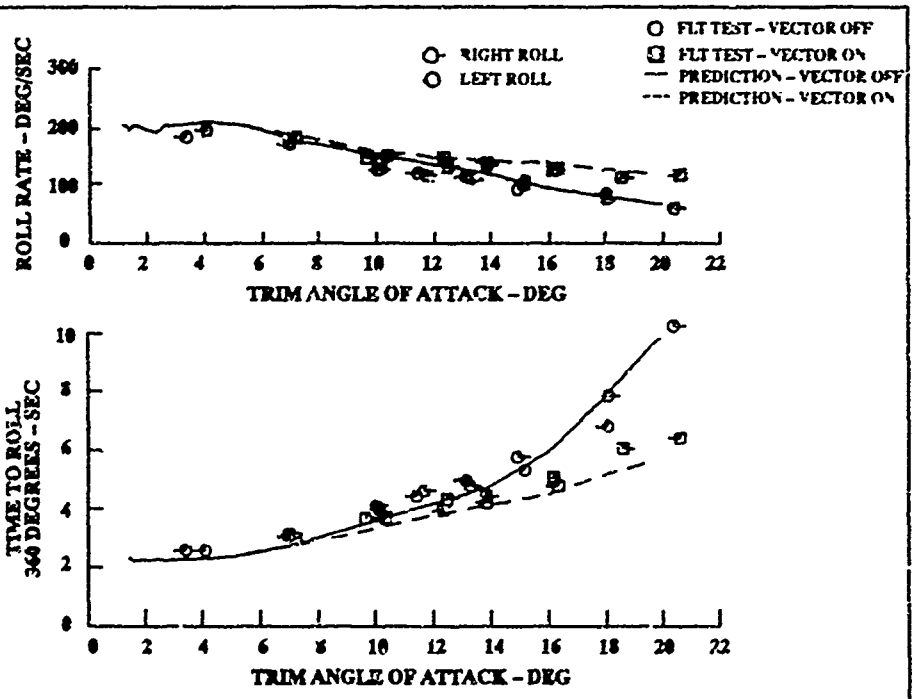

Figure 10. Roll Performance Improvements Due to Thrust Vectoring

In addition to the high angle of attack demonstrations, flying qualities maneuvers were flown to validate the benefits of thrust vectoring at lower angles of attack. One-g rolls up to 20 degrees angle of attack were performed with vectoring both on and off. As shown in Figure 10, peak roll rate was nearly doubled and correspondingly, the time to roll 360 degrees was reduced by half at 20 degrees angle of attack with thrust vectoring on.

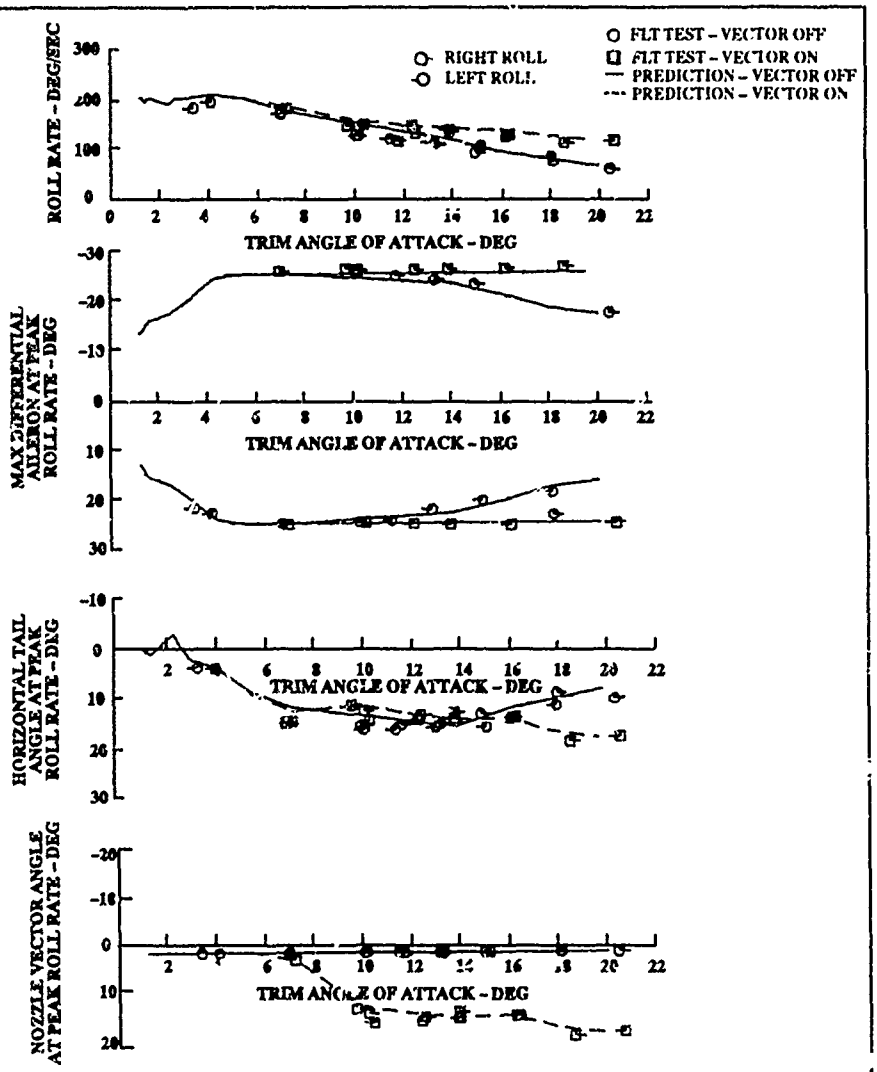

Figure 11. Effects of Thrust Vectoring on Control Surface Positions During Rolls

Figure 11 shows an example of the effect of thrust vectoring on roll rate limiting due to kinematic pitch coupling. As angle of attack increased above five degrees, the aircraft's roll rate began to decrease in a near linear manner. With thrust vectoring off, the flight control system began to limit aileron authority at approximately 9 degrees angle of attack in order to reduce roll rate and correspondingly reduce the kinematic coupling. At 14 degrees angle of attack, the horizontal tail had essentially reached its limit capability to control pitch coupling and maintain the trim angle of attack. Therefore roll rate was rapidly reduced by the flight control computers as angle of attack increased further so that the capabilities

of the horizontal tails to control pitch divergence were not exceeded.

The dashed lines and squares show the control positions with thrust vectoring on. With thrust vectoring active the aircraft's pitch control power was substantially increase and the tails were freed for roll control and for control of kinematic pitch coupling. The increased ability to control pitch divergence permitted the maximum roll surface deflections resulting in significantly increased roll rates when compared with the thrust vector off case.

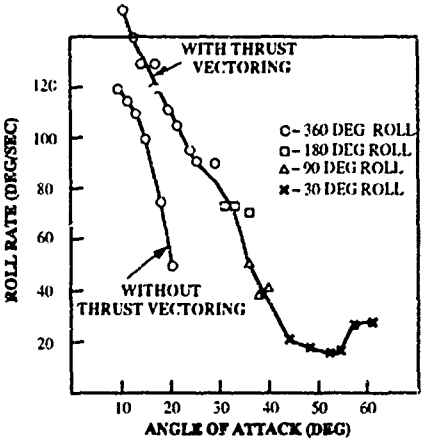

Figure 12. YF-22 Roll Rate vs. Angle of Attack

Figure 12 shows the roll rate advantage afforded by thrust vectoring over a range of angles of attack.[7] As stated previously, thrust vectoring provided much of the pitching moment authority. This freed the horizontal tails for roll and yaw rate control thus more than doubling the allowable roll rate at moderate angles of attack and allowing roll rates of 20 to 30 degrees per second above 40 degrees angle of attack.

Handling Qualities During Tracking (HQDT) tests were also conducted to evaluate thrust vectoring effects on the closed loop tracking task. At elevated load factor, where thrust vectoring became active (above 12 degrees angle of attack) the pilots preferred the tracking performance over lower angle of attack conditions where thrust vectoring was not active. As in the high angle of attack tests, the pitch response was faster and pitch attitude capture notably more precise with thrust vectoring on. The pilots characterized the handling qualities with thrust vectoring on as superb.[8]

Supersonic turn performance was also found to be improved with thrust vectoring. Pilots commented that at 1.5 Mach number the YF-22 turns were as crisp and responsive as an F-16 at 0.8 Mach number.[3] At 1.2 Mach number, 38,000 feet (11,580 m) pressure altitude, and MAX power, thrust vectoring increased the sustained turn performance, in terms of specific excess power by about 100 feet per second.[8] The improved supersonic sustained turn and roll performance was again due to the increased pitch authority made possible by thrust vectoring. Thrust vectoring reduced the horizontal tail pitch deflection required to trim and thereby reduced the supersonic trim drag and/or made more differential tail deflection available for rolling.

A comparison of roll rates between the YF-22, the F-15 and F-16 are included in Figure 13.[9] Below 5 degrees angle of attack, all three aircraft were equivalent at about 200 degrees per second. However, above 5 degrees angle of attack, the effects of thrust vectoring became evident and the YF-22 displayed an increasing roll rate advantage over the F-15. At 20 degrees angle of attack the YF-22's roll rate was more than double that of the F-15. Above approximately 25 degrees angle of attack, the YF-22 surpassed the F-16 (a design goal[4]). Both the F-15 and F-16 lost roll rate capability rapidly as 30 degrees angle of attack was approached but the YF-22 was still capable of producing roll rates of approximately 90 degrees per second.

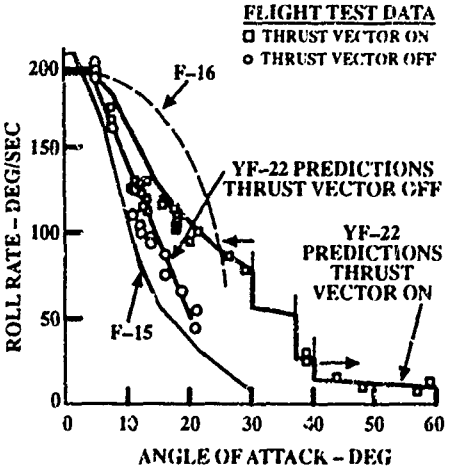

Figure 13. Roll Rate Comparison

Figure 14. shows a comparison of pitch rate between the YF-22 and the F-16 at a low speed high angle of attack flight condition.[9] The pitch authority provided by thrust

vectoring enabled the YF–22 to generate pitch rates almost five times higher than the F–16.

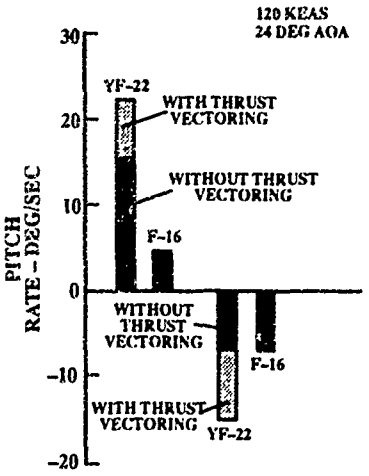

Figure 14. YF–22 Pitch Rate Comparison with the F–16 at Low Speed

4.7 Thrust Vectoring Influence Corner Speed

The capability to perform rapid and precise nose pointing at angles of attack above C_{Lmax} made the concept of "corner speed" for the YF–22 somewhat nebulas. Corner speed has been generally defined as the lowest airspeed at which maximum load factor can be attained. For aircraft restricted to maneuver at or below C_{Lmax} the maximum turn rate and minimum turn radius were achieved at this speed and the aircraft "got around the corner the fastest." Below this speed, the aircraft stalled (whatever the definition of stall is for that aircraft) and/or exceeded C_{Lmax} thus reducing lift and therefore load factor which in turn decreased turn rate and increased turn radius. Conceptually, one wanted to enter an air to air engagement near the corner speed and if possible remain near that speed during the engagement since the turn performance was near its maximum at this speed. Hopefully, your corner speed was lower than your adversary's thereby giving you an advantage in turn rate and turn radius and allowing you to turn inside your adversary and bring the aircraft's velocity vector into a position suitable for a gun or missile attack.

In the case of the YF–22 and other aircraft capable of post–stall maneuvering, minimum turn rate and radius did not necessarily occur at "corner speed." As previously stated small bank angle changes at high angle of attack produced a large change in heading. Therefore, high angle of attack maneuvering produced large changes in attitude, heading, and turn radius at speeds well below the traditionally defined "corner speed" and well below the aircraft's maximum structural load factor. The X–31 recently performed a heading change maneuver at approximately 70 degrees angle of attack that resulted in a 180 degree heading change and a turn radius of about 475 feet. The effective turn rate was 80.6 degrees per second.[10]

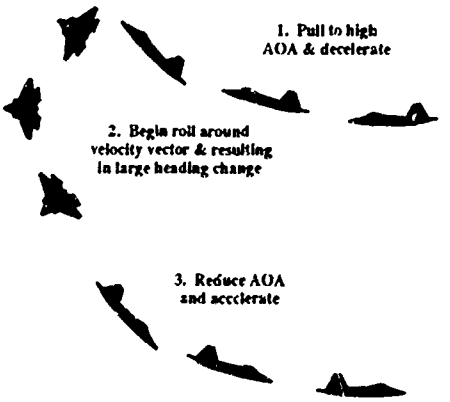

Figure 15. High Angle of Attack Heading Reversal Maneuver

The YF–22's ability to maneuver and precisely point the nose at angles of attack well above C_{max} enhanced its weapons employment opportunities. The high pitch rate capability of the aircraft made possible by thrust vectoring enabled the the aircraft to be rapidly pulled to a high angle of attack (position nose to aquire target), precisely halted at the desired angle of attack and maintained at that angle of attack for as long as desired (point nose, lock–on, and shoot), and quickly pushed down to a lower angle of attack (recover and reposition).

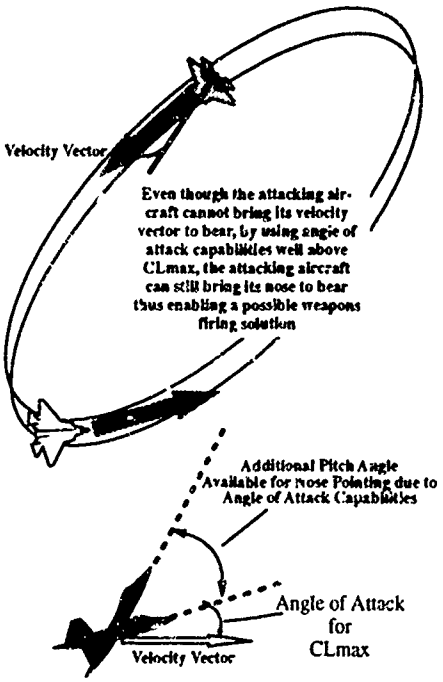

Figure 16. Nose Pointing Ability for Weapons Employment

5. CONCLUSIONS

The YF-22 demonstrated that a highly reliable thrust vectoring system, could provide unprecedented maneuver capability while maintaining the vehicle's low observable signature and could be successfully implemented in the F-22 production fighter design. Tradeoff studies showed that thrust vectoring was the most efficient and effective method of achieving the desired pitching moments without the drag and weight penalties associated with aerodynamic control.

Both the Pratt & Whitney YF119 and General Electric YF120 were proven capable of two dimensional thrust vectoring at all power settings from idle to maximum augmentation. No engine or nozzle vectoring operation problems were observed up to the maximum angle of attack demonstrated.

Thrust vectoring approximately doubled the effective pitching moment available when compared to aerodynamic controls only. The aircraft was able to maneuver and achieve desired nose positions at angles of attack well above the angle of attack for C_{Lmax}. The aircraft demonstrated trimmed flight at 60 degrees angle of attack at 82 KCAS (152 km/hr) and showed that it was controllable when performing full stick rolling maneuvers. The pitch authority provided by thrust vectoring enabled the YF-22 to generate pitch rates almost five times higher than the F-16 at the same low speed condition.

Thrust vectoring allowed substantial improvements in roll performance at high angles of attack over current fighters. The YF-22 displayed an increasing roll rate advantage over the F-15 as angle of attack increased and at 20 degrees angle of attack the YF-22's roll rate was more than double that of the F-15. Above approximately 25 degrees angle of attack, the YF-22 surpassed the F-16. Both the F-15 and F-16 lost roll rate capability rapidly as 30 degrees angle of attack was approached while the YF-22 was still capable of producing roll rates of approximately 90 degrees per second.

Thrust vectoring also contributed to enhanced handling qualities. The pilots characterized the handling qualities with thrust vectoring on as superb. Pitch attitude and angle of attack could be held to within 1/2 degree with thrust vectoring on up to 60 degrees angle of attack. During tracking tests, the pitch response was faster and pitch attitude capture notably more precise with thrust vectoring on.

Supersonic turn performance was also found to be improved with thrust vectoring. At 1.2 Mach number, 38,000 feet pressure altitude, and MAX power, thrust vectoring increased the sustained turn performance, in terms of specific excess power by about 100 feet per second.

Thrust vectoring showed impressive improvements in maneuverability and handling qualities. However, evaluation and development of tactically useful maneuvers that take advantage of the capabilities of a thrust vectored fighter have, to date, been relatively limited. The X-31 research aircraft has demonstrated maneuvering flight at 70 degrees angle of attack and has recently begun exploration of tactically useful high angle of attack, post-stall maneuvers. The F-16 VISTA aircraft is soon scheduled to begin work in this area as well. Future development efforts to enable aircraft weapon fire control systems to effectively operate during high angle of attack maneuvering and to provide useful maneuvering displays must also be undertaken if full advantage is to be taken of the post-stall capabilities made possible by thrust vectoring and demonstrated by the YF-22.

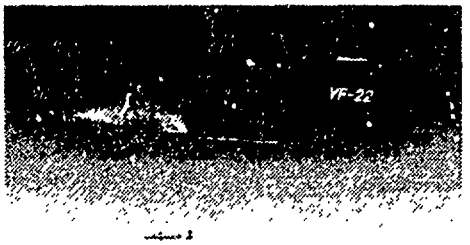

6. REFERENCES

1. Glasgow, Edsel R., Chief Engineer of Flight Sciences, Lockheed Advanced Development Company, "Supermaneuver and the F-22," Lockheed Horizons, Issue 33, January 1993.

2. Loh, General John M., Lockheed Horizons, Issue 31, August 1992.

3. Beesley, Jon S., "Report from the Future," Code One magazine, Vol 6, No 2, July 1992.

4. Clark, C. K. and Bernens, M. R., "High Angle of Attack Flight Characteristics of the YF-22," AIAA paper 91-3193

5. Abrams, Richard, Director of Flight Test, Lockheed Advanced Development Company, "YF-22 Flight Demonstration Program," Briefing to ATF Executive Committee, May 24, 1990.

6. Bernens, M. R., et al, "Test Information Sheet GP56-10FQ-040," Nov 7, 1990

7. Abrams, Richard, "YF 22 Prototype Advanced Tactical Fighter Demonstration/Validation Flight Test Program Overview"

8. "YF 22 Final Flight Test Report - Demonstration/Validation," Lockheed Aeronautical Systems Company, December, 1990.

9. Sherman N. Mullin, President, Lockheed Advanced Development Company, "T Evolution of the F-22 Advanced Tactical Fighter", 92 Wright Brothers Lecture American Institute of Aeronautics and Astronautics Aircraft Design Systems Meeting, August 24, 1992

10. Rockwell News, Volume 21, No. 9, May 21, 1993

11. Tanaka, A. Y., et al, "F/TF-15A Flying Qualities Air Force Development Test and Evaluation," AFFTC TR-76-48, July 1977.

RESULTS FROM THE STOL & MANEUVER TECHNOLOGY DEMONSTRATION PROGRAM

by

David J. Moorhouse
Wright Laboratory
Wright-Patterson AFB
2645 5th Street
Ohio 45433-7922
United States

INTRODUCTION

The STOL and Maneuver Technology Demonstration (S/MTD) program was initiated in the early 1980's with the last flight in late 1991. An F-15B aircraft was modified to incorporate four advanced technologies intended to provide current and future fighter aircraft with a Short Takeoff and Landing (STOL) capability and to increase performance over the baseline aircraft in up-and-away flight. The four technologies were:

Two-dimensional thrust vectoring/thrust reversing exhaust nozzles

Integrated Flight/Propulsion Control (IFPC)

Rough field STOL landing gear

Advanced Pilot Vehicle Interface (PVI)

The first two seat F-15B aircraft was extensively modified to the S/MTD configuration. External appearance was changed by the addition of two all-moving canards on the intakes and by modification of the aft fuselage to accommodate the rectangular shape of the 2D TV/TR nozzles. The aircraft was also equipped with a flight test noseboom for a majority of the test missions. Figure 1 illustrates the principle modifications to the baseline F-15B. A brief description of the S/MTD configuration follows, more detail is available in References 1 & 2.

The baseline Pratt and Whitney F100-PW-220 engine turbo-machinery was unchanged, supported by appropriate requirements on the nozzle design. The compressor case was modified by incorporating a transition duct which provided for transition from the circular (axisymmetric) shape to the rectangular 2D shape of the nozzles and to accommodate the increased vertical loads introduced by nozzle vectoring. The 2D nozzles incorporated hydraulically controlled convergent and divergent flaps to control nozzle throat and exit areas. The nozzle divergent flaps were also designed to vector 20 degrees up or down (i.e. pitch vectoring) with the design requirement of a "primary flight control element". Thrust reversing capability was activated by closing the convergent flaps and directing the exhaust flow through rotating vanes on the upper and lower surfaces of the nozzles. Operation of the nozzles is depicted in Figure 2 (see also Reference 3).

The original F-15 hydromechanical flight control system and analog electronic Control Augmentation System (CAS) were replaced with a four channel digital fly-by-wire Integrated Flight/Propulsion Control (IFPC) system. The IFPC system integrates aerodynamic surfaces, the engine nozzles, brakes and steering as control effectors to provide stability and controllability throughout the flight envelope. The production F-15 mechanical throttle linkage was replaced by a "power-by-wire" electronic throttle control system that utilizes electro-mechanical throttle servos to control engine power. The IFPC system redundancy management ensured overall two-fail-operate capability with no backup system, although the nozzles were fail-operate, fail-safe.

All pilot commands were integrated into natural stick, pedal and throttle actions. The S/MTD crew station displays were extensively modified by incorporating F-15E cockpit hardware. With the change to a digital control system without backup, status of the IFPC system was a primary function of the PVI. Caution lights were added with a Master Caution for critical failures. A Multi-Purpose Display was programmed to provide a complete channel-by-channel status of the system. The combination of caution lights and status display allowed the pilot to diagnose all significant failures.

Also designed into the system was the capability for Autonomous Landing Guidance to achieve the required landing performance at night or in weather without any ground-based landing aids. The APG-70 radar provided navigation capability through a radar map on a head-down display. This enabled the pilot to

Presented at an AGARD Meeting on 'Technologies for Highly Manoeuvrable Aircraft', October 1993

designate and line up with the touchdown point on the available runway. On-board software provided the elevation and azimuth steering on the Head-Up-Display. The symbology included an outline of the operating strip. Additional situational awareness was provided by projecting an InfraRed image on the HUD, supplied by a LANTIRN Navigation pod (Reference 4).

The S/MTD nose and main gear struts were internally modified to obtain optimum load/stroke characteristics for high sink rate landings and operation on repaired runways. The braking system incorporated a digital anti-skid controller for individual tire hydroplaning protection. The pilot could also pre-select an Autobrake feature, so that maximum braking with anti-skid protection was available immediately after touchdown.

This paper summarizes the configuration development, emphasizing the integration of propulsive control. Relevant flight test results are presented, with particular emphasis on the measured effectiveness of pitch vectoring and reversing. Lastly, the potential capability of future configurations is discussed.

CONTROL SYSTEM DEVELOPMENT

Although some aspects of the S/MTD development were constrained by modifying an existing aircraft, the Integrated Flight/Propulsion Control (IFPC) system was an all-new implementation between the existing cockpit controls and the control surfaces. The existing mechanical control system with analogue Command Augmentation System was replaced with a quadruplex digital fly-by-wire system. Electrical signals from Linear Variable Differential Tranducers (LVDT's) representing stick and pedal deflections were summed with appropriate sensor inputs in the Flight Controller. Control commands were sent either to new direct-drive-valve actuators for the aerodynamic surfaces or to the Nozzle Controller for vectoring and reversing commands. The Nozzle Controller integrated the commands with nozzle exit area requests from the Digital Electronic Engine Control (which was given priority in case of conflict) to position either the convergent and divergent flap positions or the reverser vane angle.

Figure 3 presents the complement of control effectors that were available on this configuration. All of these effects, including direct lift and sideforce, were fully integrated into conventional pilot cockpit controls. The design was accomplished using a combination of classical and multivariable techniques (see Reference 5). These control capabilities provided the ability to meet a stringent set of design requirements. The IFPC system was designed in specific discrete modes for demonstration purposes. The final complement of control modes is listed in Figure 4. Note that a required "SVOL" mode was implemented as three separate modes in the final design. The final content of the CRUISE and COMBAT modes is also presented.

Canard Implementation

Figure 5 summarizes how the canards were used in the control laws, i.e. scheduled with angle of attack and also used for control in various axes. The pitch control power of the canards afforded a convenient way to restore subsonic static stability. Canard deflection was scheduled as a linear function of angle of attack, with a difference between modes. The slope was the same, yielding the same level of static stability in both modes, but the intercepts were chosen to give minimum drag at 1g in the CRUISE mode and at higher load factors in the COMBAT mode. At supersonic speeds the canard schedule satisfied more than one design requirement. Of course, the configuration suffered excess stability so the canards were scheduled to reduce stability over a range corresponding to approximately 1-5g in all control modes. In addition, hinge moments were kept within limits and sufficient differential capability was retained to provide yaw control. The schedule at higher angles of attack was stabilizing to support an overall design philosophy of always having a stable pitching moment break. Tailoring static stability in this fashion also had an indirect benefit. Multivariable control theory (i.e. Honeywell's Linear Quadratic Gaussian with Loop Transfer Recovery) was used in the design process, Reference 5. An unstable configuration requires special treatment in this design process, but it was very convenient and straight forward to design to the stable configuration with canards on their angle-of-attack schedule.

In the 'enhanced' control modes (i.e. other than CONVENTIONAL) the canards were also used as short-term pitch control effectors. They deflected as a function of pilot-stick input, but then "washed out" and returned to the AoA schedule leaving the stabilator as the long term trim control. Differential canard deflection was used as a control effector in different ways. In the flaps-up modes, differential canards were used to augment the yaw control power of the rudders including dynamic stability augmentation. In the flaps-down modes, differential canard deflection was coordinated with rudder deflection to provide direct side force for crosswind landing. This was commanded by the rudder pedals on approach and by lateral stick into the wind after touchdown.

Vectoring Implementation

In simple terms, pitch vectoring was integrated into the enhanced modes not just added as an incremental control effector. Thus, Figure 6 represents the difference between two modes designed to meet requirements on flying qualities, gain and phase margin, etc. - it is the realistic increment in pitching moment capability. It shows the ability to pitch up for a 'snap shot' with maybe a half second advantage even at power for level

flight, not full capability. Equally important in combat is the reduction in time required to pitch back down again in order to regain energy. Another benefit of vectoring comes in maximum performance takeoffs. Fighters at heavy weights are frequently limited by the pitching moment required to rotate to takeoff attitude. With pitch vectoring at maximum thrust, aircraft rotation is available at the optimum speed for takeoff.

The nozzle vector angle was also on an angle-of-attack schedule to minimize drag in both CRUISE and COMBAT modes at supersonic speeds. This schedule relieved the stabilator required for trim at the high levels of static stability. Examples of the drag polars which result from the combined canard and vector schedules are given in Figure 7. Subsonically there is a zero-lift drag penalty but the benefits at higher lift coefficients are apparent. An optimum blend of the two modes would obviously be used in a production application. Drag benefits at all lift coefficients were realized at supersonic conditions.

The basic increments due to differential vectoring were small. For comparison, 20° of differential vectoring gave a rolling moment coefficient equivalent to approximately 3° of differential aileron deflection. More significant, however, the differential vectoring effect was independent of angle of attack (Figure 8). There were also sideforce and yawing moments consistent with the up-vector generating a positive pressure on the inside of the vertical tail.

Reverser Implementation

In the CRUISE and COMBAT modes, vane control to provide in-flight thrust reversing was integrated into normal throttle action, Figure 9. Pulling the throttles slowly back from maximum afterburner to intermediate (full dry power) to idle produced absolutely conventional response with the engine spooling down to the flight idle speed. Movement aft of the idle detent deployed the vanes to 45° and then to 135° with continued movement. When the vanes are at 135°, further aft movement of the throttles spooled the engine up to 100% RPM at the maximum reverse thrust point. For rapid movement of the throttle, the engine would not spool down. The pilot could therefore snatch the throttle back to command maximum reverse thrust as desired, up to the software limits. A maximum reverser command of 2g "eyeballs out" was implemented where this capability was available, and at high speeds forward deflection of the vanes was limited to avoid exceeding vertical tail bending moments.

Thrust reversing as implemented in the SLAND control mode was the key to the short landing capability, predicated on making the approach with the engine at 100% RPM and exhausting through the reverser vanes at a trim angle of approximately 60°. At touchdown the vanes were commanded forward so that thrust reversing was available with virtually no time delay. Also contributing to the landing capability was minimum touchdown dispersion achievable with this mode (see also Reference 7). The characteristics of the reverser vanes gave high-bandwidth control of the speed axis, and the control laws were designed to decouple the speed axis from the pitch axis. To achieve this the control effectors were ganged into a "moment" effector and a "thrust" effector. The thrust effector was composed of the top and bottom rotating vanes coordinated to produce zero pitching moment. Body angle was added to the thrust command to compensate for rotation of the gravity vector as the aircraft pitched. The result to the pilot was that throttle position commanded airspeed which was held constant by the airspeed feedback, and stick commanded pitch rate which was effectively flight path angle rate command because of the speed hold. This control strategy, including the differential canard implementation discussed previously, was validated by piloted simulation as facilitating landings within a "touchdown box" 60 ft long by 20 ft wide under all required conditions of wind, wind shear and turbulence.

FLIGHT TEST RESULTS

The flight testing was initiated with standard nozzles to verify functionality of the new control system (conventional modes) and the subsystems.

Envelope expansion testing proceeded routinely to the low altitude high speed flight regime. At 10K/0.8M flight conditions, the first disagreement between predicted aircraft pitch response and flight test data was noted. At 10K/0.9M, the pilot reported very low damping in both the longitudinal and directional axes. Software changes were made to account for differences in stabilator control power and pitch stability coefficients discovered during parameter identification analysis. Figure 10 shows that the transonic shift in neutral point occured at a lower Mach number than was predicted. Even though the S/MTD data base was incremented from the flight-validated F-15 model, this illustrates a typical problem of transonic wind tunnel testing. An additional problem manifested during the low altitude high speed envelope expansion phase was a reduction in longitudinal stick-free damping. The problem was caused by the mass of the stick coupling with aircraft motion and solved by installing a longitudinal stick eddy current damper. The damper increased the stick-free damping ratio from 0.03 to a value of approximately 0.6.

Reduced directional damping at low altitude high speed was traced to the presence of an additional 25 msec time lag in the yaw rate feedback loop of the flight controller, caused by an inadvertent data hold in the 40 hz control law computation. Gain changes to the

lateral acceleration feedback loop were incorporated into the control laws to produce adequate directional damping to permit continued low altitude envelope expansion. Once these changes to the flight control system were incorporated, envelope expansion continued to the end condition, 5K/0.95M, with satisfactory handling qualities in all axes.

During this initial phase of testing, an ALG backup mode using stored INS runway position information was successfully demonstrated to evaluate landing configuration flying qualities. By storing the runway position at a safe altitude, such as 10K feet, simulated landing approaches to a "runway in the sky" could be performed which afforded the pilot an opportunity to assess handling qualities prior to making an actual landing approach. This test was used with success on first flight of the aircraft. The technique does have to be combined with other testing that is designed to increase pilot gain even higher to provide a complete assessment.

First flight with the 2D engines was successfully flown on 10 May 1989. Initial testing focused on expanding the subsonic enhanced mode envelope for up and away flight (CRUISE and COMBAT modes). Handling Qualities During Tracking (HQDT) tests were accomplished using a 3g cooperative target with excellent results. CONVENTIONAL and COMBAT mode pilot ratings are all Level 1 for tracking, while the CRUISE mode (designed for flight path control) is actually better than the expected Level 2 ratings; see Reference 2 for further discussion of pilot comments and preferences. More important from a designers viewpoint, pilot comments in support of the small differences shown were exactly the same as in the ground-based piloted simulations.

Thrust reversing was functionally verified first in taxi tests building up in speed and the amount of reverse commanded. In-flight reverser operability was verified by reversing on one engine initially at Mach 0.8 at 30,000 and 40,000 ft. After that initial verification, reversing was commanded on both engines. The reversing envelope was expanded to M1.6, with parameter identification maneuvers and data analysis at M0.9 and 1.2. Figure 11 shows the deceleration capability of the S/MTD configuration compared with a production F-15 chase plane with speed brake deployed and flight idle thrust setting. It is also worth noting that this does not represent the maximum reverse thrust of the S/MTD nozzles. The forward vane angle (reverse thrust) had to be software limited at supersonic speeds to maintain vertical tail bending moments within strength limits. More reverse thrust could be available by strengthening the vertical tails, or by avoiding the interference in the design of a new configuration.

Thrust reversing was also the major factor in achieving the short landing distance. The final approach was made with the engine at 100% RPM, the nozzle exhaust closed and the efflux controlled by the reverser vane deflection. Nozzle design requirements specified that the vanes be able to go from the nominal approach position to full reverse in less than 1 second. At touchdown, the pilot could select reverse thrust which commanded the top vanes to their full forward deflection and the lower vanes to an angle determined by two schedules. An angle-of-attack schedule ensured rotation to a three-point attitude (Reference 1) and an airspeed schedule prevented hot gas reingestion. In addition, the pilot could select an Autobrake function which gave maximum anti-skid braking after touchdown. Measured landing distance of approx 1500 ft is half the dry runway capability of an F-15, and the wet runway landing distance is less than 1/3 of the F-15 value.

The flight testing also produced one particularly unpleasant surprise. Reference 1 documents the ground-effects testing and the design of control laws to mitigate an uncontrollable nose-up pitching moment with maximum forward reverser vane deflections at the touchdown speed and pitch attitude. A delay was incorporated to inhibit forward deflection of the lower vanes until one second after the weight-on-wheels indication was set in the control laws. Lower vane deflection was also scheduled with angle of attack so that it did not reach full forward until the aircraft was essentially in a three-point attitude. Lastly, a command was also introduced to give a 6 deg/sec nose-down rotation rate with no pilot input and the predicted aerodynamics. The actual landings in the SLAND mode produced nose-down rotations of approximately 18 deg/sec. Those high rates came close to bottoming the nose landing gear and were obviously unacceptable to the pilots. Analysis indicated that ground effects were the cause, not any control inputs. The obvious, and simplest, control law change was to remove the one second delay on the vane movement after touchdown. It was reasoned (i.e. hoped) that the predicted nose-up moment from the vane movement would balance the unpredicted nose-down moments that were experienced. This change was completely successful and allowed completion of the flight test program (see Reference 8 for more details).

The capability of thrust vectoring to enhance takeoff rotation was demonstrated. It was possible to maintain a precise two-point attitude at steady taxi speeds as low as 40kts. Figure 12 shows the takeoff distances that could be achieved using different rotation speeds - rotating too soon incured a loss of acceleration due to the additional drag and yielded longer distances. Also indicated in the data is the effect of rotating too quickly. The aircraft would lift off but then settle back down on to the runway. The optimum takeoff distance was approximately 25% less than a production F-15 at similar conditions. The benefits of vectoring have also been quantified up and away at low speeds. Envelope expansion was done

to 30° angle of attack. Pitch captures and nose-down recovery maneuvers from 30° AoA were flown back-to-back in CONVENTIONAL and COMBAT modes to evaluate the effectiveness of thrust vectoring. Figure 6 shows good agreement of pitching moment coefficients extracted from flight data with the predicted values. Figure 13 illustrates the additional pitch rate capability available in a recovery from high angle of attack, and also the quicker onset. The figure also shows that the control laws were not optimized for maximum effectiveness - the responses converged to the same steady state pitch rate. The S/MTD program was initiated as a full-envelope demonstration without any high-angle-of-attack emphasis. A simple linear gradient of pitch rate command vs deflection was used, and would obviously be changed in application.

A demonstration of the Autonomous Landing Guidance capability was accomplished in a night landing made at Edwards AFB without using ground-based guidance, runway lights or aircraft landing lights. Starting 30nm out the pilot designated a chosen touchdown point and rollout heading using the APG-70 radar map. The on-board software then provided steering commands via the Head-Up Display (HUD) and the Horizontal Situation Indicator. At the appropriate distance out, the pilot lowered flaps and the HUD reconfigured to the landing symbology. Both glideslope and localizer guidance were provided on the HUD, together with an outline of the Minimum Operating Strip for perspective. Nominal operating procedures would have the InfraRed (IR) image from a LANTIRN Navigation Pod also displayed on the HUD for situational awareness. For the demonstration, the IR sensor was left in the stand-by mode until a height of 200 ft to simulate breaking out of weather at that height above the runway. At an indicated 200 ft, the IR sensor was switched on and a successful short landing completed using this synthetic visual scene. Pilot comments were all favorable as far as routine use being viable.

THE FUTURE

Any prediction of the future is obviously uncertain in today's political and budgetary climates. We can, however, discuss technological advances which could continue the Wright Laboratory heritage.

Two-dimensional thrust vectoring nozzles are going into production on the F-22. Designs are also available to provide axisymmetric exhaust nozzles with the capability to vector in combinations of pitch and yaw. A General Electric design is currently flying on an F-16. The Multi-Axis Thrust Vectoring (MATV) program is investigating low-speed high-angle-of-attack control. The Advanced Control Technology for Integrated Vehicles (ACTIVE) program will fly the Pratt & Whitney vectoring nozzle design on the S/MTD aircraft in 1994 to measure full-envelope benefits, such as optimum cruise performance. It is expected that these two programs will validate full-envelope benefits for thrust vectoring nozzles as a primary flight control effector. A designer can then have confidence in the capability to trade-off the benefits of reduced tail or control size vs propulsive control in any specific design application.

CONCLUSIONS

The S/MTD program has generated flight test data to validate four specific technologies:

- 2-D thrust vectoring & reversing nozzle
- Integrated Flight/Propulsion Control
- Advanced Pilot/Vehicle Interface including Autonomous Landing Guidance
- Rough field/high sink rate landing gear.

These technologies have been integrated into an F-15B to provide mission benefits across the complete flight envelope from on-board guidance to a bad weather short landing, through significantly enhanced maneuvering benefits to supersonic performance. These technologies are either transitioning on to other aircraft, or can be considered viable design options for future aircraft. Lessons learned from the program are available in References 5-10.

REFERENCES

1. Moorhouse, D.J., J.A. Laughrey and R.W. Thomas, "Aerodynamic and Propulsive Control Development of the STOL and Maneuver Technology Demonstrator", AGARD CP 465, October 1989.

2. Moorhouse, D.J., et.al., "Handling Qualities of the STOL & Maneuver Technology Demonstrator from Specification to Flight Test", AGARD CP 508, October 1990.

3. Bursey, R., and R. Dickinson, "Flight Test Results of the F-15 S/MTD Thrust Vectoring/thrust Reversing Exhaust Nozzle", AIAA Paper 90-1906, July 1990.

4 Moorhouse, D.J., "Design and Flight Test of On-Board Guidance for Precision Landing", AIAA Paper 91-2644, August 1991.

5. Moorhouse, D.J., and R.L. Kisslinger, "Lessons Learned in the Development of a Multivariable Control System", Proceedings of NAECON 89, Dayton, OH., May 1989.

6. Leggett, D.B., D.J. Moorhouse and J.K. Zah, "Simulating Turbulence and Gusts for Flying Qualities Evaluation", AIAA Paper 90-2845, August 1990.

7. Moorhouse, D.J., "Lessons Learned from the S/MTD Program for the Flying Qualities Specification", AIAA Paper 90-2849, August 1990.

8. Moorhouse, D.J., J.G. Reinsberg and F.J. Shirk, "Study of Jet Effect & Ground Effect Interference on a STOL Fighter", AGARD Symposium on Computational & Experimental Assessment of Jets in Cross Flow, April 1993.

9. Clough, B.T., "Integrated Flight Control - Lessons Learned", AIAA Paper 90-3301, September 1990.

10. Kisslinger, R.L., and D.J. Moorhouse, "Lessons Learned in Control System Integration & Management from the S/MTD Program", SAE Paper 901849, SAE Aerotech 1990, October 1990.

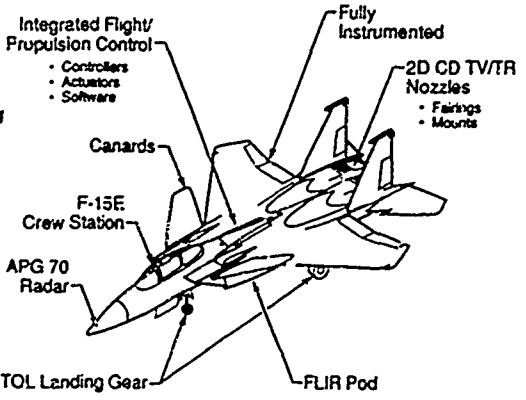

Figure 1. S/MTD Configuration

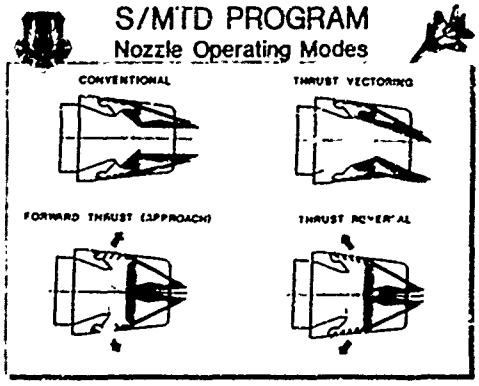

Figure 2. Nozzle Operating Modes

S/MTD PROGRAM
Control Effectors

Effector	Pitch	Roll	Yaw	X-Force	Y-Force	Z-Force
Stabilators	√	√				
Canards	√		√		√	√
Ailerons		√				√
Flaperons		√				√
Rudders			√		√	
Gross Thrust				√		
Vectoring	√	√				
Reverser Vanes	√	√	√	√		
Main Gear			√	√		
Nose Gear			√			

Figure 3. Available Control Effectors

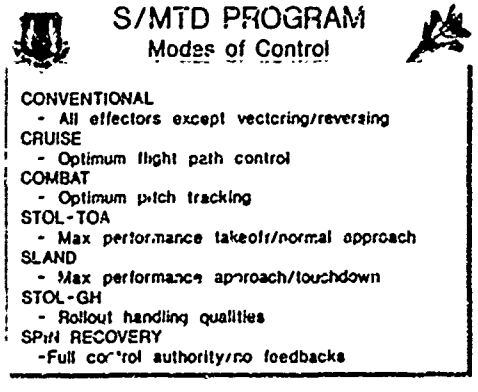

Figure 4. Flight Control Modes

S/MTD PROGRAM
Canard Usage

- Angle-of-Attack Schedule (All Modes)
  - augment longitudinal static stability
  - optimum drag
  - lateral/directional stability (high AoA)
- Control Power
  - pitch control (enhanced modes)
  - directional control (all modes)
- Direct Sideforce (Flaps Down)
  - crosswind approach (rudder pedals)
  - landing rollout (lateral stick)

Figure 5. Canard Usage

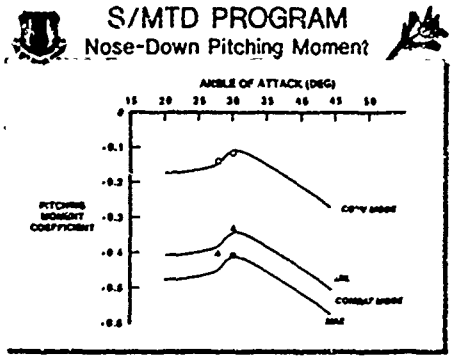

Figure 6. Pitch Vectoring Control Power

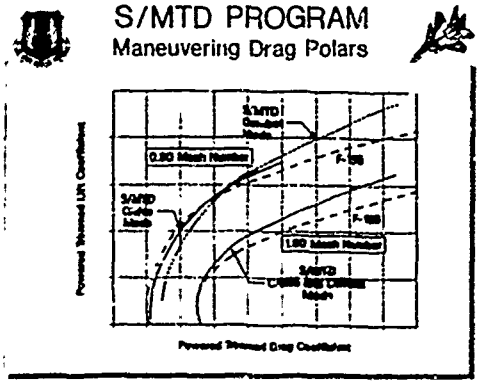

Figure 7. Maneuvering Drag Polars

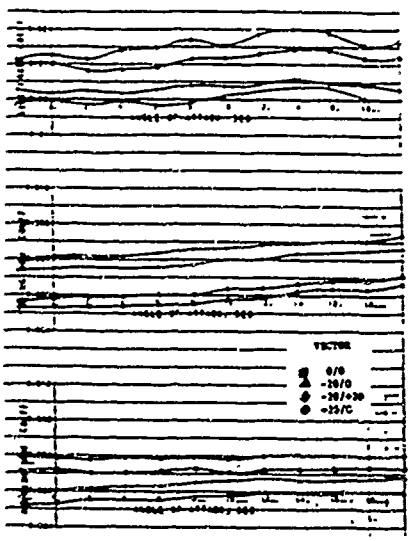

Figure 8. Differential Vectoring Effects

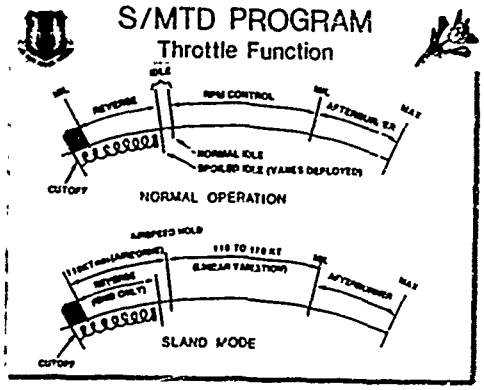

Figure 9. Throttle Geometry

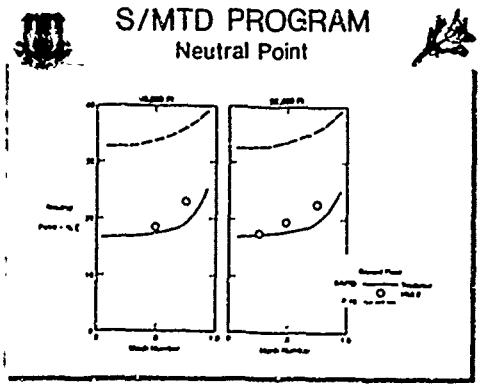

Figure 10. Neutral Point vs Mach Number

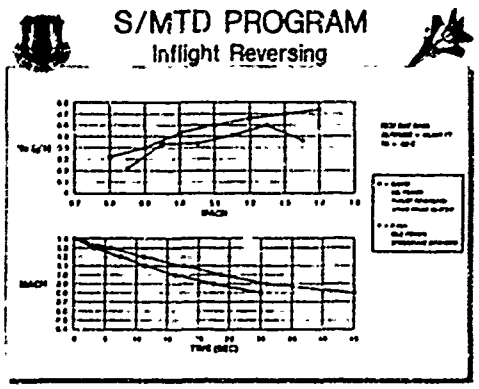

Figure 11. Inflight Reversing

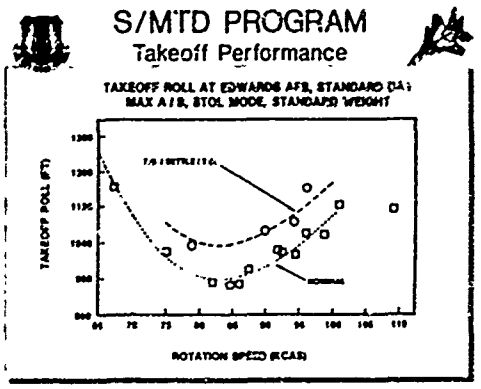

Figure 12. Takeoff with Thrust Vectoring

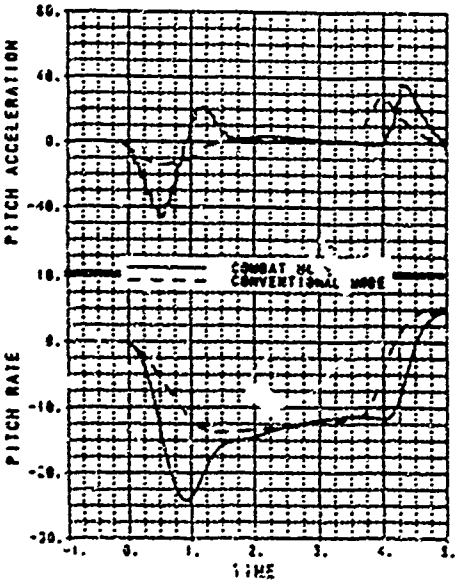

Figure 13. Pitch Response with Vectoring

ANALYSE THEORIQUE DE L'ECOULEMENT AUTOUR D'UN *RAFALE A* A GRANDE INCIDENCE

HIGH INCIDENCE FLOW ANALYSIS OVER THE *RAFALE A*

Jean-Denis MARION
DASSAULT AVIATION
DGT / DEA
78, Quai M. Dassault
92214 Saint-Cloud
FRANCE

ABSTRACT

A good high angle of attack (AoA) behaviour is a requisite for any new combat aircraft. In order to gain a better knowledge of the flow at high AoA computation over the "*RAFALE A*" has been conducted.

The aircraft is in a full nose down controls configuration : low speed, low altitude, high AoA and large control surfaces deflection. Moreover, slideslip is considered so as to assess the lateral behaviour of the aircraft in this high AoA regime.

The computational domain around the complete aircraft is discretized into an unstructured mesh and the flow is computed with a 3D inviscid (EULER) approach in finite elements.

Aerodynamical coefficients have been analyzed together with the topology of the flow in these high AoA configurations. Results have been found to yield a promising agreement concerning the flow features (loss of weathercock stability at high AoA) although absolute values of coefficients are still beyond reach of this basic methodology.

In a view to get insight into non symmetric flow as it can be found experimentally at high AoA, a modification of the boundary conditions which create a source of vorticity has been implemented. This leads to the existence of large amplitude side forces agreeing with experiments.

RESUME.

L'étude porte sur le *RAFALE A* à grande incidence en configuration de défense à piquer. Des calculs non visqueux de type EULER 3D sur un domaine discrétisé en éléments finis non structurés ont permis d'analyser le comportement à la fois des coefficients aérodynamiques et de l'écoulement tridimensionnel à haute incidence. Dans un deuxième temps, en ce qui concerne les écoulements dissymétriques de pointe avant rencontrés à très haute incidence, une modification des conditions aux limites de calcul a autorisé une dissymétrisation de l'écoulement et a créé des efforts en accord avec ceux obtenus par voie expérimentale.

LISTE DES SYMBOLES.

α	angle d'incidence.
α_{max}	angle d'incidence de portance maximale.
β	angle de dérapage.
C_p	coefficient de pression.
C_{yl}	coefficient d'effort latéral dans le repère avion.
C_{ll}	coefficient de moment de roulis dans le repère avion.
C_{nl}	coefficient de moment de lacet dans le repère avion.
C_z	coefficient de portance dans le repère aérodynamique.
C_m	coefficient de moment de tangage dans le repère aérodynamique.

1. INTRODUCTION

L'analyse du comportement d'un avion à haute incidence est complexe car entrent en jeu des phénomènes aérodynamiques à la fois encore mal identifiés et mal modélisés par les codes de calcul. En particulier, lorsque l'incidence croit, un système tourbillonnaire se développe, alimenté par les décollements prenant naissance le long de la pointe avant et des bords d'attaque en flèche [Réf. 1]. A partir d'un certain niveau d'incidence (≥50°), ces tourbillons de pointe avant subissent des déstabilisations pouvant conduire à des éclatements et à des dissymétries puis des échappements instationnaires.

La compréhension des phénomènes aérodynamiques apparaît ainsi cruciale car la dissymétrie des écoulements tourbillonnaires se traduit systématiquement sur les courbes de stabilité longitudinales et transversales de l'avion et ainsi sur sa contrôlabilité à haute incidence.

Presented at an AGARD Meeting on 'Technologies for Highly Manoeuvrable Aircraft', October 1993

L'objectif de cette étude est de montrer qu'avec les codes industriels développés chez DASSAULT AVIATION, il est désormais possible d'explorer le domaine des hautes incidences qui devient un domaine de plus en plus fréquenté par les avions de combat actuels et futurs. L'analyse, lorsque l'angle d'attaque augmente, portera principalement sur les deux aspects suivants :

* d'une part la représentativité des phénomènes aérodynamiques sur le démonstrateur ***RAFALE A*** à grande incidence,
* et d'autre part, la capacité à reproduire les asymétries notables concernant les efforts, observées expérimentalement sur une pointe avant.

2. CONFIGURATIONS ETUDIEES.

L'avion étudié dans ce domaine des hautes incidences est le ***RAFALE A*** (cf. photo 1), démonstrateur du programme d'avion de combat multimission RAFALE (1er vol le 04 juillet 1986). Les gouvernes aérodynamiques (canard, becs, et élevons) sont braquées de façon à assurer le contrôle longitudinal de l'avion à haute incidence.

Le code utilisé pour l'avion complet (cf. paragraphes 4 et 5) est un code EULER tridimensionnel, à schéma décentré implicite, appliqué sur un espace discrétisé par éléments finis tétraèdriques non structurés [Réf. 2].

La complexité de la géométrie (cf. planches 2 et 3) justifie pleinement l'utilisation de la discrétisation en éléments non structurés. La géométrie de l'avion (à part l'arrière-corps caréné) est fidèlement représentée : braquage des gouvernes, entrées d'air etc. Par contre, les jets issus des deux réacteurs ne sont pas modélisés, l'arrière-corps étant simplement caréné. Le maillage spatial est particulièrement adapté pour des calculs à haute incidence : la densité de maille restant conséquente à l'extrados de l'avion. Le maillage non structuré comporte ainsi un nombre total de noeuds supérieur à 150 000.

Pour la seconde partie de l'étude (cf. paragraphe 6), un code EULER 3D à schéma centré explicite, sur des volumes finis structurés, est utilisé sur une géométrie de pointe avant. En effet, la topologie étant essentiellement axisymétrique, un maillage structuré peut être aisément réalisé.

3. JUSTIFICATION DES OUTILS UTILISES LORS DE CETTE ETUDE.

Le code de calcul choisi pour réaliser cette étude est le code EULER tridimensionnel, développé chez DASSAULT AVIATION [Réf. 2]. Le critère de choix était l'utilisation d'un code industriel, validé et quotidiennement utilisé et de plus relativement peu coûteux par rapport à des modélisations plus fines comme un code NAVIER-STOKES avec modèle de turbulence [Réf. 1].

La justification théorique de l'utilisation de l'EULER repose sur le fait que la dynamique du tourbillon est représentable à l'aide des phénomènes relevant essentiellement du fluide parfait. Néanmoins, le processus physique de création du tourbillon per émission de rotationnel repose sur l'accumulation locale des couches limites en des lignes de glissement puis sur leur éjection. La viscosité du fluide ainsi que la turbulence ont donc un rôle fondamental dans le processus de création du tourbillon. La viscosité et la turbulence interviennent également lors de la dissipation et lors de l'éclatement éventuel du tourbillon. En négligeant les effets visqueux et turbulents, on ne pourra donc espérer modéliser précisément ni la formation des tourbillons, ni leur dissipation, ni leur éclatement.

Le calcul EULER, de plus, ne sait reproduire la formation de tourbillons secondaires issus de lignes de séparations secondaires déclenchées par le décollement des couches limites transverses induites par le tourbillon primaire.

Pour une pointe avant en incidence ou un bord d'attaque émoussé, la modélisation EULER (subsonique) ne saurait reproduire les tourbillons qui sont issus d'une ligne de glissement dont la position dépend, outre de la géométrie précise et éventuellement des irrégularités de la peau, du nombre de Reynolds. Cette dépendance du positionnement de la ligne de glissement et de l'intensité de l'émission tourbillonnaire vis à vis de la viscosité et éventuellement de la turbulence rend peu réaliste une approche fluide parfait pour ces géométries. Par contre, il apparaît que sur les bords d'attaque aigus, les gradients de pression créés par les petits rayons de courbure sont tels qu'ils positionnent correctement l'échappement tourbillonnaire en calcul EULER. Ceci est valable pour les bords d'attaque aigus de voilure et de canard.

Pour la deuxième partie de l'étude qui concernera la dissymétrisation des tourbillons de pointe avant -phénomène non encore totalement élucidé expérimentalement-, une approche EULER classique est insuffisante. Nous utiliserons alors un code EULER dans lequel on imposera des décollements en modifiant les conditions aux limites et en sollicitant la dissymétrie selon des lignes de maillage spécifiées.

Ajoutons également que le code pseudo-instationnaire employé -utilisant de plus un pas de temps local faussant la cohérence temporelle entre deux points du maillage-, force la convergence vers un état permanent qui ne saurait représenter correctement les émissions alternées pouvant être expérimentalement observées à très grande incidence (cf. simulations de [Réf. 3]).

Malgré les limitations inhérentes au code EULER, ce type de modélisation fut tout de même retenu pour sa souplesse d'utilisation et son coût relativement modeste.

4 ANALYSE DES COEFFICIENTS AERODYNAMIQUES.

Les conventions utilisées dans le cadre de cette étude sont représentées sur le schéma de la planche 4.

4.1 Configuration sans dérapage.
Un balayage en incidence fut tout d'abord étudié sans dérapage (β=0°) de façon à ne s'intéresser qu'au problème de stabilité longitudinale. Le domaine de variation recouvre le point de portance maximale :

4.1.1 *Analyse de la portance C_z.*
Pour le coefficient de portance aérodynamique C_z, La contribution des différents sous-ensembles de l'avion (voilure, fuselage, canard) a pu etre détaillée en intégrant le coefficient de pression C_p sélectivement sur chaque élément (cf. planche 5). On appellera α_{max} l'incidence de portance maximale de l'avion entier, obtenue par le calcul.
On constate alors un plafonnement de la portance de la voilure vers α_{max}-5° puis une décroissance régulière. Par contre, le fuselage augmente sa contribution jusqu'à α_{max}+5°. En ce qui concerne le canard, sa contribution augmente continûment. Du fait de son braquage initial fortement négatif, l'incidence de portance nulle n'est atteinte qu'autour de α_{max}+5°, ce qui met en évidence l'influence du champ aérodynamique de l'aile sur le canard. Notons que dans une large plage d'incidence, le canard a une contribution quasi linéaire en C_z mais qu'une saturation se décèle en extémité du domaine considéré.
La confrontation avec les résultats de soufflerie indique un accord qualitatif (cf. planche 6) satisfaisant. Les phénomènes sont reproduits bien que ni le niveau, ni l'angle d'incidence ne soient prédits avec exactitude.

4.1.2 *Analyse du moment C_m.*
Le moment de tangage C_m total croît, culmine vers α_{max} puis décroît (cf. planche 7). Le fuselage a une contribution destabilisante maximale vers cette même incidence. Le canard destabilise progressivement à mesure de sa prise d'incidence. Par contre, la voilure voit son moment de tangage devenir de plus en plus stabilisant (C_m<0).

4.2 Configuration avec dérapage.
Sur l'avion en défense à piquer, un dérapage de 5° est appliqué.

4.2.1 *Analyse de la portance C_z.*
Le dérapage fait subir à l'avion entier une légère diminution du coefficient de portance (cf. planche 8). Lorsque la contribution propre de chaque demi-avion est analysée, on constate que le demi-avion gauche (côté au vent) porte systématiquement plus que le demi avion droit (sous le vent), tandis que le demi avion de référence en dérapage nul s'intercale entre les deux niveaux précédents. Ce phénomène est cohérent avec l'effet de flèche classique d'une analyse fluide parfait qui a pour conséquence d'augmenter le gradient de portance de l'aile au vent par diminution de sa flèche apparente. Par contre, on remarque que passé α_{max}, l'aile au vent subit un accident caractéristique des avions delta : la flèche diminuant pour l'aile au vent, l'écoulement tourbillonnaire est destabilisé et le vortex d'apex éclate.

4.2.2 *Analyse de la force latérale C_{yl}.*
Le coefficient d'effort latéral exprimé dans le repère avion C_{yl} est décomposé selon ses contributions du fuselage et de la dérive (cf. planche 9). Le C_{yl} du fuselage est relativement constant. Par contre, la dérive, initialement soumise à l'effet girouette réduit son effort de rappel et l'inverse même C_{yl}<0.

4.2.3 *Analyse du lacet C_{nl}.*
Le coefficient de lacet dans le repère avion C_{nl}, est exprimé pour chaque élément constitutif (voilure, fuselage et dérive) sur la planche 10. Il fait apparaître l'effet d'inversion de stabilité de la dérive. Ceci se traduit par un coefficient C_{nl} négatif révélateur d'un couple instable.

4.2.4 *Analyse du roulis C_{ll}.*
Le coefficient de roulis C_{ll} exprimé dans le repère avion, intègre deux phénomènes précédemment mis en évidence :
* chute du rappel girouette de la dérive
* chute du différentiel du C_z voilure.
Ces deux effets (dérive et voilure) se cumulent et conduisent à une très forte diminution de la valeur du rappel en roulis (cf. planche 11).

5- ANALYSE DU CHAMP AERODYNAMIQUE.

5.1 Analyse pariétale.
Le champ des vitesses est représenté sur la peau de l'avion sous la forme de poils. Une vue latérale (cf. planche 12) présente l'effet d'incidence à dérapage nul sur la vitesse pariétale. On remarque la déflexion progressive des vecteurs vitesse avec l'incidence. A α_{max}-10°, le canard est déporteur et à α_{max}+5°, il est dans le lit du vent local.
A α_{max}+15°, on peut noter que la dérive est déventée (masque du fuselage et de la voilure).
La planche 13 présente l'extrados à α_{max}-10° et à α_{max}+5° dans le cas du dérapage. On peut y noter en particulier à l'incidence la plus élevée, la dissymétrie des demi-voilures : l'aile gauche (au vent) est déventée (éclatement du vortex) alors que l'aile droite (sous le vent) porte encore la marque du vortex.

5.2 Analyse dans le champ.
Des coupes du champ dans un plan situé à X constant au niveau du pied de dérive permettent d'analyser la raison de l'inversion de l'effet girouette à α_{max}+5° comme on avait pu le détecter à partir de l'analyse des coefficients C_y, C_{nl}et C_{ll}. Sur ces coupes, les poils de vitesse sont surimposés au champ des pressions (cf. planche 14). A α_{max}-10°, on constate une surpression

sur la face au vent de la dérive (conduisant à l'effet girouette). Les vitesses permettent de noter une prédominance du tourbillon au vent (sur la droite de la vue) par rapport à l'aile sous le vent.
Par contre, à α_{max}+5°, le champ des vitesses indique que la dérive serait alimentée de façon symétrique. De plus, la zone dépressionnaire issue de l'éclatement du tourbillon d'extrados de l'aile au vent se rapproche de la dérive et vient induire alors des pressions négatives conduisant à alors à l'inversion de l'effet de girouette.

5.3 Enseignements.
On a pu ainsi montrer, à l'aide de codes industriels relativement économiques qu'une prédiction en accord qualitatif avec l'expérience pouvait être obtenue en ce qui concerne les coefficients aérodynamiques et leur évolution en fonction de alpha pour le domaine des hautes incidences. En particulier, la perte de stabilité girouette de la dérive avec l'incidence (classique de la configuration monodérive dorsale) a pu être retrouvée par le calcul. Mais de plus, l'attrait des calculs aérodynamiques réside en l'analyse spatiale qui peut être menée en vue d'aider à la compréhension des phénomènes aérodynamiques responsables de problèmes éventuels de stabilité.

6- ETUDE DE LA DISSYMETRISATION DE LA SOLUTION.

Il a souvent été observé expérimentalement [Réf. 4] l'existence d'efforts latéraux à la fois intenses et non prédictibles sur des pointes avant coniques placées en incidence. Ceux-ci sont créés par une métastabilité du système tourbillonnaire pouvant être induite par une perturbation même minime de l'écoulement.
Une deuxième étude fut alors engagée en vue d'étudier la capacité des codes à reproduire les mécanismes d'une part d'émission tourbillonnaire sur un corps élancé et d'autre part la dissymétrisation de ce système tourbillonnaire avec l'incidence.

6.1 Déclenchement forcé des tourbillons.
Or, le code EULER, utilisé sur une pointe avant ne donne pas de tourbillons car les recompressions sont insuffisantes pour induire des décollements spontanés qui se produiraient sur les lignes de glissement.
Une procédure particulière est alors utilisée de façon à recréer artificiellemnt un décollement le long des lignes de glissement. La technique utilisée est alors la suivante. Sur la pointe avant finement maillée, un calcul EULER est réalisé. Un calcul de couche limite est ensuite conduit. Celui-ci met en évidence que les lignes de courant transitionnent par effet transversal puis décollent le long d'une ligne de glissement (cf. figure 15, où l'évolution du paramètre de forme H est représentée pour quelques lignes de courant). Le calcul EULER ne représentant pas les effets visqueux, les lignes de courant ne s'accumulent pas le long de la ligne de glissement comme on peut l'observer en réalité.
On est donc amené à introduire une modification des conditions aux limites le long de la ligne de glissement de manière à imposer un décollement le long de celle-ci à chaque itération. L'intérêt de l'utilisation du maillage structuré (I, J, K) dans cette configuration de pointe avant conique est de pouvoir aisément désigner la ligne de glissement par identification à une ligne topologique ($I=I_1$ à I_2, J_0, K_1).
La modification des conditions aux limites sur deux lignes symétriques donne effectivement naissance à deux tourbillons symétriques. On a pu remarquer que cette modification était sans effet notable à faible incidence mais qu'elle se traduisait à grande incidence par une forte émission tourbillonnaire. Cette modification des conditions aux limites s'apparente donc effectivement au phénomène physique de création de tourbillon.

6.2 Dissymétrisation des tourbillons.
Dans une deuxième étape, on a cherché à reproduire la dissymétrie observée expérimentalement sur des pointes avant à très forte incidence et à dérapage nul.
Notre calcul est ainsi rendu dissymétrique par le biais des conditions aux limites contrairement à d'autres études (cf. [Réf. 3]) qui ont joué sur une déformation géométrique pour rompre la symétrie. Ainsi, pour obtenir par le calcul une dissymetrie à β=0°, il a été nécessaire de solliciter la dissymétrie du système tourbillonnaire au niveau des deux lignes de décollement précédemment spécifiées à l'aide du calcul de couche limite. On a ensuite choisi de décaler longitudinalement une ligne par rapport à l'autre. Dans le cas présent, la ligne droite de la pointe avant est décalée de 10 cm en aval. On a pu noter une grande sensibilité des efforts latéraux vis à vis du décalage longitudinal, ce qui est cohérent avec les problèmes de répétitivité observés en soufflerie.
La planche 16 présente, dans le cas d'un calcul à 60°, les isovaleurs de l'entropie selon des coupes à X constant, vues de l'avant. Un premier tourbillon est créé par la première ligne située à gauche (n°1 à droite de la coupe). Ce tourbillon est ensuite éjectée. Un deuxième tourbillon est émis par la ligne droite (n°2 à gauche de la coupe). Celui-ci est beaucoup plus intense car les gradients de pression sont plus forts que lors de la création du tourbillon n°1. En aval, un troisième tourbillon (n° 3) est réémis par la première ligne. Cette dissymétrie de l'écoulement (cf. planche 16) se traduit par des efforts latéraux considérables dont l'amplitude est constatée être du même ordre de grandeur que celle qui a pu être observée expérimentalement à très haute incidence (≥50°).

7- CONCLUSION.

D'un point de vue général, l'ensemble des phénomènes et des tendances relevés en soufflerie ont bien été retrouvés. Sans donner des résultats quantitatifs

suffisamment fiables, le calcul permet une analyse détaillée (intégrations partielles, coupes dans le champ, etc.) et constitue déjà un complément essentiel aux essais en soufflerie pour l'identification de l'écoulement autour d'un avion à grande incidence.
Cette étude a montré que l'utilisation d'un code EULER -bien que limité par essence- sur une configuration d'avion à grande incidence peut donner des résultats facilement exploitables et dont la qualité autorise l'analyse de la nature de l'écoulement. En prenant exemple de l'avion entier *RAFALE A*, on a pu mettre en évidence le développement à grande incidence de la tendance naturelle à la perte de stabilité en lacet. De plus, un essai de modification au niveau des conditions aux limites pariétales a permis de créer une dissymétrie dans l'écoulement d'une pointe avant et ainsi de mettre en évidence par le calcul des efforts latéraux dont l'amplitude est en accord avec les ordres de grandeur relevés expérimentalement.

REMERCIEMENTS.
Cette étude fut réalisée dans le cadre du contrat STPA n° 8795012 BC 86.

REFERENCES.

[Réf. 1] : Schiff L. B., Cummings R. M., Sorenson R. L., Rizk Y. M., "Numerical simulation of high-incidence flow over the isolated F-18 fuselage forebody". J. Aircraft, *28*, 10 october 1991.

[Réf. 2] : Leclerc M.P., Mantel B., Périaux J., Perrier P., Stoufflet B., "On recent 3-D EULER computations around a complete aircraft using adaptative unstructured mesh refinements", *in* Proceed. of Second World Congress on Computational Mechanics, Stuttgart, august 1990.

[Réf. 3] : Degani D., "Instabilities of flows over bodies at large incidence", AIAA J., *30*, 1, january 1992.

[Réf. 4] : Ericsson L.E., "Fickle effect on nose microasymmetry on the high-alpha aerodynamics", J. Aircraft, *28*, 11, november 1991.

Photo 1 : *RAFALE A*

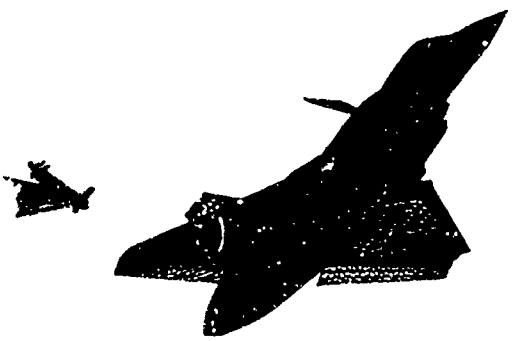

Planche 3 : Discrétisation pariétale, avion entier.

Planche 2 : Détails de la configuration du *RAFALE A* (vue ombrée du maillage).

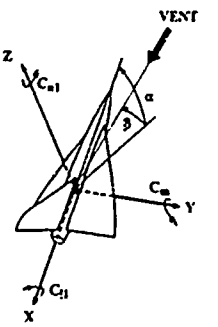

Planche 4 : Trièdres conventionnels.

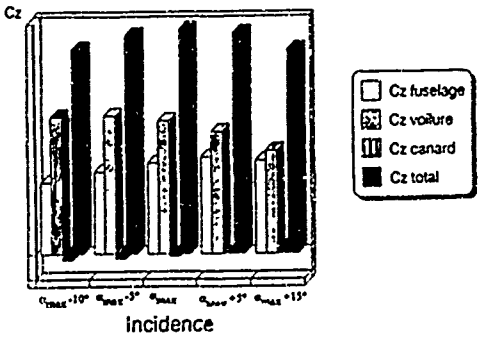

Planche 5 : Décomposition par éléments du C_z.

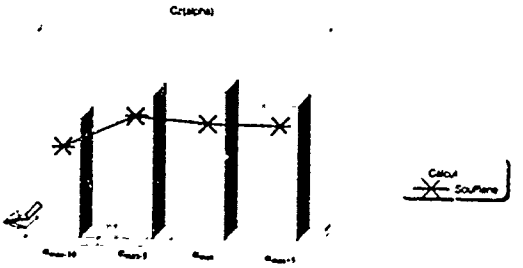

Planche 6 : CFD vs. EXPERIMENT Lift coefficient

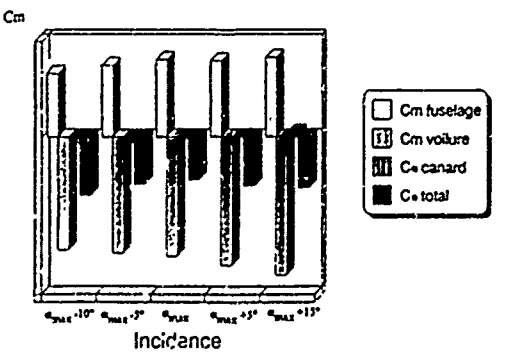

Planche 7 : Décomposition par éléments du C_m.

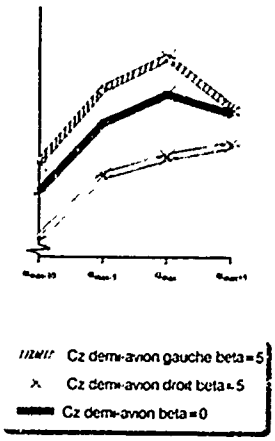

Planche 8 : ASSESSMENT OF LATERAL STABILITY
(with sideslip 5°)
Lift coefficient

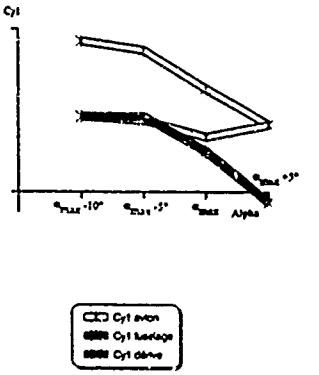

Planche 9 : Décomposition du C_{yl} avec dérapage β=5°.

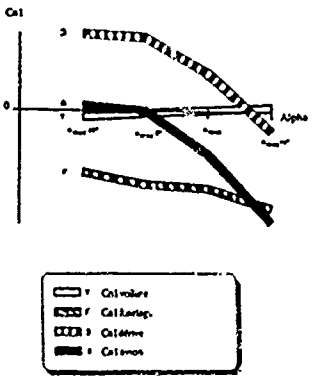

Planche 10 : Décomposition du C_{nl} avec dérapage β=5°.

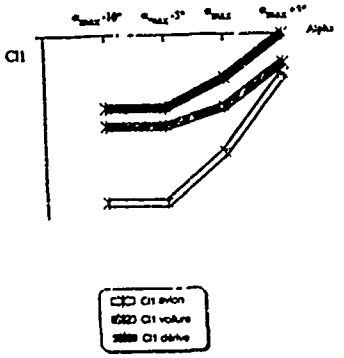

Planche 11 : Décomposition du C_{ll} avec dérapage β=5°.

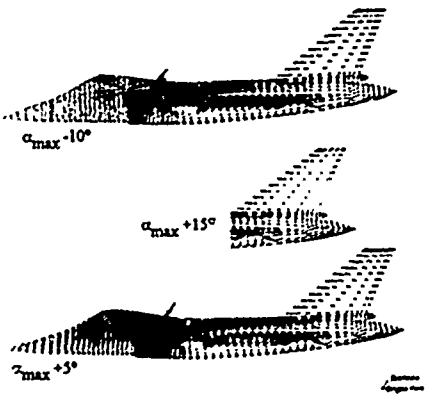

Planche 12 : Vitesses pariétales, vue de côté, β=0°.

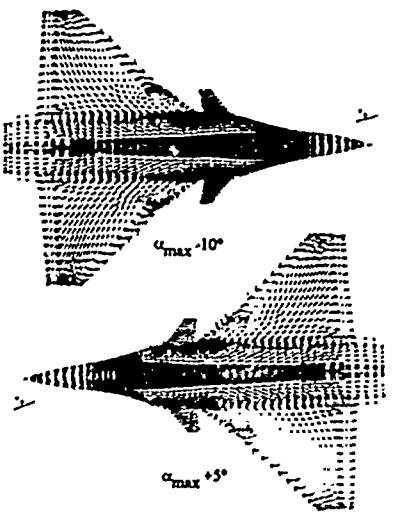

Planche 13 : Vitesses pariétales, extrados, β=5°.

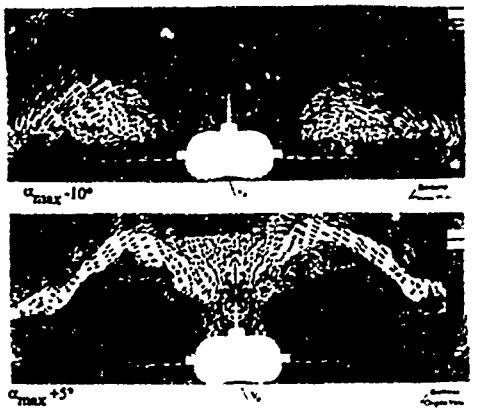

Planche 14 : C_p et trace du vecteur vitesse dans un plan X=cst au pied de dérive. Le vent vient de la droite et β=5°.

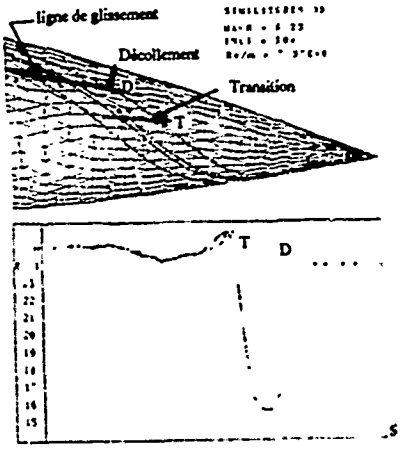

Planche 15 : Lignes de courant sur pointe avant. Evolution du paramètre de forme H.

Planche 16 : évolution de l'émission tourbillonnaire dans des plans X=cst sur la pointe avant.

DYNAMIC TESTS TO DEMONSTRATE LATERAL CONTROL USING FOREBODY SUCTION ON LARGE SCALE MODELS IN THE DRA 24FT WIND TUNNEL

Geraldine F. Edwards
A. Jean Ross
Edward B. Jefferies
Charles O. O'Leary
Aerodynamics/Propulsion Department
Defence Research Agency
Farnborough, Hampshire GU14 6TD, UK.

SUMMARY

The concept of applying suction at the nose of forebodies at high angles of attack to control the vortex flow was tested in two dynamic wind-tunnel experiments on large scale versions of the Defence Research Agency (DRA) High Incidence Research Model (HIRM1) in the DRA 24ft wind tunnel.

The first experiment with a HIRM1 wind-tunnel model mounted on a free-to-yaw rig used an analogue control system. The model was controlled at angles of attack of 28° and 32.5° by applying differential suction through small holes near the nose apex to minimise the error between demanded and measured angle of sideslip.

The second experiment used a free-flight version of HIRM1 with a digital Departure Prevention System (DPS) which was flown successfully in previous experiments. A nose suction control law, designed to maintain roll about the wind axis, was added to the DPS. The model was mounted on a rig which allowed freedom in yaw, roll and pitch, the tailplanes could move symmetrically and differentially, and the rudder was used to augment directional stability. The model could be flown at angles of attack up to about 30°, with the suction control law active, but would diverge in yaw and roll if the suction was turned off.

LIST OF SYMBOLS

F	Factor in suction control law
GM, GQ, GQD, GA, GAL	Longitudinal gains in DPS
GP, GPD, GPXF, GPH2, GPH3, GRZ, GR, GRD, GBZ	Lateral gains in DPS
g_p, g_I, g_D	Gains in ideal proportional/integral/differential controller
G_p, G_I, G_D	Gains in analogue controller
K_{PS}, K_{IS}	Gains in digital controller in suction loop
n	Lag in analogue controller
p	Gain in analogue controller
p, q, r	Roll, pitch and yaw rates, deg/sec
Q	Flow rate, cc/min or m^3/s
s	Operator in transfer functions
t	Time, seconds
V	Wind speed, m/s
x_p, z_p	Distances of cg from pivot along body axes, m
α	Angle of attack, degrees
α_L	Limiting angle of attack (i.e α_{DPS}), degrees
α_{CORR}	Corrected angle of attack from calibration of vanes, degrees
β	Angle of sideslip, degrees
η_P, η_S	Tailplane angle (Port, Starboard), degrees
ϕ	Yaw angle, degrees
μ	Gain in analogue controller
ν, ρ'	Lags in analogue controller
σ	Gain in analogue controller

Presented at an AGARD Meeting on 'Technologies for Highly Manoeuvrable Aircraft', October 1993

1 INTRODUCTION

It has been established that the vortices shed by the forebody of an aircraft become asymmetric at high angles of attack, even at zero sideslip angle, causing large sideforce and yawing moment[1]. From their symmetric positions, one of the vortices moves away from the surface, and the other moves closer, but which moves in a given direction is arbitrary. The sign of the sideforce is also arbitrary and may change as angle of attack increases, however for a given configuration at a particular angle of attack, the magnitude of the sideforce is bounded[1].

These asymmetries in the sideforce, yawing moment and rolling moment cause aircraft to depart from symmetric flight conditions, and can lead to a departure from controlled flight. The investigations[2-4] on the active control of the forebody vortices have culminated in dynamic wind tunnel tests on larger versions of the High Incidence Research Model (HIRM1)[5]. Originally it was planned to test the control system in free-flight, but changes at the range and lack of effort prevented this. The concept was therefore tested in various stages and two experiments in the DRA 24ft wind tunnel are reported here.

The first experiment used the wind tunnel version of the large model on a free-to-yaw rig, and repeated an earlier experiment[1] with the same analogue control system. The model with a longer forebody gave greater control power in yaw at a given angle of attack and control of the model was possible at α = 28° and 32.5° for tunnel speeds between 10 and 25 m/s. The second experiment used the modified free-flight model on a new rig in the DRA 24ft wind tunnel. The rig has a gimbal system allowing freedom of rotation in yaw, roll and pitch, but it was also possible to prevent rotation about the roll and pitch axes by applying brakes. The digital Departure Prevention System developed by BAe Brough[10,11] was extensively tested in free-flight and was modified[12] by BAe for this experiment. The lateral stability was enhanced and a control law added which used nose suction to maintain roll about the velocity axis, this being highly desirable for manoeuvres at high angles of attack, to keep sideslip to low levels and requires significant yawing moments from the aerodynamic controls.

2 FREE-TO-YAW EXPERIMENT

2.1 Description of model and free-to-yaw rig

A large model of HIRM1 was converted for testing in the DRA 5m wind tunnel in support of research into the prevention of departure at high angles of attack. For the free-to-yaw experiment the nose probe was removed and replaced by an ogival forebody with a sharp conical nose which had two small holes of approximately 0.75mm diameter, 7mm back from the tip, situated 30° down from the top plane of symmetry, as near to the apex as it was possible to make them. The GA of the model is shown in Fig 1. The model at the chosen angle of attack, canard and tailplane surfaces fixed, was mounted on the rig, on a single-axis gimbal (Fig 2), so that it was free to rotate in yaw about the axis normal to the fuselage. The maximum deflection in yaw could be restricted by stops. The fin did not incorporate a rudder, so the only aerodynamic control was from nose suction as a sideslip-demand system (Fig 3) to maintain demanded position. The pump generating suction was outside the tunnel, and a suction level of 1 psi (6895 N/m^2) was sufficient to generate the flow rate required. To provide a stabilising moment from the weight component, the model was ballasted aft, and a spare canard surface was fixed to the underside of the fuselage as a ventral fin to give more positive directional stability.

Transition strips, along the 80° generator, gave a turbulent separation behind the nose cone and previous tests[3,4] had shown that the longitudinal station of the change from laminar to turbulent separation (which depends on Reynolds Number) affected

the magnitude of the maximum control powers in the sideforce and yawing moment.

2.2 Flight control system and analogue controller

The Flight Control System was identical to that described in Reference 4. Two servo actuators, driven differentially by signals from the analogue controller, were connected to needle valves which changed the flow rates through the nose holes (Fig 4). A potentiometer was used to measure angle of yaw, proportional to angle of sideslip for constrained motion on a free-to-yaw rig, and the signal was used as feedback to the controller. The controller (Fig 3) was a demand system implemented on an analogue computer, ie the difference between measured and demanded angle of yaw was minimised using a proportional/integral/ differential (PID) control law.

The differential flow rate, ΔQ, is ideally given by

$$\Delta Q = F.(G_1 + G_2[1/s]+G_3[s]).(\beta_{dem} - \beta_{meas})$$

where the square brackets denote transfer functions, and F is the scaling factor required for the physical units used for ΔQ and β. However the analogue circuit was found to introduce additional lags, and the actual form of the transfer function was analysed to be

$$\Delta Q = F.(G_1 + G_2[\sigma_1/(s+\rho_1)]+G_3[ps/(s+\nu_1)]) .(\beta_{dem} - [1 + ps/(s+n)].\beta_{meas})$$

The 'differential' of the measured angle of sideslip was included to give additional damping.

2.3 Experimental responses

2.3.1 Effect of suction control

The response of the model at α = 32.5° and tunnel speed of 10 m/s, with suction on and off is shown in Fig 5. The suction controller was active for the first 21 seconds of the record, the demanded angle of sideslip was zero and the resultant angle of yaw was achieved with decreased port flow rate and increased starboard flow rate due to the negative demand from the controller. For the constrained motion in yaw, the angle of sideslip is proportional to the yaw angle but of the opposite sign, i.e $\beta_1 = -\psi \cos\alpha$, and $\dot{\psi} = r$ secs. The suction was then turned off and the model stabilised at a yaw angle of about -4.5° corresponding to a balance of the yawing moments due to the asymmetric forebody flows and sideslip, and the yawing moment due to the weight component. The controller signal was large and negative causing the port servo to close and the starboard servo to open fully (but with no flow through).

The flow rates for zero demand to the servos controlling the positions of the needle valves were set to ±30 cc/min, to enable changes in both port and starboard flow rates for negative demands to the servos. The maximum flow rate for these tests was chosen to be about 400 cc/min, and wind-off checks indicated that 390 cc/min was achieved, as indicated on the scales.

The suction pump was turned on again at about 63 seconds, and the model returned to a zero angle of sideslip, after both servos overshot the steady position. It can be seen that a small amplitude oscillation was present on the responses, the source of which has not been identified but this test demonstrated the effectiveness of the suction control to maintain zero angle of sideslip in the presence of asymmetric forebody flows.

2.3.2 Responses to steady demands

With the model at α = 32.5° and a tunnel speed of 10 m/s, the responses to a series of step changes in demanded sideslip can be seen in Fig 6. The two lowest traces show the mean levels of flow rates needed to maintain the yaw angle between 6.5° and -4°. There is a lag between the demand (second trace) and the yaw angle (top trace), but the various levels are held, except possibly for the highest demand at

t > 80sec.
Further tests showed that with increased tunnel speed (V = 25 m/s Reynolds Number = 1.5×10^6) the oscillations in the PID output and servo positions were of higher frequency and much larger amplitude, but a reason for this was not found. More discussion on this can be found in Reference 9.

2.3.3 Response to pulse demands

Computations done before the wind-tunnel tests indicated that airspeed had an effect on the lag of the response. This effect can be seen in the experimental responses in Fig 7 for $\alpha = 32.5°$. A pulse demand was applied to the PID controller and at V = 10 m/s, the response was sluggish and there was appreciable overshoot at t = 9 sec, due to the port needle valve being fully open and the starboard one closed. As the speed was increased to 15, 20 and 25 m/s, there was a decrease in the lag between the demanded and resultant yaw angle and an increase in frequency and amplitude of the PID output. The decrease in lag was similar to that in computations, but it was not possible to see any significant change in the amplitude of yaw angle due to tunnel speed.

3 FREE-TO-YAW/ROLL/PITCH EXPERIMENT

3.1 Description of model and free-to-yaw/roll/pitch r

The original plan to test the n e suction concept on a freely flyi g model dropped from a helicopter became virtually impossible due to changes at the range and low priority access to a helicopter. It was therefore decided to design a new rig for the DRA 24ft wind tunnel which would allow a model to respond in yaw, roll and pitch angle, and modify a free-flight model to be fixed to a 3-axis gimbal on the rig.

The original forebody and nose probe were replaced by the forebody and nose cone used in the free-to-yaw tests, making the external geometry of the two models identical (except that the ventral fin was not used). The canards were fixed at zero degrees to the Horizontal Fuselage Datum (HFD), but the tailplanes and rudder were driven by the flight control system, via electro- mechanical actuators. The model mounted on the new rig is shown in Fig 8, with the close-up view (Fig 8a), showing the rudder hinge line, the deflected tailplane, and the α-vane on the port side near the trailing end of the transition strip on the forebody. The bomb slip on the top of the fuselage was used for carrying the model under a helicopter for free-flight tests.

Needle valves, driven by electro-mechanical actuators responding to the FCS, controlled the flow rates through the port and starboard holes. A constant level of suction was applied to the other side of the needles, using a small electric pump installed in the fuselage.

The transducers used for flight trials were installed in the model and included rate gyros to measure roll, pitch and yaw rates, and an horizon gyro to measure pitch and roll angles. Angles of attack and sideslip together with all these signals, apart from pitch angle, were inputs to the onboard flight control system. The vanes measuring the angle of attack and sideslip were on the fuselage, and were calibrated in static tests[13]. Responses of about 30 variables could be monitored in the control room, with a maximum of 8 synchronous channels of chart records being possible.

The model was mounted on the same cranked support as the free-to-yaw rig, at mean angles of attack of between 20° and 37°. It was held above the cranked support on the 3-axis gimbal, with freedoms of ±7° in pitch and ±20° in both roll and yaw. Brakes could be applied on the pitch and roll axes to hold the model at constant angle of attack and zero bank angle respectively. The model is shown at a large angle of yaw in Fig 8b, the resulting bank angle being associated with yawing moment about the geometric body axis.

The model was ballasted to make the centre of gravity as near as possible to the centre of rotation for the gimbal system. Longitudinally the cg needed to be less than 0.02m from the pivot point for the available aerodynamic pitching moment from the tailplanes (at the low speeds) to balance the moment due to the weight. It was also found that the roll control available was not sufficient to counteract the unstable moment from the weight if the cg was more than about 0.003m above the pivot. The longitudinal cg position could be changed fairly easily, with ballast being required at the rear, but it was difficult to reduce the height of the cg above the HFD. The wing is above the HFD and is relatively heavy, so 50lbs of lead shot was put on the floor of the model, about 10% of unballasted model weight of 550lb (250kg). This did not reduce the cg height sufficiently to give roll control, but the available volume restricted addition of more ballast.

Some experiments were conducted with a 10lb weight held on a rod fixed to the rear of the model, about 0.7m below the HFD, and control was found to be marginal.

To improve recovery from extreme angles of yaw and roll the edge of the cut-out in the floor of the model was packed with foam rubber reducing the effects of hitting the stops. The final experiments were conducted with a 20lb weight fixed 0.7m below the fuselage just ahead of the pivot.

3.2 Flight control system and digital controller

The control system for these experiments was much more complicated than the analogue controller described in Section 2.2, and a full description of the control laws designed by BAe is given in Reference 13.

The Departure Prevention System[11] for HIRM1 was successfully tested in free flight, to α = 30° approximately and it was decided to modify the system to extend control up to α = 32°, and also to add a control law to maintain roll about the wind axis using nose suction to generate the required yawing moments. The block diagrams for the departure prevention system and the nose suction control system are shown in Fig 9.

The longitudinal control law could be either a pitch-rate demand system or an angle-of-attack limiter, switching automatically between the two. It could also be used as an α-demand system by applying a constant high level of pitch rate demand and setting the α limit to the required angle, and was used in this way for these experiments. The required angle-of-attack could be changed within ±7° about the chosen mean angle of the model on the rig.

The roll control was a roll-rate demand system with roll damper, using differential tailplane for roll control, and a cross-feed to rudder to enhance roll performance. The roll control law was switched out and the Automatic Bank Angle Recovery System (ABRS) became effective for 5 seconds if the bank angle exceeded a set limit. (The directional control law was also switched out). This Recovery System was needed for flight experiments, and was used as a back-up to the roll brake on the rig, to prevent large bank angles. The directional control system was a rudder demand system, with augmentation of lateral/directional stability using rudder proportional to angle of sideslip, and a yaw damper.

The control laws required angles of attack and sideslip, so the corrected values had to be calculated from the vane signals, using the calibration data[13]. The mean of the port and starboard vane signals was substantially independent of angle of sideslip and flow rate. The difference between the readings was related to sideslip, but was affected by the forebody vortices. This meant that applying flow rate affected the indicated angle of sideslip, which could be corrected in the calibration, but the random asymmetry at zero angle of sideslip and zero flow rates could not be included in the correction.

The additional control law using nose suction, minimised the yaw rate about the wind axis (p.sin α - r.cos α) in order to maintain rolling about the wind axis and prevent large angles of sideslip. The required changes in flow rate were applied differentially to port and starboard needle valves, so the initial flow rates were set at equal non-zero values to allow decreases as well as increases in the flow rate. The differential flow rate was given by

$$\Delta Q = F.(K_{fs} + K_{ls}[1/s]) .(p.\sin\alpha - r.\cos\alpha) \quad cc/min$$

with K_{fs} = 50 and K_{ls} = 150 for F = 1.0 and the roll rate p and yaw rate r in deg/sec.

The Flight Control computer was extensively bench-tested using a free flight model and a mathematical model[14] of the aerodynamic forces and moments, to simulate the motion in free flight. The responses of the mathematical model were used as inputs to the Flight Control laws, and the resulting outputs were used to drive the actuators of the tailplanes, rudder and the needle valves. The loop was closed by feeding the control positions to the mathematical model.

A problem was encountered where the signal to the differential tailplanes increased, at arbitrary rates and random sign, with a drift in angle of sideslip, tending to result in a divergent response. The source of the drift was investigated[9] but could not be eliminated.

However it was found that:-

a) there was no drift if the integrators were switched out of the control loops and
b) it was possible to maintain control of the model by introducing pilot demands to roll rate via pulses through a joy-stick-type controller, the sign and duration of the pulses being judged by the 'pilot'.

On this basis it was decided to use the Flight Control System in the wind-tunnel tests.

3.3 Computed responses

Initially it was thought prudent to allow the model to respond in yaw only but controlled by the lateral laws of the digital Flight Control System. This was achieved by keeping the roll and pitch brakes on. Before 'flying' the model on the rig, responses were computed using the equations of motion[7], yawing moments from the mathematical model and a complete FCS, for various longitudinal positions x_f of the cg relative to the pivot, over an α range from 20° to 32.5°. The model was found to be stable. A set of responses with α = 30°, V = 20 m/s and the cg and pivot point coincident is shown in Fig 10a.

With the roll brake off the response was very similar but more oscillatory for the same flight conditions (Fig 10b, set(i)). The effect of the cg position 0.02m behind the pivot was also checked but had very little effect (set(ii)). The response shown in set(iii) was for α = 32.5° and was more oscillatory but reached a stable trimmed state.

When the pitch brake was released, the longitudinal control law became effective and the mean tailplane deflection defined a realistic trim state. Computations for α_t = 27.5°, $x_f = z_f = 0$ are shown in Fig 11a,b the mean vane reading of 47.6° from the calibration used in the mathematical model.

Computations were also made with the integrators excluded from the control laws (Fig 11c), as the FCS could be used in this state. The response was more damped than the corresponding 'integrators in' response, with a final α = 16.8° (vane reading 32.3°) where the nose suction control is ineffective. The trim state could not be reached since the error between the demanded and measured angle of attack cannot be minimised without an integrator in the loop.

Checks were also made to see if control could be maintained with the cg above the pivot and a few conditions were

found where the departure in roll could theoretically be held, at higher wind speeds, for z_p = 5mm, but it was felt that control was unlikely to be possible in practice.

The behaviour of the model during tunnel run-up with the FCS active was also investigated, finding that the model reached a near steady state by the time the wind speed was constant.

3.4 Experimental responses

As stated in 3.1, the model vertical cg location was lowered by the addition of a 20 lb mass fixed on a bar 0.7 m below the fuselage. The interference effects of the bar and mass on the aerodynamic forces and moments were judged to be small.

With the model at mean α = 25°, (α_{DEM} = 26.6°), and V = 15 m/s, control could be maintained at small constant yaw angles with the roll brake on, and the integrators switched in. This is illustrated in the first 12 seconds of record in Fig 12a, although roll demands via the joy-stick were used prior to this to prevent divergence of the differential tailplanes. The corrected α_{MEAN} about 24° and the tailplane deflection about -13°, indicate that the longitudinal position of the cg is ahead of the pivot.The roll brake was released at t = 12.5 seconds and the model moved to trim angles of bank and yaw. The model was then centralised by small roll demands and a rudder pulse was demanded (Fig 12b), causing the yaw angle to change sign and the bank angle to become positive. The roll demands at 33 seconds gave differential tail movements and changes in yaw and bank angles as expected.

The final configuration with the model at α = 25.5° and cg slightly aft of the pivot, was achieved by putting 2.1kg of ballast inside the rear of the model. The first 25 seconds of responses in Fig 13 (with the integrators switched out and the roll brake off) show a lightly damped oscillation in yaw with the two α vanes at different levels indicating an angle of sideslip in the control laws so the rudder moved to augment directional stability. When the integrators were switched in, the model slowly diverged in angles of bank and yaw with constant differential tail and slowly decreasing rudder deflection. However control was maintained by small continuous inputs to rudder and roll demands via the joystick, as can be seen starting at t = 56 seconds.

The gains in the control law for maintaining roll about the wind axis were determined using a mean flow rate of 180 cc/min and maximum flow rates of 1600 cc/min at speeds of about 40 m/s. The actuators of the needle valves controlling flow rate were adjusted to give these limits and a mean flow rate at zero demand. It was possible to increase the gains by increasing the level of suction, and this gave much tighter control.

The responses in Fig 14 were for changes in α_{DEM} with oscillations similar to those on the free-to-yaw rig, the frequency was lower but the limit cycle character was the same. A detailed description of further tests can be found in Reference 9 and although it was not possible to manoeuvre the model on the rig at very high rates, the response generated did show that the suction control was effective, and could be implemented successfully.

4 CONCLUDING REMARKS

The two experiments described here are the culmination of a research programme into controlling forebody flows at high angles of attack to generate yawing moment for the enhancement of manoeuvring capability.

The yawing moment due to differential flow rate has been used successfully to control a free-flight scale HIRM1 model on a free-to-yaw rig. An analogue controller minimised the error between demanded and measured yaw angle, maintaining zero yaw when asymmetric forebody flows were present, and moving the model to demanded positions. The directional stability was marginal at these angles of attack, so was

augmented by a ventral fin.

The nose suction control law has been added to an existing Flight Control System and the free-flight model of HIRM1 was successfully controlled on a free-to-yaw/roll/pitch rig. The FCS requires further development, but the responses indicate that the principles of using forebody vortex control via nose suction have been demonstrated. Rolling about the wind axis can be maintained by the nose suction control for the restricted manoeuvres possible on the free-to yaw/roll/pitch rig. The main conclusions of the whole research programme are listed in Reference 9.

REFERENCES

1 Fiddes S P;'Separated flow about cones at incidence -Theory and experiment'. RAE TM Aero 2055, 1985.

2 Mundell A R G;'Low-speed wind tunnel tests on the use of air jets to control asymmetric forces and moments occurring on aircraft at high incidences'. RAE TM Aero 1984, 1984.

3 Heydari F;'Active yaw control of a generalised missile body at high angles of attack by means of nose suction'. RAE TM Aero 2140, 1988.

4 Ross A J, Jefferies E B, Edwards G F; 'Control of forebody vortices by suction at the nose of the DRA High Incidence Research Model: Wind Tunnel tests'. RAE TM Aero 2172,1990.

5 Ross A J, Jefferies E B, Edwards G F; 'Control of forebody vortices by suction at the nose of the DRA High Incidence Research Model'. RAE TM Aero 2194, 1990.

6 Ross A J, Jefferies E B, Edwards G F; 'Aerodynamic data for the effects of nose suction on a High Incidence Research Model with a large forebody'. (App. by D G Mabey). RAE TM Aero 2204, 1990.

7 Ross A J, Jefferies E B, Edwards G F; 'Dynamic wind tunnel tests on control of forebody vortices with suction'. AGARD CP 496, Paper 17, 1991. RAE TM Aero 2206, 1991.

8 Ross A J, Jefferies E B, Edwards G F; 'Wind tunnel tests on control of forebody vortices by suction for several forebodies on the DRA High Incidence Research Model'. RAE TM Aero 2230, 1991.

9 Ross A J, Jefferies E B, Edwards G F; 'Dynamic tests on large scale High Incidence Research Models (HIRM1) in the DRA 24ft wind tunnel with control of forebody vortices by nose suction' DRA TR 92067, 1992.

10 Naseem M A; 'High Incidence Research Model (HIRM): Flight Control System'. BAe Note YAC 386, 1987.

11 Naseem M A, Ross A J; 'Development and implementation of flight control system for a research drop model'. Seventh Bristol International Conference on Remotely Piloted Vehicles, 1988. (BAe Note YAD 386).

12 Naseem M A; 'High Incidence Research Model (HIRM): Flight Control System Design (Nose Suction)'. BAe Note YED 8064, 1992.

13 Ross A J; 'Calibration of air data instruments on the High Incidence Research Models in the DRA 5m wind tunnel'. RAE TM Aero 2109, 1987.

14 Smaller K; 'Definition of HIRM1 aerodynamic models: Nose suction effects'. (TSIM and LUCOL representations). BAe Note YAD 5332, 1992

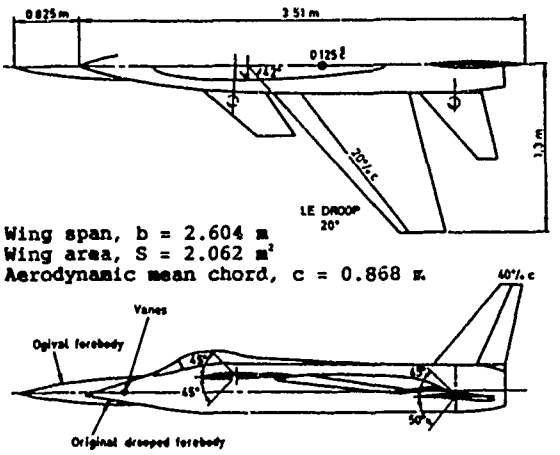

Fig 1 General arrangement of model (HIRM 1)

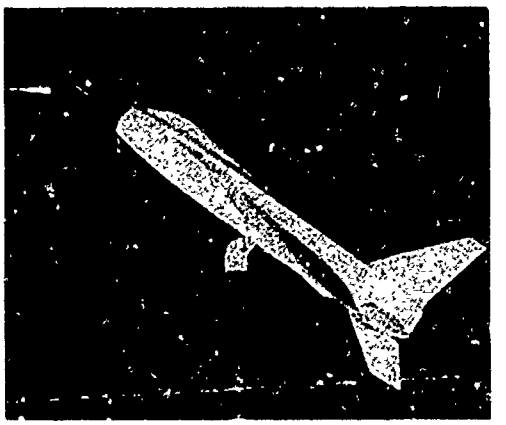

Fig 2 Model on free-to-yaw rig

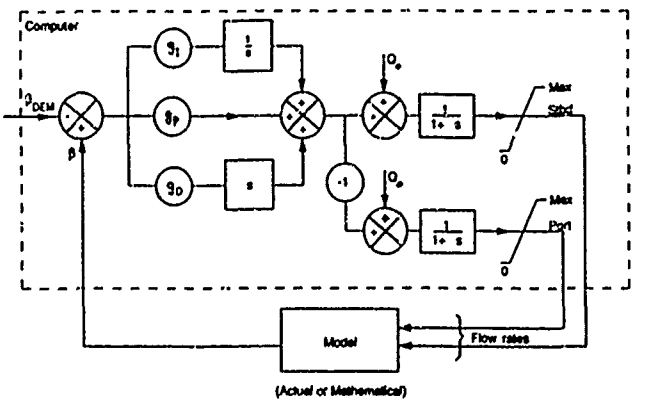

Fig 3 Block diagram of sideslip demand system

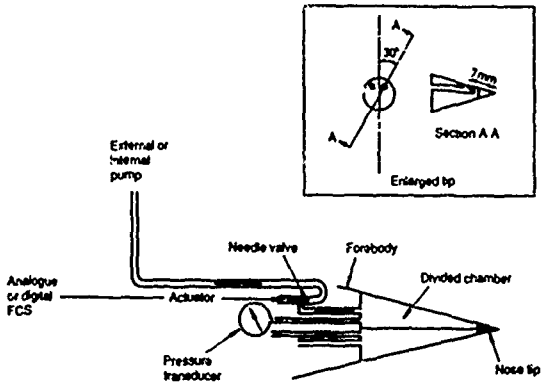

Fig 4 Sketch of suction system

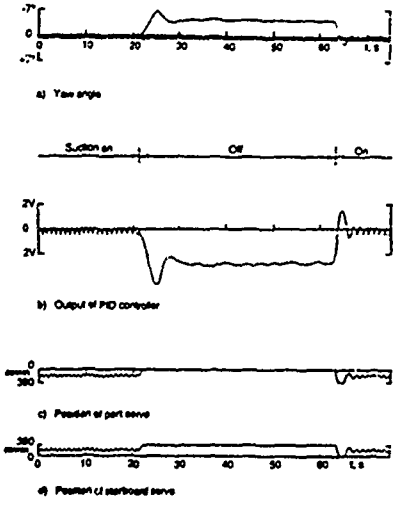

Fig 5 Effects of turning suction off and on, α = 32.5, V = 10 m/s (free-to-yaw rig)

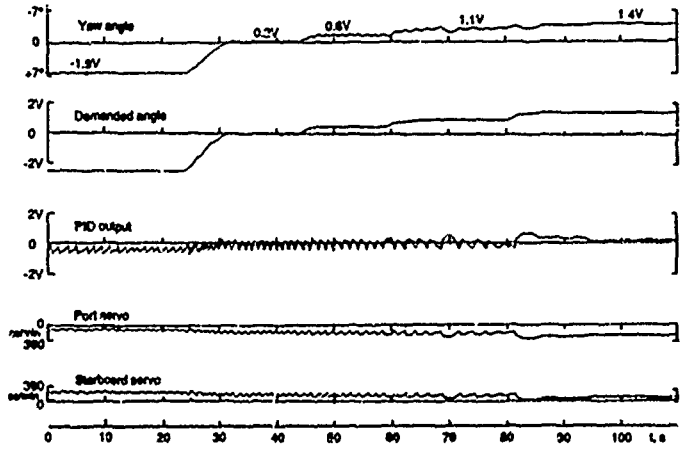

Fig 6 Response to various levels of demanded angle-of-sideslip α = 32.5, V = 10 m/s (free-to-yaw rig)

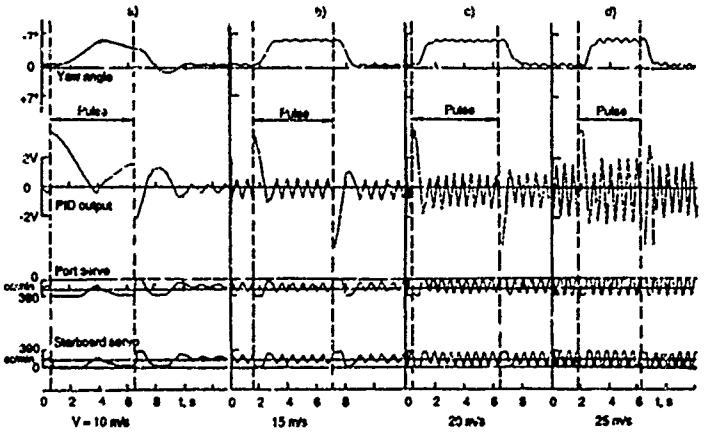

Fig 7 Effect of airspeed on responses to pulse inputs, α = 32.5 (free-to-yaw rig)

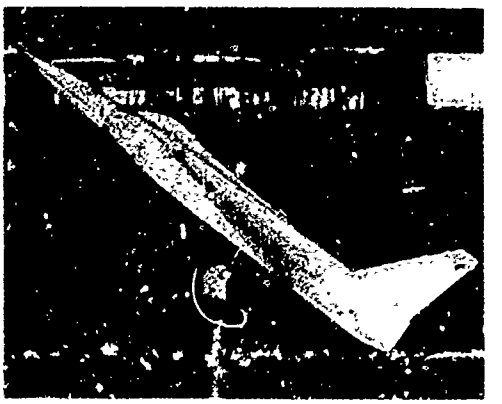

Fig 8a Model on free-to-yaw/roll/pitch rig, external ballast below mid-fuselage

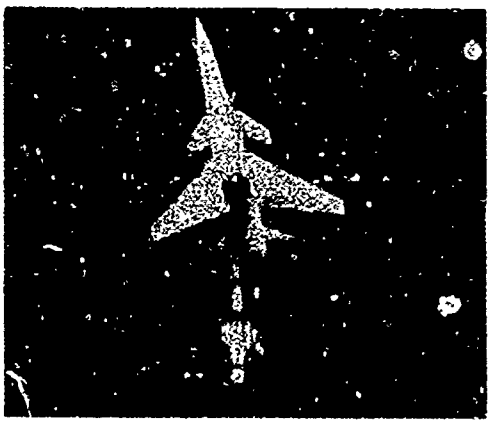

Fig 8b Model at large yaw angle on free-to-yaw/roll/pitch rig

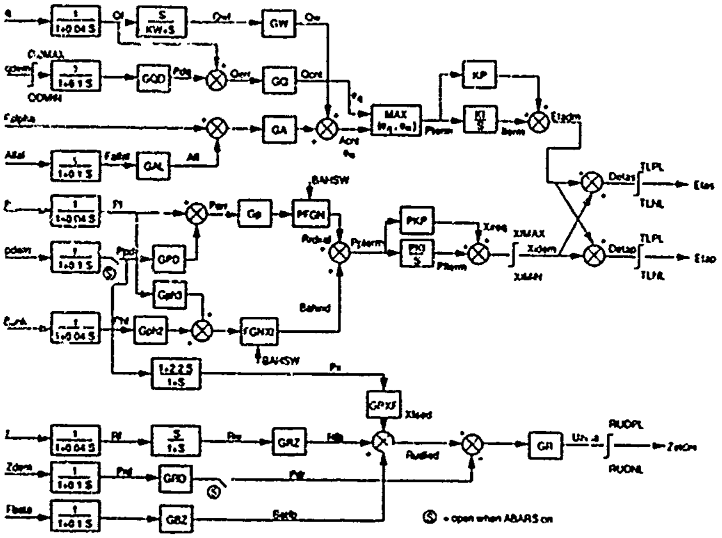

Fig 9a Block diagram of Departure Prevention System (DPS)

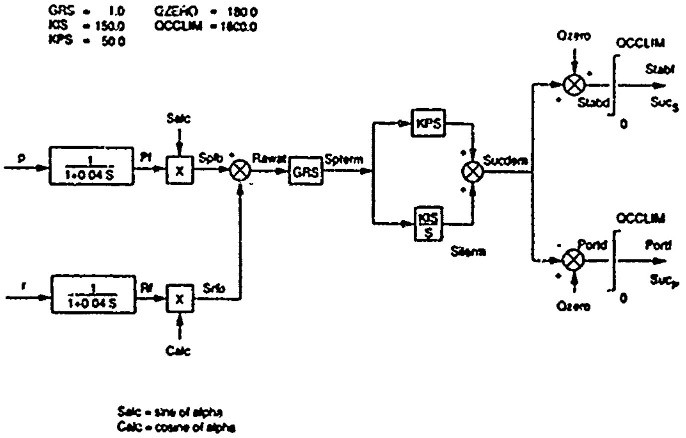

Fig 9b Block diagram of nose suction control system

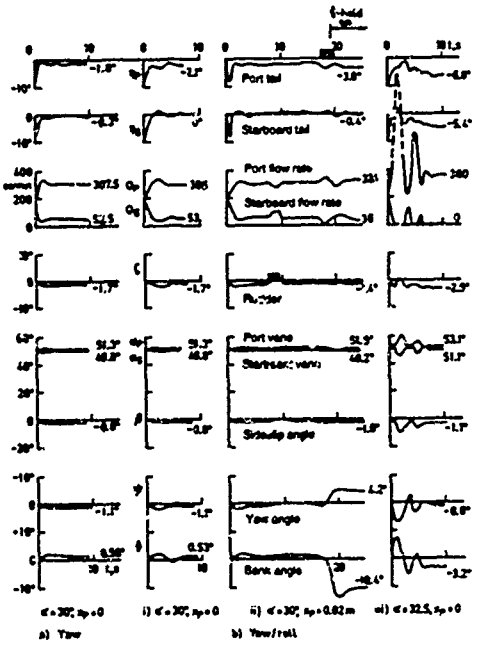

Fig 10 Computed responses for free-to-yaw/roll/pitch rig, constrained by brakes, V = 20 m/s

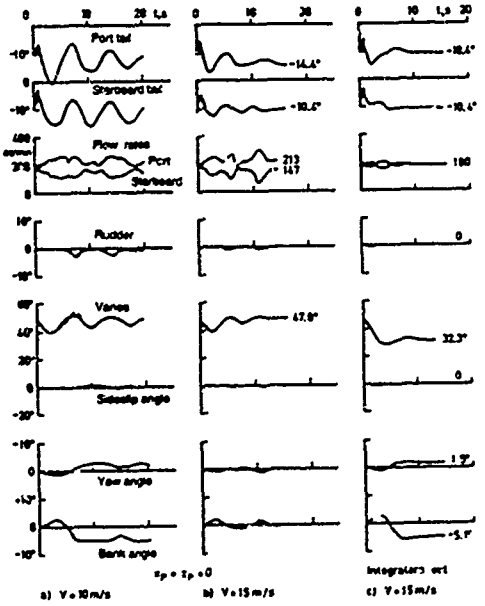

Fig 11 Computed responses for free-to-yaw/roll/pitch rig, α_L = 27.5°

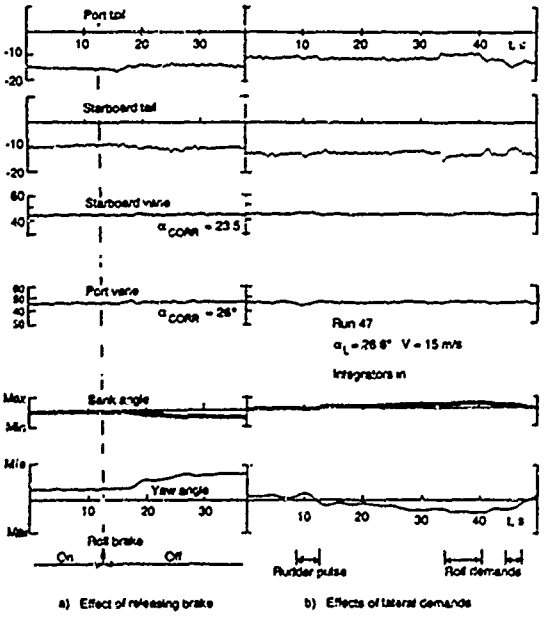

Fig 12 Responses with roll brake on and off, ballast weight below mid fuselage (free-to-yaw/roll/pitch rig)

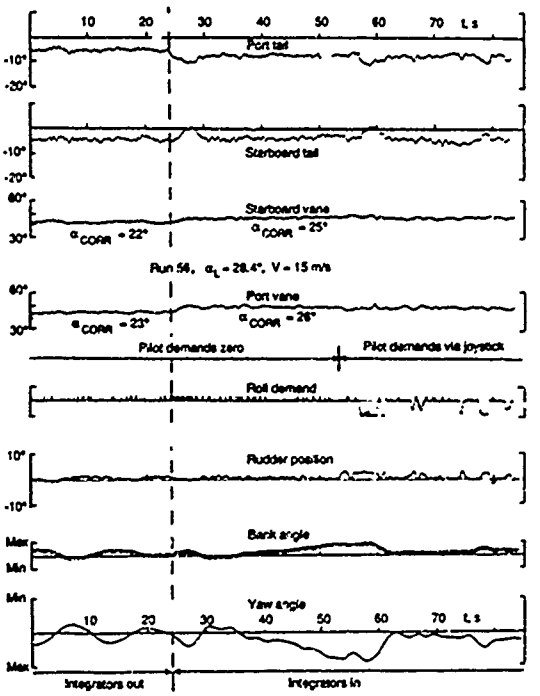

Fig 13 Effects of integrators and demand inputs, α = 25.5, V = 15 m/s (free-to-yaw/roll/pitch rig)

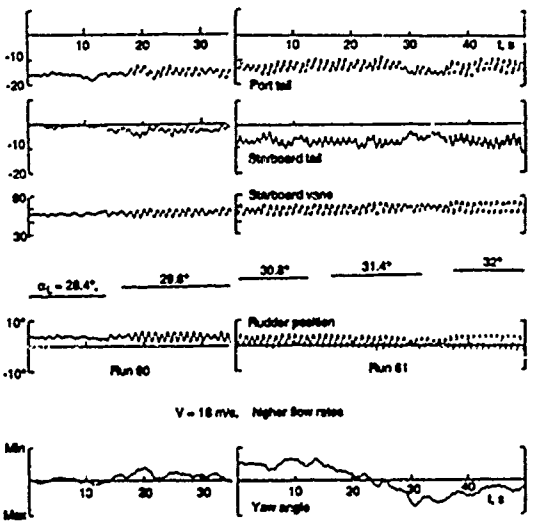

Fig 14 Responses to changes in demanded angle-of-attack, higher flow rates (free-to-yaw/roll/pitch rig)

Outils pour la caractérisation aérodynamique et l'évaluation des performances à haute incidence

O. Renier
ONERA-IMFL
5, Boulevard Paul Painlevé
59000 Lille
France

RESUME

L'ONERA-IMFL dispose d'outils contribuant à l'étude des comportements des avions d'armes manoeuvrant à grande incidence. Des montages de simulation dynamique en soufflerie permettent de caractériser l'aérodynamique stationnaire et instationnaire à basse vitesse lors de sollicitations en roulis aérodynamique et en dynamique de tangage. L'analyse de la donnée et la modélisation aérodynamique est facilitée par utilisation de logiciels spécifiques. L'emploi des techniques d'analyse des systèmes dynamiques non linéaires conduit à la détermination des cartes de stabilité de l'aéronef dans tout le domaine de vol ainsi qu'à l'évaluation de performances de manoeuvres. La validation des prévisions de comportement est réalisée par des essais en vol de maquette en soufflerie verticale ou en laboratoire.

Ces outils ont été utilisés pour l'étude du contrôle en lacet à grande incidence par des gouvernes de pointe avant. La robustesse du concept de virures d'avant-corps vis-à-vis de sollicitations dynamiques a été mesurée en soufflerie. Des essais en vol de maquette ont validé les comportements prévus.

ABSTRACT

ONERA-IMFL develops techniques for high AOA manoeuvring aircraft behaviour studies. Specific wind-tunnels tests -coning and oscillatory coning motions, constant pitch rate tests- provide information about steady and unsteady, low speed aerodynamics. Specific software facilitates data analysis and aerodynamic modelling. Application of non-linear dynamic systems analysis techniques allows stabilities calculations and performance evaluation. For some manoeuvers, behaviour predictions can be validated with model flight tests in vertical wind-tunnel or in laboratory. These techniques have been used for forebody yaw control studies. Sensitivity of strakes efficiency to aircraft dynamic motions was measured in wind-tunnel facilities. Model flight tests confirm expected behaviours.

NOTATIONS

α, β	incidence, dérapage
ψ θ, ϕ	angles d'Euler
C_l, C_m, C_n	coefficients aérodynamiques de moment de roulis, tangage, lacet
C_x, C_y, C_z	coefficients aérodynamiques de force axiale, latérale, normale
α', β'	vitesses de variation d'incidence $d\alpha/dt$ et de dérapage $d\beta/dt$
θ', θ''	vitesse et accélération angulaires $d\theta/dt$, $d^2\theta/dt^2$
λ	angle entre les vecteurs rotation Ω et vitesse aérodynamique V

1. INTRODUCTION - CONTEXTE GENERAL

Depuis de nombreuses années un intérêt croissant est porté à la manoeuvrabilité des avions de combat à grande incidence. Dans ce contexte des dispositifs aérodynamiques susceptibles de limiter des instabilités latérales rencontrées sur les aéronefs sont étudiés. Les travaux menés à ce jour ont permis de montrer que le siège de ces instabilités est en particulier localisé au niveau de la pointe avant. Les tourbillons générés par le contournement de la pointe par l'écoulement prennent en effet des positions dissymétriques pour certaines valeurs d'incidence, engendrant localement une force latérale, donc un moment de lacet global important (fig. 1).

Des dispositifs de types "strakes" ont fait l'objet d'études paramétriques assez complètes [1]. Disposées de chaque côté du nez de l'avion, ces surfaces fixent les lignes de décollement sur la pointe et symétrisent l'écoulement. Mais en jouant sur leur position relative, il est possible d'imposer le sens de la dissymétrie (fig. 2). D'un moyen d'atténuation de l'instabilité, les virures deviennent potentiellement un moyen de contrôler le moment de lacet à grande incidence (fig. 3).

Dans ce contexte, les travaux de l'ONERA-IMFL ont porté sur l'application de ce concept sur une géométrie réaliste d'avions d'armes de formule delta-canards, à ajuster les caractéristiques de dimensionnement et de positionnement des virures et à étudier l'efficacité de ce dispositif lors de sollicitations dynamiques en soufflerie ou en essai en vol.

La démarche générale d'étude des phénomènes grandes incidences à l'ONERA-IMFL est donnée figure 4. Elle suit un schéma classique d'analyse des phénomènes physiques: caractérisation expérimentale, analyse et modélisation des mesures, simulation des comportements, validation expérimentale. Les outils sont ici adaptés au domaine de vol basses vitesses, grandes incidences, dynamique élevée.

Ces diverses étapes sont fortement interactives et des rebouclages sont nécessaires. De nouveaux trop complexes à l'analyse vont nécessiter des compléments d'essais, voire la création de moyens d'essais nouveaux. De même, des corrélations non satisfaisantes entre les essais de validation et les simulations numériques conduisent à reconsidérer la représentativité du modèle aérodynamique ou encore la validité de certaines hypothèses expérimentales.

Presented at an AGARD Meeting on 'Technologies for Highly Manoeuvrable Aircraft', October 1993.

A ce schéma s'ajoute une étape appelée évaluation de performances. Le calcul, à partir d'un modèle représentatif de l'avion, de critères correspondant à des capacités de réalisation de certaines manoeuvres permet la comparaison entre des formules géométriques différentes.

Dans ce document nous présentons une rapide description des moyens d'essais grandes incidences de l'ONERA-IMFL. Des résultats relatifs à l'étude en soufflerie des voilures d'avant-corps serviront de base d'illustration.
La mise en oeuvre des essais en vol de maquette en laboratoire et leur exploitation seront présentées.
Enfin on évoquera les outils d'analyse pour l'étude des stabilités à grande incidence et l'évaluation des performances en manoeuvre.

2. LES OUTILS EXPERIMENTAUX POUR LA CARACTERISATION

Le rôle de ces outils est de caractériser l'aérodynamique d'une maquette au voisinage de trajectoires représentatives dans l'espace des variables et des commandes [2]. Ceci implique la simulation dynamique de mouvements privilégiant la rotation de l'avion autour du vecteur vitesse (l'angle entre les vecteurs vitesse et rotation est faible) de même que des mouvements à forte dynamique de tangage (ces deux vecteurs sont quasiment orthogonaux).
L'ONERA-IMFL dispose de deux outils pour soufflerie basses vitesses. Le premier d'entre-eux, appelé montage dynamique "PQR", est spécifique à l'étude de la dynamique de tangage. Le second est une balance rotative originale, axée sur l'étude des roulis aérodynamiques et capable d'essais couplés oscillatoires en α et β.

2.1 Le montage dynamique "PQR"

Ce montage équipe la soufflerie S2L4 de l'ONERA-IMFL depuis 1990. Dès sa conception, les critères de discrétion en vrille et une dynamique élevée en tangage ont été intégrés. Il en résulte un dispositif mécanique dont le schéma descriptif est donné fig 5. Il reproduit les trois degrés de liberté correspondant aux angles d'Euler, communément utilisés en mécanique du vol. Les angles de cap et d'assiette latérale (Ψ et Φ) sont réglables mais constants en cours d'essai. L'assiette longitudinale Θ est asservie à un actionneur de puissance et peut évoluer rapidement en cours d'essai. Grâce à un système d'asservissement adapté, des lois quelconques $\Theta(t)$ peuvent être imposées à la maquette: harmonique, rampe, arbitraire (fig. 6), dans la limite de la bande passante. L'ensemble du dispositif a été dessiné de façon à réduire les interactions avec la maquette et présente une discrétion optimale pour les grandes incidences (fig. 7).

Ce montage permet donc :

- la caractérisation des effets dynamiques instationnaires lors de variations d'incidence de grande amplitude. Celles-ci peuvent être obtenues soit par des essais de type harmonique ou par des essais à vitesse de tangage constant (fig. 8);

- la simulation de l'évolution de l'incidence au cours d'une manoeuvre de type montage axe avion à grande incidence et retour au vol normal. L'intérêt de ce type d'essai est évident, puisqu'il permet de mesurer de façon réaliste l'aérodynamique instationnaire effectivement rencontrée lors d'une manoeuvre typique de combat aérien.

La figure 9 illustre un des intérêts de ce montage. Il s'agit de l'influence de la variation d'incidence sur la dissymétrie en lacet à grande incidence. Ce type d'essai met en évidence les phénomènes de retard à l'établissement de la dissymétrie. Dans le cadre de l'utilisation de voilures de pointe avant à des fins de contrôle en lacet, un tel comportement doit être évidemment pris en compte.

2.2. La balance rotative

Cet outil a été développé à l'ONERA-IMFL en 1976 et équipe la soufflerie verticale SV4. Sa cinématique comporte six degrés de liberté (fig. 10) associés aux paramètres de description traditionnels de la vrille. L'expérience acquise en plus de quinze années d'exploitation ont montré l'intérêt de ce type de montage tournant et son adéquation à la caractérisation aérodynamique, stationnaire et instationnaire à grande incidence.

En effet un large domaine d'incidence dérapage est accessible pour caractériser l'aérodynamique au cours de rotations stationnaires. Les variables incidence, dérapage, taux de rotation sont constants. Les mesures effectuées permettent d'accéder aux termes d'amortissement en roulis aérodynamique (Cl_q ou Cl_{pA}). Les essais effectués avec du dérapage sollicitent également l'aérodynamique en vitesse de tangage. Sous certaines hypothèses ils permettent l'identification de termes d'amortissement en tangage (Cm_q, $Cm_{\dot{\alpha}}$).

En utilisant un degré de liberté spécifique à ce montage à savoir λ, angle entre les vecteurs vitesse et rotation, les essais en rotation deviennent instationnaires au sens où au cours de l'essai l'incidence et le dérapage évoluent périodiquement (fig. 11). De tels essais mettent en évidence le décrochage dynamique (fig. 12) sur les caractéristiques de portance et de tangage. Là aussi sous certaines hypothèses les contributions instationnaires peuvent être évaluées et mises en corrélation avec une variable dynamique comme $d\alpha/dt$. Les caractéristiques latérales lors de tels essais sont plus complexes à analyser, en raison du couplage cinématique des deux variables sensibilisantes $\alpha(t)$ et $\beta(t)$.

Cet outil a récemment été utilisé pour évaluer l'influence de la rotation sur l'efficacité des voilures sur le moment de lacet. La figure 13 présente les mesures $Cn(\beta)$ pour trois configurations extrêmes du dispositif (nez avec voilures, avec une seule voilure à gauche, à droite). Elle illustre la robustesse de ce concept puisque les efficacités mesurées en statique demeurent. Les termes d'amortissement sont ici peu affectés.

2.3. Outils complémentaires

Deux autres techniques expérimentales de soufflerie viennent compléter ceux précédemment décrits. Les visualisations d'écoulement sont aussi utilisés pour aider à la compréhension des phénomènes aérodynamiques. En particulier les techniques d'enduit visqueux permettent de matérialiser les lignes d'écoulement pariétales ainsi que les zones décollées. Dans l'étude de voilures d'avant-corps, la mise en évidence des lignes de décollement sur la partie avant, leur déplacement selon divers paramètres (présence de la voilure, position, incidence globale) contribue à l'analyse

de l'influence de ces paramètres sur les mesures d'efforts aérodynamiques globaux (fig. 14).

Les techniques de mesure de pression pariétales ont également été développées pour des essais sur la balance rotative. Une application en a été faite pour étudier le champ de pression sur un cône en incidence au cours de mouvements en rotation stationnaire ou instationnaire (fig. 15) [5]. Effectuées alors dans une configuration lisse (sans vrilles) le déplacement des lignes d'arrêt et de décollement selon le sens de rotation est fortement corrélé avec l'incidence et le dérapage local au niveau de la pointe. Le comportement du champ de pression se déduit dans ce cas des caractéristiques mesurées en statique.

3. LES OUTILS D'ANALYSE

3.1. La modélisation

L'ensemble des mesures issues de la phase de caractérisation aérodynamique en soufflerie constitue une masse d'informations volumineuse. Le nombre de paramètres d'entrée est élevé puisqu'il faut compter parmi eux ceux qui caractérisent les essais dynamiques.

La phase d'analyse consiste dans un premier temps à mettre en évidence les relations entre les paramètres d'entrée et les variables de sortie, ici les coefficients aérodynamiques globaux. A grande incidence, cette étape est rendue plus difficile du fait de l'existence de non-linéarités, d'hystérésis, de phénomènes dynamiques fortement dépendants du temps. Cette phase s'appuie essentiellement sur la visualisation de la donnée. La superposition de séquences d'essais correctement choisies peut mettre en évidence des effets simples de configurations (gouvernes, dérapage,...) mais aussi des effets temporels comme le décrochage dynamique de voilure. Dans le cas où cette approche n'aboutit pas, la projection de la donnée selon des coupes dans l'espace de la base de données permet la recherche de variables sensibilisantes.

Ce travail permet dans un second temps de définir une stratégie de modélisation. Pour chaque coefficient, on détermine les variables sensibilisantes, on évalue l'additivité des effets, on met en évidence le poids des phénomènes instationnaires. Une structure de modèle, adaptée à la nature des phénomènes observés peut alors être choisie.

A cette étape des logiciels de modélisation spécifiques permettent d'identifier de façon aisée certains termes ou coefficients du modèle. C'est ainsi que pour représenter les phénomènes stationnaires, l'ONERA-IMFL dispose d'un logiciel d'identification ou l'expression générale d'une fonction à déterminer est la suivante :

$$F(X) = \sum \prod F_i(X_i)$$
$$X \in \mathbb{R}^n$$
$$F_i : \mathbb{R}^n \longrightarrow \mathbb{R}$$

Cette définition est récursive, c'est-à-dire que chaque fonction Fi peut être elle-même définie comme somme de produits de fonctions. Les fonctions terminales sont définies comme des polynômes multi-variables ou des fonctions tabulées multi-entrées. Chaque fonction Fi peut être identifiée séparément sur un sous-ensemble de la base de données.

Ce type de formulation est tout à fait adaptée à la représentation des coefficients aérodynamiques stationnaires. L'utilisation de fonctions tabulées permet en outre de modifier aisément le modèle, ou encore de l'enrichir si des informations complémentaires sont disponibles. Un coefficient de moment de tangage peut ainsi être défini comme :

$$Cm(\alpha, \beta, \delta m, q) = Cm1(\alpha,\beta) + Cm2(\alpha, \delta m) + Cm3(\alpha)qL/V$$

La représentation des phénomènes instationnaires est plus complexe. A l'étape de l'analyse de la donnée, certains aspects temporels (déphasage, retards) peuvent être mis en évidence. Si ces aspects s'avèrent directement liés à une variable d'entrée caractérisant la dynamique, (la variation d'incidence par exemple), sous l'hypothèse d'additivité des différents effets aérodynamiques on s'intéresse à la contribution purement instationnaire définie comme:

$$\Delta Ci_{dyn} = Ci_{global} - Ci_{stationnaire}$$

La quantité stationnaire pouvant être obtenue depuis un modèle stationnaire identifié au préalable. L'analyse par visualisation de cette quantité ΔCi_{dyn} en fonction des variables d'entrée permet de confirmer ou infirmer l'hypothèse d'additivité

La figure 16 illustre la validité de cette hypothèse pour la modélisation des caractéristiques longitudinales mesurées en rotation instationnaire. La structure est la suivante:

$$Ci_{global} = Ci(\alpha, \beta) + Ci(\alpha, q) + \Delta Ci_{dyn}$$
$$\Delta Ci_{dyn} = H(\alpha, sgn(\alpha),...) \, d\alpha/dt$$
$$H \quad \text{fonction de transfert}$$

Dans d'autres cas, l'analyse de la donnée suggère directement une structure de modèle. Une illustration en est donnée avec les essais réalisés sur le montage dynamique "PQR" (fig. 9) et déjà évoqués plus haut. La caractéristique statique du moment de lacet, avec sa dissymétrie provoquée par la présence d'une vrille sur la pointe avant se trouve décalée lorsque l'incidence varie rapidement. L'assimilation de ce comportement à un phénomène de retard conduit à proposer une structure de modèle de type:

$$Cn_{global} = H(\alpha, d\alpha/dt,...) \, Cn_{statique}$$

Une fonction de type filtre ou retard pur peut être choisie pour H.

3.2. Calcul des stabilités

La prévision du comportement de l'aéronef à grande incidence est un problème délicat. En effet, les équations de la mécanique du vol constituent un système complexe où apparaissent toutes les non-linéarités aérodynamiques, les hystérésis, les couplages longitudinal- latéral, inhérentes au vol post- décrochage. L'approche classique consistant à étudier le système linéarisé autour d'un point de vol n'est plus applicable.

La théorie des bifurcations des systèmes dynamiques non linéaires apporte à ce problème des éléments de réponse. Elle ne peut prédire le comportement exact de l'avion mais

permet le calcul des stabilités du système sur l'ensemble du domaine de vol.

Si la formulation générale des équations est

x' = f(x, u),
x vecteur d'état,
u vecteur des commandes,

La résolution numérique x'=0 fournit les surfaces d'équilibre du système. La stabilité en chacun de ces points est donnée par les valeurs propres de la matrice Jf matrice jacobienne de f. L'ensemble des points pour lesquels au moins une valeur propre a une partie réelle nulle est appelé ensemble des points de bifurcations. En projetant cet ensemble sur l'espace des commandes on obtient la surface de bifurcations. Cela signifie que si le système traverse cette surface, le nombre d'états d'équilibre possibles et leurs stabilités changent.

Cette technique, appliquée à l'étude du vol à grande incidence permet de déterminer les zones critiques du domaine de vol comme par exemple des équilibres très stables à grande incidence où les commandes sont peu influentes.

La figure 17 illustre une application réalisée à l'ONERA-IMFL sur un modèle d'avion d'armes [4]. Sur la surface d'équilibre projetée dans le plan (α, δl, δm) apparaissent les zones de vrilles et de tonneaux. La surface présente également un repliement dont les bords correspondent à des points de bifurcations. Le déplacement de la commande δl peut provoquer le passage brutal d'un mouvement de tonneau à un mouvement de vrille.

La théorie des bifurcations fournit donc une photographie des stabilités de l'avion à grande incidence. Elle constitue à ce titre un outil utile pour l'évaluation de lois de commandes. Les performances de ces lois se traduisent en particulier par la disparition des zones instables calculées dans le cas de l'avion muni de ces commandes "naturelles".

La technique des bifurcations ne fournit que des états d'équilibres asymptotiques qui sont théoriquement atteints au bout d'un temps infini. Dans la pratique les résultats des calculs de stabilités sont complétés par des simulations numériques du mouvement afin de fournir des indications sur les mouvements transitoires et sur l'ordre de grandeur du temps nécessaire pour passer d'un état d'équilibre à un autre.

3.3. Evaluation des performances

La comparaison entre deux aviors d'armes ou entre plusieurs formules géométriques s'effectue au travers de quantités appelées critères, représentatives de la capacité d'un aéronef à réaliser une manoeuvre donnée.

Aux grandes incidences les critères statiques habituellement utilisés sont généralement peu adaptés à qualifier toutes les manoeuvres envisageables notamment lors de phases transitoires, de changement d'attitude pour les manoeuvres de pointage, d'accélération ou de décélération.

Des notions nouvelles sont aujourd'hui introduites pour qualifier ces manoeuvres, telles la manoeuvrabilité, l'agilité, la maniabilité, la contrôlabilité,... Ces concepts visent à quantifier les capacités de modification de trajectoire (manoeuvrabilité), ou d'attitude (agilité). La maniabilité caractérise le faible temps de réponse à [illegible] sollicitations en roulis ou en tangage. D'autres critères [illegible] de simulations de combats aériens [illegible] le nombre d'opportunités de tirs, le [illegible] [3]...

Ces critères s'appliquent sur un modèle complet et représentatif de l'avion intégrant [illegible] particulier les caractéristiques des commandes de vol. Une évaluation préliminaire des performances [illegible] avant l'étape de conception des commandes de vol. Elle consiste à considérer l'avion en boucle ouverte et à évaluer la capacité aérodynamique à réaliser des manoeuvres types en supposant possible le calcul instantané de la commande idéale. Elle s'appuie sur des techique de simulations numériques du mouvement en boucle fermée.

3.3.1. Techniques de découplage des systèmes non linéaires

Cette approche de l'étude des systèmes non linéaires consiste à transformer un système comportant des couplages en un système partiellement découplé et se prêtant ainsi à la commande. Elle s'appuie sur des hypothèses quant à la formulation des équations du système:

x' = a(x) + b(x) u,
y = c(x)
z vecteur d'état,
u vecteur des commandes
y vecteur d'observation

Ce système suppose l'état linéaire vis-à-vis de la commande. Cette technique consiste à déterminer f(x) et g(x) telles que :

u = f + gw

de façon à ce que le système puisse s'écrire :

$$d^{(\alpha_i)} y_i / dt^{(\alpha_i)} = w_i,$$

w nouveau vecteur de commande.

Si cette détermination est possible, on obtient un système dont une partie observable est totalement découplée et de dimension égale à la dimension du vecteur de commande.

Cette technique peut être appliquée aux équations de la mécanique du vol. On caractérise une manoeuvre type par la poursuite d'objectifs donnés et définis en fonction du temps. La dérivation de ces objectifs fournit le nouveau vecteur de commande w et le système complet peut être intégré.

Ainsi une manoeuvre de pointage longitudinal pourra être caractérisée par l'évolution $\Theta(t)$ désirée et le maintien du vol symétrique (assiette latérale nulle, cap constant) et être obtenue a priori à l'aide des trois commandes conventionnelles de l'avion.

La capacité de l'avion à réaliser une telle manoeuvre est établie si l'on peut trouver les évolutions temporelles de la commande en respectant les limitations en débattement $[u_{min}, u_{max}]$ et en vitesse $(du/dt)_{max}$.

Cette technique peut être utilisée pour évaluer l'impact de paramètres sensibilisants (aérodynamiques, inertiels,...) sur la faisabilité de la manoeuvre. La sensibilité au paramètre modifié est directement liée à la modification des historiques

u(t) nécessaires pour poursuivre les objectifs fixés (fig. 18). Cette technique est rapide à mettre en oeuvre et donne des résultats intéressants dans la mesure où l'on compare des configurations géométriques relativement proches et que les trajectoires x(t) pour chacune d'elles sont peu différentes [8] [9].

3.3.2. Techniques d'optimisation de trajectoires

Dans le cas de la comparaison de formules géométriques plus différenciées, l'approche précédente ne peut s'appliquer. La technique d'optimisation de trajectoires consiste à définir une manoeuvre à partir de ses états initial et final, un ensemble de contraintes courantes ou finales à respecter et à déterminer par les algorithmes appropriés la trajectoire répondant à ces conditions. Le critère peut être défini comme le temps minimum pour réaliser la manoeuvre. Cette méthode s'adapte à tous types d'engins, puisque la meilleure trajectoire est calculée pour chacun d'eux.

La figure 19 illustre une application réalisée à l'ONERA [11]. La manoeuvre considérée est une manoeuvre de pointage longitudinal à 60°. Dans le premier cas, l'incidence de l'avion est limitée à 45°, dans le second à 50°. Un gain de temps de 30 % est ainsi obtenu en relachant la contrainte sur l'incidence.

Cette technique est optimale au sens où elle exploite pleinement le potentiel de l'avion pour réaliser un objectif donné dans un temps minimum. Elle est en revanche plus lourde à mettre en oeuvre et d'autant plus coûteuse en temps machine que le système est de dimension importante. Elle se combine aussi avec la méthode précédente puisqu'elle fournit une trajectoire optimale de référence autour de laquelle une étude de sensibilité peut être menée.

4. LES OUTILS DE VALIDATION

L'étude du comportement d'un aéronef à grande incidence conduit au travers des différentes étapes précitées (caractérisation en soufflerie, modélisation aérodynamique, étude des stabilités, simulations numériques) à établir des prévisions de comportement.

En raison de la dynamique caractérisant les évolutions à grande incidence, les aspects transitoires prennent une place prépondérante dans les prévisions. Ces transitoires ne peuvent être reproduits et caractérisés en amont par des essais en soufflerie en raison des limitations cinématiques de ceux-ci. La prévision est donc au travers une simulation numérique le résultat lié à une aérodynamique extrapolée depuis des essais statiques et dynamiques élémentaires. Seuls les essais en vol sont en mesure de valider ces phases transitoires.

L'ONERA-IMFL dispose de moyens d'essais en vol de maquettes d'avion adaptés pour l'étude de certains mouvements transitoires. Ce sont la soufflerie verticale et un laboratoire de vol libre.

4.1. La soufflerie verticale

La soufflerie verticale est traditionnellement le moyen d'essai spécifique à l'étude de la vrille sur maquette. L'équilibre entre les forces de gravité et les forces aérodynamiques dues au vent ascendant permettent en effet une observation aisée des comportements d'une maquette en mouvement hélicoïdal. Le respect des conditions de similitude de Froude (masse et inerties maquette) permet dans la plupart des cas une extrapolation des résultats à l'avion échelle 1.

L'ONERA-IMFL s'est doté de moyens supplémentaires pour l'exploitation quantitative des essais en vol en soufflerie. Un dispositif mécanique appelé lanceur permet de donner à la maquette des conditions initiales de vol en attitude et en rotation réglables et parfaitement répétables. La maquette est équipée de capteurs accélérométriques dont les mesures sont acquises et stockées sur des mémoires embarquées puis relues en fin d'essai.

Deux systèmes trajectographiques fixes sont installés dans la soufflerie. L'un d'eux est constitué de deux bases photographiques synchronisées, fournissant par traitement les attitudes de la maquette. Le second est constitué de quatre caméras placées dans le collecteur de la soufflerie. L'analyse des images vidéo permet de repérer et d'identifier des marqueurs situés sur la maquette. Un traitement spécifique fournit les attitudes et la position du C.G. de la maquette à tout instant.

L'exploitation de l'ensemble des mesures disponibles conduit à la restitution du vecteur d'état et des coefficients aérodynamiques globaux au cours du temps. La figure 20 illustre une application de l'exploitation d'essais en vol de vrille sur un avion d'armes. Les coefficients globaux restitués sont comparés à ceux calculés à partir d'un modèle aérodynamique identifié dans cette même soufflerie depuis des essais sur balance rotative. Cette comparaison montre le bon recoupement dans la zone correspondant à la vrille stabilisée et peu perturbée. Elle montre aussi les limitations du modèle pour représenter le mouvement transitoire entre les conditions initiales (incidence 90°) et la vrille établie (incidence 40°).

La soufflerie verticale se prête également à la représentation de mouvements plus marginaux comme la manoeuvre d'abattée ou tumbling. L'étude consiste à analyser la dynamique de tangage à laquelle est soumise l'avion suite à une montée en attitude verticale et à l'annulation de la vitesse aérodynamique. En soufflerie la maquette est initialement placée en incidence négative puis est lachée dans le vent. L'analyse des signaux embarqués permet d'évaluer le facteur de charge affectant la structure de l'avion [10].

4.2. Le laboratoire de vol libre

La nécessité d'approcher par des essais en vol des manoeuvres dynamiques sur des trajectoires plus tendues que celle réalisables en soufflerie verticale ont conduit l'ONERA-IMFL à moderniser une station d'essais en vol en laboratoire.

Cette installation a pour vocation à l'origine l'étude de la perte de contrôle et l'entrée en vrille d'une maquette à partir du vol normal à faible incidence. A cette fin une maquette d'avion est mise en vitesse, portée par un chariot mobile montée sur une catapulte. Puis elle est laissée libre de voler dans un volume autorisant une évolution de type hélicoïdal le long d'une trajectoire parabolique (fig. 21).

Des améliorations ont porté sur le dispositif de mise en

vitesse de la maquette et les outils trajectographiques. Elles permettent la restitution complète de l'état aérodynamique pendant le vol.

Ce moyen peut reproduire certaines manoeuvres dynamiques comme le pointage longitudinal à grande incidence, ou valider l'action de gouvernes nouvelles comme les virures d'avant-corps.

Manoeuvre de pointage longitudinal. Ce moyen a été utilisé pour étudier la dynamique de tangage à grande incidence sur une géométrie delta canard [6]. Une maquette, instrumentée et équipée de commandes sur les gouvernes de profondeur (élevons et canards) est tirée avec des conditions initiales de vol équilibré en portance, mais déséquilibrée en tangage de façon à monter rapidement en incidence. Au bout d'un temps de vol d'une demi-seconde les gouvernes sont braquées à piquer pour permettre la récupération du vol normal.

La restitution des essais conduit à caractériser les évolutions de l'incidence et de la vitesse de tangage lors de telles manoeuvres, pour différentes lois de braquages de gouvernes (fig. 22). Elle a permis de mettre en évidence la portance instationnaire. En revanche des comparaisons des coefficients aérodynamiques restitués avec ceux calculés depuis un modèle identifié sur balance rotative ont montré des écarts liés à une représentation inadéquate des phénomènes instationnaires développés en mouvement de dynamique de tangage.

Manoeuvre en lacet à grande incidence. Dans le cadre de l'étude des virures d'avant-corps on a abouti à la réalisation d'essais en vol de maquette pour valider ce concept. Dans ce but, une maquette représentative d'un avion d'armes de formule delta canards a été équipée d'une centrale gyrométrique et d'une commande de rentrée des virures d'avant-corps.

La maquette est tirée dans des conditions initiales d'équilibre longitudinal à incidence élevée correspondant à la zone d'efficacité des virures. Des essais ont été effectués pour différents historiques des positions des virures. La figure 23 illustre l'évolution du moment de lacet au cours du vol dans les deux cas suivants: virures rentrées, virures sorties. La dissymétrie naturelle du moment de lacet (virures rentrées) conduit la maquette à dépointer à gauche ($r<0$). La présence des deux virures sorties en permanence permet de symétriser les écoulements tourbillonnaires générés à la pointe avant, le vol demeure sensiblement symétrique.

Sur cette même figure deux autres cas sont présentés. La maquette est tirée virures sorties, puis au bout d'un temps assez court l'une ou l'autre virure est rentrée. L'effet sur le mouvement en lacet est immédiat. La rentrée de la virure gauche (resp droite) induit un virage à gauche (resp droite). La vitesse de lacet évolue de façon linéaire dans le sens attendu conformément aux essais en soufflerie.

5. CONCLUSION

L'ONERA-IMFL dispose d'outils contribuant à l'étude des comportements des avions d'armes manoeuvrant à grande incidence.

Des montages de simulation dynamique en soufflerie permettent de caractériser l'aérodynamique stationnaire et instationnaire à basse vitesse lors de sollicitations en roulis aérodynamique et en dynamique de tangage.
L'analyse de la donnée et la modélisation aérodynamique est facilitée par utilisation de logiciels spécifiques.
L'emploi des techniques d'analyse des systèmes dynamiques non linéaires conduit à la détermination des cartes de stabilité de l'aéronef dans tout le domaine de vol ainsi qu'à l'évaluation de performances de manoeuvres.
La validation des prévisions de comportement est réalisée par des essais en vol de maquette en soufflerie verticale ou en laboratoire.

Ces outils ont été utilisés pour l'étude du contrôle en lacet à grande incidence par des gouvernes de pointe avant. La robustesse du concept de virures d'avant-corps vis-à-vis de sollicitations dynamiques a été mesurée en soufflerie. Des essais en vol de maquette ont validé les comportements prévus.

Dans le cadre des études relatives à la prévision des comportements des avions hautement manoeuvrants il convient de considérer:

- le besoin d'évolution des outils expérimentaux. Les montages de simulation dynamique doivent être capables de mouvements approchant davantage les trajectoires réelles du vol pour être représentatifs de l'aérodynamique instationnaire. Ces outils doivent être également bien identifiés au plan des interactions maquette- montage, problème sensible sur les montages de simulation sophistiqués. Le groupe de travail AGARD WG16 sur les balances rotatives contribue à cette évaluation ;

- la complémentarité de l'approche aérodynamique (reconnaissance des écoulements, visualisations des tourbillons, cartes de pression...) pour une meilleure compréhension des phénomènes décrochés et faciliter la modélisation ;

- la difficulté de modéliser certaines caractéristiques instationnaires (les coefficients latéraux en particulier) ;

- l'intérêt des gouvernes nouvelles basées sur le contrôle de tourbillons ;

- le nécessaire rebouclage entre les différentes étapes (caractérisation, analyse et modélisation, prévisions et validation) et en particulier avec les essais en vol échelle 1, seul moyen de vérifier la validité des prévisions établies à partir de données de soufflerie à plus faible nombre de Reynolds

- la stratégie à adopter vis-à-vis de l'intégration de commandes de vol dans des essais au sol.

REFERENCES

1. G. N. Malcom "Forebody Vortex control" in "Aircraft dynamics at high AOA: experiments and modelling" AGARD Report n° 776 Paper 6

2. O. Renier "Characterization of unsteady aerodynamic phenomena at high AOA" in "Manoeuvring dynamics" AGARD CP 497, May 1991, Paper 11

3. F. Bournonville , L. Planckaert "Evaluation des performances des avions" Rapport ONERA-IMFL n°92/23

4. "Rotary Balance Testing for Aircraft Dynamics" AGARD AR 265 pp 189-191

5. F. Descatoire "Supermanoeuvrabilité des avions de combat: Etude de corps simples en écoulement hélicoïdal à grande incidence" Rapport ONERA-IMFL n° 87/64

6. J.L. Cocquerez, O. Renier, P. Simon, C. Hugon "Manoeuvrabilité des avions d'armes à grande incidence. Essais de la maquette du Mirage 2000 avec canards dans la stations B5" Rapport ONERA-IMFL n° 91/28

7. O. Renier "Manoeuvrabilité des avions d'armes à grande incidence (IV)" Rapport ONERA-IMFL n°92/35

8. F. Descatoire, O. Renier, L. Planckaert, C. Hugon "Manoeuvrabilité des avions d'armes à grande incidence (III)" Rapport ONERA-IMFL n°90/68

9. C. Delaval, F. Descatoire , O. Renier "Travaux relatifs à la manoeuvrabilité des avions d'armes à grande incidence" Rapport ONERA-IMFL n° 90/13

10. F. Descatoire , O. Renier, "Travaux relatifs à la supermanoeuvrabilité des avions d'armes" Rapport ONERA-IMFL n° 89/16

11. M. Do Khac P. Guicheteau "Mécanique du vol à grande incidence. Prédiction de la perte de contrôle, lois de commande et optimisation de manoeuvres" Rapport ONERA RT 49/5148 SY

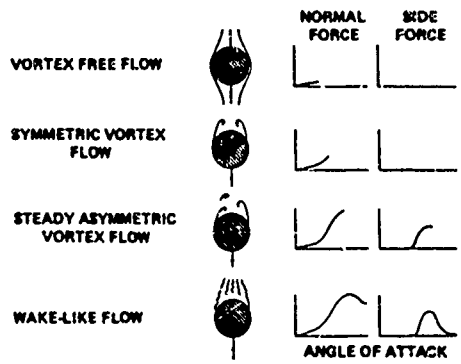

Fig1. Les différents régimes tourbillonnaires sur une configuration ogive- cylindre en incidence [1]

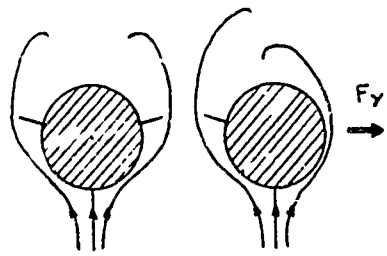

Fig2. Influence des virures de pointe avant sur le développement des tourbillons de pointe avant

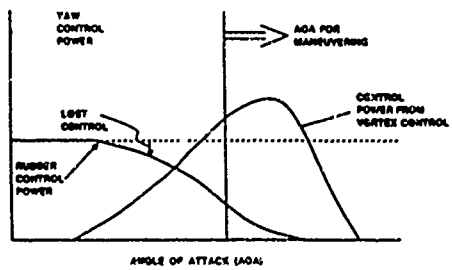

Fig3. Illustration du potentiel de contrôle en lacet des virures d'avant corps.

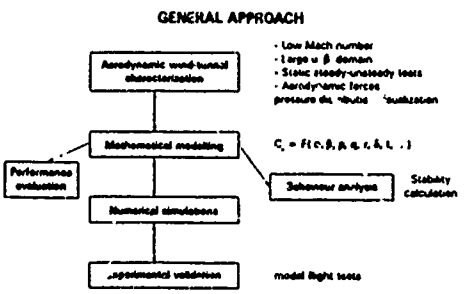

Fig4. Démarche générale d'étude des grandes incidences à l'ONERA-IMFL

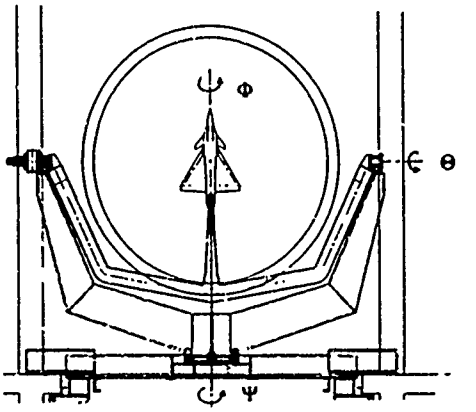

Fig5. Coupe du montage dynamique de soufflerie "POR

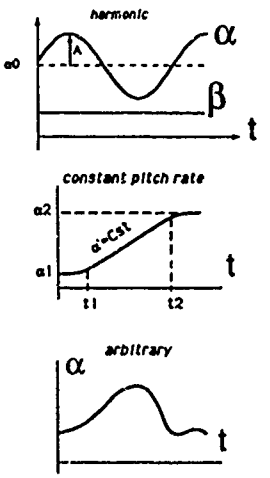

Fig6. Les différents essais dynamiques réalisables sur le montage "POR"

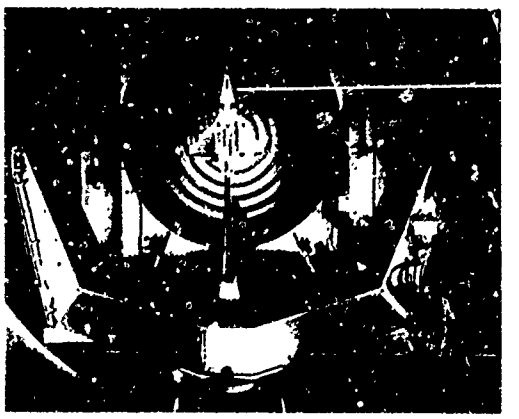

Fig7. Maquette de l'avion Rafale sur le montage "POR"

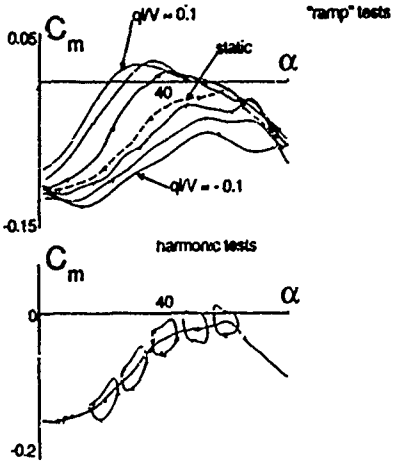

Fig8. Effets des variations d'incidence sur la stabilité en tangage. Essais harmoniques (f°=.05) et essais de type rampe (/q°/<.1)

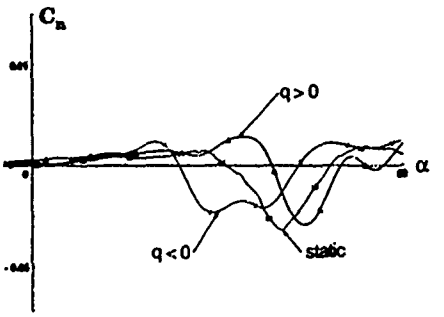

Fig9. Influence de la variation d'incidence sur le moment de lacet(q°=t°»±.03)

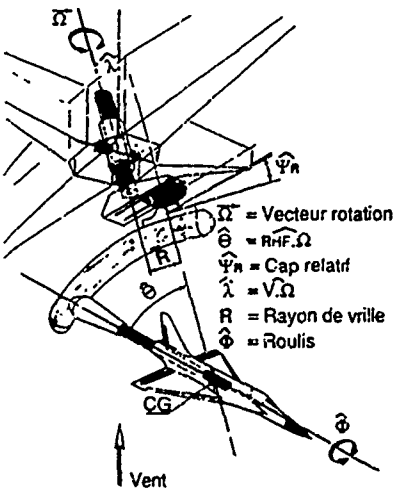

Fig10. Cinématique de la balance rotative de l'ONERA-IMFL

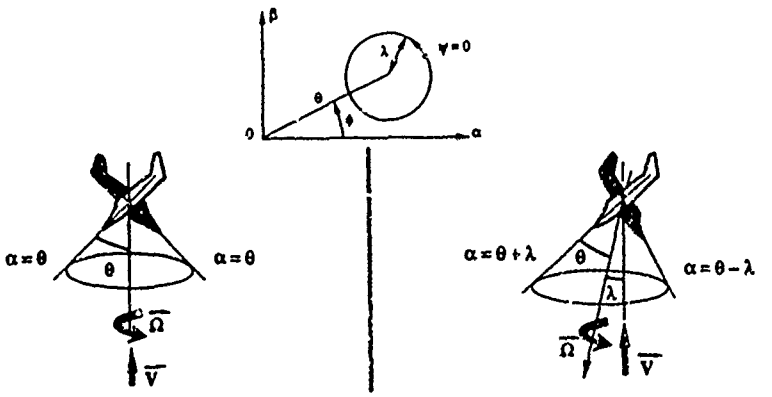

Fig11. Essais dynamiques réalisables sur la balance rotative: essais coniques et coniques oscillatoires

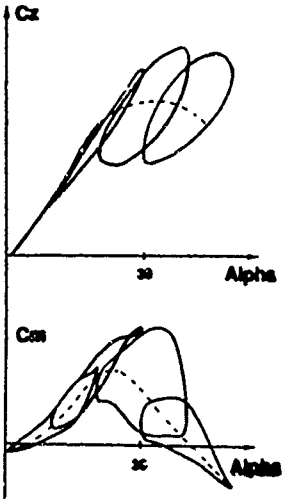

Fig12. Caractéristiques longitudinales mesurées en rotation conique oscillatoire

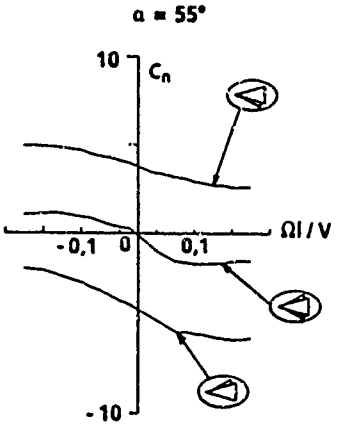

Fig13. Amortissement en roulis aérodynamique CnΩ. Influence des virures de pointe avant.

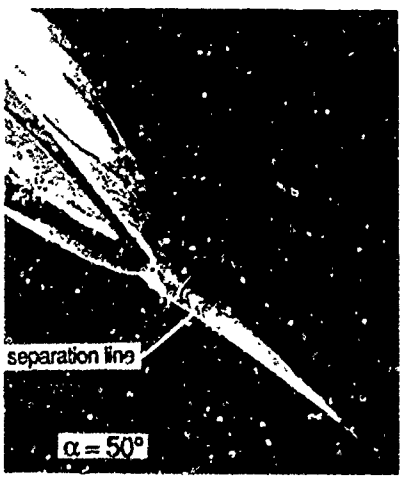

Clean forebody

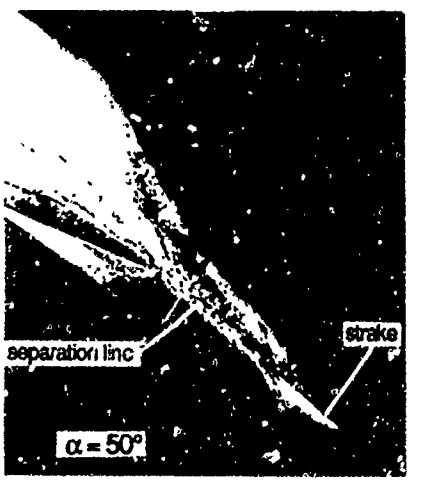

Forebody equiped with
a single right hand side strake

Fig14. Visualisation de l'écoulement pariétal par enduit visqueux. Influence des virures sur la position des lignes de décollement

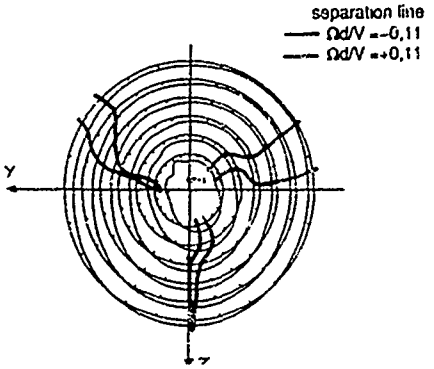

Fig15. Cône équipé de prises de pressions pariétales sur balance rotative. Cartes des pressions aux cours d'essais en rotation stationnaire

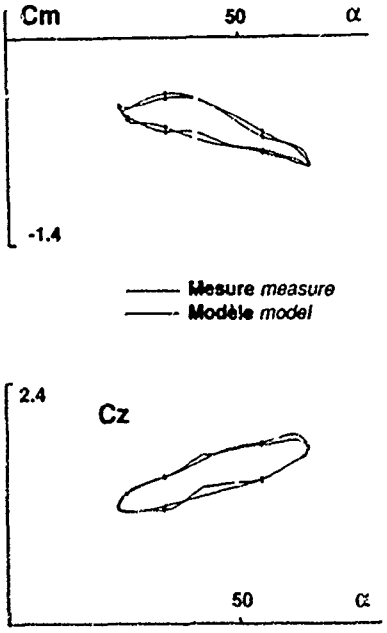

Fig16. Comparaison modèle mesure sur un essai conique oscillatoire

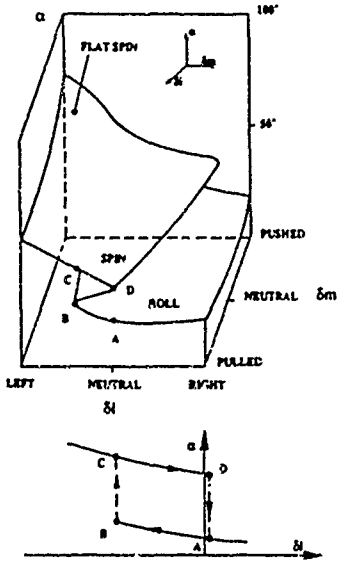

Fig17. Surface des équilibres à grande incidence dans l'espace (α,δl,δm)[4]

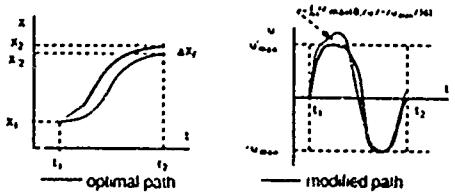

Fig18. Application des techniques de découplage de systèmes. Evaluation de la sensibilité d'une manoeuvre à des variations du modèle

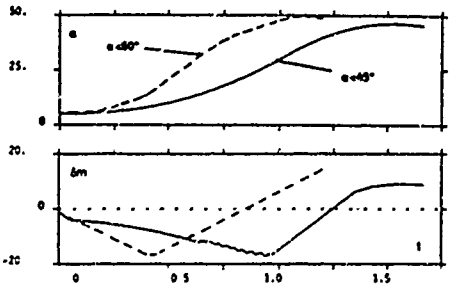

Fig19. Techniques d'optimisation de trajectoires. Application à une maneuvre de pointage longitudinal.

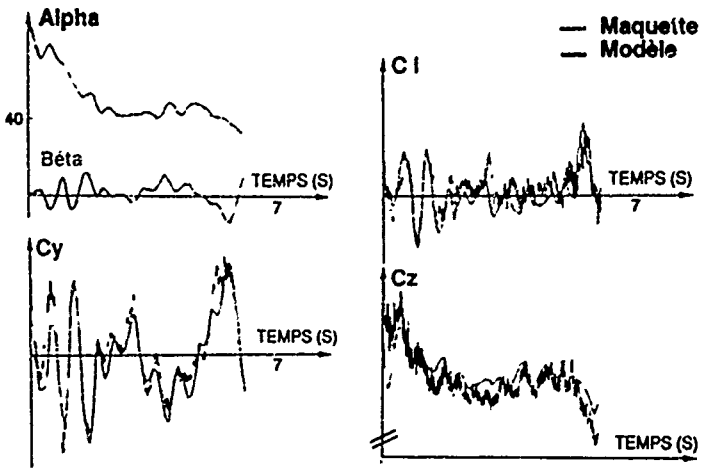

Fig20. Restitution d'essais en vol en soufflerie verticale. Comparaison modèle mesure.

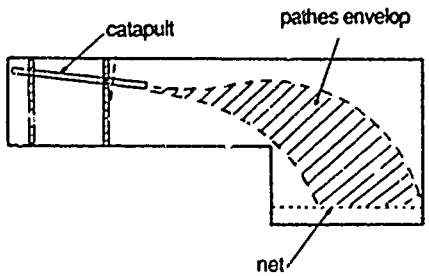

Fig21. Laboratoire d'essais en vol de maquettes

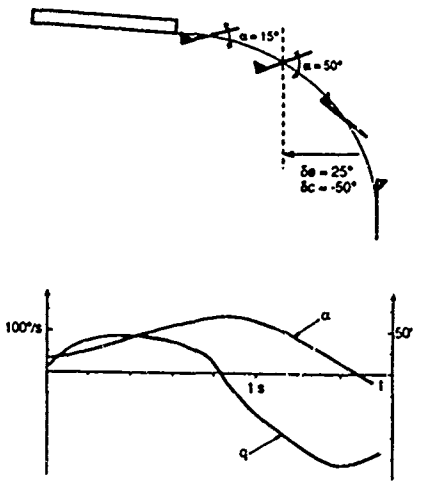

Fig22. Essais en vol de maquette. Manoeuvre de pointage longitudinal.

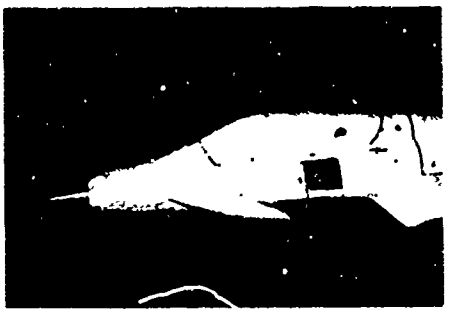

Fig24. Maquettes d'avion d'armes équipée de virures rétractables

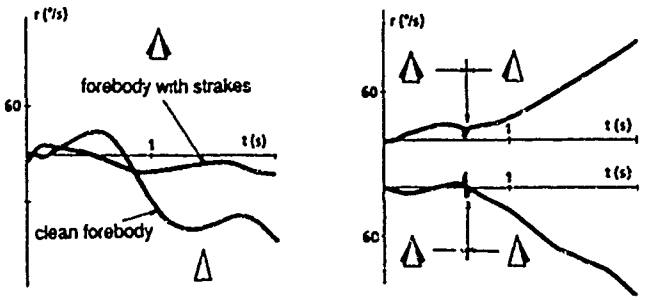

Fig23. Essais en vol de maquette. Valiation de l'effet des virures de pointe avant sur le moment de lacet.

Yaw Control by Tangential Forebody Blowing

N J Wood and W J Crowther
School of Mechanical Engineering
University of Bath
Bath, Avon BA2 7AY, UK

SUMMARY

Aircraft yaw control at high angles of attack by tangential forebody blowing has been investigated experimentally. Tests were performed in the University of Bath 2.1mx1.5m low speed wind tunnel using an approximately 6% scale generic combat aircraft model fitted with blowing slots in the nose cone. Six component strain gauge balance force and moment data was measured for angles of attack up to 90° for various slot geometries and locations. The effect of slot azimuthal location is demonstrated and a slot stall phenomenon described. A geometry dependent forebody/wing flow-field coupling has been identified which can lead to unexpected yawing and rolling moments. The primary source of yawing moment is shown to be the enhanced area of attached flow on the blown side of the forebody rather than direct vortex influence.

The optimum slot extent and location depend on the angle of attack range over which control is required. For regions where steady vortex asymmetry is present, slots near the apex of the forebody produce severe control reversals at low blowing rates which can be minimised by placing the slots away from the apex. For control in regions where the flow is dominated by periodic vortex shedding long slots offer efficient control to 90° angle of attack. The most suitable compromise for wide range control would appear to be a short slot placed away from the apex of the forebody.

SYMBOLS

b	Wing Span (0.66m)
C_L	Rolling Moment Coefficient (L/(qSs))
C_N	Yawing Moment Coefficient (N/(qSs))
C_Y	Side Force Coefficient (Y/(qS)
C_μ	Jet Momentum Coefficient ($mV_j/(qS)$)
l	length of slot
L	Rolling Moment (+ve port wing up)
m	Jet mass flow
N	Yawing Moment (+ve nose to starboard)
q	Free stream dynamic pressure
S	Wing reference area ($0.15m^2$)
s	Wing semi-span
V_j	Jet Exit Velocity
x	location of upwind end of jet
Y	Side Force (+ve to starboard)
α	Angle of attack
θ	Slot azimuthal location

INTRODUCTION

Aircraft able to manoeuvre freely at high angles of attack exhibit a number of potential advantages over aircraft with more limited flight envelopes. Enhanced turn performance and the ability to perform prolonged manoeuvres at high pitch and sideslip angles are examples of possible improvements. Rapid heading reversal is such a manoeuvre and significant reductions in the execution time have been demonstrated as a function of the angle of attack limit[1].

Flight at high angles of attack does introduce additional complexity into the flowfield around the aircraft and the flow is often separated and unsteady. This results in a reduction of the effectiveness of conventional moving surface controls and a susceptibility to lateral oscillations and divergence[2]. In particular, instabilities associated with the steady vortex pair emanating from the forebody of the aircraft may result in a destabilising yawing moment of significant magnitude (nose-slice). In many instances, the resulting moments from forebody vortex asymmetry are larger than the restoring control power available from the rudder. Thus to maintain lateral control authority at high angles of attack it is necessary to develop alternative methods for the generation of yawing moment.

Since it is the forebody vortex asymmetry which is the cause of this characteristic, it is logical to attempt to correct the instability by direct control of the forebody flow. This has been the focus of a number of related research programmes. It is also important to understand the nature of the flow to be controlled and it's dependence on angle of attack, figure 1. At low to moderate angles, the flow is stable and symmetric. As the angle of attack increases, a steady asymmetry may appear both in the vortex positions and the location of the crossflow separations and a strong yawing moment may be produced. Further increases in angle of attack produce a flow which is unsteady but generally periodic as evidenced by the alternate shedding of the forebody vortices. Under these conditions, the time-averaged yawing moment will return to zero and the nose-slice instability disappears. It is this higher angle of attack range which offers many potential improvements in manoeuvre envelope and therefore any control device must be capable of generating

Presented at an AGARD Meeting on 'Technologies for Highly Manoeuvrable Aircraft', October 1993.

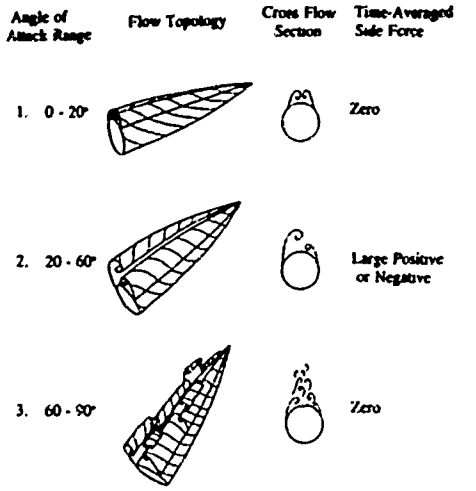

Figure 1: Flow Field Regimes for a Slender Body at Incidence.

yawing moments in regions of either steady vortex asymmetry and/or periodic vortex shedding.

The control of forebody vortices by mechanical or pneumatic devices has been the subject of a number of recent research programmes[3]. Many of the mechanisms offer high potential control gain over certain regions of the flight envelope but reduce in effectiveness in the region dominated by periodic shedding. It is the intent of this programme to investigate the generation of yawing moment over a wide range of angles of attack by the application of tangential forebody blowing. It is important to differentiate between vortex control and flow control techniques since vortex control in itself is generally insufficient to produce yawing moments over the entire range of angles of attack.

Tangential Forebody Blowing (TFB)

Examination of typical pressure distributions around a forebody in the range of angle of attack where asymmetric vortices are present shows that the majority of the out of plane moment arises from the differential attached flow around the forebody. Since the vortices themselves act more directly on the upper surface of the forebody, they are only important in maintaining the asymmetric equilibrium which produces the differential locations of the separation lines. Mechanical strakes provide a very effective mechanism for correcting forebody vortex asymmetry[4] but then consequently are only able to provide limited controlled asymmetry. Discrete air jets[5] have the disadvantage of requiring knowledge of the vortex location for optimum operation and are therefore relatively ineffective in generating control power.

TFB is essentially different from other forms of forebody flow management in that direct control is exerted on the forebody cross flow separation lines and the presence of a vortex is not strictly necessary for the production of control forces. Since the majority of the control moment results from the attached flow around the forebody it is expected that TFB will be effective in not only controlling the asymmetry but also in subsequently controlling the moment. The tangential mass injection is also able to suppress the unsteady shedding since the separation points become dependent primarily on the wall jet attachment and are relatively insensitive to cross flow instabilities. Thus it is likely that TFB will be able to exert control through the angle of attack range including that where periodic shedding is present, beyond 60°.

The concept of TFB is based on the phenomenon of Coanda jet attachment to convex surfaces. Curvature of the surface enhances the entrainment of the external fluid and accelerates the transfer of momentum from the jet to the surrounding flow and as a result, separation of the outer flow is suppressed. Previous examples of the application of curved wall jets to flow control include circulation control aerofoils[6], blown trailing edge flaps[7] and more recently the control of vortical flows over delta wings[8].

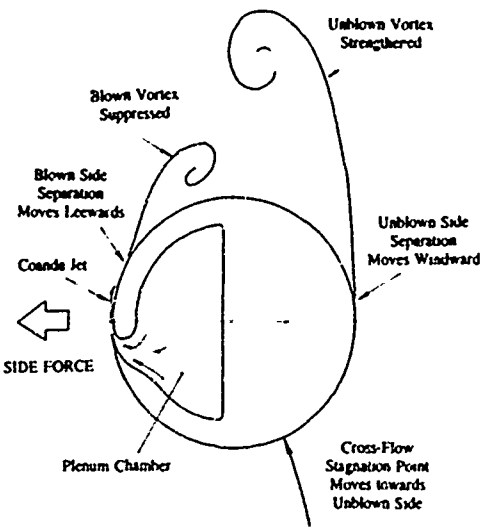

Figure 2: Fluid Mechanism for Tangential Forebody Blowing.

The present application to the control of forebody flows is presented as figure 2. For a simple circular

forebody section, the addition of jet momentum delays the flow separation on that side, reduces the adjacent vortex strength and relocates it closer to the leeward surface. This motion of the adjacent vortex causes the opposite vortex to move away from the surface and to strengthen. Subsequently, the opposite separation points must move to windward enhancing the induced side force. In addition, the stagnation point moves towards the unblown side representing a form of circulation in the crossflow plane. Thus the production of side force/yawing moment on a forebody is not dissimilar to the control of circulation on conventional elliptic aerofoils. The primary source of yawing moment has been shown to be the modified area of attached flow rather than modified vortex influence.

The present research intends to investigate the mechanisms by which yaw control may be developed over a wide range of angles of attack (up to 90°) using TFB and to identify factors affecting the efficiency of such a device.

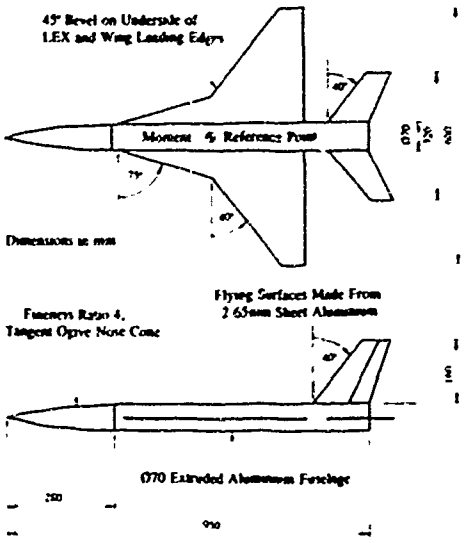

Figure 3: Wind Tunnel Model.

EXPERIMENTAL APPARATUS

The wind tunnel model is shown in figure 3. The configuration was determined through a parametric study of current combat aircraft shapes, with an emphasis on establishing a simplified but representative forebody and wing geometry.

The basic components of the model are a 70mm diameter extruded aluminium fuselage, 2.65mm thick aluminium sheet flying surfaces and a fineness ratio 4 tangent ogive nose cone made from vacuum formed plastic. The model is modular in design permitting a variety of wing planforms to be evaluated. A cross section through the nose cone is shown in figure 4. The length of the slot can be varied by partitioning off sections with adhesive tape and the slot height can be varied by adjusting screws set a small distance in from the slot lip. Slot angular position is varied by rotating the whole nose cone assembly relative to the fuselage.

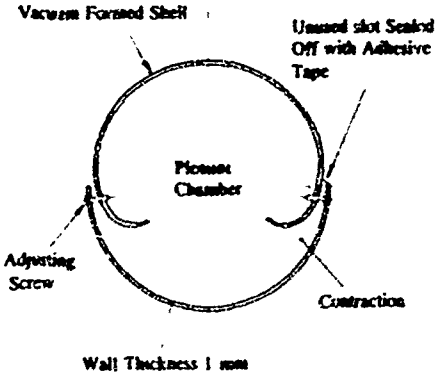

Figure 4: Cross Section through Vacuum Formed Nose Cone.

Three different nose cones were manufactured. For slot azimuthal location tests, a nose cone with a single slot on the port side and another with a slot on the starboard side were fabricated. When the optimum slot azimuthal location had been determined, a further nose cone was made with slots on either side, at the optimum location.

The wind tunnel model was mounted on a pantograph high angle of attack mechanism capable of 0 to 90° in pitch. Forces and moments were measured on a 6-component sting balance (kindly loaned by DRA Farnborough) mounted within the model near the centre of gravity. The moment reference point is shown on figure 3. The data acquisition system was fully automated and acquired balance data at 1000Hz. A sample period of 1 second was averaged to provide mean force and moment results. Repeatability on force and moment coefficients was shown to be well within 5%.

Throughout this work a non-dimensional momentum coefficient, C_μ has been used to present the effect of blowing on the model forces and moments. Unlike equivalent mass flow parameters, momentum has been shown to provide the best collapse of results which include variations of both slot geometry and free stream conditions. For fixed slot geometry and

incompressible flow either parameter may be used with equal effectiveness.

Jet flow parameters were derived from measurements of supply volume flow rate and plenum static pressure. This removes slot area from the parameter determination calculations and thus allows for variations in slot discharge coefficient and minimises the effect of any slot distortion at different plenum pressures. Unless otherwise stated, a slot 240mm long starting 30mm from the forebody apex was used.
The off-body velocity contours were obtained from an Aerometrics® two component laser anemometer. A 1m focal length transmitter provided a fringe spacing of 8 microns and water droplets produced from a commercially available automobile paint spray gun provided copious amounts of 4 micron seed. A Doppler Signal Analyzer (DSA®) was used to analyze the output signals and averages of 1000 validations were used to produce mean and rms velocities.

RESULTS AND DISCUSSION

All results presented were obtained at a Reynolds number of 1.5×10^6 per metre.

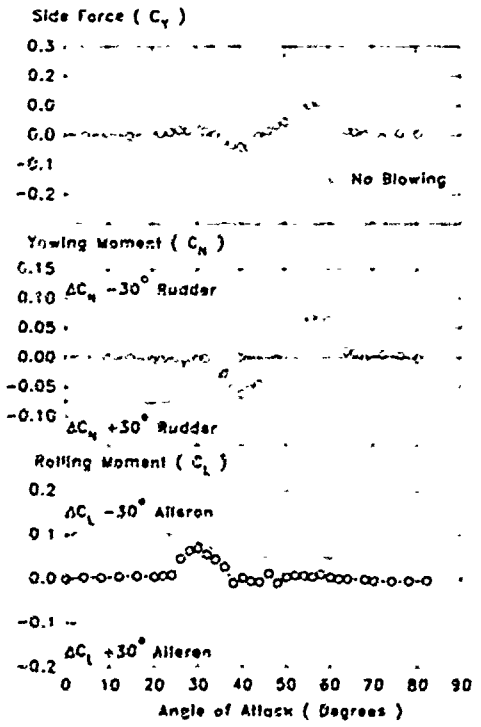

Figure 5. Unblown Force and Moment Data.

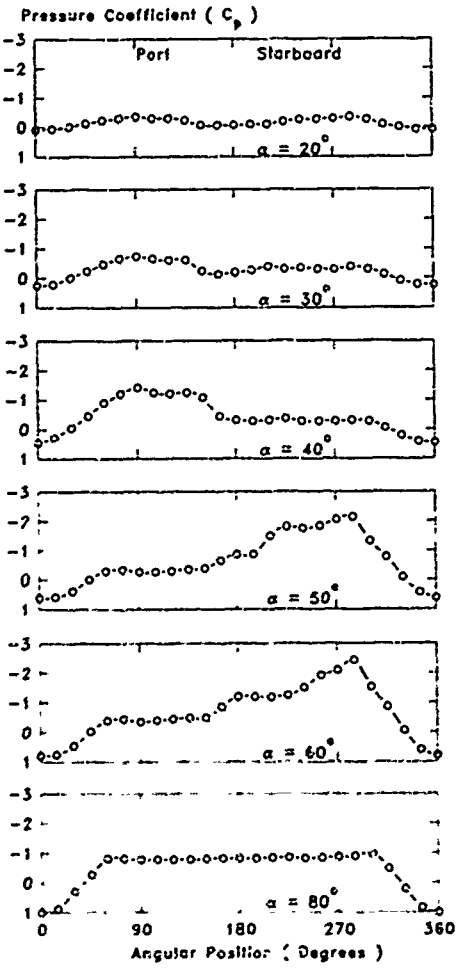

Figure 6: Unblown Pressure Distributions around Forebody.

Baseline Unblown Data

Unblown sideforce, rolling moment and yawing moment data is shown in figure 5. The results can be correlated with three types of vortex configuration. For angles of attack up to 25° the vortices are steady and symmetric resulting in zero lateral forces and moments. Between 25° and 60° a steady asymmetric vortex patterns appears. The yawing moment data exhibits the classic nose-slice response to steady asymmetric vortices at around 35° angle of attack and a reversal at 48° as the vortex pair switches to a mirror image configuration. Pressure distributions around the forebody clearly show this reversal of the vortex asymmetry, figure 6. Note that above 35° angle

of attack the destabilising moments generated by the forebody flow asymmetry are larger than the restoring moments available from the rudder. Beyond 60° the flow is dominated by periodic vortex shedding and the time-averaged lateral forces and moments return to zero.

The rolling moment is zero apart from regions between 20° and 35° and around 45°. Flow visualisation studies have shown that these regions mark the extent of a region in which the forebody and LEX flowfields are coupled and that asymmetric forebody vortices result in asymmetric bursting of the LEX vortices, figure 7. The resulting asymmetric pressure distributions, primarily on the LEX, produce the observed rolling moments. The magnitude of this coupling has been shown to be somewhat dependent on the wing planform and in particular the presence of the LEX.

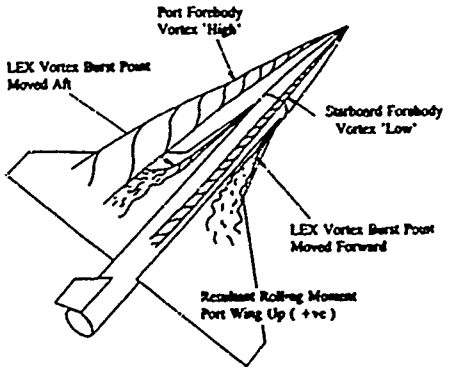

Figure 7: Diagram of LEX/Forebody Vortex Coupling taken from Flow Visualisation.

Blown Force and Moment Data

The effects of blowing are shown in figure 8 for fixed blowing momentum. Unless otherwise stated, all results are for the longest slot configuration starting at the apex and at the 90° azimuth location. A key feature of the data is the presence of a non-linear yawing moment response at 20° angle of attack at the initiation of the forebody/LEX coupling. Note that in this region, port side blowing produces a negative rolling moment and vice versa. This is consistent with a forward motion of the blown side LEX vortex burst location and an opposite, aft motion on the unblown side. A similar phenomenon has been reported by Gee et.al.[9] from numerical studies of forebody slot blowing on an F-18 configuration.

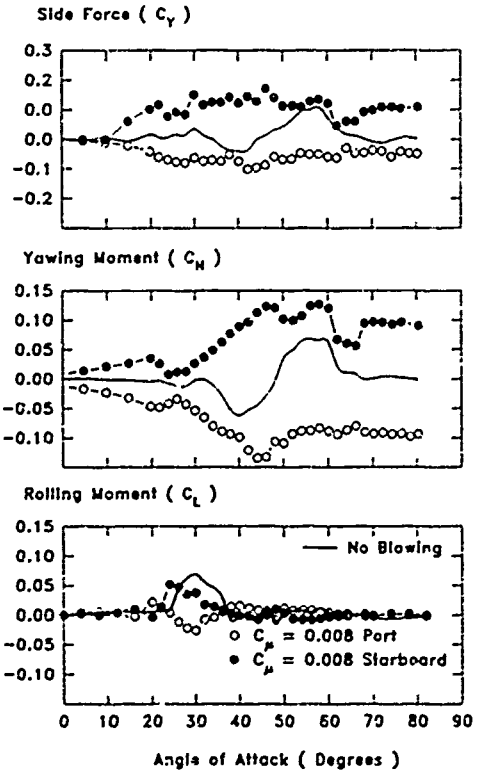

Figure 8: Blown Force and Moment Data.

Figure 9 shows the response to varying blowing momentum at fixed angles of attack. Generally, port side blowing produces a nose-to-port (negative) yawing moment and starboard side blowing a nose-to-starboard (positive) yawing moment. However, at low blowing rates, a control reversal appears in the angle of attack region where steady vortex asymmetry has been observed. This phenomenon is associated with a reversal of the intended fluid response to increasing blowing momentum. At very low blowing levels, the blown side separation point moves towards the windward generator resulting in reduced areas of attached flow and a strengthened blown side vortex. The mechanisms which cause this reversal are unclear but it is possible to note some observations.

(i) The sign of the unblown vortex asymmetry does not affect the resulting control reversal.

(ii) Since the wall jet separation is dominant compared to the external boundary layer it is possible for the jet to precipitate premature separation. Thus the slot azimuthal location could be important in producing the reversal.

(iii) The presence of vortices generated at the ends of the blowing slots may contribute to a change in the crossflow equilibrium which requires the forebody vortices, and hence the separation points, to relocate.

(iv) The control reversal is only apparent in the angle of attack range at which the vortices are steady and asymmetric.

(v) The longitudinal slot location will be shown to minimise the control reversal.

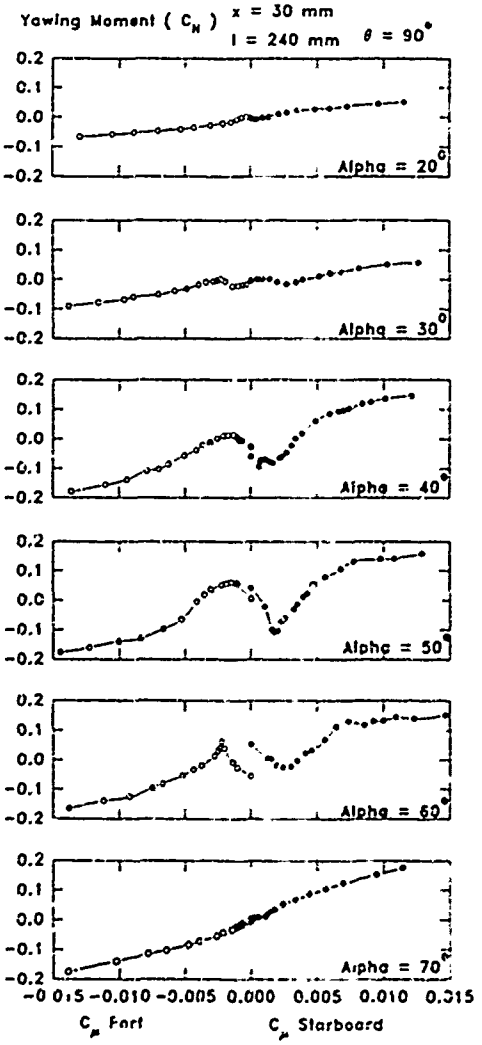

Figure 9: Blown Control Response at Increasing Angle of Attack.

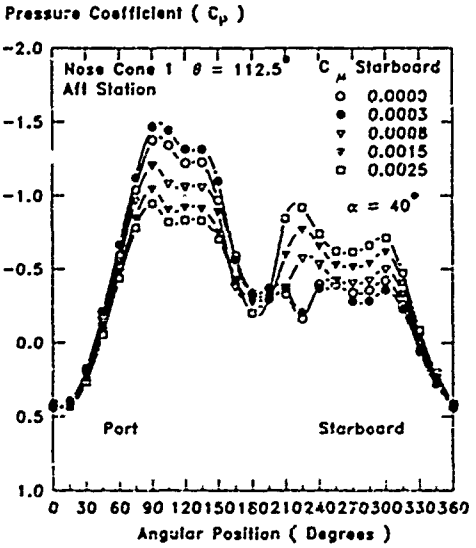

Figure 10: Pressure Distributions around the Forebody for low Blowing, $\alpha = 40°$.

Figure 10 shows pressure distributions around the forebody at conditions which exhibit control reversal and show the increased suction on the unblown side. It is difficult to identify the motions of the separation locations from these distributions but the sensitivity of the yawing moment to those locations may be inferred. Note that the blowing momentums shown are restricted within the region of control reversal.

Recognising that the primary source of yawing moment from slot blowing is due to increased regions of attached flow on the blown side, it is possible to represent the yawing moment response to increasing blowing momentum as the sum of two separate contributions, figure 11. The first order response is to delay separation on the blown side. The degree to which this can produce yawing moment is limited by the contraction of the attached flow region due to jet end effects and the reducing effectiveness of the attached flow when resolved in the side force plane. Hence the gradual reduction in moment production with increasing blowing. The rate of increase in yawing moment with blowing is determined also by the angle of attack. At higher angles, the jet is issuing into a crossflow more nearly aligned with the jet exit direction (normal to the slot) and the interaction is enhanced.

Superimposed on this response is the interaction with the steady asymmetric forebody vortices and the

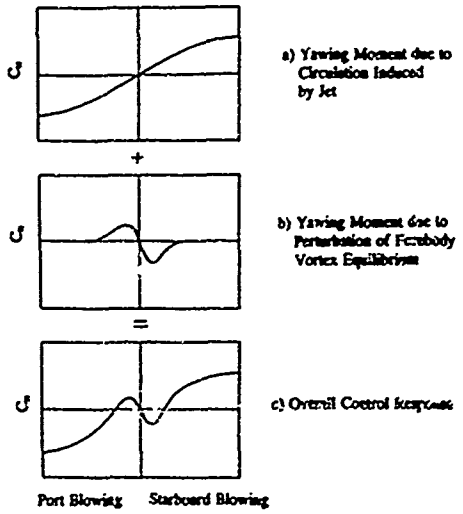

Figure 11: Contributions to Yaw Control.

resulting control reversal. The superimposition of these two effects produces the observed control response. The magnitude of the second order response is related to the increasing strength of the forebody vortices with increasing angle of attack.

Velocity Contours

Figure 12 shows the results of a brief LDA survey at the point of the forebody/LEX junction for both unblown and blown conditions at 40° angle of attack. The velocities recorded were aligned with the free stream direction but can still provide useful information regarding the location of the forebody vortices and the effects of blowing.

Unblown, the vortex asymmetry can be seen and the asymmetric acceleration of the fluid around the forebody can be related to, and is consistent with, the yawing moment measured from the sting balance. The vortex indicated is referred to as the "high" vortex, the other being located outside the measurement region and closer to the forebody surface.

Blowing was introduced at a rate which allowed only the first order response to be present ($C_\mu = 0.01$). At this momentum level, the wall jet can be seen to delay separation past the leeward generator, and then to leave the surface on the unblown side. The trajectory of the jet away from the surface can be identified as can the fluid acceleration on the blown side. The reversal of the yawing moment should be obvious.

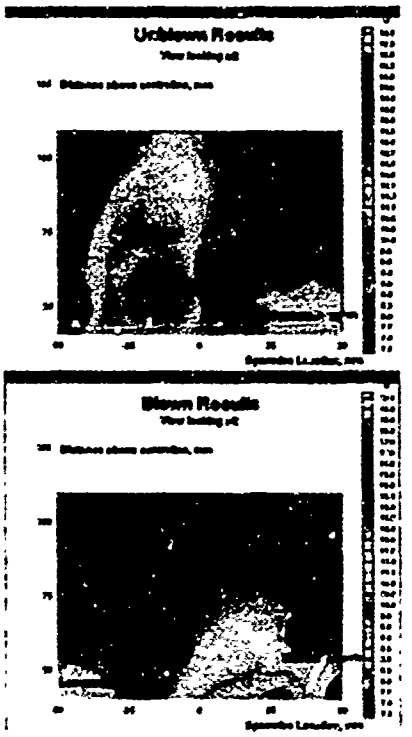

Figure 12: Off Body Velocity Contours, Blown and Unblown, $\alpha = 40°$.

Slot Location

Figure 13 shows the effects of changing the slot length for each of the three vortex regimes. At low angles of attack the response is essentially independent of the slot length and control can be established with very short slots. In regions dominated by steady vortex asymmetry, lengthening the slot extends the region of control reversal. However this may also be an indication that the extent of the reversal is dependent more on the local velocity ratio rather than momentum. Reducing the slot height at constant momentum may well reduce the extent of the reversal. At high angles of attack, where the forebody flow is dominated by periodic vortex shedding, increasing the length of the slot produces significant gains in efficiency. This may be related to the increased area of attached flow which results from the gradually increasing radius of the forebody away from the apex.

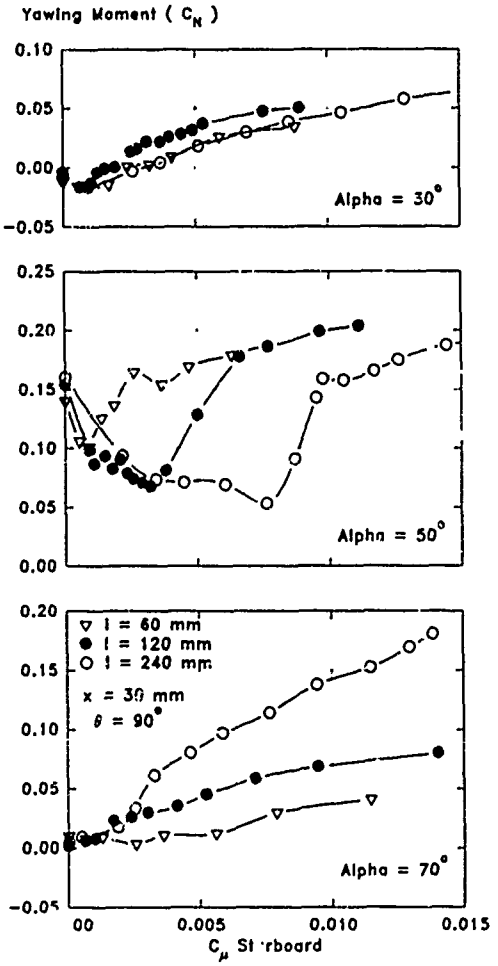

Figure 13: Effect of Slot Length on Blown Control Response.

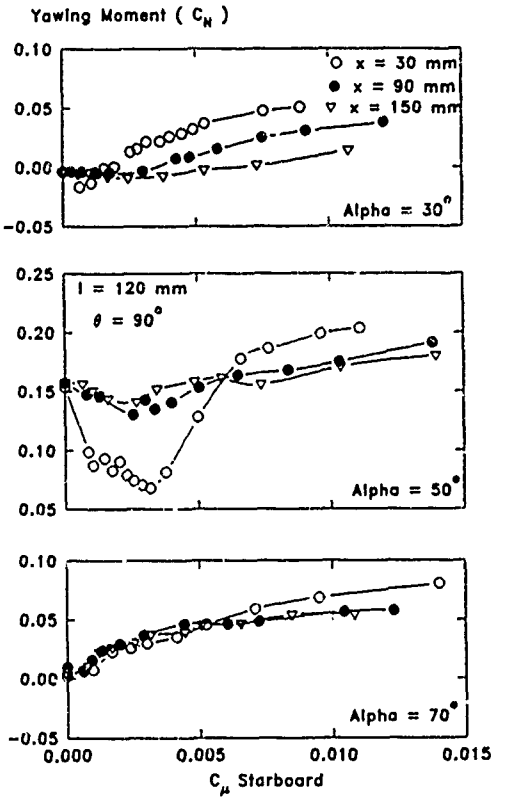

Figure 14: Effect of Slot Position on Blown Control Response.

The effect of slot longitudinal location is shown in figure 14. For efficiency at low angle of attack, it is essential to place the slots as far forward as possible; a conclusion reached by many other researchers. At mid-range angles of attack moving the slot aft reduces the control reversal with little effect on the eventual gain of the system. Of more interest are the results for high angles of attack where slot longitudinal location has little effect on the response to increasing blowing. Thus it may be possible to configure a relatively short slot (to minimise mass flow) away from the apex (to minimise interference with the radome and the occurrence of control reversal at low blowing) as an optimum configuration for extreme angle of attack control. The lack of sensitivity to longitudinal position at these angles is suggested to be due to a cancellation of the effect of reduced area of attached flow and increased distance from the centre of gravity.

The effect of slot azimuthal location for the single slotted nose cone models is shown in figure 15. The dominant trend is that, for a fixed blowing rate, larger yawing moments are produced in response to movement of the slot towards the leeward generator. The slot efficiency keeps increasing until a position at which a phenomenon referred to as slot stall appears at high angles of attack. The slot stall is characterised by a sudden detachment of the wall jet from the surface resulting in a loss of control of the cross flow separation. This phenomenon has also been observed on delta wings with tangential leading edge blowing. As the azimuthal location of the slot moves towards the leeward generator the angle of attack at which slot stall occurs decreases. This phenomenon is also characterised by a hysteresis loop which may spread over 20° angle of attack. The optimum location of the slot would appear to be near the 90° azimuthal

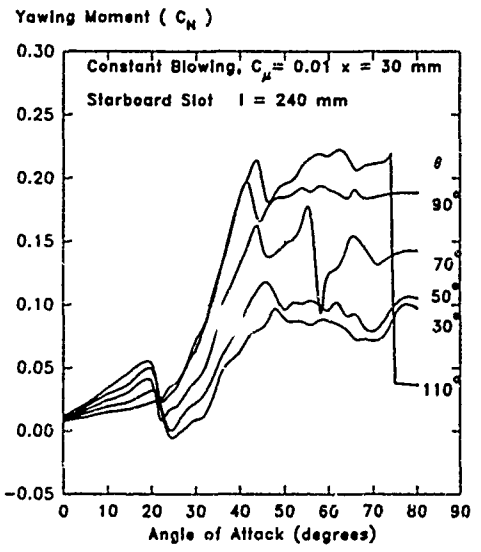

Figure 15: Effect of Slot Azimuthal Location on Control Response at Fixed Angle of Attack.

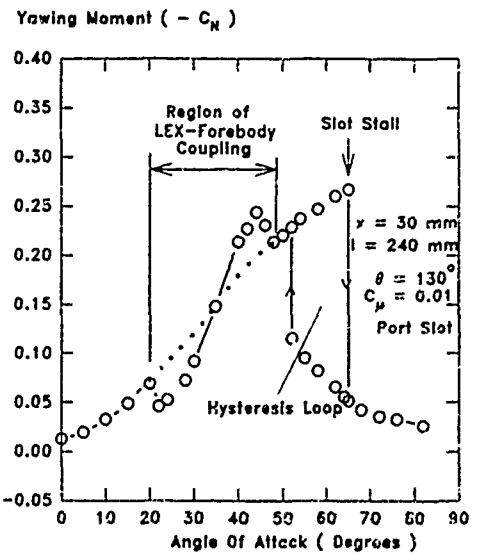

Figure 16: Summary of Control Response Identifying Vortex Coupling Region and Slot Stall.

location. This variation of control effectiveness with azimuthal location may be used to identify possible response in the presence of sideslip. It should be noted however, that a circular cross section is perhaps the most sensitive to azimuthal location due to the relatively weak pressure gradients in the crossflow.

It has been determined that the cross-flow separation in the vicinity of the slot was generally laminar for all these tests. At larger scale and higher speeds it is expected that the cross-flow separation would be turbulent. This should not affect the performance of TFB providing the azimuthal location of the slot exit is modified to account for the delayed separation.

Figure 16 summarises the overall yawing moment response to tangential forebody blowing. Each of the non-linear regions associated with LEX/forebody coupling and slot stall may be minimised by configurational optimisation. If control is sought primarily for high angle of attack (>60°) then a system capable of controlling the periodic shedding process is necessary. Since it has been shown that an efficient mechanism for yawing moment development is the production of increased attached flow around the forebody, tangential forebody blowing appears to be a good candidate for further investigation. A short slot away from the apex offers simplified installation with acceptable response at very high angles of attack. Preliminary estimates for full scale applications show that 2% of engine mass flow would be sufficient to provide yaw control up to 90° angle of attack.

CONCLUSIONS

Tangential Forebody Blowing has been shown to be an effective device for the development of yawing moment to very high angles of attack. The primary mechanism is the control of the area of attached flow on the side of the forebody rather than influence resulting from vortex control. This enables control of both steady asymmetric forebody vortices and, at higher angles of attack, periodic shedding.

For low angle of attack control, short slots near the apex of the forebody are most suitable although these may be superfluous in the presence of even the smallest fin/rudder combination.

For control in regions with steady asymmetric vortices, slots positioned near the apex produce significant control reversals for low blowing rates. For a modest loss in efficiency, slots positioned some way removed from the apex have been shown to minimise this reversal.

For high angle of attack control, TFB is capable of controlling the periodic shedding of the forebody vortices and producing significant lateral control. Long slots extending from the apex appear to offer the highest gain but adequate control can be achieved

with the upwind end of the slot some distance from the apex. This combination of a medium length slot clear of the apex would appear to offer the best compromise.

A further coupling between TFB and the wing planform has been identified which may result in undesirable roll/yaw interactions depending on the proximity of a LEX to the blowing slot. A slot stall with a large hysteresis has also been identified and is a function of the azimuthal location of the jet exit.

REFERENCES

1. Herbst, W. "Dynamics of Air Combat", J.Aircraft, *20*, 7, pp594-599
2. Ross, A. "High Incidence - The Challenge to Control Systems", Lecture presented to the R.Aero.Soc., January 1990
3. Malcolm, G., "Aerodynamic Control of Fighter Aircraft by Manipulation of Forebody Vortices", AGARD CP497, Paper 15, November 1991
4. Malcolm, G., Ng, T., Lewis, L. and Murri, D., "Development of Non-Conventional Control Methods for High Angle of Attack Flight Using Vortex Manipulation", AIAA Paper 89-2192, July 1989
5. Gittner, N. and Chokani, N., "An Experimental Study of the Effects of Aft Blowing on a 3.0 Calibre Tangent Ogive Body at High Angles of attack", AIAA Paper 91-3252, September 1991
6. Wood, N. and Nielsen, J., "Circulation Control Aerofoils as Applied to Rotary Wing Aircraft", J. Aircraft, *23*, 12, December 1986, pp865-875
7. Englar, R., "Further Developments of Pneumatic Thrust-Deflecting Powered Lift Systems", J. Aircraft, *25*, 4, April 1988, pp324-333
8. Wood, N. and Roberts, L., "Control of Vortical Lift on Delta Wings by Tangential Leading Edge Blowing", J. Aircraft, *25*, 3, March 1988, pp236-243
9. Gee, K., Rizk, Y., Murman, S., Lanser, W., Meyn, L. and Schiff, L., "Analysis of a Pneumatic Forebody Flow Control Concept about a Full Aircraft Geometry", AIAA Paper 92-2678, June 1992

CONTROL OF LEADING-EDGE SEPARATION ON A CAMBERED DELTA WING

by

P.R. Ashill and G.L. Riddle
Building 17
Defence Research Agency
Bedford, MK41 6AE
United Kingdom

SUMMARY

Wind tunnel studies of flows over a cambered delta wing of 60° leading-edge sweep at low speed have shown that the flow separates on a forward part of the curved upper surface. Although not apparent in surface pressure distributions, this separation strongly influences the position of the onset of leading-edge separation. The present paper describes a wind-tunnel study into the use of sub boundary-layer vortex generators, in the form of thin wires, to control the flow along and toward the upper-surface separation line The control is effective because it shifts the position of the onset of leading-edge separation downstream, ensuring increased leading-edge thrust, mainly through a reorganisation of the separated flow further downstream. The flow mechanisms are described, as well as the effects of wire number. Multiple wires can provide a reduction of about 16% in the lift-dependent drag factor. The implications of the study for the subsonic flight characteristics of supersonic combat aircraft are described and suggest that the vortex generators offer genuine improvements in subsonic manoeuvre performance.

NOTATION

A	Wing aspect ratio
C_D	overall drag coefficient
C_{DE}	excrescence-drag coefficient, based on frontal area of excrescence and local dynamic pressure
C_{D_p}	overall parasitic-drag coefficient
C_f	local skin-friction coefficient
C_L	overall lift coefficient
C_m	pitching-moment coefficient, about reference point shown in Fig 3b
C_m'	reduced pitching moment coefficient, Fig 14
C_p	static pressure coefficient
C_x, C_z	overall axial and normal force coefficients, axial force positive downstream, normal force positive in lift direction
c_x, c_z	local axial and normal force coefficients based on local wing semi-span
c_0	wing centre-line chord (Fig 3b)
d	wire diameter
K	lift-dependent drag factor
M	free-stream Mach number
n	number of wires
P	point on wing leading edge where flow changes from attached to separated
R	Reynolds number based on free-stream conditions and geometric mean chord
R_1	reattachment line (Fig 2)
S_1, S_2, S_3	separation lines (Fig 2)
u_τ	wall friction velocity, $= \sqrt{(\tau_w/\rho)}$
s	local wing semi-span made non-dimensional by centre-line chord
s_m	geometric mean semi-span of wing made non-dimensional by centre-line chord
S	wing planform area (Fig 3b)
WVG	wire vortex generator
x,y,z	cartesian coordinate system, made non-dimensional by centre-line chord and with origin at virtual apex of wing (Fig 3b)
x_p	axial position of point P
x_n, x_{n1}	axial stations defining positions of wires (Fig 4)
α	angle of incidence
δx_n	axial distance between wires (Fig 4)
Δ	increment due to wire(s)
η	non-dimensional spanwise position, = y/s
τ_w	wall shear stress

NB. Unless otherwise stated, all coefficients are based on free-stream dynamic pressure and overall-force coefficients are based on wing planform area S.

1 INTRODUCTION

Modern combat aircraft are expected to fulfil multiple roles, which means that they have to be able to operate over a wide range of combinations of lift coefficients and Mach numbers (Fig 1) These requirements mean that the wing has to be able to provide lift efficiently in a wide variety of flow conditions. At least three different approaches to attain these objectives might be considered:

i) produce a compromise design, ie one which is not optimum at any given condition,

ii) make use of variable geometry; and

iii) design for a prime condition in the lift coefficient-Mach number plane, accepting that the aerodynamic performance of the wing may be much poorer than that of shapes that are optimum at other conditions.

Presented at an AGARD Meeting on Technologies for Highly Manoeuvrable Aircraft, October 1993.

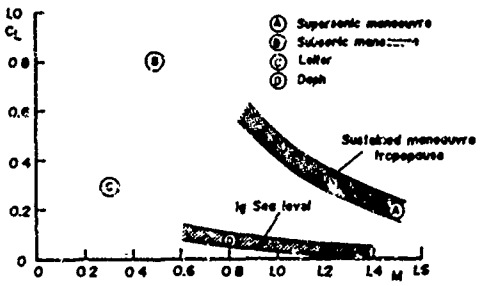

Fig 1 Typical operating conditions for hypothetical combat aircraft

The present paper is mainly concerned with wings designed using the third approach. The principal design point of the type of wing considered is a sustained manoeuvre condition at supersonic speeds (Case A in Fig 1). Wing shapes designed to achieve efficient manoeuvre at supersonic speeds have been the subject of extensive study in the USA, mainly at Grumman Aerospace and at NASA Langley Research Center. Mason and Miller[1] and others[2,3] considered a particular class of supersonic wing featuring significant camber and having relatively-blunt leading edges. Spanwise camber was shown to weaken the cross-flow shock wave above the wing, thus reducing wave drag, while a blunt leading edge ensured that the flow at the leading edge was attached. Wings of this type have also been studied at the Defence Research Agency (DRA, formerly RAE) Bedford. Experimental studies, performed at supersonic speeds in the 8ft x 8ft Wind Tunnel at Bedford in collaboration with NASA, Langley Research Center, confirmed the soundness of the potential-flow design methods used by NASA[4] and of Euler methods for complex configurations used in UK[5].

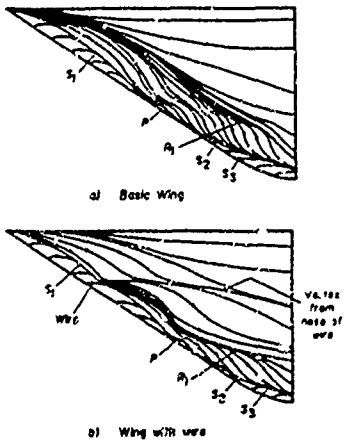

Fig 2 Sketches of upper surface oil-flow visualisations showing types of flow studied

As well as studying the supersonic aerodynamics of these wings, DRA has also investigated their behaviour at subsonic manoeuvre conditions. Investigations in the Mach-number range 0.5 to 0.8 revealed the flows to be complex and to vary significantly with Reynolds number[6]. In order to gain an improved understanding of the factors affecting the scale (or Reynolds-number) sensitivity of these flows at low cost, a detailed study has since been performed in the 13ft x 9ft Low Speed Wind Tunnel at Bedford of flows over one of the wings previously studied at higher Mach number. An illustration of the character of the flows over this wing is provided by a sketch of a surface oil flow on the upper surface (Fig 2a). The sketch shows that the flow may be divided into two regions, one upstream of the point P (on the leading edge), where the leading-edge flow is attached, and the other downstream of it where leading-edge separation occurs, revealing a flow with a part-span separation S_2, reattaching at R_1, and a secondary separation of the flow outboard at S_3. In the upstream region, separation occurs on the curved part of the upper surface at S_1. Although this three-dimensional separation is a weak feature, in that it is not apparent in surface pressure distributions, it has a profound influence on the flow through its effect on the boundary-layer flow towards the point P. At this point the separation line S_1 effectively joins or intersects the leading edge. This suggests the possibility of controlling the leading-edge separation by influencing the behaviour of the boundary layer in the region of the separation line S_1. Fig 2b shows that a sub boundary-layer vortex generator, in the form of a thin wire placed upstream of S_1, induces a vortex which controls the flow towards and along the separation line in such a way as to move the point P downstream. The movement of this point has the obvious consequence of increasing the extent of the leading edge over which the flow is attached, resulting, it might be thought, in an increase in leading-edge thrust. However, the discussion later in this paper will show that there are less obvious consequences which lead to larger reductions in drag.

Section 2 describes the details of the experiment. Section 3 discusses detailed aerodynamic aspects of these boundary-layer control devices and of how their effectiveness, in terms of increased leading-edge thrust or reduced drag, is influenced by the number of wires. The implications of these results for the flight characteristics of combat aircraft are considered in Section 4. Conclusions are presented in Section 5.

2 EXPERIMENTAL DETAILS

2.1 Wind tunnel, model, equipment and techniques

The tests were performed in the 13ft x 9ft Wind Tunnel, which has an atmospheric-pressure working section, so that changes in wind speed result in changes in both Reynolds number and Mach number. The wind tunnel has a maximum operating speed of about 90m/s and low turbulence levels. For example, at a wind speed of 61m/s, turbulence levels in a working section reference plane have been measured to be 0.014% in the longitudinal direction and 0.063% in the lateral direction.

The model used for this study is illustrated in Fig 3, which shows a photograph (Fig 3a) and a sketch (Fig 3b). As indicated in the figure, the model comprises the port half of a wing-body configuration mounted on an under-floor, mechanical balance measuring four components of force or moment. The wing has a leading-edge of 60° sweep, with a Küchemann-type tip, and with streamwise sections of 4% local thickness to chord ratio. The leading-edge radius is virtually constant at 0.13% centre-line chord, c_0, over the whole span. Fig 3b illustrates the camber distribution, showing the pronounced curvature of the wing in the spanwise direction and the characteristic inverse camber of the wing section near the body side.

a) Model in Working Section

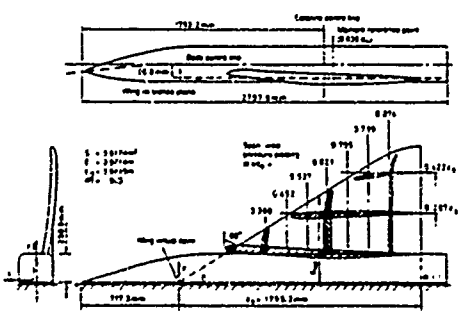

b) Sketch of Model, illustrating geometry and notation

Fig 3 Details of the model

Static pressures were measured on the wing surface at 7 spanwise stations along the model axis (Fig 3b) at a total of 300 orifices, each of 0.5mm diameter and drilled normal to the surface. The orifices were concentrated in the region of the leading edge so that local axial force or leading-edge thrust could be determined accurately. The axial position of each of these stations is defined by x, the axial distance from the apex of the wing, made non dimensional by centre-line chord. The pressures were measured using electro-mechanical scanning of pressure transducers of range ±34.5 kN/m². As well as being used to study the character of the flow, these measurements were used to investigate local and overall pressure forces on the wing. In addition, pressure measurements were used to infer the non-dimensional axial position of the point P, x_p; this was achieved by plotting the pressure coefficient at an orifice close to that for minimum pressure against angle of incidence at each axial measurement station. The angle of incidence at which this pressure increases rapidly with angle of incidence was noted and taken to indicate the angle of incidence at which 'P' coincided with the measurement station or the onset of leading-edge separation. The downstream shift of 'P' due to a wire or wires was then found by comparison between plots of x_p against angle of incidence.

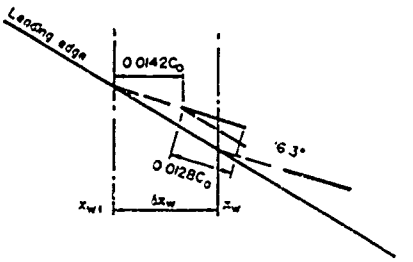

Set	n	x_{w1}	δx_w
1	2	0.368	0.0843
2	3,7	0.284	0.0843
3	7,14 28,56	$x_{w1}(n/2)$ = $c_{w1}(n) + \delta x_w(n)$ $x_{w1}(56) = 0.2094$	$\delta x_w(n/2)$ = $2\delta x_w(n)$ $\delta x_w(56) = 0.0106$

Fig 4 Definition of wire geometries

Fig 4 illustrates the geometry, position and orientation of each of the wire vortex generators (WVG's, patent pending). In the tests to be described the wires were of diameter d = 0.51mm (0.00028c_0) and of length 22.9mm (0.0128c_0). The wires were stuck with a contact adhesive and were pressed down so that the height of the wire crest above the wing surface was equal to wire diameter. The position is defined by a particular axial station, x_w, which the nose of the wire is downstream of by a fixed distance 0.0142c_0, and the angle between the axis of the wire and the wing leading edge in the wing chord plane was set at 16.3° in the tests to be described. As well as single wires, configurations with multiple wires were tested. Three sets were studied, as defined in the table in Fig 4, by the value x_w of the most upstream wire, x_{w1}, the non-dimensional axial distance between them, δx_w, and the number of wires n. In the case of Set 3, the largest number of wires tested was 56, the corresponding value of x_{w1} being shown in Fig 4; the other members of the set were obtained by successively removing every other wire, beginning with the most upstream wire. The values of x_{w1} and δx_w for the other members of the

family are determined by the simple recurrence relationship given in the table.

In all the tests, boundary-layer transition was allowed to occur naturally*. The reason for this is that transition cannot readily be fixed near the leading edge of wings at high angles of incidence and low speed owing to the combined problems of a) the need to fix transition upstream of the suction peak, which is close to the leading edge, and b) the difficulty of fixing transition in the region of rapid acceleration upstream of the peak. As is shown in Section 3.1, a consequence of not being able to fix transition is that the effect of Reynolds number on the wing flow is large at low Reynolds numbers. However, the tests were performed at a higher Reynolds number where the effects of Reynolds number on the flows is small.

Oil-flow visualisations were performed for a selection of conditions using a mixture of diesel oil and a pigment that was sensitive to ultra-violet light.

No corrections were applied to the data for wind-tunnel wall interference because the investigation was primarily concerned with changes in aerodynamic characteristics due to the vortex generators.

2.2 Test conditions

Unless otherwise stated, the tests were performed at a free-stream speed of 61m/s. The corresponding nominal test Reynolds number based on the geometric mean chord of the wing, R, and the Mach number, M, are, respectively, 3.9×10^6 and 0.18. The free-stream speed was chosen on the basis of observations of Reynolds-number effects on the flow to be discussed in Section 3.1. The range of angles of incidence, α, tested was between 8° and 18°, the angle of incidence being the angle between the free-stream direction and the body axis (Fig 3b). Force and pressure measurements were made at intervals of 1° for angles of incidence between 8° and 10°, reducing to intervals of 0.25° at higher angles of incidence. A number of surface oil-flow visualisations were made at angles of incidence between 13° and 18°.

2.3 Presentation of data

Data for overall forces are presented in the form of axial and normal force coefficients. Here axial and normal force coefficients are, respectively, taken positive in the x and z directions (Fig 3b). Unless otherwise stated, overall forces are obtained from the mechanical balance. The effects of the WVG's on overall forces, local forces and the axial shift of the point P are presented as increments and are indicated by the symbol Δ.

* The wires were always downstream of any laminar short bubbles. Hence the only way that the wires could have influenced boundary-layer transition was by an upstream effect on wing pressure distribution. However, the indications from pressure measurements were that this effect is negligible.

3 RESULTS AND DISCUSSION

3.1 Basic-wing flows

As noted earlier, the main aim of the present study was to investigate the influence of wire vortex generators on the aerodynamic characteristics of the wing. However, it was appreciated that, even at low speeds, the performance of the devices might depend on the type of flow over the wing and that the flow in the wind tunnel might differ from that at higher Reynolds numbers, typical of those in flight. For this reason, the flow over the basic wing, ie the wing without control devices, was studied over a range of wind speeds up to a value close to the maximum available in the wind tunnel. The change in the aerodynamic behaviour of the wing with wind speed is illustrated in Fig 5, in which axial-force coefficient is plotted against Reynolds number based on geometric mean chord, R, (and Mach number, M) for three angles of incidence. Between the Reynolds numbers 2×10^6 and 3×10^6, there is a rapid change in axial force coefficient with Reynolds number, but at higher wind speeds the variation is more gentle. There are good reasons for believing that the rapid change is due to the variation in Reynolds number rather than to changes in free-stream Mach number (between 0.10 and 0.14). Calculations of the local Mach number of the flow component normal to the leading edge, using measured pressure distributions, indicate that this Mach number is less than 0.5 in the corresponding speed range, suggesting that compressibility effects are likely to be of secondary importance to those due to Reynolds number. Rapid changes of flow over a range of Reynolds number based on leading-edge radius similar to that of the present wing have been found in the wind-tunnel study of a swept-panel wing[7] of sweep 60° and also on wings with high-lift devices[8].

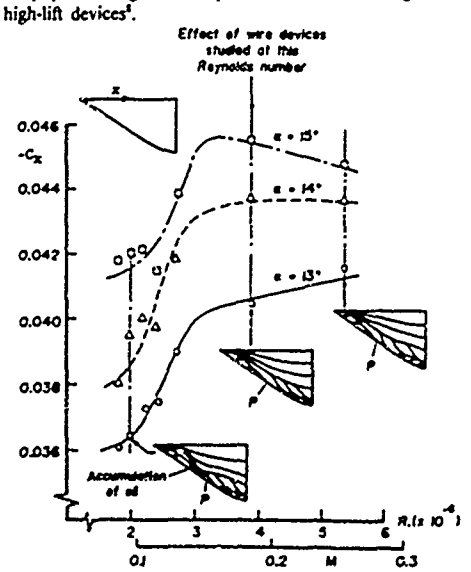

Fig 5 Effect of Reynolds number (and Mach number) on axial-force coefficient

Examination of surface oil flows (Fig 5) provides an explanation for this change. At Reynolds numbers above about 3×10^6, the mechanism for leading-edge separation at the point P is turbulent separation, possibly just downstream of (turbulent) reattachment of a 'short' bubble. This is the type of flow described in the Introduction. At lower Reynolds numbers, on the other hand, the mechanism for flow breakdown at 'P' is the bursting of the laminar separation bubble at the leading edge, indicated in the surface oil flows by a concentration of oil near the leading edge. This type of flow would be expected to be much less sensitive to the control of the flow upstream of the turbulent separation line than the flows at higher Reynolds number, and limited studies of the effect of a WVG over the range of wind speeds considered confirmed this. Thus, in what follows, results are presented for flows with turbulent leading-edge separation at the wind speed 61m/s, corresponding to a mean chord Reynolds number of 3.9×10^6 and a Mach number of 0.18.

3.2 Effect of single devices

3.2.1 Flow near the wire

The use of conventional, vane-type vortex generators to control boundary layers on wings is well documented[9]. These generators are designed to protrude outside the boundary layer with the aim of transferring high energy air in the inviscid flow into the lower-energy flow within the boundary layer. The trailing or streamwise vorticity that promotes this mixing is generated in the same way that a wing creates trailing vorticity, ie by generating circulation around streamwise sections. Since a large part of this type of device lies in the high dynamic-pressure flow outside the boundary layer[10], a significant drag penalty is caused. In contrast, sub boundary-layer vortex generators are, typically, buried within about 20% of the boundary-layer thickness, where the velocity deficit is greatest. Consequently, they have a much lower parasitic drag than that of vane vortex generators, but they are still effective in transferring energy from the outer regions of the boundary layer to the low energy regions near the wing surface[10]. Sub boundary-layer vortex generators are placed too deep within the boundary layer to create circulation effectively; instead, they provide trailing vorticity by conversion of boundary-layer vorticity[11].

The application of vortex generators has, up to present, mainly been to the control of separation on wings of low sweep. As far as the authors are aware, no research has been published on the use of vortex generators to control separations on highly-swept wings. For flows of this type, additional, and arguably more important, flow mechanisms have to be taken into consideration. An illustration of such a mechanism is provided by Fig 6, which shows a view of a surface oil flow and a sketched interpretation in the near region of a WVG. Here, the wire is of diameter 0.51mm, which is slightly larger than the (calculated) displacement thickness of the boundary layer just upstream of the wire. Thus the device is well within the boundary layer. The flow around the wire is complex, with a topology that is difficult to interpret. However, one important feature of the flow that is readily evident is the 'scarf' vortex wrapped around the nose of the wire. This vortex results from the conversion of boundary-layer vorticity into vorticity which is parallel to the local streamwise direction, as implied above. The mechanism for effecting this change is separation of the boundary layer just upstream of the nose of the wire.

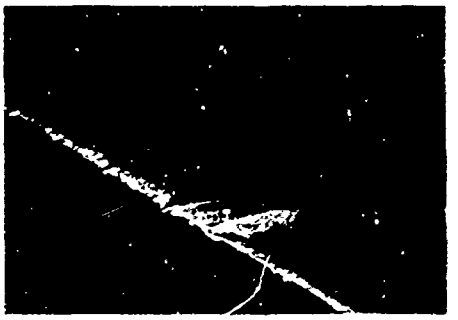

Oil Flow

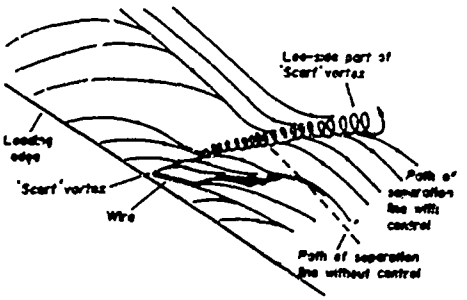

Interpretation of Flow

Fig 6 Surface flow close to wire showing its effect on flow approaching separation line

As shown in Fig 6, the wire is at incidence to the local flow so that the part of the 'scarf' vortex on the lee side of the wire is much stronger than that on the windward side, and it is the lee-side vortex that has the dominant effect on the flow further downstream. Therefore it is reasonable to suppose that the strength of this vortex depends on the angle between the wire axis and the local flow direction within the boundary layer. This vortex alters the flow beneath it both in the direction normal to and along the separation line further inboard, as illustrated schematically in Fig 7. The sense of the vortex is such that it increases the velocity of the flow toward and just upstream of the separation line, while reducing the velocity of the flow along the separation line. The effect of this is to displace the separation downstream at a given spanwise position by a significant amount, typically up to about 1% of centre-line chord. This shift results, in turn, in a downstream displacement of the point P, with the consequences referred to above and to be discussed in detail below.

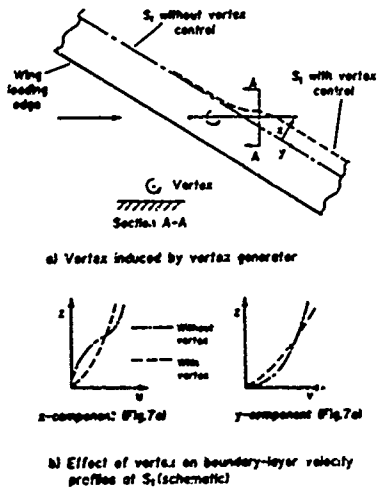

Fig 7 Sketches illustrating explanation for effect on wire on flow approaching separation line

Sub boundary-layer devices use various ways to convert boundary-layer vorticity into streamwise vorticity. The mechanism described above for the WVG's is somewhat different from that of sub boundary-layer devices of the Kuethe type[11], in which a wave element diverts the boundary-layer vorticity, or of the Wheeler type[12], in which separation of the flow over an aft face appears to alter the direction of the vorticity. Usually, devices of this type are arranged so that they generate a vortex pair of more or less equal strength, in contrast to the dominant lee-side vortex of the present device.

In some respects, the action of a WVG is similar to that of a fence in that the device reduces the boundary-layer drift towards the outer wing. However, fences alter nearby pressure distributions by means of the 'reflection effect'[13], off-loading the wing and starting a new boundary layer outboard of the fence, while diverting the boundary layer just upstream of the fence in the downstream direction[14]. Such an effect must surely be negligible for sub boundary-layer devices such as WVG's. Mabey et al[15] noted that small fences and notches could have significant effects on unsteady-flow characteristics However, the wire devices discussed in this paper are much smaller, as a proportion of wing mean chord, than those studied by Mabey . ences have been tested on an uncambered delta wing with round leading edges of 60° sweep by Johnson and Rao[16] and Rao and Johnson[17], but their devices are much larger than those considered here and presumably have significantly higher parasitic drag than WVG's.

3.2.2 Effect on overall flow

Fig 8 shows that the effect of a single wire at x_w = 0.452 on normal-force coefficient, axial-force coefficient and the axial position of the point P. The increments in normal and axial-force coefficients are determined both from balance measurements, with the precision shown, and from appropriate integration of pressures measured on the wing. The figure indicates that the agreement between the two methods is good, particularly for axial force, which is a consequence of concentrating the orifices near the leading edge, as noted before. The effect of the WVG is to reduce both normal-force and axial-force coefficients significantly over the range of angles of incidence 12° to 16.5°. Fig 8 reveals a generally satisfactory correlation between the downstream shift of point P and the reductions in normal-force coefficient and axial-force coefficient (or increase in leading-edge thrust). In particular, there is a good correlation between the respective ranges of angle of incidence. Thus the reductions in force coefficients are entirely consistent with the tendency for the WVG to increase the region of the wing over which the leading-edge flow is attached. This change has the effect of reducing the 'non-linear' normal force associated with leading-edge vortex flows and of increasing leading-edge thrust. However, there are subtle differences which need to be understood, as follows

i) Both the normal and axial-force curves have two minima, one at α = 14° and the other at α = 15.5°, whereas the curve of Δx_p against angle of incidence has only one maximum at α = 15°.

ii) The maximum reduction in axial force occurs at the turning point with the higher angle of incidence.

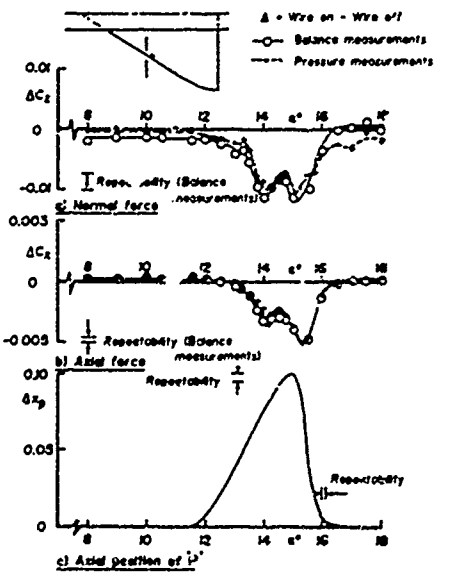

Fig 8 Effect of single wire (x_w = 0.452) on overall force coefficients and axial position of point P

Explanations for these differences are suggested in the following two figures. Fig 9a shows the variation with angle of incidence of increments in local normal force, $\Delta c_n s/s_m$, and local axial force, $\Delta c_a s/s_m$. These increments are deduced from pressure distributions at the pressure measurement stations. Here c_n and c_a are local normal and axial-force coefficients based on local wing semi-span; s is local wing semi-span and s_m is geometric mean semi-span of the wing (in both cases made non dimensional by centre-line chord c_0). Also shown are the loci of the point P for the wire on and wire off cases. In the region to the left or above the wire-on locus, the leading-edge flow with control is attached, while to the right or below it is separated. Fig 9a shows that, in the former region, there are reductions in axial force or leading-edge thrust, as expected. Similarly, there are reductions in normal force. Depending on angle of incidence, contributions of similar or even greater magnitude compared to those in the attached-flow region are apparent in the separated-flow region. Thus, by shifting the point P downstream, the WVG changes the character of the separated flow downstream of point P in such a way as to increase suctions on forward-facing surfaces of the wing and hence to increase the thrust.

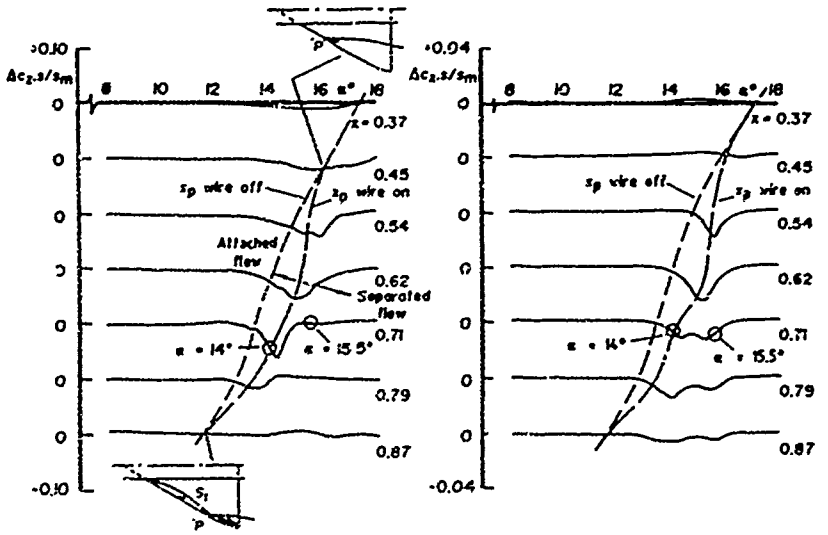

a) Local normal and axial forces

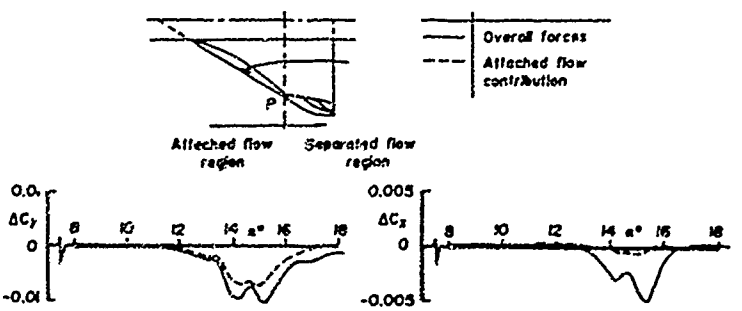

b) Analysis of contribution to overall forces

Fig 9 Local normal and axial forces and analysis of overall forces, single wire $x_w = 0.452$

Fig 9a also shows that the two loci of the point P merge at $x = 0.45$, ie close to where the wire is situated. In other words, the wire ceases to be effective once it is downstream of the point P, or, more precisely perhaps, downstream of the separation line S, as might be expected from the discussion in Section 3.2. The loci also merge at $x = 0.87$: this point is upstream of the trailing edge, where it might be expected to be, because the flow at the highly-swept leading edge in this region is dominated by local conditions rather than those further upstream.

By integrating the local pressure forces over the part of the wing where the leading-edge flow is attached, it is possible to analyse the relative contributions of the attached-flow and separated-flow regions with the wire on. The result is shown in Fig 9b. The attached-flow region provides most of the normal force coefficient but only a small part of the axial-force coefficient. This implies that the major part of the overall increase in leading edge thrust comes from a reorganisation of the separated flow so that it increases suctions on the forward facing surfaces on the drooped leading edge. This is an important result, since it implies that the observed increments in leading-edge thrust are conditional on the wing having significant forward-facing regions on the upper surface near the leading edge. Thus an uncambered wing of the same planform and thickness distribution would not provide the scope for such large increases in leading-edge thrust. Fig 9b shows, furthermore, that the undulations in the curves of the attached-flow contributions are much less obvious than those in the corresponding overall-force curves, particularly for axial force. This suggests that the main reason for the undulations is changes in the nature of the effect of the WVG's on the separated-flow region with angle of incidence. This suggestion is reinforced by the fact there are no undulations (or even inflexions) apparent in the curve of the axial-shift in the point P against angle of incidence (Fig 8). This leads to a possible explanation as to why the reduction in axial force coefficient is larger at $\alpha = 15.5°$ than at $\alpha = 14°$ at the higher angle of incidence a larger part of the leading edge has separated flow than at the lower angle of incidence, hence the scope for increasing the thrust is greater at $\alpha = 15.5°$ than at $\alpha = 14°$

Further information on the change in the effect of the WVG between the attached-flow and separated-flow regions is illustrated by pressure distributions at the station $x = 0.705$ for $\alpha = 14°$ and $\alpha = 15.5°$ in Figs 10 a&b. Results are shown for plots of static pressure coefficient, C_p, against non-dimensional spanwise position $\eta s/s_m = y/s_m$, and of $C_n ds/dx$ against z/s_m, where z is non-dimensional ordinate of the wing. Integration of the first plot provides local normal force while integration of the second graph provides a major contribution to local axial force*. For $\alpha = 14°$ (Fig 10a), the WVG changes the local leading edge flow from separated to attached (as may be seen in Fig 9a). For $\alpha = 15.5°$ (Fig 10b), the leading-edge flow remains separated. Here the beneficial effect of the WVG in reorganising the separated flow to give increased leading-edge thrust (with little change in local normal force) is seen clearly.

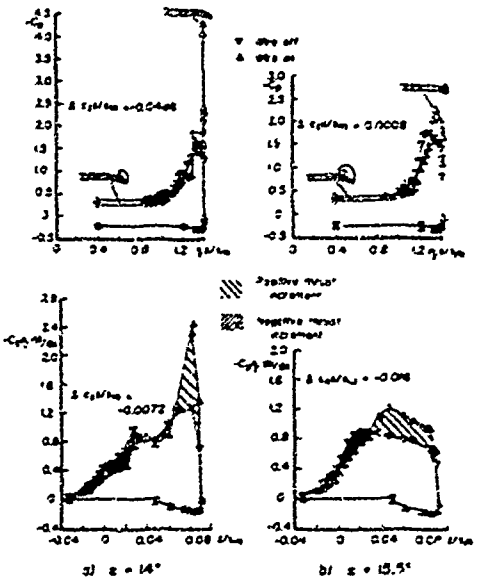

a) $\alpha = 14°$ b) $\alpha = 15.5°$

Fig 10 Pressure Distributions at $x = 0.705$ Single wire at $x_w = 0.452$

3.3 Multiple wires

It is reasonable to suppose that, as the number of WVG's on the wing is increased, the downstream shift of 'P' and the resulting increase in leading-edge thrust becomes larger. However, the mutual interference between the WVG's has to be taken into account. Fig 11 illustrates a source of favourable interference, which has an important bearing on the effectiveness of multiple devices. The figure shows plots of the reduction in overall axial-force coefficient and the shift in the axial position of 'P', respectively, for single WVG's at $x_w = 0.37$ and 0.45 and for two devices, one at each of these positions. For $\alpha = 16.3°$ it is seen that the combined effects of two devices is greater than the sum of the individual contributions both in terms of the magnitude of the axial-force increment and the downstream shift of 'P'. A single device at $x_w = 0.45$, Case A, has no effect on the flow, and the sketch at the bottom of the figure shows that this is because the device is downstream of the separation line S_1. The single device at $x_w = 0.37$ (Case B), on the other hand, is upstream of the separation line and consequently moves this line and the point P downstream. This movement is sufficiently large to ensure that a second device placed at $x_w = 0.45$ then becomes effective (Case C) and continues to be effective over an increased range of angle of incidence.

* For a conical wing this integral provides the exact value of local axial-force coefficient. For this nearly-conical wing the error obtained by using only this term to determine the change in local axial-force coefficient due to the WVG's is less than 10% for the two cases shown.

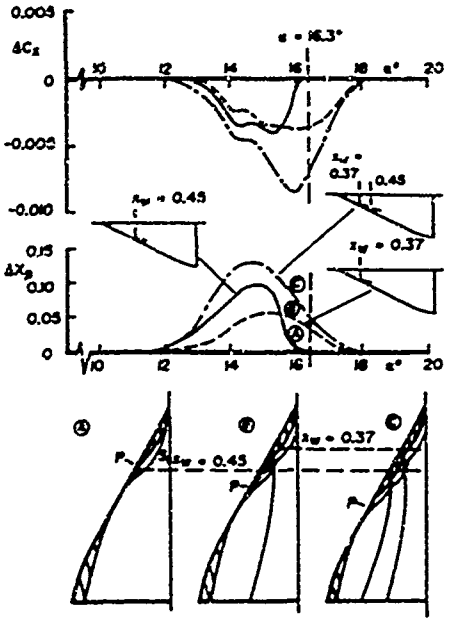

Fig 11 The influence of one wire on another

A further favourable consequence of increasing the number of wires is that the maximum reduction in axial-force coefficient is increased. The curve with two peaks for the single-wire at $x_w = 0.45$ is replaced by a curve in which the peak at the higher angle of incidence has virtually overwhelmed the peak at the lower angle of incidence, the latter being replaced by an inflexion in the curve. For the two-wire case, the peak value in leading-edge thrust occurs at a higher angle of incidence than that for the peak value in the axial shift of point P. A study of local forces similar to that described in Section 3.2.2 shows that these observations can be explained by the increased contribution of two wires to leading-edge thrust in the separated-flow region compared with that of the single wire. As with the single wire, the main contribution to leading edge thrust comes from the effect of the wires on the separated-flow region. However, for angles of incidence below 16°, the contribution from the attached-flow region is significantly higher for two wires than for the single wire.

There is a suggestion in Fig 11 of an adverse interference between the two wires, insofar as the maximum value of the downstream shift of point P for two wires is less than the sum of the shifts of the two individual wires at the same angle of incidence. On the other hand, the maximum reduction in axial-force coefficient for the two-wire case is greater than the sum of the corresponding contributions of the single wires at the same angle of incidence. This emphasises that, overall, there are benefits from increasing the number of WVG's.

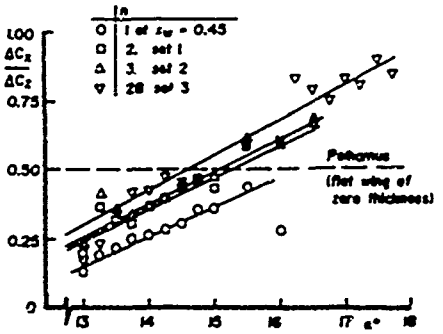

Fig 12 Ratio of $\Delta C_z/\Delta C_z$ versus angle of incidence

It is interesting to study the ratio $\Delta C_z/\Delta C_z$, which provides a measure of the efficiency of the devices in converting the loss in normal force to a gain in leading-edge thrust. According to Polhamus' leading-edge suction analogy[18], this ratio has the value 0.5 for an uncambered, untwisted wing of zero thickness and of leading-edge sweep 60°. The variation of this ratio with angle of incidence for various wire configurations is shown in Fig 12, which indicates that, for each wire configuration, the ratio increases with angle of incidence in a roughly linear way, being less than 0.5 at low values of angle of incidence. Possible reasons for this trend are as follows. Since the wing has round leading edges and is cambered, regions of the leading edge where the flow is separated will provide some thrust. This is particularly true at the low end of the angle of incidence range where the 'centre of area' of the separated vortex sheet is relatively close to the leading edge. Thus, without control, there are suctions on forward-facing parts of the wing in the separated-flow region, implying a significant thrust from this region. Hence, in this range of angle of incidence, changing the leading-edge flow from separated to attached by WVG's does not yield the benefit predicted by Polhamus' analogy, which is based on the idea that there is zero leading-edge thrust in the separated-flow condition. It has already been shown that, at higher angles of incidence, WVG's reorganise the separated-flow region downstream of the point P, changing it from one with the 'centre of area' of the separated vortex sheet well inboard to another where this centre is close to the forward-facing part of the wing surface. This seems to explain why the factor exceeds the value given by Polhamus' analogy at high angles of incidence.

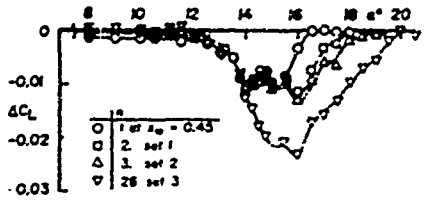

a) Lift coefficient versus angle of incidence

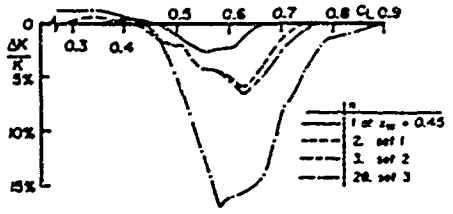

b) Lift-dependent drag factor versus lift coefficient

Fig 13 Effect of various wire configurations on lift coefficient and lift-dependent drag factor

Up to this point, the discussion has concentrated on axial and normal force increments. However, the aircraft designer is more concerned with changes of lift at constant angle of incidence, drag at constant lift and pitching moment also at constant lift. Changes in lift coefficient at a given angle of incidence are shown in Fig 13a for various wire sets. Reductions in the lift dependent drag factor $\Delta K = \Delta C_D \pi A / C_L^2$ are shown as a percentage of the lift-dependent drag factor of the datum (wire-off) configuration in Fig 13b plotted against lift coefficient for the same wire sets as Fig 13a. The maximum reduction occurs at a lift coefficient of about 0.6 for all wire configurations, and the largest reduction of all the wire configurations shown, of approximately 16%, is obtained with 28 wires. This is a significant reduction and suggests the potential for improvement, by the use of WVG's, in the subsonic manoeuvre performance of combat aircraft with highly-swept wings. Fig 13b also shows that the effect of increasing the number of wires from 2 and 28 is to increase the range of lift coefficients by about 0.1 over which the WVG's are effective in reducing drag.

The influence of the WVG's on pitching moment is illustrated in Fig 14, where pitching moment coefficient, C_m, has had subtracted from it a term that is linearly dependent on lift coefficient, in order to obtain a scale which shows the small increments clearly. The reduced pitching moment coefficient, C_m', of the datum, no-wire case is seen to be

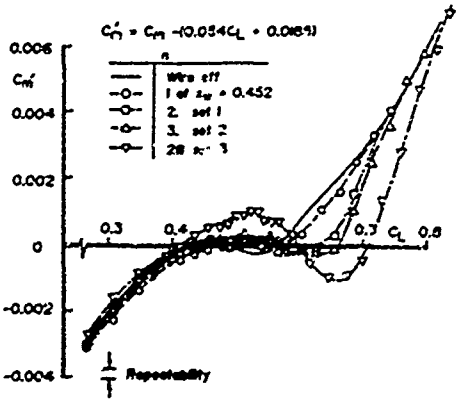

Fig 14 Effect of wire vortex generators on pitching moment - lift curve

close to zero between the lift coefficients 0.4 and 0.55 but, at higher lift coefficients, there is a pronounced pitch up as the separated-flow region moves upstream. The effect of the wires is to increase the value of lift coefficient at which this increase in pitching moment occurs, this value increasing with number of wires up to 28. Similar effects have been observed with fences[17]

Since no measurements were made of unsteady forces on the model, it is not possible to show the effect of WVG's on buffet characteristics. However, since the wires have been shown to reduce the extent of leading-edge separation, it is probable that they will exert a favourable effect on wing buffet characteristics[19], delaying the light buffeting criterion to higher lift coefficients. However, the moderate and heavy buffeting criteria will probably be unaltered.

4 IMPLICATIONS FOR AIRCRAFT PERFORMANCE

The discussion of the implications of the present study of WVG's for combat-aircraft performance starts with a brief review of the influence of Reynolds number. The most important changes with Reynolds number are likely to be those due to changes in boundary-layer thickness (relative to wire diameter) and to changes in the cross-flow velocities in the boundary layer. The former determines the degree to which the WVG is submerged within the boundary layer, while the latter decides the effective angle of the axis of the device to the direction of the oncoming boundary-layer flow. Changes in boundary-layer thickness with Reynolds number are difficult to predict owing to the variation in boundary-layer state near the leading edge[3]. However, the indications of limited experiments on the effect of wire diameter on a given flow (not presented) are that changes in boundary-layer thickness for a given wire diameter will not have a significant effect on the performance of WVG's provided the wire is not wholly submerged in the viscous sub-layer at wind-tunnel scale. Similarly, experiments on the effect of wire angle (also not presented) suggest that changes in boundary-layer cross flow are unlikely to influence the

characteristics of WVG's noticeably. Thus, as far as scale effects are concerned, wind-tunnel tests may reasonably be used to optimise the size and orientation of WVG's provided that low Reynolds effects associated with bubble bursting are avoided, as in the present study.

Since the present tests were performed at low speed, it is worthwhile to speculate as to how the effects of WVG's at Mach numbers representative of subsonic manoeuvre (eg Case B, Fig 1) might differ from those described here. One change is that the flow close to the leading edge will become supercritical at high subsonic speeds, with the further, strong possibility of a shock wave downstream. This shock wave may cause turbulent separation, depending on its strength, and therefore may determine the position of the turbulent separation line S_1. Further studies are therefore desirable to investigate the arrangement of WVG's to give best performance at high subsonic speeds. It is possible that the turbulent separation on the upper surface may no longer have a role in controlling the leading-edge separation. However, tests made at high subsonic Mach numbers on the datum wing suggest that this is unlikely to be the case[4]. These tests showed that flows with a part-span leading-edge separation are also sensitive to small excrescences at high Reynolds numbers (in this case caused by small cover plates near the leading edge).

The benefits of WVG's described in this paper have to be set against possible parasitic drag penalties in high-speed dash or manoeuvre conditions. Here parasitic drag is defined as the drag of the WVG or WVG's in the presence of the wing. Such penalties, it might be argued, could be especially severe for multiple-wire configurations. In order to obtain an indication of the parasitic drag penalties of the wires, calculations have been made for the following cases.

1) Supersonic manoeuvre at the Tropopause (flight scale)

$M = 1.5$, $C_L = 0.2$, $R = 56 \times 10^6$ (Case A, Fig 1)

2) Subsonic dash at sea level (flight scale)

$M = 0.8$, $C_L = 0.1$, $R = 100 \times 10^6$ (Case D, Fig 1)

3) Low-speed manoeuvre (wind-tunnel scale)

$M = 0.18$, $\alpha = 12°$, ($C_L = 0.4$), $R = 3.9 \times 10^6$

4) Low-speed manoeuvre (Reynolds number as for Case 2))

$M = 0.18$, $\alpha = 12°$, ($C_L = 0.4$), $R = 100 \times 10^6$

The first two conditions are representative of those of high-speed flight for a typical delta-wing combat aircraft, while the third case is one studied in the present investigation. This case is included in order to provide a link between the wind-tunnel measurements and calculated values of parasitic drag in high-speed flight. Comparison of values for the third and fourth cases yields an indication of Reynolds number effects between the wind tunnel and flight.

In all cases, the ratio d/c_0 (= 0.000283) and the wire angle are taken to be the same as for the wind-tunnel tests. Furthermore, the axial position of the wire was taken as $x_w = 0.452$. In the calculations the following assumptions have been made:

i) Wire vortex generators may be treated as individual elements for the calculation of parasitic drag.

ii) The changes in forces acting on the wire may be divided into components normal and parallel to the wire axis. Each of these components is taken to be the same as that on a wire in a uniform two-dimensional flow with a velocity equal to the appropriate component of the external-flow velocity of the approaching flow. The drag of the wire is then obtained by resolving the components in the free-stream direction.

iii) For the calculation of the normal-force component, end effects of the wire are ignored.

Hoerner[9] and, more recently, Gaudet and Winter[11] have provided a great deal of data for the drag increments due to various types of excrescences. In particular, Gaudet and Winter correlated their data for excrescence drag coefficient, C_{De}, of a number of types of excrescences in the form

$$\frac{C_{De}}{C_f} = f\left(\frac{u_\tau d}{\nu}\right)$$

Here C_f is local skin-friction coefficient and the drag coefficient is based on the frontal area of the excrescence. All the parameters are based on flow conditions just upstream of the wire, and friction velocity

$$u_\tau = \sqrt{\frac{\tau_w}{\rho}}$$

and viscosity are based on wall conditions.

The required boundary-layer parameters are determined by using an integral method for calculating boundary layers on infinite swept wings[12]. Allowance for wing taper is not needed because the WVG's are close to the leading edge, where the flow is similar to that over an infinite swept wing. Transition of the boundary layer on the wing is taken to be at the reattachment line for the two high-speed cases (1 and 2) and at the high Reynolds number, low-speed case (4); for the wind-tunnel case it is taken to be at the transition line of the short bubble, inferred from oil-flow visualisations. In all cases the pressure distributions used in the calculations were obtained from wind tunnel tests.

The normal force of each wire is derived from data given by Gaudet and Winter for a square ridge, using the appropriate component of velocity and skin friction. Information on the drag of long excrescences with blunt noses and tails is scarce but, from information given by Gaudet and Winter on fairings, a value of unity for axial force coefficient, based on

frontal area and local dynamic pressure appears reasonable for rough estimates. The results obtained for the parasitic drag coefficient of individual wires, C_{D_p}, (based on free-stream dynamic pressure and wing planform area) are shown in the table below, and are negligible.

Case	M	R x 10^{-6}	C_{D_p} x 10^7
1	1.5	56	2.26
2	0.8	100	3.39
3	0.18	3.9	11.59
4	0.18	100	18.82

If the parasitic drag penalty of multiple wires can be inferred from these results by addition, it will remain insignificant even with 28 wires (eg, for Case 4 the penalty ΔC_D = 0.00005). Therefore wing high-speed performance should not be compromised by WVG's considered in this paper.

It is also worth noting that the values of parasitic drag coefficient for the two high-speed flight cases (1 and 2) are much lower than that low-speed, high Reynolds-number case (4). This may be explained by the observation that, at high-speed conditions, the velocity of the flow in the vicinity of each wire is much lower, as a proportion of free-stream speed, and is more closely aligned with the wire axis than for the low speed, high incidence case. The parasitic drag coefficient of the wind-tunnel case (3) is somewhat lower than that of the corresponding high Reynolds-number case (4), showing the adverse effect of Reynolds number in reducing the thickness of the boundary layer compared with wire diameter and hence exposing the wire to flows of higher dynamic pressure. However, the value for the wind-tunnel case (3) is also much larger than those of the two high-speed cases. The value for Case 3 may be compared with measurements in the wind tunnel. For angles of incidence of 12° and below, the WVG's are not effective in controlling the flow (see Fig 8), hence measured increments in drag coefficient at low angles of incidence provide an indication of the parasitic drag penalty of the wires. However, the measured values of the increments in drag coefficient for a single wire at low angles of incidence are within the range of repeatability of the experiment which is small (±0.0002). The same comment applies to the calculated value in Case 3 above and also to the measured and calculated values for 28 wires. This provides further evidence that the parasitic-drag penalties of WVG's in high-speed flight are likely to be small.

The present study has other implications for flight performance of combat aircraft which are related to manufacturing tolerances in the leading-edge region of the wing. It has been shown that small excrescences can have significant effects on the force and pitching-moment characteristics of highly-swept wings at manoeuvre conditions, suggesting the need for careful monitoring of the wing shape in the leading-edge region.

Finally, the present paper has been concerned with the control of separations on the upper surface of a wing designed primarily for efficient supersonic manoeuvre. However, WVG's may also prove useful for wings with variable-droop leading edges designed primarily for efficient subsonic manoeuvre. Flows over wings of this type feature adverse pressure gradients in the region of the junction of the droop and the main wing, which possibly will cause upper-surface separations similar to those described in this paper. These separations may also determine the position of the origin of the leading-edge separation on the outer wing. Thus WVG's may be useful for controlling flows over wings of this type.

5 CONCLUSIONS

A wind-tunnel investigation into the effect of sub boundary-layer vortex generators on the flow over a cambered delta wing with leading edges that are both highly swept and round suggests the following conclusions.

1) A small, wire vortex-generator placed on the wing in the attached turbulent boundary layer close to the wing leading edge, at an angle of 16° to the leading edge in plan view, produces a vortical disturbance. This disturbance is caused by the conversion of boundary-layer vorticity into trailing vorticity. The vortical disturbance controls the boundary-layer flow toward and along a separation line on the curved upper surface of the wing, moving that separation line downstream.

2) This separation line effectively intersects or joins the leading edge, so that a further consequence of the control is that the position of the onset of leading-edge separation is shifted downstream, causing, in turn, reduced normal force and increased leading-edge thrust.

3) This increased leading-edge thrust arises mainly from a reorganisation of the separated leading-edge flow further downstream. The 'centre of area' of the suctions on the wing surface underneath the separated vortex is moved towards the forward facing parts of the wing surface.

4) An increase in the number of wires enlarges the range of angles of incidence over which the wires are effective in increasing leading-edge thrust.

5) A reduction in lift-dependent drag factor of up to about 16% is shown to be achievable by using multiple (28) wire vortex generators. The wire configuration giving this reduction should have an insignificant parasitic drag penalty in subsonic dash and supersonic manoeuvre conditions.

6) Wire vortex generators delay the wing pitch-up to a higher lift coefficient, the value of this lift coefficient increasing as wire number is increased.

Thus this paper shows that sub boundary-layer vortex generators provide effective control of separations on the upper surface of highly-swept, cambered wings for supersonic

combat aircraft, thereby giving significant improvements in performance at subsonic manoeuvre conditions.

KNOWLEDGMENTS

This work was supported by the British Ministry of Defence. The authors wish to thank Mrs I Gaudet for her work in computing the pressure forces and Mr M Stanley for his assistance with the wind tunnel tests and data reduction.

REFERENCES

1 Mason W.H., and Miller D.S., "Controlled supercritical cross-flow on supersonic wings - an experimental validation." AIAA-80-42 July 1980.

2 Miller D.S., Pittman J.L., and Wood R.M., "An overview of two non-linear supersonic wing design studies." AIAA-83-082 January 1983.

3 Mason W.H., Siclari M.J., and Miller D.S., "A supersonic manoeuvre wing designed for nonlinear attached flow." AIAA-83-0425 January 1983.

4 Rose O.J., Miller D.S., Pittman J.L., Ashill P.R., and Fulker J L., "Full potential analysis of a supersonic delta wing/body" Journal of Aircraft. Vol 26, No 3, March 1989, pp 235-240.

5 Fulker J.L., and Ashill P.R. "A theoretical and experimental evaluation of a numerical method for calculating supersonic flows over wing-body configurations." AGARD-CP-437, pp 12.1 - 12.11, 1989.

6 Ashill P.R., Fulker J.L., Simmons M.J., and Betts C.J., "Flow features of highly-swept wings at subsonic and supersonic speeds." ICAS-90-3.9.1 October 1990.

7 Ashill P.R., and Betts C.J., "A study of the flow around the leading edge of a highly-swept wing in a low-speed wind tunnel." Proc. ASME Fluids Engineering Conference, Symposium on Transitional and Turbulent Compressible Boundary Layers', Washington DC, 21-24 June 1993.

8 Woodward D.S., Hardy B.C., and Ashill P.R., "Some types of scale effect in low speed, high-lift flows." ICAS-88-4.9.3, 1988.

9 Pearcey H.H., "Shock-induced separation and its prevention by design and boundary-layer control." 'Boundary Layer and Flow Control, its Principles and Application', Vol 2, Ed G V Lachmann, Pergamon Press, Oxford, 1961

10 Holmes A.E., Hickey P.K., and Murphy W.R., "The application of sub-boundary layer vortex generators to reduce canopy "Mach rumple" interior noise on the Gulfstream III." AIAA 87-0084, January 1987.

11 Kuethe A.M., "Effect of streamwise vortices on wake properties associated with sound generation." Journal of Aircraft, Vol 9, No 10, Oct 1972, pp 75-78.

12 McCormick D.C., "Shock-boundary layer interaction control with low-profile vortex generators and passive cavity." AIAA-92-0064, January 1992.

13 Weber J., Lawford J.A., and Haines A.B., "The reflection effect of fences at low speeds." ARC R&M 2977, 1956.

14 Haines A.B., "Some notes on flow patterns observed over various sweptback wings at low Mach numbers (in RAE 10ft x 7ft high speed tunnel)." RAE Technical Note Aero 2350, September 1954.

15 Mabey D.G., Welsh B.L., and Pyne C.R., "The development of leading-edge notches to improve the subsonic performance of wings of moderate sweep." European Forum on Aeroelasticity and Structural Dynamics, Aachen 1989.

16 Johnson, T.D. Jr., and Rao D.M., "Experimental study of delta wing leading-edge devices for drag reduction at high lift." NASA CR 65846, February 1982.

17 Rao D.M., and Johnson T.D Jr., "Investigation of delta wing leading-edge devices." Journal of Aircraft, Vol 8, No 3, March 1981, pp 161-167.

18 Polhamus E.C., "Predictions of vortex-lift characteristics by a leading-edge suction analogy." Journal of Aircraft, Vol 8, No 4, 1971, pp 193-199.

19 Mabey D.G., "A review of scale effects in unsteady aerodynamics." RAE Technical Report 91007 (1991) Prog. Aerospace Sci, Vol 28, 1991, pp 273-321.

20 Hoerner S.F., "Fluid-Dynamic Drag." Published by the Author, 1965.

21 Gaudet L., and Winter K.G., "Measurements of the drag of some characteristic aircraft excresences immersed in turbulent boundary layers." AGARD-CP-124, pp 4.-1 - 4.-11, October 1973.

22 Ashill P.R., and Smith P.D., "An integral method for calculating the effects on turbulent boundary-layer development of sweep and taper." The Aeronautical Journal, Vol 89, No 882, February 1985, pp 43-54.

AERODYNAMIC DESIGN OF SUPER MANEUVERABLE AIRCRAFT

by

R.D. Irodov and A.V. Petrov
Central Aerohydrodynamic Institute (TsAGI)
Zhukovsky-3, Moscow Region, 140160
Russia

SUMMARY

The main peculiarities of aerodynamic design of highly maneuverable aircraft are examined. The possibilities of improving the aerodynamic characteristics of aircraft at high angles of attack by use of high-lift devices and powered-lift systems (boundary layer control, blowing over wing, engine thrust vectoring) are shown. The conditions of controllable maneuver at high post-stalled angles of attack ($\alpha \leq 90$deg.) are established. Results of experimental investigations on the influence of wing planform and locations of aircraft components (wing, empennage) on the longitudinal stability and controllability at high angles of attack are presented. A comparative analysis of aerodynamic and maneuver performance of aircraft of various configurations (conventional, three-surface, canard) is performed.

LIST OF SYMBOLS

CL	lift coefficient increment;
Cn	normal force coefficient;
CJ	jet momentum coefficient;
Cm^{CL}, Cm^{α}	pitch moment coefficient derivatives;
S	area;
T	gross engine thrust;
R	turn radius;
H	altitude;
V	speed;
W	weight;
CM	center of mass;
α_n	control surface true angle of attack;
φ	control surface deflection angle;
ε	downwash angle;
t	time;
nxa	longitudinal load factor;
nza	lifting load factor;
$\dot{\psi}$	turn rate;
XCM	CM position;
XF^{α}	aerodynamic center position;
X_p	center of pressure position;
X_s	sailing center position

1. INTRODUCTION

Principal requirements currently being imposed on advanced fighters are: increased radius of action supersonically and enhanced maneuvering capabilities subsonically. The first requirement defines the choice of aerodynamic configuration: a canard configuration with a thin, moderate-aspect ratio wing having a leading edge sweep angle of 45...50deg. This configuration enables the supersonic aerodynamic efficiency to be increased as compared to the conventional two-surface configuration due to lesser aerodynamic center displacement with Mach number and accordingly lesser trim drag penalty. The second condition calls for substantially widening the angle-of-attack range, that is, operating well beyond a maximum of 20...25deg. Inherent in preceding-generation fighters, since the conventional means for enhancing aircraft lifting characteristics within the limits of their linear variations are practically exhausted. At this point, two avenues of investigations can be set off:

1) enhancement of maneuvering capabilities within the subcritical range of angles of attack, increase in the maximum lift coefficient Cmax and stall angle of attack (Fig.1) using powered-lift systems (PLS) for improving the parameters of classical maneuverability: lifting load factor nza, turn radius R and rate $\dot{\psi}$;

2) use of post-stall angles of attack in maneuvering, that is, reaching angles of attack on the order of 90deg. with substantially decreasing flight speeds (Fig.2); this enables the aircraft fore-and-aft axis (weapon pointing direction) to be rotated up to 90deg. relative to the flight path and the flight direction to be changed through rotating the aircraft about its longitudinal axis at near-zero forward speed, that is, the supermaneuverability to be realized.

Transition to angles of attack up to 90deg. can be either dynamic, that is, without trimming at limit points, or steady-state, that is, with the trim being provided at $\alpha = 90$deg. In the latter case, the PLS can be employed in the form of jet controls developed for VTOL aircraft.

Investigations conducted at the TsAGI have shown that the indicated potentialities of significantly improving maneuvering performance can be realized either on the canard aircraft with a tail elevator or on the aircraft of conventional two-surface configuration with an additional horizontal canard (HC, three-surface configuration) [1,2]. Thus, the contradictory requirements being imposed on advanced fighters can be met in the framework of the same canard configuration or its variants.

2. AERODYNAMICS OF MANEUVERABLE AIRCRAFT AT HIGH SUB-STALL ANGLES OF ATTACK

Fighter maneuvering characteristics nza, R, $\dot{\psi}$ are the best at angles of attack 30...35deg. and at maximum aerodynamic lift. This being so, aerodynamic means should be used for improving the lifting characteristics and reducing the required thrust-to-weight ratio of an aircraft.

The problem of improving the lifting characteristics of modern fighters of conventional two-surfaces configuration at high angles of attack is solved by using adaptive high-lift devices on wing panels and their leading edge extensions (LEX), with the latter generating stable vortex flow over the wing up to 30...35deg. angles of attack.

The investigations conducted at the TsAGI in the 1970s have shown that much the same effect can be obtained both with the conventional (pronounced-fuselage) configuration featuring a sharp-edged LEX on the wing and with the so-called integrated configuration. The basis for this configuration is formed by a lifting surface of a complex planform which combines three volumetric elements: the fuselage nose with the cockpit and equipment and two engine nacelles with side-wing inlets. Designed according to the first arrangement are the fighters F-16, F-18, YF-22, and designed according to the second one are the fighters MiG-29, Su-27, YF-23.

Similar characteristics can be obtained with a close-coupled canard-wing configuration. Favorable canard-wing interference allows obtaining high lifting characteristics and aerodynamic efficiency at high angles of attack and providing stability and controllability at stall and post-stall angles of attack.

Experimental investigations have shown that with the same area-to-wing area ratio the lift increment produced by the LEX is greater than that produced by the installed HC mainly due to higher strength of vortices generated by the highly swept LEX (Fig.3). Untrimmed values of Cmax for the conventional two-surface configuration with the LEX are somewhat greater than those for the canard configuration, with their planform areas being equal. But at the same overall dimensions, taken with accounting for

Presented at an AGARD Meeting on 'Technologies for Highly Manoeuvrable Aircraft', October 1993.

aerodynamic arrangement and center-of-mass (CM) position considerations, the realized planform area for the canard configuration can be greater than that for the conventional two-surface configuration, due to the installation of lifting surface on the rear fuselage. Under these conditions, at subsonic speeds untrimmed lift values will be the same for both the configurations, while in the trimmed case the canard configuration will produce the greater lift.

Lifting characteristics of both the configurations can be enhanced with the aid of wing leading and trailing edge high-lift devices both at moderate and at high angles of attack (Fig.4). An additional improvement of the lifting characteristics can be attained by the use of PLSs [5-7]: wing leading and trailing edge boundary layer control, spanwise axisymmetric jet blowing, thrust vectoring (TV) through nozzle rotations (see Figs.1,4).

The use of the powered-lift systems on the conventional configuration fighter allows the available lifting load factor in subsonic sustained maneuvering regimes to be enhanced by 0.6...0.8 and the deceleration/acceleration characteristics at M=0.4...0.6 to be improved considerably (Fig.5). The use of the internally blown flap system (BLC) or the spanwise blown system on the wing with deflected flaps is most effective.

3. AERODYNAMICS OF MANEUVERABLE AIRCRAFT AT HIGH POST-STALL ANGLES OF ATTACK

In increasing angle of attack beyond reaching the Cmax, aircraft lifting characteristics decrease and the drag continues to increase (see Fig.2). As angle of attack increases a lift decreases, the share of the thrust T increases which enters as a component of resulting force into expressions for longitudinal and lifting load factors:

$$n_{xa} = \frac{T\cos\alpha - D}{W}, \quad n_{za} = \frac{T\sin\alpha + L}{W}$$

At very high angles of attack (α=70-90deg.) in the wing-axis coordinate system the greater part of the aerodynamic force is the aircraft drag (normal force in the body-axis system) and the thrust substitutes for the lift. If the effective power-plant thrust exceeds the weight of a fighter it can fly without loss of height ($n_{za} \geq 1$) down to speeds approaching zero ($V \to 0$) while increasing angle of attack up to 90deg. In doing so, the radius of horizontal steady turn diminishes drastically ($R \to 0$). Thus, the potentialities of using high post-stall angle of attack in steady flight are defined by thrust-to-weight ratio $T/W > 1$, aerodynamic configuration and measures aimed at providing the control of aircraft and operating stability of its power plant over the whole angle-of-attack range ($\alpha \leq$ 90deg.). It is advisable to conduct the analysis of high-angle-of-attack aerodynamics with the body axis coordinate system, i.e. using the normal force as a function of angle of attack (see Fig.2). The function $Cn(\alpha)$ has three characteristic portions. 1 - linear increase in the normal force with angle of attack, which corresponds to attached or steady vortex flow around the wing; 2 - decrease in the increment rate of the normal force with angle of attack due to the separation onset on the wing and to breakdown of steady vortex flow over the wing; 3 - normal force stabilization as result of establishment of a developed unsteady separated flow over the wing. To enable reaching high post-stall angle of attack (on the order 90deg.) at low subsonic speeds, the aircraft must be able to be trimmed in the static conditions and have a sufficient pitch-down moment margin over the operational angle-of-attack range.

This means that the function $Cm(\alpha)$ of a supersonic fighter must be essentially nonlinear:

$Cm\alpha > 0$ under trim conditions at sub-stall angles of attack;
$Cm\alpha < 0$ under trim conditions at post-stall angles of attack.

The nature of the function $Cm(\alpha)$ at $\varphi = 0$ is determined by the normal force as a function of angle of attack and the CM position relative to the normal-force application point (center of pressure, $\bar{x}_p$). Control surface deflection displaces the center of pressure and, consequently, the curve $Cm(\alpha)$ in the pitch up or pitch down direction (in accordance with the deflection sign and the position of the control surface relative to the aircraft CM) by the value determined by control effectiveness.

The center-of-pressure position of isolated wings with low and moderate aspect ratios at $\alpha \to$ 90deg. shifts from a point that depends on the wing planform at low angles of attack (aerodynamic center), to the wing's center of area, which is, by definition, at the 50 percent mean aerodynamic chord ("sailing center", $\bar{x}_s = 0.5$, Fig.6) [1,3,4]. The smaller are the wing's sweep angle and aspect ratio, the greater is this shift. The shift is maximum for a forward-swept wings.

The aerodynamic center of the wings with complex planforms at α = 0. .5deg. is near the sailing center and can coincide with it (Fig.7).

The mounting of a horizontal tail or a canard shifts the aerodynamic center and the center of pressure of configuration respectively backward or forward. In the case of the canard the forward shift of the aerodynamic center at $\alpha = 0$ is greater than the center-of-pressure shift at α = 90deg. The horizontal tail shifts the center of pressure backward greater than the aerodynamic center due to a difference in the values of downwash at these surfaces. As a result of the mounting of these surfaces the distance between the points indicated increases for configurations with simple wing planforms (Fig 8).

The indicated backward shift of the center of pressure and the normal force stabilization at high angles of attack result in a substantial qualitative change in the behavior of the relationship $Cm(\alpha)$ in the range of α = 0. .90deg. at different CM positions of aircraft.

In the case of a forward CM position (1) with the CM being ahead of the center of pressure ($\bar{x}_p$) at zero control surface deflection ($\varphi = 0$) (Fig.9,a), the function $Cm(\alpha)$ takes the form that is characteristic of static stable aircraft (Fig.9,b). If for all angles of attack the aircraft's CM remains behind of the center of pressure at ($\varphi = 0$) (3), the expression is characteristic of unstable aircraft, but the curve flattens out after the critical angle of attack due to stabilization of the normal force (see Fig.9,b).

When the CM position is between the aerodynamic center at α = 0 deg and the center of pressure at α = 0 deg. (2), the curve $Cm(\alpha)$ takes the characteristic form with two trim points-unstable at low angles of attack ($\alpha_{trim} = 0$ at $\varphi = 0$) and stable at high ones (see Fig.9,b). Such form of the function $Cm(\alpha)$ enables aircraft to be trimmed at post-stall angles of attack (Fig 10). For reaching angles of attack on the order of 90deg. a overshoot in angles of attack is used beyond the angle corresponding to the stable trim at the maximum control surface deflection, φ_{max}, while the subsequent return to the required α_{trim} independently of the effectiveness of control surfaces is realized because of availability of high pitch-down moments owing to the configuration and the CM position.

Thus, the possibility of safely reaching extremely high angles of attack in flight depends to a large extent on the relative position of the two characteristic points, namely, the aerodynamic center at α = 0...5deg. and the center of pressure at α =90deg., i.e. on the aircraft's aerodynamic layout. If the two points practically coincide (wing with leading edge kink, see Figs.7 and 8), the choice of CM position cannot provide the nonlinear behavior of the function $Cm(\alpha)$ required for safely reaching α = 90deg. To reach extremely high angles of attack, an automation of the pitch-control channel is needed with the necessary provision of effective control at angles of attack near 90deg.

Control surface effectiveness is determined by the value of lift (normal force), depending on the true angle of attack

$$\alpha_n = \alpha + \varphi - \varepsilon$$

According to experimental data, the normal force on the horizontal tail or the canard varies approximately proportional to angle of attack up to $\alpha_n \approx 40$deg. At $\alpha_n > 40$deg the normal force is stabilized and, consequently, the control surface practically loses its effectiveness, but the pitch moment varies proportionally to the cosine of control surface deflection angle (Fig.11):

$$cm(\alpha,\varphi) = -k \cdot C_n \cdot l \cdot \cos\varphi,$$

where k is dynamic pressure ratio at control surface location, l is the arm of the control-surface normal force.

At positive deflection the canard loses effectiveness occurs at lower angles of attack than the horizontal tail of the conventional wing-tail configuration (see Fig.11) due to greater downwash near the canard. The function $\Delta C_m(\varphi)$ is practically linear and it retains the linearity up to sufficiently high angles of attack at negative deflection angles of the control surfaces. Effectiveness-optimized control is realized by means of an all-moving surfaces (or tail elevator) for a stable aircraft and with the help of the all-moving canard for an unstable one. Thus, to be trimmed, a highly-maneuverable fighter at canard configuration must have tail control surfaces, which are effective at high angles of attack. The possibility of longitudinal trim and safely reaching high post-stall angles of attack in the case of conventional configuration aircraft can be enlarged by mounting an additional canard (three-surface configuration) (Fig.12).

Extremely high angles of attack (on the order of 90deg.) in a dynamic regime can be reached by an aircraft of canard configuration with an elevator as well as by an aircraft of conventional two-surface configuration and three-surface configuration with properly chosen planform and CM position (Fig.13).

CONCLUSION

1. For supersonic fighters to operate at high post-stall angles of attack for subsonic maneuvering, it is advantageous to use a canard configuration with a tail elevator and nozzle vectoring at the tail or a three-surface configuration (with canard and horizontal tail). The canard configuration with a tail elevator is preferable because it provides higher Cmax values compared to the conventional two-surface configurations due to thrust vectoring and a higher trimmed lift-to-drag ratio at supersonic speeds owing to the absence of trim drag penalty due to small shift of the aerodynamic center.

2. For fighters not intended for prolonged supersonic cruise and having no thrust vectoring system, a three-surface configuration can be chosen whose subsonic lifting capabilities can be substantially increased by high-lift devices and powered-lift systems.

3. For safely reaching extremely high angles of attack (on the order of 90deg.) the CM of aircraft with any configuration must be located between the aerodynamic center at $\alpha = 0$ and the center of pressure at $\alpha = 90$deg. ($\varphi = 0$). The required relative positions of these points must be provided by a proper choice of the wing planform and control surface parameters. It is necessary to provide a pitch-down moment margin and effective roll and yaw control at all angles of attack.

REFERENCES

1. I.G.Bashkirov, R.D.Irodov, L.A.Kurochkin, S.B.Novoselcev, L.N.Onkova.
"Aerodynamic configurations of advanced fighters."
Aviation science and technology, 1 (601), 1993 (in Russian).

2. R.D.Irodov, I.A.Kurochkin, A.I.Maksimenko, S.B.Novoselcev, A.A.Pavlenko, L.N.Onkova
"Aerodynamics of the advanced fighter." Proceedings of TsAGI, 1989 (in Russian).

3. I.G.Bashkirov, L.I.Bushueva, N.N.Dolzhenko, R.D.Irodov
"Investigations of the aerodynamic characteristics of maneuverable aircraft models at angles of attack $\alpha = 0...90$deg. in the TsAGI T-105 wind tunnel." Aviation science and technology, 2, 1993 (in Russian).

4. I.G.Bashkirov, R.D.Irodov
Influence of wing planform and aircraft configuration over pitch moment for angles of incidence from 0-90deg."
International conference on Aircraft flight safety. Zhukovsky, Russia, 1993.

5. N.M.Mitrohin, A.V.Petrov
"The use of powered-lift systems for improving aerodynamic characteristics of maneuverable aircraft."
Proceedings of TsAGI, 1989 (in Russian).

6. B.N.Minajlov, A.V.Petrov
"An investigation of thrust vectoring effectiveness at high subsonic speeds."
Proceedings of TsAGI, 1989 (in Russian).

7. A.V.Petrov
"Aerodynamics of aircraft with powered-lift systems."
Proceedings of the second sino-russian symposium on aerodynamics. CAE, Beijing, 1992.

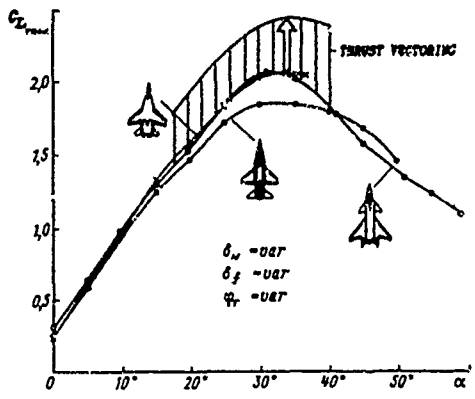

Fig.1. Combat aircraft aerodynamics

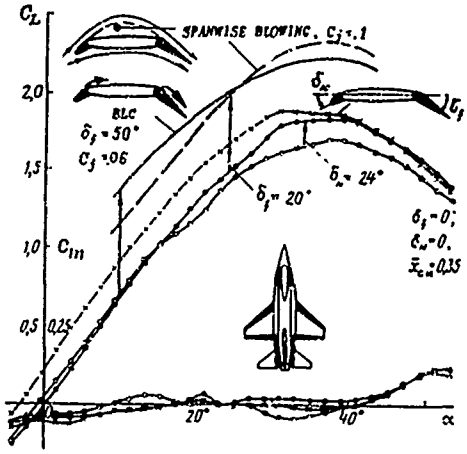

Fig.4. High-lift and powered-lift systems

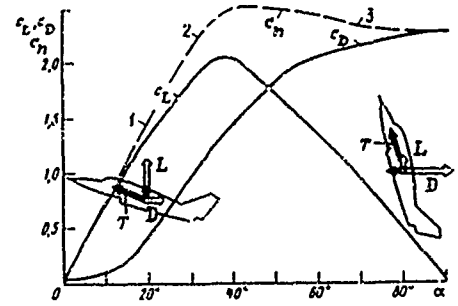

Fig.2. Combat aircraft aerodynamic characteristics vs angle of attack

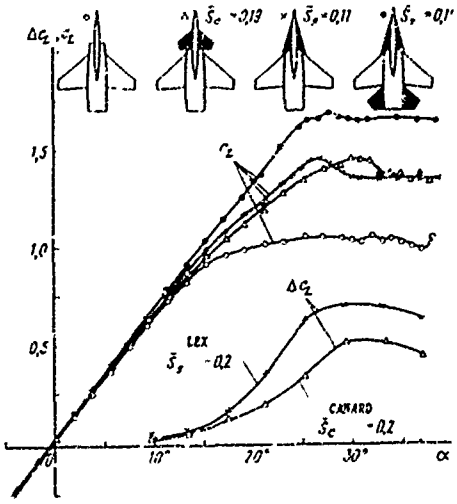

Fig.3. Effect of LEX, canard and tail upon lift augmentation

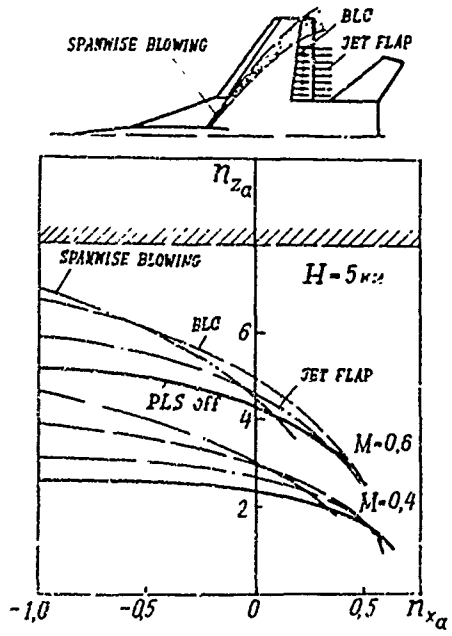

Fig.5. Load factors increment by use of PLS

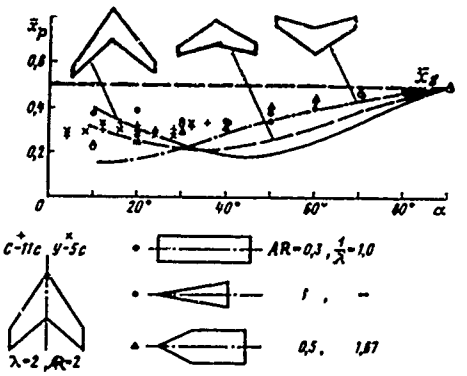

Fig.6. Wing form influence on center-of-pressure location

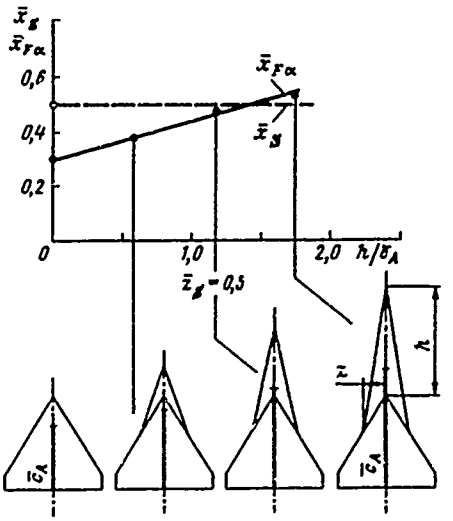

Fig.7. Relative location of the aerodynamic and sailing centers

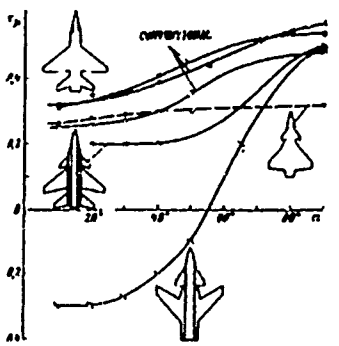

Fig.8. Effect of aerodynamic configuration and angle of attack on center-of-pressure location

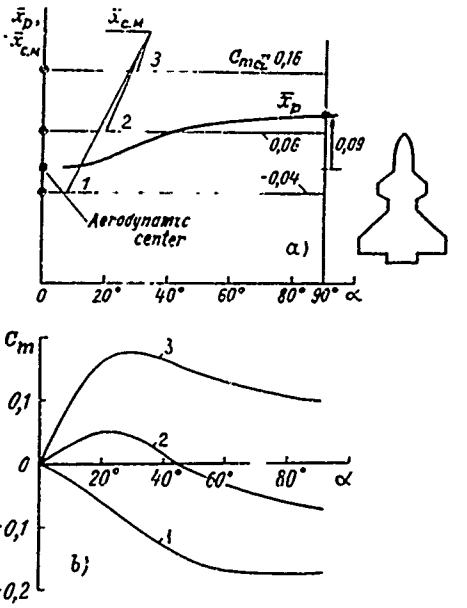

Fig.9. Relative center-of-pressure and center-of-mass locations (a) and its effect on Cm vs α (b)

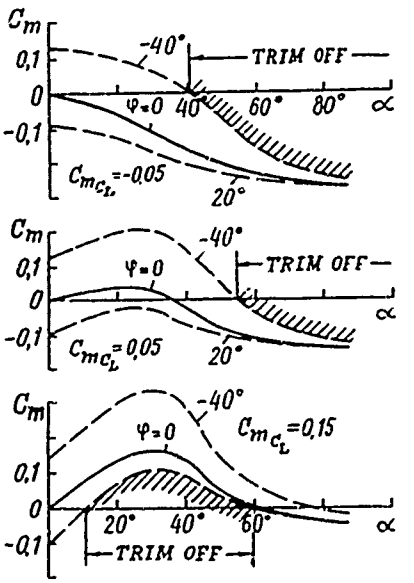

Fig.10. Aircraft pitch trim

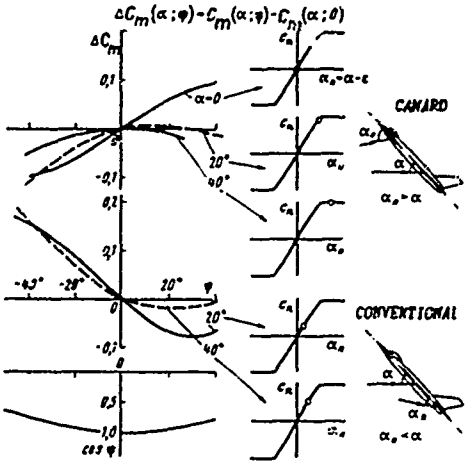

Fig.11. Tail and canard effectiveness

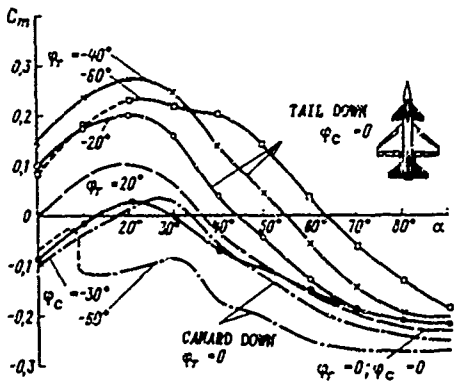

Fig.12. Pitching moment vs α for the three-surface configuration at various canard and tail deflections

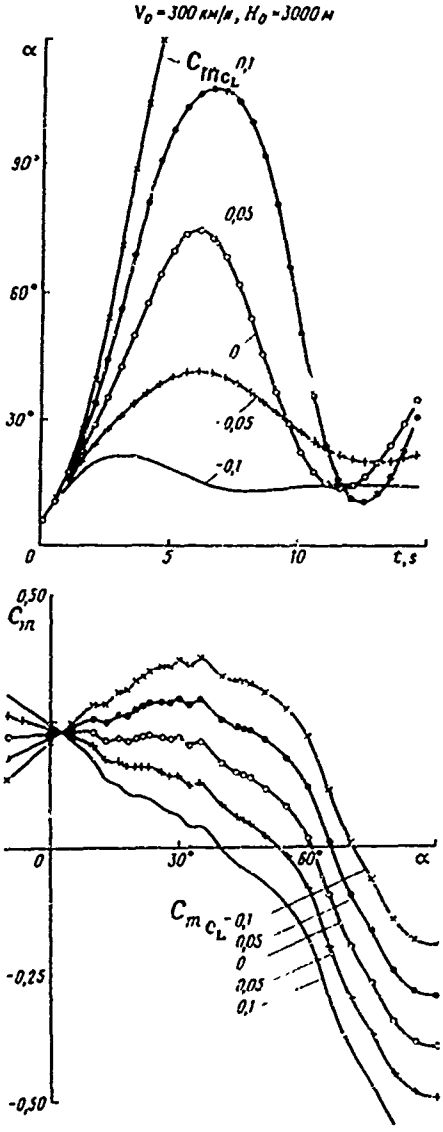

Fig.13. Pull-up/push-over manoeuvre for different static stability margins

X-31A CONTROL LAW DESIGN

by

H. Beh and **G. Hofinger**
Deutsche Aerospace AG
Military Aircraft LME212
Postfach 801160
D-81663 Munich
Germany

1. SUMMARY

This paper presents an overview on the X-31A flight control law design philosophy and the technical realization of the design. After an introduction in the FCS hardware configuration the basic control law structure and the method used for feedback gain calculation are presented. Several elements as the feedforward path, gravity effect compensation, inertial & gyroscopic coupling compensation and the pilot command system are discussed in more detail. Simplified block diagrams of the basic flight control mode in the longitudinal and lateral/directional axis follow. Finally the implementation of the thrust vectoring system including engagement and disengagement procedure is shown.

2. LIST OF SYMBOLS AND ABBREVIATIONS

AoA	Angle of Attack
A/C	Aircraft
CPU	Central Processing Unit
DASA	Deutsche Aerospace (former Messerschmitt-Bölkow-Blohm MBB)
EFM	Enhanced Fighter Maneuverability
FCC	Flight Control Computer
FCL	Flight Control Laws
FCS	Flight Control System
IMU	Inertial Measurement Unit
IO	Input/Output
LVDT	Linear Variable Data Transducer
PST	Poststall
RI	Rockwell International
TV	Thrust Vectoring
Φ	bank angle
Θ	pitch attitude
α	angle of attack
α_c	angle of attak command
β	sideslip
β_c	sideslip command
δ_{SF}	symmetrical trailing edge command
δ_{DF}	differential trailing edge command
δ_C	canard command
δ_R	rudder command
κ	thrust vectoring command yaw axis
σ	thrust vectoring command pitch axis
$\cos\mu \cos\gamma$	direction cosine
$\sin\mu \cos\gamma$	direction cosine
J	performance index
V	aircraft speed
g	gravity constant
n_y	sideforce
n_z	load factor
p	roll rate body axis
q	pitch rate body axis
r	yaw rate body axis
x_p	pilot command roll axis
x_q	pilot command pitch axis
x_r	pilot command yaw axis

Indices

e	experimental axis
k	nodal line axis (flight path axis)
w	wind axis
c	command

Vectors and matrices

$\underline{x}$	pilot command vector
$\underline{u}$	surface command vector
$\underline{u}_c$	steady state actuator command vector
$\underline{x}$	state variable vector
$\underline{y}$	output vector
$\underline{x}^T$	transpose of vector $\underline{x}$
$\underline{x}_k$	vector $\underline{x}$ @ time k
$\underline{\underline{A}}$	system matrix
$\underline{\underline{B}}$	input matrix
$\underline{\underline{C}}$	output matrix
$\underline{\underline{K}}$	feedback matrix
$\underline{\underline{P}}$	Riccati gain matrix
$\underline{\underline{Q}}$	weighting matrix of performance index
$\underline{\underline{R}}$	weighting matrix of performance index
$\underline{\underline{X}}^T$	transpose of matrix $\underline{\underline{X}}$

3. INTRODUCTION

The X-31A post stall experimental aircraft was developed to demonstrate enhanced fighter manoeuvrability by using thrust vectoring to fly beyond stall limits. The goal of the EFM program is to demonstrate the tactical advantage of a fighter aircraft being capable to manoeuvre and maintain controlled flight including the poststall regime up to 70 degrees AoA.

Two fighter type X-31A aircraft were built by Rockwell International and Deutsche Aerospace under contract with the Advanced Research Projects Agency (ARPA) and the German Ministry of Defense (GMoD).

Presented at an AGARD Meeting on 'Technologies for Highly Manoeuvrable Aircraft', October 1993.

Since the first flights of aircraft #1 on October 11th 1991 and aircraft #2 on January 19th 1992 the two aircraft have accumulated a total of 268 flights (145 on aircraft #1 and 123 on aircraft #2) until August 20th 199. The conventional envelope was cleared to 0.9 Mach, 40 kft pressure altitude, 485 kcas and 30 degrees AoA. Symmetrical loads were cleared between 7g's and -2g's. Shortly after PST flight test was started both aircraft were transferred from the RI flight test facility at Palmdale Cal. to the NASA Dryden Flight Research Facilities (DFRF) at Edwards Airforce Base by late January 1992 to continue the PST envelope expansion flight test. Since then more than 100 PST clearance flights have been accomplished and the PST envelope is now cleared up to 70 degrees AoA, between 10 kft and 30 kft pressure altitude, a maximum of 4g's during PST entry and a maximum of 225 kcas entry speed. In the meantime tactical flight test has started to demonstrate the EFM capability of the X-31A aircraft.

4. X-31A FLIGHT CONTROL SYSTEM

The X-31A aircraft is a longitudinal unstable (time to double amplitude as low as 200 msec) delta wing A/C with canard configuration The primary aerodynamic control surfaces are symmetrical trailing edge flaps and canard for the longitudinal axis and differential trailing edge flap and rudder for the lateral/directional axes In addition a thrust vectoring system is added to the engine exhaust nozzle utilizing three paddles. Each paddle covers an angular section of 120 degrees around the exaust nozzle and can be deflected up to 35 degrees into the plume, leading to a thrust deflection in the pitch and yaw axis of more then 10 degrees This TV system is used to augment the aerodynamic control power during low speed and PST flight.

The X-31A flight control system is a full authority digital fly by wire system. It consists of three identical FCC's (two CPU's each) supported by a so called tie-breaker FCC. This tie-breaker is like the other FCC's but with just one CPU. It selects the healthy FCC lane in case of a second FCC failure, which gives a quadruplex system reliability. The safety critical flight control components are electrically quadruplex and connected to all four FCC's These are the pilot inceptors (stick and pedal), the rate gyros, the accelerometers and the actuators of trailing edge flap, canard and rudder. The safety critical actuators (primary control surfaces) are hydraulically duplex. The other components are not considered safety critical, but are necesary to fullfil the EFM requirements and to be able to fly within the PST regime. These are AoA and sideslip sensors located at the noseboom, air data computer, inertial measurement unit and the actuators of the thrust vectoring paddles, leading edge flap, speedbrake and engine air intake These components are electrically duplex, except the IMU which has a selftest monitoring feature The nonsafety critical actuators (secondary control surfaces) are hydraulically simplex. A failure of a nonsafety critical component

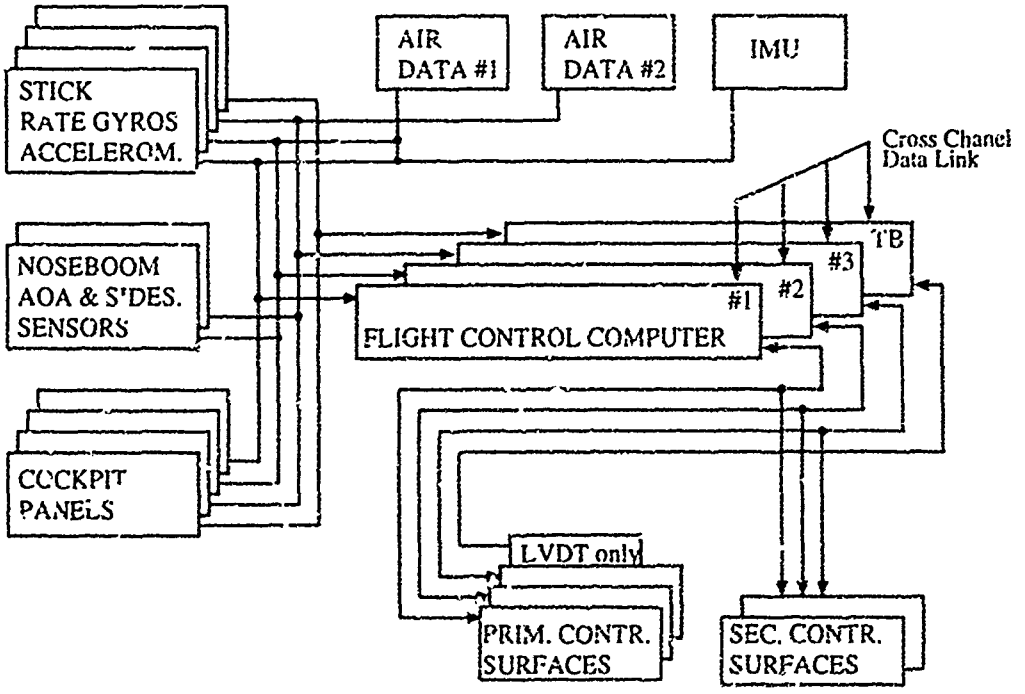

Fig1: X-31A flight control hardware configuration

must be monitored by the redundancy management and reported to the flight control laws. Fig. 1 gives an overview over the flight control system architecture.

In the basic flight control system mode all feedback signals are used to calculate the actuator commands There are two basic modes, because the TV can be enabled and disabled by the pilot. But PST flight is prevented by the FCL as long as TV is disabled. For takeoff and landing TV is automatically disabled for safety reasons. Depending on the actual sensor failure situation, reversionary modes provide a step by step system degradation, i.e.

- R1 - inertial measurement unit disengage mode
- R2 - flow angle disengage mode
- R3 - fixed gain mode in case of an airdata failure

The most degraded mode, R3, still has save flying home capability. In fig. 2 the step by step degradation is shown; note that the more degraded mode includes the disengagements of the less degraded modes, i.e in R3 mode the IMU and flow angles are also disengaged. The arrows illustrate the possible degradations in case of a hardware failure. The degraded modes are also pilot selectable in a nonfailure situation for flight test purposes.

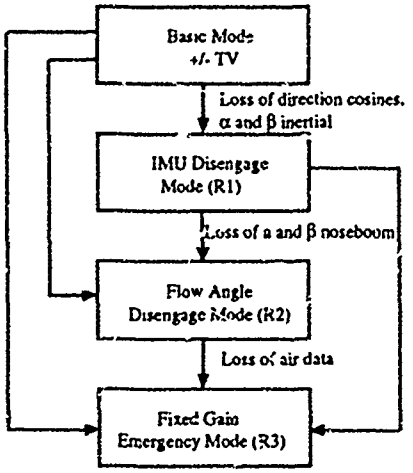

Fig 2: Flight Control System Modes

For safety reasons a spin recovery mode was introduced into the flight control laws. This mode must be selected by the pilot. There are classical direct links from stick and pedal to canard, trailing edge flap, rudder and thrust vectoring, giving the pilot full surface deflection authority. A proportional and integral pitch rate feedback is the only closed stabilization loop in the spin recovery mode.

5. BASIC STRUCTURE OF THE CONTROL LAWS

The X-31A flight control laws have three main external interfaces i.e.:

the pilot command vector $\underline{P}$ (x_p, x_q, x_r),

the sensed feedback vector $\underline{y}$ (p, q, r, α, β) and

the actuation command vector $\underline{u}$ (δ_{SF},δ_{DF},δ_C,δ_R ,σ ,κ).

Within the PST flight envelope the pilot command vector consists of wind axis roll rate command (x_p), angle of attack command (x_q) and sideslip command (x_r). At high dynamic pressure flight conditions load factor command replaces angle of attack command.

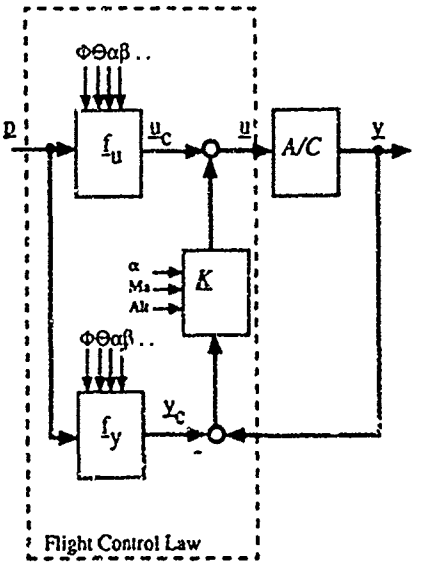

Fig. 3: Basic structure of the X-31A FCL

Fig. 3 shows the X-31A flight control laws in a closed loop together with the aircraft dynamics There are three subunits within the flight control laws, the linear feedback unit K and the nonlinear feedforward units f_u and f_y. The feedforward unit f_u calculates the necessary steady state command vector $\underline{u}_c$, i.e. the trimmed surface deflections, for the pilot command vector $\underline{P}$ depending on the actual flight condition and aircraft configuration data (e.g. c.g., weight). In parallel f_y calculates the corresponding steady state command vector $\underline{y}_c$. That means for all feedback signals an associated command signal must be calculated from the pilot input.

The actuator commands are calculated with the following

vector equation:

$$\underline{u} = \underline{K} * \left(\underline{y} - \underline{y}_c\right) + \underline{u}_c \quad \text{(Eqn. 1)}$$

Thus the actuator command vector u is the sum of the steady state command vector (trimmed surface deflections) and the feedback difference vector multiplied by the feedback gain matrix.

5.1 Determination of the Feedback Gain Matrix K

The feedback gain matrix K is determined using the linearised aircraft model split into longitudinal respectively lateral/directional motion. All additional dynamics (e.g actuation and sensor models) are not considered. This leads to fourth order models. Using the z-transform the vector difference equations are

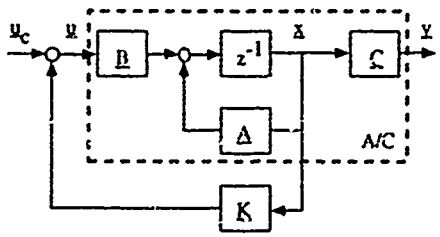

$$\begin{aligned} \underline{x}_{k+1} &= \underline{A}\underline{x}_k + \underline{B}\underline{u}_k \\ \underline{y}_k &= \underline{C}\underline{x}_k \end{aligned} \quad \text{(Eqn. 2)}$$

The feedback matrix is mathematically calculated using the optimal linear digital regulator design. Thereby the main task for the designer is the definition of the weighting matrices Q and R of the quadratic performance index J (Eqn. 3). The minimization of the performance index for infinite time results in a time constant optimum feedback matrix K. This matrix is calculated (Eqn. 4) using the system and weighting matrices and the matrix P which is the solution of the "Matrix Riccati Equation" (Eqn. 5):

$$J = \frac{1}{2}\sum_{k=0}^{\infty}\left(\underline{x}_k^T \underline{Q}\, \underline{x}_k + \underline{u}_k^T \underline{R}\, \underline{u}_k\right) \quad \text{(Eqn. 3)}$$

$$\underline{K} = \left(\underline{B}^T \underline{P} \underline{B} + \underline{R}\right)^{-1} \underline{B}^T \underline{P} \underline{A} \quad \text{(Eqn. 4)}$$

$$\underline{P} = \underline{A}^T \left[\underline{P} - \underline{P}\underline{B}\left(\underline{B}^T \underline{P}\underline{B} + \underline{R}\right)^{-1} \underline{B}^T \underline{P}\right] \underline{A} + \underline{Q} \quad \text{(Eqn. 5)}$$

This equation is often referred to as the algebraic Riccati equation. The stability and handling analysis is carried out with the full high order system. If this check shows unsatisfactory results the weighting matrices have to be adjusted and the optimization procedure is repeated.

5.2 Calculation of the Feedforward Paths

The feedforward paths are calculated independently from the feedback path using the steady state equations of motion of the aircraft. Steady state is interpreted in this context as the resulting stable flight condition with constant pilot inputs (e.g. steady state wind axis roll). When taking into account all influences in calculating the steady state vectors $\underline{y}_c$ and $\underline{u}_c$, the functions f_y and f_u describe the inverse steady state model of the aircraft. They include all direct link and all compensation paths (e.g gravity effects, inertial coupling, speedbrake moment compensation ...) and are dependent on configuration and flight condition. Constraints as complexity, model fidelity or computer power do not allow the full implementation of all paths, therefore some of them must be simplified or omitted at all. The steady state feedback difference error is a measurement of this simplification.

5.3 Inertial and Gyroscopic Coupling Compensation

The gyroscopic moments are square dependent on the angular rates and therefore not considered in the linearised model. At high angular rates these moments cannot be neglected. Uncompensated these moments would lead to unacceptably large deviations and the aircraft reaction would be lagged by its dynamic. Introduction of an integral feedback would help, but it introduces overshoots. The better solution is a feedforward compensation acting instantly (just lagged by sensor and actuation dynamics) against the disturbances. The small remaining deviations due to model uncertainties are controlled by the feedback loops. Fig. 4 and fig. 5 show the block diagram of the longitudinal respectively lateral/directional inertial and gyroscopic coupling compensation. The constants c are dependent on the inertias of the aircraft and the engine. These are used to calculate a normalised compensation moment out of the rates in front of the gains k. These gains are functions of flight conditions. The outputs are the necessary

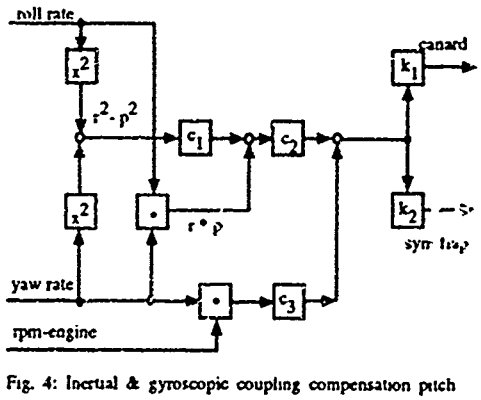

Fig. 4: Inertial & gyroscopic coupling compensation pitch axis.

surface deflections to compensate the inertial and gyroscopic moment.

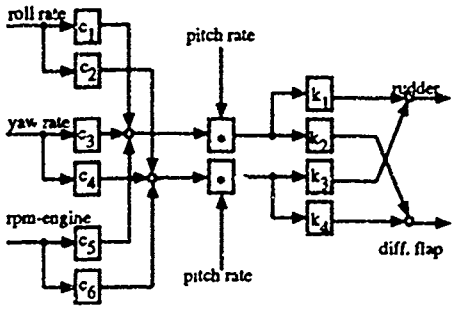

Fig. 5: Inertia & gyroscopic coupling compensation lateral/ directional axis.

5.4 Gravity Effect Compensation

The simplest description of the force equation is in the flight path axes system. Here the forces in y- and z-direction (ny and nz) consist just of the centripedal force and the gravity.

$$n_{k_z} = \frac{V_k}{g} q_k + \cos\mu\cos\gamma \qquad \text{(Eqn. 6)}$$

$$n_{k_y} = -\frac{V_k}{g} r_k + \sin\mu\cos\gamma \qquad \text{(Eqn. 7)}$$

They will be used to calculate the flight path rate command signals out of the commanded g's and gravity components.

$$q_{k_c} = \frac{g}{V_k}(n_{k_{z_c}} - \cos\mu\cos\gamma) \qquad \text{(Eqn. 8)}$$

$$r_{k_c} = \frac{g}{V_k}(-n_{k_{y_c}} + \sin\mu\cos\gamma) \qquad \text{(Eqn. 9)}$$

For this the body axes acceleration commands are transformed into flight path axis.

With the dependency of the rates from gravity additional moments due to aerodynamic damping come into the exact equation, the compensation of these moments is neglected.

The time differential of the gravity component leads to angular accelerations. These moments are compensated by a feedforward command.

5.5 Additional Control Structure Elements

The simplified model, used for the determination of the feedback matrix, may lead to a high order system with reduced stability and/or degraded handling qualities. With filters in the feedback and feed forward loops this can be improved again. Failed or missing feedback signals have to be substituted by observers.

If the calculation of the feedforward signals is missing some steady state term (in case of a hardware failure), a steady state error (difference between commanded and sensed signal) will remain. Washout filters in the feedback loop are used to drive this error to zero. Here just the high frequency part of the feedback signal will be used.

Limitations due to loads, control power, sensors and pilot accelerations are kept with scaling and rate limiting of the pilot command loop.

6. LONGITUDINAL FLIGHT CONTROL LAWS

The pitch stick position is scaled in the flight control laws from -1.0 (max push) to +1.5 (max pull). This position corresponds directly to an AoA or load factor command. At low dynamic pressure flight conditions the FCL is in the AoA comand mode. Here a command of -1.0 corresponds to -10 deg AoA, +1.0 corresponds to +30. deg AoA and +1.5 corresponds to +70. deg AoA. If PST is disabled the AoA command is limited to +30. deg. A force detend in the stick feel system at +1.0 gives the pilot information whether he has pulled into PST or not. At high dynamic pressure -1.0 commands approx. -2.4 g's and +1.0 commands 7.2 g's. Pulling over the detend does not change the maximum command of 7.2 g's (this is the aircraft's load limit). The switch over between these two command systems is at the flight condition where 30 deg AoA results in the maximum load factor of 7.2 g's. This is around 380 psf. Depending on the stick command the associated command is calculated, i.e. in the angle of attack command flight regime the associated load factor command is calculated and vice versa. PST flight is only possible if the aircraft is in the angle of attack command mode.

Fig. 6 presents a simplified block diagram of the longitudinal flight control laws for the AoA command mode. On the left hand side the pilot input (in this case AoA command) and the main feedback sensor signals AoA and pitch rate are shown. The calculated output canard command, symmetric trailing edge flap command and the thrust vectoring command for the pitch axis are on the right hand side. Within the block diagram three areas are surrounded by a dashed line. They reflect the main units as described before.

6.1 Direct Link Longitudinal Axis (f_{ll})

The direct link path in the upper right corner of fig. 6 calculates the steady state canard and trailing edge flap positions out of the commanded angle of attack and the actual flight condition. Derived from trimmed conditions with wings level and max. dry power the according canard and trailing edge flap deflections are stored in a set of two trim-tables. The additional degree of freedom with two control effectors is used to optimize for minimum drag at low angle of attack and lateral stability (aerodynamic stability derivatives are dependant on canard position) at high angle of attack. This set is called the "cruise" trim schedule. But this schedule results in high landing speeds, therefore a second set of trim tables was calculated with the goal of maximum lift at landing angle of attack. This "high lift" schedule is also stored in the flight control computer. The pilot can switch from one schedule to the other, but the "high lift" trim schedule is restricted for takeoff and landing. For simplification only one set of trim tables is shown in fig. 6.

A lag filter with a time constant corresponding to the angle of

attack response of the aircraft is used in front of the trim-tables to compensate the pilot command lead error to the aircraft response.

The canard and trailing edge deflections to compensate the inertial and g) ' .opic moments as defined in fig.4 are added to the output of the trim-tables and this sum forms the steady state trim commands.

The aerodynamic control power is sufficient for trimming, therefore thrust vectoring is not used.

6.2 Calculation of pitch rate command (f_y)

The pitch rate command calculation is shown on the left side of fig. 6. First the associated n_z command is derived from the AoA command, using a stored trimmed lift table, dynamic pressure and an estimated aircraft weight. From that the direction cosine of the gravity in the aircraft z-axis is subtracted and multiplication with the gravity constant divided by aircraft speed results in the pitch rate command (Eqn. 8).

6.3 Feedback Loops Longitudinal Axis

The feedback loops are shown on the lower right corner of fig. 6. Inputs are the differences between commanded and actual AoA and pitch rate. These deltas are multiplied by the gains stored in three-dimensional tables as functions of altitude, mach number and AoA and the results are summed up. This sum is a normalised pitching moment the feedback loops ask for. Downstream this pitching moment is distributed with factors to canard, symmetrical flap and pitch axis thrust vectoring command. These factors depend on the flight condition and the actual engine thrust level. They are calculated in the flight control laws using stored tables. There are two different distributions stored in the flight control laws, with and without thrust vectoring. Without thrust vectoring this factor is set to zero and the others are raised accordingly.

It is the designer's choice to select an appropriate distribution of the different pitching moment producers during the optimization of the feedback gains. The $\underline{x}_k$ and $\underline{u}_k$ vector of equation 2 for the longitudinal axis reads:

$$\underline{x}^T = \left[\nu_k, \alpha, q, \Theta\right] \quad u = \left[\delta\right] \qquad \text{(Eqn. 10)}$$

In this equation δ is a linear combination of canard, symmetrical trailing edge deflection and pitch thrust vectoring. For the elements of the performance index weighting matrices only their relative value to each other is important, therefore the control weighting matrix can be set to one. For the state weighting matrix a diagonal matrix was chosen with zeros in the speed and pitch attitude rows. This results in small feedback gains for speed and pitch attitude which are neglected because of their small influence on angle of attack motion. The Phugoide cannot be controlled with these feedbacks, but the resulting Phugoide is within the handling quality requirements. The frequency and damping of the angle of attack mo-

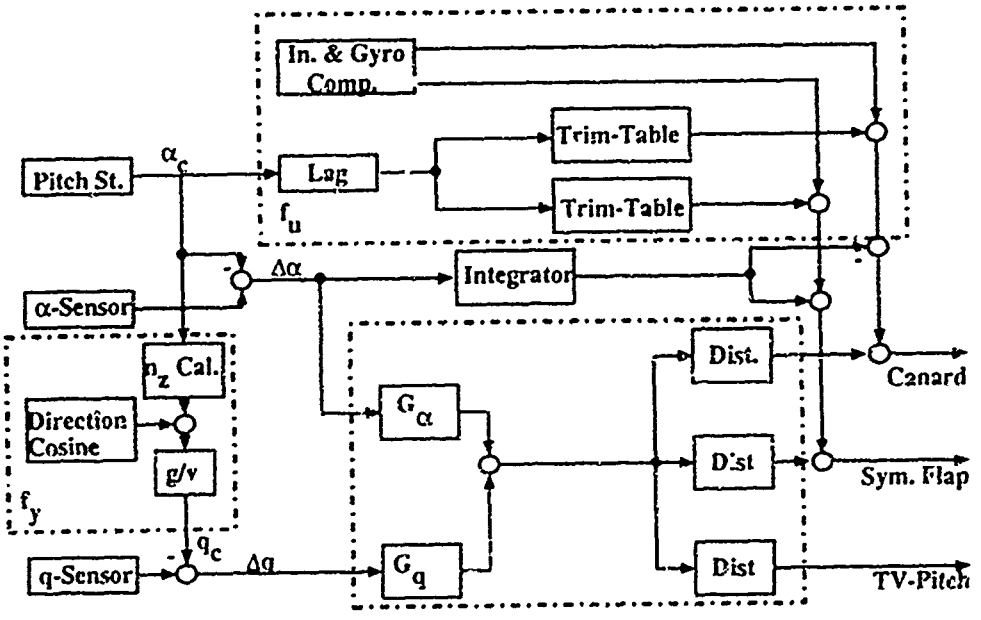

Fig. 6 . Simplified block diagram of the X-31a longitudinal flight control laws. (Basic Mode, α-Command)

tion is chosen with the values of q_α and q_q.

$$\underline{Q} = diag\left[0, q_\alpha, q_q, 0\right] \; ; \; \underline{R} = [1] \qquad \text{(Eqn. 11)}$$

In addition an angle of attack resp. load factor error integral is implemented which has not much influence on the angle of attack motion. The Phugoide remains unchanged with angle of attack integral and is more damped with load factor integral.

7. LATERAL/DIRECTIONAL FLIGHT CONTROL LAWS

Roll stick position is scaled in the flight control laws from -1. (max. left) to +1. (max. right). Depending on the flight condition a maximum wind axis roll command $p_{c\,max.}$ is calculated (up to 240 deg/sec @ low AoA and high dynamic pressure). The maximum roll rate is scaled with flight condition such, that the available control power will be used as much as possible for the steady state roll, with sufficient control power left for stabilization and departure prevention. This maximum command multiplied by the scaled roll stick input gives the wind axis roll rate command p_c.

The rudder pedal command is calculated in a similar way. Here $\beta_{c\,max}$ is calculated as a function of AoA and aircraft speed (up to 12 deg @ low AoA and low speed). This maximum command multiplied by the scaled rudder pedal gives the sideslip command β_c. During rapid rolling the sideslip command is blended to zero, to use the whole control power for rolling (roll priority).

Fig. 7 shows a simplified block diagram of the lateral/directional flight control laws. The large box in the center marked "Gains" represents a matrix multiplication of a combined feedback and feedforward matrix (5 columns 3 rows) by the input vector (p_c, Δp, Δr, $\Delta\beta$, β_c) resulting in surface commands for rudder, differential trailing edge flap and yaw thrust vectoring.

7.1 Direct Link Lateral/Directional Axes (f_{ll})

In the lateral/directional axis direct links exist from the wind axis roll rate command as well as from the sideslip command to the trailing edge flaps (differential), rudder and thrust vectoring. They are calculated by multiplying the commands with gains. The gains are stored in tables and interpolated depending on flight condition. The direct link commands correspond to the deflections calculated in a steady state flight condition.

The direct link yawing moment is fed to the aerodynamic rudder at angles of attack up to 30°. At post stall conditions the rudder becomes ineffective. Thus direct link is blended to thrust vectoring which takes over the full authority in yaw at 45° AoA.

As with the longitudinal flight control law the surface deflections to compensate the inertial and gyroscopic moments

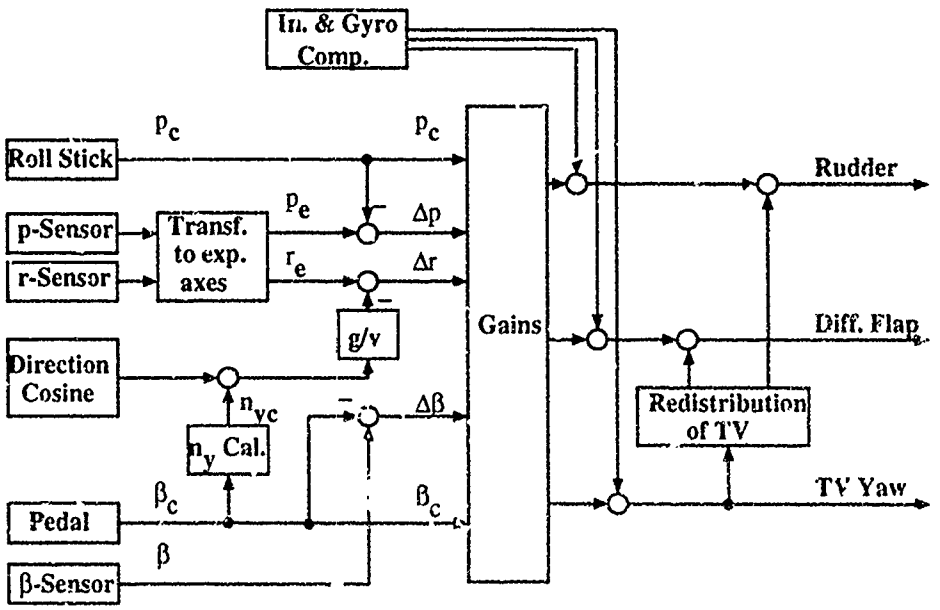

Fig. 7 Simplified block diagram of the X-31a lateral/directional flight control laws (Basic Mode)

as defined in fig. 5 are added to the surface commands.

7.2 Calculation of yaw rate command (f_y)

The yaw rate command is not directly a pilot input, thus it has to be calculated in the flight control laws. First the associated n_y command is derived from the sideslip command, using a stored sideforce table, dynamic pressure and an estimated aircraft weight. From that the direction cosine of the gravity in the aircraft y-axis is subtracted and multiplication by the gravity constant divided by aircraft speed results in the wind axis yaw rate command (Eqn. 4).

7.3 Feedback Loops Lateral/Directional Axes

Similar to the longitudinal control laws the differences of the commanded and actual sideslip, wind axis roll and yaw rate are multiplied by gains depending on AoA, altitude and mach number. The thrust vectoring gains depend also on estimated thrust. If thrust vectoring is switched off this command is redistributed to rudder and differential flap. Thrust vectoring nearly gives a pure yawing moment, in the stored redistribution tables a combination of rudder and differential flap is precomputed depending on flight condition giving also a pure yaw moment.

The feedback gain matrix is determined by the optimal control theory. The $\underline{x}_k$ and $\underline{u}_k$ vectors of equation 2 for the lateral/directional axes read:

$$\underline{x}^T = \left[\beta, p_w, r_w, \Phi\right]$$
$$\underline{u}^T = \left[\delta_{DF}, \delta_R, \delta_{TV}\right] \qquad \text{(Eqn. 12)}$$

The weighting matrices are defined as shown below. The Φ-column and -row elements are set to zero and the Φ-feedbacks which have only marginal influence on Dutch Roll and Roll mode are neglected. The diagonal elements of the matrix Q mainly define the eigenvalues of the lateral/directional aircraft motion. The other elements are used to decouple the yawing and rolling motion. The control power is weighted with the diagonal matrix R. A Spiral mode stabilization needs a Φ-feedback or the feedback of an equivalent signal, but the resulting Spiral mode fulfills the handling quality requirements.

$$\underline{Q} = \begin{bmatrix} q_\beta & q_{\beta p} & q_{\beta r} & 0 \\ q_{\beta p} & q_p & q_{pr} & 0 \\ q_{\beta r} & q_{pr} & q_r & 0 \\ 0 & 0 & 0 & 0 \end{bmatrix}$$

$$\underline{R} = \begin{bmatrix} r_{\delta_{DF}} & 0 & 0 \\ 0 & r_{\delta_R} & 0 \\ 0 & 0 & r_{\delta_{TV}} \end{bmatrix} \qquad \text{(Eqn 13)}$$

8. THRUST VECTORING COMMAND DISTRIBUTION

The longitudinal and lateral/directional flight control systems command effective thrust deflections in pitch and yaw directions. These have to be transformed into the associated vane actuator commands. For this the pitch and yaw commands are transformed into polar coordinates where the maximum effective deflection can easily be limited with engine parameters without changing the direction of the command. Stored thrust vectoring tables depending on desired thrust deflection as well as engine parameters are used to calculate the vane deflections in two steps. First the plume boundary vane position is calculated, then the thrust deflection vane commands are superimposed. At vane deflections larger than 26° geometric clearance is not guaranteed, therefore a software limitation is introduced which allows only one paddle to deflect more than 26°. When thrust vectoring is switched off the two lower vanes (#2 & #3) can be used as airbrakes.

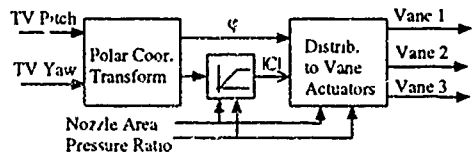

Fig. 8 Thrust vectoring command distribution

9. ENGAGEMENT/DISENGAGEMENT OF THRUST VECTORING

The thrust vectoring system can be switched on and off by the pilot. In case of a failure thrust vectoring is automatically blended out. This blending is implemented in the flight control software in such a way that the aerodynamic surfaces get additional commands which produce the same overall moment as with thrust vectoring. As long as sufficient aerodynamic control power is available there is no difference in the moments with and without thrust vectoring. With small pilot commands this is valid in the whole conventional flight envelope and for the pitch axis even in the post stall regime. In all these cases the linear handling qualities are nearly unchanged with thrust vectoring in and out. In case of a thrust vector failure in post stall no sufficient yawing moment is available. To keep the sideslip as low as possible, the rudder as well as the differential flap command is blended out during recovery to low angle of attack. Due to the reduced control power, the roll performance is also reduced with thrust vectoring off.

10. WEIGHT AND THRUST ESTIMATION

For calculation of the load factor command out of the angle of attack command and vice versa as well as for thrust estimation information about the aircraft weight is necessary. For the calculation of the effective thrust deflection information about the aircraft thrust is necessary, because the resulting moment is proportional to the thrust. No sensed signals for weight or thrust are available, therefore these values are estimated with the lift and drag equations which are transformed into body axes. To minimize the dynamic error of these steady state models the following limitations are included.

- lag filters reduce high frequency effects
- the estimations are rate limited
- the estimated values are bounded
- during extreme maneuvres the estimation holds the last value.

The overall accuracy of the estimations depend on the accuracy of the aerodynamic model.

With a new softwareload an engine model was introduced to improve thrust estimation.

11. POST STALL (PST) MODE

The control law structure does not change with the introduction of the PST-mode. Only the breakpoints in the gain tables and angle of attack dependent scalings are extended to the larger angle of attack range. Flying into the PST is only possible if all of the given prerequisites are fulfilled. If this is the case the pilot can pull to angles of attack larger then 20°. To prevent the pilot from unintentional PST entries a detent is introduced in the stick force spring at 30° angle of attack command. If one or more of the prerequisits are not longer fulfilled, or in case of a failure the angle of attack command is automatically reduced to 30°.

12. CONCLUDING REMARKS

Flight test confirmed the design approach and the control law structure concept including the thrust vectoring system to be successful. The aircraft dynamics were rated by the pilots close to existing level 1 handling quality requirements throughout the whole envelope. Within the post stall envelope no settled requirements exist, however the pilots rated the handling and performance of the airplane as excellent, impressive and well satisfactory.

During the last two years of flight test no significant control law structure changes were necessary. The only major modification was the introduction of limited integral feedbacks of sideslip and roll rate error. This was necessary due to unpredicted large asymmetries in the lateral/directional axis encountered during flight test at AoA's greater than 40°.

Two updates of the aerodynamic model shortly before first flight and during flight test showed the flexibility of the optimal control approach. This was demonstrated by a redesign of the feedback gains performed in less than one month.

X-31A SYSTEM IDENTIFICATION APPLIED TO POST-STALL FLIGHT - AERODYNAMICS & THRUST VECTORING -

D. Rohlf
E. Plaetschke
S. Weiss
DLR Institut für Flugmechanik
Lilienthalplatz 7, 38108 Braunschweig, Germany

SUMMARY

Flight testing of the X-31A post-stall experimental aircraft started in October 1990. By the end of 1992, the X-31A flight regime had been expanded to 70 deg angle of attack and a significant number of flight tests with dynamic post-stall maneuvers had been performed.

Within the international 'Combined X-31A Flight Test Team', DLR (German Aerospace Research Establishment) contributes its system identification experience and capabilities to the determination of aerodynamic parameters and thrust vector control effectiveness from flight test data.

After a brief description of the applied hard and software, this paper presents recent results from flight test data compatibility checking. The identification models used for separated evaluation of longitudinal and lateral-directional motion are introduced, emphasizing the model reductions necessary for X-31A high angle of attack applications. Identification results of selected aerodynamic parameters are shown in comparison to wind-tunnel predictions. The identification of the X-31A thrust vector control effectiveness is addressed and preliminary results are presented as well. An outlook of future identification activities with respect to nonlinear/instationary effects in the high angle of attack regime is given.

NOMENCLATURE

Symbols

CD, CL, CY	coefficients of drag, lift, and side force
Cl, Cm, Cn	coefficients of roll, pitch, and yaw moment
*K_*	calibration factor error
*T_*	time delay error
*Δ_*	zero offset error
*δx_, δy_, δz_*	alignment error angles around x, y, z axes

Abbreviations

AC	aerodynamic center
ADC	airdata computer
ADS	aerodynamic data set
AoA	angle of attack
ASA	acceleration sensor assembly
DoF	degrees-of-freedom
FCL	flight control laws
HQ	handling qualities
INU	inertial navigation unit
ML	maximum likelihood
NB	nosebcom
PID	parameter identification
PST	post-stall
RSA	rate sensor assembly
SI	system identification
TV	thrust vector(-ing)

Control Deflection Angles

CAN	canard
KAPPA	thrust vector in yaw
RUD	rudder
SIGMA	thrust vector in pitch
TEA	asymmetric trailing edge flap (aileron)
TES	symmetric trailing edge flap (elevator)

1. BACKGROUND

Within the scope of the MoA (Memorandum of Agreement) 'A Joint Enhanced Maneuverable Fighter Aircraft Research, Development, and Flight

Presented at an AGARD Meeting on 'Technologies for Highly Manoeuvrable Aircraft', October 1993.

Test Program' between ARPA (Advanced Research Program Agency) and GMOD (German Ministry of Defense), the X-31A research aircraft (*Figure 1*) was designed to demonstrate maneuvering capabilities beyond stall limits (post-stall maneuvering). To meet this design key, new technologies were applied including e.g. high angle of attack aerodynamics and flight control system integrated pitch/yaw thrust vectoring.

Two basically identical demonstrator aircraft have been built by the main contractors RI (Rockwell International Corporation's North American Aircraft) and DASA (Deutsche Aerospace formerly MBB, Germany). Flight testing started with the first flight of aircraft no.1 on October 11, 1990. Before the end of 1992 both aircraft had accomplished a significant number of flights covering the entire AoA regime from about -5 deg to 70 deg. These flight tests included dynamic PST maneuvering as well as the required milestone maneuvers of 360 deg rolls at 70 deg AoA in both directions.

Within the international 'Combined X-31A Flight Test Team', the task of DLR is to extract aerodynamic parameters and thrust vector control effectiveness from flight test data by using SI/PID methods. Both sets of results are essential to validation and update of the X-31A data base used for control law design and simulation.

As published in [1] and [2], DLR was able to achieve reliable SI results covering the conventional angle of attack regime in spite of some deficiencies (from the view of an SI engineer) in the provided flight test data. The application of SI to high AoA/PST flight data, however, poses some major challenges to be discussed in the following.

2. HARD/SOFTWARE EQUIPMENT

To be near to the flight test facility and to run the DLR software for interactive data analysis and system identification on a familiar computer environment, a mobile computer system was first set up by DLR at the RI facilities in Downey (Los Angeles) and then moved to NASA-Dryden at Edwards AFB. To cope with large amounts of flight test data and increasing computational demands, the computer system was gradually supplemented. *Figure 2* gives an overview of the latest configuration.

The following software packages are currently used for on-site data analysis:

GetData	reading flight test data
DA	data conversion and signal calculation
DIVA	interactive data analysis
ADSA	analysis of aerodynamic data set
ML	system/parameter identification using output error method
NLKAL	system/parameter identification using filter error method

GetData is a DLR-modified version of the NASA software package described in [3]. It is used to read the flight test data (provided on CD-ROM) and to convert it to the DLR data format used by the following analysis programs.

DA is used for further data conversion and signal calculations such as scaling, filtering and numerical differentiation. This program is applied only to those time slices which have been selected for further evaluation.

DIVA is used for analysis of time and frequency dependent data [4]. For system identification purposes it serves mainly as a plot routine.

ADSA gives access to the wind-tunnel based aerodynamic data set of the X-31A. Various data set functions and derivatives can be calculated and plotted.

ML is an implementation of the maximum likelihood output error method for estimation of parameters in nonlinear systems [5]. The latest version of this algorithm is documented in [6]. This program is used for

- trim value estimation (see [2]),
- validation of data compatibility and signal calibration,
- estimation of aerodynamic model parameters and thrust vector control parameters,
- verification of estimated parameters (see [2]),
- estimation of equivalent model parameters and subsequent calculation of handling qualities parameters (see [7] and [8]).

NLKAL is an implementation of the maximum likelihood filter error method for estimation of parameters in nonlinear systems [9]. Up to now, this program has been used only for the estimation of lateral-directional derivatives. Compared to ML, NLKAL has two significant advantages

- it is well suited for unstable systems,
- it accounts for process noise induced e.g. by forebody vortices.

Disadvantages are that NLKAL requires more CPU-time than ML and that possible modeling errors are concealed because they are considered as process noise by the algorithm.

3. DATA COMPATIBILITY CHECKING

Prior to the estimation of aerodynamic parameters, a flight path reconstruction (FPR) is carried out

routinely to secure flight test data compatibility. Within the FPR a set of instrumentation errors is identified for each aircraft which should remain constant as long as the measurement system is not changed. The latest FPR model includes

- alignment errors for each sensor package,
- zero offset, scale factor error and time delay for each sensor,
- geodetic wind components, assumed to vary linearly with altitude (wind shear).

The inertial navigation unit (INU) serves as reference for the estimation of the alignment errors of the other three sensor packages: acceleration sensor assembly (ASA), rate sensor assembly (RSA), and noseboom sensors (NB). The estimated wind components are compared to the onboard calculated wind, but differences are, in general, not weighted in the ML cost function to be minimized.

The FPR is based on 6-DoF kinematic equations of aircraft motion. Inputs are the

- load factors *NX, NY, NZ* (ASA signals) and
- angular rates *P, Q, R* (RSA signals).

Outputs are the

- true airspeed and airflow angles *VTAS, ALPHA, BETA* (NB signals),
- geodetic velocity components *VKXG, VKYG, VKZG* (INU signals),
- Euler angles *PHI, THETA, PSI* (INU signals) and
- altitude *H* (ADC signal).

Before the inclusion of alignment error and wind shear estimation, the data compatibility check had to be carried out separately for each maneuver [2]. At present, all SI/PID relevant maneuvers from the flights of one day are collected and evaluated in a single identification run. The example in *Figure 3* shows that the FPR model output reproduces the measured flight test data very well within the entire flight regime. Major differences are only to be seen in the fit of the *BETA*-signal.

The following parameters are currently included in the FPR model:

- zero offset errors
  Δ_NX, Δ_NY, Δ_NZ, Δ_P, Δ_Q, Δ_R;
- calibration factor errors
  K_P, K_Q, K_R, K_VTAS, K_ALFA;
- time delay errors
  T_VTAS, T_ALFA, T_BETA, T_PHI, T_THETA, T_PSI;
- alignment errors
  δy_RSA, δz_RSA, δy_NB, δz_NB;
- wind shear parameters
  VWXG, VWYG, VWZG, VWXG_H, VWYG_H, VWZG_H.

This set of parameters was chosen from all possible parameters by neglecting minor effects and by selecting only parameters which are uncorrelated. Furthermore, only error parameters whose values remained constant during the evaluation of the flights of several days (precondition: no changes in the instrumentation system) were retained in the model. As expected, the identified set of instrumentation errors is slightly different for each of the two X-31A aircraft.

4. IDENTIFICATION OF THRUST VECTOR EFFECTIVENESS (Conventional AoA regime)

The TV effectiveness was identified indirectly in the conventional AoA regime (below 30 deg AoA), based on flight tests with and without operative thrust vector system. Because of the high correlation between the aerodynamic control and TV deflections, the aerodynamic parameters were estimated first from flight tests *without* operative TV system. In a second step, these estimates were kept constant for the estimation of the TV effectiveness from flight test data at the same flight condition, but *with* TV system engaged. Any effects not described by the model from the first step are then attributed to the TV system.

Above 30 deg AoA, this procedure is not practicable (flight safety does not allow to disengage the TV system). Therefore, the effectiveness either from the aerodynamic control surfaces or from the TV system could be estimated in the high AoA/PST regime, assuming in each case correct predictions of the fixed parameters.

The X-31A identification makes use of an engine model which has originally been derived for simulation purposes from data of the engine manufacturer and from cold jet static model tests conducted to determine thrust vector characteristics. Gross thrust *F*, thrust deflection angles in pitch and yaw, *SIGMA* and *KAPPA*, inlet force, and angular momentum of the engine are calculated as functions of power lever angle, mach number, pressure altitude, nozzle pressure ratio, and exhaust nozzle throat area. Thrust vector forces and moments are tied together by the distance between thrust impact point and aerodynamic center, *xthac*. Linearization with respect to the TV deflection angles - they generally do not exceed 10 deg - leads to two nondimensional TV derivatives which are linear functions of the normalized thrust (Detailed information may be found in [10]):

$$CmSIGMA = xthac/\bar{c} \cdot F/(\bar{q}S)$$

$$CnKAPPA = xthac/b \cdot F/(\bar{q}S)$$

Figure 4a shows flight measured data and identified model output of two pilot generated pitch doublet maneuvers of a flight with operative TV system. The model output is simulated with aerodynamic parameters as derived from a corresponding maneuver with TV disengaged. Initial states and trim values are estimated but TV is neglected (i.e. TV effectiveness is set to zero). A significant mismatch between measurement and model output is visible. After additional estimation of the TV derivatives, a nearly perfect curve fit is obtained *(Figure 4b)*. A similar behaviour has been observed in the case of yaw maneuver evaluation.

The identified TV derivatives in pitch and yaw are presented in *Figure 5*. Here, *CmSIGMA* and *CnKAPPA* are plotted versus normalized thrust. The error bars indicate the uncertainty levels of the parameter estimates. They correspond to the standard deviations as obtained from the Cramér-Rao lower bound multiplied by a factor of 20. This large factor was chosen to account for the uncertainties in the previously estimated aerodynamic parameters. The broken lines represent the thrust model predictions for the X-31A.

The TV effectiveness in pitch *CmSIGMA* follows the predictions in general, while the estimated TV effectiveness in yaw *CnKAPPA* is obviously lower than predicted. The relatively large scatter in the results may be caused by possible errors in the engine and thrust deflection models used, and by the above mentioned errors in the estimates of the aerodynamic parameters. Furthermore, only flight test data with pilot generated doublet inputs were available which are non-optimal for PI purposes. These deficiencies, however, do not affect the general trends of the results.

5. AERODYNAMIC MODEL IDENTIFICATION (High AoA/PST regime)

The application of SI/PID to X-31A high AoA/PST flight data poses three major challenges due to

- *instabilities* of the basic/uncontrolled aircraft (aerodynamics/flight mechanics design),
- *high correlations* in aircraft states and control deflections (FCL design for aircraft stabilization), and
- *process noise* induced e.g. by forebody vortices.

The *instabilities* of the basic/uncontrolled X-31A aircraft lead to numerical problems in the ML output error algorithm (possible divergence of the integrated solution or overflow, see [11] and [12]) during the identification of aerodynamic parameters. Therefore, a *numerical stabilization* procedure was included in the algorithm. As the artificial stabilization affects the identification results, its degree was reduced step by step and the final results were obtained without stabilization (see chap. 5.1). These problems do not occur when the *ML filter error method* is used (see chap. 5.2) because here the solutions are stabilized by the filter update. Another method which is capable of handling unstable systems is the *ML output error method* in the frequency domain because here numerical integration is avoided. This method has been successfully applied to X-31A flight test data from conventional flights [13].

The *high correlations* in aircraft states and control inputs, however, could not be avoided during flight test because it is mandatory that the control laws command all control effectors simultaneously for aircraft stabilization and maneuvering. These problems would be overcome only by PID flight tests with *single effector excitation*.

In X-31A high AoA flight, small vortices are separating stochastically from the aircraft nose. This causes *process noise* in the flight data of the lateral-directional motion. Therefore, the *ML filter error method* is applied (see chap. 5.2).

In the maneuvers evaluated so far, the longitudinal and lateral motion were excited separately and no cross coupling effects were visible. Both motions are therefore identified separately using measured signals for lateral-directional terms in the longitudinal motion and vice versa. Due to this procedure, the identification is applicable to flight test data derived in wings level flight as well as in steady turns. The structure of the aerodynamic model was defined according to the ADS to facilitate comparison with the data set predictions and eventual updates of the data base values. The longitudinal motion is therefore formulated in the experimental reference frame whereas the lateral-directional motion is written in body axes.

For the estimation of aerodynamic parameters and thrust vector control parameters, all sensor positions are taken into account as well as aircraft weight, e.g. location, and moments of inertia which are derived as functions of measured fuel quantity from the X-31A weight and balance data. Measured signals, used either as inputs or as outputs, are corrected according to the results of the preceding data compatibility check.

So far, the flight tests were mainly directed to HQ/FCL investigations (e.g. pilot commanded doublet inputs in pitch/yaw/roll axis and bank-to-bank maneuvers) and are therefore not well suited for PID purposes. Due to the high correlations in the various control deflections and aircraft response, it

was necessary to reduce the SI models described in [1]. Some parameters (e.g. canard effectiveness) were set constant at their ADS-predicted values realizing that errors in these values affect the estimates of the other derivatives. In other cases, influences of two correlated parameters were combined into one derivative (e.g. aileron/rudder effectiveness and yaw/roll damping).

5.1 Longitudinal Motion

Drag, lift and pitching moment coefficients, *CDRAG, CLIFT* and *CmAC*, define the aerodynamic model for the longitudinal motion. It contains the following parameters:

CD0, CDALPHA, CDTES,
CL0, CLALPHA, CLTES,
Cm0, CmALPHA, CmTES, CmQ, CmCAN,
and CmSIGMA.

To avoid high correlations between the parameter estimates, e.g. between *CD0* and *CDALPHA*, the model is written in terms of deviations of the state and control variables from their trim values. In this way, the coefficients *CD0, CL0* and *Cm0* represent the values of *CDRAG, CLIFT* and *CmAC* at the respective trim point. Their estimates depend directly on the thrust as calculated from the thrust model which, however, seems to provide incorrect values for high power settings. The trim values of the individual variables are estimated in a preceding step.

Two typical longitudinal HQ/FCL test maneuvers are presented in *Figure 6*. Due to dynamic pitch stick inputs, the FCL command simultaneous deflections of canard *CAN*, symmetric trailing edge flaps *TES*, and thrust vector in pitch *SIGMA*. The control commands are additionally correlated to the aircraft states (in particular pitch rate *Q*) due to the feed back in the FCL. Consequently, not all pitching moment derivatives *CmALPHA, CmQ, CmTES, CmCAN*, and *CmSIGMA* can be estimated independently from those maneuvers. In the course of high AoA/PST maneuver evaluation, the following procedure was found to be adequate:

- *CmCAN* and *CmTES* were kept fixed on their ADS predictions,
- *CmSIGMA* was estimated (TV influence increases with AoA in contrast to *CmTES*),
- some other parameters (e.g. *CmQ* and *CDTES*) were occasionally kept fixed on their ADS predictions (otherwise these parameters would diverge to unreasonable values because of their small influence in the respective maneuver),
- if necessary, quadratic terms (e.g. *CDTES2*) were included.

The use of ADS predictions for *CmCAN* was justified by earlier evaluations of flight tests with single surface excitation in the conventional AoA regime using the X-31A flutter test box [2].

The flight conditions in which the longitudinal motion was evaluated, are presented in *Figure 7* as Mach versus AoA. After adding strakes at the aft-body of the X-31A, the longitudinal handling qualities were rated well and only a few pitch doublet maneuvers were flown in the high AoA/PST regime. Representative identification results are shown in *Figure 8* in comparison to the respective predictions. Drag and lift due to angle of attack, *CDALPHA* and *CLALPHA*, are well identifiable and close to the predictions. The longitudinal stability *CmALPHA* shows relatively large scatter and greater discrepancies to the predictions which by themselves have no clear dependence on AoA.

The identified thrust vector effectiveness is presented in *Figure 8d* for the X-31A with aft-strakes. Here, *CmSIGMA* is related to the normalized thrust and therefore, the X-31A thrust model predictions are constant for all flight conditions. The estimated TV effectiveness shows large scatter, and the values at low AoA differ significantly from the predictions. This may be caused by possible errors in the engine/TV model, as mentioned above, and by the fixing of the trailing edge flap effectiveness *CmTES* at its ADS predictions.

5.2 Lateral-directional Motion

Figure 9 illustrates the problems facing the parameter identification from pilot generated maneuvers at higher AoA. It shows a bank-to-bank roll around the velocity vector at 54 deg AoA, 0.26 Mach and 27 kft (8200 m) altitude. The FCL commands not only lead to highly correlated control deflections of aileron and TV, *TEA* and *KAPPA*, but also to highly correlated roll and yaw rates, *P* and *R*. Furthermore, little excitation in lateral acceleration and sideslip make the identification of lateral force derivatives rather inaccurate. To gain higher accuracy, single surface excitation is a prerequisite.

For the identification of the lateral-directional motion, some modification compared to the earlier SI/PID [2] were made to account for the deficiencies in the evaluated high AoA/PST flight test data:

- The parameter estimation was executed by using *NLKAL* to account for process noise and to overcome stability problems, as mentioned above.
- Due to the high correlations between roll rate and yaw rate, the derivatives *CYP, ClP and CnP* resp. *CYR, ClR, and CnR* could not be

estimated separately. Therefore, combined derivatives *CYP**, *ClP* and CnR** were introduced.

- The above mentioned correlations between the thrust deflection angle in yaw, *KAPPA*, and the aerodynamic control deflections make it impossible to estimate the TV effectiveness in yaw, *CnKAPPA*, together with the aerodynamic control parameters. For this reason, *CnKAPPA* was fixed on 65% of the predicted value as identified previously.
- The rudder effectiveness was set to zero for AoA above 40 deg because the rudder command is faded out by the FCL for high AoA.

Thus, beside the initial values of the states, the following aerodynamic parameters were generally estimated from maneuvers in high AoA/PST flight:

CY0, CYBETA, CYP, CYTEA, CYRUD,*
Cl0, ClBETA, ClP, ClTEA, ClRUD,*
Cn0, CnBETA, CnR, CnTEA, CnRUD.*

The high AoA/PST flight conditions evaluated so far in the lateral-directional motion, are shown in *Figure 10* as Mach versus AoA. In *Figure 11*, three of the derivatives listed above, namely *CYBETA*, *ClTEA*, and *CnR** are presented in comparison to their ADS predictions. The sideforce due to sideslip, *CYBETA*, shows large scatter. This could be expected as there is nearly no excitation in the lateral acceleration. The derivative *ClTEA* is the parameter which was best identifiable. The results indicate that the decline in aileron effectiveness starts earlier than predicted, at about 30 deg AoA. The combined yaw damping

$$CnR^* = CnR + CnP \cdot P / R$$

also shows large scatter due to insufficient excitation of the aircraft eigen motion. The predictions for *CnR** were calculated from the ADS values of *CnP* and *CnR* by setting

$$P / R = cot\ (ALPHA).$$

which corresponds to the ratio for ideal rolling around the velocity vector.

6. NONLINEAR/INSTATIONARY EFFECTS

To support the X-31A flight testing with respect to flight envelope expansion and aerodynamic data set validation, SI/PID has been applied so far to pilot maneuvers which were flown with relatively small and slow changes of flight conditions around the respective trim point. The future evaluation of large amplitude and high dynamic maneuvers however, calls for the inclusion of nonlinear and instationary effects in the identification models.

Typical maneuvers that generate instationary effects in the longitudinal aerodynamics are pitch steps and abrupt pullup maneuvers as repeatedly flown by the X-31A. These maneuvers are characterized by AoA variations around the aerodynamic lift maximum in combination with high pitch rates. The time histories of an abrupt pullup and a quasistatic deceleration maneuver are shown in *Figure 12a*. The corresponding aerodynamic lift *CL_ae* is plotted versus AoA in *Figure 12b*. In the case of the abrupt pullup maneuver, the hysteresis in *CL_ae* due to dynamic lift effects can be seen clearly.

On the basis of lately achieved PID results, DLR will develop a longitudinal PID model which includes both, nonlinear and hysteresis effects for the X-31A high AoA regime. Thus, the identification of instationary effects as described above will become applicable.

7. CONCLUSIONS

X-31A system identification was carried out for angles of attack up to 70° and Mach numbers up to 0.9. The identification was mainly based on pilot generated doublet inputs and bank-to-bank maneuvers which are non-optimal with respect to SI/PID. The FCL-caused high correlation in the control effector deflections and in the state variables enables only reduced/combined parameter identification. Due to the non-optimal excitation of the aircraft motion, the SI/PID results show partly large uncertainty levels and scatter, especially in the lateral-directional aerodynamics. Nevertheless, the X-31A aerodynamic data set could be verified on the whole with the exception of some obvious discrepancies in the lateral-directional motion.

The thrust vector effectiveness could be identified separately in the AoA regime below 30 deg. The TV effectiveness in pitch is close to the predictions whereas the TV effectiveness in yaw is lower than predicted.

Within a X-31A follow-on program under discussion, future SI/PID is scheduled to be directed to:

- supersonic PID with single surface excitation (aerodynamic control surfaces only),
- high AoA PID with single effector excitation (aerodynamic control surfaces and thrust vector),
- nonlinear/instationary aerodynamics as occurring in case of large amplitude/high dynamic maneuvers.

8. ACKNOWLEDGEMENTS

The authors would like to thank Mr. Erwin Kunz, DASA, and his team for all their support and for fruitful discussions.

9. REFERENCES

[1] Rohlf, D., Plaetschke, E. and Weiss, S.: *X-31A Model Evaluation and Validation via System Identification.* AIAA Atmospheric Flight Mechanics Conference, 12-14 August 1991, New Orleans, LA, Paper 91-2875

[2] Weiss, S., Plaetschke, E., Rohlf, D. and Galleithner, H.: *System Identification for X-31A Project Support - Lessons Learned so Far.* AGARD FMP Symposium 'Flight Testing', 11-14 May 1992, Chania, Crete, Greece, Paper 14

[3] Maine, R.E.: *Manual for GetData Version 3.1 - A FORTRAN Utility Program for Time History Data.* NASA TM 88288, October 1987.

[4] Wulff, G. and Zoellner, M.: *DIVAIMIMO Flight Test Data Analysis for the X-31A Demonstrator.* AIAA Atmospheric Flight Mechanics Conference, 12-14 August 1991, New Orleans, LA, Paper 91-2852

[5] Jategaonkar, R.V. and Plaetschke, E.: *Maximum Likelihood Parameter Estimation from Flight Test Data for General Non-Linear Systems.* DFVLR-FB 83-14, 1983.

[6] Weiß, S.: *NLHPIL - Ein Programm zur Maximum-Likelihood-Parameterschätzung für nichtlineare Systeme - Benutzeranleitung.* DFVLR-IB 111-87/29, 1987.

[7] Huber, P., Weiss, S. and Galleithner, H.: *X-31A Initial Flying Qualities Results Using Equivalent Modeling Flight Test Evaluation Techniques.* AIAA Atmospheric Flight Mechanics Conference, 12-14 August 1991, New Orleans, LA, Paper 91-2891

[8] Huber, P. and Galleithner, H.: *X-31A High Angle of Attack and Initial Post Stall Flight Testing.* AGARD FMP Symposium 'Flight Testing', 11-14 May 1992, Chania, Crete, Greece, Paper 11

[9] Jategaonkar, R.V. and Plaetschke, E.: *Identification of Moderately Nonlinear Flight Mechanics Systems with Additive Process and Measurement Noise.* J. Guidance, Vol.13, No.2, March-April 1990, pp 277-285

[10] Plaetschke, E. and Weiß, S.: *Identification of Thrust Vector Control Effectiveness from X-31A Flight Test Data.* Z. Flugwiss. Weltraumforsch. 17 (1993), pp. 235-238.

[11] Maine, R.E. and Murray, J.E.: *Application of Parameter Estimation to Highly Unstable Aircraft.* AIAA Atmospheric Flight Mechanics Conference, Williamsburg, Virginia, August 18-20, 1986, Paper No. 86-2020.

[12] Plaetschke, E.: *Identifizierung instabiler flugmechanischer Systeme mit einem Ausgangsfehlerverfahren.* Z. Flugwiss. Weltraumforsch. 12 (1988), pp. 233-240.

[13] Kaletka, J. and Fu, K.H.: *Frequency-Domain Identification of Unstable System Using X-31 Aircraft Flight Test Data.* AIAA Atmospheric Flight Mechanics Conference, Monterey, California, August 9-11, 1993, Paper No. 93-3635.

10. FIGURES

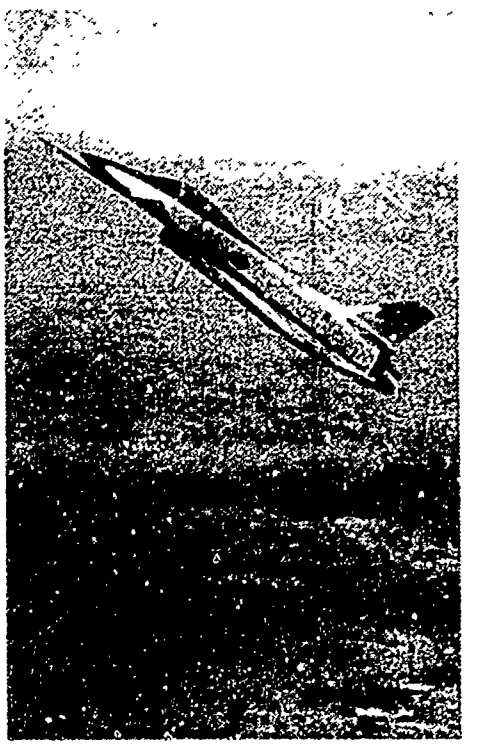

Figure 1. X-31A in high AoA flight

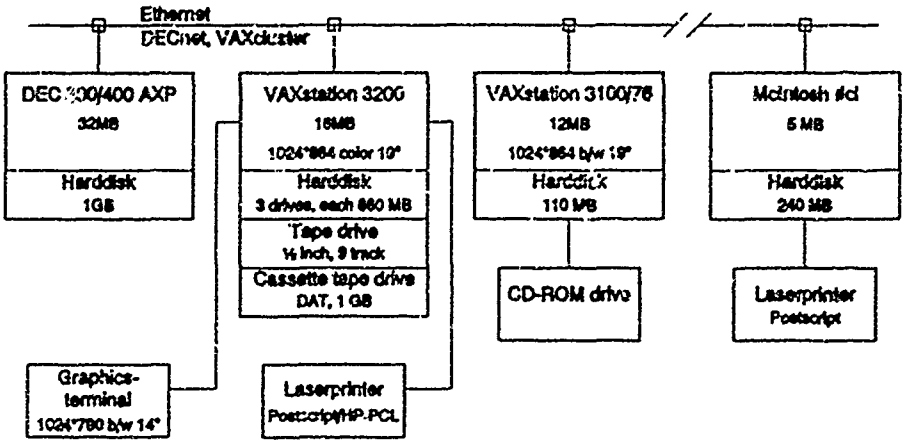

Figure 2. DLR computer system for X-31A on-site flight test data evaluation

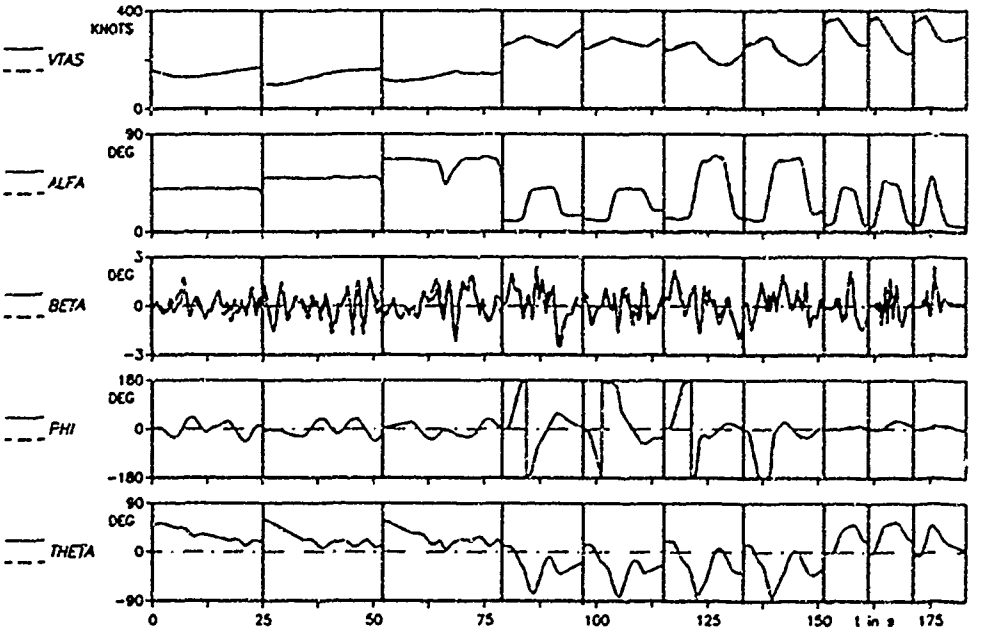

Figure 3. 6-DOF flight path reconstruction for data compatibility check (a/c 1, flights 121-123)
—— flight test data, ---- model output

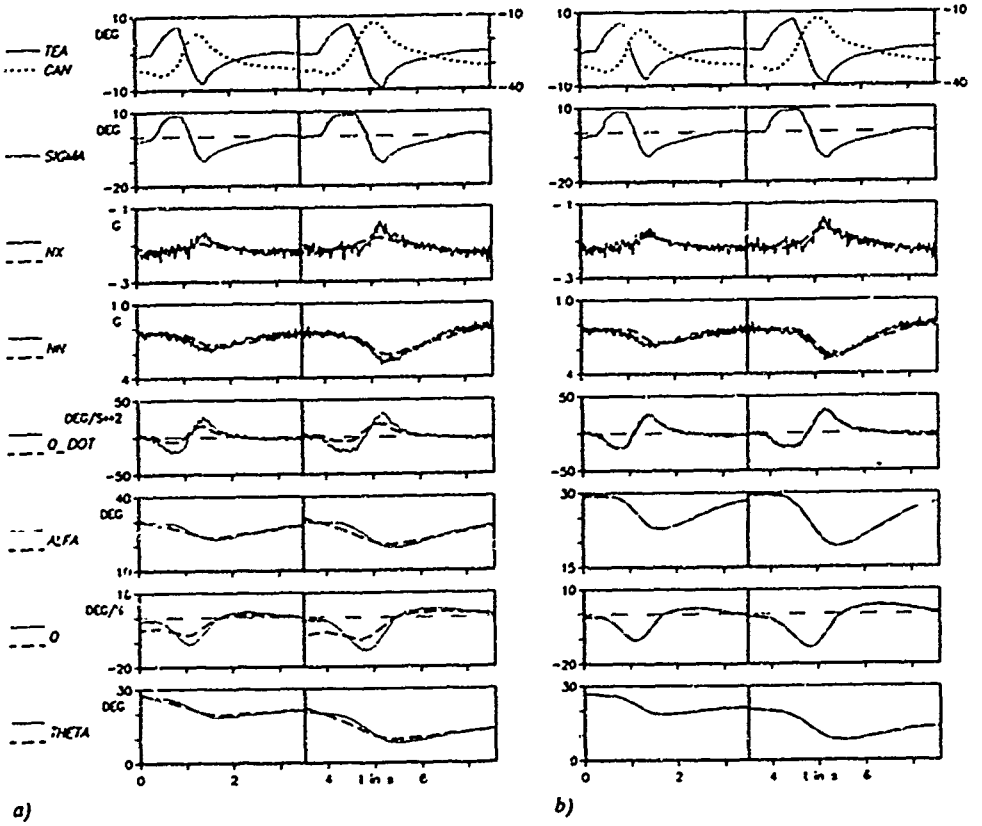

Figure 4. **TV effectiveness identification: Pitch doublet maneuvers from TV engaged flight**
—— flight test data, — model output
a) model without TV derivatives, *b)* model with TV derivatives included

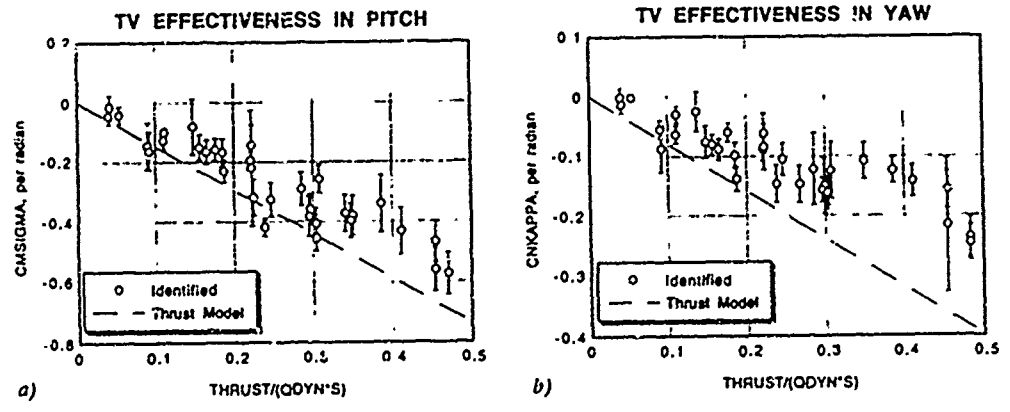

Figure 5. **TV effectiveness identification: Identified derivatives** *a)* in pitch, *b)* in yaw

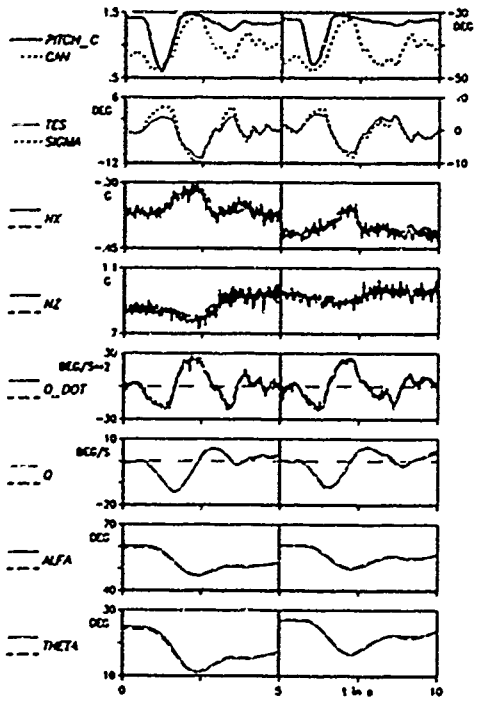

Figure 6. Long. Aero-PID (ML output error method): Pitch doublet maneuvers
(a/c 1, flight 80: 56 deg AoA, 0.28 Mach, 32 kft Alt)
——— flight test data, —— model output

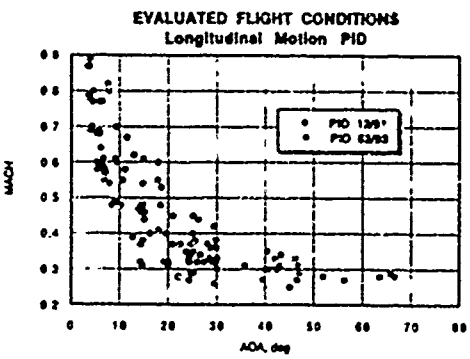

Figure 7. Long. Aero-PID: Evaluated flight conditions

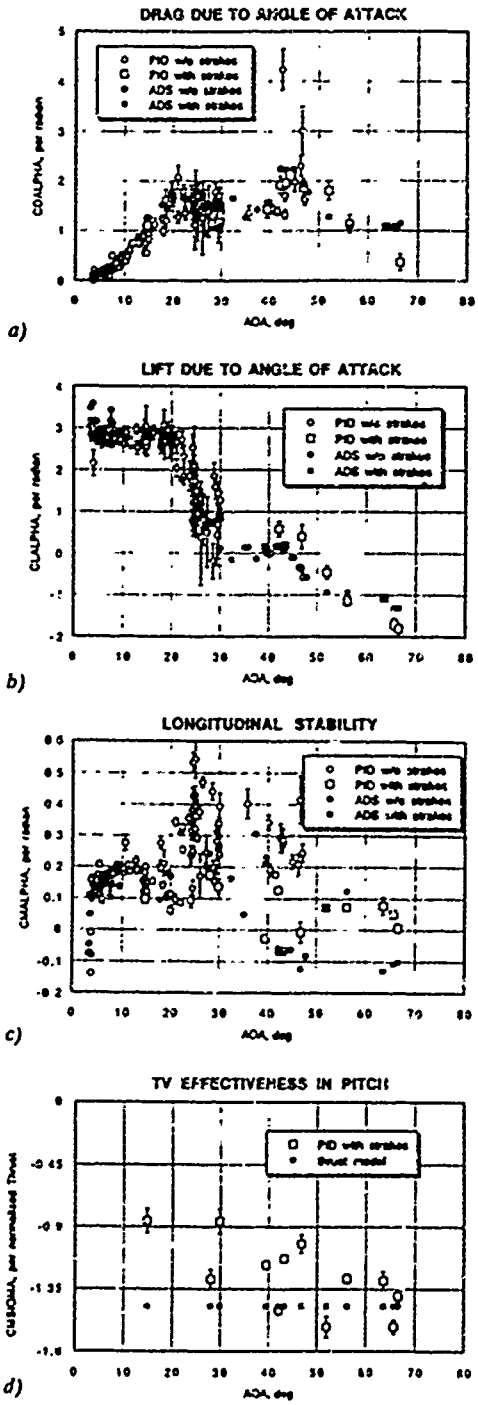

Figure 8. Long. Aero-PID: Identified derivatives

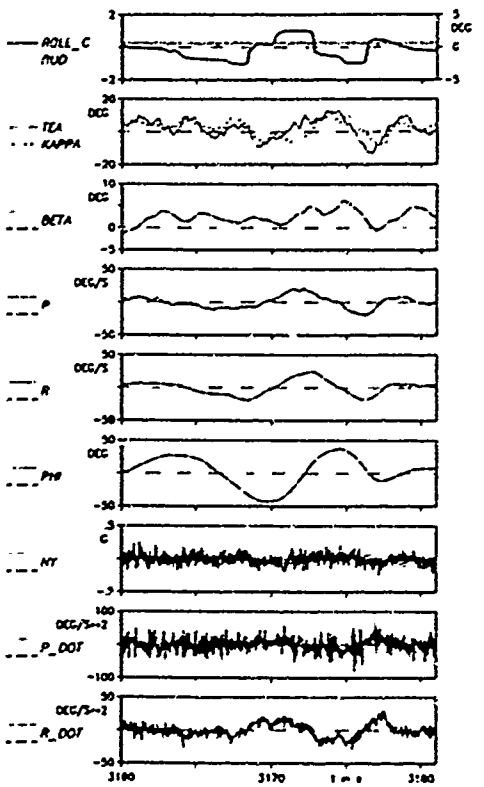

Figure 9. Lat.-dir. Aero-PID (ML filter error method): Bank-to-bank maneuver
(a/c 2, flight: 62: 54 deg AoA, 0.25 Mach, 27 kft Alt)
—— flight test data, ---- model output

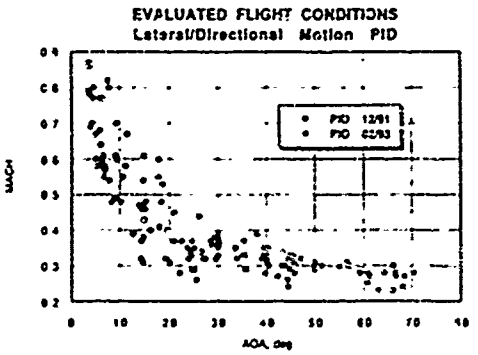

Figure 10. Lat/dir. Aero-PID: Evaluated flight conditions

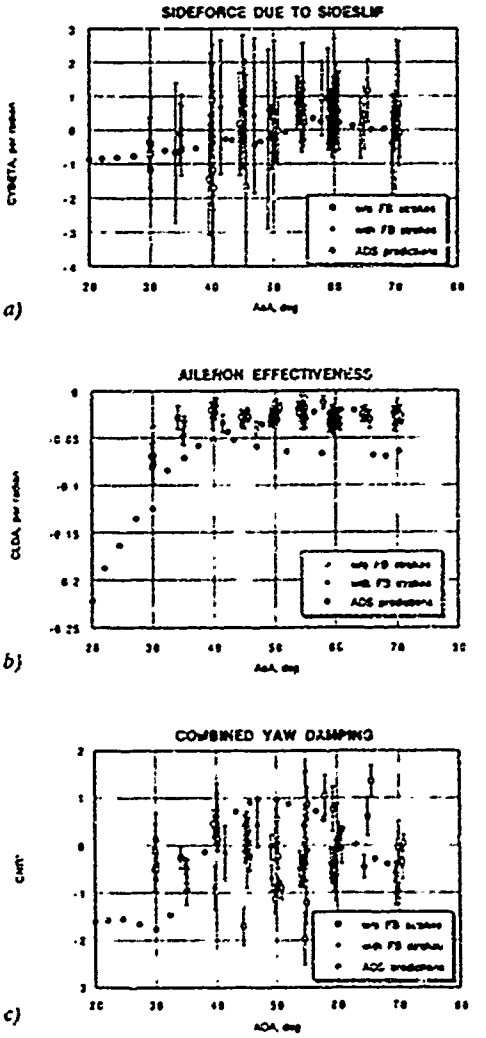

Figure 11. Lat/dir. Aero-PID: Identified derivatives at high AoA

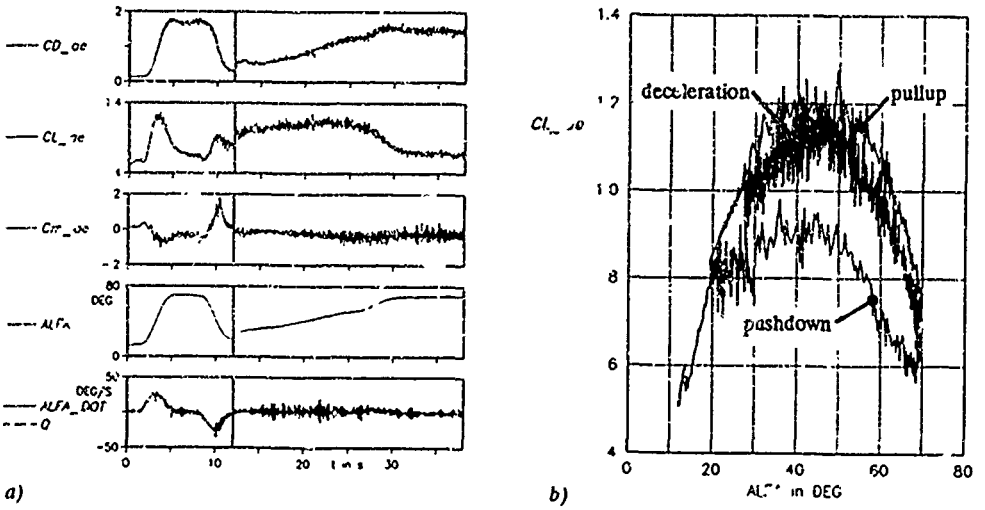

Figure 12. **Dynamic lift effects:**
a) Abrupt pullup and quasistatic deceleration maneuver, *b)* Ca. lated lift coefficients

X-31 TACTICAL UTILITY – INITIAL RESULTS

by

David E. Canter and **CDR Allen W. Groves, USN**
Naval Air Warfare Center, Aircraft Division
Flight Test and Engineering Group
Strike Aircraft Test Directorate (SA60)
NAS Patuxent River, MD 20670-5304
United States

1. SUMMARY

The X-31 is a research aircraft built to explore the tactical benefits of enhanced fighter maneuverability which is possible through the use of thrust vectoring. This paper gives background information on the program and on the aircraft. The high angle of attack envelope expansion phase is covered; detailing aircraft modifications that were required. The tactical utility phase of testing, including simulation and flight testing, is discussed. Helmet mounted display and supersonic thrust vectoring tests planned for the near future are briefly discussed.

2. INTRODUCTION

2.1 Background

The X-31 is a research aircraft under evaluation by an International Test Organization (ITO) at Edwards AFB, CA. The program is sponsored by the U.S. Advanced Research Projects Agency (ARPA) and the German Federal Ministry of Defense (FMOD). The U.S. Navy was selected to act as ARPA's agent for the management of the program. The ITO is made up of contractor and government organizations from the U.S. and the Federal Republic of Germany. The U.S. government participants include the Navy, the National Aeronautics and Space Administration (NASA), and the U.S. Air Force. The principal U.S. contractor is Rockwell International (RI). The German government participation includes the FMOD, the German Air Force, the German Aerospace Research Establishment (DLR), and WTD-61 (the government flight test center). The principal German contractor is Deutsche Aerospace (DASA).

The program utilizes six project pilots, one each from the U.S. Navy, NASA, U.S. Air Force, German Air Force, WTD-61, and Rockwell International. The X-31 stems from efforts in both countries to develop highly maneuverable aircraft. Rockwell had experience working on the remotely piloted Highly Maneuverable Aircraft Technology (HiMAT) program in the early 1980's, while DASA's Dr. Wolfgang Herbst had long been a proponent of the use of post-stall maneuvering to gain the edge during close-in-air combat. Numerous simulations had validated Dr. Herbst's theoretical concepts. In 1986, ARPA let a contract to design, build, and flight test two aircraft to prove the concepts of enhanced fighter maneuverability (EFM). Principal to EFM is the use of thrust vectoring to achieve aircraft control at low airspeeds where conventional aerodynamic control is no longer possible.

The four original program goals were: 1) rapid demonstration of EFM maneuvering concepts, 2) validation of a low cost, international prototyping concept, 3) development of design requirements and a data base for future aircraft designers, and 4) investigation of the tactical benefits of EFM technology. As such, primary design drivers were cost and time. This led to the substantial use of off-the-shelf components which were already flight qualified. Another critical design requirement for EFM performance was a high thrust-to-weight ratio. This led to extensive efforts to keep the aircraft's weight as low as possible. The requirements of a rapidly built, low cost, low weight aircraft drove most of the decisions made in the design process. To keep weight down, no weapons system or radar were included; nor was the aircraft given the capability for in-flight refueling. However, certain safety requirements, such as a hydrazine powered emergency power unit and emergency air-start system were included despite their weight. DASA had responsibility for the flight control laws, wings, and thrust vector paddles. RI had overall design integration responsibility. Design of the aircraft began in 1987, construction began in 1989, and the first flight of aircraft number one was in October 1990.

The first 110 flights were conducted from RI's Palmdale, CA facility. During these flights, flutter testing was completed as well as the majority of the conventional angle-of-attack (AOA) envelope flying qualities and loads testing. The initial high AOA or post-stall (defined as AOA's greater than 30°) flight testing was performed with testing up to 52° AOA. In

Presented at an AGARD Meeting on 'Technologies for Highly Manoeuvrable Aircraft', October 1993.

January 1992, the aircraft were flown to Edwards, AFB. The decision was made to move the flight test operations to NASA's Dryden Flight Research Facility to take advantage of their expertise in high AOA flight research, and to add valuable resources (in terms of personnel and support facilities) to the program. At approximately the same time, the Air Force became involved with the program, supplying engineering and pilot support. Since the first ITO flight in April 1992, over 200 test missions have been flown at NASA Dryden, with over 300 total flights using both X-31s. All envelope expansion required to support the tactical utility testing has been completed and the tactical utility phase of flight testing has begun.

2.2 Aircraft Description

The X-31 is characterized by a low mounted double-delta wing, forward mounted canards, three carbon-carbon paddles for vectoring engine exhaust, a single vertical tail with a conventional rudder, and an F-18 bubble-type canopy enclosing a single pilot cockpit. The aircraft is equipped with an extended nose mounted air data boom, has conventional speedbrakes mounted on both sides of the aft fuselage, and has an air inlet lip which schedules down with AOA to provide adequate air flow to the engine at high AOA. The aircraft's external dimensions are given in figure 1.

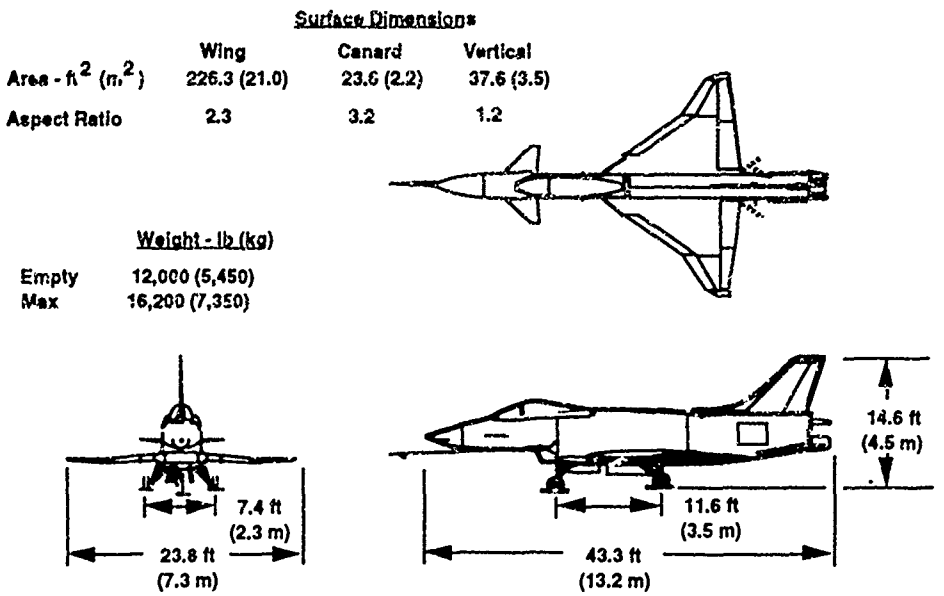

Figure 1. X-31 Dimensions

The aircraft is approximately the size of an A-4 Skyhawk. The X-31 weighs 12,000 lb (5,450 kg) empty and can carry up to 4,200 lb (1,900 kg) of fuel. The aircraft is equipped with a single General Electric F404-GE-400 engine rated at 16,000 lb (71,200 N) maximum thrust for uninstalled, sea-level, standard day conditions. To date, the engines have performed flawlessly during high AOA operations. Once selected by the pilot, the operation of the thrust vectoring vanes (TVV) is transparent, with the flight control system dividing the required surface deflections between the TVV's and the conventional control surfaces. Depending upon the flight condition (AOA, center of gravity, etc.), the X-31 unaugmented airframe is statically unstable both longitudinally and lateral-directionally. The aircraft also has unstable (propelling) roll damping above 25° AOA.

2.3 Flight Control System

The flight control system of the X-31 is a full authority, multi-feedback digital fly-by-wire system. The aircraft has three primary flight control computers and a fourth computer which is used as a tie-breaker for flight control sensor redundancy management. Longitudinally, the pilot control stick commands Nz (through an Nz prediction based on AOA) at high

airspeeds and commands AOA at low airspeeds. Laterally, pilot stick commands stability axis roll rate. Directionally, pilot rudder pedal commands sideslip. The maximum sideslip command decreases from approximately six degrees at 30° AOA to zero degrees at 45° AOA.

There are two trailing edge flaps (TEF's) per wing which are deflected in unison. The TEF's are the primary control surfaces for pitch and roll. The TEFs are prioritized for pitch then roll control; however, no priority is assigned to the TVV's between pitch and yaw. The TEFs are used to compensate for the nose up pitching moments created by engine gyroscopic and inertial coupling effects.

The canards were included on the aircraft to ensure sufficient aerodynamic nose down moments to recover from high AOA in the case of a TVV malfunction. The canards only move symmetrically and remain unloaded, staying at the same angle (trailing edge up) as the aircraft's AOA, up to about 45°. Upon a nose down command, the canards can then move to their maximum deflection of 70° (trailing edge up) to create a nose down pitching moment.

When not used for thrust vectoring, the TVV's can be used as speedbrakes, extending into the freestream when commanded by the pilot. They can be used independently or with the conventional speedbrakes. However, flight testing has shown that little deceleration performance is gained when using the TVV's in addition to the conventional speedbrakes. If extended as speedbrakes, the flight control logic will retract the TVV's while decelerating above 30° AOA.

The aircraft is equipped with leading edge flaps (LEF's) to provide optimal camber at low AOA's and to improve stability and control characteristics at higher AOA's. The LEF's move symmetrically and are scheduled as a function of AOA.

2.4 EFM

To the X-31 program, EFM means the ability to pitch and roll the aircraft at high AOA/low airspeed flight conditions where conventional aircraft are unable to maneuver. Simulations and analyses have determined that this capability greatly increases an aircraft's lethality during close-in combat. The ability to maneuver at higher AOA's can only be achieved with thrust vectoring, since standard flight control surfaces are ineffective at low dynamic pressure. The X-31 performs coordinated (zero sideslip) stability axis rolls. Stability axis rolls are a combination of body axis roll and yaw rate. The relationship is given by the following equation (for the zero sideslip case):

$$P_{stab} = P_{body} * \cos(AOA) + R_{body} * \sin(AOA)$$

The effect that increasing AOA has on the components that make up P_{stab} is illustrated in figure 2.

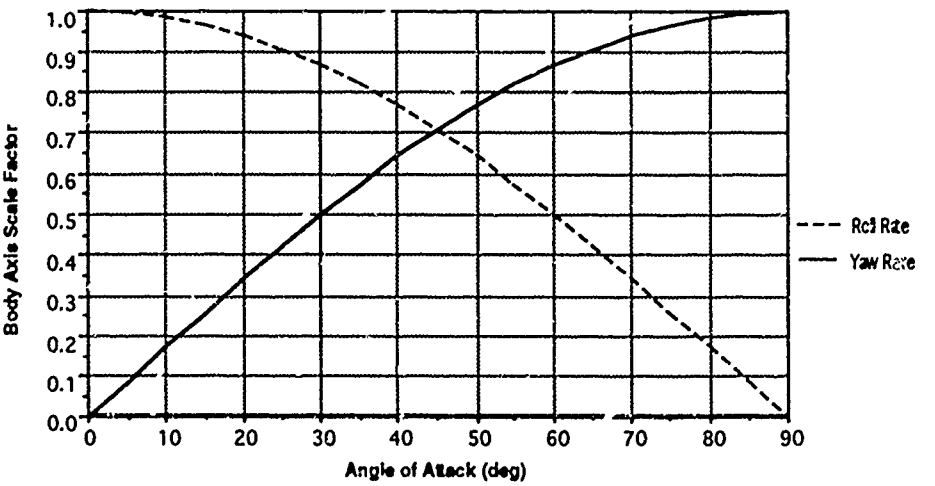

Figure 2. Effect of AOA on Body Axis Rate Contribution to Coordinated Stability Axis Roll Rate

This relationship is very important to understanding one of the X-31's main advantages during close-in-combat. As can be seen from figure 3, the X-31's stability axis roll rate at 150 KCAS (278 km/h) / 70°

AOA is approximately 45 °/s. This means that the aircraft has a body axis yaw rate of 42 °/s. Typically, the flight path is rotated downward 70 to 90° during sustained 70° AOA maneuvering. For these values of flight path and AOA, a 42 °/s body axis yaw rate causes heading to change at approximately the same rate; giving the aircraft a maximum *turn rate* of almost 42 °/s at 150 KCAS (278 km/h). By comparison, current fighters have a maximum turn rate of only about 10 °/s at this flight condition. Maximum turn rate is not the sole determining factor in a close-in combat engagement, but this example clearly indicates the enormous potential benefit of thrust vectoring. It should be noted, however, that the X-31 was designed to have high specific excess power (Ps) and high agility at low AOA's along with the additional capabilities offered by thrust vectoring. Thrust vectoring was viewed as an addition to, not as a substitute for, a good basic fighter aircraft design.

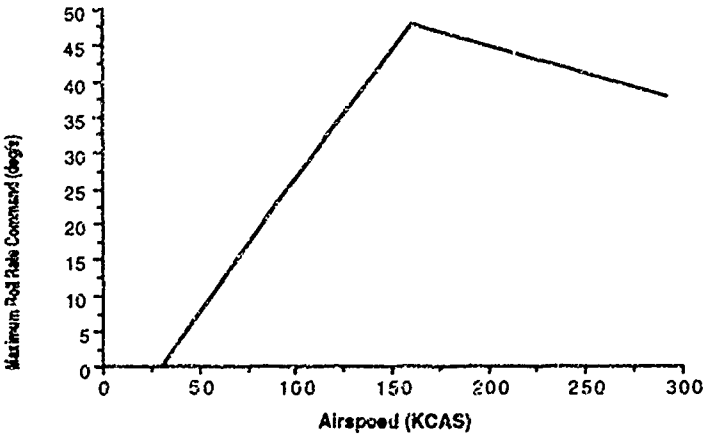

Figure 3. Maximum Roll Rate Command at 70° AOA (Flight Control Software OFP V117)

3. HIGHLIGHTS OF ENVELOPE EXPANSION

The progress made by the X-31 team during envelope expansion has been remarkable. In slightly over a year, the aircraft progressed from not being permitted to fly above 50° AOA to being able to perform virtually any desired high AOA maneuver up to the designed limit of 70° AOA. This progress was the result of hard work and dedication by the ITO personnel. Some of the highlights of the steps toward the current highly capable X-31 are discussed below.

3.1 Aft Strakes

During one of the early PST expansion flights, while performing a slow deceleration to 52° AOA in aircraft #2, the pilot was forced to apply full lateral stick to maintain wings level flight. This proved to be a very interesting and important test point. The pilot did not realize it at the time, but he had lost roll control authority. That was due to the fact that the pitch priority control system was using considerably more symmetric TEF deflection (trailing edge down) than was predicted to maintain the commanded AOA. This in turn limited the amount of differential TEF deflection available for roll control. Further analysis determined that there was a significant change in aircraft pitching moment due to a change in the aft fuselage made during the latter phase of design. The original design, which was used for the majority of the wind tunnel tests, had externally mounted pods which contained the lower TVV actuators. The pods were then enclosed in a simpler, constant-area aft fuselage design for ease of construction. It turned out that the original design's external TVV actuator housings gave the aircraft considerably more nose down pitching moment and served a strake-like role. After considering a number of alternatives to solve the pitching moment problem (control law re-design, nose ballasting), it was decided that aft mounted strakes would be the best solution. Several designs were proposed and investigated in the wind tunnel at NASA Langley. The location finally decided upon was a compromise of performance and ease of installation. The strakes were installed on the lower aft fuselage, under the speedbrakes. They are 65 in (165.1 cm) long and 6 in (15.2 cm) wide and are inclined 13° leading edge down (the same angle as the fuselage at that point). Provisions were made to bolt/unbolt various sized and shaped strakes if required. Once the first set of strakes were installed on the aircraft, the pitching moment was much closer to the

value that was used in the control law design. This change is shown in figure 4. With this change in place, 1 g envelope expansion to 70° AOA was completed.

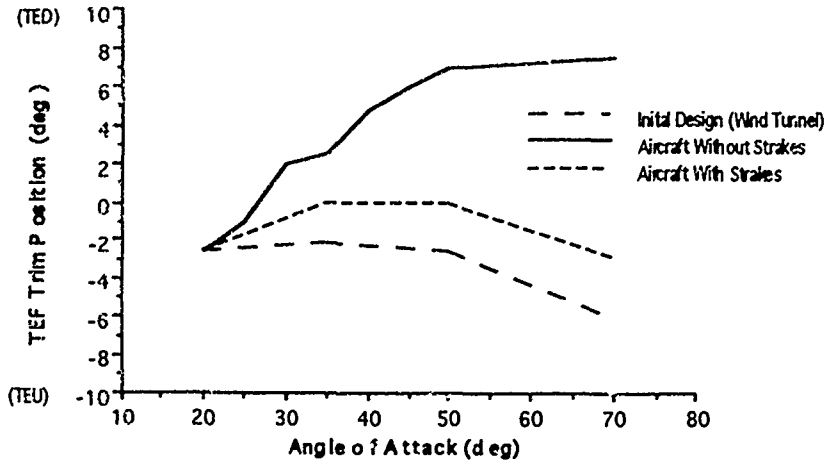

Figure 4. Influence of Aft Strakes on Trim Trailing Edge Flap Position

3.2 AOA Limiter

During early post-stall flight testing, prior to the addition of aft strakes, with the limit of 50° AOA in place, inadvertent overshoots as high as 60° were seen. This was not unexpected, given the high longitudinal stick sensitivity for commanding AOA in post-stall. As seen in figure 5, 0.2 in (0.5 cm) of aft stick movement equates to a 5° AOA command.

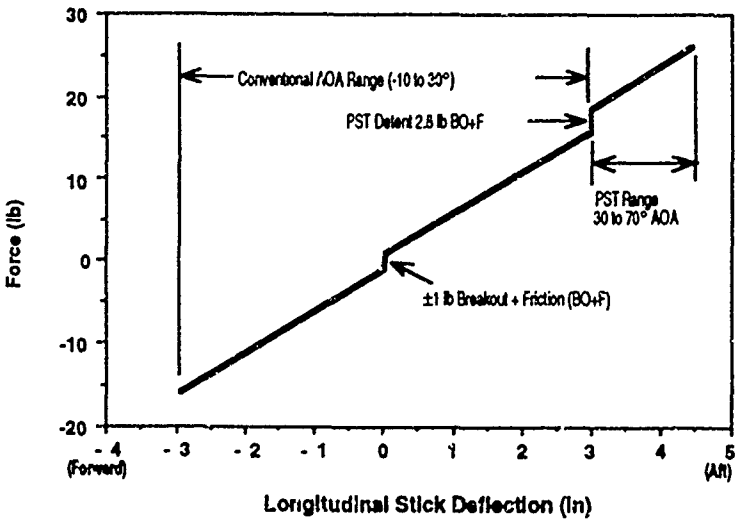

Figure 5. X-31 Longitudinal Stick Force vs. Deflection

It was thought that the control stick characteristics would be acceptable for tactical utility flight test; however, more precise AOA control was desired for the clinical envelope expansion maneuvers. For this reason, a pilot selectable AOA limiter was introduced into the flight control software. It selects, in 5° increments, the maximum AOA command for full aft stick. It contributed greatly to being able to precisely reproduce flight conditions to gather data for analysis and was of major benefit during envelope expansion.

3.3 Nose Modifications

The next aerodynamic challenge for the X-31 at high AOA was yaw asymmetry. Once we began flying above 50° AOA, pilots reported numerous side force kicks which they referred to as "lurches". It was also noted that aircraft two was more susceptible to these lurches than was aircraft one. Thus began an intense period of measuring and weighing the two aircraft to see if any external differences could be detected. No glaring external differences could be determined. NASA aerodynamicists suggested the addition of "grit" to the nose area as a way of reducing the aerodynamic asymmetries by forcing symmetric flow separation. Grit (a substance with individual grains the size of very small pebbles) was then added in thin (approximately 1/4 inch (1/8 cm)) strips to the radome and noseboom. The grit strips seemed to reduce the asymmetries to an acceptable level and the envelope expansion continued. The next major hurdle was entries to PST at elevated Nz values. During the first flight investigating this area, using aircraft two, a departure from controlled flight occurred. The test maneuver was a split-s from 0.4 Mach at 30,000 ft (9,100 m) to 60° AOA. On the previous two maneuvers to 45° AOA no indications of an impending departure had been seen. On the departure maneuver, a large yaw asymmetry was encountered above 50° AOA which caused a rapid build-up in sideslip and a departure at 58° AOA. The aircraft quickly self-recovered after 320° of heading change with maximum AOA and yaw rates of 76° and 70°/s, respectively. This flight, in late November 1992, was a major setback for an aircraft which had been designed to be "departure proof" with "carefree" handling. Considerable work began on both control law and aerodynamic fixes to the aircraft to prevent such a departure from reoccurring. Had this flight test point been performed with aircraft one instead of aircraft two, the departure may not have occurred; thus delaying the necessary improvements. For this reason, the departure was, in the long run, a very good thing for the X-31 program.

Asymmetric forebody vortex shedding was seen as the cause of the problem and it needed to be controlled more effectively than it was with the grit strips alone. It was critical to force the vortices to burst at the same point on the left and right sides of the nose. In order to force symmetric transition of the vortices, it was decided to try using strakes mounted on the nose. Strakes of various sizes and locations were investigated in the wind tunnel at NASA Langley. In addition, a study of previous research indicated that aircraft with blunt nose tips had less severe asymmetries than aircraft with very sharp nose tips. The nose tip of the X-31 was very sharp, having essentially a zero radius of curvature. While carefully measuring the nose of the 13% scale wind tunnel model, it was determined that the model had always had a "blunt" nose, with approximately the same radius of curvature (0.6 in or 1.5 cm) as planned for the X-31. So, in order to investigate the effects of nose tip radius on asymmetric behavior, the model's nose actually had to be made *sharper*.

The wind tunnel and design studies resulted in the nose tip being blunted to a radius of 0.6 in (1.5 cm). Nose strakes measuring 0.6 in (1.5 cm) wide by 20 in (50.8 in) long were placed horizontally down the fuselage, starting from the tip of the nose. The effect on the yawing moment characteristics as a function of sideslip angle are shown in figure 6. The wind tunnel data given is for 60° AOA. As can be seen, the combined changes to the aircraft's nose greatly lessened its static directional instability at 60° AOA. The significant difference in data between the model's original blunt, unstraked nose and the aircraft representative sharp nose may help to explain why the departure was not predicted before it occurred.

The modifications were made to the aircraft's nose within two weeks of the completion of wind tunnel testing. With the modifications completed, envelope expansion testing continued, based upon the positive wind tunnel predictions.

While flight testing pressed on, engineering work continued on improving the aircraft's control laws and control power. These are discussed in section 3.5.

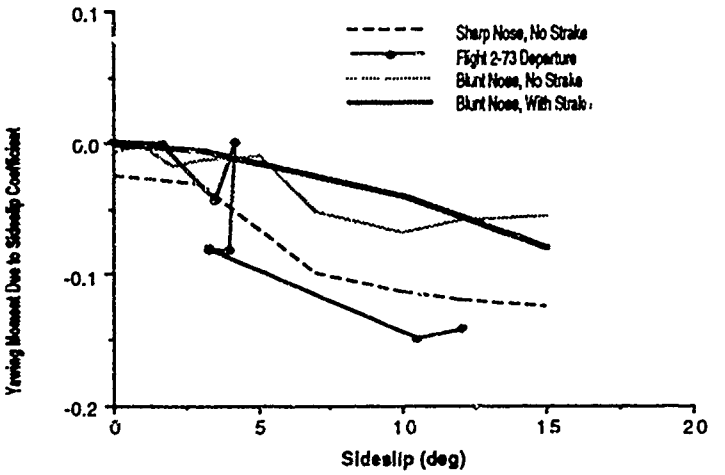

Figure 6. Effect of Nose Modifications on Yawing Moment Characteristics at 60° AOA

3.4 Noseboom Modifications

The next major improvement to the aircraft involved improving sideslip control. This was a fairly complicated issue. The aircraft uses inertial navigation unit (INU) data as truth data. The INU data is compared with flight control sensor data for redundancy management purposes.

With respect to air data information, the INU is updated with pitot-static, AOA, and angle of sideslip (AOSS) from the noseboom. The initial control laws only updated the INU with noseboom data up to 35° AOA. Above 35° AOA, the INU continued to use its last update. During flight testing at high AOA, descending altitude conditions, changes in wind direction and/or magnitude could cause a significant difference between the INU calculated and noseboom values of AOA and AOSS. The flight control laws were using the INU supplied values as the truth data and were attempting to match the commanded AOA and AOSS to the feedback values from the INU. This caused the control system to chase spurious values of AOA and AOSS. The more critical of the two was control of AOSS. As seen in figure 6, the aircraft was not able to tolerate a large magnitude of sideslip at high AOA. As test experience increased, the range of AOA for updating the INU with noseboom AOA and AOSS was increased to 50°. The pitot-static updating of the INU for velocity calculation was maintained at 35° due to the large velocity position error of the probe above 40° AOA For this problem, ITO engineers came up with the idea of using a Kiel type pitot-static probe on the tip of the noseboom. Wind tunnel data from reference 1 (dating from the 1950's) indicated that position error remained very small up to approximately 65° for the Kiel probe. Since the X-31 was designed to fly and maneuver at 70° AOA, the probe was canted down 10° from the noseboom, increasing its range of effectiveness to approximately 75° AOA. To our knowledge, the X-31 is the first aircraft to use a Kiel probe. We suspect that this is due to the fact that reference 1 stated that there are problems with shielded probes (such as the Kiel) supersonically.

When the aircraft was flown above 60° AOA for the first time, a bounded oscillation was seen on the noseboom AOSS vane. It occurred at approximately 62° AOA and was at 4 Hz with a magnitude of ± 15°. The drift between INU and noseboom AOA and AOSS was still present above 50° AOA and it was desired to extend the range of updating the INU to 70° AOA. This would not be possible with the AOSS vane oscillation. Here, a similar approach was taken as for the Kiel probe: the AOSS vane would be canted down 20° from the noseboom. This idea was designed, wind tunnel tested, and installed on the aircraft. After a sufficient number of flights to verify the operation of the new air data boom configuration, the flight control software was modified to use all of the noseboom information up to 72° AOA for updating the INU. The new noseboom and associated control law changes have virtually eliminated erroneous AOA and AOSS signals at high AOA.

3.5 Flight Control Law Changes

During the course of envelope expansion, many improvements were made to the flight control laws. The TVV deflection tables were revised to improve their effectiveness. The trailing edge flap rate limit was increased from 60 to 80 °/s when the engine core RPM is at 84 % or higher (one of the entry conditions for post-stall flight). Post-stall AOA roll / yaw command gains were adjusted. A new, more accurate thrust estimation algorithm was added. This made the estimation of TVV control power more accurate and in turn lead to larger TVV restoring moments. A very important addition was architecture for a limited authority integral path to control uncommanded roll rate and sideslip in the post-stall regime. These are only the highlights of many adjustments and additions that were made to the control laws which combined to greatly improve the aircraft's handling qualities and stability.

3.5.1 Increased Thrust Vector Vane Travel

The departure pointed out the need to obtain as much control power from the thrust vectoring system as possible. The engine thrust and paddle size were fixed, so the only possibility was to increase the TVV range of travel. This was a major effort that required a substantial control law modification. The original travel was limited, via software and hardware slugs in the TVV actuators, to 26°. This value prevented vane-to-vane impact. Analysis determined that the maximum usable travel for the paddles was 35° into the engine exhaust plume. Extensive analysis by DASA was required to revise the control law TVV tables to allow for this increased travel. Additionally, major changes by RI in redundancy management were required, because only software would now prevent vane-to-vane collisions. Once the required changes were made, and the aircraft began flying with increased TVV travel in June 1993, aircraft control was greatly improved.

3.6 Lateral Stick Command Scaling

During high AOA rolling maneuvers, it was discovered that some of the pilots had a difficult time achieving a full roll command. The reason for this was anthropometric - the pilots were hitting their legs with the control stick before they reached the lateral stops. Figure 7 helps to illustrate this problem. To command high AOA, the stick is almost all the way aft, nearly hitting the pilot's ejection seat. At full aft stick, the lateral stick interference problem is the most severe. This interference is aggravated by the stick height. With the seat up to the desired height for out of cockpit field-of-view, the stick grip is not much above the pilot's thigh. This means that his hand is between his thighs holding the stick grip, so that the width of his hand (and obstruction from his kneeboard) also restricts lateral stick deflection. Investigation into a solution revealed that a hardware fix would be difficult, so a software solution was devised. The solution was to scale the lateral stick command in the software, linearly varying it with longitudinal stick such that only half lateral stick deflection would be required at full aft stick for a full roll command. Handling qualities engineers were concerned that this change would increase lateral stick sensitivity and would remove tactile cueing such that pilots would not hit the stick stop and would not know if they had a full roll command. After manned simulations showed no adverse sensitivity effects, the software change was incorporated. Subsequent flying has verified that the lateral stick sensitivity was not adversely effected; however, some pilots do not like the lack of tactile cueing of a full roll command. Over all, the change has had little effect on handling qualities. This is likely due to the fact that full lateral stick commands (for high stability axis roll rates) are short duration events during tactical engagements. Furthermore, any lateral stick problems are largely masked by the high longitudinal stick forces and AOA sensitivity.

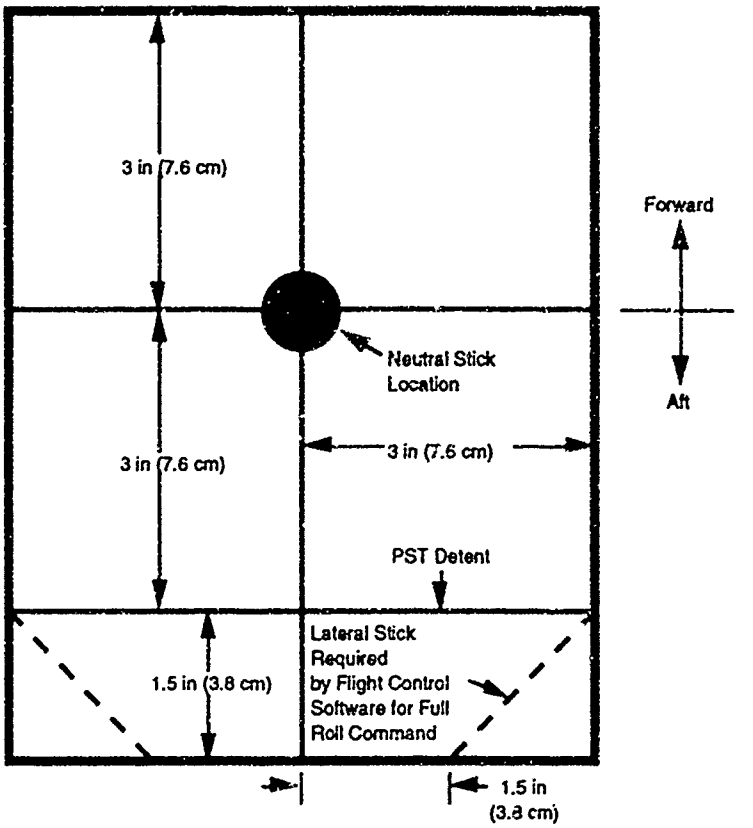

Note: Outer border indicates mechanical stops of stick.

Figure 7. X-31 Control Stick Range of Motion

3.7 Aircraft Differences

Throughout the program, envelope expansion has been carried on by whichever aircraft was airworthy at the time. At almost all times, one of the aircraft was down for an inspection or modification. The initial post-stall 720° rolls were flown with aircraft two. Its asymmetric characteristics led to excessive trailing edge flap deflection being required to control left rolls at 40° AOA. Shortly thereafter, the aircraft went into an extensive 100 hour inspection and modification period. When the 720° rolls were repeated with aircraft one, no problems were identified and the aircraft was fully cleared for multiple rolls in post-stall. It was with aircraft one, which has a significantly lower asymmetry level than aircraft two, that the post-stall envelope expansion was completed. As of early October 1993, aircraft two has returned to flight status and post-stall testing to determine its characteristics. The goal is for both aircraft to have the same flight envelope, if at all possible. Regression testing is not desirable from a cost and time perspective, but the aircraft differences have made it mandatory.

3.8 Cleared Post-Stall Envelope

The cleared post-stall envelope was in part determined by what would be required for tactical utility flight testing. As shown in figure 8, several factors determined the requirements of this envelope. It should be noted that all portions of the envelope were verified through flight test. The maximum post-stall entry speed for tactical testing was selected as 225 KCAS (417 km/h). The maximum altitude expected to be reached during the engagements was less than 30,000 ft

MSL (9,100 m), since the engagements would start at 23,000 ft MSL (7,000 m). The minimum altitude in the specially designated X-31 test area was 11,000 ft MSL (3,300 m). To ensure a recovery to less than 30° AOA by the minimum altitude, recoveries from post-stall would have to begin at 13,000 ft MSL (4,000 m). This determined the lower altitude boundary. The minimum airspeed boundary of 70 KTAS (130 km/h) was required since that is the lowest airspeed that the air data computer can calculate. The aircraft was tested to airspeeds as low as 48 KCAS (89 km/h) at 25,000 ft (7,600 m). The cleared PST envelope has been sufficient for tactical utility testing to date.

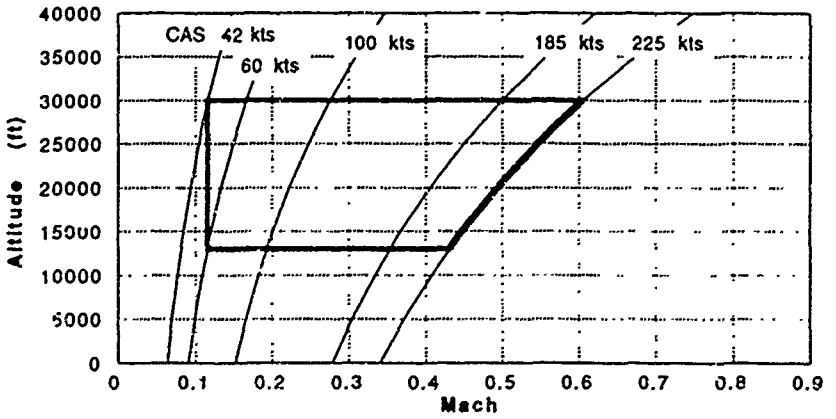

Figure 8. X-31 Envelope Cleared for Post-Stall Flying

4. SIMULATION EFFORTS

As with any modern flight test effort, simulation has played a very important role in the X-31 program. It was early simulation studies that demonstrated a dramatic increase in exchange ratios during close-in-combat for aircraft equipped with multi-axis thrust vectoring. Simulation was used extensively during the envelope expansion phase for flight test maneuver development and rehearsal, and for predictions of aircraft response. Additionally, tactical dome versus dome simulations have played a key role in the program. The two main uses of dome-to-dome simulation were intensive two week periods known as Pinball I and Pinball II.

4.1 Adversary Selection

Prior to the start of Pinball I, it had been decided that the principal adversary aircraft would be the F/A-18. Ideally, the engagements would be between a PST capable and a non-PST capable X-31. This way, the only variable (other than pilot skill) would be whether or not PST was used. However, due to the frequent inspection intervals required of these experimental aircraft, it was assumed that it would be very difficult to have both X-31's flying simultaneously. This assumption has proven to be accurate. Also, the original program plan was for the tactical utility phase of testing to take place at the NAWC AD facility at Patuxent River, MD where many F/A-18s would be available for adversary support. Fortunately, the choice of adversary did not have to change when the decision was made to complete flight testing at NASA, since NASA also maintains a fleet of F/A-18 support aircraft.

4.2 Pinball I

Pinball I was conducted in September 1990 at the IABG research facility in Ottobrunn, Germany (near Munich). IABG was chosen as the location for Pinball I for several reasons. The IABG facility is next to the main DASA engineering complex, has two dome simulators, and they have extensive experience with the evaluation of air combat engagements. The purpose of Pinball I was to support flight test efforts by: a) selecting the best starting conditions for the air combat engagements and b) developing a Rule of Thumb (ROT) weapon system for both pilots to use during these engagements.

Out of this testing, four principal setup conditions were identified. They are shown in figure 9. Three of the setups have both aircraft initially at 325 KCAS (602 km/h), separated by 3,000 ft (914 m). The difference between the three lies in the orientation of the aircraft; either defensive (DEF), offensive (OFF), or neutral in a high speed line abreast (HSLA). The fourth setup selected is slow speed line abreast (SSLA). It varies from HSLA in that the two aircraft are only 1,500 ft (457 m) apart and start at a lower airspeed of 215 KCAS (398 km/h). These four initial conditions allow PST to be utilized and evaluated in a range of options.

Since the X-31 has no weapons system, a ROT weapons system was created. It specified generic, yet realistic requirements for a gun and a heat-seeking missile. The ROT specified minimum tracking time required for a kill, maximum allowable off boresight angle, maximum allowable AOA for the missile, and minimum and maximum ranges for both weapons.

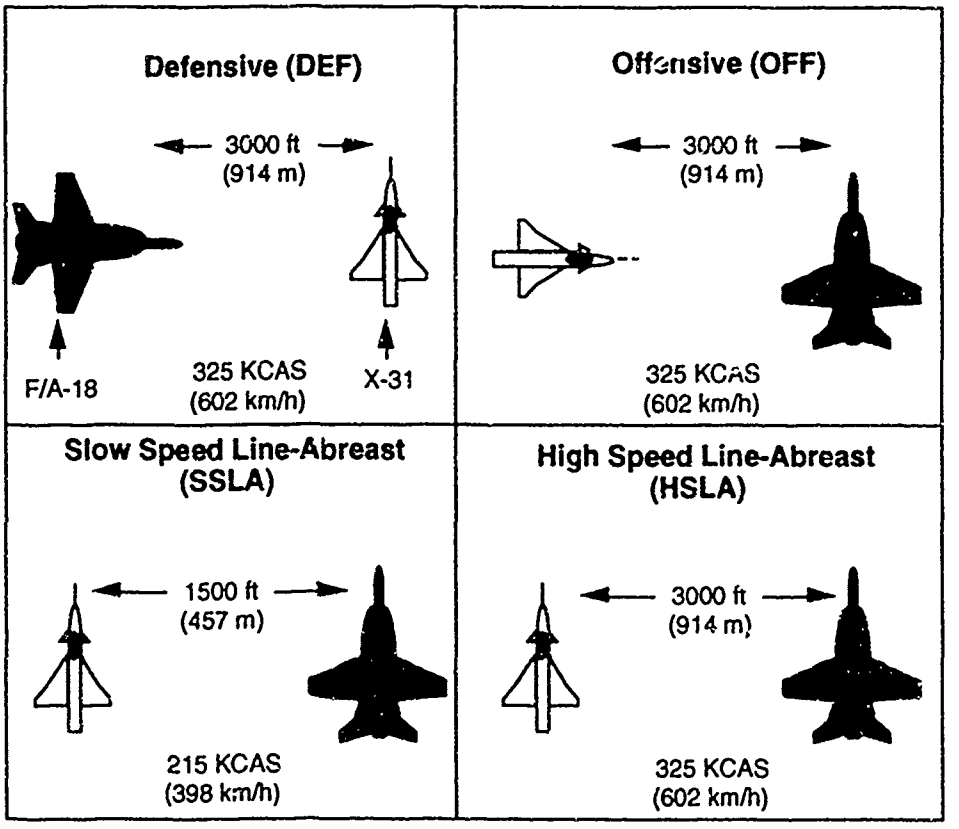

Figure 9. Starting Conditions for X-31 Tactical Engagements

4.3 Pinball II

The Pinball II exercise was conducted at IABG in April 1993. Its purpose was to act as a training buildup for the pilots and engineers who would conduct the engagements and also to perform a larger number of engagements than would be possible in the limited flight test program in order to create a statistical data base of the results. Many runs were able to be flown since the engagements were limited to 90 seconds and the simulator could very quickly be reset to the initial starting conditions.

The Pinball II exercise was a great success in terms of the pilots and engineers learning what to expect during flight test.

4.4 Cross-Country Link

It was realized that it would be beneficial to the program to have a dome-to-dome simulation facility available locally to support the tactical utility test phase. It would be useful for pilot proficiency and to evaluate new setups, new maneuvers, and the impact of aircraft changes on combat performance. NASA Dryden does not have a dome simulator; however, two of the other ITC participants each have a dome simulator. RI has a dome at their Downey, CA facility. It has been used for X-31 support since the beginning of the program. The Navy, at their NAWC AD Pax River, MD test facility has a dome simulator which is regularly used to support various programs including the X-31 and F/A-18. RI had been working in the area of linking simulations via computer networks. After considerable efforts by both parties, the concept was proven in August 1993. Unfortunately, there have been equipment problems and the dome-to-dome capability has yet to perform as envisioned. Data rate transfer and time delays have not presented a technical difficulty and it is hoped that this capability will be fully demonstrated in the near future

5. TACTICAL UTILITY FLIGHT TEST

The tactical utility flight test (TUFT) phase of the program was planned in several portions. Tactical maneuvers against a cooperative F/A-18 were flown first, followed by basic fighter maneuvering. The planned final phase is unlimited close-in combat.

5.1 Tactical Maneuvers

The purpose of the tactical maneuvers was to look at some basic post-stall air combat maneuvers in a structured, low risk way. This was in following with flight test buildup procedures. The maneuvers selected were pitch rate reserve, J-turn, helicopter (helo) gun attack, and flat scissors. Flying these maneuvers served as a bridge between the clinical flight test inputs and the free-for-all maneuvering of air combat. This helped the pilots and engineers get used to seeing the aircraft fly in a more unrestrained fashion. For instance, the AOA limiter, which had been used for the majority of the envelope expansion, was not used during these maneuvers. Since the tactical maneuvers were short, scripted looks at post-stall maneuvering, they were actually started before the 225 KCAS (417 km/h) envelope was cleared. These maneuvers were initially flown using the 185 KCAS (343 km/h) and 18,000 ft (5,500 m) minimum altitude post-stall envelope available at that time. A minimum separation of 1,000 ft (300 m) was maintained at all times during these maneuvers.

5.1.1 Pitch Rate Reserve

Pitch rate reserve means that, for whatever flight condition the aircraft is flying, it still has a reserve pointing capacity with PST. For instance, the X-31 could be turning at 30° AOA unable to bring its nose to bear on the F/A-18. However, since the X-31 can achieve 70° AOA, it can pull its nose to the target and achieve a firing solution. Two types of pitch rate reserve maneuvers were flown: a guns and a missile reserve. The guns reserve called for the X-31 to achieve a guns tracking solution. The missile pitch reserve required the X-31 to pull lead on the target so that the aircraft could be unloaded to a lower AOA (30°) that was called for by the ROT for a missile shot. The main result of these maneuvers was a tendency for pitch overshoots due to the longitudinal stick sensitivity in post-stall. This tendency was not as large as had been previously feared, and it could be managed with a moderate amount of pilot compensation.

5.1.2 J-turn / Helo Gun Attack

The J-turn, also known as the Herbst maneuver, consists of a rapid pitch up to high AOA followed by a full stick stability axis roll rate command to perform a 180° heading change. This was one of the prime maneuvers utilized during the envelope expansion phase of the program. During the tactical maneuver phase, however, there was an F/A-18 flying a pre-defined turn to act as a target. The initial setup was created such that, as the X-31 completed the J-turn, it would be able to attempt acquiring the F/A-18 for a gun or missile shot. After several of these were performed, it became apparent that this setup would work very well to set up a helo gun attack. In the helo gun attack, the X-31 uses a high AOA roll to rotate at a high rate (looking like a helicopter doing a pedal turn) to acquire and track the target. The lessons learned from these maneuvers were that the lateral acquisition and tracking task required less pilot compensation than for the pitch reserve and that there was a control harmony problem. The problem was that up to 3 in (7.6 cm) of lateral stick was required for a full roll command whereas only very small changes in the longitudinal stick created large changes in AOA. Again, this tendency could be compensated for by the project pilots, all of whom are very experienced test pilots and/or very experienced fighter pilots. The stick mechanization of the X-31 would not, however, be desirable for a production aircraft.

5.1.3 Flat Scissors

A flat scissors maneuver involves two aircraft, usually close to one another and at low airspeed, turning toward one another and reversing after overshooting flight paths. This process is repeated until one aircraft can maneuver behind the other to achieve a firing solution. Key aircraft characteristics to success in flat scissors are the ability to fly slower than the target so that it flies out in front of you, and high roll rates in order to rapidly change flight path. These characteristics are supposed to be strengths of the X-31 design. Also, the flat scissors is a common maneuver during slow speed air combat; thus it was a logical practice maneuver to perform. The X-31 could easily decelerate behind the F/A-18 by pulling to high AOA. However, if the X-31 was pulled to too high of an AOA, it began to sink in altitude in relation to the F/A-18. The X-31's high roll rates at low airspeed were advantageous during this maneuver. It was noted however, that due to the high nose attitude of the aircraft at low airspeed, it was often difficult to maintain sight of the target. This is an area which needs to be solved by future designers, that of maintaining sight and situational awareness of the target during a high AOA fight.

5.2 Agile Vu

It is very difficult to visualize an aerial engagement if you are not one of the participants. Even then, its difficult for a pilot to remember the precise details of as many as six engagements which take place over the span of 20 minutes. It is also important to demonstrate the results of your testing For all of these reasons, it was highly desirable to obtain a visualization tool with which to view the engagements. Fortunately, such a program was already in existence. Its name is "Agile Vu". It is a software program which is run on a Silicon Graphics work station. It was developed by McDonnell Aircraft Company under contract to NAWC AD, Warminster. It was originally developed for researching agility. The program requires aircraft position and attitude information as a function of time. More than one aircraft can be displayed simultaneously. The user then has the option of many different view points, scale factors, time history plots, etc. It was originally planned to use Agile Vu only for post-flight analysis. Since that time, however, Agile Vu has been adapted to run real-time during flights in the NASA mission control room. It is also possible to display the range between the two aircraft on Agile Vu. This feature has been helpful in setting up the tactical engagements. Agile Vu shows great promise as an analysis tool for the TUFT.

5.3 Basic Fighter Maneuvering

The primary purpose of the basic fighter maneuvering (BFM) phase was training for the final, close-in-combat (CIC) phase. There were 17 BFM sorties flown between August and September 1993 with 15 flights conducted during one two week period. All of the BFM flights were very successful and were conducted in a safe fashion, with the aircraft performing flawlessly.

Many important lessons were learned during BFM. The four setups defined during Pinball I were used. However, the first BFM sorties used 185 KCAS (343 km/h) as a starting speed, since the envelope expansion was not yet completed. On those flights, only the OFF setup was tested. For the BFM, rules of engagement (ROE) very similar to those used by the U.S Navy and Air Force were adopted for safety. The ROE establish radio protocol, set the minimum separation distance, and specify many other safety related items. Initially, a 1,000 ft (300 m) minimum distance between aircraft was used, but after sufficient training, this was reduced to 500 ft (150 m). The principal difference between BFM and the CIC phase is that the pilots pre-briefed their initial move prior to each engagement. Either the F/A-18 or X-31 always went high or low as the first move. After this first move, however, the aircraft were free to maneuver at will. Since training was the main BFM objective, certain rules that will apply during CIC were not used. For instance, fights were allowed to last longer than 90 sec (with a maximum of about 120 sec), and a weapon solution did not require the engagement to end. Engagements continued from the initial "fight's on" call until the X-31 pilot felt that he had achieved his training objectives or until the minimum altitude "hard deck" of 13,000 ft (4,000 m) was reached.

An important element in flight is that it is considerably more difficult and time consuming to achieve starting setups than in the simulator. In the simulator, the OFF and DEF set up was with both aircraft at a wings-level 1 g flight condition. In flight, the only way to achieve those setups is to have one aircraft turning across the other aircraft's flight path, attempting to be on a perpendicular flight path at the correct range and airspeed. The aircraft typically used a 2 g turn such that they were already in a 60° bank with a turn rate at the start of the engagement.

Another important difference between the flight test and the simulation is the aircraft's envelope. In the simulation, post-stall could be used any time the aircraft was below 325 KCAS (602 km/h) and 0.7 Mach. During the 325 KCAS (602 km/h) BFM starts, the

pilot must rapidly decay his speed to 225 KCAS (417 km/h), the current software PST entry limit, to maneuver above 30° AOA. It has not yet been determined if this difference will have a significant adverse effect on the comparison of the flight and simulation data.

Old rules of air combat still apply, such as: small aircraft like the X-31 are hard to see; aircraft flying out of the sun are hard to see; and if you lose sight, you will lose the fight.

The new rule says that PST used at the wrong time results in the F/A-18 getting the first shot opportunity. The main X-31 advantages are in high yaw rate capability and in pitch pointing the nose. The X-31's capabilities lead, when used properly, to positional advantage and decreased time to a weapons solution.

The X-31 demonstrated amazing flying qualities and performance during these maneuvers and made a strong case for the benefits of thrust vectoring during close-in-air combat. The aircraft handling was characterized as "care-free" by the pilots. It was also noted that this is both good and bad. It is very desirable from a safety and mission effectiveness standpoint. However, most aircraft have some traits or characteristics (such as noise, buffet, wing rock) which "tell" the pilot what his AOA is. In the X-31, the buffet level is approximately the same at 70° as it is at 12° AOA. This led most pilots to ask for a tone to provide them with AOA cueing.

It was very common for the pilots to inadvertently input rudder pedal commands. This usually happened as the pilot was twisting his body around to look for the F/A-18, ie. "checking six". The pilots tended to push on the rudder pedal on the opposite side of the direction they were twisting. It was simply a matter of trying to get leverage to help pivot their torso. Some pilots, depending on the type of aircraft they had air combat experience in, instinctively input rudder pedal commands while trying to roll the aircraft at high AOA. These pilots did this as a reflex, since they knew that the rudder pedal command fades to zero between 30 and 45° AOA.

The high stick forces required for flying at high AOA caused many of the pilots to fly with two hands on the control stick. The throttle position was always at maximum afterburner, so they did not need a hand for power modulation. They did need to remove their left hand from the stick to transmit on the radio, since the mic button is on the throttle. Frequent UHF calls were required during BFM to give information required by the ROE, such as "I'm going high" or "blind". The requirement to frequently let go of the stick with their left hand was a nuisance during the engagements.

5.4 Close-In-Combat

The close-in-combat phase of the TUFT is scheduled to begin in mid October 1993. It is planned that a minimum of 24 CIC flights will be flown, allowing each of the six project pilots to fly four sorties. It will be conducted in a fashion very similar to the BFM flights. The main difference will be that there is no pre-briefed initial move for either pilot. Engagements will continue until one of the following occurs: a valid kill is achieved (as determined by the control room), the 90 sec time limit is reached, the minimum altitude is reached, or a "knock it off" call is transmitted by either pilot or the control room for an unsafe condition. Data will be collected from both the X-31 and F/A-18 along with time space position indication (TSPI) data from ground-based tracking radars for both aircraft. Included in the downlinked aircraft data is weapons select and firing switches and AOA. The aircraft and TSPI data will allow for real-time calculations of ROT parameters for kill determination. The data will also be stored for post-flight data analyses using the same measures of effectiveness that were used to analyze the Pinball II simulation data.

6. ADDITIONAL NEAR-TERM TESTING

There are additional tests planned for the X-31 to take place between October 1993 and March 1994. The additional tests planned involve Helmet Mounted Displays (HMD), audio cueing, and quasi-tailless supersonic thrust vectoring.

6.1 HMD

The HMD research is designed to see if the pilot's situational awareness / spatial orientation suffers or needs augmenting during PST air combat maneuvering. Helmets with HMD have only been used in western fighters for night-vision applications; thus there is a strong impetus to see how an HMD helmet can support a pilot during a day, air combat engagement. Aircraft two has been modified to include hardware and software to support HMD research. Flying should begin in late October 1993.

6.2 Audio Cueing

Audio cueing will be researched, initially, through the use of an AOA aural cue (as a variable frequency tone) to the pilot to improve situational awareness of aircraft

state during PST air combat. An AOA tone was used during Pinball II and proved to be useful. If other potentially useful aural cues are determined, the interesting, new concept of three dimensional audio will be explored.

6.3 Quasi-Tailless Supersonic Thrust Vectoring

Aside from enhanced slow speed maneuverability, thrust vectoring offers other options for future aircraft designers. It may be possible to build aircraft with the same levels of maneuverability that today's aircraft enjoy, with the addition of thrust vectoring to allow the reduction of the size (or the elimination of) the vertical tail, gaining the required levels of stability and control from the thrust vectoring. Reducing or eliminating the vertical tail could yield benefits in performance (lower drag) and possibly reduce radar signature (increase stealthiness). The program plans to fly (in early 1994) the X-31 at 1.2 Mach, use the rudder to create a yaw command (to simulate an external aircraft disturbance) and then use the thrust vectoring to create the restoring yaw moment. If this phase is successful, the aircraft may eventually fly with a reduced vertical tail and, much later, without a vertical tail - using only thrust vectoring for yaw control.

7. CONCLUSIONS

The X-31 has been an excellent proof-of-concept vehicle for high AOA flight and air combat maneuvering. It has proven to have excellent handling qualities and performance with only minor deficiencies noted. Major differences in controllability have been seen between the two X-31s. This points out that minor, difficult-to-measure differences between aircraft can greatly affect high AOA flying characteristics. Much has been learned about the aerodynamic, flight control system, and air data system requirements to support aggressive high AOA maneuvering for an unstable aircraft.

The tactical utility lessons learned to date indicate that post-stall maneuverability is not a revolution to air combat, it is an evolutionary step which supplements existing tactics. The technology of thrust vectoring is not exotic, it is available now to designers of the next generation of aircraft.

The X-31 continues to have excellent potential for future research efforts in many areas, such as: helmet mounted displays, audio cueing, and the use of thrust vectoring for supersonic flight stabilization.

8. ACKNOWLEDGMENTS

The authors would like express their sincere gratitude to the following individuals for their assistance in the preparation of this paper and/or the symposium presentation: Dave Rodrigues, Dave Dowdell, Dave Webber, Evan Lum, Peter Huber, Fred Knox, Barry Smith, Jose Villeta, B.F. Tamrat, Susanne Weiss, Roy Mills and Dave Eubanks.

9. REFERENCES

1. Gracey, W., "Measurement of Aircraft Speed and Altitude", New York, NY, John Wiley & Sons, Inc., 1981 (ISBN 0-471-08511-1), p 39

EFA FLYING QUALITIES SPECIFICATION AND ITS UTILISATION

M. Marchand, R. Koehler, H. Duda
DLR-Institute of Flight Mechanics
Lilienthalplatz 7, D 38108 Braunschweig (GE)

E. Buchacker
BWB-WTD61
Flughafen, D 85007 Manching (GE)

K. Elbel
IABG
Einsteinstr. 20, D 85521 Ottobrunn (GE)

1. INTRODUCTION

The European Fighter Aircraft (EFA) was designed as a highly augmented, basically unstable aircraft. Its Stability and Control System (FCS) is of a much higher complexity than that used in earlier aircraft, eg the Tornado To ensure, that safe operation and optimum performance are not degraded due to possible handling qualities deficiencies, new methods had to be used for both the development and the assessment of the aircraft. This paper describes the specifications and the methods used in customer assessment prior to first flight. An overview of these methods is provided in the following paragraphs

2. FLYING QUALITIES SPECIFICATION USED

In order to ensure a good flying aircraft, useful design guidelines are necessary, as well as a clear concept of how to certify and qualify the aircraft for service use. The effort invested in generating an adequate Flying Qualities Specification for EFA (HQDD = Handling Qualities Definition Document, Ref 2) is described in Ref 1. In addition, accompanying contractor documents are required, which define special requirements to be applied during the design and clearance process

Analysis of the requirements laid down in these documents demonstrated that the requirements could be grouped in the following way:

Requirements to be demonstrated by manned simulations or flight tests:

- Requirements which explicitly ask for pilot comments and therefore need tests with a pilot at the controls (ground based simulation or flight tests)
- Requirements which need pilot-in-the-loop tests (PIO, tracking)

Requirements to be demonstrated by numerical analysis:

- Requirements which basically deal with trimmed flight conditions and average gradients accompanying deviations from trim
- Requirements based on linear system analysis
- Requirements which allow for nonlinear system behaviour

3. ASSESSMENT METHODS APPLIED

Due to the diversity of requirements, a number of different methods have been applied in customer assessment. An overview of these methods follows.

3.1 Manned Simulations/Flight Tests

3.1.1 Methods Used in Preparation of Simulations and Flight Tests

In order to provide general support for both simulator and flight tests for HQ assessments, the requirements to be applied together with manoeuvres to be performed and the associated questions for the pilot debriefing have been defined in accordance with the Handling Quality Definition Document for EFA (HQDD, Ref 2). A list of the manoeuvres is provided in Table 1. Most of the manoeuvres can be used to obtain both pilot comments and test data for several requirements simultaneously. This is shown by the examples listed in Table 2. Manoeuvres in respect of any given requirement can be selected from this Table, and it can also be seen which requirements these manoeuvres can provide data for. For instance, the manoeuvre "PULLUP" contributes to the assessment with respect to seven different criteria.

Finally, pilot actions and the questions to be answered by the pilot were defined for each manoeuvre to be performed (see Table 3)

3.1.2 Simulation Tests Performed

Official assessments have been performed using different ground simulation facilities available within the European Fighter Aircraft (EFA) partner nations to support qualification and certification work for the customer and the National Airworthiness Authorities prior to first flight. These were:

- The Advanced Flight Simulator (AFS) at DRA Bedford (Ref 4). The AFS was heavily used because of its ability to simulate aircraft motion, which was felt especially important for simulation of take off, approach and landing.
- The dual dome air combat simulator at IABG (Ref 6) This was mainly used for the simulation of the up and away Cat A flight phases where motion simulation for fighter aircraft is not possible with existing systems and not as crucial as for the Cat C flight phases
- The DASA EFA development simulator (Ref 7) In order to avoid any failures or misinterpretations which could arise due to differences in software and hardware standards, the same simulator as used by the contractor had to be used for the final official check.

The activities described below are mainly those simulations performed in Germany at IABG.

Presented at an AGARD Meeting on 'Technologies for Highly Manoeuvrable Aircraft', October 1993.

Simulations performed at the IABG Dual Flight Simulation (DFS) Facility

The government-owned simulation facility at IABG, Ref 6, was selected for the evaluation of Cat A flight phases only. Due to the inherent limitations of the simulator visual system, it was agreed that all governmental handling quality tests for the take-off and landing flight phases would be conducted at DRA Bedford's Advanced Large Motion Amplitude Flight Simulation (AFS) Facility, which provides good visual ground representation and includes the motion system.

The IABG facility has been optimised for use as a Weapon System Simulator, in particular for air to air combat in a realistic environment. The EFA contractor supplied the configuration-controlled data to be installed for the simulation, based on the DFS hardware/software environment. In order to provide the pilot with the proper visual reference cues necessary for the evaluation of the handling qualities, a target with manoeuvring and non-manoeuvring capability, which had been preprogrammed, pregenerated and stored, was provided in the dome.

Since EFA is a co-operative European programme, Official Flight Test Centres from all participating Nations were involved. The handling qualities evaluations were carried out in the course of two one-week simulation exercises performed in April and May 1992:

The first test period was designed to scan the entire flight envelope to be cleared, including the test manoeuvres developed, in order to determine which parts of the envelope and which type of manoeuvres were to be evaluated in depth by test pilots of the four nations involved. The evaluation methods used and the hardware and software involved were also tested, together with the assignments of the evaluation team. This team consisted of one German test pilot and some 20 engineers and scientists from various institutions of the four nations. Data was recorded in respect of 125 parameters at intervals of 12.5 ms or multiples, depending on the sensitivity of the parameter, and processed off-line using the software described below. Standard time history plots of the most important flight mechanical parameters were available for the debriefing shortly after the pilot left the cockpit. Due to the constraints imposed on the project by lack of time and financial pressure, the fast generation of evaluation material in hard copy and immediate report writing were considered to be of particular importance. It thus proved possible for the team to release a preliminary report of the findings within three days of completion of the tests.

This "dry run" provided valuable information as to which parts of the flight envelope initially to be cleared required thorough investigation and which type of test manoeuvres should be included in the final test plan for the four nation test period to be held in May 1992. In this test period, five test pilots from all nations were involved, together with several scientists for analysis of the results. The total clock time recorded for the first week of testing amounted to 30.75 hours productive data generation, with each participating nation allowed similar periods of pilot time in the cockpit.

The final simulation test plan can be divided into four major test blocks, see Table 4.

During familiarisation, both cockpits were manned and the pilots selected the manoeuvres and flight conditions under the guidance of the test engineers. This method proved to be very effective in familiarising the pilots with the aircraft simulated in a short time. Each pilot was allowed approximately 1.5 hrs to familiarise himself with the aircraft before productive data recording. During this familiarisation period, both pilots and engineers could request data recording of activities of particular interest. All other test blocks utilised only one simulator dome at a time.

The last block of manoeuvres, "Tracking with Target Offsets", should perhaps be explained in detail. The test team had gained some experience in evaluating air to ground tracking performance utilising lamps laid out in a pattern on the ground as targets. These lamps were switched on randomly within the pattern, and the pilot's task consisted of tracking the lit target. The results of this test are provided at Ref 3. This principle was transferred to the air to air target tracking tasks. During the manoeuvre, the target was changed randomly every 15 seconds to a position either 30 or 60 mils removed from the pilot's current manoeuvre path, see Fig 1. During these changes, the overall pilot-in-the-loop-system is excited with a higher bandwidth and the pilot is forced to act with a higher workload and gain than in classical tracking tests. Under such conditions, any PIO tendencies present can be more easily detected. Various test conditions and manoeuvres were flown, eg flight level and Mach number, turbulence ON and OFF (Dryden Model, Mil 8785C), constant g turns, wind-up turns, barrel rolls, etc. The target positions were selected in such a manner that the pitch axis could be evaluated separately from the combined pitch and roll manoeuvres. Coarse acquisition rating and fine tracking rating were enabled by large offsets of the target and the time available to the pilot before each successive target change.

The Cooper Harper and PIO rating scales as published at Ref 4 were used for the evaluation of handling qualities. After completion of each pilot's test session (duration 45 min to 1 hr), a questionnaire based on the manoeuvres flown during the session was completed, automatically printed and used at the debriefing. Answers were stored electronically for processing together with the answers provided after other pilot test sessions. In this way, all pilot replies and ratings recorded could be quickly sorted and summarised in tables. The tables containing the ratings and the comments were then compared with the HQDD requirements evaluated in individual tests, see Table 5 and Fig 2. All pilot comments provided in the questionnaire were thus directly linked to the corresponding requirements.

All five pilots from the four nations involved provided comparatively similar ratings, which enabled excellent assessment of the aircraft handling qualities. Examples of the results are presented at Figs 2, 3 and 4.

Comparison of Figs 3 and 4 shows that the influence of turbulence injected into the simulation was clearly experienced by the pilots as task intensification. The Dryden model was used for turbulence simulation.

3.1.3 Analysis of Simulation Data

In addition to the evaluation of pilot comments and ratings, the recorded time histories of the simulation runs were evaluated to provide additional information and as confirmation of the simulation results. Evaluations were performed using software tools provided by DLR and IABG, eg:

- quick look plots of time histories and cross plots
- statistical evaluations and plots of tracking errors
- determination of maximum values and gradients
- calculation of power spectra and frequency responses from 3-2-1-1-manoeuvres
- application of HQ criteria in the time and frequency domains.

In the time domain, a large number of criteria were applied successfully and in general, the results correlate well with pilot assessments. In contrast, some problems occurred in frequency domain evaluations, which were caused by the limited frequency content of the manoeuvres. As shown at Fig 5, the confidence level of the frequency response data (expressed in terms of coherence function) is poor at frequencies above 0.6 - 0.8 Hz (or 4 - 5 rad/sec).

In addition, results are often poorly defined due to the scatter of the frequency response data. In future simulation and flight tests, pilot inputs should be of higher frequency contents and more accurate system identification methods will be applied with regard to evaluation.

3.2. Numerical Analysis from Mathematical Models

Numerical evaluations form an important part of the overall HQ assessment and are often (eg during the design phase) the only way to demonstrate the handling qualities of an aircraft. The industry provided the actual versions of data sets needed for the customer assessment of EFA (aerodynamic data, mass and inertial data, flight control laws, etc). Based on this data, computing programs were developed for different kinds of evaluation and applied at DLR. These programs include the following:

- calculations of reference states and gradients
- nonlinear evaluations
- synthesis and analysis of linear models
- LOES (Low Order Equivalent System) approximation
- application of criteria in both time domain and frequency domains.

3.2.1 Trim Calculations and Steady State Criteria

Some requirements deal with parameters of a reference state and with gradients of steady state conditions. The calculations were performed in accordance with the following steps:

- determination of a trim condition
- determination of a reference state which may differ from the trim condition
- determination of steady state conditions with small parameter deviations from the reference state (for sensitivity and gradient calculations)
- comparison of results calculated for several reference states, eg to check the linearity of steady state responses with regard to the corresponding control inputs.

An example is given at Fig 6.

The above method was applied to the following handling quality evaluations:

- airspeed response to attitude changes
- flight path stability
- control forces in manoeuvring flight
- pitch axis control power in unaccelerated flight
- pitch manoeuvring capability
- lateral-directional characteristics in steady sideslips
- lateral-directional control in crosswinds.

3.2.2 Nonlinear Evaluations

Time domain evaluations form an important part of the numerical assessment. A large number of characteristics can be derived from step response simulations and conclusions can be drawn from the type and magnitude of the aircraft responses. Simulations were therefore performed for each flight condition with step inputs in pitch, roll and yaw demand. The evaluation of the time histories can be performed visually (eg to look for critical sideslip or pitch excursions during roll manoeuvres), or automatically (eg to evaluate roll and flight path time constants).

The main advantage of time response evaluations is that the effects of nonlinearities can be easily shown. The validity of linear characteristics in large amplitude manoeuvres can be investigated by varying the input amplitude. For instance, in order to confirm the validity of the PIO assessment in the case of full stick amplitudes, it was possible to demonstrate that an increase in pitch stick amplitude was accompanied by an increase in phase lag at frequencies close to the critical frequency ω_{180}, whereas gain was decreased significantly. Fig 7 provides an example of nonlinearities in the pitch control path.

3.2.3 Linear Model Evaluation

Synthesis of Linear Models:

Linear aircraft models are required for investigations in the frequency domain and the application of criteria using eigenvalues, Nichols plots, transfer functions or Low Order Equivalent Models. With regard to conventional aircraft, the evaluation of linear models from the nonlinear model function $\dot{\underline{x}} = f(\underline{x}, \underline{u}, t)$ can be performed by linearisation of the function f in respect of the aircraft state variables and system inputs. This approach is often inapplicable to nonlinear models of highly augmented aircraft, consisting as it does of a large number of first or second order filter elements described by digital filter macros, so that the function f(x,u,t) is not directly available for the complete flight control system.

The synthesis of the high order linear models was therefore performed separately in respect of the subsystems basic aircraft, flight control system, sensors, actuators, etc. The model of the basic aircraft was evaluated using the conventional linearisation method, whereas the models of flight control system, sensors and actuators were expressed in terms of several transfer functions. The complete closed loop high order model was then generated with the help of the computer software package MATLAB (see Fig 8).

Verification of the High Order Linear Model:

Due to the high complexity of the system, the linear model generated contains several potential error sources, and verification of the linear model is a very important factor. Verification can be performed via comparison of linear and

nonlinear time responses, whereby problems arise from the high system order of the linear model in time domain. When the full hardware models were implemented, the complete closed loop model was approximately of 70th order with regard to both longitudinal and lateral motion. This fact renders performance of time domain analysis difficult due to the numerical problems which arise when operating with 70x70 transition matrices with an extreme spread of eigenvalues. Therefore, when time domain analysis has to be performed, reduced order hardware models representing characteristics up to approximately 4 Hz, were implemented into the complete closed loop model. This produced linear models of approximately 40th order with a much lower spread of eigenvalues, so that no numerical problems arose when using the MATLAB tools to generate linear time responses. The differences in the complete closed loop models with reduced and full hardware assumptions are negligible in respect of investigations in low frequency range or in time domain.

The results of the comparison of linear and nonlinear time responses recorded in respect of a large number of flight conditions and input signals can be summarized as follows:

Curve matching in nearly all the steady state flight cases with small input amplitudes (5%) investigated was so good, that hardly any differences were discovered between linear and nonlinear time responses. The curve matching became poorer in extreme flight conditions (high angle of attack, high load factors) and with higher input amplitudes, see Fig 9. For example, at 30% input amplitude, due to a nonlinear filter block in the longitudinal flight control laws, the differences between the linear and nonlinear time responses were much higher than those at 5% input amplitud., see Fig 9a. No such nonlinear filter block exists in the lateral control laws, so that here curve matching was good, even at amplitudes of 40%. At very high amplitudes of 100% the nonlinearities, emanating mainly from the rate limiters, became higher, so that the differences between the curves were increased, see Fig 9b

3.2.4 Criteria Applied

Time Domain Analysis:

Time domain criteria can be used either with linear or nonlinear system responses. Due to the very good curve match between linear and nonlinear time responses with regard to moderate flight conditions and input amplitudes (see para 3.2.3), the linear model was used for the evaluation of the following criteria:

- effective roll time constant
- flight path angle time delay

The time constant was calculated in both criteria by using a tangent at the time response curve, whereby different time constants were calculated in accordance with tangent placement, see Fig 10. Therefore, in a given time window, time constants were calculated in respect of several tangent placements and the maximum time constant recorded as criterion result. As shown below (see Fig 15), the results are quite consistent with frequency domain derived time constants

High Order System (HOS) Analysis in Frequency Domain:

In frequency domain analysis, no numerical problems arise from the high system order of the linear model, so that the full hardware models can be implemented into the complete closed loop model. Comparison showed that in high frequency range (> 1 Hz) linear models with full hardware assumptions obviously possessed other characteristics than the models with reduced order hardware assumptions. For example, when evaluating the PIO phase rate criterion, the phase rate evaluated was very sensitive with regard to the selected hardware assumptions. This fact meant that different linear models had to be applied to the analysis of time and frequency domains.

The following frequency domain criteria were applied:

- open-loop stability margins (longitudinal and lateral)
- a set of pitch response criteria (Nichols plot boundaries as shown in Fig 11, bandwidth, PIO phase rate and amplitude limits)
- PIO phase rate limits for roll axis
- Neal-Smith criterion
- a modification of the PIO analysis rules included at Ref 5, see Tables 6 and 7

Most of these criteria form part of the relevant EFA Requirements, whereas the Neal-Smith criterion and the R H Smith PIO analysis rules are taken as additional tools to provide the evaluating engineer with a different view of handling characteristics in possible problem areas.

Application of PIO Assessment Rules

During the discussion of assessment results presented by Industry, it became clear that the prediction of PIO tendencies could not be based on the application of only one single criterion. In particular, the limits for the crossover gain (at -180 degree phase angle) of the pitch attitude response were discussed and additional investigations performed. The industry also applied the bandwidth criterion (taken from MIL-STD-1797). The influence of the non-linear pitch response to pilot inputs was investigated at DRA Bedford using the Nichols plot, phase-rate and bandwidth criteria. An effort was made at DLR to apply the PIO theory presented by Ralph R Smith and included at Ref 5, which is described briefly in the following paragraph:

Table 6 provides a definition of the two PIO categories. From the eigenvalues evaluated, it follows that Type II PIO is unlikely. Therefore, effort was concentrated on the assessment with regard to Type I PIO. The rules finally applied are outlined in Table 7. The original rules included at Ref 5 were amended, in that evaluation step 4 was modified and evaluation step 8 added. A simplified definition of the relative bandwidth was introduced at evaluation step 4. Evaluation step 8 introduces a check as to whether stick forces are high enough to prevent the pilot from providing giving large amplitude periodic inputs. Since there are a many uncertainties in the definition of the boundaries used in the evaluation, the rules should be applied as a tool for detecting possible problem areas rather than as a strong yes-or-no decision criterion. Possible tolerances of system dynamics as well as the uncertainties of the boundaries applied should also be taken into account.

Low Order Equivalent System (LOES) Analysis:

The POLYKO Method developed at DLR was used to determine the characteristics of so-called "Low Order Equivalent Systems" (LOES) (a short description of this method is provided at Annex A of Ref 1). In contrast to earlier

assessments made (eg in respect of Tornado), LOES evaluations for the FFA provided doubtful results containing only limited information in respect of handling characteristics, which meant that alternative criteria using high order models or simulated time responses had to be applied instead of LOES criteria. Some of the experiences are discussed here in a few words.

Short-period mode evaluation: In a number of flight conditions it was observed that the HOS (high order system) response had more than one pair of eigenvalues in the short-period frequency range, the influence of which was not totally cancelled by corresponding zeros. One of these modes influenced mainly the pitch rate, the other more the load factor response. Results of the LOES approximation then depended on the choice of signal mainly used in the evaluation, as demonstrated in Fig 12. In other cases, the identified LOES model does not match the given data sufficiently. This is most obvious in the low-g or high-g cases investigated. An example of a 0-g flight condition is provided at Fig 13. In such cases, the alternative high order criteria must be used and the LOES characteristics treated only as additional information, eg as indication of whether low damped modes exist or not. Generally, it can be concluded that an aircraft cannot respond in the "classical" sense if pitch rate and normal acceleration responses cannot be approximated simultaneously.

Approximation of lateral LOES models: It was generally observed that the application of a global lateral model containing Dutch roll, roll and spiral modes did not produce any satisfactory results. This was because the results of the parameters to be determined were very strongly correlated, so that no unique solution could be found. The experience gained from the application of different model structures is summarized in Table 8 as rules for a step-wise approach. Explanations are provided in the following paragraphs in respect of the items contained in this table.

Evaluation of the spiral mode time constant: With regard to the spiral mode, a value can be taken from the HOS response. This is because the high frequency FCS modes have little influence in the frequency range of the spiral mode. The HOS value can be used in the approximation, eg in evaluation step 4a, to fix the spiral time constant.

Evaluation of roll time constant: As shown in Table 8, there are two different definitions of roll time constant and therefore two different situations for the evaluation (see evaluation steps 2 and 3 in this table). Determination of the **roll time constant as an eigenvalue** of the LOES would require the spiral mode to be included in the model. However, the experience gained showed that in most cases the roll time constant identified was highly correlated with equivalent time delay and other parameters. On the other hand, when determining the **effective roll time constant** (T_{Reff}) as a characteristic of the roll step response, including the effects of other modes and delays, the LOES model must not contain the spiral mode explicitly. If an equivalent time delay is identified, it must be added to the roll time constant to provide the total value of T_{Reff} (see evaluation step 3). Further investigations and comparisons with time domain results showed, that the evaluation should also consider the frequency range below the roll mode, even if the curve fit in this region is poor, as shown at Fig 14. It was shown that the lowest evaluated frequency should be not greater than 0.1 rad/sec for the low speed cases and not greater than 0.3 rad/sec for medium and high speed cases. A comparison of time domain and LOES derived results is provided at Fig 15.

Evaluation of Dutch roll parameters: When using the full lateral 4th order model with all parameters free, it was not possible to find a unique solution to the approximation problem. Parameters which were highly correlated were the equivalent delay t_β and the high frequency zero of the sideslip/rudder transfer function. In order to avoid correlations, at least T_{Spiral} and t_β should be fixed (T_{Spiral} at the HOS value and t_β eg at 0 or 0.1 sec corresponding to the Level 1 limits). As a consequence, only the frequency and damping of the Dutch roll mode can be taken from the full lateral LOES models.

Alternatively, the Dutch roll characteristics can be taken directly from the HOS model (see evaluation step 4b) if the classical modes (roll, Dutch roll, spiral) are clearly defined by the pole-zero constellation of the transfer functions and well separated from FCS modes.

4. CONCLUDING REMARKS

We are confident that using the specifications, methods and tools developed during our efforts and described in this paper will assure the safety required for first flight clearance and beyond.

It was important to us not to rely on one single approach, but to employ different methods and tools, pilot-in-the-loop tests as well as purely theoretical approaches.

During pilot-in-the-loop simulation, we took great care to design tasks from which pilots could gain a clear view of handling qualities of the proposed first flight configuration.

The pilot is the only universal test tool. All other tools employed suffer from constraints in one or several areas and sound engineering judgement is needed in their application.

5. REFERENCES:

[1] E. Buchacker, H. Gallenmüller, R. Koehler, M. Marchand: Development of MIL 8785C into a Handling Qualities Specification for a New European Fighter Aircraft. AGARD-CP-508, 1990.

[2] Handling Qualities Definition Document for EFA, Issue D, 1990.

[3] R. Koehler, E. Buchacker, D. J. Biezad: GRATE - A New Flight Test Tool for Flying Qualities Evaluation. AGARD-CP-452, 1989.

[4] A. D. White, J. R. Hall, B. N. Tomlinson: Initial Validation of an R&D Simulator with Large Amplitude Motion. AGARD-CP-513, 1992.

[5] R. H. Smith: A Theory for Longitudinal Short-Period Pilot Induced Oscillations. AFFDL-TR-77-57, 1977.

[6] W. Schattenmann, H. Seuß: A Brief Description of the IABG Air Combat Simulator (DFS). IABG-WTS-TN-70-1989.

[7] H. Eibl, H.-G. Offenbeck, H. W. Pongratz: Development and Evaluation of an "Attack and Maneuvering System" with Combat Development Simulators as Main Development Tool. AGARD-CP-513, 1992.

A) Terminal Operations	
TAXIING	taxiing
TO RUN NOR	normal takeoff run
TO RUN DRY	takeoff run on a dry runway in lieu of a wet runway
TO RUN WET	takeoff run on a wet runway
TAKEOFF	takeoff
TO XWINDS	takeoff in crosswinds
F LOSS CO	thrust loss, takeoff continued
F LOSS AB	thrust loss, takeoff aborted
F LOSS TO	thrust loss during takeoff
LANDING	landing
L XWINDS	landing in crosswinds
WAVE OFF	wave-off, go-around
ROLLOUT NOR	normal rollout
ROLLOUT DRY	rollout on a dry runway in lieu of a wet runway
ROLLOUT WET	rollout on a wet runway
F LOSS RO	thrust loss during rollout
F LOSS AP	thrust loss in approach
B) Tests of Longitudinal and Lateral-Directional Handling Qualities	
ACC DEC	acceleration and deceleration
PUSHOVER	pushover
WUT SPD	wind up turn at constant speed
STEEP TURN	steep turn
PULLUP	pullup
FL CO CONST	level flight with cockpit controls fixed
FL CO ZERO	level flight with cockpit controls free
TURN -YAWC	turn with yaw controls free
TURN +YAWC	turn with yaw controls used for coordination
SIDESLIP	sideslip
RO STEP MAX	rolls with full roll control
RO MAX BETO	rolls with yaw controls used for coordination
C) Tests of Miscellaneous Handling Qualities	
AIR TRACK	air to air tracking
PATH TRACK	flight path tracking
CONFIG CHNG	configuration change
FCS MODE CH	FCS Mode change
ASYM LOADS	asymmetric loads
F LOSS FL	thrust loss in flight
FAILURES	failures
2 ENGIN OFF	2 engine failure
GUST	flight in atmospheric disturbances
PIO	PIO tests

Table 1 List of simulator tests suited for HQ assessments

TESTS	HQDD-REQUIREM. 3.2.1.1	3.2.1.1.2	3.2.2.1.3	3.2.2.2.1	3.2.2.2.2	3.2.3.1.2	3.2.3.2.1	3.2.3.2.2	3.2.3.2.7	3.3.1.1.5	3.3.2.6	3.3.2.7	3.3.4.1.3	3.3.4.2	3.3.5	3.3.6.1	3.3.6.2	3.3.6.3.1	3.3.6.3.2	3.3.7.1	3.4.4.1	3.4.10	3.5.2.1	3.6.1	3.6.1.2	3.6.3	3.6.3.1
B LONG LAT																										
ACC DEC		C																						M	C	C
PUSHOVER		C			M	M			C	M																
WOT S/O		C		M	M	M																				
STEEP TURN		C				M	M														C	C				
PULLUP		C		M	M	M	M		M													C				
FL TO CONST	C		M				M			M																
FL TO ZERO	C		M				M			M													C	M		
TURN +RAMP											M	M		C												
TURN +RAMP											M	M		C												
SIDESLIP														C	C	C	C	C	M	C		C				
PC STEP MIX													M	M	M											
[illegible]																										

Legend M Test is mandatory C Test can contribute in respect of the requirement

Table 2 Matrix of tests and requirements

Test Symbol	Pilot Actions	Questions	Requ. #
ACC DEC	After trimmed wings-level straight flight rapid acceleration at maximum augmented thrust from 250 knots to V_{max}. Then rapid deceleration by the most critical combination of changes in power, actuation of deceleration devices, steep turns and pullups performed by normal pilot techniques.	Are the magnitude and rate of the trim changes small enough to cause no difficulty in maintaining straight level flight or the desired load factor by normal pilot techniques?	3.2.1.1.2
		Does the trim device operate rapidly enough to enable the pilot to maintain his control forces yet not so rapidly as to cause oversensitivity or trim precision difficulties?	3.6.1.3 3.6.1 3.6.3.1
		Did the operation of secondary control devices impose excessive control forces?	

Table 3 Example of test definition and corresponding questions and requirements

FAMILIARIZATION:
• doublets in pitch-, roll- and yaw-axis
• sideslips
• other manoeuvres on pilot experience and desire
CLASSICAL HQ-MANOEUVRES:
• acceleration/deceleration
• symmetrical pushover/pullup
• windup turns at constant speed
• steep turn with reversal
• continuous roll (4x360 degree)
• continuous roll reversal
TRACKING (ACQUISITION AND FINE TRACKING):
• level flights
• constant g-turns and windup turns
• roll reversals (both unloaded and loaded)
• barrel rolls
TRACKING WITH TARGET OFFSETS:
• level flights
• constant g turns and windup turns
• barrel rolls

Table 4. Testplan for the 4-Nations Simulations performed at IABG Dual Simulation Facility

Requirement #, Question	Test Pilot 1 2 3 4 5	Pilot Comments
HQDD 3.2.2.1.3 HQDD 3.3.1.1		
Do any sustained residual oscillations in normal or lateral accelerations or in pitch, roll, or yaw attitude (in calm air) interfere with the pilot's ability to perform the tasks required in service use of the aircraft?	1 3 4 5	(Collection of comments of the test pilots 1,3,4,5) ....

Table 5 Arrangement of comments from different pilots according to requirement number

PIO CATEGORIES

PIO Type	induced by ...
I	... dynamic response of the closed loop pilot control of pitch attitude
II	... non-tracking control or disturbances

Table 6. PIO Categories (from Ref 5)

PITCH PIO ANALYSIS
MODIFIFIED ASSESSMENT RULES FOR TYPE I PIO

Evaluation Steps	Questions	Answers (Example)
1. Define a model for pilcted pitch control (Neal-Smith-Criterion)		
2. Close pitch attitude loop	Is the closed loop resonant?	yes
3. Compute transfer function and spectrum of normal acceleration (a_{zp} for pitch loop closed)		
4. If a_{zp} shows a resonant peak, determine relative width ν of the peak and resonant frequency ω_R	Is the spectrum resonant (e.g., if $\nu < 0.5$) or lightly damped ?	no
5. Calculate the amplitude ratio normal acceleration/pitch rate at frequency ω_R	Is $\lvert a_{zp}/q \rvert > 0.012$ g/deg/sec ?	yes
6. Close the a_{zp}-loop with pilot delay = 0.25 sec, pilot gain adjusted to give crossover frequency at ω_R		
7. Calculate phase of open-loop a_{zp}-response (including pilot delay) at ω_R	Is the phase angle < -180 deg ?	yes
8. Calculate critical pilot gain (i.e. gain for unstable closed loop) and compare with limits from stickforce/g requirements	Is the critical gain less than the upper Level-1-limit ?	yes
Conclusion	**Is PIO Type I a strong possibility? (Are all the answers "yes" ?)**	no

Table 7. Pitch PIO Analysis based on the assessment rules from Ref 5

STEPWISE APPROACH FOR LATERAL LOES APFROXIMATION

LOES-Mode to be evaluated	Recommended Approach	Transfer function to be used in approximation
1. Spiral mode T_{Spiral}	Take T_{Spiral} from HOS-Response, if possible	Denominator of lateral HOS
2. Roll mode T_R (eigenvalue)	Difficult to evaluate (strongly correlated with equivalent time delay)	(p/δ_a)
3. Effective roll mode time constant T_{Reff}	Use 1st order model with time delay, $\frac{K}{1+Ts}\exp(-\tau s)$, $T_{Reff} = T + \tau$	p/δ_a
4a. Dutch roll mode frequency and damping from LOES	Use 4th order model with fixed T_{Spiral} and fixed τ_β (otherwise results are strongly correlated)	p/δ_a and β/δ_r
4b. Dutch roll mode frequency and damping from HOS	Take eigenvalues directly from HOS, if roll and dutch roll modes are clearly identifiable and well separated from FCS-modes	p/δ_a and β/δ_r

TABLE 8. Stepwise approach of LOES-Determination for the lateral modes

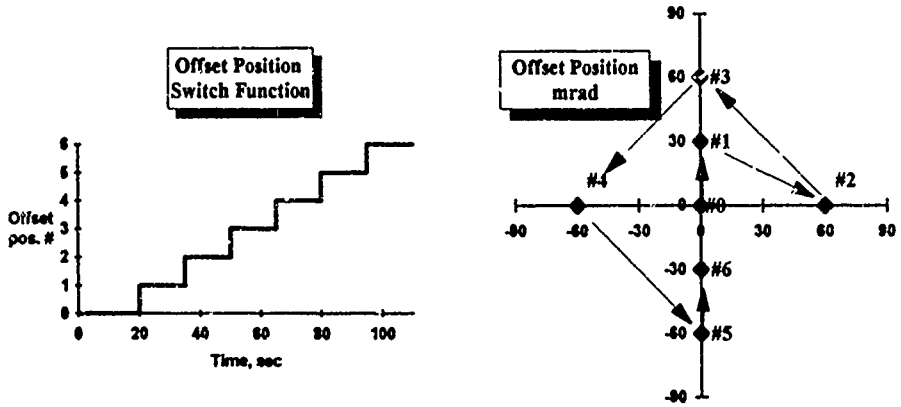

Fig. 1 Offset of jumping target in air-to-air tracking simulation

Pilot Ratings in Constant g Turns

Pilot	GE		UK		IT		SP		∅	
Rating	HQR	PIO	HQR	PIO	HQR	PIO	HQR	[illegible]	HQR	PIO
Without turbulence										
Reacquisition	5	3	5	3	3	1	4	2	4	2.5
Fine Tracking	2	1					2	2	2	1.5
With turbulence										
Reacquisition			7	3	7	4	7	4	7	4
Fine Tracking							6	4	6	4

Fig. 2. HQR (Cooper-Harper-HQ-Ratings) and PIO-Ratings during tracking in constant g-turns
(Ratings as given by pilots from four nations and average rating)

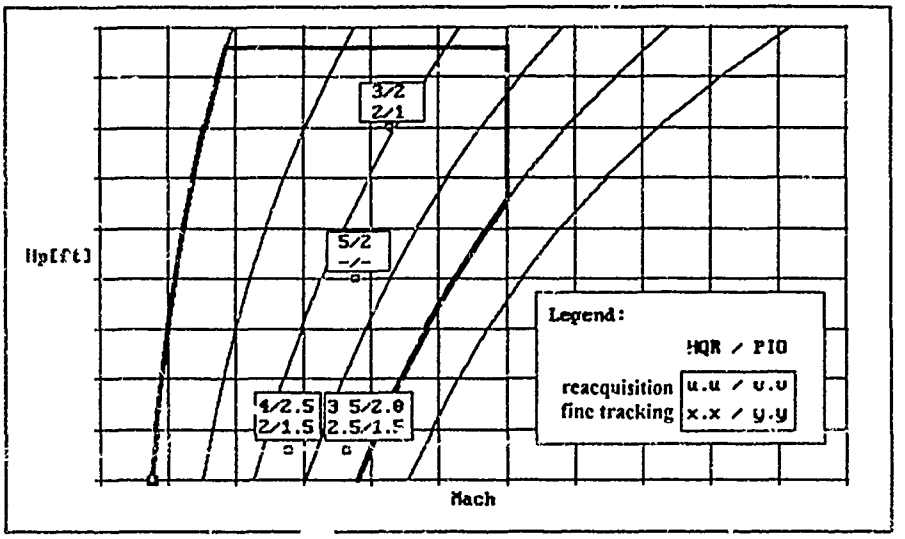

Fig. 3. Pilot ratings during tracking exercises 'constant g' without turbulence

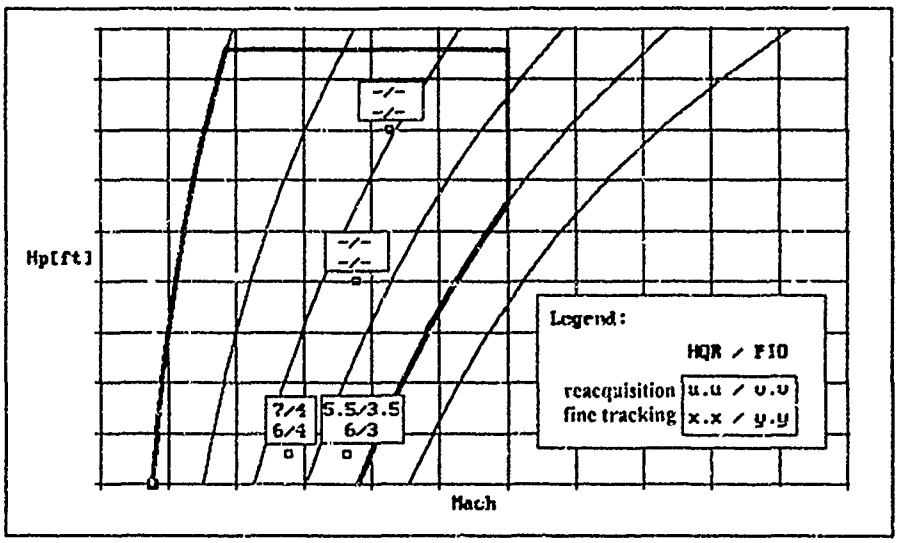

Fig. 4. Pilot ratings during tracking exercises 'constant g' with turbulence

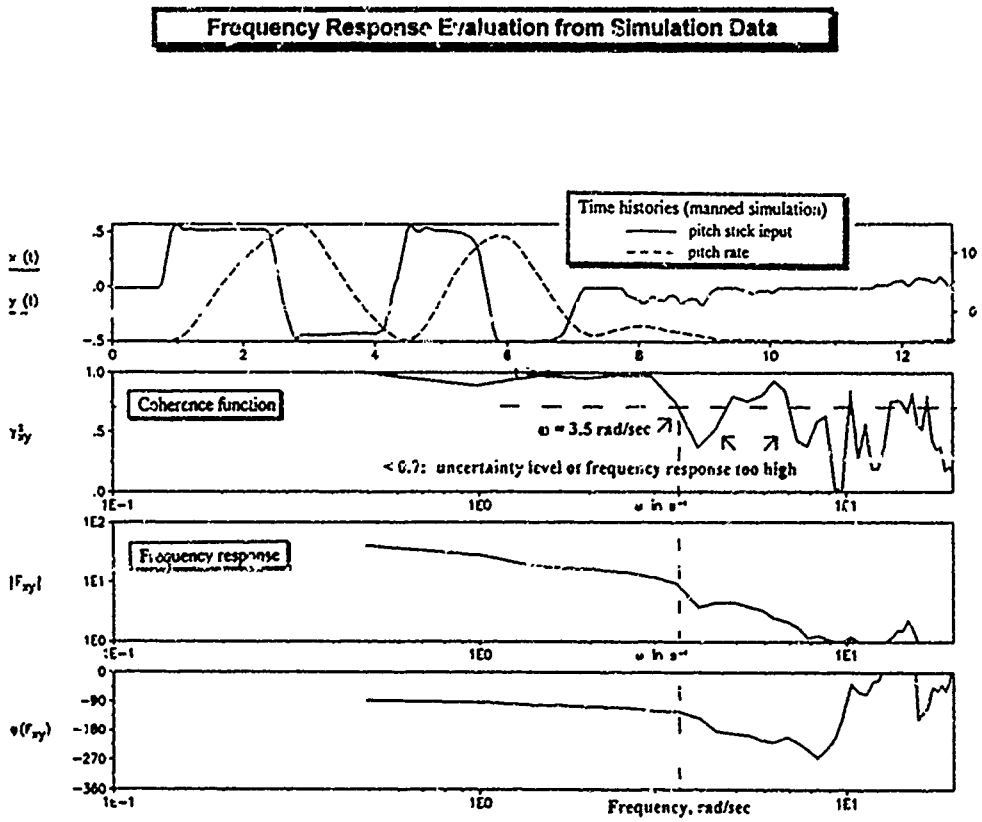

Fig. 5. Example of frequency response evalation from ground simulation data (time histories, coherence function, magnitude and phase of frequency response)

Diagram of flight path stability

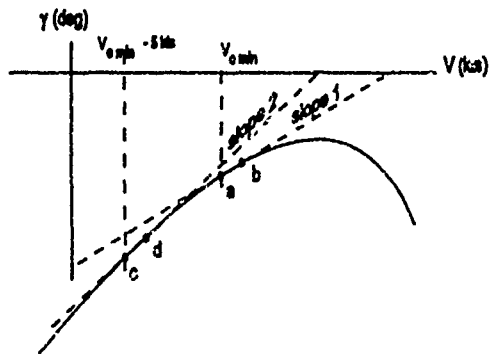

Evaluation of steady state parameters

slope 1: $\left(\frac{\Delta\gamma}{\Delta V}\right)_{V_{trim}} = \frac{\gamma_b - \gamma_a}{V_b - V_a}$

slope 2: $\left(\frac{\Delta\gamma}{\Delta V}\right)_{V_{trim}-5kts} = \frac{\gamma_d - \gamma_c}{V_d - V_c}$

difference of slopes:

$$\Delta\left(\frac{\Delta\gamma}{\Delta V}\right) = \left(\frac{\Delta\gamma}{\Delta V}\right)_{V_{trim}} - \left(\frac{\Delta\gamma}{\Delta V}\right)_{V_{trim}-5kts}$$

Calculations of reference state conditions

Refer. state	Input parameters for calculation	Output parameters
a	cockpit control forces $V_a = V_{o\,min}$ $\gamma_a = \gamma_{approach}$	cockpit control trim positions
b	cockpit control trim positions $V_b = V_a + \Delta V$	$\gamma_b = \gamma\,(V_{trim} + \Delta V)$
c	cockpit control trim positions $V_c = V_a - 5$ kts	$\gamma_c = \gamma\,(V_{trim} - 5kts)$
d	cockpit control trim positions $V_d = V_c + \Delta V$	$\gamma_d = \gamma\,(V_c + \Delta V)$

*) ΔV = small change of speed

Criteria parameters:

slope 1 and difference of slopes:

$$\left(\frac{\Delta\gamma}{\Delta V}\right)_{V_{trim}}, \Delta\left(\frac{\Delta\gamma}{\Delta V}\right)$$

Fig. 6. Example of steady state HQ evaluations (Flight path stability criterion)

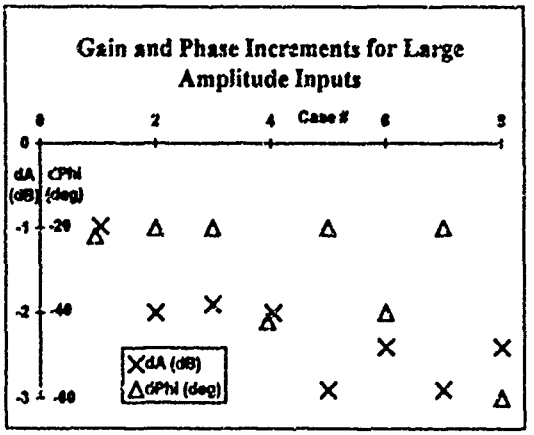

Fig. 7. Influence of large input amplitudes on pitch rate T.F. (measured in the crossover frequency region of the a_{zp}-loop from sweep stick inputs up to 60 %)

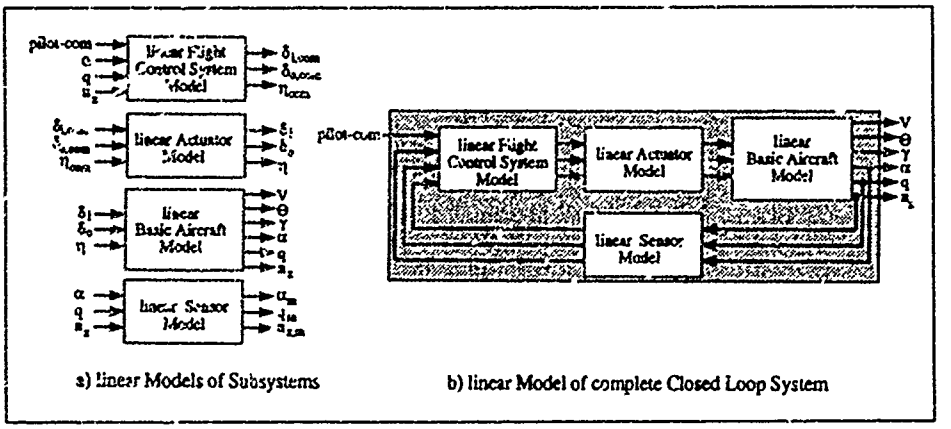

Fig. 8. Synthesis of linear high order models (Longitudinal motion)

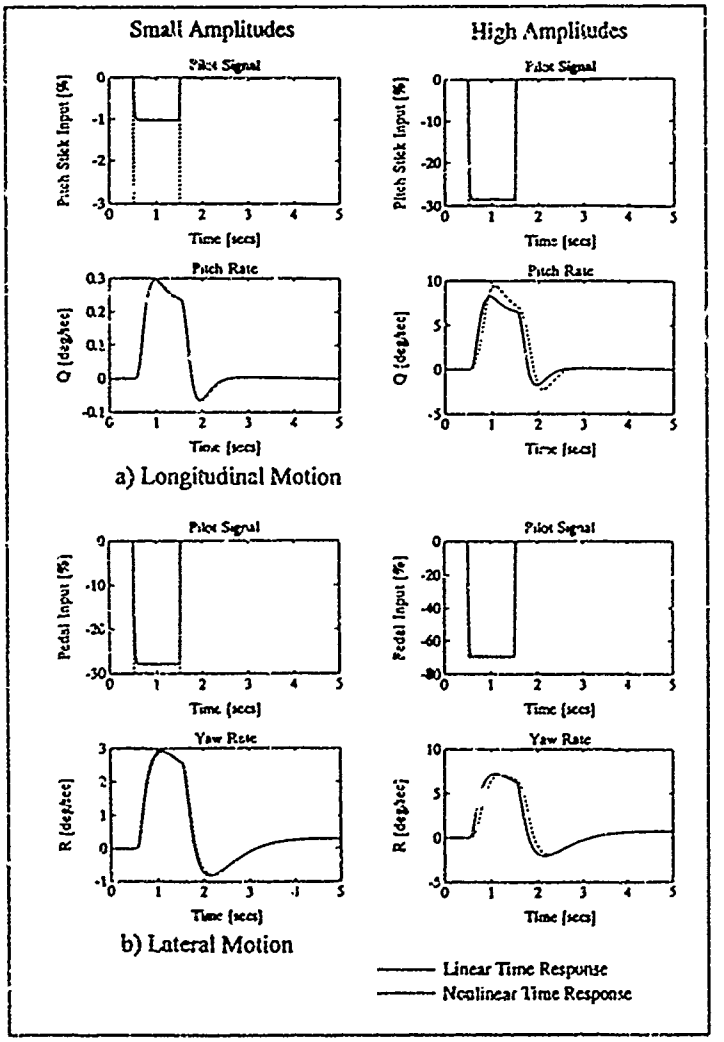

Fig. 9. Comparison of nonlinear responses with time histories from linearized models for small and large pilot command inputs

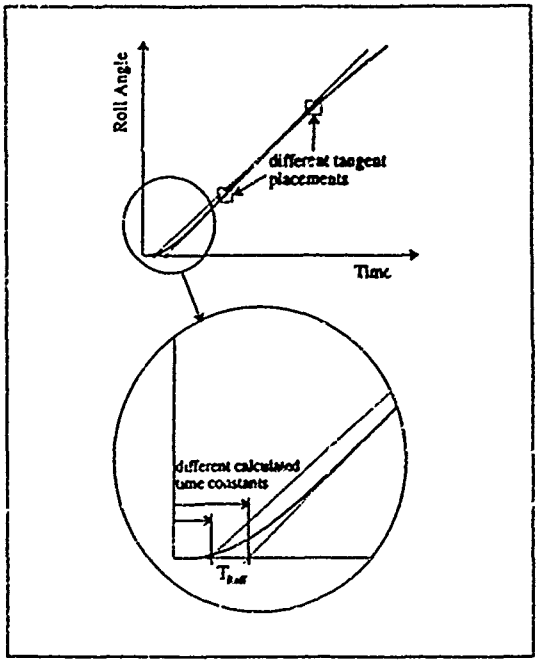

Fig. 10. Uncertainty of effective roll time constant from time domain evaluations

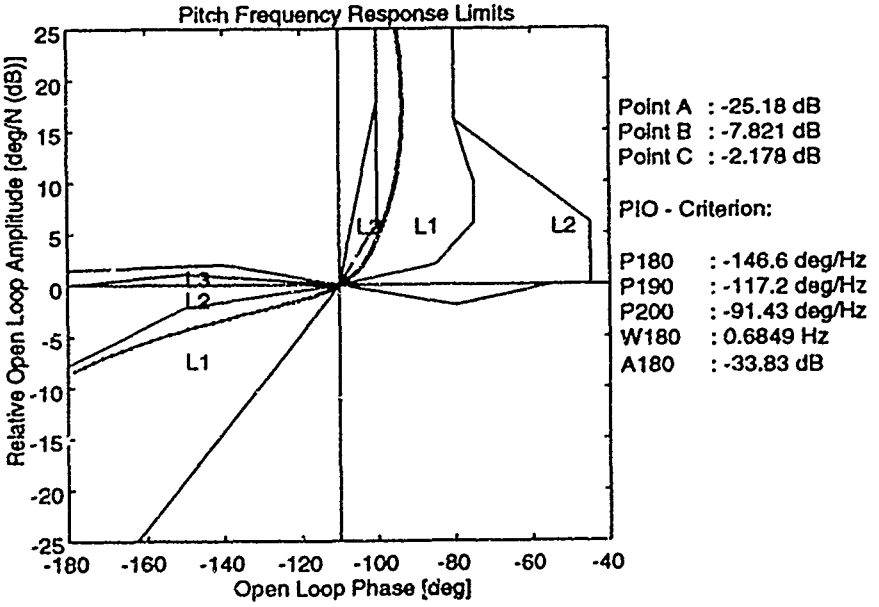

Fig. 11. Example of HQ assessment using frequency domain criteria
(Pitch attitude transfer function and PIO phase rate and amplitude boundaries)

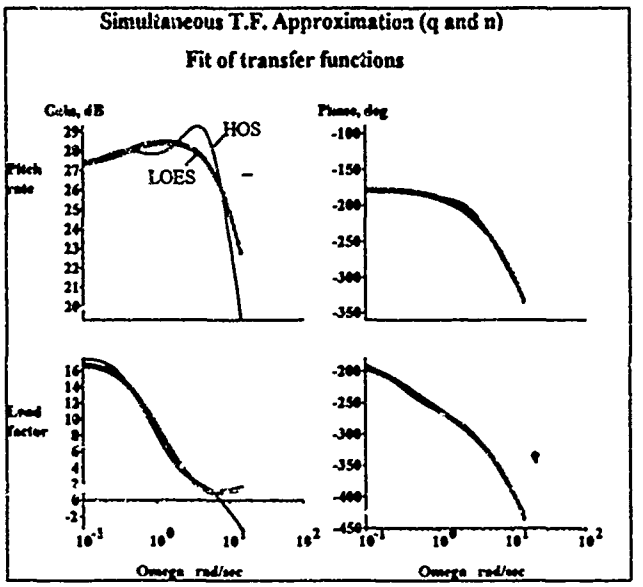

Fig. 12..Curve fits and resulting LOES eigenvalues from simultaneous and single transfer function approximation

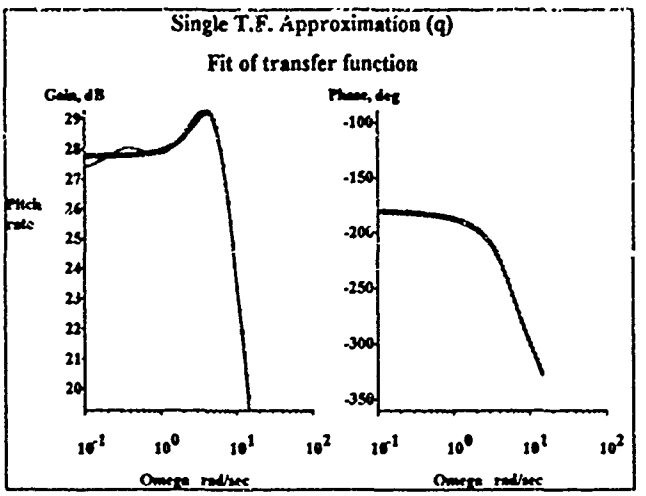

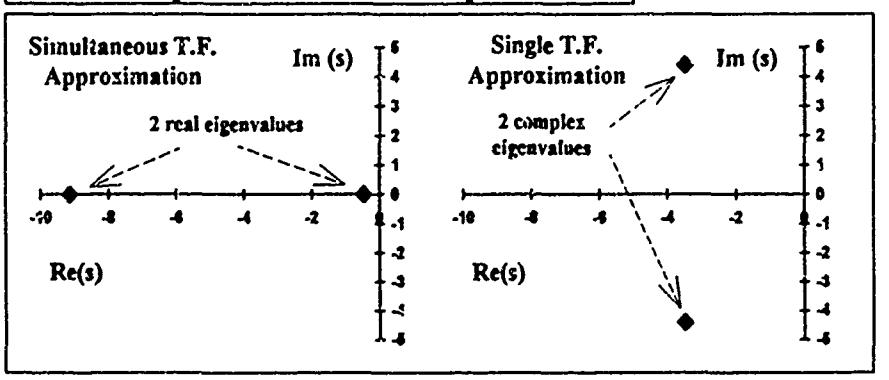

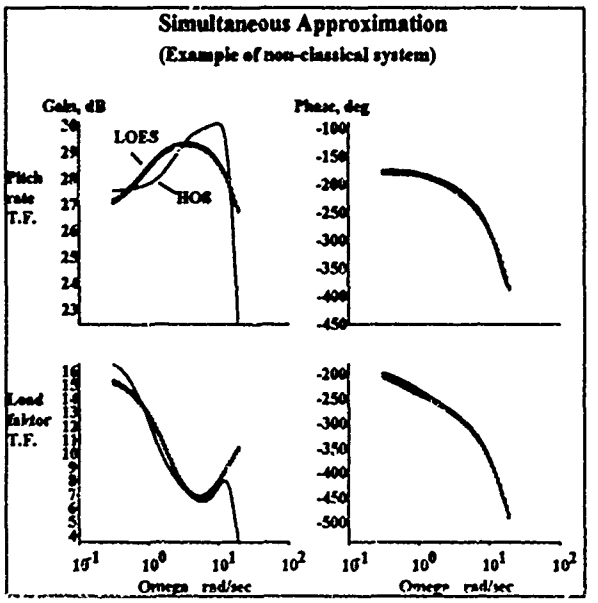

Fig. 13. Example of LOES approximation for non-classical system characteristics

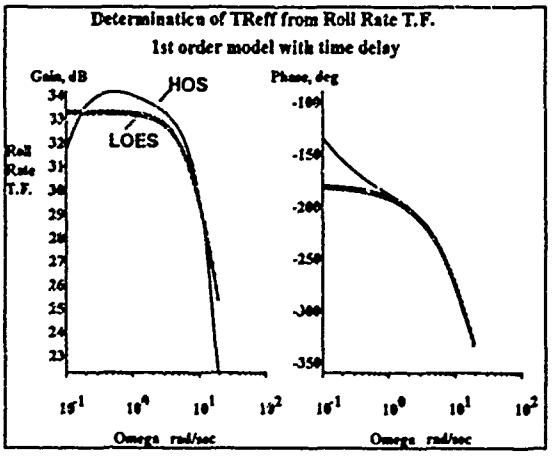

Fig. 14. LOES-approximation for determination of effective roll time constant according to step 3 of Table 8.

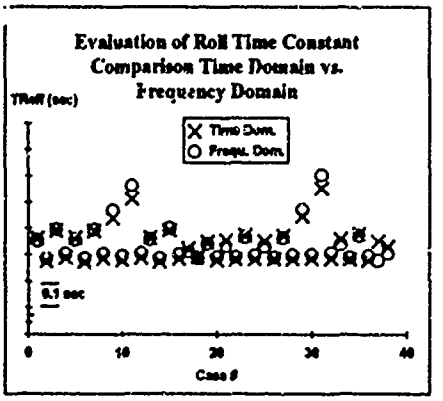

Fig. 15. Comparison of time domain and frequency domain results

APPLICATION OF CURRENT DEPARTURE RESISTANCE CRITERIA TO THE POST-STALL MANOEUVERING ENVELOPE

Robert M. Seltzer
Jeffrey F. Calvert

Air Vehicle And Crew Systems Technology Department
Naval Air Warfare Center, Aircraft Division, Warminster
Warminster, PA 18974-0591, USA

SUMMARY

This paper presents an analysis of current departure resistance and high angle of attack (HAOA) flying qualities parameters with respect to applicability and utility in design and assessment of today's enhanced maneuverability aircraft. Modern fighter/attack aircraft possess extremely non-linear aerodynamic databases and highly complex flight control systems. In addition, these aircraft require both departure resistance and mission effective HAOA maneuvering capability. The limitations of using traditional departure susceptibility parameters such as $C_{n_{\beta_{DYN}}}$ and LCDP to address departure resistance and agility design and analysis issues are analyzed and presented herein. Discussion includes the design philosophy and tradeoffs of improving static versus dynamic departure resistance. In addition, the utility of open or closed-loop departure parameters derived from linear and/or decoupled equations of motion representing highly non-linear aircraft is addressed. Finally, a general methodology outlining the application and validity of current departure susceptibility parameters to the modern aircraft HAOA flight regime is provided with recommendations.

LIST OF SYMBOLS

A. Aircraft motion, position, and attitude

h	Pressure altitude
M	Mach number
N_y	Aircraft lateral acceleration, g's
P, Q, R	Roll, pitch, and yaw angular rates about aircraft x, y, z body axes
U, V, W	Components of velocity along aircraft x, y, z body axes
V_T	True Velocity, $\sqrt{U^2 + V^2 + W^2}$
α, β	Angle of attack and sideslip angle
δ_i	Control surface deflection, (i= A=aileron, D=differential trailing-edge flap, R=rudder, C=canard)
μ	Wind axis roll angle
ψ, θ, ϕ	Yaw, pitch, and roll Euler angles between inertial axis and aircraft body axis

B. Aerodynamics

C_ℓ C_m, C_n	Aerodynamic non-dimensional, rolling, pitching, and yawing moment coefficients, $\ell/\bar{q}Sb$, $M/\bar{q}Sb$, $N/\bar{q}Sb$
ℓ, M, N	Rolling, yawing, and pitching moment about aircraft body axis
ℓ_i', N_i'	Total incremental change in rolling and yawing acceleration due to incremental change in state variable quantity (subscript), $\ell_i' = \{\ell_i + (I_{xz}/I_x)N_i\}/[1-(I_{xz}^2/I_xI_z)]$ $N_i' = \{N_i + (I_{xz}/I_z)\ell_i\}/[1-(I_{xz}^2/I_xI_z)]$
$C_{n_{\beta_{DYN}}}$	Open-loop Lateral-Directional Departure Susceptibility Parameter
LCDP	Closed-loop Lateral Control Departure Parameter
T_{ϕ_1}, T_{ϕ_2}	First order time constants of an over damped roll attitude numerator
T_{θ_1}	First order time constant of the pitch attitude numerator which can result from unsymmetrical flight

C. Aircraft Parameters

b	Wing span
$\bar{c}$	Mean aerodynamic chord
I_x, I_y, I_z	Moment of inertia about aircraft x, y, z body axes
I_{xy}, I_{xz}, I_{yz}	Cross moment of inertia
m	Mass of aircraft
S	Wing reference area

D. Miscellaneous Definitions

A, B, C, D, E	Coefficients of fourth order polynomial, $As^4 + Bs^3 + \quad + E$
DR	Lateral-directional Dutch roll mode
g	Acceleration due to gravity
$\bar{q}$	Dynamic pressure
P	Phugoid Longitudinal mode
R	Lateral-directional roll mode, Rudder
RHP	Right-half plane
RS	Roll-spiral lateral directional mode
s	Laplace operator, $(s=\sigma \pm j\omega)$
S	Lateral-directional spiral mode
SP	Short period longitudinal mode
TV	Thrust vectoring
λ	Eigenvalue
ω_n, ζ_n	Natural frequency and damping ratio with subscript
$\approx$	Approximate
$\equiv$	Defined
[ ]	Square matrix
$\Delta(s)$	Characteristic equation

E. Subscripts

APP	Apparent
APPROX	Approximate
ARI	Aileron rudder-interconnect
B	Body axes
C	Canard
COP	Coupled stability axis system (Ref (5))
DR	Lateral-directional Dutch roll mode
D, DTEF	Differential trailing edge flap deflection
DYN	Dynamic
o	Trim, reference or nominal value
R	Lateral-directional roll mode, Rudder
SEC	Secant
S	Lateral-directional spiral mode
s	Stability axes
TV	Thrust vectoring

Presented at an AGARD Meeting on 'Technologies for Highly Manoeuvrable Aircraft', October 1993.

1. INTRODUCTION

The importance of being able to confidently predict when an aircraft has the potential to depart controlled flight is not only a safety issue, but it is also paramount in maintaining mission effectiveness in the close-in-combat (CIC) environment. The CIC environment today, and in the near future is projected to be characterized by (1) short duration maneuvering, (2) an increased importance placed on the transition between beyond visual range (BVR) and within visual range (WVR) maneuvering, and (3) expansion of the combat arena into the low-speed post-stall flight envelope regime. These three characteristics require more aggressive maneuvering and improved agility in current and future aircraft designs. Improved agility will result in aircraft capable of higher turn rates, increased control of acceleration and deceleration capability, and most importantly, provide nose-pointing capability (although at the potential expense of energy conservation).

The focus on improving high speed performance and flying qualities characteristics has led aircraft designs to have long slender nose shapes with fuselage loaded mass/inertia characteristics, and reduced static stability airframe designs. To address these design characteristics the modern aircraft utilizes a highly augmented flight control system with control-surface control surfaces. Understanding, predicting and designing for departure resistant aircraft (without sacrificing desired levels of maneuverability) has spurred the development of many aircraft departure susceptibility criteria and guidelines that originate with the development of the basic directional weathercock stability derivative C_{n_β}. The four mentioned modern aircraft attributes have prompted the necessity to revisit the application and appropriateness of classical departure parameters and susceptibility criteria to today's complex designs. This paper discusses the major departure resistance criteria specifically focusing on their applications and limitations relative to third and fourth generation fighter class aircraft. In providing guidelines for the analytical determination of aircraft departure susceptibility, the intent is not to endorse one criteria over another, or to reiterate what is recommended in Mil. STD 1797A (reference 1)). Rather an attempt is made to point out the departure susceptibility prediction techniques which are most appropriate at various stages of the design. In this paper, application of the departure parameters will be analyzed using specific examples from the X-31A data base.

2. AIRCRAFT MODEL

To be able to predict and analyze aircraft departure susceptibility and HAOA flying qualities with acceptable accuracy depends primarily on the ability to formulate a valid aerodynamic mathematical model. For the purposes of this paper, it is assumed that the desired HAOA aerodynamic quantities (i.e. C_{m_α}, C_{n_β}, $C_{n_{\dot\beta}}$, $C_{n_{pq}}$, etc.) are accurately measured in a wind tunnel, or computed analytically within a good confidence level. However, for a number of reasons this is not a straight forward task for the HAOA flight regime and the assumption that the aerodynamic data can be accurately determined (either experimentally in a wind tunnel, or analytically using empirical or computational methods) can be presumptuous and lead to false conclusions. For this reason good engineering judgement is called for to conduct sensitivity analyses where appropriate.

Of particular interest to the flight dynamics engineer in terms of predicting an aircraft's tendency to depart from controlled flight, are those flow phenomena that significantly vary with angle of attack, and that can result in asymmetric effects even when the aircraft maintains a zero sideslip attitude. Two significant phenomena of this kind that characterize today's fighter configurations are (1) the formation, asymmetric shedding, and breakdown of forebody vortices, and (2) the formation and asymmetric bursting of wing leading edge vortices. These phenomena become even more complex if an oscillatory motion (i.e. pitch oscillation) is superimposed on the primary steady flight trajectory (reference(2)). These HAOA flow phenomena have large effects on all of the aerodynamic characteristics of the aircraft including of course the static and dynamic aerodynamic stability parameters. The most important of these effects on the dynamic stability parameters are (1) large nonlinear variations of the aerodynamic stability derivatives with angle of attack, sideslip angle, controller deflection(s), and Mach number, (2) large oscillatory intervals in wind tunnel test derived dynamic stability derivative data due to significant variations of the data as a function of frequency and amplitude of the oscillatory rate (i.e. stability axis roll rate), (3) significant aerodynamic cross-coupling between longitudinal degrees of freedom (i.e. C_{m_β}, C_{n_α}) and (4) time-dependent (i.e. those represented by time rate of change of the aerodynamic angles $\dot\alpha$, $\dot\beta$) and hysteresis effects. Note that each of these four effects are strongly configuration dependent. Reference (2) discusses these effects in great length, but for the purposes of this paper the focus will be on the impact these elements have on the methodology required to accurately predict aircraft departure susceptibility.

3. STABILITY AND THE RIGID AIRCRAFT EQUATIONS OF MOTION

An aircraft departure is generally defined to be a divergent large amplitude, uncommanded aircraft motion (i.e. pitch up, nose slice, roll reversal, etc.). This definition can be further refined (see reference (3)) and a distinction can be made between open-loop and closed loop departures. An open-loop departure denotes an aircraft instability with respect to an initial flight condition. That is even if the pilot does not move the controls, small perturbations in the aircraft states build up until the aircraft can no longer be controlled. In a closed loop departure the basic aircraft may or may not be unstable, but the addition of a pilot and/or flight control system (FCS) loop closure creates an unstable vehicle/pilot system. Thus, the closed loop departure has to do with the stability of the aircraft due to pilot/FCS control inputs and loop closures.

Analytically predicting the occurrence of an aircraft departure from controlled flight is invariably based on the assumptions used to formulate the math model (aircraft equations of motion (EOM) including the flight control system as necessary) which describes the response of the aircraft to initial conditions, atmospheric disturbances and system failures (i.e. propulsion, flight control system, etc.)

Like all physical systems, the six degree-of-freedom EOM describing the dynamics of a rigid aircraft are nonlinear and have time varying parameters. The concept of nonlinear system stability is very much different than that of linear systems. For a linear system stability, or the lack of it, is a property of the constant parameter linear system, and stability is determined by the eigenvalues of the system. In addition, the stability of a linear system is unaffected by the initial conditions or the forcing functions. Care must be taken when applying this last statement such that the assumptions inherent to the development of the linear model are not violated.

In contrast, a nonlinear system may be stable for one input or initial condition, and unstable for another. That is, stability for a nonlinear system is generally not a system property, but a property of a particular solution corresponding to a given initial condition of the nonlinear system. There unfortunately exists no convenient method for the determination of the stability of a nonlinear system in general. In most cases this forces attention to be focused on the stability of a nonlinear system in the region of a desired trim solution. The reformulation of the nonlinear math model into a linearized set of equations about a series of defined reference points is an effective and widely used technique to begin to understand the stability characteristics of a nonlinear system. This method is justifiable provided that the magnitudes of the perturbation quantities and the chosen operating point used to define the linear model reproduces the nonlinear system dynamics adequately over a sufficient time span. Each of the models then provides stability information valid for a particular region of the flight envelope and permits analysis using the more insightful simplified linear techniques. However, care must be exercised to avoid extrapolating the results beyond the valid linear region. When the linearizing assumptions are not justified the analysis of the mathematical model must be carried out using one or more of the nonlinear analysis methods (see reference (4)).

The stability or Jacobian [A] matrix formulated from the nonlinear body axis rigid EOM is given in figure (1) and is completely general with the only assumptions being (1) that the aircraft is symmetrical about its xz plane, (2) that attitude (θ), and bank angle (ϕ), perturbations are small (approximately less than 15 degrees), and (3) the $w(\dot{\beta})$ and $w(\Omega)$ dynamic translational rate derivatives ($L_{\dot{w}}$, $N_{\dot{w}}$, L_{Ω}, N_{Ω}, $Y_{\dot{w}}$, $Z_{\dot{w}}$) are zero. From this complete six degree-of-freedom (DOF) matrix representation of the EOM, all of today's linear departure susceptibility criteria, as specified in the Military Flying Qualities specification, MIL-F-1797A, and more recent technical papers (references (5) - (8)), can be derived. To arrive at the analytical relationships of each of the linear departure susceptibility criteria, simplifying assumptions associated with the complete six DOF linear EOM are employed. The motivation, as with many flight dynamic applications, is to reduce the complexity of the problem and provide engineering insight. This is especially important when designing for departure resistance early in the design phase where limited aerodynamic data is available and major configuration layout decisions (including controller size), are being made.

Table I chronologically cites the major departure susceptibility criteria developments including the associated researcher(s), referenced work(s), and the analytical expression(s). It should be noted that some of the departure susceptibility criteria developments shown in Table I are more closely classified as stability parameters as opposed to parameters that have been correlated with aircraft departure susceptibility. Also note that linearization of the nonlinear rigid body EOM is common to the derivation of each. This points to the need to obtain parameters which simplify the problem and allows the designer/analyst engineer to predict, assess, and modify the HAOA aircraft stability design characteristics early in the design phase.

4. DEPARTURE ANALYSIS OF A PRELIMINARY X-31A CONFIGURATION

Using the aerodynamic data base of an early X-31A configuration (references (17)-(20)), the application, advantages, and deficiencies of the major departure susceptibility criteria are discussed (see Table I). The flowchart of figure 2 illustrates the appropriate utility of each of the criteria as a function of the assumed aerodynamic math model.

4.1 X-31A Aircraft Aerodynamics

The X-31A static stability and control derivatives were computed from the nonlinear aerodynamic data base of reference (16) using both a central and forward numerical difference technique (tangent slope linearization method) as given by equation (1).

Central Difference

$$C_{z_x} = \frac{(\Delta C_z)_x|_{x_o+\Delta x} - (\Delta C_z)_x|_{x_o-\Delta x}}{2\Delta x} \qquad \text{EQ(1b)}$$

Forward Difference

$$C_{z_x} = \frac{(\Delta C_z)_x|_{x_o+\Delta x} - (\Delta C_z)_x|_{x_o}}{\Delta x} \qquad \text{EQ(1a)}$$

For purposes of this analysis, the sideslip derivatives, C_{y_β}, C_{n_β}, and C_{ℓ_β} were computed from the nonlinear database using the secant method (defined in reference (12)). The secant method is analogous to the forward difference technique, except that x_o is equal to zero. The differencing interval for each independent variable (i.e., M, α, δ_j, etc.) was chosen to correspond to the smallest interval associated with the nonlinear database. The sideslip stability derivative data (figure 3) were calculated as a function of M, α, and β. The control effectiveness derivatives (figure 4) were calculated as a function of M, α, and δ_j. Taken from reference (18), the dynamic derivative data (figure 5) is shown as a function of α. Throughout the analysis, it was assumed that the canard and leading-edge flap control deflections followed their respective 1-g trim schedules.

Table I Chronology of Major Departure Stability Parameters and Criteria

DATE	DEPARTURE PARAMETER(SY CRITERION	RESEARCHER(S) (REFERENCES)
<1950	Lateral-directional Aerodynamic Static Stability $C_{n_\beta} > 0 ; C_{l_\beta} < 0$	Unknown
	Open-loop, Symmetric, Lateral-directional Static Stability $C_{n_{\beta_{DYN}}} > 0$	Moul & Paulson/NASA, Langley (Ref: (9))
	Closed-loop, Symmetric, Lateral-directional Static Stability LCDP > 0	
1971	Open-loop, Symmetric, Lateral-directional Static Stability $\alpha_\beta > 0$ (equivalent to $C_{n_{\beta_{DYN}}} > 0$)	Jenny/McDonnell Douglas (Ref: (10))
	Closed-loop, Symmetric, Lateral-directional Static Stability $\alpha_\beta > \alpha_S$ (equivalent to LCDP > 0)	
1971	Combined Open/Closed-loop, Symmetric, Lateral -Directional Static Stability Criteria, $C_{n_{\beta_{DYN}}}$ vs. LCDP Criterion Plane	Weissman/Air Force, Wright Lab (Ref. (11))
1976	Revised	Titiriga & Skow/Northrop (Ref. (12)
1980	Revised	Johnston/Systems Technology Inc (Ref (13))
1974	1. Closed-loop, Asymmetric Stability $1/T_{\theta 1} > 0$	Johnston/Systems Technology Inc (Ref (14))
	2. Open-loop Asymmetric Stability Parameters - Aerodynamic, L'_α, N'_α - Kinematic, Z_p, Z_r	
1978	Open-loop, Asymmetric Lateral-Directional Static Stability Coupling Stability Parameters $N_{\beta_{COP}}$, $M_{\alpha_{COP}} > 0$	Kalviste/Northrop (Ref (15)
1980	1. Closed-loop, Symmetric, Lateral-Directional Stability $1/T_{\phi 1} > -0.5$, $1/T_{\phi 2} > 0$	Johnston/Systems Technology Inc. (Ref (13))
	2. Closed-loop, Asymmetric, Lateral-Directional Stability $\omega^2_{\phi_{COP}} \cdot (\omega^{\phi}_{SP_{COP}})^2 > 0$	
1983	Closed-loop, Symmetric Flight (States Only) $C_{n_{\beta_{ATP}}} > 0$	Pelikan/McDonnell Douglas (Ref (16))
1989	Dynamic Stability Parameters, $L_{\beta_{COP}} \cdot M_{\alpha_{COP}} \cdot M_{\dot{\alpha}_{COP}} < 0$ and $N_{\beta_{ACTIVE}} \cdot N_{\beta_{COP}} > 0$	Kalviste/Northrop (Ref (5))
1988/1990	Routh-Hurwitz Dynamic Stability Parameters A, B, C, and AB-C > 0, where: $\lvert\Delta(s)\rvert_{LAT/DIR} = s^3+As^2+Bs+C$	Chody & Skow/Eidetics (Ref (7) & (8)

4.2. HAOA STABILITY PARAMETERS AND DEPARTURE RESISTANCE CRITERIA

4.2.1. $C_{n_{\beta_{DYN}}}$ Stability Parameter

The $Cn\beta_{DYN}$ stability parameter can best be understood and applied as derived from the general aircraft linear, rigid body, EOM (without flight control system augmentation) by considering the stability of the linear, uncoupled lateral/directional dynamics (i.e., β_o=0 ϕ_o=0 degrees, R_o, P_o=0 deg/sec and no aerodynamic cross-coupling or translational rate derivative effects considered). The state-space representation of this linear model using a *body-axis* coordinate system is given in equation (2) (Reference (21))

$$\begin{bmatrix} \dot{v} \\ \dot{p} \\ \dot{r} \\ \dot{\phi} \end{bmatrix} = \begin{bmatrix} Y_v & Y_p + W_o & Y_r - U_o & g\cos\theta_o \\ L'_v & L'_p & N'_r & 0 \\ N'_v & N'_p & N'_r & 0 \\ 0 & 1 & \tan\theta_o & Q_o\tan\theta_o \end{bmatrix} \begin{bmatrix} v \\ p \\ r \\ \phi \end{bmatrix} + \begin{bmatrix} Y_{\delta_D} & Y_{\delta_R} \\ L'_{\delta_D} & L'_{\delta_R} \\ N'_{\delta_D} & N'_{\delta_R} \\ 0 & 0 \end{bmatrix} \begin{bmatrix} \delta_D \\ \delta_R \end{bmatrix} \quad \text{EQ (2)}$$

To test for stability the Routh-Hurwitz Stability Criterion is applied to the characteristic equation of the linear system A matrix given by equation (3)

$$|\lambda I - A| = 0 \text{ , or } A\lambda^4 + B\lambda^3 + C\lambda^2 + D\lambda + E = 0 \qquad \text{EQ (3)}$$

Solving for the coefficients of the characteristic equation (EQ (3)) yields,

$$A = 1$$
$$B = -(Y_v + L'_p + N'_r)$$
$$C = N_v(U_o - Y_r) - L'_v(Y_p + W_o) + L'_p(Y_v + N'_r) + (Y_v N'_r - N'_p L'_r)$$
$$D = N'_r[L'_v(Y'_p + W_o) - Y_v L'_p] + N_v[L'_p(Y_r - U_o) - L'_r(Y_p + W_o)] + N'_p[Y_v L'_r - L'_v(Y_r - U_o)] + g\cos\theta_o(N'_v \tan\theta_o - L'_v)$$
$$E = -g\cos\theta_o[L'_v N'_p \tan\theta_o + N'_v(L'_p \tan\theta_o - L'_r) - L'_v N_r]$$

A dynamic system becomes unstable and divergence will occur when one or more of the roots of the characteristic equation (eigenvalues) becomes positive. According to the Routh-Hurwitz Stability Criterion, the characteristic equation described by the quartic of equation (3) will have positive eigenvalues (RHP poles) if any of the coefficients A, B, C, D, E or if the combination of coefficients $BCD-AD^2-B^2E$ becomes negative. The $Cn\beta_{DYN}$ parameter is specifically derived from the C-coefficient. Rearranging and simplifying the C-coefficient to non-dimensional form, yields,

$$C = C_1 + C_2 + C_3 \qquad \text{EQ (4)}$$

$$C_1 = C'_{\ell_\beta}(\cos\alpha - \frac{\rho Sb}{4m}C_{Y_r}) - C'_{n_\beta}\left(\frac{I_z}{I_x}\right)_\beta(\sin\alpha - \frac{\rho Sb}{4m}C_{Y_p})$$

$$C_2 = \frac{\rho Sb^3}{8I_x}\left[C'_{n_r}C_{Y_r} - C'_{\ell_r}C_{Y_p}\right]$$

$$C_3 = C_{Y_\beta}\left[C'_{n_r} + \left(\frac{I_z}{I_x}\right)_\beta C'_{\ell_p}\right]$$

To arrive at the expression for $Cn\beta_{DYN}$ most often seen in the literature, the terms of equation (4) containing products of derivatives are assumed to be small in magnitude (second order) as compared to the other terms (i.e., thereby omitting terms C_2 and C_3), and the terms $(\rho Sb/4m)C_{Y_r}$ and $(\rho Sb/4m)C_{Y_p}$ are assumed small in the C_1-term relative to $\cos\alpha$ and $\sin\alpha$ respectively. Applying these simplifications, the well known expression for $Cn\beta_{DYN}$ can be derived as given in equation (5).

$$Cn\beta_{DYN} = C'_{n_\beta}\cos\alpha_o - (I_z/I_x)C'_{\ell_\beta}\sin\alpha_o \qquad \text{EQ (5)}$$

In general terms, positive static stability is a necessary property of a linear system if it is to be dynamically stable. In the case of an aircraft, the $Cn\beta_{DYN}$ criteria (>0) defines the minimum requirement for positive open-loop lateral-directional static stability. A minimum value as correlated with departure susceptibility is debatable. Reference (16) suggests $Cn\beta_{DYN} > 0.004$ 1/deg.

In order to better understand the underlying validity of the above simplifications to the C-coefficient, used to derive the $Cn\beta_{DYN}$ parameter expression, X-31A data was used to study lateral-directional static stability based on various forms of the $Cn\beta_{DYN}$ parameter (see table II). The analyses showed that $Cn\beta_{DYN}$, $(Cn\beta_{DYN})_{APPROX}$ and $(Cn\beta_{DYN})_{TOT}$ are essentially equal in value at all the flight conditions analyzed. This can be seen as presented in figure 6(a). Therefore the effects of using the prime derivatives (which include the effects of I_{xz}) and the C_2 and C_3 terms are concluded to be negligible relative to the nominal values of $Cn\beta_{DYN}$ calculated using the classical, simplest form of the equation.

TABLE II Variants of the $Cn\beta_{DYN}$ parameter investigated

PARAMETER	DESCRIPTION
$Cn\beta_{DYN}$	As defined by equation (5)
$(Cn\beta_{DYN})_{APPROX}$	As defined by equation (5) except using the unprimed stability derivatives (i.e., I_{xz}=0).
$(Cn\beta_{DYN})_{SEC}$	As defined by equation (5), except the stability derivatives were calculated using the secant-based technique
$(Cn\beta_{DYN})_{TOT}$	As defined by equation (4). Includes dynamic derivative terms, i.e., C_2 and C_3.

Additionally, comparison of the calculated $(Cn\beta_{DYN})_{SEC}$ shows a very close comparison to $Cn\beta_{DYN}$ over the AOA range investigated (see figure 6(b)). This can be interpreted to mean that the yawing and rolling moment sideslip derivatives for the X-31A are reasonably linear with sideslip angle for $|\beta| \leq 10°$.

From the $Cn\beta_{DYN}$ versus α plot of figure 6(a) it can be concluded that the X-31A configuration overall exhibits stable unaugmented lateral/directional static stability characteristics across its AOA envelope at M=0.2. The data also reveals three areas of interest where reduced levels of lateral/directional static stability may wish to be further investigated with respect to FCS augmentation requirements. These regions are, (1) the low AOA region of -10 to 0 degrees AOA, (2) 15 to 25 degrees AOA , and (3) the 40 to 45 degree AOA ranee. Regions (1) and (2) are areas where the X-31A exhibits its lowest values of $Cn\beta_{DYN}$. In region (3) the data indicates a very large, sudden, negative decrease in $Cn\beta_{DYN}$.

It should be noted that $Cn\beta_{DYN}$ remains positive throughout the AOA range investigated even though the directional stability derivative $Cn\beta$ does become significantly negative at higher AOA. The reason for this is because the $(I_z/I_x)_\beta$ term applies a multiplying factor greater than 11 to the effective dihedral derivative, $C\ell_\beta$. This causes the dihedral effect, which tends to increase with AOA, to dominate the lateral/directional static stability characteristics of the X-31A about the velocity vector which results in improved departure resistance from a static perspective.

As a good approximation, the $C_{n\beta_{DYN}}$ parameter can be related to the Dutch roll natural frequency as given by equation (6).

$$C_{n\beta_{DYN}} \equiv (I_{zB}/\bar{q}Sb)\omega^2_{n_{DR}} \qquad EQ\,(6)$$

The assumption is that $N_{\dot{\beta}}\dot{\beta}$ and $\mathcal{L}_r r$ and the gravity term of equation (2) are negligible with respect to the Dutch roll mode dynamics (see reference (22)).

The $C_{n\beta_{DYN}}$ stability parameter, and its variants, have been successfully applied as an aircraft departure susceptibility parameter with good accuracy on aircraft such as the F-4, F-106B, F-15 (see reference (8)), AV-8B (see reference (23)), and F/A-18, (see reference (16)). Its good correlation with flight test data comes as no surprise in cases where the aircraft departure is due to unstable lateral-directional statics, whereby an aperiodic divergence associated with a negative value of $\omega^2_{n_{DR}}$ as determined primarily by a negative $C_{n\beta_{DYN}}$ value. In these cases, independent of the aircraft dynamic stability characteristics the aircraft will depart controlled flight and/or be very difficult to control because the aircraft is sufficiently statically unstable.

4.2.2. $C_{n\beta_{APP}}$ Stability Parameter

To assess the effectiveness of the use of available yaw and roll control power to augment a bare airframe with unstable static directional stability (as indicated by a negative $C_{n\beta_{DYN}}$ value), or conversely to determine an aircraft's static directional stability degradation due to adverse control effects, Pelikan, (Reference(16)), developed the $C_{n\beta_{APP}}$ parameter given by equation (7).

$$(C_{n\beta})_{APP} = \left[\frac{(\Delta C_n)_\beta + (\Delta C_n)_{CONTROLS}}{\bar{q}}\right]\cos\alpha \qquad EQ\,(7)$$
$$-\left(\frac{I_x}{I_y}\right)_B\left[\frac{(\Delta C_l)_\beta + (\Delta C_l)_{CONTROLS}}{\beta}\right]\sin\alpha$$

(Note, an aircraft is considered to be departure resistance when $(C_{n\beta})_{APP}$ is greater than zero for the sideslip range of interest(reference (16))

In a broad sense, $C_{n\beta_{APP}}$ addresses the relationship between the restoring, or propelling, angular accelerations that result when the aircraft is perturbed in sideslip and the angular accelerations that result from the forcing moments due to control deflections.

By assuming either a sideslip-to-roll-control augmentation control law (as represented by the gain, $K=\delta_{roll}/\beta$) or a sideslip-to-yaw control law structure (as represented by the gain, $K=\delta_{yaw}/\beta$), Equation (7) can be rewritten as given in equation (8).

$$(C_{n\beta})_{APP} = \left[\frac{(\Delta C_n)_\beta}{\beta} + \frac{K(\Delta C_n)_{CONTROLS}}{\beta}\right]\cos\alpha \qquad EQ\,(8)$$
$$-\left(\frac{I_x}{I_z}\right)_B\left[\frac{(\Delta C_l)_\beta}{\beta} + \frac{K(\Delta C_l)_{CONTROLS}}{\beta}\right]\sin\alpha$$

In this form, it can be seen how $C_{n\beta_{APP}}$ can be used to develop preliminary departure resistance control law design structures. Aircraft which exhibit poor lateral-directional departure resistance characteristics can be the result of unstable statics ($C_{n\beta_{DYN}} < 0$), or the adverse effects of the aerodynamic controllers (i.e., generation of large values of adverse or proverse yaw). The $C_{n\beta_{APP}}$ parameter addresses both of these issues and defines a method to assess whether sufficient control power exists to augment $C_{n\beta_{DYN}}$ to desirable levels for departure resistance.

As noted in reference (24) and the original work published by Pelikan (reference (16)), the concept of using the secant method for calculating the stability derivatives rather than using the local tangent value of the slope is an attempt to remove local aerodynamic nonlinearities from the problem. There is no theoretical basis for using the secant linearization method and the results (as Pelikan observed) may not always agree with local stability results obtained using tangent slope derived stability derivatives (i.e., $C_{n\beta_{DYN}}$ vs. $C_{n\beta_{APP}}$ with neutral controls). Though F/A-18 departure correlation was found to be better using the secant based derivative method, it is believed that further validation/correlation with flight test data is needed to support use of the secant slope linearization method that is the basis of the $C_{n\beta_{APP}}$ departure susceptibility parameter.

4.2.3. Routh-Hurwitz Dynamic Stability Criteria

With the advent of improved HAOA aerodynamic designs that provide good static stability characteristics and increased available control power, it no longer suffices to consider departure susceptibility based solely on the information provided by the $C_{n\beta_{DYN}}$ parameter. The fact that an aircraft possesses lateral-directional static stability (i.e., $C_{n\beta_{DYN}} > 0$) does not imply that the aircraft is dynamically stable. In fact, many of today's HAOA capable fighter aircraft exhibit static stability but unstable (or propelling) dynamics due to the dominance of the forebody aerodynamics of these aircraft.

The X-31A aircraft is an example of this fact. It's aerodynamic roll and yaw damping characteristics (C_{l_p} and C_{n_r}) between approximately 20 to 50 degrees AOA are propelling as shown in figure 4. In terms of the X-31A bare airframe unaugmented stability, the propelling yaw and roll damping characteristics manifest themselves in the B-coefficient term of the lateral/directional characteristic equation. By applying the Routh-Hurwitz Stability criteria to the B-coefficient (see equation (9)) the data indicates that the bare airframe is dynamically unstable between approximately 28 and 50 degrees AOA, with the greatest instability occurring at approximately 38 degrees (see figure 7). The B-coefficient term can be shown to be directly related to the aircraft roll mode eigenvalue

$$B = -[C_{n_r} + (I_z/I_x)_s\, C_{l_p}] > 0 \qquad EQ\,(9)$$

Throughout the X-31A preliminary aerodynamic design the interchange of desired bare airframe static characteristics with desired dynamic stability characteristics was apparent during the numerous design testing iterations. The tradeoff between static and dynamic stability characteristics was carefully considered and the decision was made to weigh static characteristics more heavily, and effect desired

dynamic stability through advanced FCS augmentation (i.e., blended thrust vectoring control).

It is interesting to note that if the fundamental method used to improve departure resistance is to modify the flight control laws to increase the unaugmented value of $C_{n_{\beta_{DYN}}}$ to acceptable levels (via either an N_y or β-feedback structure) the results may be less than expected. As pointed by equation (10), this is because the damping of the Dutch roll mode is approximately inversely proportional to the undamped Dutch roll natural frequency (i.e., the square root of $N_{\beta_{DYN}}$), which is directly proportional to the aircraft's lateral/directional static stability (as shown in equation (6)).

$$\zeta_{DR} \cong -\frac{1}{2}\left[N_r / \sqrt{N_{\beta_{DYN}}}\right] \qquad \text{EQ (10)}$$

Thus it will often be necessary to augment the Dutch roll damping characteristics (via either stability axis rates or estimated sideslip rate ($\hat{\beta}$) feedback) concurrently with desired increases in lateral/directional static stability, $C_{n_{\beta_{DYN}}}$. This limitation of the $C_{n_{\beta_{DYN}}}$ and $C_{n_{\beta_{APP}}}$ stability parameters has led to the formulation of departure resistance criteria proposed by Chody and Skow (References (7) and (8)) which address individually each of the Routh-Hurwitz stability coefficients of the lateral-directional characteristic equation quartic.

4.2.4. Lateral Control Departure Parameter (LCDP)

When the conditions are satisfied that permit the longitudinal and lateral/directional EOM to be decoupled, the 3-DOF N_δ^ϕ / Δ transfer function can be represented by equation (11) below.

$$\frac{N_\delta^\phi}{\Delta} = \frac{K_\phi[s^2 + 2\zeta_\phi \omega_{n_\phi} + \omega^2_{n_\phi}]}{(s + 1/T_s)(s + 1/T_R)[s^2 + 2\zeta_{DR}\omega_{n_{DR}} + \omega^2_{n_{DR}}]} \qquad \text{EQ (11)}$$

The LCDP parameter is derived based on determining conditions for which the roll attitude to roll control input transfer function, N_δ^ϕ / Δ, is non-minimum phase (i.e., N_δ^ϕ, contains a zero in the right half plane of the s-plane). The Routh-Hurwitz Stability Criteria is applied to the polynomial of equation (12) to determine when the non-minimum phase condition is satisfied.

$$N_\delta^\phi = A_\phi s^2 + B_\phi s + C_\phi \qquad \text{EQ (12)}$$

The numerator polynomial, N_δ^ϕ, can be determined by taking the determinant of the matrix given by equation (13).

$$N_\delta^\phi = \begin{vmatrix} s - A_{11} & -A_{12} & -A_{13} & 0 \\ -A_{21} & s - A_{22} & -A_{23} & -\ell_\delta \\ -A_{31} & -A_{32} & s - A_{33} & -N_\delta \\ -A_{41} & -A_{42} & -A_{43} & 0 \end{vmatrix} \qquad \text{EQ (13)}$$

A_{nm} = the elements of the decoupled lateral/directional body-axis A-matrix given in EQ(2)

According to the Routh-Hurwitz Stability Criterion, the quadratic polynomial given by N_δ^ϕ is guaranteed to have no RHP zeros if each of the coefficients, A_ϕ, B_ϕ, and C_ϕ, as given in equation (14) have positive values.

Moul and Paulson (reference (9)), found that negative values of the C_ϕ coefficient were associated with lateral/directional departures.

$$A_\phi = 1 + \left(\frac{N'_{\delta_A}}{\ell_{\delta_A}}\right)\tan\theta_o \qquad \text{EQ (14)}$$

$$B_\phi = (N'_p \tan\theta_o - N'_r - Y_v) + \frac{N'_{\delta_A}}{\ell_{\delta_A}}\left[\ell'_r - \tan\theta_o(\ell'_p + Y_v)\right]$$

$$C_\phi = (U_o + W_o \tan\theta_o)\cdot\left[N'_v - \ell'_v\left(\frac{N'_{\delta_A}}{\ell_{\delta_A}}\right)\right]$$

$$+ Y_v\left(N'_r - \ell'_r\left(\frac{N'_{\delta_A}}{\ell_{\delta_A}}\right)\right] - \tan\theta_o\left[N'_p - \ell'_p\left(\frac{N'_{\delta_A}}{\ell_{\delta_A}}\right)\right]$$

In the derivation of LCDP, the condition for C_ϕ, having a positive value was simplified to the expression given in equation (15) by assuming that the Y_v is second order, and simplifying the first term by assuming the use of stability axis (where $U_o = V_T$ $W_o = 0$; and $\theta_o = \gamma_o$ which is assumed to be zero. Also recall $N_\beta = N_v V_T$; $\ell_\beta = \ell_v V_T$) yields,

$$(C_\phi)_s \cong (N'_\beta)_s - (\ell'_\beta)_s\left[\frac{N'_{\delta_A}}{\ell'_{\delta_A}}\right]_s > 0 \qquad \text{EQ (15)}$$

$$\equiv \text{LCDP} > 0$$

In non-dimensional terms equation (15) is expressed as,

$$\text{LCDP} \cong (C'_{n_\beta})_s - (C'_{\ell_\beta})_s\left[\frac{C'_{n_{\delta_A}}}{C'_{\ell_{\delta_A}}}\right]_s > 0 \qquad \text{EQ (16)}$$

As a good approximation, the LCDP parameter can be related to the numerator natural frequency zero, ω_ϕ, as given by equation (17).

$$\text{LCDP} = (I_{z_s} / \bar{q}Sb)\cdot\omega^2_\phi \quad (\text{assumes } \gamma_o = 0^\circ) \qquad \text{EQ (17)}$$

The LCDP departure susceptibility parameter is also applicable to aircraft with an aileron-to-rudder interconnect proportional to bank angle. This expression is given by equation (18).

$$(\text{LCDP})_{\phi\rightarrow\text{ARI}} = (C'_{n_\beta})_s - (C'_{\ell_\beta})_s\left[\frac{C'_{n_{\delta_A}} + KC'_{n_{\delta_R}}}{C'_{\ell_{\delta_A}} + KC'_{\ell_{\delta_R}}}\right] > 0 \qquad \text{EQ (18)}$$

$$\text{Where} \quad K = \frac{\delta_R}{\delta_A}$$

Additionally, Weissman of reference (25) provides an expression for LCDP that addresses systems augmented with aileron proportional to roll attitude plus rudder proportional to sideslip angle. This expression is given by equation (19).

$$(LCDP)_{\substack{\beta\to\delta_R \\ \phi\to\delta_A}} = (C_{n_\beta})_s - (C_{l_p})_s \left[\frac{C_{n_{\delta_A}}}{C_{l_{\delta_A}}}\right]_s \qquad \text{EQ (19)}$$

$$+ K\left[\frac{C_{n_{\delta_A}}}{C_{l_{\delta_A}}} C_{l_{\delta_R}} - C_{n_{\delta_R}}\right]_s > 0$$

$$\text{Where} \quad K = -\frac{\delta_R}{\beta}$$

It should be noted that for highly augmented aircraft the use of any feedback to the rudder and/or yaw thrust vectoring will alter the roll numerator zero, ω_ϕ, and hence the effective LCDP value. This is demonstrated by the modified LCDP expressions given in equations (18) and (19). Provided that all the assumptions used in the development of LCDP are valid for the aircraft being analyzed, the key point is that these dynamic feedbacks are beneficial. Here, beneficial means that the FCS feedforward and feedback control logic effect rudder deflection and/or yaw thrust vectoring to oppose any roll control induced yaw, and thus, tends to make LCDP more positive. Therefore, for highly augmented aircraft the airframe alone LCDP parameter will likely be conservative (reference (26)).

Figure 8 depicts a plot of LCDP versus angle of attack for the X-31A for M=0.2 and neutral controls. The data shows that LCDP drops below -.001 (LCDP = -.001 1/deg corresponds to the region A/B boundary of the Weissman Departure and Spin Susceptibility Criterion, see figure 9) between 38 and 42 degrees AOA. This indicates that the unaugmented X-31A is susceptible to a mild closed-loop rolling departure if the only feedback control structure utilized was roll rate and/or roll attitude feedback to the differential trailing edge flaps (note, a roll attitude/roll rate feedback structure is *not* representative of the actual X-31A control law structure). In addition to the negative values of LCDP, three sharp decreases occur The first drop occurs between 10 and 25 degrees AOA and is attributed to the inverting and decreasing magnitudes of $C_{n\beta}$ and $C_{l\beta}$ thereby decreasing LCDP to near zero. The second drop in LCDP, beginning at approximately 35 degrees AOA, is primarily caused by proverse yaw due to $C_{n\delta_{DTEF}}$ approaching zero and eventually becoming adverse for α>50 degrees as AOA increases. With $C_{n\delta_{DTEF}}$ approximately zero in the 45-55 degree AOA range, LCDP becomes essentially a function of $(C_{n\beta})_s$ which also becomes negative in this AOA range. The third, and final sharp decrease in LCDP occurs at approximately 56 degrees AOA and is caused by the corresponding sharp reduction in $(C_{n\beta})_s$ that also occurs at 56 degrees AOA and continues to 65 degrees AOA. Over the 56-65 degree AOA range the lateral-directional control derivatives and effective dihedral remain essentially constant.

A representative plot of the X-31A LCDP values versus AOA with δ_D = -10 degrees is presented in figure 8(b). A comparison of the LCDP values with the LCDP Weissman Criterion boundaries indicate that all values are greater than -.001 1/deg over the AOA range investigated. The point of presenting this plot is to illustrate the appreciable differences between the LCDP values calculated for the neutral δ_{DTEF} case and the -10 degree deflection case. At least in the case of the X-31A, this points out the sensitivity of the LCDP parameter to the nonlinear characteristics of the δ_{DTEF} roll controller.

4.2.5. Predicting Departure Resistance With Respect To Asymmetric Flight

Both the $C_{n\beta_{DYN}}$ and LCDP Lateral-directional stability parameters, along with all of their variants, are based on decoupling the lateral-directional EOM set from the longitudinal EOM set. In doing this, the effects of longitudinal-lateral/directional dynamic coupling introduced due to aerodynamic coupling, asymmetric flight conditions (β_o and/or $\phi_o \neq 0$), and/or the effects of maneuvering (P_o, Q_o, $R_o \neq 0$, i.e., inertial coupling effects) on aircraft stability are ignored. The root locus plots of figure 10 illustrate the effect of an asymmetric/non zero sideslip condition on the bare airframe dynamics of the X-31A for both a low and HAOA flight condition. Figure 10(a), 10(b) and 10(c) typify the unaugmented $\phi(s)/\delta(s)_{DTEF}$ dynamics at low AOA (M=0.2, α=16.6 degrees) for β=0°/3-DOF model, β=0 °/6-DOF model, and β=5°/6-DOF model respectively. As can be seen by comparing the root loci plots of figures 10(b) and 10(c), the modal shapes associated with the asymmetric flight condition have not changed from the zero sideslip flight condition. However, the magnitude of the Dutch roll dipoles (numerator zero and denominator pole) frequency and damping characteristics clearly have changed. In this case the frequency of both dipoles increased, while the damping decreased.

For the high-AOA flight condition, three root loci plots are presented. Figure 10(d) depicts the HAOA $\phi(s)/\delta(s)_{DTEF}$ dynamics for zero degrees sideslip and assumes the longitudinal and lateral-directional dynamics can be decoupled (i.e., 3-DOF). In Figure 10(e), decoupled longitudinal and lateral-directional dynamics is not assumed (i.e., the 6-DOF root locus is plotted) and in figure 10(f) the bare airframe 6-DOF $\phi(s)/\delta(s)_{DTEF}$ dynamics are calculated assuming 5 degrees of sideslip.

Analysis of the HAOA root loci case reveals three observations relevant to conducting analytical departure resistance predictions. Comparing the zero sideslip 3-DOF (figure 10(d)) and 6-DOF (figure 10(e)) root loci plots, the Dutch roll eigenvalues are essentially unaltered. In contrast, the location of the ω_ϕ dipole has changed significantly. The natural frequency of the ω_ϕ dipole has increased slightly, but the noticeable change is the relatively large increase in the dipoles damping characteristics. These observed Dutch roll modal shape changes are attributed to the aerodynamic cross-coupling terms ℓ_w and N_w which are accounted for when using the 6-DOF math model. Note, for the low-AOA case (comparing figure 10(a) and 10(b)) the ℓ_w and N_w terms are not significant and hence the Dutch roll modal shape remains the same.

Returning to the HAOA case, when non-zero sideslip effects which introduce kinematic lateral/directional-longitudinal coupling are considered (figure 10(f)), it is observed that the Dutch roll mode now becomes unstable due to negative damping (note, $C_{n\beta_{DYN}}$ *remains* stable). Additionally, the

ω_ϕ dipole which was minimum phase (LCDP > 0) with zero sideslip conditions has now become non-minimum phase with a RHF zero at $1/T_{\phi_1} = -0.6$. In the simulation study of reference (13) it was determined that a value of $1/T_{\phi_1} > -0.5$ was indicative of a departure resistant airframe. The authors suggested that $1/T_{\phi_1}$ values greater than -0.5 apparently limit the closed-loop first-order divergence to a rate slow enough for pilots to respond and recover. Conversely, a $1/T_{\phi_1}$ zero location less than 0.5 resulted in divergence rates so fast that the pilots can not prevent departure.

It is important to observe that by the LCDP criteria (3-DOF, β=0°) the X-31A bare airframe is deemed departure resistant. However, by considering the coupling effects introduced by only 5 degrees of sideslip angle, the X-31A bare airframe is actually departure susceptible (Region B of the Weissman Departure Susceptible Criterion Plane) based upon the $1/T_{\phi_1} > -0.5$ criteria. The implication for the X-31A aircraft with regard to departure resistance is the importance that must be placed on maintaining zero sideslip at HAOA via the thrust vectoring control system. Of course, use of the X-31A's active yaw thrust vectoring controller significantly alters and improves the bare airframe root loci plot of figure 10(f) such that departure susceptibility for this flight condition is not predicted. From a departure resistance analysis perspective, these observations point out that to understand the complete HAOA stability and departure characteristics of an aircraft, the effects of dynamic maneuvering and associated asymmetric flight conditions must be considered. Reference (3) more fully discusses the impact of asymmetric flight and dynamic maneuvering as they relate to the aircraft modal characteristics and ultimately HAOA stability, control, and departure.

To assess the effectiveness of the control law design to compensate for longitudinal-lateral/directional cross-coupling and steady maneuvering effects, the $1/T_{\phi_1}$ and $1/T_{\theta_3}$ departure parameters (references (13) and (25) respectively) can be used. These departure parameters are most appropriate due to the fact that they address the fully coupled 6-DOF airframe including the complete FCS augmentation. These parameters, combined with the results of Kalviste's research (reference(5) and (15)), address the factors most relevant to the general departure susceptibility problem.

In *theory*, HAOA departures can now be avoided by implementing a properly designed FCS that utilizes available thrust vectoring control power over and beyond what was traditionally available using conventional aerodynamic controllers. The caveat to this statement, that *sufficient* control power *is available*, and that the FCS is properly designed, *should not* be assumed. Recent flight tests of the X-31A have revealed zero-sideslip yawing moment asymmetries, C_{n_0}, on the order of 0.04. These asymmetries occur at approximately 50° AOA and are explained by the asymmetric shedding of the forebody vortices. Asymmetries of this magnitude were not only not predicted, but were not able to be compensated for, even with the available TV control power, without first reducing the value of C_{n_0} by altering the X-31A forebody aerodynamics. This was accomplished by the addition of a forebody strake, use of forebody gritting, and blunting the forebody nose radius. The caveat that the FCS is properly designed for HAOA flight assumes robustness of the flight control law design to uncertain aerodynamics, sensor errors, and unmodelled dynamics. This assumption is likewise not always valid even when applying the many available multi-variable linear robust control design methodologies since the bounds assigned to these uncertainties are not well defined.

5. CONCLUDING REMARKS

There is typically no one analytical criteria that can be applied to an aircraft design and provide a global analysis of the susceptibility of an aircraft to depart from controlled flight. Not only are there certain analytical criteria that more appropriately apply to some configurations than others, but there is also valuable information to be gained from experimental and piloted simulation methods that can not be obtained using analytical methods due to their inherent assumptions and limitations. Taken from reference (27), table III summarizes one suggested use of the existing departure resistance criteria/stability parameters as they apply in the course of an aircraft design evolution.

$C_{n_{\beta_{DYN}}}$ is a viable departure prediction parameter when an aircraft departure is due to instability in static lateral directional stability because departure is pending independent of the aircraft dynamic directional stability characteristics. Adequate $C_{n_{\beta_{DYN}}}$ characteristics does not by itself provide for dynamic stability. The modern fighter must possess both departure resistance and HAOA maneuverability. Therefore, the effects of unstable (propelling) dynamic derivatives associated with forebody aerodynamics prevalent in the modern fighter must be addressed.

Furthermore, $C_{n_{\beta_{DYN}}}$ and LCDP are departure prediction parameters derived from decoupled, linearized EOM which inherently assume symmetric (β_0, $\phi_0 \neq 0°$), steady-state (P_0, Q_0, R_0 = 0 deg/sec) flight conditions. The near future fighter will conduct controlled aggressive maneuvering up through 90 degrees AOA at any flight attitude. This flight regime is extremely non linear requiring highly augmented flight control systems. Unlike linear systems, nonlinear system stability is effected by the initial conditions and forcing function, and it does not necessarily follow that stability of the developed linear model is also indicative of the non-linear system stability.

Fortunately, *judicious* extraction of linear models at numerous flight conditions spanning the aircraft flight envelope has been shown to produce good correlation between stability of the linear and nonlinear aircraft systems even for highly dynamic trajectories (reference (3)). $C_{n_{\beta_{DYN}}}$ and LCDP are a result of simplifying the lateral-directional characteristic equation coefficient that approximates the aircraft Dutch-roll frequency modal characteristic. The advent of modern computational power facilitates the calculation of the eigenvalues directly associated with the complete airframe/flight control system model. Unlike $C_{n_{\beta_{DYN}}}$ or LCDP, the eigenvalues allow the designer to assess both the static and dynamic stability characteristics of

the aircraft. Therefore, classical HAOA departure analyses should now be augmented using the calculated aircraft eigenvalues to provide valuable information regarding dynamic stability.

Finally, if dynamic stability is to be provided through the use of a highly augmented flight control system, the designer must address the difficult issue of control power and control margin requirements. This is especially true when one considers that the X-31A, F-22, F-18 HARV and future post-stall capable aircraft are not designed to avoid departure susceptible portions of the flight envelope. Rather they are designed for carefree maneuvering in these regions by exploiting new means for generating control power (i.e., thrust vectoring) and improved HAOA aerodynamic design.

Table III Recommended Methodology For Evaluation/Determination of Aircraft Departure Susceptibility

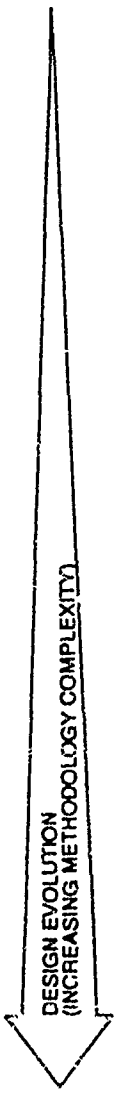

DATA ANALYSIS REQUIREMENTS	APPROPRIATE /RECOMMENDED CRITERIA AND/OR METHODOLOGY
o Aircraft Inertia Data & Static Lateral-Directional Aerodynamic Data	Determine Significance of aerodynamic cross-coupling (i.e., see vector polygon method of reference (13)) a. If Cross-Coupling is significant apply Kalviste's Coupled Stability Criteria b. If cross-coupling is not significant apply STI/Weissman's LCDP versus $C_{n_{\beta_{DYN}}}$ criterion.
o Dynamic Stability Derivative Data	Apply Chody/Skow's criteria to address the possibility of lateral-directional dynamic instability (i.e., due to negative Dutch roll damping or unstable roll mode).
o Evaluate the effects of asymmetric flight	Applicable stability parameters include STI's $1/T_{\theta_3}$ and $1/T_{\phi_1}$ and Kalviste's Coupled Stability Parameters.
o Assess/determine the effects of maneuvering	Kalviste's (1989) Dynamic Stability Parameters address the effects of steady maneuvering flight Likewise, the STI's $1/T_{\theta_3}$ and $1/T_{\phi_1}$ parameters also apply. Additionally, pilot-in-the-loop simulation and experimental tether and drop model testing is highly recommended.
o Assess/determine the effects of the FCS	The closed-loop criteria, $1/T_{\theta_3}$ and $1/T_{\phi_1}$ apply equally well to fully augmented aircraft. The LCDP parameter can be modified to address various FCS loop closures. FCS loop-closure effects can be considered in the Chody and Kalviste (1989) parameters using augmented stability derivatives (i.e., $(L_p)_{AUG} = L_p + K \cdot L_\delta$).
o Assess/determine the impact of uncertain and/or unmodelled aerodynamics.	Experimental tether wind tunnel and drop model testing (NASA, Langley).

6. RECOMMENDATIONS

Because the primary departure susceptibility criteria parameters are based on linearized decoupled EOM, several factors must be considered throughout the design evolution of a given aircraft configuration when addressing departure susceptibility. The following paragraphs outline recommendations for utility of current departure criteria on modern and future aircraft. The rationale for the recommendations not directly addressed in this report are covered in detail by reference (27).

When analyzing departure resistance of the modern combat aircraft, the designer should conduct analysis of both open-and-closed-loop departure susceptibility. As a prerequisite to the analysis, careful measurement and thorough analyses of wind tunnel static aerodynamic data parameters should be conducted. This includes: (1) assessing the effects of Reynolds number during HAOA wind tunnel testing; (2) testing in small increments of α and β to define non-linear aerodynamic data regions; (3) investigating the existence of aerodynamic cross-coupling ($C_{m\beta}$, $C_{l\alpha}$, $C_{n\alpha}$) and zero sideslip asymmetric phenomena (C_{l_0} and C_{n_0}); and (4) influence of control surface deflections on bare-airframe aerodynamic data parameters.

In addition, departure resistance analysis applied to modern designs should include the influence of the aerodynamic dynamic derivatives. Sensitivity analyses of the HAOA aerodynamic characteristics (i.e., $C_{m\beta}$, $C_{l\alpha}$, $C_{n\alpha}$, $C_{l\beta}$, C_{lq}, etc.) should be addressed. Furthermore, the effects of longitudinal-lateral/directional dynamic coupling introduced due to maneuvering flight conditions including, asymmetric flight (β_0, $\phi_0 \neq 0$ degrees) and inertial coupling effects (P_0, Q_0, $R_0 \neq 0$ deg/sec), need to be addressed.

The effects of flight control system augmentation modify the effective bare-airframe aerodynamic characteristics, and thus the effective aircraft departure resistance characteristics. The FCS effects must therefore be addressed when analyzing/predicting aircraft departure resistance. In addition, the effects of system non-linearities should be assessed using man-in-the-loop simulation to address: (1) the effect of the pilot on overall system stability; (2) the effect of control system non-linearities such as position and rate limiters, hysteresis, non-linear dynamic maneuvering effects, and atmospheric disturbances; (3) evaluation of failure states and degraded flight control system modes, and, (4) verification and validation of analysis results using the linear departure susceptibility criteria.

Finally, analytical and pilot simulation results should be supported with available experimental methods including water tunnel tests (for flow visualization), tethered model and drop model testing. The results can then be applied to validate and refine the predicted HAOA and departure susceptibility characteristics of the subject aircraft to provide the best estimate of aircraft departure susceptibility and enhanced maneuverability.

7. REFERENCES

1. Anonymous, "Military Standard Flying Qualities of Piloted Aircraft," MIL-STD-1797A, 30 Jan. 1990.
2. Ruckemann-Orlik, K.J., "Aerodynamic Aspects of Aircraft Dynamics at High Angles of Attack," Journal of Aircraft, Vol. 20, No. 9, September 1983.
3. Stengel, R. F., and P. W. Berry, "Stability and Control of Maneuvering High Performance Aircraft," NASA-CR-2788, April, 1977.
4. Roskam, Jan, "Linear or Nonlinear Analysis Methods: When and How?," AGARD CP-235, 1978.
5. Kalviste, J. and B. Eller, "Coupled Static and Dynamic Stability Parameters", AIAA Paper 89-3362, Atmospheric Flight Mechanics Conference, Boston, Massachusetts, 14-16 August 1989.
6. Chody, J.R., Hodgkinson, J. and A.M. Skow, "Combat Aircraft Control Requirements for Agility," AGARD Paper No. 4, Madrid, Spain, October 2-5, 1989.
7. Chody, J., "High Angle-of-Attack Departure Criteria," Eidetics TR-88-013, 7 October 1988.
8. Skow, A., and W. Porada, "Development of Improved High Angle of Attack Departure Criteria," Eidetics International, Report No. TR-90-010, August 1990.
9. Moul, M. T. and J W. Paulson, "Dynamic Lateral Behavior of High Peerformance Aircraft," NACA RM-L58E16, August, 1958.
10. Hodgkinson, J., "Prediction of Lateral and Directional Divergence at High Angles of Attack," McDonnell Aircraft Co. Report No. EN844, 15 October 1971.
11. Weissman, R., "Criteria For Predicting Spin Susceptibility of Fighter-Type Aircraft," ASD-TR-72-48, June, 1972.
12. Titiriga, A., Jr., Ackerman, J. S., and A. M. Skow, "Design Technology for Departure Resistance of Fighter Aircraft," Stall Spin Problems of Military Aircraft, AGARD Conference Proceedings No 199, June 1976.
13. Johnston, D., Mitchell, D., and T. Myers, "Investigation of High Angle of Attack Maneuvering Limiting Factors, Part I Analysis and Simulation," AFWAL-TR-80-3141, September, 1980.
14. Johnston, D. E., et al., "Investigation of Flying Qalities of Military Aircraft at High Angles of Attack, Volume I- Technical Results," AFFDL-TR-74-61, June 1974.
15. Kalviste, J., "Coupled Static Stability Analysis for Nonlinear Aerodynamics," AIAA Paper 83-2068, AIAA Atmospheric Flight Mechanics Conference, August, 1983.
16. Pelikan, R. J., "F/A-18 High Angle of Attack Departure Resistance Criteria for Control Law Development," AIAA Paper 83-2126, Gatlinburg, TN, 14-17 August, 1983.

17. Hayes, P., Schellenger, H., Sharff, R., and K. Davey, "Lateral-Direction Aerodynamic Dataset for Flight Control Analysis of the X-31A, Revsion A (Vols. I&II)," Rockwell International Report TFD-88-1268L, 10 Feb. 1989.

18. Schellenger, H., "Aerodynamic Damping Dataset for Flight Control Analysis of the X-31A Aircraft," Rockwell International TFD-89-1392L, 8 Sep 1989.

19. Dickes, Edward, "Analysis of Static and Rotational Aerodynamics at High Angles of Attack for Rockwell X-31A Preliminary Configuration," Bihrle Applied Research, Report No. BAR 88-1, January 1988.

20. Goodman, Alex and Ronald Altman (of Tracor Hydronautics), "An Experimental Study to Determine the Subsonic Static and Dynamic Stability Characteristics of a 0.19 Scale Model of the X-31A Aircraft Operating at High Angles of Attack," Rockwell International TFD-88-1493L, 11 May 1987.

21. Henderson, C., Clark, J., and M. Walters, "V/STOL Aerodynamics and Stability & Control Manual," Report No. NADC-80017-60, 15 January 1980.

22. McRuer, D., Ashkenas, I., and G. Dunstan, "Aircraft Dynamics and Automatic Control," Princeton University Press, Princeton, NJ, 1973.

23. Tinger, H. I., "Analysis and Application of Aircraft Departure Prediction Criteria to the AV-8B Harrier II," AIAA Paper 87-2561, 1987.

24. Lutz, F. H., Durham, W. C., and W. P. Mason, "Development of Lateral-Directional Departure Criteria," Final Report for NASA/LRC Project NCC1-158, June 1992.

25. Weissman, R., "Status of Design Criteria for Predicting Departure Characteristics and Spin Susceptibility," Journal of Aircraft, Vol. 12, No. 12, December 1975.

26. Johnston, D. E. and R. K. Hefley, "Investigation of High-AOA Flying Qualities Criteria And Design Guides," AFWAL-TR-81-3108, December, 1981.

27. Seltzer, R. M., "Investigation of Current and Proposed Aircraft Departure Susceptibility Criteria With Application to Future Fighter Aircraft," Report No. NADC-90048-60, 31 May 1990

$$\dot{\bar{x}} = \text{A-MATRIX} \cdot \bar{x}$$

$$\begin{bmatrix} \dot{u} \\ \dot{v} \\ \dot{w} \\ \dot{p} \\ \dot{q} \\ \dot{r} \\ \dot{\psi} \\ \dot{\theta} \\ \dot{\phi} \end{bmatrix} = \begin{bmatrix} X_u & R_0 & X_w - Q_0 & 0 & X_q - w_0 & V_0 & 0 & g\cos\theta_0 & 0 \\ -R_0 & Y_v & P_0 & Y_p + W_0 & 0 & Y_r - U_0 & 0 & -g\sin\phi_0\sin\theta_0 & g\cos\phi_0\cos\theta_0 \\ Z_u + Q_0 & -P_0 & Z_w & -V_0 & Z_q + U_0 & 0 & 0 & -g\cos\phi_0\sin\theta_0 & -g\sin\phi_0\cos\theta_0 \\ 0 & \mathcal{L}'_v & \mathcal{L}'_w & \mathcal{L}_p & \frac{I_z - I_y}{I_x} \cdot R_0 & \mathcal{L}'_r - \frac{Q_0(I_z - I_y)}{I_x} & 0 & 0 & 0 \\ M_u + M_{\dot{w}}\left(Z_u + Q_0\right) & M_v - M_{\dot{w}}P_0 & M_w - M_{\dot{w}}Z_w & -M_{\dot{w}}V_0 + \frac{I_z - I_y}{I_x} \cdot R_0 & M_q + M_{\dot{w}}\left[Z_q + U_0\right] & \frac{I_z - I_y}{I_x} \cdot P_0 & 0 & -M_{\dot{w}}g\cos\phi_0\sin\theta_0 & -M_{\dot{w}}g\sin\phi_0\cos\theta_0 \\ 0 & N'_v & N'_w & N'_p + \frac{I_x - I_y}{I_z} \cdot Q_0 & \frac{I_x - I_y}{I_z} P_0 & N_r & 0 & 0 & 0 \\ 0 & 0 & 0 & 0 & \sin\phi_0\sec\theta_0 & \cos\phi_0\sec\theta_0 & 0 & \begin{matrix} Q_0\sin\phi_0\sec\theta_0\tan\theta_0 \\ + R_0\cos\phi_0\tan\theta_0\sec\theta_0 \end{matrix} & \begin{matrix} Q_0\cos\phi_0\sec\theta_0 \\ - R_0\sin\phi_0\sec\theta_0 \end{matrix} \\ 0 & 0 & 0 & 0 & \cos\phi_0 & \sin\phi_0 & 0 & 0 & \begin{matrix} -R_0\cos\phi_0 \\ -Q_0\sin\phi_0 \end{matrix} \\ 0 & 0 & 0 & 1 & \sin\phi_0\tan\theta_0 & \cos\phi_0\tan\theta_0 & 0 & \begin{matrix} Q_0\sin\phi_0\sec^2\theta_0 \\ +R_0\cos\phi_0\sec^2\theta_0 \end{matrix} & \begin{matrix} Q_0\cos\phi_0\tan\theta_0 \\ -R_0\sin\phi_0\tan\theta_0 \end{matrix} \end{bmatrix} \begin{bmatrix} u \\ v \\ w \\ p \\ q \\ r \\ \psi \\ \theta \\ \phi \end{bmatrix}$$

Figure 1. Six Degree-of-Freedom Linear Bare Airframe Stability (or Jacobian) A-Matrix (Reference (27)

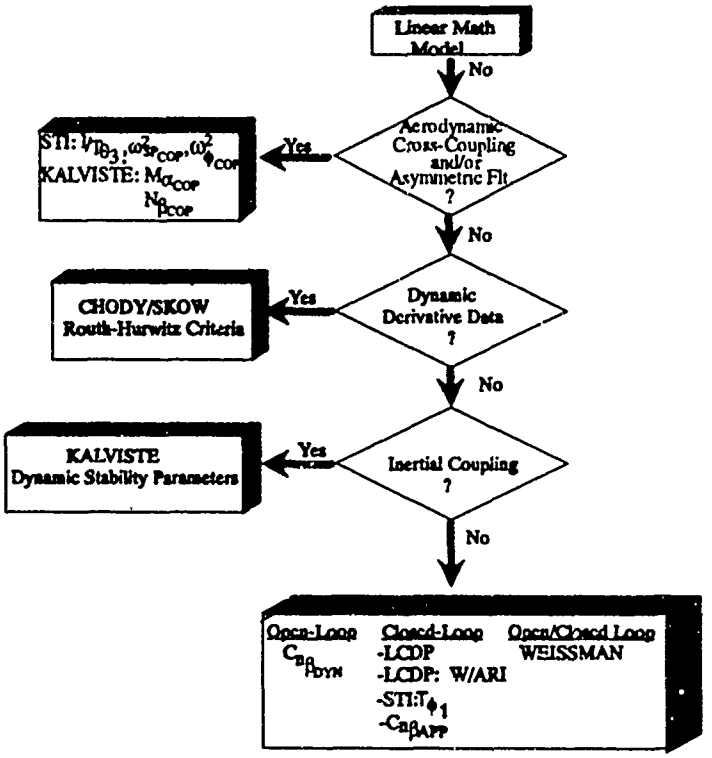

Figure 2. Utility Of Departure Parameters As A Function Of The Aerodynamic Math Model

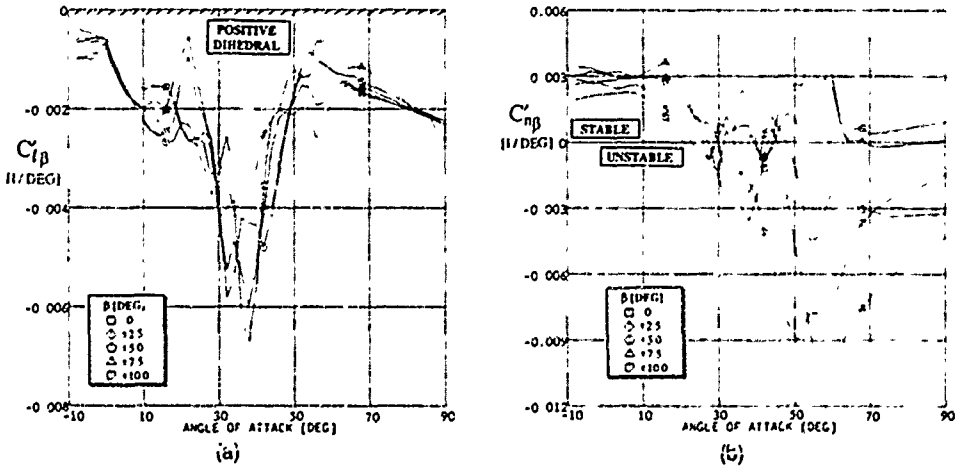

Figure 3. Prsliminary X-31A Lateral-Directional Static Stability Derivative Data (Reference (17))

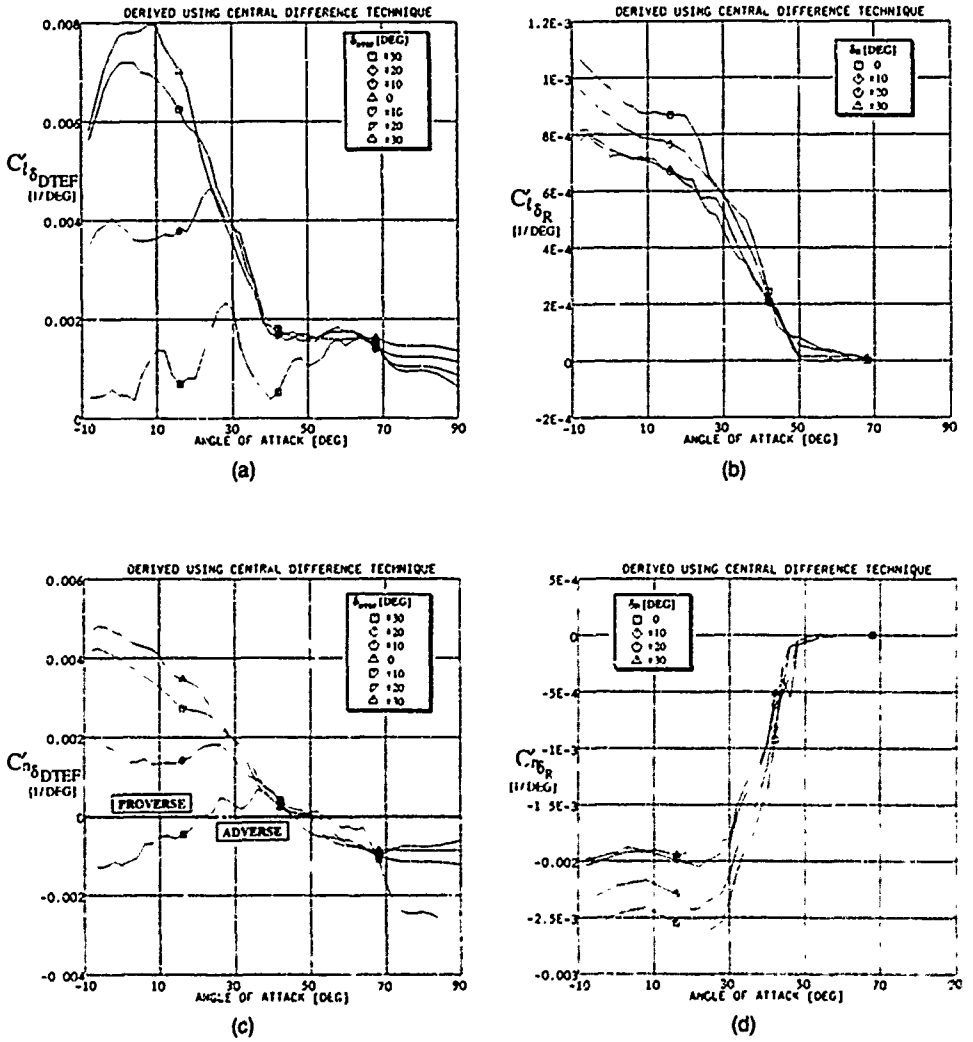

Figure 4. Preliminary X-31A Lateral-Directional Control Derivative Data (Reference (17))

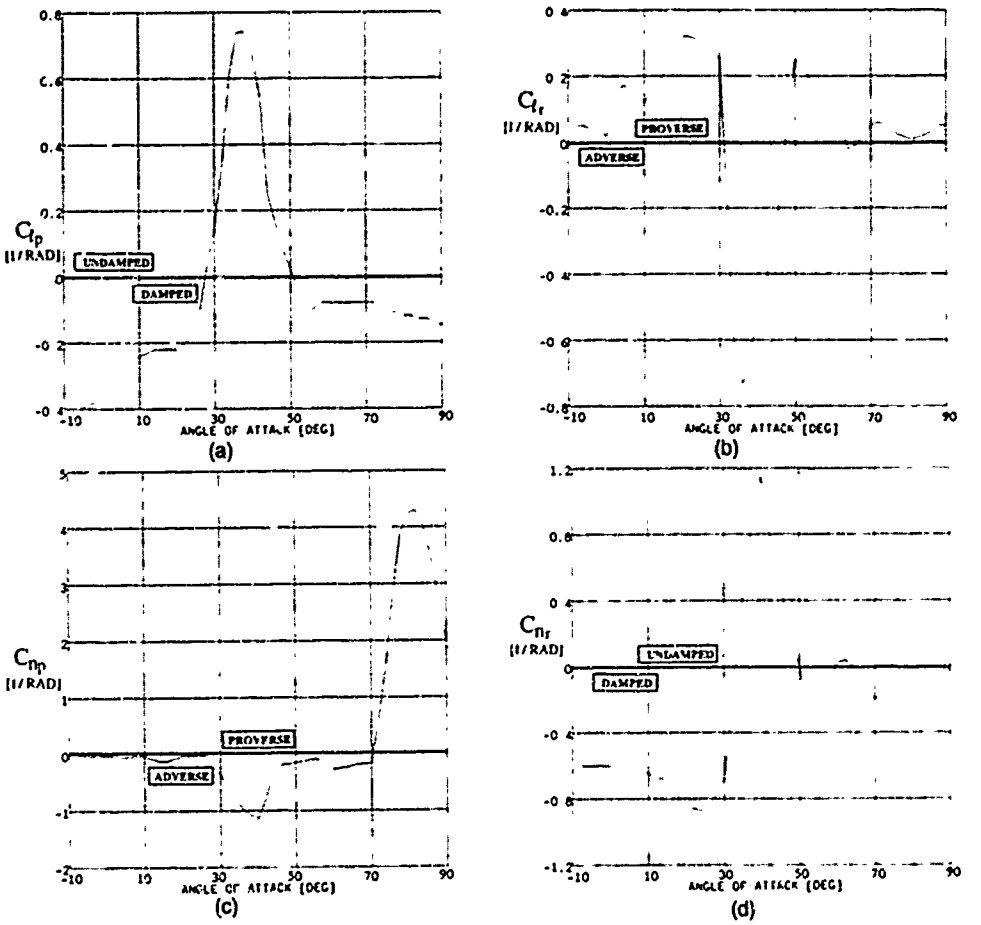

Figure 5. Preliminary X-31A Lateral-Directional Dynamic Stability Derivative Data (Reference (18))

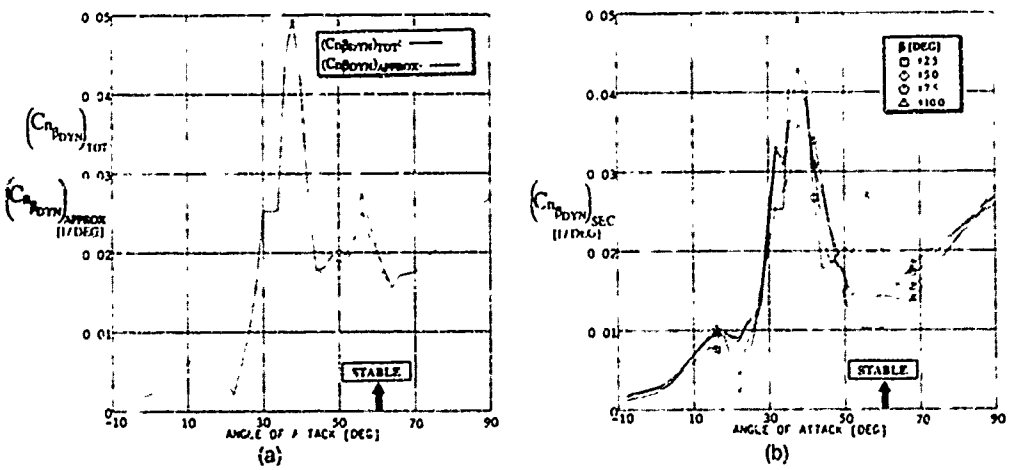

Figure 6. $(Cn_{\beta DYN})_{TOT}$, $(Cn_{\beta DYN})_{APPROX}$ and $(Cn_{\beta DYN})_{SEC}$, Versus Angle of Attack

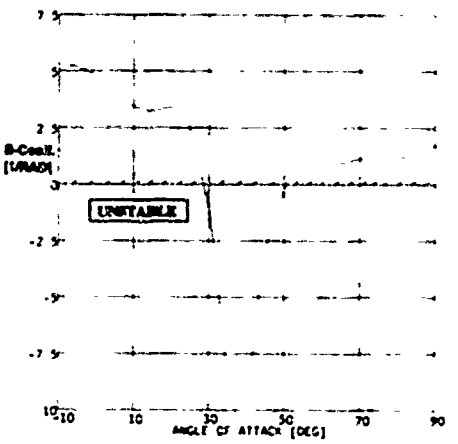

Figure 7. Lateral-Directional Characteristic Equation B-Coefficient Versus Angle of Attack (M = 0.2)

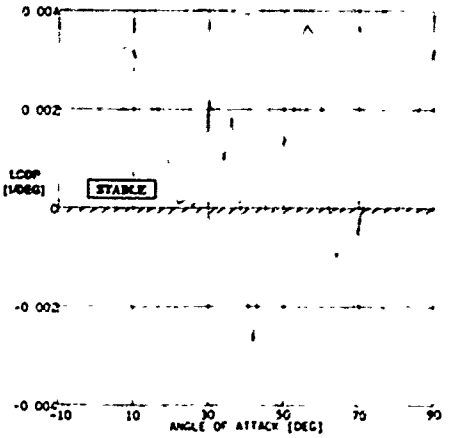

Figure 8(a). LCDP Versus Angle of Attack ($M=0.2/\ \delta_{DTEF} = 0°$)

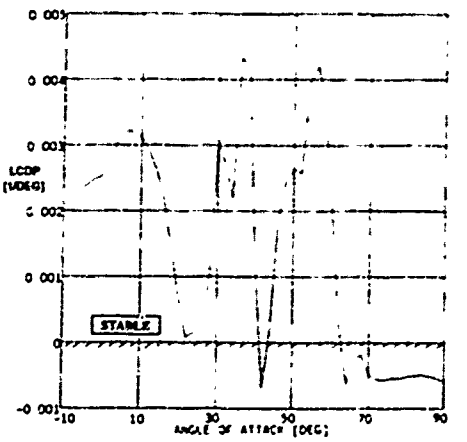

Figure 8(b). LCDP Versus Angle of Attack ($M=0.2/\ \delta_{DTEF} = -10°$)

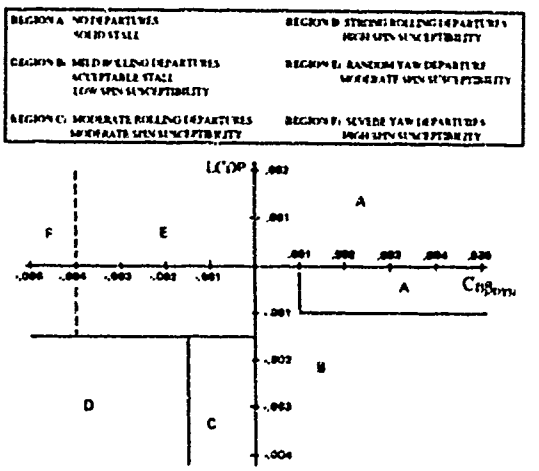

Figure 9. Weissman LCDP Versus $C_{n_{\beta_{DYN}}}$ Departure Susceptibility Plane As Modified By Skow & Titiriga of Reference (26)

LOW-AOA CASE:
UNAUGMENTED ϕ/δ_{DTEF} ROOT LOCI (M=0.19, α=16.6°)

HAOA CASE:
UNAUGMENTED ϕ/δ_{DTEF} ROOT LOCI (M=0.10, α=56.4°)

KEY	
DR	Lateral-Directional Dutch Roll Mode
P	Longitudinal Phugoid Mode
R	Lateral-Directional Roll Mode
RS	Coupled Roll-Spiral Mode
S	Lateral-Directional Spiral Mode
SP	Longitudinal Short Period Mode

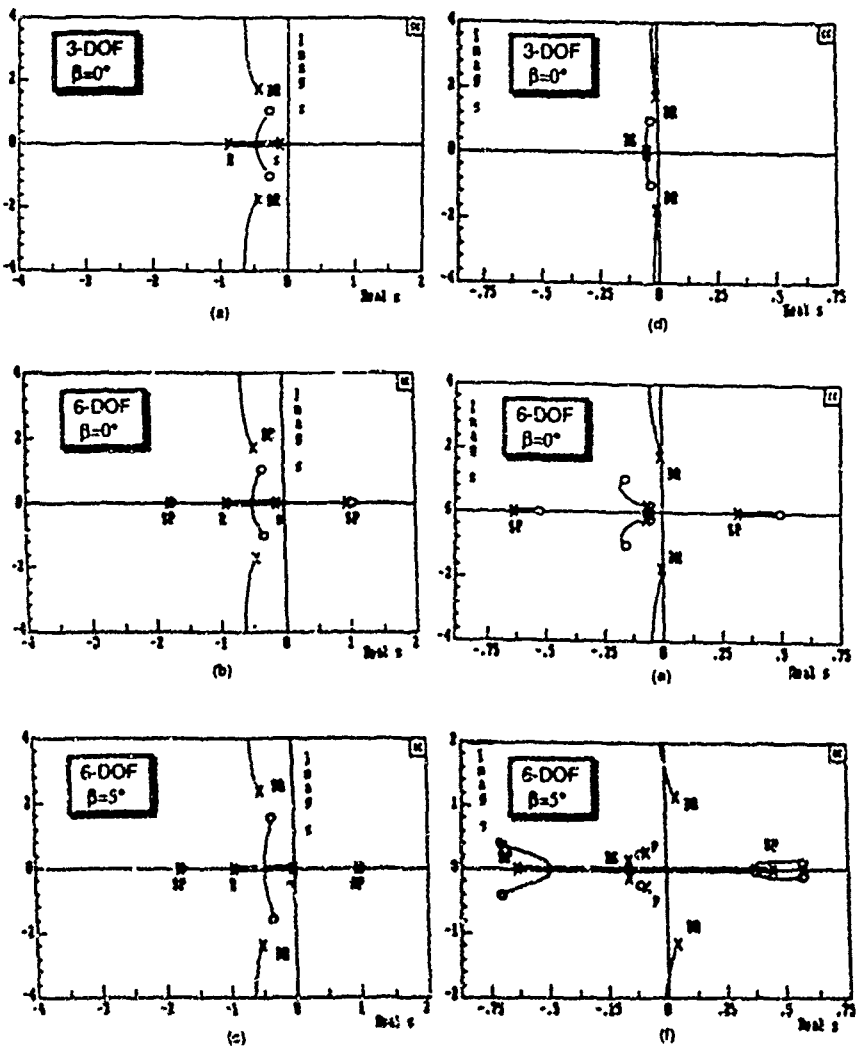

Figure 10. Example Of Unaugmented X-31A Low AOA & HAOA Dynamics And The Effects Of Sideslip

FLYING QUALITIES EVALUATION MANEUVERS

by

Thomas J. Cord and David B. Leggett
Flight Dynamics Directorate
Wright Laboratory
Wright Patterson AFB
Ohio 45433-7531
United States

David J. Wilson, David R. Riley and Kevin D. Citurs
McDonnell Douglas Corporation
P.O. Box 516
St. Louis, Missouri 63166-0516
United States

Abstract

An initial set of aircraft maneuvers has been defined to augment the evaluation methods currently used by the flying qualities and flight test communities. These maneuvers are meant to employ the full range of available aircraft dynamics and to be applied over the full aircraft flight envelope. They include several closed-loop tasks and are the start of a set of demonstration maneuvers (of the type now used in the rotorcraft flying quality specification) for aircraft requirements. A primary goal was to establish a tie between design parameters, aircraft attributes and the operational usage environment while maintaining control of the evaluation process. The approach was to concentrate on aircraft dynamics which occur in daily operations and to create pilot tasks which use those conditions to relate to important aircraft characteristics. Existing evaluation methods concentrate on comparing quantitative data to charts in MIL-Standards which predict flying qualities. The maneuvers discussed here directly measure the ability of the pilot to perform the tasks of interest and at the same time maintain a tie to the design community.

A contract for "Standard Evaluation Maneuvers (STEMS)", was let to McDonnell Douglas Aerospace with subcontracts to Douglas Aircraft, Fighter Command International and Hamilton and Associates, with participation by engineers and pilots from the Naval Air Warfare Center, the Air Force's Flight Test Center, 4950th Test Wing and Wright Laboratory. A maneuver development process based on pilot and engineering experience and ground-based simulation was established. This process was exercised to create an initial set of twenty maneuvers applicable to highly maneuverable aircraft. A flight test plan to investigate in flight the ability of these maneuvers to provide improved evaluation of aircraft flying qualities was also written. If flight test validation of these maneuvers is available before the 1996 revision to MIL-STD 1797, Flying Qualities of Piloted Aircraft, they will be proposed for inclusion in that document.

Introduction

The ideal aircraft-weapon system would not limit the pilot. Maximum angle of attack, load factor, speed, pitch- and roll-rate capability and minimum speed, would all match the pilot's needs and ability to accomplish the mission. The aircraft would respond quickly and precisely to every command. Weapons would be available in any attitude, during any motion. All information would be accurate and presented simply enough to permit the pilot to clearly decide on the correct tactics no matter what the situation. All system failures would be identified and corrected without pilot action. Atmospheric disturbances would be sensed and countered automatically. It is within the realm of technology to solve, individually, these problems.

The ideal pilot would not limit the aircraft-weapon system. He could withstand extreme load factors, would never become disoriented, and would absorb, process and act on all information presented to him. He would never make a tactical mistake. Technology has little influence in this area. Infinite training would, however, minimize pilot-induced limitations.

In an ideal world sufficient time and money would always be available to create the systems and train the pilots in their use.

What we have to work with is of course different. Resources are limited, requirements in the operational and technical disciplines conflict and schedules never permit the perfect solution of any problem. It is in this environment that we must be able to weigh cost versus capability and trade among the different technologies to achieve a system that meets a reasonable set of operational goals.

Two of the items necessary to design and build aircraft to meet those goals are: first, criteria for the various disciplines which correlate aircraft design parameters with operational effectiveness and account for interactions among the technical disciplines; and second, a means to evaluate the product as the design progresses. The effort reported here assumes that a decent set of said criteria exists and concentrates on finding ways to augment evaluation methodology so that the piloted aircraft system can be examined in its full dynamic flight envelope.

Background

Flying qualities is the relationship among the pilot, his vehicle/ weapon system and the mission he is to fly. They are quantified in terms of task performance, pilot workload and loss of control. As such, it is taxed to the extreme by high-performance aircraft since by their nature, the tasks demand the most from both pilot and vehicle. The capability of each technical discipline is expanding and we are seeing more and more conflict among what used to be isolated technologies. As we integrate the increased potential these disciplines offer, evaluations may best be based directly on how well the pilot can use the aircraft to perform the design mission.

Early in an aircraft project, predictions of flying qualities are made based on aircraft and flight control system parameters such as short period frequency, time delay, damping and several criteria which define acceptable boundaries for these parameters. Often, the applicability of these predictions depends on how similar the new configuration and the task of the airplane are to historical data used to generate the regions of goodness. The first real evaluation of flying qualities takes place in a ground-based simulator. This may be continued in flight by using the Total In-Flight Simulator (TIFS), the NT-33 variable stability aircraft, ATTAS, etc. Finally, flight test of the actual vehicle is conducted. In many cases, however, flight test has been more concerned with flight envelope expansion and performance measures than with flying qualities. Often, the parameters used to predict flying qualities are gathered rather than directly assessing how well the pilot can use the aircraft. Several tasks are flown in which the pilot is trying to achieve a

Presented at an AGARD Meeting on 'Technologies for Highly Manoeuvrable Aircraft', October 1993.

particular level of performance; landing, air-to-air refueling, formation flying. In some cases Handling Qualities During Tracking (HQDT) is used to evaluate the essence of air combat tracking capability. But the whole spectrum of how the airplane will be used is not typically studied.

Two important changes in the area of flying qualities are being proposed: 1) placing more emphasis on specific tasks and dynamics that the aircraft will require to perform its mission (task-oriented flying qualities) rather than the current general categories of high-performance, medium-performance, terminal performance, and 2) including direct evaluation of the ability of the pilot to fly tasks similar to those to be flown operationally.

Maneuver Development Process

The maneuver development process is shown schematically in Figure 1. The initial set of maneuvers was defined with the high-angle-of-attack (AOA) flight envelope of a highly maneuverable fighter as the primary application.

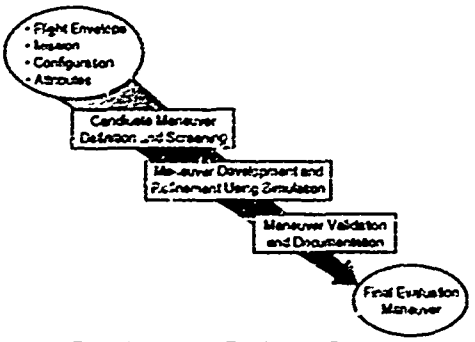

Figure 1 Maneuver Development Process

Maneuver Definition and Screening

A group of engineers and pilots with experience in specification, design, flight test and operational use of flying qualities and agility was assembled. They "brainstormed" a large set of preliminary maneuvers from their individual perspectives. The engineers started with aircraft attributes similar to those shown in Figure 2 and the pilots used operational scenarios like those shown in from Figure 3. The project engineer then gathered these partial descriptions of maneuvers, as documented in Figure 4, and combined them into a series of nearly 200 evaluation maneuvers. A qualitative screening was then performed, with the goal of identifying testable maneuvers which would be related to both the design and the operational communities. This resulted in approximately thirty maneuvers for further consideration.

- Longitudinal Flying Qualities
- Lateral Flying Qualities
- Directional Flying Qualities
- Axial Flying Qualities
- Multi-Axis Flying Qualities
- Pitch Authority
- Roll Authority
- Pitch Control Margin
- Roll Coordination
- Pitch Performance
- Roll Performance
- Turn Performance
- Axial Performance
- Maneuverability
- Energy Maneuverability
- PIO Tendencies
- Departure Resistance
- Frontside/Backside Operation

Figure 2 Current List of Aircraft Attributes

Development and Refinement through Simulation

At this point, the maneuvers were still vague. A simulation

- Guns Tracking
- Shift Targets
- Turn Reversal
- Weapons Acquisition
- Nose Intimidation
- Guns Defense
- Collision Avoidance
- Vertical Lead Turn
- Missile Jink
- SAM Break
- Vertical Reposition
- Vertical Attack
- Attack Abort - Bugout
- Min Time Nose High Reversal
- Aerial Refueling
- Formation Flying
- Precision Landing
- Side-Step Approach & Landing

Figure 3 Example Operational Scenarios

was conducted to establish flight techniques and initial geometries, to assure flyability and repeatability, to generate high quality data and to maintain operational relevance of the dynamic environment used by the maneuver. Performance criteria for Cooper-Harper pilot opinion ratings were also defined.

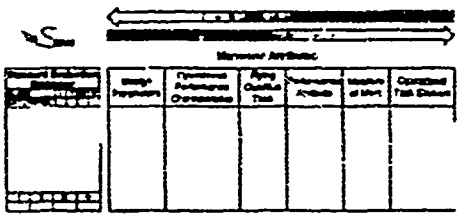

Figure 4 Original Maneuver Description Form

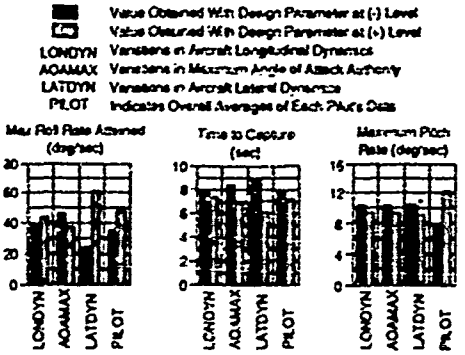

Figure 5 Example Data Analysis for Dual Attack Maneuver

A Design of Experiments (DOE) technique, Reference 2, was used to establish the sensitivity of task performance to aircraft design attributes, varied over a range suggested by experience and Reference 1, and to pilot variability. The goal was to have maneuvers which were sensitive to design parameters and insensitive to pilot variation. An example of the data analysis is shown in Figure 5. For the maneuver to be judged worthwhile, changes in the measure of merit must be larger for different design parameters than for different pilots. Figure 5 then shows that the Dual Attack maneuver would be a good maneuver in that the time to capture measure changes more for LATDYN variation than for pilot variation. Note: the pilot variation shown is for the test pilot and the operational pilot which flew the maneuver in the simulator. Maximum pitch rate would not be a good measure to test with this maneuver, however, since by far the largest change is seen between the two pilots. Maximum roll rate achieved tends to be sensitive to both LATDYN and pilot differences.

Simulation data and pilot commentary on the flight

techniques and flying qualities of each maneuver were then studied and a revised set of maneuvers defined. Potential human factors, such as g-induced loss of consciousness and disorientation were also taken into account.

Maneuver Validation

A final entry into simulation was made to verify that the maneuvers developed could identify characteristics of aircraft other than the model used in the development. This included a test on a transport-class model where appropriate. Limited in-flight validation of the flyability of some maneuvers was also done by the USAF Test Pilot School students in two separate class projects.

Initial Maneuver Set

Most of the maneuvers developed and tested, to date, augment existing, conventional envelope maneuvers such as "Handling Qualities During Tracking." An attempt was made to build upon the agility research conducted in References 3 and 4. The maneuver development process described earlier resulted in the identification of 20 maneuvers. These maneuvers were proven through piloted simulation to be maneuverable as well as provide useful data for the design process. The maneuvers are primarily designed for fighter aircraft in air-to-air combat. Many of the maneuvers were developed to evaluate extended flight envelope capabilities in terms of post-stall/low speed maneuvering because of relatively recent improvements in aircraft capability in this flight regime. A few maneuvers were developed for heart of the envelope operation and for a transport aircraft in order to validate the maneuver development process over a wider range of aircraft classes and flight phases.

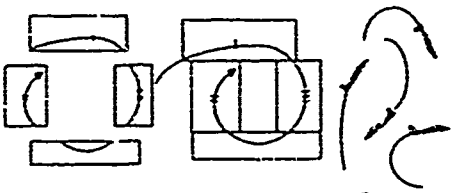

Figure 6 Maneuvers Categories

The maneuvers can be loosely categorized as individual maneuvers, maneuver sequences, or freestyle maneuvers as illustrated in Figure 6. It is difficult, and probably unnecessary, to strictly classify each maneuver as one of these types since some maneuvers contain elements of each. However, these categories are a general indicator of the nature of the maneuver. Individual maneuvers, such as a full stick pitch pull, are the most basic elements of a maneuver and cannot be broken down further. Maneuver sequences are combinations of individual maneuvers. A pop-up ground attack maneuver can be thought of as a maneuver sequence because the pilot pulls to a desired pitch attitude, climbs to a given altitude, rolls inverted, pulls to and captures a target, then rolls back to wings level while tracking the target. Freestyle maneuvers allow the pilot a great deal of freedom because only the start and end conditions are specified. The pilot can use any technique to transition from one state to another.

Individual maneuvers are used to gather quantitative data because they contain less pilot variability. They isolate a single task and tend to be simple and repeatable. Maneuver sequences are more complex to analyze. They are composed of several tasks, each of which often depends upon the outcome of the previous task. As a result, it may be used to see how a configuration transitions between tasks. High quality quantitative data tends to be more difficult to obtain from maneuver sequences because of the added variability. Freestyle maneuvers result in much better qualitative data than quantitative data. The freestyle maneuvers may be best suited for demonstrating unique capabilities of an aircraft and comparing various techniques to perform a maneuver objective.

The STEMS maneuvers allow the evaluation of a range of aircraft characteristics, Figure 7. Some maneuvers isolate a single axis while others are multiple-axis tasks and are useful for evaluating inter-axis harmony. Some maneuvers are more useful for qualitative data gathering, whereas others are much better suited for quantitative analyses. The nature of the maneuvers vary from virtually open-loop tasks to tight, closed-loop tracking tasks. Several design parameters were evaluated for each maneuver. Figure 7 also shows some of the design parameters that were successfully evaluated through qualitative and/or quantitative data. The limited time available did not allow all design parameters to be tested for each maneuver, so the lack of a check mark may simply indicate that testing was not conducted. Each maneuver will be briefly described here; however, Reference. 5 and 6 should be reviewed for complete details.

STEM 1: Tracking During High AOA Sweep

This is a good maneuver to evaluate longitudinal, lateral, and directional precision flying qualities over a wide range of AOA. It has a strong link to operational requirements and is a direct extension of the HQDT technique. It can be used to quickly evaluate tracking over a wide AOA range and identify potential problem areas. If any problems are uncovered, then the High AOA Tracking maneuver (STEM 2) can be used to isolate an AOA for closer investigation. Pilot comments constitute the primary source of data.

The target aircraft starts directly in front of and cospeed with the evaluation aircraft at approximately 350 knots. The target enters a descending constant 4g turn at a sink rate of about 2500 feet per minute. The evaluation aircraft performs a pure pursuit gun track, adjusting power to allow a slow buildup of angle of attack until tracking can no longer be maintained. Two evaluations can be conducted. The first is to evaluate spot tracking capability. This should be done using a fixed 10 mil diameter reticle, noting any changes in flying qualities over the entire angle-of-attack range. The second is to evaluate the ability to make rapid aim point changes on the target. Perform single axis repositioning of the aim point of 50 mils every 5 or 10 degrees angle of attack, acquire and track with a fixed 50 mil reticle.

Two variations are suggested. First, stabilize at 5 degree increments in angle of attack. This allows an extended tracking evaluation as long as the is excess energy. Second, combine tracking and repositioning in to one run. This may not allow sufficient evaluation time depending on both target and test aircraft characteristics.

STEM 2: High AOA Tracking

This maneuver was developed and extensively tested under McDonnell Douglas Aerospace (MDA) and NASA sponsored research, References 7 and 8. This maneuver is designed to isolate the spot tracking and aim point correction characteristics at a specific AOA. It can be used to isolate an axis or evaluate multi-axis capabilities. Specific variations of this maneuver were defined and tested at 30 degrees, 45 degrees, and 60 degrees AOA. Pilot comments and ratings constitute the primary source of data and have been successfully used to develop flying qualities criteria.

Target begins co-speed, co-heading and 1500 feet in front of the evaluation aircraft. Target aggressively rolls and pulls to a constant angle of attack descending turn, adjusting bank angle to maintain a predetermined airspeed. The test aircraft rolls in behind the target and goes to a lag position. The pilot can then pull up into a stabilized tracking solution at the desired angle of attack and evaluate the ability to tightly track a point on the target or reposition the aim point about

Maneuver Number and Name	Env.		Axis			Data		Precision				Type			Design Parameters								
	Conventional	High AOA	Longitudinal	Lateral-Directional	Axial	Quantitative	Qualitative	No Capture	Gross Capture	Moderate	Tight Control	Individual Maneuver	Maneuver Sequence	Freestyle Maneuver	Short Period Freq.	Short Period Damping	Maximum AOA	Lon. Command Type	CG Location	Maximum Roll Rate	Roll Time Constant	Engine Time Constant	Vectoring Rate Limits
1. Tracking During High AOA Sweep		X	X	X			X				X	X			X	X				X	X		
2. High AOA Tracking		X	X	X			X				X	X			X	X				X	X		
3. High AOA Lateral Gross Acquisition		X		X		X	X			X		X	X							X	X		X
4 Dual Attack	X	X	X	X			X			X	X	X	X	X			X						X
5. Rolling Defense		X	X			X		X				X							X	X			
6. Maximum Pitch Pull	X	X	X			X		X				X			X	X	X						
7. Nose-Up Pitch Angle Capture	X	X	X			X	X			X		X	X		X	X							
8. Crossing Target Acq and Tracking	X	X	X	X			X			X	X		X	X	X	X				X	X		
9. Pitch Rate Reserve		X	X			X		X				X			X	X	X						
10 High AOA Longitudinal Gross Acq		X	X			X	X			X		X	X		X	X							X
11. Sharkonhausen	X	X	X	X		X	X			X	X			X			X						
12. High AOA Roll Reversal		X		X		X		X				X	X							X	X		
13 High AOA Roll and Capture		X		X		X	X			X		X	X							X	X		
14. Minimum Speed Full Stick Loop	X	X	X		X		X	X					X										
15. Minimum Time 180° Heading Change	X	X	X	X	X		X		X					X									
16. 1-g Stabilized Pushover		X	X			X		X				X											
17. J-Turn		X	X	X			X		X				X		X			X		X			
18 Tanker Boom Tracking	X		X	X	X		X			X	X	X			X	X				X			
19. Tracking in Power Approach	X		X	X	X		X			X	X	X	X		X	X				X			
20. Offset Approach to Landing	X		X	X	X		X			X	X	X	X		X	X				X		X	

Figure 7 General Characteristics and Design Parameters Evaluated with Initial STEMS Maneuvers

50 mils on the target. Separate evaluations of the longitudinal and lateral axes should be conducted. Throttle changes may be required to keep the test angle of attack. When the angle of attack exceeds the test range, break off and reestablish the tracking solution at the test angle of attack.

STEM 3: High AOA Lateral Gross Acquisition

This maneuver was developed and extensively tested under MDA and NASA sponsored research. It can be used to isolate high AOA lateral acquisition flying qualities at a specific AOA. Specifically, the controllability of the capture and the roll rate achieved can be evaluated. It has been used successfully at 30 degrees, 45 degrees, and 60 degrees AOA under the NASA and MDA efforts. Pilot comments and ratings are the primary data generated from this maneuverand have been used to develop flying qualities criteria. Measure of merit data may also be obtained with this maneuver, though it is primarily intended for flying qualities evaluations.

The target starts approximately 1500 feet in front of and 1000 feet above the evaluation aircraft, rolls and pulls to establish a constant angle of attack descending turn. Bank angle is used to maintain a predetermined speed. When the target rolls, the evaluation pilot hesitates until the target is 10 to 20 degrees off of the nose (depending on test angle of attack and configuration lateral dynamics). At that time, he pulls quickly to the test angle of attack and advances the throttle to the test setting. After obtaining the test angle of attack, the pilot rolls aggressively to capture the target within an 80 mil vertical band or reticle. Initiation of the roll defines the beginning of the measurement portion of the maneuver. Limit evaluation to the lateral axis as much as possible by accepting a pitch bias on the capture.

STEM 4: Dual Attack

This maneuver is an operationally relevant task that exercises rapid multiple-axis acquisitions of two target aircraft. The targets fly straight and level with a 90 degree heading difference and the evaluation aircraft maneuvers between them to alternately acquire each target. The ability to reach high AOA and subsequently control the aircraft is highlighted. In particular, the advantages of good roll performance can be demonstrated. The pilot can evaluate loaded roll capabilities as well as the ability to unload, roll, and pull to each target.

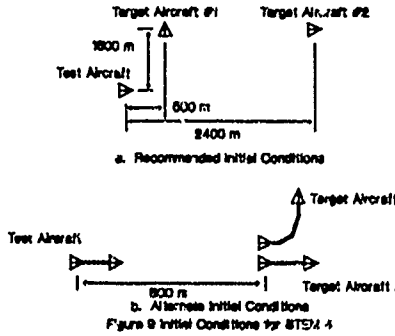

Figure 8 Initial Conditions for STEM 4

The initial geometry, see Figure 8, and aircraft speeds of this maneuver are described in Reference 6 and have several possible variations, depending on test aircraft characteristics. The test aircraft maneuvers to capture target #1 within an 80 mil reticle in minimum time. This solution is held for two seconds, at which time a loaded roll is performed to capture the second target. Again use the 80 mil reticle and hold for two seconds. Two other methods can be used in transition from one target to the other. First, an unloaded roll and pull to the target can be used to emphasize pitch performance to a direct compare to the loaded roll case. Second, a freestyle maneuver may be allowed. The test can continue by switching between targets, each conversion requiring a larger angular transition. In the latter case, the targets must turn

into the test aircraft when not being tracked in order to not have the evaluation pilot lose visual contact with them.

STEM 5: Rolling Defense

This maneuver is primarily intended as a control law evaluation maneuver to verify the nose-down pitch authority available while rolling. Additional information about roll coordination and maximum roll rate may also be obtained. This maneuver yielded good, repeatability numerical data. Some pilot comments were also generated, but the maneuver tended to be very dynamic and somewhat difficult to comment on.

The maneuver is begun above the desired test speed, with a level turn to achieve the test angle of attack. As the speed decays, angle of attack and bank angle for level turn are maintained. When airspeed reaches test conditions, the pilot applies full roll controls (roll over the top) to reverse bank angle while maintaining angle of attack. As the aircraft passes through the opposite 90 degree of bank, apply full forward stick while keeping in full roll controls. (Note, this can be flown with constant longitudinal stick instead of angle of attack. This is easier to fly but introduces some inconsistency in the conditions at pushover.) The maneuver ends as angle of attack goes below 10 degrees. This maneuver should be used at a variety of angles of attack and airspeeds. In particular, the critical inertial coupling and nose down pitching moment conditions should be flown.

STEM 6: Maximum Pitch Pull

This represents a fundamental element of several maneuvers. It isolates an aggressive, open-loop longitudinal input to determine the maximum pitch capabilities of an aircraft. This maneuver generates good quantitative data because it is a very simple, repeatable maneuver that isolates the pitch axis. Some pilot comments can also be obtained but it cannot be used for flying qualities development because it is an open-loop maneuver.

Low speed conditions:

To setup the maneuver, perform a wings level deceleration at a predetermined power setting to the test airspeed. Stabilize flight path angle and set the test power level. The maneuver begins with an aggressive full longitudinal stick pull and any other appropriate pitch up controls. Bank angle should be kept within 5 degrees. Timing of the maneuver begins when the longitudinal stick is employed and ends when the aircraft pitch rate has gone to zero or the pitch angle has passed through the vertical.

It is recommended that a variety of airspeeds and power settings be investigated with this maneuver, especially if thrust vectoring is used by the test configuration.

High speed conditions:

Start above test altitude and below test speed. Dive to test conditions at approximately -15 degrees flight path angle while at the desired power setting. The remainder of the maneuver is the same as the low speed case. Caution, this maneuver has the potential for GLOC (g-induced loss of consciousness) at some flight conditions.

STEM 7: Nose-Up Pitch Angle Capture

This maneuver isolates an aggressive longitudinal capture task. Most of the measures of merit were dominated by pilot variability because of the closed-loop nature of the task. Time to capture was also calculated and was not effective because of the large amount of pilot technique required. However, this maneuver generates useful pilot comments and Cooper-Harper ratings.

The target aircraft in this maneuver flys straight and level at an airspeed slightly below the evaluation aircraft airspeed. The evaluation aircraft setup is the same as the previous STEM. Geometry of the two aircraft is best determined by simulation, with the target aircraft preferred at long range in order to maintain angles during the maneuver. When the target is at the test capture angle, the pilot captures it within an 80 mil horizontal band (or reticle) in minimum time. The capture angle selected should be less than maximum pitch angle available, otherwise the performance limit may mask closed-loop flying quality deficiencies. A display may be used in place of the target aircraft although blurred images due to high rates may preclude this option.

STEM 8: Crossing Target Acquisition and Tracking

This maneuver allows the acquisition and tracking abilities of an aircraft to be exercised through a multiple-axis acquisition of a target aircraft. The ability to pull to moderately high AOA, stop the pitch rate, laterally track a target while unloading in AOA, and then transition to longitudinal tracking are tested.

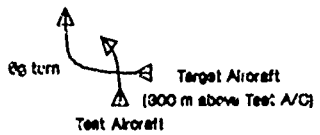

Figure 10 Initial Conditions for STEM 8

The target begins at corner speed with a 90 degree crossing angle, see Figure 10, 1000 feet above the test aircraft. After passing above the test vehicle, the target initiates a 5 to 6 g level turn towards the test aircraft. This turn is continued until the maneuver is complete. The test vehicle begins at 1 g level at minimum velocity. As the target passes overhead, the pilot pulls up and aggressively captures the target. The target should remain within a 30 mil reticle for 2 seconds. Difficulty can be varied by changing the initial altitude difference and target load factor. Increasing the test aircraft speed to corner speed and a point between corner and minimum speed allows a broad range of aircraft characteristics to be evaluated.

STEM 9: Pitch Rate Reserve

This maneuver is intended to demonstrate the reserve pitch authority available from a loaded condition. This maneuver was adapted from the "Angular Reserve" maneuver in Reference 3. Several measures of merit successfully correlated the simulation data indicating the ability to use quantitative data from this maneuver. Some pilot comment data was obtained using this maneuver, but it was limited because of the open-loop nature of the maneuver.

The pilot establishes a level turn at the desired angle of attack and airspeed and selects the test power setting. The pilot then rapidly applies full aft stick and holds that control until the pitch rate drops below the initial value.

STEM 10: High AOA Longitudinal Gross Acquisition

This maneuver is intended to isolate the flying qualities characteristics of an aircraft during a high AOA longitudinal capture task. This maneuver was developed and tested under MDA and NASA sponsored high AOA flying qualities criteria development efforts. This task has been used to develop flying qualities criteria for 30 degrees, 45 degrees, and 60 degrees AOA. A few measures of merit were found to successfully correlate the design parameters; however, this task primarily produces flying qualities comments and ratings.

The evaluation aircraft begins in trail of the target aircraft, approximately at 3000 feet range. The target enters a constant angle of attack descending turn, with control of bank

angle to maintain speed. The evaluation pilot allows the target to attain a predetermined angle off and then rolls into the target's maneuver plane and sets the throttle to test position. The evaluation pilot must hesitate until the lag position is such that the capture will occur at the test angle of attack. This does require some practice. The acquisition should be aggressive and result in a capture within an 80 mil horizontal band. After the capture, the pilot unloads and allows he target to drift to some offset (value controls angle of attack at capture) and repeats, thus allowing several acquisitions from one setup. Target flight path can be steepened to increase evaluation airspeed. Simulator practice appears to be valuable for both initial geometry and target profile definition.

STEM 11: Sharkenhausen

This maneuver allows the acquisition capabilities of an aircraft to be exercised through a multiple-axis acquisition of a target a craft. The ability to pull to moderately high AOA and maintain good lateral control is emphasized. Some measures of merit were found to correlate to design parameter variations; however, the data is very dependent upon initial range. This implies that the task may be limited to simulation use. This maneuver produced qualitative data that can be used as an overall check of the aircraft's ability to rapidly point and track a crossing target.

The task is initiated with a co-speed, head-on target aircraft that is greater than 8000 feet downrange, 5000 feet to the right, and 5000 feet higher than the evaluation aircraft. The target aircraft maintains straight and level flight at constant airspeed. At 8000 feet range, the evaluation pilot attempts to capture the target as rapidly as possible and then track the target. Capture in an 80 mil reticle for 2 seconds was required. The range at which acquisition is begun has a strong influence on the ability to do this task. One measure of merit may be the minimum range at which a tracking solutions can be achieved without resorting to a tail chase. If tracking cannot be obtained in the first pass, it should be called off. It is also recommended that this maneuver be performed over a wide range of initial velocities.

STEM 12: High AOA Roll Reversal

This maneuver allows the investigation of high AOA roll performance in a relatively stabilized flight condition. Roll onset as well as the aircraft response to a large cross-check input can be evaluated. This maneuver was originally suggested in Reference 3 but developed and tested under the STEMS research. Overall, this maneuver was more effective at generating numerical data than pilot comments but some useful comments were obtained.

Setup for this maneuver is accomplished by performing a split-S from above test airspeed and altitude, then pulling to the test AOA. Set thrust as required. The data gathering portion of the maneuver begins after the pitch attitude increases to the point that the velocity vector is pointed directly downward. At that time, the pilot applies a full roll control input and holds it until the heading has changed by a predefined amount An outside reference point approximately 180 degrees away was used in this effort. The pilot then applies full opposite roll control until returning through the initial heading.

This maneuver is designed for post-stall angles of attack and will be difficult to use at lower angles because of a more severe bending of the flight path from vertical before the reversal. The maneuver from Reference 3 is well suited to evaluations at lower angles of attack. The change in heading angle should be sufficient to allow maximum roll rate to develop.

STEM 13: High AOA Roll and Capture

This maneuver is intended to isolate the flying qualities characteristics of an aircraft during a high AOA lateral capture task. The maneuver is initiated the same as STEM 12, but the pilot performs a lateral capture instead of reversing the roll. A heading change of 360 degrees was used here. Since this maneuver is used at high AOA, the pilot actually captures a heading angle through the use of roll control. Currently data is only available for one pilot so final conclusions on the data cannot be made. However, initial indicators for quantitative data look promising and the pilot comments and ratings received from this maneuver appear to be valuable. If the longitudinal flight control system does not command angle of attack directly, it may be best for the pilot to hold pitch attitdue rather than angle of attack in order for him to concentrate on the lateral task.

STEM 14: Minimum Speed Full Stick Loop

This maneuver is intended to define the minimum airspeed required to retain control throughout a loop for a longitudinal stick snatch technique. Information on pitch authority at low speeds in the vertical as well as roll stability information may also be obtained. It does not represent the minimum airspeed at which a loop can be flown using energy-maneuverability principles. It is flown in a iterative, build-up feshion to identify an airspeed band in which the loop cannot be completed. The maneuver is started at a low speed and a maximum pitch pull is performed. The initial speed is successively increased until an 80 degree pitch attitude is attained. The maneuver is then attempted at 100 knots faster than the speed required to reach 80 degree pitch attitude. This start speed is then successively reduced until the minimum pitch rate drops below 5 degrees per second or the lateral control becomes deficient. This maneuver tends to be more of a demonstration and envelope expansion maneuver rather than a design evaluation maneuver.

STEM 15: Minimum Time 180 degree Heading Change

This maneuver is intended to demonstrate the possible options that a pilot has available to change the aircraft heading by 180 degrees. It should include testing of convention methods such as level turns, split-S, and slices as well as new techniques such as a J-Turn. Only the initial and final conditions are specified for this maneuver. This maneuver is not intended for quantitative data except for a rough estimate of time required to change heading. It is primarily useful as an operationally relevant maneuver to demonstrate the various maneuvering options available to the pilot.

STEM 16: 1-g Stabilized Push-over

This maneuver allows a stabilized evaluation of the nose-down pitch authority at high AOA. This maneuver was developed and tested under NASA/USN research, Reference 9. It is included as one of the initial STEMS maneuvers because of its applicability to high AOA and the fact that it is a relatively newly developed maneuver. This maneuver generates very consistent quantitative data because of its simple, repeatable technique. Pilot comments and Pitch Recovery Ratings can also be used from this maneuver.

The pilot establishes a stabilized, wings level high AOA condition by smoothly applying aft stick from level flight to capture a predetermined pitch attitude. He then aggressively applies full forward stick. The pilot continues to hold forward stick until the AOA drops below 10 degrees. Testing should be done at the angle of attack for minimum nose down pitching moment, points where nose down pitching moment is questionable, maximum angle of attack or angle of attack for maximum lift. Various throttle settings should also be tested, especially if thrust vectoring is used. A pitch attitude capture could also be used to finish the maneuver to demonstrate that the motion can be controllably stopped. The maneuver can also be flown from an inverted initial position to check recovery from negative load factors or angles of attack.

STEM 17: J-Turn

This maneuver requires the simultaneous use of high AOA

pitch and roll authority. It serves as a good demonstration maneuver for high AOA maneuverability. This maneuver is intended to emulate the maneuvering requirements of a tactic developed during the Multi-System Integrated Controls (MuSIC) thrust vectoring tactical utility studies, Reference 10. This maneuver also resulted in some pilot comments but seems to be best suited as a maneuver to demonstrate high AOA roll and pitch authority.

From straight and level flight which is aligned with some landmark, the pilot simultaneously applies full pitch and roll control inputs until the aircraft has completed a 180 degree heading change. Then the pilot removes the roll control input and continues to pitch the nose back up to the horizon.

STEM 18: Tanker Boom Tracking

This maneuver is intended to evaluate high gain flying qualities. This is an existing maneuver at the Air Force Flight Test Center but was tested here for further validation and because it may not be a well-recognized evaluation maneuver. The maneuver consists of tracking the refueling probe of a tanker from a predefined range. The evaluation pilot can track a steady probe or the boom operator can move the probe to create tracking errors. This task was more difficult to fly in fixed-base piloted simulation than believed to be in flight. It appeared that PIO tendencies were exaggerated and it was more difficult to control the range to probe. These were attributed to the reduced pilot cues. It is still believed to be a valuable task for flying qualities ratings; however, fixed-base simulation may result in an overly pessimistic evaluation.

STEM 19: Tracking in Power Approach

This maneuver is intended to evaluate the precise tracking capabilities in a landing configuration. It can be performed at a safe altitude before precision landings are attempted. This was an existing maneuver but was tested here for further validation and because it may not be a well-recognized evaluation maneuver. The maneuver consists of tracking a target aircraft from approximately 1500 ft range while in a power approach mode and at approach airspeed. It is valuable to have the target perform a sequence of heading changes to generate a more demanding task. Additional testing and validation of the this maneuver is recommended; however, it appears to be a promising maneuver for flying qualities comments and ratings.

STEM 20: Offset Approach to Landing

This maneuver provides a demanding flying qualities task to test the ability to control flight path and speed while the aircraft is configured for approach. This maneuver has been used extensively to evaluate aircraft approach to landing flying qualities. Aircraft speed control was found inadequate for the model tested during this research and that tended to dominate the pilot comments. Testing was suspended because of the amount of data and testing that has already been conducted in other research. This maneuver is included in STEMS because it has been a valuable evaluation tool in several development programs.

Maneuver Selection Guidelines

Maneuver selection guidelines have been developed to help the user select the most appropriate maneuver to test rather than blindly using all of the maneuvers. The best maneuver to use for an evaluation depends upon the data and information that is being sought. Therefore, a user must first identify the type of aircraft to be evaluated, its intended mission, and the aircraft attributes to be tested. This information can be used in conjunction with a cross reference table, which is provided with the maneuvers, to identify potentially useful maneuvers. The maneuver description sheets and background information can then be further examined to determine the best maneuvers for the specific test objectives. Examples of information that may help identify the most appropriate evaluation maneuver includes the following: type of data generated (qualitative and/or quantitative), operational applications, pilot performance objectives, flight testability, etc. Finally, examples of the maneuvers can be viewed through the use of AGILE-VU, Reference 11, to provide a better appreciation for the maneuver prior to selecting it for testing. Examples of existing maneuvers may be obtained from WL/FIGC.

The maneuver selection guidelines and evaluation maneuvers can be used early in the design process to help identify and correct design deficiencies. Most of these maneuvers can be used throughout the design cycle and into flight test for final flying qualities validation. The overall objective is to provide a more capable operational aircraft by including operationally representative evaluation maneuvers early in the design of an aircraft.

Lessons Learned

Several valuable lessons were learned while evolving and using the maneuver development process. Some of these lessons will be summarized here to improve the quality of new evaluation maneuvers and minimize the time required to develop them.

Use of Piloted Flight Simulation

Piloted flight simulation was found to be an effective tool in the development and evaluation of maneuvers. Different approaches and techniques to fly a maneuver could be tried quickly and eliminated from consideration. Additionally, a quick appreciation could be gained for the type of data generated and the aircraft characteristics evaluated. The maneuver can then be refined to produce better quality data. Other types of simulation, without a human pilot in the loop, may also be useful to develop or screen maneuvers but were not investigated during this research.

Pilot and Engineer Involvement

It is recommended that both pilots and engineers be involved throughout the development of new evaluation maneuvers. There may be some overlap of knowledge, but each tends to have a specialized background that can improve the value of the maneuver. In general, engineers were needed to determine the constraints on the maneuver and the data obtained from the maneuver. The pilots were invaluable in maintaining operationally representative conditions and defining techniques for the maneuvers. Both pilots and engineers had important suggestions to improve the flyability and repeatability of the maneuvers.

Operational and Test Experience

The influence of pilots with operational and test experience is also important because of the desire to link the maneuvers to operational requirements. Pilots with operational experience have a good understanding of how the aircraft will really be used in training and operation, and they have significant experience and knowledge of tactics and techniques. Flight test experience is important to increase the overall quality of the maneuver and data by improving the maneuver setups and execution for better repeatability.

Data Quality Review

It is very important to review the data generated from a maneuver and have an understanding of its sensitivity to design parameter variations. It may be misleading to develop a maneuver with a single set of aircraft dynamics and then use it to evaluate design modifications or other aircraft. The data must be checked to evaluate the amount of pilot variability expected in the data. The pilot variability should then be compared to the changes observed due to design parameter variations to determine which pieces of data can be used in the design process. This data review should be applied to both quantitative and qualitative data.

Observations From DOE Testing

Many of the simulation test matrices used during this research were based on Design of Experiment (DOE) techniques. Fractional factorial matrices were used to minimize the data requirements so that as many maneuvers as possible could be developed. The DOE test techniques worked well for quantitative data, but it was difficult to analyze the qualitative data since multiple design parameters were being varied simultaneously. Also, it can be difficult to efficiently expand testing after an initial data set is taken. Simple test matrices could be augmented to include additional design parameters, but more complex matrices could not be augmented. As a result, it is very valuable to perform a quick, qualitative check of the intended test matrix prior to gathering a complete data set.

Summary and Recommendations

This research resulted in an initial set of 20 standard evaluation maneuvers and the definition of a maneuver development process. These maneuvers are meant to augment current evaluation maneuvers and the maneuver development process is intended to help the creation of additional maneuvers. It is strongly recommended that STEMS be maintained as a "living" document that can be used as a reference guide for evaluation maneuvers. New and existing evaluation maneuvers should be included in STEMS to make it more widely applicable. The vast majority of the initial maneuvers were developed for the evaluation of fighter aircraft, high AOA dynamics. However, the maneuver development process was shown to work for the conventional flight envelope and for other aircraft classes. Finally, continued documentation of the use of the STEMS maneuvers and resulting lessons learned is encouraged because it can provide valuable reference information for future users. Such informations should be sent to Wright Laboratory, Attention: T. Cord at Wright-Patterson Air Force Base.

References

1. Anon., "Military Standard, Flying Qualities of Piloted Vehicles," MIL-STD-1797A, 30 January 1990.

2. Box, G. E., Hunter W. G., and Hunter J. S., Statistics for Experimenters, John Wiley and Sons, New York, NY 1978.

3. Lawless, A.R., and Butts, S.L., "Aircraft Agility Measurement Research and Development," AFFTC-TIM-91-01, June 1991.

4. Butts, S.L., and Purifo[illegible] D., "X-29A High Angle-of-Attack Agility Flight Test Results," AFFTC-TIM-91-02, September 1991.

5. Wilson, D.J., "Aircraft Maneuvers for the Evaluation of Flying Qualities and Agility - Maneuver Descriptions and Selection Guide," WL-TR-93-3082, August 1993.

6. Wilson, D.J., "Aircraft Maneuvers for the Evaluation of Flying Qualities and Agility - Maneuver Development Process and Initial Maneuver Set," WL-TR-93-3081, August 1993.

7. Wilson, D.J., and Riley, D.R., "Flying Qualities Criteria Development Through Manned Simulation for 45 Degrees Angle of Attack - Final Report," NASA CR-4435, April 1992.

8. Wilson, D.J., Riley, D.R., and Citurs, K.D., "Flying Qualities Criteria for 60 Degrees Angle of Attack," NASA report to be published in 1993.

9. Ogburn, M. E., et al, "High-Angle-of-Attack Nose-Down Pitch Control Requirements for Relaxed Static Stability Combat Aircraft", NASA Conference Publication 3149, October 1990.

10. anon., "Multi-System Integrated Control", WRDC-TR-90-6001, June 1990.

11. Boland, J. R., et al., AGILE-VU User's Manual, Naval Air Warfare Center and McDonnell Douglas Aerospace publication, 1992 (available thru NAWC Warminster, Attn: Bob Seltzer).

Study Findings on the Influence of Maneuverability and Agility on Helicopter Handling Qualities

Matthew S. Whalley
Aerospace Engineer
U.S. Army Aeroflightdynamics Directorate
MS 210-7, Ames Research Center
Moffett Field, CA 94035-1000
USA

1. SUMMARY

Three piloted simulation studies were performed by the U.S. Army Aeroflightdynamics Directorate to examine the influence of maneuverability and agility on helicopter handling qualities and to provide an expanded basis for the dynamic response requirements in Aeronautical Design Standard 33C, Handling Qualities Requirements for Military Rotorcraft. The experiments focused on aggressive tasks such as air-to-air combat and target acquisition and tracking. The first experiment focused on yaw agility requirements in the form of attitude quickness and bandwidth. The second experiment focused on pitch and roll agility and maneuverability requirements in the form of bandwidth, angular rate, and attitude quickness. The third experiment focused on maneuverability requirements in the form of normal and longitudinal load factor envelope for both conventional and compound helicopters. Findings from the three studies are presented in the form of Cooper-Harper handling qualities ratings, pilot commentary, and task performance.

2. INTRODUCTION

Maneuverability and agility (M/A) has been a topic of research for many years in both the fixed and rotary wing communities. It is generally agreed that maneuverability is some measure of the maximum achievable time-rate-of-change of the velocity vector and that agility is the measure of the maximum achievable time rate-of-change of the acceleration vector. It is also agreed that good M/A is a key requirement for success in highly dynamic missions such as air-to-air combat. Unfortunately, a precise definition of M/A and a quantification of the amount required has not yet been agreed upon. As an alternative, M/A will be represented here using the existing handling qualities dynamic response criteria from the current Army handling qualities specification, *ADS-33C, Handling Qualities Requirements for Military Rotorcraft* (Ref 1).

ADS-33C is a comprehensive document containing handling qualities requirements for all phases of helicopter operations including air-to-air combat. The intent of the document is to ensure that no limitations on flight safety or on the capability to perform intended missions will result from deficiencies in handling qualities. ADS-33C contains quantitative dynamic response requirements for small, moderate and large amplitude responses. The small amplitude requirements consist of short term response to control inputs requirements and are defined in terms of bandwidth in the frequency domain. The moderate amplitude response requirements are defined in the time domain in terms of the ratio of peak rate response for a given attitude change and is referred to as attitude quickness. The large amplitude response requirements are expressed in terms of peak rate capabilities.

Three piloted simulation experiments were performed to examine the influence of maneuverability and agility on helicopter handling qualities in terms of the specification requirements contained in ADS-33C. The experiments are referred to in this paper as 1) the yaw agility experiment, 2) the pitch and roll maneuverability and agility experiment, and 3) the normal and longitudinal load factor experiments.

2.1 Yaw agility experiment

ADS-33C contains several quantitative requirements pertaining to the response of the yaw axis to control inputs. Of particular interest during this experiment were Sections 3.3.6 and 3.4.7.1; the moderate-amplitude heading changes in hover (attitude quickness) and bandwidth in forward-flight requirements. However, only the attitude quickness results will be discussed in this paper.

The ADS-33C hover and low speed moderate-amplitude heading changes requirement, section 3.3.6, states,

"The ratio of peak yaw rate to change in heading, $r_{pk}/\Delta\Psi_{pk}$, shall exceed the limit specified in [Figure 1]. The required heading changes shall be made as rapidly as possible from one steady heading to another and without significant reversals in the sign of the cockpit control input relative to the trim position."

The attitude quickness requirement applies to attitude changes ranging from 10 to 60 deg. Attitude changes of less then 60 deg. are covered by the bandwidth criteria (see section 2.2), while attitude changes of greater than 60 deg. are covered by a minimum angular rate capability requirement.

The requirement characterizes not only how quickly the pilot can effect a heading change, but also how precisely. This is achieved through the variables used by the requirement. $\Delta\Psi_{pk}$ refers to the maximum heading change associated with establishing a new heading. Using this number has the effect of penalizing any overshoots that occur. $\Delta\Psi_{min}$ refers to the minimum undershoot which occurs during the course of establishing a new heading thereby penalizing undershoots.

Because of the implied impact on design, it was felt necessary to perform a careful investigation to supplement the current basis for the ADS-33C yaw attitude quickness requirement.

Presented at an AGARD Meeting on 'Technologies for Highly Manoeuvrable Aircraft', October 1993.

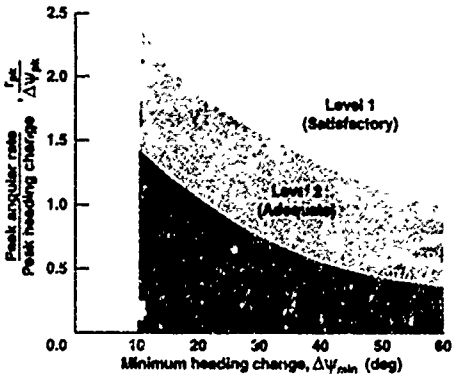

Figure 1. Requirements for moderate-amplitude heading changes – hover and low speed, target acquisition and tracking. (redrawn from ADS-33C)

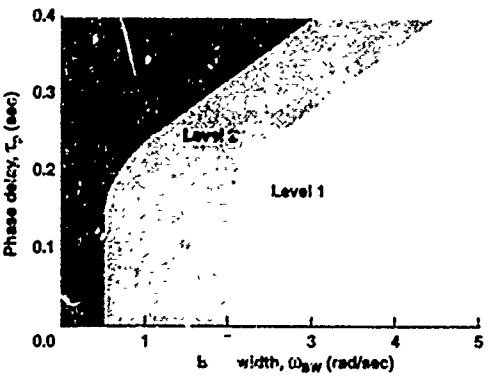

Figure 2. Roll bandwidth requirement (redrawn from ADS-33C)

2.2 Pitch and roll maneuverability and agility experiment

ADS-33C contains requirements for the pitch and roll response. Of particular interest to this experiment were Sections 3.4.5.1, 3.4.5.2, and 3.4.5.3. These sections pertain to the bandwidth, attitude quickness and control power of the pitch and roll axes in forward flight above 45 knots. However, only the roll bandwidth requirement will be discussed in this paper.

The ADS-33C requirement for bandwidth is shown in figure 2. The bandwidth and phase delay parameters are obtained from frequency responses as defined in figure 3. Bandwidth, as defined in the specification, is referenced to the aircraft with all augmentation loops closed, but not with the pilot in the loop. The frequency response data required to measure the bandwidth parameters must include all of the elements of a typical analog or digital flight control system; e.g., anti-aliasing filters, bending mode filters, stick filters, actuators, computational delays, etc. Bandwidth is measured from a frequency response (Bode) plot of angular attitude response to cockpit controller force. As shown in figure 3, two bandwidth frequencies are measured: the frequency for 6 dB of gain margin ($\omega_{BW_{gain}}$), and the frequency for 45 degrees of phase margin ($\omega_{BW_{phase}}$). This describes the margin above the (augmented) vehicle's response in which the pilot can double his gain or add a time delay or phase lag without causing an instability. The phase delay parameter characterizes the shape of the phase curve beyond the bandwidth frequency.

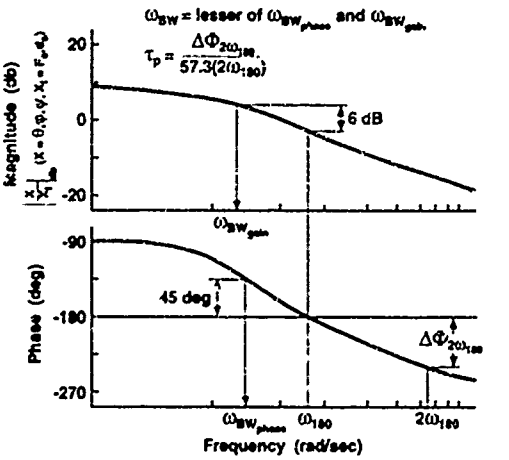

Figure 3. Bandwidth definition.

2.3 Normal and longitudinal load factor/maneuverability experiment

To change the magnitude and direction of the velocity vector one has to apply a force. Obviously, then, the major contributor to good maneuverability is the ability to generate normal, longitudinal, and lateral load factor. In a conventional helicopter, acceleration is generated by changing the magnitude and direction of the main rotor thrust. In a compound helicopter, acceleration is generated by using a combination of the magnitude and the direction of the main rotor thrust and the magnitude of the auxiliary thrust.

Maneuverability was examined in the context of these facts during this experiment. Namely, the effects that variations in the load factor envelope have on handling qualities and mission performance for some representative "aggressive" tasks were investigated. By taking this approach, it was expected that a set of data would be generated from which information regarding the relationship between maneuverability, mission performance, and handling qualities could be obtained.

3. DESCRIPTIONS OF THE THREE EXPERIMENTS

All three investigations were conducted using the NASA Ames Research Center Vertical Motion Simulator (VMS) (fig. 4, ref. 2). The VMS is unique among flight simulators in its large range of motion (table 1). This large motion capability provides cues to the pilot that are critical to the study of handling qualities. The cockpit was configured as a single pilot cockpit with a three window computer generated imagery (CGI) display. Conventional helicopter controllers were used. A head-up display (HUD) provided the pilot with critical aircraft state and targeting information.

A stability derivative helicopter math model termed the Enhanced Stability Derivative Model (ESD) was used as the ownship. The ESD model is a derivative of the TMAN model developed for the Helicopter Air Combat simulation experiments (refs. 3-5). Earlier versions of the ESD model have been used for other handling qualities experiments (refs. 6 and 7).

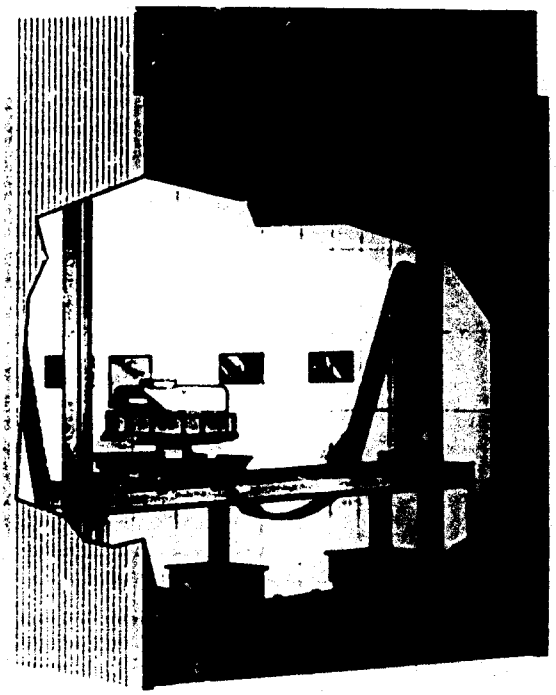

Figure 4. NASA Ames Vertical Motion Simulator.

Table 1. Vertical Motion Simulator motion limits.

	Displ. (ft)	Rate (ft/sec)	Accel. (ft/sec2)
Long.	±4	±4	±10
Lat.	±20	±8	±16
Vert.	±30	±16	±24
	(deg)	(deg/sec)	(deg/sec2)
Pitch	±18	±40	±115
Roll	±18	±40	±115
Yaw	±24	±46	±115

The ESD model is a simple, non-linear, generic helicopter math model intended for use as a handling qualities research tool. It includes the effect of load factor on the pitch and roll rate damping derivatives, the effect of forward speed on the force derivatives, a collective trim curve, and a ground effect model. The attitude response is rate-type in pitch, roll, and yaw with automatic turn coordination above fifty knots. The model does not include control or response coupling.

Both the pitch and roll maneuverability and agility and the normal and longitudinal load factor/maneuverability experiments contained air-to-air tasks which used an automated air-to-air adversary termed the AUTOmated MANeuvering (AUTOMAN) opponent (Refs. 8, 9). AUTOMAN was developed by Grumman Corporation under contract to the U.S. Army Aeroflightdynamics Directorate.

Four types of data were collected during these experiments. Real time variables of interest such as position, attitude, and rates were recorded continuously. Performance measures such as time on target were recorded and printed out at the end of each run. Qualitative pilot opinion was gathered for each configuration in the form of commentary and a Cooper-Harper rating (CHR) (ref. 10).

To minimize the effects of training, each pilot was given several hours to practice the tasks. During this time, task performance was communicated to the pilot at the end of each run. Data were not collected until both the pilot and the investigators were convinced that the pilot had achieved the necessary skill level. After a minimum of three representative runs were recorded, the pilot would give commentary and assign a CHR.

3.1 Yaw agility experiment

3.1.1 Experimental variables

There were two experimental variables used during the yaw agility experiment: yaw damping, N_r, and yaw actuator rate limit, $\delta_{p_{lim}}$. N_r ranged from -0.5 to -4.0 sec^{-1} and $\delta_{p_{lim}}$ ranged from 50 percent/sec to unlimited. The effect of yaw actuator rate limit is shown in figure 5. The yaw control effectiveness, N_{δ_p}, was adjusted for each configuration such that a maximum yaw rate of 60 deg/sec was attainable in hover regardless of the amount of yaw damping.

3.1.2 Tasks

Three tasks were flown during the experiment – the target acquisition in hover task, the 180 degree turn in hover task, and the target tracking in forward flight task. However, only the target acquisition in hover task will be discussed in this paper. The target acquisition in hover task was designed to evaluate the location of the existing attitude quickness boundaries. Figure 6 illustrates the task setup. The helicopter was initialized in a 10 foot hover with no target present. When the pilot indicated he was ready, a target was made to appear which would be at some angular offset from the helicopter heading. Upon seeing the target, the pilot would yaw the aircraft to acquire and hold the target within ±1 deg of the boresight for two seconds. A solid tone in the headset would indicate to the pilot when he had the target within ±1 deg of his boresight reticule. After the pilot had held the target within the required pointing constraints for two sec, the headset tone would switch from solid to intermittent at which point the pilot would squeeze the trigger to "shoot" the target. The target would then immediately disappear and reappear at a new location. The task of acquiring the target was then repeated using a different target location. This

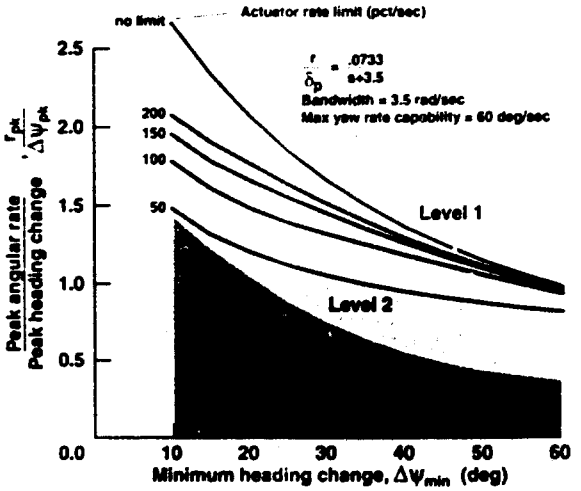

Figure 5. Effect of actuator rate limit on attitude quickness

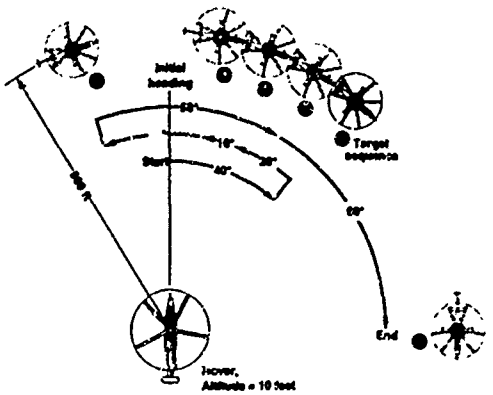

Figure 6. Target acquisition in hover task.

process would continue until six targets had been acquired. The targets were positioned such that one heading change each of 10, 20, 30, 40, 50, and 60 deg would be required. The sequence and direction of the heading changes were ordered randomly. The pilot was required to maintain his horizontal position within 25 feet of his starting point throughout the task.

The performance standards for this task were based on the quickness and precision with which the yaw maneuvers were performed. Desired performance required that all six targets be acquired within 35 seconds with no more than 3 overshoots of the ±1 deg acquisition zone. Adequate performance required that all six targets be acquired within 40 sec with no more than 6 overshoots. The performance standards were established early in the simulation by having several pilots perform the task very aggressively using a "good" configuration and then measuring their performance. Using performance standards that had been established this way led to the desired effect of driving each pilots' aggressiveness to a consistently high level.

3.1.3 Experiment results

This section contains a discussion of the qualitative and quantitative data gathered for the target acquisition task. Data are presented in the form of task performance measures, CHRs, and pilot commentary. The data shown are a summary of the data gathered from all six pilots who participated.

An effort has been made to determine the level of confidence in the data. The range within which the true mean will occur with a ninety percent probability has been calculated using the *t* test (ref. 11). This confidence interval is indicated using error bars on the task performance plots and CHRs summary plots. Stated more simply, the true mean of the entire pilot population has a ninety percent chance of occurring within the range indicated by the error bars. This information is useful in that it reflects both the sample size and variation of the data collected.

Figure 7 contains a summary of the CHRs, the total time to acquire all six targets, and the number of acquisition overshoots which occurred. The symbols indicate the location of the mean and the error bars indicate the 90 percent confidence interval. The numbers adjacent to the mean indicate the number of data points collected for that configuration. For this task, 208 runs were performed and 57 CHRs were assigned. The dashed lines on the CHR plots indicate the boundaries between Level 1

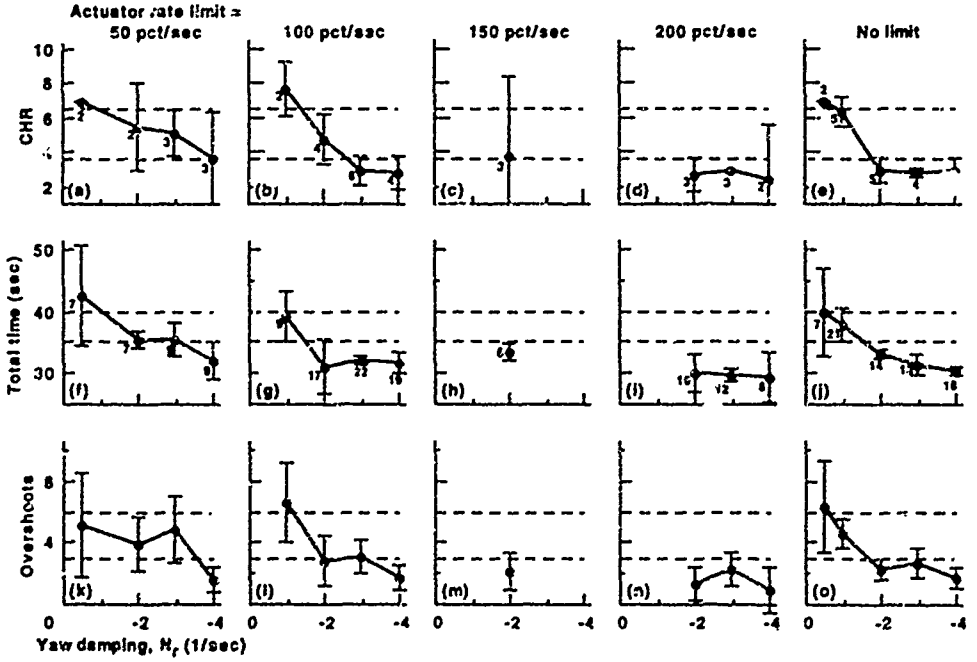

Figure 7 Target acquisition in hover results. (a-e) Cooper Harper ratings; (f-j) time to acquire all six targets, (k-o) number of overshoots.

(satisfactory), Level 2 (adequate), and Level 3 (unsatisfactory) handling qualities. The dashed lines on the total-time plots indicate the desired and adequate performance standards of 35 and 40 sec. The dashed lines on the overshoot plots indicate the desired and adequate performance standards of 3 and 6 overshoots.

In general, it can be seen that there is a good correlation between the task performance and the CHRs. This does not imply that the pilots relied merely on the performance standards in assigning CHRs. On the contrary, it is clear from the pilot commentary that the pilots were primarily assessing their overall workload. For example, for a decidedly Level 3 configuration (actuator rate limit = 50 percent/sec, N_r = -0.5 sec^{-1}) pilot B states:

"[This configuration is] characterized by sluggish response – sluggish response on the initial target acquisition phase and oscillatory and unpredictable response in the target tracking phase. Very unpredictable response in the termination of the target tracking... It has nonlinear characteristics in that respect as well as the sluggish response. And the result is that the requirement for the pilot to exercise a lot of lead and the principal result is the inability to make even adequate performance standards..." (CHR 7)

A Level 2 configuration (actuator rate limit = 50 percent/sec, N_r = -3.0 sec^{-1}) received the following commentary from pilot B.

"The configuration was characterized by good initial response, very snappy initial response which leads you to believe it is going to be a good configuration until you try to arrest the initial acquisition phase which results in lack of precision and overshoot of the desired arresting point. And in addition the target tracking phase is oscillatory. ...The deficiencies are more than annoying because they really do demand a very specific control strategy and a fair amount of forethought, to accomplish the task. So the deficiencies are moderately objectionable. The demands on the pilot involve at least moderate compensation.." (CHR 5)

Finally, a Level 1 configuration (actuator rate limit = 100 percent/sec, N_r = -4.0 sec^{-1}) receives the following assessment from pilot C,

"That configuration was clearly optimal, that is, it was very easy to fly. ...was good for target acquisition and it was good for fine tracking. In one or two cases where the pipper was going off it was easy to stop it and bring it back to center... crisp and easy to accelerate to maximum yaw rate..." (CHR 2)

It can be seen in figure 7 that yaw damping, N_r, had a stronger influence on handling qualities than did actuator rate limit. CHR results ranged from Level 1 to Level 3 for the range of yaw damping examined, regardless of the actuator rate limit. In contrast, the actuator rate limit increased the CHRs only slightly for the 100 percent/sec case and more for the 50 percent/sec case. The actuator rate limit was not investigated at values lower than 50 percent/sec because it was felt that this value was already less than would practically exist in any production aircraft.

Figure 8 shows an interpretation of the CHR data which suggests a location for the attitude quickness Level 1 and Level 2 boundaries for an assumed idealized control input shape. The results suggest that the existing ADS-33C yaw attitude quickness boundaries might be relaxed without sacrificing satisfactory handling qualities.

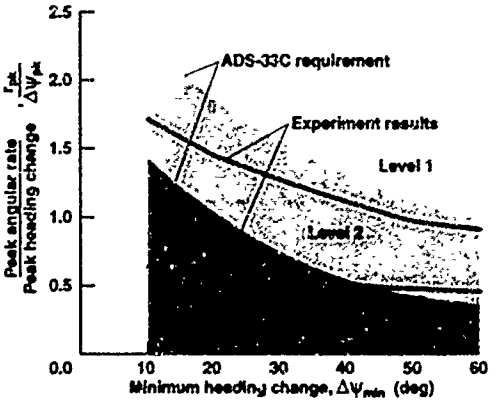

Figure 8. Target acquisition in hover attitude quickness results.

3.2. Pitch and roll maneuverability and agility experiment

3.2.1 Experimental variables

To limit the size of the configuration matrix, a baseline configuration was established for the pitch and roll maneuverability and agility experiment from which each of the experimental variables was varied individually. The baseline configuration and experimental variable ranges were established iteratively based on pilot commentary gathered during the initial phases of the experiment. Table 2 gives a summary of the range of configurations that were examined during this experiment.

The bandwidth was varied via the pitch and roll damping derivatives and ranged from 0.5 rad/sec to 5.0 rad/sec. The maximum pitch and roll rate were varied via the control sensitivity derivatives and ranged from 30 deg/sec to 120 deg/sec. The attitude quickness was varied via an actuator rate limiter that ranged from 10 percent/sec to unlimited.

The baseline configuration had a pitch bandwidth of 3 rad/sec, a roll bandwidth of 4 rad/sec, a maximum pitch rate capability of 60 deg/sec, a maximum roll rate capability of 100 deg/sec, and unlimited actuator rate limit in both the pitch and roll axes.

Table 2. Experimental variables.

	Baseline	Variation
Pitch Bandwidth (rad/sec)	3	0.5–5.0
Roll bandwidth (rad/sec)	4	0.5-5.0
Max pitch rate (deg/sec)	60	30–120
Max roll rate (deg/sec)	100	30–120
Pitch actuator rate limit (pct/sec)	No limit	10–50
Roll actuator rate limit (pct/sec)	No limit	30–120

3.2.2 Tasks

Two tasks were flown during the experiment: the abeam task and the mountain task. The objective of both tasks was the same – to track the AUTOMAN for as long as possible using the ownship boresight reticule. In addition, the pilot was required to maintain less than 0.1 g lateral acceleration, one ball width, while tracking. Pilots were encouraged to maintain airspeed above forty-five knots. Each run was limited to 25 seconds. Only the abeam task will be described in this paper.

The initial conditions for the abeam task are shown in figure 9. The target was positioned 2000 feet in front of, and 100 feet be

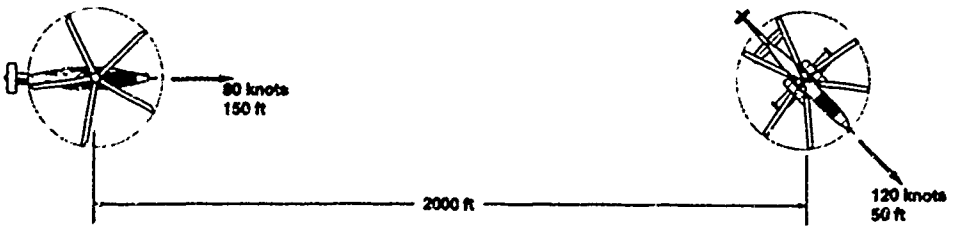

Figure 9. Abeam air-to-air task initial conditions.

low the ownship with a heading 135 degrees away to the left or right. The ownship was initialized at its maximum maneuvering speed, 80 knots, while the target was initialized at 120 knots. Line-of-sight existed for both aircraft over hilly terrain. The initial target heading was randomly set to either the left or the right before each run to introduce some variability to the task.

Task performance standards were based on the longest continuous tracking period measured during the run. Tracking time accumulated whenever the AUTOMAN cg was within 30 feet of a vector defined by the ownship boresight (azimuth and elevation less than $\tan^{-1}(30/\text{range})$), and the ownship lateral acceleration was less than 0.1 g. Performance for the longest tracking period was categorized as unsatisfactory (less than 1.5 seconds), adequate (greater than or equal to 1.5 and less than 3.0 seconds), or desired (greater than or equal to 3.0 seconds). These levels were established during early fixed-base operation to ensure a baseline level of aggression among the pilots. Task performance was indicated to the pilot via audio tones in the headset.

3.2.3 Experiment results

Because of the large volume of data gathered, the only experimental variable discussed in detail is roll bandwidth. Also, only the data from the abeam task are shown because of the similarity of the results of the two tasks. Results are presented in the form of task performance, CHR's, and pilot commentary. The data shown are a summary of the data gathered from all four pilots who participated.

Figure 10 shows a summary of the CHR data plotted versus roll bandwidth for both tasks. Figure 11 shows a summary of the task performance plotted versus roll bandwidth for the abeam task.

The CHR's indicate that a minimum bandwidth of approximately 1.0 rad/sec is required for Level 2 handling qualities. Pilot commentary supports this observation. The comments for the 0.5 rad/sec bandwidth case refer primarily to maintaining control of the aircraft while the comments for the 1.0 rad/sec case refer to the configurations ability to meet task performance requirements.

The roll bandwidth required for Level 1 is not as obvious. The mean CHR is best at 3.5 rad/sec, but only borderline Level 1/Level 2. Examination of the individual ratings reveal, however, that eight Level 1 ratings were given with all but one of them occurring above 3.5 rad/sec. Considering these facts, the best estimate is that a minimum bandwidth of 3.5 rad/sec is required for Level 1 handling qualities.

The task performance data shown for the abeam task in figure 11 is representative of both tasks. The performance data show dramatic improvement out to 3.0 rad/sec and then level off. Both the total time on target and the maximum

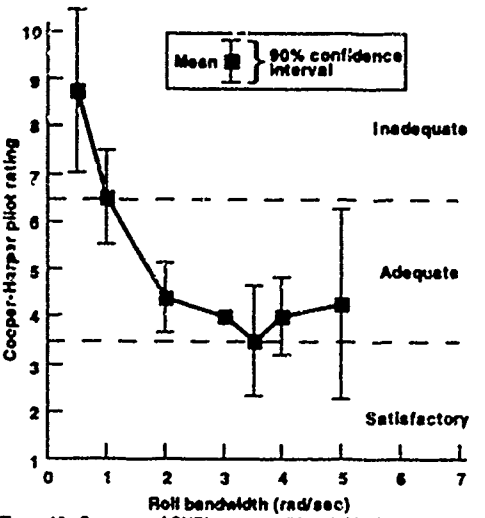

Figure 10. Summary of CHR's versus roll bandwidth for all pilots for both tasks.

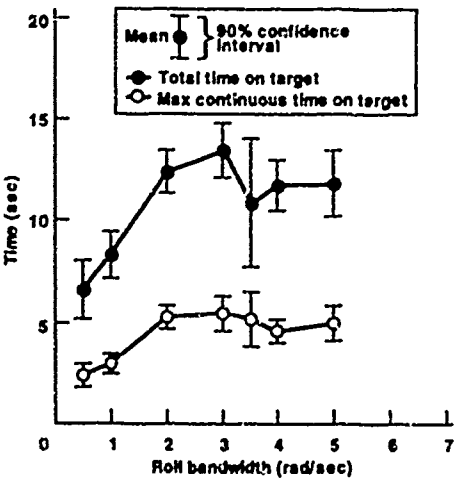

Figure 11. Summary of tracking performance versus roll bandwidth for all pilots for the abeam task.

continuous time on target show the same trend. These results correlate well with the pilot opinion data.

The current ADS-33C requirement calls for a roll bandwidth of 2.0 rad/sec for Level 2 and 3.5 rad/sec for Level 1. The data presented here indicate that the Level 2 requirement could be reduced. Good agreement with the Level 1 requirement was found.

3.3 Normal and longitudinal load factor/maneuverability experiment

An auxiliary thruster with a selectable force or u_{body}-command system was added for the normal and longitudinal load factor/maneuverability experiment. The math model assumed axial flow through a 10 ft diameter propeller and included the effects of both power and stall limitations. The total power available was shared between the main rotor and the propeller.

Four inceptors for the control of the auxiliary thruster were examined during the early stages of the simulation (fig. 12). The four were: 1) a thumbwheel on the cyclic grip that contained a center detent but no spring gradient; 2) a thumb joystick on top of the cyclic grip; 3) a twist grip on the collective that contained only friction; and 4) a beep switch on the collective head. The thumbwheel and the collective twist grip were used as either direct X-force-command or u_{body}-command. The collective beep switch and the cyclic thumb joystick were used as either X-force-rate-command or u_{body}-rate-command. This resulted in the eight auxiliary thruster control possibilities shown in table 3.

Table 3. Auxiliary thruster control inceptor/response types.

Inceptor	Response Type
cyclic thumb joystick	force rate
cyclic thumb joystick	u_{body} rate
cyclic thumbwheel	force
cyclic thumbwheel	u_{body}
collective beep switch	force rate
collective beep switch	u_{body} rate
collective twist grip	force
collective twist grip	u_{body}

3.3.1 *Experimental variables*

Normal and longitudinal load factor envelope were varied during this experiment. Table 4 shows the configuration test matrix. Maximum continuous normal load factor capability was varied from 1.5 to 5.0 g (at 80 kt). Maximum longitudinal load factor capability was varied only for the thrust augmented cases and was varied from 0.1 to 1.0 auxiliary thrust/weight ratio. The transient load factor limit was set equal to 1.33 times the maximum continuous load factor capability at 80 kt.

3.3.2 *Tasks*

Three tasks were flown during the experiment — the abeam air-to-air task, the mountain air-to-air task, and the return-to-cover task. The abeam and mountain tasks were the same as in the pitch and roll maneuverability and agility experiment.

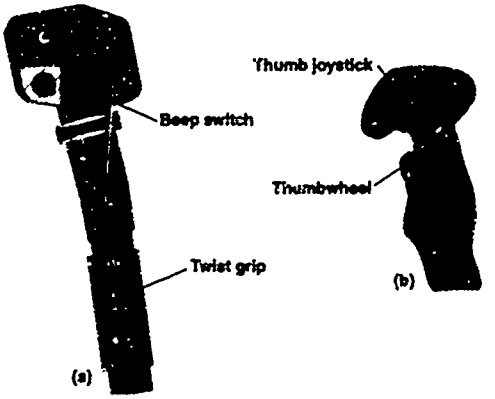

Figure 12. Location of auxiliary thrust control inceptors. (a) collective grip; (b) cyclic grip

Table 4. Configuration test matrix

N_z (g)[a]	Auxiliary thrust/weight					
	0	0.1	0.2	0.33[b]	0.6	1.0
1.5	AMM_2R			AM		
1.75	AMR			AM		
2.0	AMM_2R	A		AM		
2.5	AMR			AM		
3.0	AMR	AM	AM	AMR	AMR	AR
3.5	AMM_2	M	M	AM		
4.0	AMR			AM	AM	
5.0	AMR			AM		

A - Aberm air-to-air task

M - Mountain air-to-air task

M_2 - Mountain air-to-air task, low capability adversary

R - Return-to-cover task

[a] Maximum continuous capability at 80 knots.

[b] This level of thrust/weight represents the average value of several compound helicopters surveyed

3.3.3 Experiment results

This section contains a discussion of the results of adding longitudinal force control by means of an auxiliary thruster. The results from variations in load factor capability and auxiliary thrust level are presented in the form of task performance, CHRs, and pilot commentary. The data shown are a summary of the data gathered for all four pilots who participated unless otherwise noted.

The eight different auxiliary thruster inceptor/control response types were examined to determine the best candidate for the remainder of the experiment. The mean CHRs and some sample pilot commentary from the abeam air-to-air task for each of the eight different combinations are shown in table 5.

Generally, the pilots preferred the u-body command systems over the force-command systems. This was because the force command systems required the pilot to monitor the quantity and duration of force that was applied in order to achieve the desired airspeed or closure rate. This required adding the auxiliary thrust displayed on the HUD into the instrument scan and trying to estimate the amount of auxiliary thrust required for the desired response. The u-body command systems maintained the set airspeed automatically.

Of the inceptors examined, the cyclic joystick was preferred for its location, orientation, force characteristics, and the ability to make incremental inputs. The cyclic thumbwheel was found to be too sensitive. The collective beep switch, although found to be satisfactory, was generally not preferred because of its "all or nothing" input type. The collective twist grip was found to have poor force/displacement characteristics; the forces were ratchety and it lacked a discernible detent.

It is interesting to note though that one pilot favored the collective beep switch because of its location on the left side. He said he felt that the auxiliary thruster was a "power-type" control and should therefore be grouped with the collective.

The cyclic joystick with the u_{body}-rate command system was used to generate the rest of the data presented in this section.

Figure 13 shows the CHRs and task performance results for the air-to-air tasks with and without the auxiliary thruster. Figure 13(a) shows the mean CHRs from both the abeam task and the mountain task.

Figure 13(b) shows the task performance results. The data shown for the auxiliary thruster were for a thruster which had a maximum thrust/weight capability of 0.33.

The results indicate a significant improvement in both handling qualities and task performance when the auxiliary thruster was added. In general, there was 1.0 to 1.5 CHR improvement with the auxiliary thruster. The CHRs also indicate that the pilots were satisfied with an approximately 3.0 g configuration with the auxiliary thruster as compared to a 3.5 to 4.0 g configuration without the auxiliary thruster.

Table 5. Sample pilot commentary and mean CHRs for auxiliary thrust inceptors.

Inceptor (see figure 12)	Command system: force rate	Command system: u_{body} rate
cyclic thumb joystick	*"I had to work at it a lot more to maintain the airspeed control... I was the integrator in the process of trying to establish the new airspeed"* **mean CHR = 5.5**	2.9
collective beep switch	*"Again it is more work load because you select some power, you take your finger off, and to actually get to the speed that you wanted you have to deselect the power. That is twice as much as you are doing before."* 4.8	*"I didn't particularly like all or nothing on the switch. It was difficult to get an incremental change in there. And I think that is a benefit with having it up on the [cyclic joystick]; to be able to get that incremental change."* 3.5
cyclic thumbwheel	force	u_{body}
	"Once you are in a dynamic situation, and you are trying to slow down and speed up, it is too sensitive..., in that it is all too easy to select full aft or full forward and get the full thrust which then decreases your speed too quickly or increases your speed too quickly, making it very difficult to control." 5.8	*"It is actually nice to have a reference, an idea of what speed you have set with this the X-force controller, but this, at the moment is too sensitive."* 5.8
collective twist grip	*"I don't like the throttle arrangement, it is much too stiff, there is uncertainty about it's position and what the neutral position is"* *"This throttle is all screwed up."* 6.0	*"I never knew where I was in the position and it was even difficult to find the trim position... the way this is reacting now, I would say that it is almost unusable."* 5.5

Note: Maximum N_z capability = 3.0, auxiliary thrust/weight = 0.33

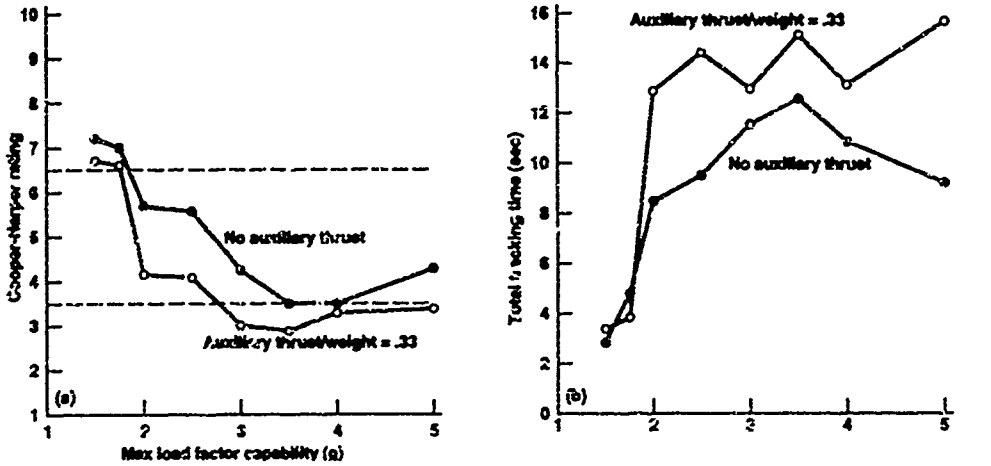

Figure 13. Air-to-air task results with and without auxiliary thrust. (a) mean CHRs for both tasks; (b) task performance results.

The pilot commentary indicates that the improved speed control that the auxiliary thruster afforded was a major factor in the improved CHRs. Pilot B stated,

"You could use [the auxiliary thruster] quite easily to slow yourself down, increase your turn rate or to speed yourself up to get into a better position without having to sort of lower the collective and bring the nose up so that your tracking has gone to worms."

Pilot A commented,

"During the initial part of this run, it looks like since the target is so far away from you that you can go ahead and use positive x-force to increase your speed quickly to get it up to a desired velocity for rate of closure. Once the adversary started turning, you could increase your rate of turn in an attempt to track him by using the negative X-force."

Pilot commentary also indicated that at very high levels of 'g' capability the x-force was not as useful because of the already inherent superiority of the ownship. Also, at very low 'g' capability the x-force was viewed as unable to make up for the degree of deficiency.

Figure 14 shows a summary of the mean CHRs given for all of the auxiliary thrust configurations. The data shown represent the average of both air-to-air tasks. The data have been shaded to indicate the CHR Level: Level 3 ratings are black, Level 2 rating are gray, and Level 1 ratings are unshaded. The location of the AH-56A Cheyenne is shown for comparison purposes.

The data indicate that some load factor capability can be traded for auxiliary thrust capability without significantly degrading handling qualities. It can be seen that a 3.0 g configuration with an auxiliary thrust/weight of 0.33 achieved better CHRs than a 4.0 g configuration without auxiliary thrust. Configurations with auxiliary thrust/weight levels as low as 0.2 are seen to possess significant handling qualities advantages over those without.

The data in figure 14 indicate that the configurations with auxiliary thrust/weight levels of 0.6 and 1.0 did not have significant handling qualities advantages over those with 0.33 thrust/weight levels.

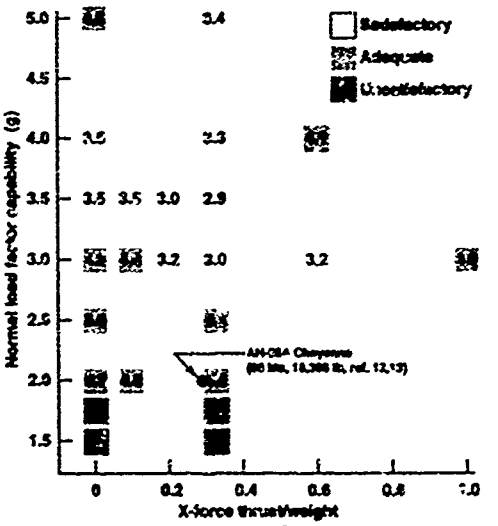

Figure 14. Mean CHRs versus load factor capability and auxiliary thrust capability.

4. CONCLUSIONS

Three piloted simulation studies were performed by the U.S. Army Aeroflightdynamics Directorate to examine the influence of maneuverability and agility on helicopter handling qualities and to provide an expanded basis for the dynamic response requirements in Aeronautical Design Standard 33C, Handling Qualities Requirements for Military Rotorcraft. The experiments focused on aggressive tasks such as air-to-air combat and target acquisition and tracking.

The results of the target acquisition in hover task from the yaw agility experiment suggest that the ADS-33C yaw attitude quickness boundaries might be relaxed to the levels indicated in figure 8 without sacrificing the ability of the pilot to make precise heading changes in hover.

Good agreement with the ADS-33C roll bandwidth requirement was seen for the pitch and roll maneuverability and agility experiment. Task performance results correlated well with pilot opinion ratings.

The normal and longitudinal load factor/maneuverability experiment showed that the addition of auxiliary thrust can provide a significant improvement in handling qualities. Auxiliary thrust levels as low as 0.2 thrust/weight were shown to have significant handling qualities and mission performance advantages over those configurations without auxiliary thrust. It was also shown that integration of the auxiliary thrust inceptor with the pilot's other controls is critical. Poor implementation can actually make the vehicle more difficult to fly than if there was no auxiliary thrust at all. Of the auxiliary thruster/control systems examined, a u_{body}-rate command/u_{body}-hold system with a cyclic joystick inceptor was found to provide the best handling qualities. Some normal load factor capability could be traded for auxiliary thrust capability without sacrificing satisfactory handling qualities. Increasing auxiliary thrust levels to 0.6 thrust/weight and higher did not yield further handling qualities improvements over those cases with 0.33 thrust/weight

5. REFERENCES

1. Anon., "Handling Qualities Requirements for Military Rotorcraft, U. S. Army AVSCOM Aeronautical Design Standard, ADS-33C", Aug. 1989.

2. Danek, G., "Vertical Motion Simulator Familiarization Guide", NASA TM-103923, Jan 1993.

3. Lewis, M. S. and Aiken, E. W., "Piloted Simulation of One-on-One Helicopter Air Combat at NOE Flight Levels", NASA TM-86686, Apr. 1985.

4. Lewis, M. S., Mansur, M. H. and Chen, R. T. N., "A Piloted Simulation of Helicopter Air Combat to Investigate Effects of Variations in Selected Performance and Control Response Characteristics", NASA TM-89438, Aug. 1987.

5. Lewis, M. S., "A Piloted Simulation of One-on-One Helicopter Air Combat in Low Level Flight", J. AHS, Volume 31, No. 2, pp. 19—26, Apr. 1986.

6. Whalley, M. S. and Carpenter, W. R., "A Piloted Simulation Investigation of Pitch and Roll Handling Qualities Requirements for Air to Air Combat", *in* "Proceedings of the 48th Annual Forum of the American Helicopter Society", Jun. 1992.

7. Whalley, M.S., "A Piloted Simulation Investigation of the Normal Load Factor and Longitudinal Thrust Requirement for Air-to-Air Acquisition and Tracking", *in* "Proceedings of an AHS Technical Specialist's Meeting" , San Francisco, CA, Jan. 1993

8. Austin, F. and George, D., "Automated Control of an Adversary Aircraft for Real-Time Simulation of Air-to-Air Combat", Grumman Corp. Report RE-786, Aug. 1991.

9. Austin, F., George, D. and Bivens, C., "Real-Time Simulation of Helicopter Air-to-Air Combat", *in* "Proceedings of the 47th Annual Forum of the American Helicopter Society", Phoenix, Arizona, May 1991.

10. Cooper, G. E. and Harper, R. P., "The Use of Pilot Rating in the Evaluation of Aircraft Handling Qualities", NASA TN-5153, Apr. 1969.

11. Bethea, R. M. and Rhinehart, K. R., "Applied Engineering Statistics", Marcel Dekker, Inc., New York, 1991, pp 63-65.

12. "Substantiation Technical Data, AH-56A Attack Helicopter, Books 1 and 2", Lockheed Report LR 25271, CDRL Item A009, USAAVSCOM Contract DAAJ01-72-C-0513(P60), May 31, 1972.

13. Sirota, W.W., Petach, A.M., East, A.W., and Carlson, R.M. "AH-56A Performance Report", Lockheed Report LR 22707, USAAVSCOM Contract DAAE13-66-0-3667(H), July 29, 1970.

Operational Agility
An Overview of AGARD Working Group 19

by
K.McKay
British Aerospace Defence
Warton Aerodrome
Preston, PR4 1AX
Lancashire, England

Summary

The environment in which a fighter pilot is required to operate is subject to continual change. This change arises from advances in technology and the altering world political situation. The only prediction that can be made with any confidence is that this change process is bound to continue with an unpredictable rate.

In dealing with change, it is easy to prescribe a process but extremely difficult to implement the process with success. Success requires anticipation, reaction, re-evaluation and modification of tactics and processes. The need for change must be recognised and accommodated. Such an approach, whether applied to fighter airplanes or any field of human endeavour translates to agility.

In undertaking this work, the Group encountered many definitions of agility, some of which represented widely differing viewpoints. Often, in the past, protagonists of the varying ideas have fallen into heated arguments as to who is right. Fortunately, within the Group, we have been able to stand back and examine the arguments with a dispassionate approach which has enabled us to understand the various arguments and see the common ground, rather than the differences.

From our deliberations and discussions, the answer has emerged that no one was wrong, that all were right, at least in part. However, few had taken the time to stand back and take an all embracing view. Had they done so, then the message that all were trying to put forward might have had a wider and more sympathetic audience.

All of the agility concepts that have been put forward have some merit. What was required was a way to relate the ideas and be able to apply them in a manner that is both reasonable and logical from both the viewpoints of the designer/supplier of aircraft and the customer/user of the vehicles that result.

In defining a Weapon System, it is essential to examine the component parts and their interaction, whether this be airframe, propulsion system, sensors, cockpit and avionics or the weapons themselves and establish balance and synergistic integration between all of the components appropriate to the intended role and missions of the aircraft. It is the need to achieve balance and integration that is the prime driver for understanding Operational Agility as a set of concepts, supported by metrics which fit into a generalised framework, capable of evaluating a complex combat aircraft design with a view to maximising the effectiveness of that design within affordable cost limits.

The activities of the Group have produced such a framework, derived from the various flight mechanics based concepts, but which would appear to be generalisable to cover the other systems, either as individual systems, or as a total Weapon System. Their is further work required to confirm that this framework will stand, but our initial investigations are very promising.

This points the way forward for future aircraft. Achievement of this design balance requires all of the Weapon System attributes to be studied, evaluated and weighed against each other, together with the cost implications, to determine the optimum solutions. This may imply significant compromises if the roles and perceived threats are too diverse. A consequence is that future design specifications and requirements will need to be prepared in a different way from that traditionally used, in order that the correct design balance for a given set of applications can be achieved.

Presented at an AGARD Meeting on 'Technologies for Highly Manoeuvrable Aircraft', October 1993.

Introduction

The flying characteristics and flying qualities have been major interests of the Flight Mechanics Panel of AGARD for many years. A subcommittee of the Panel has addressed this area specifically. Recently, the subcommittee sponsored Working Group 17, which examined the "Handling Qualities of Unstable Highly Augmented Aircraft", published as reference 1 and a Symposium on Flying Qualities, reference 2.

Stemming from these activities, it was recognised that flying qualities and traditional aircraft performance parameters did not characterise the capability or effectiveness of combat aircraft, although they do offer a guide. Other learned groups had reached a similar conclusion. The subject that arose from these realisations was "agility".

Recognising that this was an incomplete or immature concept and that a wide variety of sometimes disparate views existed, the Panel formed a further Working Group, WG.19, consisting of specialists from AGARD member countries, to study the subject under the title of, as originally proposed, "Functional Agility" or as now preferred by the members of WG.19, "Operational Agility".

The final report of WG.19 is due to be published as reference 3 in the near future.

Objectives of Working Group 19

The specific objectives for Working Group 19 were defined by the previous Working Group, WG17, as follows:-

- To provide definitions, which are universally acceptable, of the terminology involved in agility.
- To collate the results of lessons learned from experiments on agility.
- To define metrics or figures of merit for use in design and evaluation.
- To explore and document the theoretical foundations.
- To explore the operational payoff of balanced capabilities between the airframe, systems and weapons
- To highlight any specialised aspects applicable to rotorcraft.
- To indicate possible means of evaluation in flight.
- To recommend areas for further research and development activities, including possible collaborative projects.

Five working sessions were held at places of special interest to the group, between the years of 1991 and 1993. Venues were:-

- Edwards AFB, Lancaster, California, United States.
- STPA, Paris, France.
- Sikorsky Aircraft, Stratford, Connecticut, United States.
- Aermacchi, Varese, Italy.
- British Aerospace, Warton, United Kingdom.

Working Group 19 is now in the process of finalising its report, which will be available for general distribution in the near future.

The Background to Operational Agility

To understand the background to Operational Agility it is worth considering some of the historical background to agility.

The first air to air conflicts occurred in the Great War. Here, aircraft were, for the most part marginal with regard to performance, stability and controllability. Indeed, many combat losses could be attributed to these shortcomings rather than the action of the enemy. However, some of the aircraft were regarded, and still are, as models of the agile fighter, particularly in the hands of an expert pilot or "ace". The basic skills required were the ability to remain in control and shoot accurately.

For subsequent conflicts, the same basic skills were required, although airframes were better stabilised and controlled and had increased power available, resulting in higher speeds. With radar and radio, it became possible to receive guidance towards the targets that the ground control perceived as the prime threat. Weapons remained visual range, however, but regardless of this,

the increased speeds and the added information changed the difficulty of the pilot's task due to the implications on his situational awareness and choice of tactics. Increasingly, the combat results became more clouded by the interaction of the systems available to the pilot and his ability to assimilate the information provided.

The advent of jets, airborne radar capability, missiles and counter offensive equipment have all tended to complicate the picture whilst attempting to improve the ability to perform the same basic tasks, i.e.. finding the opposition and shooting him down. Korea demonstrated the benefits of high performance combined with good handling, to the detriment of the Communist forces. However, some lessons were forgotten, and had to be relearned in later conflicts.

A classic modern example derives from the Falklands conflict, where the Sea Harrier had significantly less performance than the opposing Mirage and Dagger aircraft, but was able to acquit itself very successfully because of its radar, weapons, the back-up of ship-borne control radar and information and not having to operate at the extremes of its range. Further examples come from the USAF and USN aggressor training schools, where the success of the F-5 in the hands of very skilled, combat experienced pilots caused a number of upsets in training combats against apparently more capable opponents.

As a direct consequence, over recent years, there has been a growing recognition that studying traditional performance parameters and Flying Qualities does not adequately characterise the differences between aircraft or their relative effectiveness.

Considerably more is involved in understanding what makes an aircraft effective and many workers have been attempting to qualify what the extra something is and quantify its measurement. The studies of agility are a direct result.

Figure 1 provides an approximate illustration of the increasing complexity of the fighter pilot's task which have resulted from the introduction of increasing technology aimed at assisting him increase the effectiveness with which he can operate. If it is assumed that the workload in combat is always maximum, then his ability to attend to each system is significantly reduced. An aircraft in which this can be achieved with success can certainly be described as agile.

The Working Group has defined, therefore, our subject of "Operational Agility" as a full system capability, including the sensors and other onboard electronic systems and the weapons. Systems which are not onboard to which the aircraft systems must relate have not been considered, specifically.

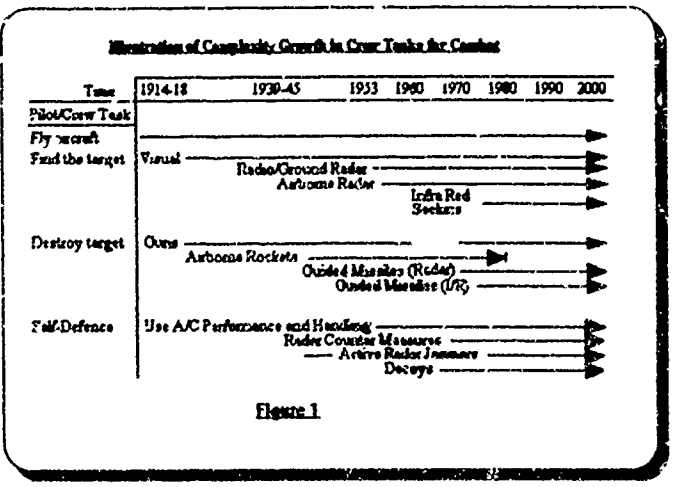

Figure 1

Definitions of Agility Terminology

In developing the subject of Operational Agility the Group has had to derive a terminology which adequately describes the intended meanings, such that we were clear within our own work. Before describing the activities and conclusions in detail, it is worth presenting the terminology which resulted.

A set of definitions has been arrived at which are consistent with the proposed methodology for evaluation and specification of the aircraft and its associated onboard systems. These definitions are:-

Operational Agility - the ability to ***adapt*** and ***respond***, ***rapidly*** and ***precisely***, with ***safety*** and ***poise***, to maximise mission effectiveness.

Airframe Agility - the physical properties of the aircraft which relate to its ability to change, rapidly and precisely its flight path or pointing axis and to its ease of completing that change.

Systems Agility - the ability to rapidly change mission functions of the individual systems which provide the pilot with his tactical awareness and his ability to direct and launch weapons in response to and to alter the environment in which he is operating.

Weapons Agility - the ability to engage rapidly the characteristics of the weapon and its associated onboard systems in response to hostile intent or counter measures.

Transient Agility is a continuously defined property reflecting the instantaneous state of the system under consideration.

The Form of the Working Group Final Report.

From the earliest discussions within the Group, it was clear that the starting point for most people working with agility problems was often in the Flight Mechanics and Controls area. Most of the arguments regarding how to characterise agile aircraft had their origins in these disciplines, but some authors were advocating a broader approach. The objectives of the Group required us to adopt this broad approach, but it was recognised that the "traditional" aspects had to be dealt with.

Accordingly, the report was to be split into four prime sections to deal with the aspects of Operational Agility which we considered to be most significant. Both fixed wing and rotorcraft aspects are addressed throughout the report and a considerable synergy between the two communities became apparent.

These sections are:-

- Airframe Agility - this section has been further subdivided to give detail appraisals of:
    - Vehicle Flight Mechanics applied to Agility. This details the equations which can be utilised to describe the flight path and rotation/translation of the vehicle in question. As such, this provides the theoretical background to Airframe Agility.
    - The Agility Metrics. This provides details of the metrics which have been developed to date. During preparation of this survey, it was realised that there was a form appearing which looked to applicable to any aircraft system, not just the Flight Mechanical aspects. Paper 24 of this symposium will address this work in some detail.
    - Handling Qualities and Airframe Agility. It was recognised that there is a strong relation between these areas, which is addressed here. Paper 23 of this symposium relates to this section. One of the concerns which has been raised during the work of the Group relates to whether or not there is an upper limit to agility, whether this be the airframe or any other system. This is perhaps most readily understood in terms of the airframe agility. Some of the upper limits are comparatively easy to describe, as they result from the limitations of the structure or rate at which controls move. However, there are concerns that very high performance may be dangerous to use, as the more aggressive the use of the airframe, then the more the handling qualities may degrade. In very high workload situations, this may result in unsafe characteristics but the situation is likely to be difficult to quantify as it will depend on the aggressiveness of the pilot. If high performance is dangerous to use, then pilots will avoid using it, hence flying qualities can provide major restrictions on the agility of a particular airframe.
    - Design for Airframe Agility. This describes the design process for an agile aircraft, highlighting the iterative nature and increasing level of detail involved. It deals with the use of the various agility metrics, in combination with the more traditional aircraft performance parameters and flying qualities, and when these various aspects apply. Both fixed wing and rotorcraft design aspects are addressed.
    - Airframe Agility Evaluation. This section deals specifically with the use of the proposed metrics in the evaluation process, providing a useful guide to airframe designers when agility is a design driver.
- Subsystems Agility. This section addresses the less traditional aspects which it was realised will play a significant part in whether or not a vehicle can be regarded as Operationally agile. This is the recognition of the total Weapon System. The primary areas addresses relate to:-
    - Mission Oriented Systems. This looks at the aircraft onboard systems, such as

sensors, and examines their influence on the overall agility. Examples of the transient metrics which can be applied to the typical onboard aircraft systems are presented. This should enable designers to decide the type of metric, within the proposed framework, which will be appropriate to their particular system.

- Weapons Agility. A key feature of an Operationally agile vehicle relates to the weapons which it must deploy. This section looks at some of the issues which are involved. Paper 27 examines some of the issues covered.

- **Pilot-Vehicle Interface**. This section deals with the aspects of the agile vehicle which relate to the design of the cockpit and the interface to the pilot. There are two main parts:-

  - Physiological Aspects. This looks at the various aspects of the design which relate to the pilot physiological concerns and his performance under various stresses. Paper 22 of this symposium examines some of the aspects which relate.

  - Pilot Aiding. This section addresses some of the systems which can assist the pilot of a vehicle with high levels of agility and also gives a brief overview of some of the aspects of multi-mission capability. Paper 21 examines some of the issues which are involved for the ground attack scenario.

- **Evaluation**. Evaluation forms an essential element of understanding Operational Agility. At the outset, this was thought to address the flight test of agile vehicles, as this is an area that is being studied in many countries. However, it was soon realised when this section came to be drafted, that evaluation is a continuous process, running from concept, through to the end of the vehicles Service life. As such, evaluation should play a significant role in the design and procurement of agile Weapon Systems. The key issues addressed are:-

  - Evaluation Techniques. Here the report looks at the methodologies for evaluating agile aircraft and systems and proposes techniques which might be applied to this end. The concept of the Mission Task Element for this purpose is seen as a central element.

  - Data Gathering & Reduction. Currently, there is little information available which enables the designers and system specifiers to see how the current aircraft systems are actually utilised by the aircrews who have to fly with them. There is clearly a need to establish what really happens, and under all conditions, if realistic evaluation techniques are to be established.

Each major section of the report draws its own conclusions, enabling the report to be read either as a total entity or as a series of individual, stand-alone documents. The conclusions are all drawn together at the end, together with the recommendations for further activities.

The major item which runs though the report is the need for the unified methodology, which is summarised in more detail here, as are the conclusions and recommendations.

An Operational Agility Methodology

Test and evaluation is an exacting process for even simple designs and articles. The term test is worthy of some discussion, before we turn to evaluation. The definition contained in 'The Glossary: Defense Acquisition Acronyms and Terms', prepared by the Defense Systems Management College, is as follows:-

- A "test" is any programme or procedure which is designed to obtain, verify, or provide data for the evaluation of: research and development; progress in accomplishing development objectives; or performance and operational capability of systems, subsystems, components and equipment items.

It is evaluation which transforms test results into useful information.

Evaluation is an essential element in the process of development of any system. For maximum effectiveness, it has to be combined with a satisfactory methodology by which the evaluation can proceed. One of the key outputs of the Working Group relates to the statement of such a methodology which may be adapted for application to any aircraft or system development project.

From the work on correlating the various metrics, an overall form has emerged with a regular pattern to it.

On further examination, the Group found that the emerging structure could be applied to any system associated with the airborne vehicle, and that there was a route to quantifying the worth of the system in relation to each of the other systems.

For any individual project, the generalised methodology must be adapted to a specific set of evaluation methodology and metrics which should be decided at the beginning of the design cycle. The reason behind this is that the metrics are a function of the roles which the vehicle must fulfil.

Recognition of this allows the same methodology to be applied to any category of vehicle, on much the same way as Handling Quality specifications . The key to success is to consider the evaluation process before the engineering detail design process has started.

From the agility definitions, the necessary methodology and evaluation techniques become evident. The detail will look similar to that proposed in Table 1.

Fundamental to this is the concept of Mission Task Elements. The process is to break down all of the mission related tasks which have to be performed into their component parts, going down to whatever level of detail is necessary to capture all of the activities and the information exchanges which relate to the decision processes. Using such techniques, it is possible to analyse any function or system onboard the vehicle and it helps focus the mind on the actual processes which are in place with the pilot in the cockpit, at any stage of his task. These are already in use in the rotary wing world, but are only just being taken on board by the fixed wing community.

In the early stages of design, even at the conceptual stage, this technique can be used to determine what is required to perform any task and allows a study of all of the design options available such that the most effective way of achieving the task results.

As shown in the table, the methods range from the very simple to the complex Operational Test and Evaluation exercises A concept which is worth pursuing further, in this relation, is that of onboard simulation of systems, to simulate the necessary stimuli and gauge the response.

Conclusions

The Group has completed its study of Operational Agility with this report. In undertaking the study, a greater understanding has been reached of those subjects which influence Operational Agility and how these subjects, via the use of Operational Agility concepts, may be related to the combat effectiveness of the Weapon Systems.

In reaching this understanding the Group has proposed definitions of the agility terminology which it is hoped will prove universally acceptable.

To go with these definitions, the Group has arrived at a methodology for assessment of the various component systems which contribute to the Operational Agility or combat effectiveness of a Weapon System. This methodology is described in detail in the Working Group report

Its application allows the relative worth of the differing systems to be evaluated against each other.

On further examination, it would appear that ***the methodology could be used for any class of flight vehicle, although the values of the metrics would need to change appropriately.*** The parallel with Flying Qualities criteria as applied to different classes of aircraft is striking, although this was not intentional.

Specific Conclusions:

1) There is a mismatch between the Weapons and the Airframe capabilities.

A great deal of effort has been expended in developing the airframes to be highly agile but this has not necessarily been matched by the equivalent development of the weapons that the airframes carry. This does not imply that there has been no activity, there has, but there needs to be a concurrency in the development if the total effectiveness is to be maximised.

2) The way in which aircraft and their associated systems are specified is in need of review and revision.

Current combat aircraft specifications and requirements are not really appropriate for the complex, integrated vehicles which have to result from attempting to meet the requirements. The very complexity of the vehicles often means that decisions relating to the design options may not take into account all the influences, leading to engineering difficulties and expense later in the processes of development and procurement.

The concepts involved in Operational Agility can assist in the process of determining what the specification and requirements should contain and in the design and subsequent evaluation of the vehicle that results. The object should be to define the function and purpose, then establish the methodology and means of evaluation prior

to issue of detail engineering design specifications. To achieve this, there needs to be close interface and teaming between the customer, end user and possible designers and suppliers of equipment, airframes, etc.

3) The achievement of a cost effective design balance and the maximisation of Weapon System combat effectiveness are central to the concepts of Operational Agility.

There has been a problem of vocabulary which has inhibited communication in this field. However, the report of the Working Group should assist by providing the necessary definitions of agility terminology by which the communication can be established. The key is to recognise the broad scope that Operational Agility encompasses, and to be specific about which aspect or system is being discussed.

To achieve the design balance not only needs the definitions of agility, it also requires standardised agility figures of merit, together with a proven quantification methodology applicable from concept through design, test and into operational contexts. The role for the vehicle will give rise to differing weighting factors for the agility attributes, influencing the design balance.

The proposed metrics structure seems to logically characterise the airframe agility, i.e., transient, experimental and operational. However, there is insufficient data at present to clearly determine the tactical meaning of airframe agility metric results. This conclusion strongly relates to the second conclusion regarding the tactical meaning of agility.

4) There is a need for Global data acquisition.

In order to understand and quantify the Operational Agility of a Weapon System, there is a need to gather data on all the systems simultaneously, in order to determine the actual usage that is being made of all the systems at any time. Additionally, there is a need to record data under realistic operating conditions, including combat use and even actual war. The capability exists now to gather the information and to handle the database that results. The implication is that the data acquisition would need to be structured with all the potential users in mind and should be sufficiently flexible to accommodate changing and growing needs.

5) Combat success requires more than an agile airframe.

Use of the proposed Operational Agility methodology should enable the crucial aspects of each contributing system to be identified. The object will be to focus on the time delay of each aircraft subsystem with the aim of reducing the delays without over-emphasis on a specific system aspect which could potentially lead to increases in time delays by other components, including the pilot.

Clear understanding the time delays for mission functions enables identification of actions to automate, i.e. housekeeping, leaving the crews limited attention time to more critical tasks such as the tactical situation.

6) Quickness parameters provide best means to bound agility.

The concepts of quickness parameters are comparatively well developed for rotary wing vehicles, as exemplified by ADS33C. For fixed wing, the concept is still in its infancy, but it would appear to be well worthwhile developing as an analysis tool, particularly if the vehicle will have to demonstrate high levels of agility in its class.

Flying qualities need to be considered in the early design process. The concept of an "agility factor" for this phase of work where the focus is on probability of mission success or failure combined with a mission task element method of analysis will assist in mission effectiveness trade studies.

The Operational Agility structure is applicable to mission oriented and weapons agility.

7) Airframe agility is designed in from the outset.

Only in exceptional circumstances can it be added later, implying the basic design was not balanced properly.

Operational Agility concepts can and should be applied at the outset of the design process, starting even with the Operational Analysis [illegible]. The objective is to determine the correct design balance between airframe aspects, weapons and the onboard systems with a view to maximising the operational effectiveness at an affordable cost and to ensure that there is adequate growth potential in the aircraft to take it through its Service life.

Typically, combat aircraft have to remain in Service for around 20 to 25 years. During this time, the onboard systems can be upgraded many times, as the changing needs of the operational environments dictate. However, the airframe is much harder to make any fundamental changes to, implying that the flexibility has to be built in at the outset.

Provided this is recognised early in the design process, before detail work starts, then it is more easily accommodated. Adding capability later is always more expensive, and may need major structural repair work.

8) Rapid prototyping of crew stations is an agility enabler.

Modern crew station design focuses on the tasks for the specific missions which are to be performed. The objective is to be more effective in an overall performance sense and to be able to respond to changes in the external environment more adeptly than at present. This requires an understanding as to how the crew interface with the systems in order that the appropriate displays of information, as opposed to data, can be implemented. The process can and should be used to decide which functions are to be automated, rather than what can be automated.

9) Changing combat situations result in dynamic missile envelope conditions that press the ability of the mission systems to present up-to-date information.

The key here is the need for the systems to display information, not data, but in a form that the pilot can readily relate to and with a speed that is commensurate with the changing situation. Under some circumstances, it may even be appropriate for the system to take action and then inform the crew that it has already dealt with a situation, for example in response to an external threat. Again, rapid prototyping alloyed to adequate simulation and evaluation will prove to be key enablers of such technology.

10) Pilot-Vehicle Integration for the expanded flight envelopes provides a major challenge with regard to displays

When at high angles of attack, new forms of displays are required to ensure that awareness of the flight path vector is maintained. Recovery from high angle of attack manoeuvres, using 45° or more is accompanied by the feeling that the aircraft is not reducing angle of attack initially. The aircraft appear to maintain AoA and reduce flight path angle. This places additional burden on developing means to inform the pilot as to what is happening, particularly if the correct things are taking place, but it does not feel natural.

11) Integration of propulsion systems into agile airframes places special requirements on the propulsion unit and its integration into the design.

Engine response times need improving for carefree handling. The goal should be to obtain maximum power on the same time as the pilot can achieve his desired AoA.

Thrust vectoring offers a powerful control effector. A careful cost/benefit analysis is required for each individual project study. It may not always be beneficial or necessary to include such technology to achieve the desired effectiveness. PST should not be considered if it drives the configuration such that it penalises the aircraft over the rest of its design flight envelope.

12) The study of Operational Agility is still immature.

On the limited evidence available to the Working Group, the concept does appear to be valid and examples have been provided in the report. However, the concept requires the establishment of a suitable vocabulary and unification of existing work. The definitions derived by the Group could provide a basis for further work in this area, which would appear to offer a worthwhile reward in terms of the operational effectiveness enhancements that could result.

Recommendations

There are a number of recommendations which result from the studies of this Working Group. These are as follows:-

1) The Mismatch of Missiles and Weapons with Airframes.

There is need for some form of formal discussion relating to the mismatches in development of missiles, or weapons in general, and airframes. The Group believes that this could best be addressed by a Symposium to illustrate the current problems and identify possible ways forward. It is noted that such an activity could relate or be a part of the proposal for a Symposium on Weapon System Integration which has been raised within the Flight Mechanics Panel.

2) The Need for a Database Relating to the Systems Use in Operations

There is a need for data to be obtained from service which can be made available to the whole community involved in aircraft design, assessment and operation. The capability to provide the necessary information exists and so handle the database that results. The Group recommend that a new working group could usefully address the problem, with a view to providing the necessary database. This new group would need the

services of experts in operational use, design, and information systems technology. The objective would be to recommend ways of achieving a database of use to all disciplines involved in the design and procurement of Operationally Agile aircraft.

3) The Tactical Meaning of Agility Metrics needs to be Established

Work needs to be undertaken to establish the tactical meaning of agility metric results, such that the value of Operational Agility studies can be quickly established and the resulting designs be shown to be more effective in a manner which fits the needs of the operators and purchasers.

4) Additional Studies Required.

Further studies are recommended in the following areas before a complete understanding of Operational Agility will be quantified:-

- Subsystem agility concepts and the possible metrics need to be developed further with more examples of application of the proposed structure to test its fitness.
- Develop more rotary wing metrics compatible with the Operational Agility structure particularly for the airframe, which currently lags the work done in the fixed wing areas.
- Develop a complete library of mission task elements which can be used in the development and assessment of Operational Agility for either fixed or rotary wing vehicles.
- As the upper bounds on agility remain to be determined, there is a need to gather more quickness parameter data. At present, the quickness parameter concepts are used by the rotary wing community, but it would appear applicable and useful for fixed wing applications as well. It is recommended that further work be done on this concept for fixed wing application.
- Further analysis of the relation of flying qualities and vehicle performance to define the upper limits on airframe agility is needed, particularly if aggressive use of the airframe causes the handling qualities to degrade. This requires dedicated evaluation tasks where both the objectives and success criteria are clearly defined.
- Develop an "aggressiveness" rating system to parallel Cooper-Harper.

5) Establish the Influences on Awareness of High Rate and Acceleration Manoeuvres.

The effect of high angular and linear rates and accelerations under varying visual reference conditions needs to be established if agile airframes and displays with which the pilot can interface correctly are to be achieved. The concern here is that what might be perfectly acceptable under planned flight test conditions will be of little use or even dangerous when manoeuvring aggressively at maximum rate or rate of change of any flight condition, particularly in a dynamic combat environment. Use of high rate manoeuvres may be particularly dangerous under less that ideal visual conditions or when pilots are distracted by combat demands.

6) Establish the Influence of Prolonged Exposure to Sustained 'g' at Moderate Levels.

Determination of the relationship between sustained high 'g' below the level causing loss of consciousness and loss of situational awareness. This is a direct corollary of the previous recommendation.

7) Revise the Way in Which Future Aircraft Specifications are Written.

Specifications should be written to define the function to be achieved, from which the levels of performance can be derived in conjunction with the appropriate trade studies. Each new airframe project should be assessed in its own right to establish which technologies are affordable or relevant. Technology should not be included for its own sake. No one item should be inviolate, all items in the detail engineering specification should be tradable to ensure the correct design balance results.

8) Adopt Concurrent Engineering Methods.

A concurrent engineering approach between customer and supplier will help to ensure that the necessary objectives are achieved.

Achievement with respect to the Objectives:

At its outset, the Group was given a set of eight objectives to achieve, if possible, as described in the preface to the full report.

The achievements against each of the set objectives are as follows:-

1) To provide definitions, which are universally acceptable, of the terminology involved in agility.

The Group has derived definitions that can be applied, which seem to make sense and which ought to prove to be universal in their application. Hopefully, provision of the appropriate terminology can help alleviate some of the differences which have arisen in the past.

2) To collate the results of lessons learned from experiments on agility.

Currently, many of the flight experiments are still ongoing and the Group has had limited access to the very latest information. We have been able to use information which has been published, together with whatever the members have been able to bring to the table. However, this objective has not been fulfilled completely, but only partially.

3) To define metrics or figures of merit for use in design and evaluation.

No new metrics have been defined by the Group, rather the existing metrics have been placed into a unifying framework, which should be applicable not only to the airframe, but also to the other systems and subsystems which contribute to the Operational Agility or combat effectiveness of the Weapon System. This objective has been fulfilled to the best of our ability.

4) To explore and document the theoretical foundations.

The theoretical foundation for airframe agility has been explored and documented in Chapter 2.1 of the report.

5) To explore the operational payoff of balanced capabilities between the airframe, systems and weapons.

A methodology for completing this investigation has been proposed, with examples showing how it might apply across a number of different systems. The need to undertake studies early in the design and development programme has been clearly enunciated as a key to providing an Operationally Agile Weapon System.

6) To highlight any specialised aspects applicable to rotorcraft.

In undertaking the work, the synergy that has evolved between fixed and rotary wing vehicles has been marked. We have seen that the two communities are tending to come together, although there will always be marked differences. These differences stem from the differing functions that the vehicles perform, and the implications that this has for the technologies involved. We have learned from each other. Specific lessons from each are included.

7) To indicate possible means of evaluation in flight.

Having established a methodology for dealing with Operational Agility, the report concludes with a Chapter on evaluation. Our realisation is that evaluation has to be part of the process from the design outset and is not purely a flight test function. Indeed, evaluation methodology may influence the design process considerably.

8) To recommend areas for further research and development activities, including possible collaborative projects.

Concluding Remarks

Summarising, the Group believes that it has met the objectives which were set for it, with the possible exception of item 2, relating to the lessons learned from experiments on agility. However the scope of the activity which has resulted has taken us into a far wider realm than the original proposal envisaged. The major consequence of this is that a better perspective of the integrated airframe and systems has resulted.

The Group's view is that the study of Operational Agility is in a similar situation to that seen by the Flying Qualities community some twenty years or more ago when faced with fly-by-wire, highly augmented airframes for the first time. Much remains to be accomplished before Operational Agility attains the same status as Flying Qualities currently has. However, the benefits which should accrue from better understanding of Operational Agility will encourage a rapid progression. In particular, when funds are restricted, it is essential that there is an adequate understanding of where funds are best targeted for any project. The Operational Agility methodology derived by the Group should be able to provide major assistance to making logical decisions.

This report should enable the reader to share that perspective.

Finally, it is considered that the Group has met the objectives which were set out for it and that this report summarises the understanding which has resulted from the activities.

There is still much to do and understand, particularly with regard to interfacing all of the technologies which can influence combat aircraft Operational Agility.

The driver will remain effective combat aircraft at a cost affordable to the customer.

References

1) Handling Qualities of Unstable Highly Augmented Aircraft.

AGARD AR279, Wuennenberg et al.

2) Flying Qualities.

AGARD CP-508.

3) Operational Agility.

AGARD AR314, McKay et al.

(To be published)

OPERATIONAL AGILITY ASSESSMENT WITH THE AM-X AIRCRAFT

by

Renzo Bava
Alenia Flight Mechanics Group
Corso Marche 41 Turin
Italy

Ugo Rossi
Aermacchi Flight Mechanics Group
Via Sanvito 80 Varese
Italy

Sergio Paloni
A.M.I. Flight Test Center
Aeroporto Pratica di Mare
00040 Pomezia (Roma)
Italy

ABSTRACT

Relating to the activities performed by WG 19 a common area of interest was individuated by Aermacchi, Alenia and the Flight Test Center of the Italian Air Force to investigate the application of the agility concept to conventional aircraft.

Agility metrics and manoeuvres have been developed to evaluate the operational effectiveness of a modern fighter in the new combat scenarios that evolved following the introduction of advanced technologies.

Agility metrics and manoeuvres, however, may be effectively adopted to evaluate also operational effectiveness of a conventional aircraft since those metrics have been developed to reproduce synthetically the new operational scenarios.

The AM-X Ground Attack aircraft was hence chosen as a testbed to verify the applicability of the Agility concept to conventional aircraft and to assess the possible benefits for operational training.

The research activity is being carried out by simulator and flight tests to compare simulator cueing effectiveness against the real A/C and to investigate simulator effectiveness for agility training.

Single axis agility manoeuvres performed by simulator will be validated through up-coming flight tests. Results from this activity will be used to plan and perform further simulation test with complex multi-axis closed loop agility tasks.

This activity proved that Agility metrics and manoeuvres are applicable also to conventional A/C as well, and are effective in evaluating it within a highly dynamic combat environment.

Operational Agility may be improved with adequate pilot training and simulator may be used as an effective tool for it. Anyway, particular attention must be paid to the definition of the training program to overcome shortcomings of the simulator cueing system.

SYMBOLS

δ_{ls}	Longitudinal stick deflection
δ_{lat}	Lateral stick deflection
δ_{ped}	Pedal deflection
δ_e	Elevator deflection
δ_s	Stabilizer deflection
δ_a	Aileron deflection
δ_{sp}	Spoiler deflection
δ_r	Rudder deflection
α	Angle of attack
γ	Dive angle
ϑ	Pitch attitude
q	Pitch rate
ϕ	Roll attitude
p	Roll rate
r	Yaw rate
β	Sideslip angle
ψ	Nose heading angle
M	Mach Number
H	Altitude
CRU	Cruise Flaps
MAN	Manoeuvre Flaps
AOA	Angle of Attack

Presented at an AGARD Meeting on 'Technologies for Highly Manoeuvrable Aircraft', October 1993.

C/F	Crossfeed
Δ	Parameter Variation

1.0 INTRODUCTION

A process of continual evolution among the aeronautic technologies has seen a gradual improvement in aircraft combat performance, and, thanks to greater integration of on-board systems and pilot interface techniques, an improvement in their operational capabilities.

Today's pilots are confronted with operational scenarios more and more complex, in which they must administer each of these systems, and at the same time take full advantage of the high performance level of each.

Given that the overall efficiency of the system in five scenarios is not guaranteed by the standards currently used in the design / development phase, there arises the need to establish new criteria and requirements in order to complement the existing ones.

The result was a new body of research, originally oriented toward the identification of new criteria for evaluating the characteristics of advanced vehicles, namely controllability and manoeuvrability, and at the same time, for evaluating the degree to which each characteristic contributes toward attainment of the overall mission goal for which the aircraft was designed.

Under this systems aspect, researchers have had to expand the scope of these criteria, going beyond the performance of the airframe to include other elements of the weapon system, such as man-machine interface, engines, avionics and armament, in order to evaluate "the ability to adapt and respond, rapidly and precisely, with safety and poise to maximize the mission effectiveness", an ability summarized by the term *Operational Agility*.

The methodologies of evaluation already developed, which then become design criteria as well, have been studied for eventual adaptation and application possibilities in the design of an advanced trainer and fighter.

To investigate the validity of this concept, a joint research program has been put into action using as a primary instrument the R&D simulator, and flight tests to validate the results.

2.0 OBJECTIVES

The objectives of the research program are the following:

- Evaluate a conventional aircraft against the classical agility metrics
- Verify the simulation validity for agility assessment
- Define the operational application of the agility manoeuvres considered
- Quantify the utility of the manned simulation for agility versus operational training

3.0 AIRCRAFT AND TOOLS DESCRIPTION

Aircraft

The AM-X aircraft (figure 1) is a subsonic, single seat, single engine, dedicated attack aircraft developed within a framework of a joint Italian and Brazilian programme. Both Air-Forces had requirements for an aircraft whose primary mission would be "ground support at and just beyond the forward edge of battle" supporting the land and naval forces and having capability to provide:
- close interdiction
- close air support
- reconnaissance

and possibility of:
- air self-defense

Therefore the main design aims were about an aircraft capability to operate at low altitude subsonic speed with the following characteristics:
- large external store capability for ground attack
- air to air missile and gun for the air defense
- low sweep, medium thick wing to adopt a sophisticated "High Lift System" for adequate
. take-off and landing performances.
- single seat, high visibility cockpit
- advanced avionic systems for navigation and weapon aiming with head-up
- high survivability to continue the mission despite considerable battle damage.
- safe return-home capability following total electrical and hydraulic failure.

The AM-X flight control system has been designed as a "fail operative" system with a mechanical "back-up". A fly-by-wire F.C.S. provides three axes control, trim and compensation employing a dual-dual digital computer, in addition to analog motion dampers for all three axes. The hydraulic system is a dual-source, dual-redundant throughout. Normal functioning is still ensured after the first electrical and/or hydraulic failure whereas after the second electrical failure the controls are provided by hydraulically assisted back-up linkage on ailerons and elevator. These revert to manual following the second hydraulic failure, degrading the flying qualities to level 3 for the longitudinal and lateral stick forces in cruise as well as in landing flight phases.

Flight Simulator

The ALENIA Flight simulator has played a very important role since the very beginning in the development of AM-X aircraft. It continues to support

flight testing on the instrumented prototypes relevant to handling and manoeuvrability of aircraft modifications. At the moment an activity is in progress to investigate ground attack capability with safety indication for ground avoidance and several attack or automatic guidance mode.

Part of an expanding simulation complex, the AM-X simulator is a fixed base, fully instrumented cockpit with a real "head up display", in an inflatable dome with 10m diameter. A "control loading system" is available for a quick change of stick characteristics and a "G-suit, G-seat" system is available to improve the usable cue environments.

After many years of data correction and model improvement, the simulation program has achieved a high fidelity and reproduced correctly the aircraft response and performance both within the flight envelope and post stall region.

4.0 AGILITY METRICS AND MANOEUVRES TESTED

Even though Agility definitions and related metrics did become a quite large family all of them refer to the optimum combination of quickness and precision or, similarly, to the combination of manoeuvrability and controllability.

On the basis of the research work done by AGARD WG 19 "Operational Agility" Agility metrics and manoeuvres have been divided in the following classes (see Ref.1):

Transient metrics: property of response that varies in time

Experimental metrics: small task completion

Operational metrics: mission task element completion

Among these, experimental metrics can be further classified considering those tasks involving FRL (Fuselage Reference Line) aiming independently of flight path (nose pointing agility) and those involving flight path orientation (flight path agility).

Test activity was developed with the intent of analyze A/C agility characteristics initially on each axis separately, then on multiple axis and subsequently, in the completion of a mission task element. Hence experimental and operational metrics and manoeuvres have been considered.

- Single axis agility manoeuvres

Starting from set up condition capture an end state in minimum time with significant precision from an operational stand-point manoeuvering the A/C separately on his pitch, roll and yaw axis.

- Multiple axis agility manoeuvres

Starting from set up condition capture an end state in minimum time with significant precision from an operational stand-point manoeuvering the A/C on more axis at the same time.

For the single axis tasks, reported in Table 4.1, the metric adopted is the "time to capture" a state change or the time necessary to maintain an end state within specified tolerances starting from defined set-up conditions. Doing so it has been possible characterize with a single parameter identify the combination of manoeuvrability and controllability of an A/C.

Test Procedure and Data Reduction

An attack configuration with a medium weight and CG position at 5000 feet of altitude was considered being representative of an operational condition.

The tested manoeuvres are described in figure 2.

To complete the evaluation of both test technique (agility manoeuvres) and quality of the response, a questionnaire has been prepared which will constitute part of the pilot rating at the completion of each set of manoeuvres (Figure 3).

The data reduction has been carried out evaluating the time-to-capture, defined as the time from the pilot first input to the instant when the end state control parameter enters and remains within a specified tolerance range around target value for a defined length of time.

5.0 EXPERIMENTAL AGILITY SIMULATION RESULTS

Pitch Pointing Agility

Figure 4 reports the results obtained with the "Pitch Angle Capture" task in terms of time to achieve the desired pitch attitude angle change versus the pitch attitude angle change. Negative and positive pitch attitudes up to 60 deg have been achieved with a push-down or a pull-up manoeuvre from level flight and with several g-entry. The 90 deg pitch angle variation instead has been achieved with a level turn manoeuvre and the results do not reflect the trend of the vertical plane manoeuvres.

Compared with some actual production aircraft (Ref.6) pitch pointing performances were generally a bit lower, but one should keep in mind the operative role of the aircraft Compared against some experimental aircraft, however, the performance parameters are not very different

Pilot ratings between 3 and 5 were assigned to this kind of task with generally better comments given to "manoeuvre flaps/slats" than to "cruise flaps/slats" setting.

Inspite of a fast transient response, the main problem faced during the assessment was a quite difficult capture of final attitude because of uncommanded pitch oscillation. This problem, mainly accentuated with the "cruise flaps/slats" setting, is essentially due to the sharp non-linearity of the aerodynamic characteristic CL versus Cm at high incidence values. This phenomenon, depicted in figure 5 is classical for a conventional aerodynamic configuration.

The flight test results confirmed the above hypothesis and figure 6 shows, during a pull-up manoeuvre, an uncommanded pitch rate oscillation starting as AOA enters the non-linear region.

The best agility results achieved performing pitch down manoeuvres ($\Delta C = -30 deg$ on figure 4) confirmed the more linear aerodynamic characteristics for negative incidence.

The assessment highlighted, for a conventional aircraft, the dependence of pitch agility on AOA transient. Figure 7 shows different pitch agility results for the same task. The maximum agility performance is reached when the manoeuvre is performed at AOA value very near the operative limit.

For this reason, a very aggressive manoeuvre doesn't always yield the maximum pitch agility. During the simulation assessment, in the absence of actuation cues, the pilot tended to make abrupt stick inputs with g-onset generally exceeding 15 g's/sec. A more gentle manoeuvre permits a better control of the incidence achieving the best performance.

During the AM-X development, to enhance the pitch characteristic, reducing the pilot workload, an automatic flap selection (auto-manoeuvre), based on pitch rate and incidence sensed values, has been in-flight tested. Figure 8 shows a comparison of the same pitch manoeuvre with and without the control device. Despite the low rate of slat and flap actuation, a small slat deflection contributes to improved response from the very beginning, eliminating the pitch oscillation and reducing buffet and lateral unsteadiness associated with approaching the maximum AOA limits, thereby improving steady-state performance.

Simulation results indicate that the auto-manoeuvre device reduces pitch pointing agility times by up to 20%.

Roll Agility

Roll agility manoeuvres such as level wing capture from -90 deg bank attitude (90 deg bank variation) and 90 deg bank capture from -90 deg bank attitude (180 deg bank variation) have been assessed during the simulation study.

The global pilot rating for this task was 2 or 3 at medium-high speed and 4 at low speed.

Figure 9 shows the 90 deg bank variation results in terms of time to capture and maintain the desired bank angle within a defined threshold as a function of g-entry.

With a threshold of 10 deg of bank attitude a large results dispersion has been obtained. The poorest results at the beginning of the assessment were due to the low pilot training for this specific task. Familiarisation with the task led to a very good performance very similar to some actual production aircraft notoriously very agile for the operational role they cover.

The pilot technique affects significantly the time spent in the acquisition phase. If control technique is applied incorrectly the global time can double.

Specific training helps the pilot, for both low and high g-entry manoeuvres, to anticipate the lateral stick reversal necessary to capture the desired bank angle.

Figure 11 shows, for the same flight condition, the aircraft roll response and level wing capture with two different stick reversal anticipation.

Figure 10 demonstrates the degree to which proper anticipation of stick reversal can affect roll agility both low and high g-entry. The manoeuvre performed with optimum stick reversal leads to a global roll agility result in line with "MIL Spec. time to bank" requirement. Infact, providing adequate roll damping, the acquisition phase becomes very short compared with to the previous transient and steady state phases.

Unlike the pitch agility, roll agility can be significantly improved through adequate pilot training.

Of course, if in some region of the flight envelope, the flying qualities degrade the above conclusion is not guarantied. At low speed for example, the degradation of lateral-directional tracking characteristic leads to difficult bank angle captures. The higher pilot workload was the reason for the worse pilot rating.

Moreover, at the flight envelope limit, beyond the 80% of the normal load factor limits, even if no specification is given for the roll performances, from an operational stand-point it is desirable to maintain a suitable lateral manoeuvrability avoiding the roll capability as being a limiting factor for the maximum angle of attack allowed.

In the AOA range approaching the stall, due to a rapid collapse of the lateral-directional stability along with a control effectiveness reduction, the AM-X exhibited a lateral manoeuverability degradation, with lateral unsteadiness build-up and possible departure condition if the stall was aggravated by the lateral control.

Performing a roll manoeuvre increasing the incidence angle, the deficiencies were at first evident as a roll hesitation and then as a roll reversal.

Figure 12 shows the in-flight results relevant to an objectionable situation. With a sustained full lateral stick, at an angle of attack near to the stall, a large adverse sideslip build-up generates a roll acceleration inversion with a consequent roll-reversal.

Predictions using the Weissman departure criteria, reported in figure 13, shows that the aircraft, in the original configuration, exhibited a rapid loss of LCDP which becomes negative at α-values lower than the α-stall by a few degrees. Point I is the corresponding point for the in-flight manoeuvre of figure 12.

During the AM-X development, to enlarge the aircraft operability, these poor characteristics have been carefully examined undertaking corrective actions both via aerodynamic changes (ventral strakes) and via FCS modifications (lateral-directional interconnection).

To improve the roll performances within this area, up to the stall, a roll-to-yaw interconnection has been designed which causes the rudder to be deflected as a function of the lateral and longitudinal stick displacement. The advantages associated with this solution are shown in figure 14: the $LCDP - vs - Cn_{\beta_{dyn}}$ curve, in the α range up to the stall moves toward the positive value of LCDP.

Flight tests confirmed the predicted improvement for the roll characteristics up to the stall angle as can be seen in the "time-histories" presented in figure 15 related to points II and III on the previous analytical criteria. The roll manoeuvre performed at the α-stall (point III) is still acceptable, even if the low LCDP contributes to generate continuous roll rate oscillation.

Improvements in terms of roll rate versus angle of attack (shown in figure 15), removing the roll departure conditions, has permitted a definition of a safer permissible AOA limits allowing the pilot to concentrate more on the battle field operations than on avoiding the AOA limit.

Flight Path Agility

Figure 16 shows the simulation results in terms of time to acquire the Normal load factor versus flight speed. Several g-entry conditions for pull up and push down manoeuvre have been tested.

Only the "manoeuvre flaps/slats" configuration has been considered for this task avoiding the objectionable pitch characteristics which affect the longitudinal task (pitch pointing agility) with flaps/slats up.

Even when the task was executed with the load factor cue presented on the H.U.D. with an alphanumeric format with a refreshment frequency of 10 Hz, the pilot rating was satisfactory and within a range from 2 to 3.

Results show similar best time-to capture for both positive and negative load factor variations.

Results showed generally low dispersion for the pull up manoeuvre. The high g onset, greater than 10 g/sec consent to achieve very rapidly the desired load factor, while the pitch oscillation at high incidence, fairly small with the manoeuvre flap configuration, do not affect the phase of final precise acquisition.

Compared with pull-up manoeuvre results, push-down manoeuvre at high speed showed a larger dispersion. This effect has been attributed to the greater control surface effectiveness at low incidence, which provides pitch down acceleration higher than at high AOA, causing load factor overshoot and increasing the pilot workload in the acquisition phase.

Also for this task the results are strongly affected by pilot technique particularly for push down manoeuvre where the behaviour is less predictable and pilots take longer to adapt. Being g-load and g-unload the basic of fight manoeuvering it is hence possible to improve agility and operational effectiveness through specific training.

Yaw Pointing Agility

Figure 17 shows the results, from simulation, of the yaw pointing agility task. The time to acquire and maintain 5 deg of heading angle change, with no change in bank angle, is plotted versus the speed.

A degradation from high to low speed has been highlighted with a pilot rating from 3 to 5.

At low speed, the main problem was the high pilot workload to maintain wing level. Large lateral stick displacement was required to counteract the high sideslip build-up, and oscillations increased significantly the time to capture the desired attitude change.

From an operational point of view, this task would be useful for evaluating fine target tracking adjustments prior to weapon release.

6.0 OPERATIONAL AGILITY SIMULATION RESULTS

Considering the primary role of the AM-X, namely ground attack, some phases of the final approach to the target have been examined as a composition of several agility segments with the final task to achieve the weapon release condition in the shortest time.

Figure 18 shows a possible approach to the target. A turn with almost -90 deg bank in dive is followed by a roll manoeuvre to level the wing within a threshold of +/- 10 deg with a final target acquisition

Note: The threshold of +/-10 deg, used in the roll agility assessment, is the bank angle range within which the ground avoidance algorithms are reliable. This function provides the break-away cross to be displayed on the HUD indicating to the pilot the last possible moment to initiate a pre-defined pull-up manoeuvre for the dive recovery maintaining a limited altitude margin from the ground.

The final target acquisition is achieved in the last weapon aiming phase positioning the steering line and pipper of the "Continuous Computed Impact Point" (CCIP) on the target. The "Weapon Aiming Display Driving" provides the display of this function on the H.U.D.

The global attack manoeuvre can be divided into several agility segments.

1 High-g's turn with 90 deg of heading variation

  From a 5 g-entry condition turn at 7 g's up to achieve 90 deg of heading variation. With almost 90 deg of bank the manoeuvre corresponds to a 90 deg of pitch acquisition on a horizontal plane.

2 Unload from 7 g's to 1 g maintaining the 90 deg of bank angle

3 Roll manoeuvre from -90 deg to level wing in dive

  This manoeuvre is concluded when the bank angle is within the threshold of +/- 10 deg

4 Weapon aiming and release

  This phase includes the fine yaw pointing, positioning the steering line of the CCIP on release window

5 Pull up manoeuvre at break-away cross display, to achieved the defined load factor necessary for ground avoidance

Although the last manoeuvre is performed after the main objective of weapon release has been completed, the agility time to achieve the steady state condition is an important part of the weapon delivery effectiveness. For a given margins, a faster time to achieve steady state load factor, permits a lower altitude where the break-away cross appears, and a release point closer to the target.

The figure 19 compares the results, in term of agility time, of the individual manoeuvre segment. When final weapon aiming is free from closed loop pilot/vehicle/display system deficiencies, the total agility time to achieve weapon release window is not very different from the sum of the times for each individual agility tasks presented in par.5. However problems arise whenever such closed-loop deficiencies do not permit easy tracking and prolong the total time to reach the weapon release window (Ref.8)

Figure 20 shows, for several types of bomb, the optimum weapon aiming envelope in terms of speed, altitude and dive angle, which were deemed necessary to guarantee satisfactory target tracking, with significant reduction of the time to achieve the weapon release window and consequently the time of exposure to threats.

Figure 21 shows a similar ground attack manoeuvre. In this case the aircraft starts from an inverted flight (almost 180 deg bank) in climb, followed by a roll manoeuvre up to wing level and a push-down for the acquisition of a certain dive angle .

This kind of manoeuvre, from an operational stand-point, is similar to the pop-up manoeuvre used to pass over a hill and roll in on the target in dive.

The overall attack manoeuvre can be divided into several agility segments:

1 Roll manoeuvre from -180 deg to wing level

  This manoeuvre is concluded when the bank angle is within the threshold of +/- 10 deg

2 Push-down manoeuvre to achieved the desired dive angle

3 Weapon aiming

4 Pull up manoeuvre at the break-away cross display, to achieved the defined load factor necessary for ground avoidance

At the beginning, operational pilots, coming from other ground attack aircraft, were accustomed to perform the first two manoeuvre segments with a diagonal stick command (Ref.9). The intent of the rolling push-down manoeuvre was the achievement of higher roll rate in order to reduce the overall time of target acquisition.

With the AM-X the large proverse sideslip build-up due to pitch-down produced very high roll rate (greater than 300 deg/sec) reducing the time to achieve the wing level attitude but increasing significantly the pilot workload and the time to stop the aircraft at wing level.

Figure 22 presents, from manned simulation, the time histories of such a manoeuvres. Despite the gentle roll, the manoeuvre with combined push down does not permit an easy bank control at wing level attitude.

In some case of rapid rolling, during the capture phase, the high roll sensitivity and the large bank overshoot required large lateral stick displacement, causing a very dangerous lateral overcontrol considering the low altitude.

This combined manoeuvre was prohibited and a specific "warning" introduced in the "Flight Manual".

Figure 23 compares the total agility time to achieve, from the inverted flight, the wing level and 30 deg of dive angle, performing several commands in sequence. Performing roll followed by push down manoeuvre led to the best performance with 20% of time less than a pull down followed by a roll and 30% less than a combination of roll and push down manoeuvre.

7.0 CONCLUSIONS

The Agility concepts were originally developed as a methodology to better evaluate and compare the operational effectiveness of advanced air-to-air fighters. Nevertheless this on-going research, is showing that agility concepts may be effectively applied to the evaluation of aircraft of different roles, e.g. a conventional, ground-attack aircraft like AM-X.

The study was supposed to be mainly conducted by simulation, with flight tests only for validation of results. Even though agility manoeuvres tested were of large amplitude, the lack of some external cues (g-force) did not negatively influenced pilot opinion of the simulator that have been well accepted for this kind of testing.

The agility assessment permitted to identify some problems concerning the conventional configuration of the tested aircraft. The agility tasks on the longitudinal plane pointed out some deficiencies for large attitude acquisition that have been attributed to the strong aerodynamic non-linearity at high AOA typical of the configuration tested.

Due to the low predictability of response it would be difficult to improve pitch agility through specific pilot training alone. An automatic flaps/slats selection device instead, permits a global agility time reduction of about 20% with full pilot attention on the battle field.

The roll agility task highlighted a greater predictability of response. An effective enhancement is expected with adequate pilot training on the manoeuvre technique.

The agility manoeuvres used revealed some flying qualities characteristics quite interesting from an operational point of view. Of particular interest is the fact that the methodology study did permitted to assess the performance of the entire weapon system, thus including in the assessment the interaction of the pilot with the system as well.

Following the operational assessment, definition of an "optimum weapon aiming envelope" was deemed necessary to improve overall weapon system effectiveness, while limitation of large combined stick inputs during the ground attack phase, were considered for safety.

Future test activity planned is the simulation of more complex agility manoeuvres up to the completion of mission task elements and flight test trials to validate the simulation results.

The objective of this part of activity will be to optimize the operational application of the aircraft allowing to draw guidelines for an improved operational pilot training.

REFERENCES

Ref.1 "Operational Agility", AGARD WG 19, July 6 1993

Ref.2 "Qualitative and Quantitative Comparison of Government and Industry Metrics", Journal of Aircraft, March 1990, Bitten

Ref.3 "Aircraft Agility the Science of the Opportunities", Paper AIAA 89-2015, M.Dorn

Ref.4 "Agility as a Contribution to Design Balance", Paper AIAA 90-1305, A.Skow

Ref.5 Parametric Effect of Some Aircraft Components on High-Alpha Aerodynamic Characteristics", AGARD CP ..., Visintini, Fertile, Mentasti,

Ref.6 "Flight Testing for Aircraft Agility" Paper AIAA-90-1308-CP, S.L.Butts, A.R.Lawless

Ref.7 "Relationships Between Agility Metrics and Flying Qualities", Paper AIAA 90-1003, D.R.Riley, M.H. Drajeske

Ref.8 "Flying Qualities Experience with the AM-X Aircraft", AGARD CP-508, R.Dava

Ref.9 "AM-X Flight Simulator, From Engineering Tool to Training Device", AGARD CP.513, A.Armando, P.Castoldi, F.Fassi

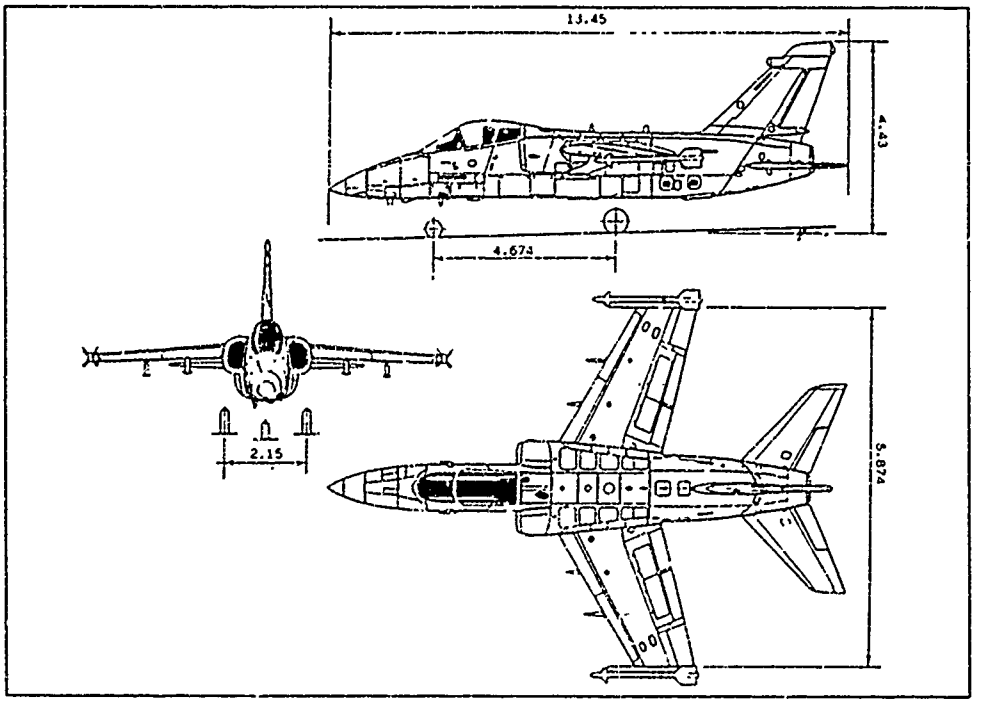

Fig.1 - AM-X Three View

PITCH ANGLE CAPTURE

OBJECTIVE

CHANGE BODY AXIS PITCH ANGLE AND STABILIZE AT THE TARGET PITCH ANGLE IN MINIMUM TIME

FLIGHT TEST TECHNIQUE

a. WINGS LEVEL TECHNIQUE

- TRIM AT TARGET AIRSPEED AND ALTITUDE
- PULL TARGET LOAD FACTOR TO ACHIEVE DESIRED ATTITUDE CHANGE
- HOLD AT FOR t=1 sec WITHIN +-3° WINDOW

b. WING BANKED TECHNIQUE

- ACHIEVE SET UP LOAD FACTOR IN LEVEL TURN
- UPON REACHING PREDETERMINED LANDMARK BANK TO 90° +-5°
- PULL TARGET LOAD FACTOR TO ACHIEVE DESIRED HEADING CHANGE
- HOLD (y) FOR t=1 sec WITHIN +-3° WINDOW

BANK ANGLE CAPTURE

OBJECTIVE

CHANGE FROM A BANKED CONDITION AND STABILIZE AT TARGET BANK ANGLE IN MINIMUM TIME MAINTAINING TARGET LOAD FACTOR WITH A TACTICALLY SIGNIFICANT LEVEL OF PRECISION

FLIGHT TEST TECHNIQUE

- STABILIZE A LEVEL TURN AT INITIAL CONDITIONS
- ACHIEVE STEADY 60° BANK
- ROLL TO +90° (0°) (over the top) HOLDING LOAD FACTOR
- HOLD +90° (0°) BANK FOR t=1 sec WITHIN +-5° WINDOW

LOAD FACTOR CAPTURE

OBJECTIVE

CHANGE LOAD FACTOR Nz AND STABILIZE AT THE TARGET nZ IN MINIMUM TIME WITH A TACTICALLY SIGNIFICANT LEVEL OF PRECISION

a. WING LEVEL TECHNIQUE

- ACHIEVE SETUP AIRSPEED, ALTITUDE AND LOAD FACTOR
- PULL (PUSH) TO ACHIEVE DESIRED LOAD FACTOR CHANGE
- HOLD Nz FOR t=1 sec WITHIN +- 5g WINDOW

b. WING BANKED TECHNIQUE

- SET TARGET SPEED +- 10 KTS AT TARGET ALT +/-100 ft INITIAL Nz +- 5g IN A LEVEL TURN
- ROLL TO 90° +- 5° BANK
- UPON REACHING 90° BANK ACHIEVE DESIRED Nz
- HOLD Nz FOR 1 sec, +- 5g BANK 90°

LEVEL YAW

OBJECTIVE

ACHIEVE HEADING CHANGE IN STEADY SIDESLIP WITH WINGS LEVEL IN MINIMUM TIME

FLIGHT TEST TECHNIQUE

- STABILIZE AT INITIAL CONDITIONS
- APPLY FULL RUDDER PEDAL FORCE AND HOLD (WINGS LEVEL)
- HOLD HEADING CHANGE FOR t>2 sec WITH WINGS LEVEL

Fig.2 - Single Axis Agility Manoeuvres Tested

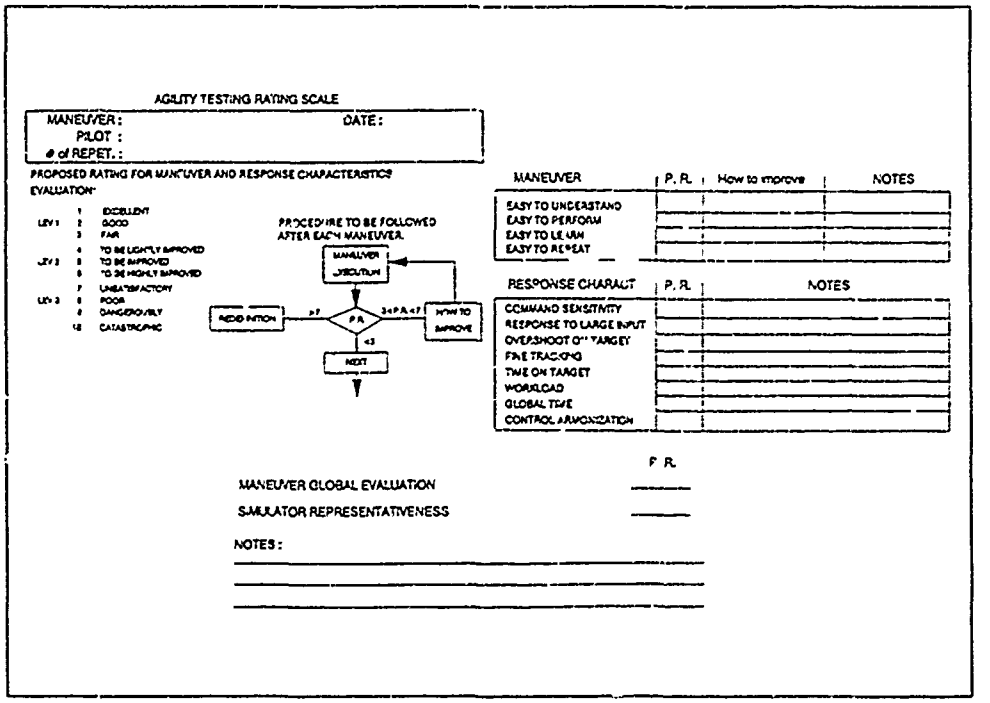

Fig.3 - Pilot Rating Questionnaire

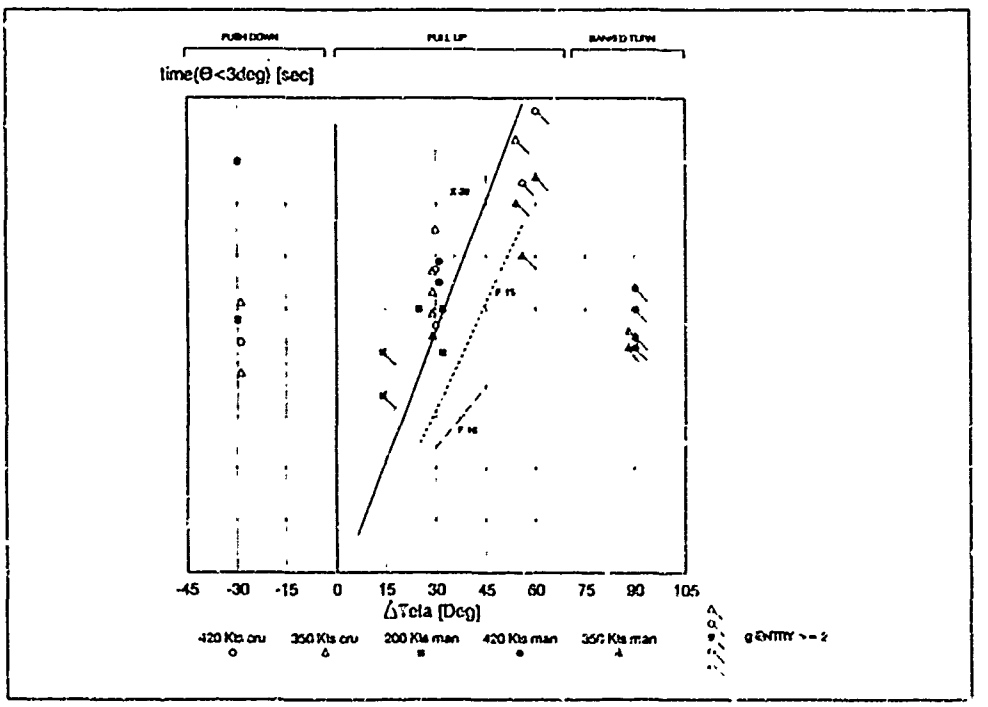

Fig.4 - Pitch Pointing Agility Results

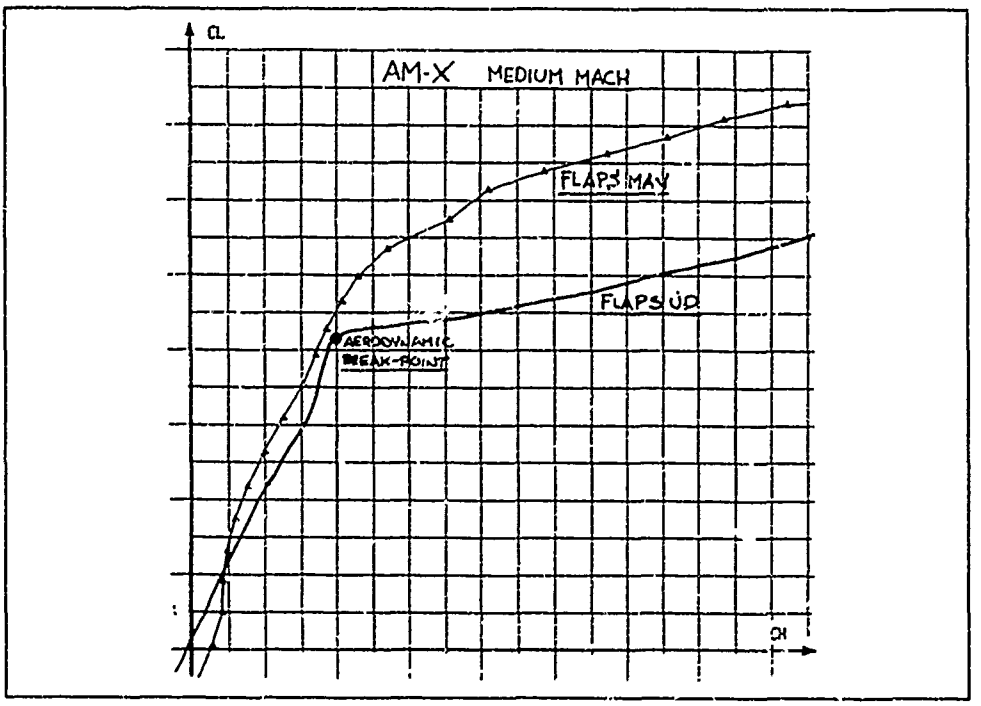

Fig.5 - Non-Linear Aerodynamic Characteristics Cl & Cm

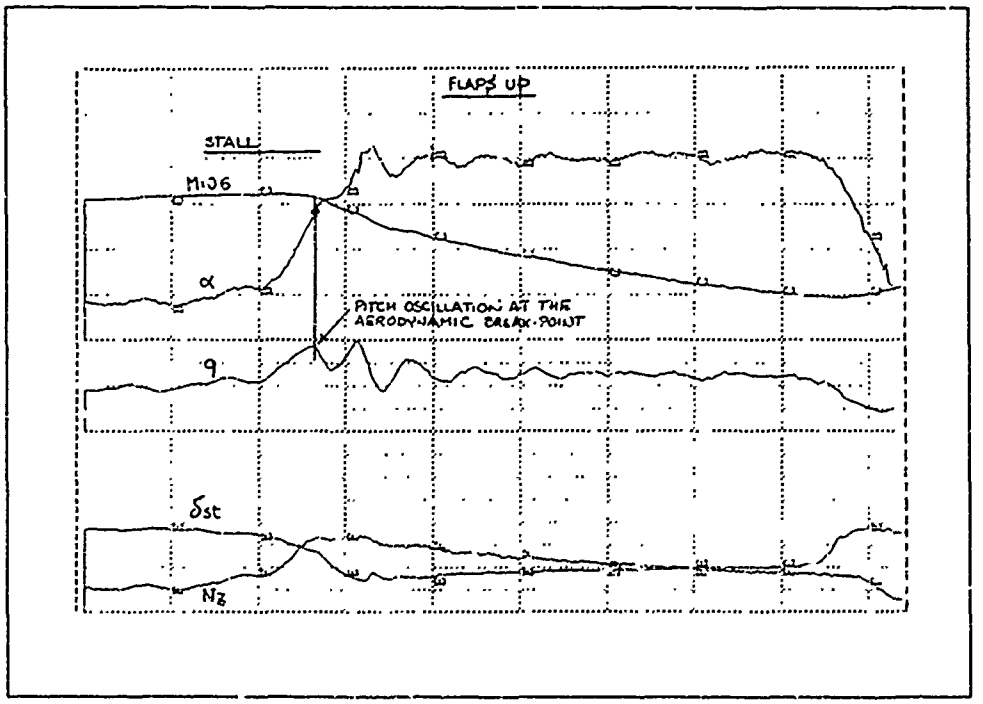

Fig.6 - In-Flight Test: Large Longitudinal Manoeuvre

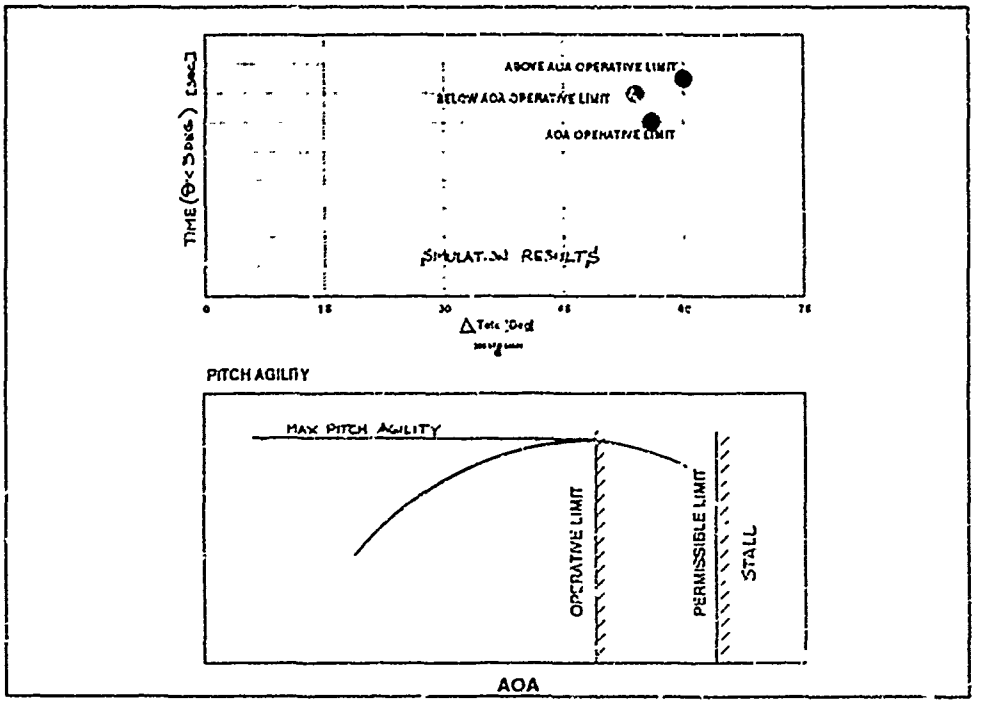

Fig.7 - Maximum Pitch Agility for a Conventional A/C

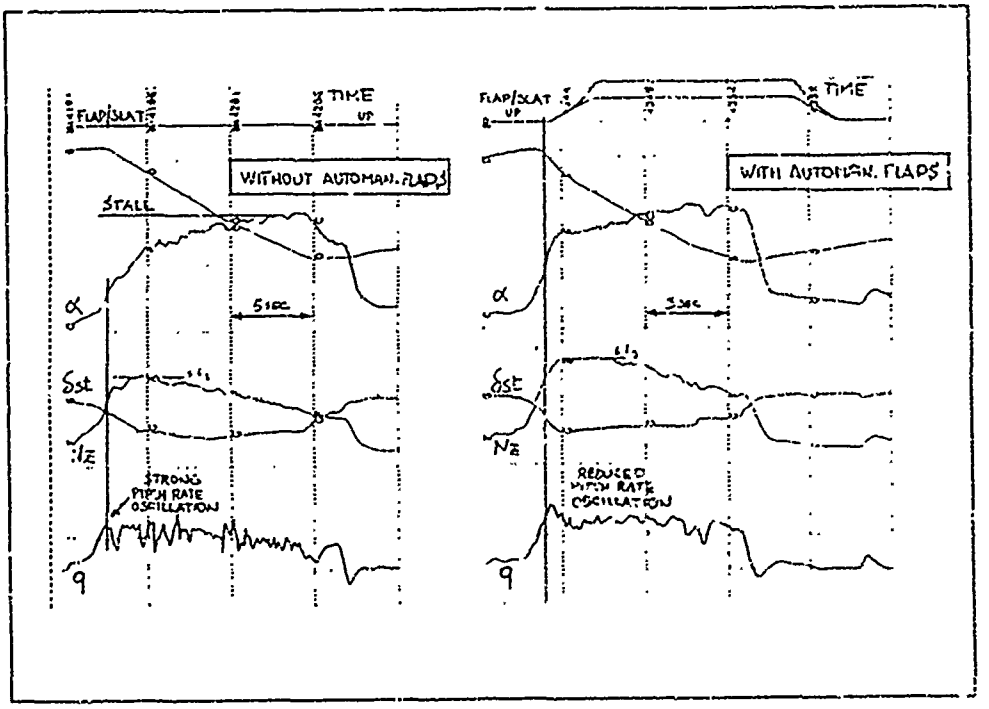

Fig.8 - In-Flight Test: Automatic Flaps/Slats Selection

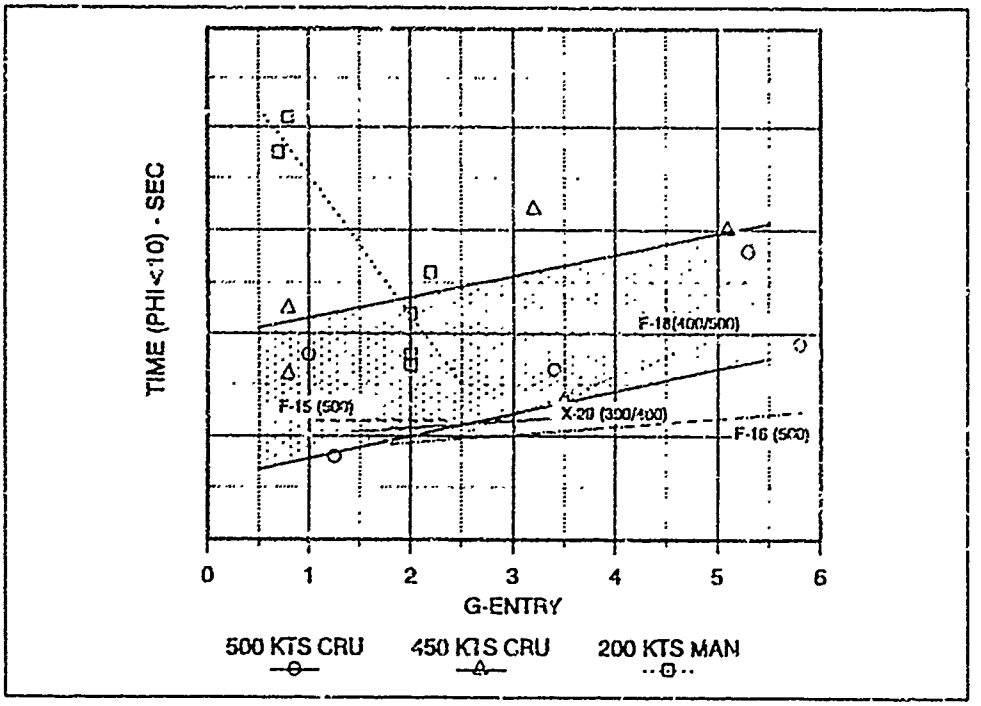

Fig 9 - Roll Agility Results: Level Wing Capture from -90 deg Bank

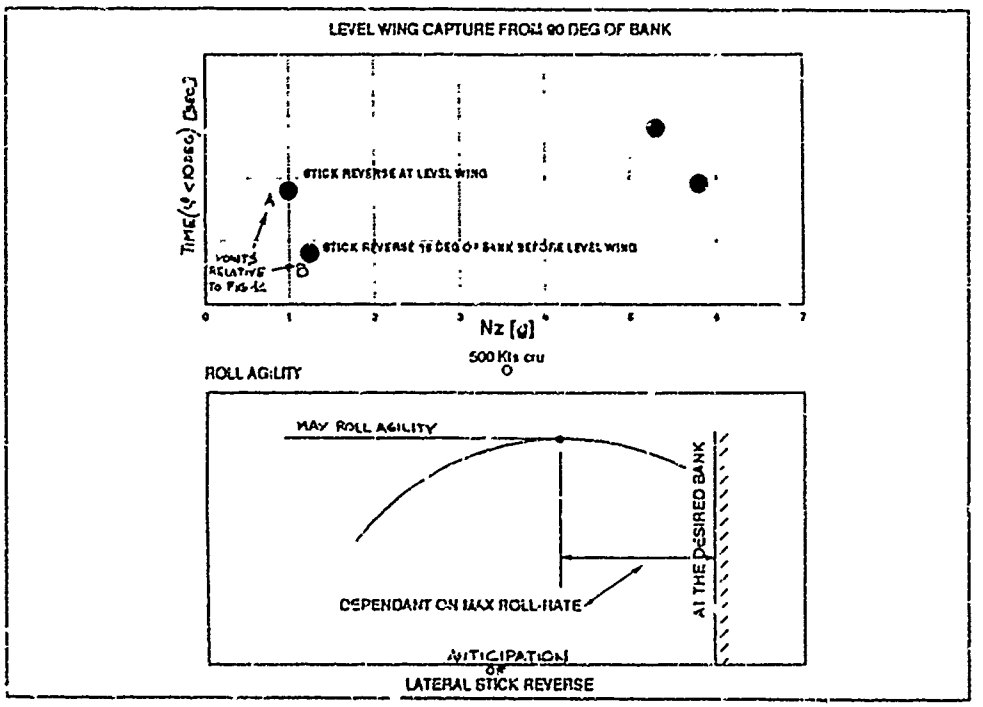

Fig.10 - Effect of Stick Reverse Anticipation on Bank Acquisition

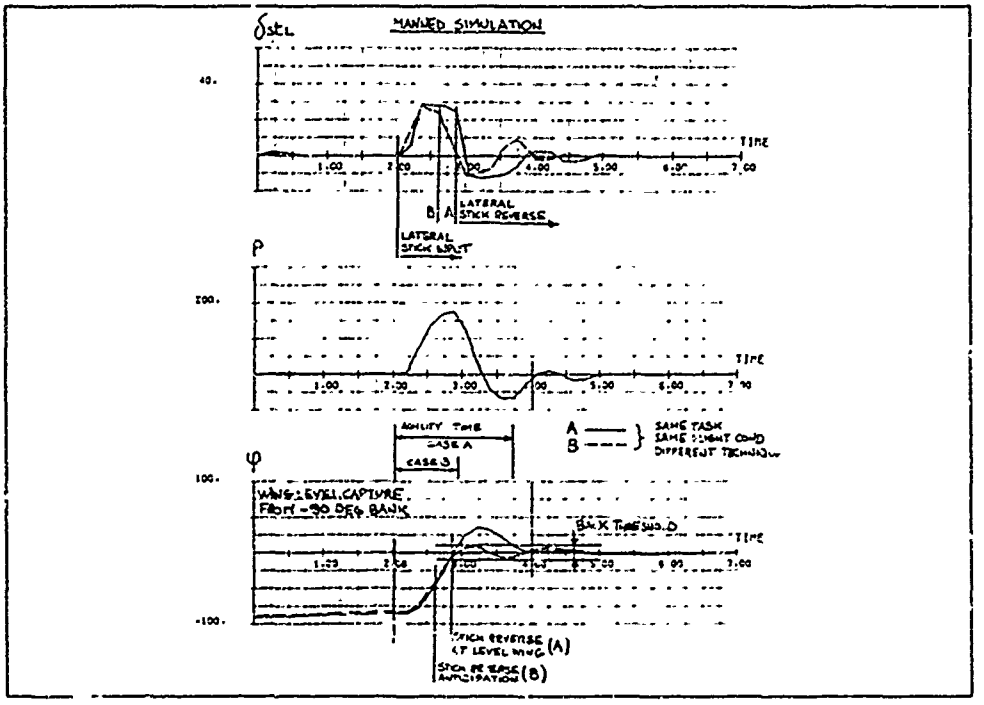

Fig.11 - Roll Agility Time Response

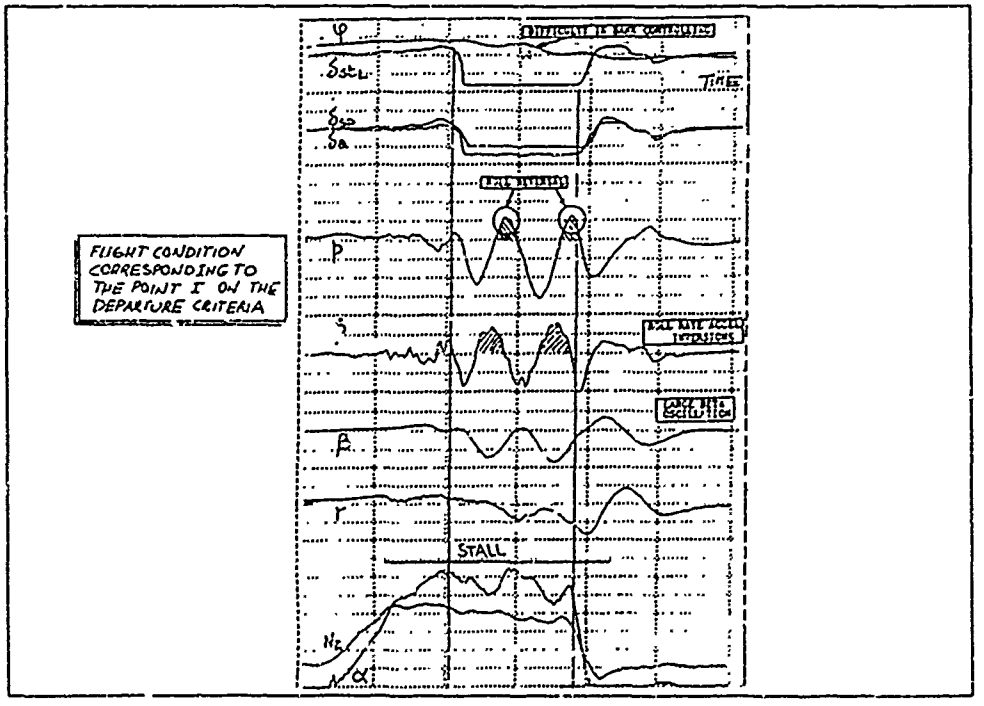

Fig.12 - In-Flight Test: Uncommanded Roll Reversal at High AOA

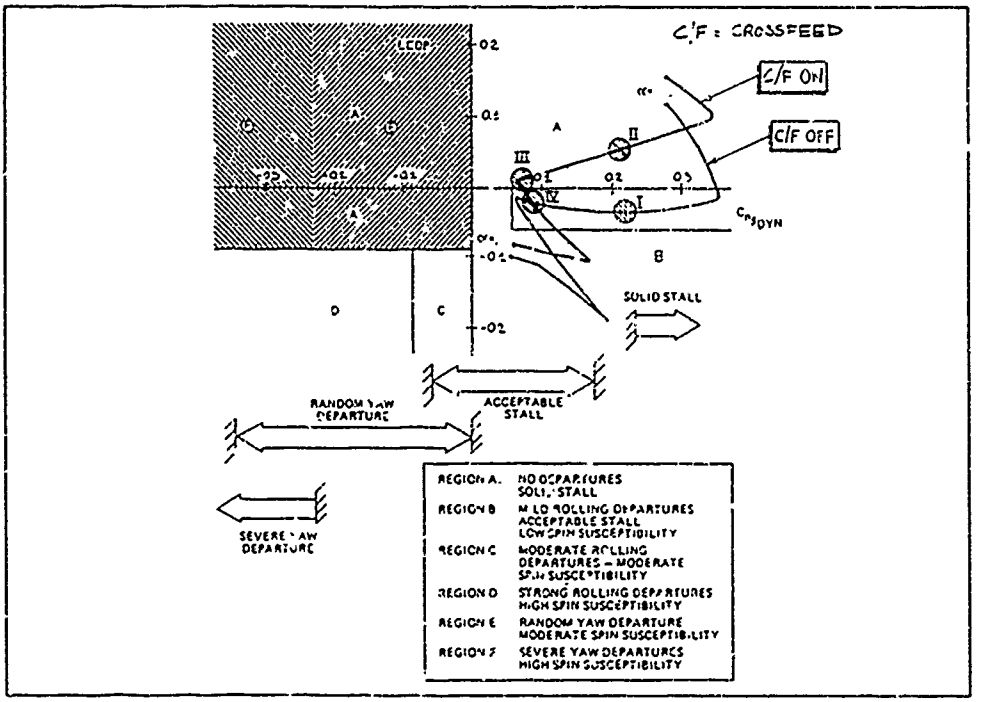

Fig.13 - Objectionable Roll Characteristics Prediction

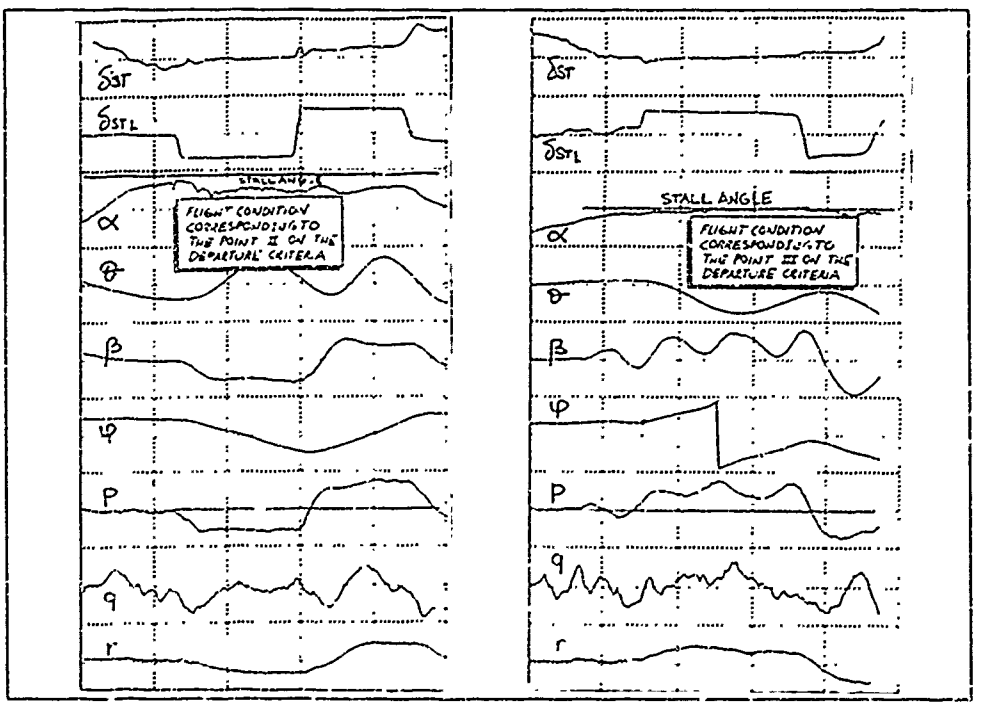

Fig.14 - Improvement of Roll Characteristics with Corrective Actions

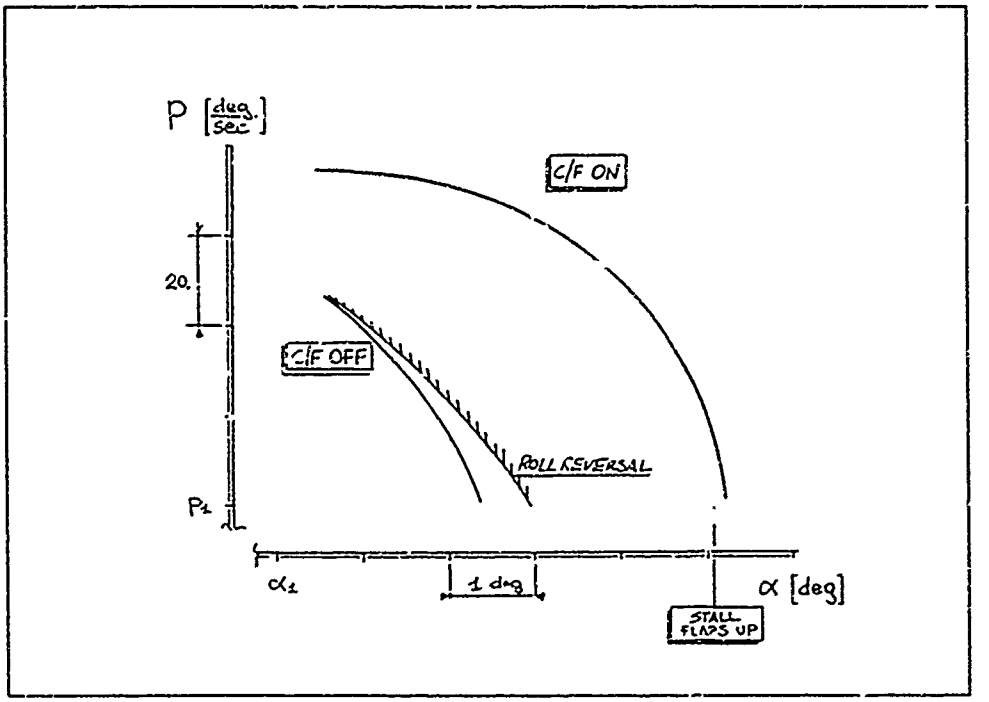

Fig.15 - Roll Performance/Agility Improvement Versus AOA

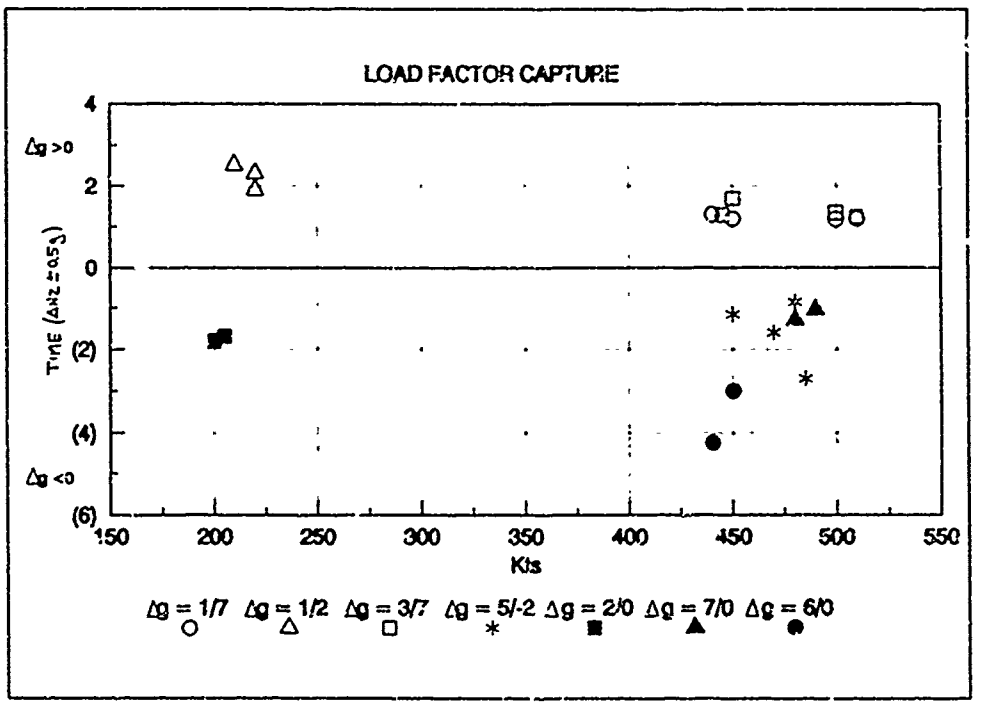

Fig.16 - Flight Path Agility Results: Load Factor Capture

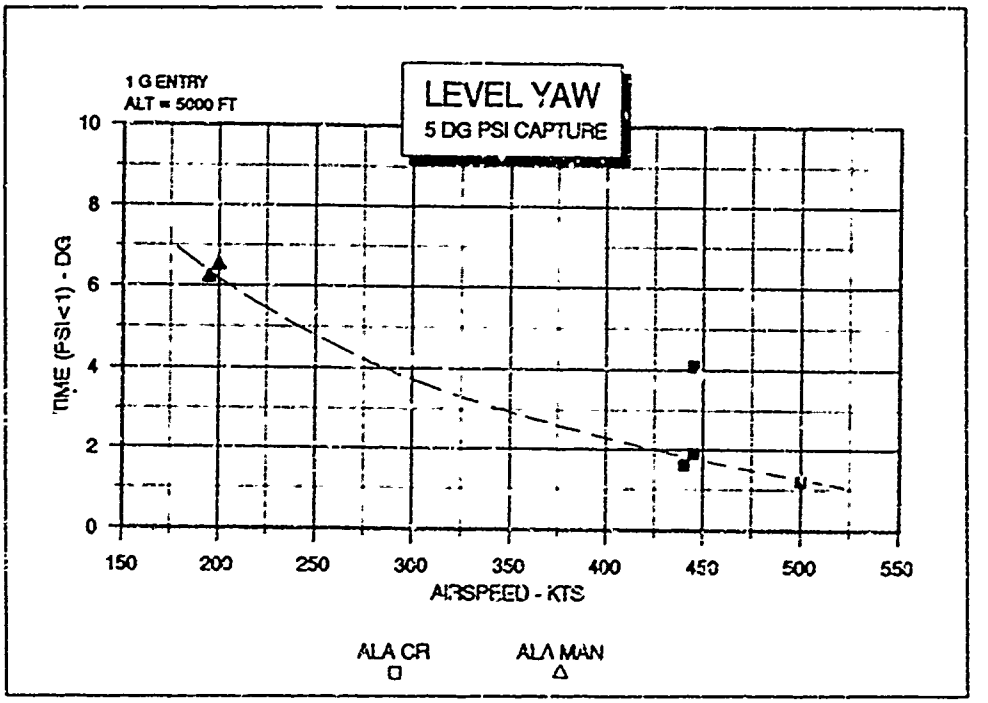

Fig.17 - Yaw Pointing Agility Results

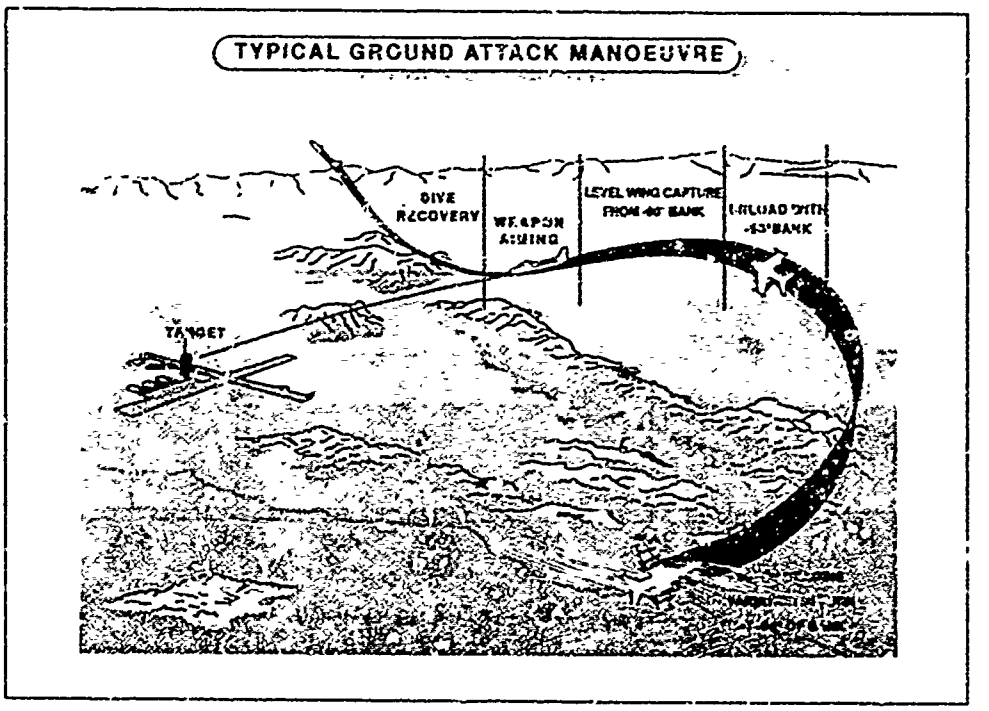

Fig.18 - Typical Ground Attack Manoeuvre

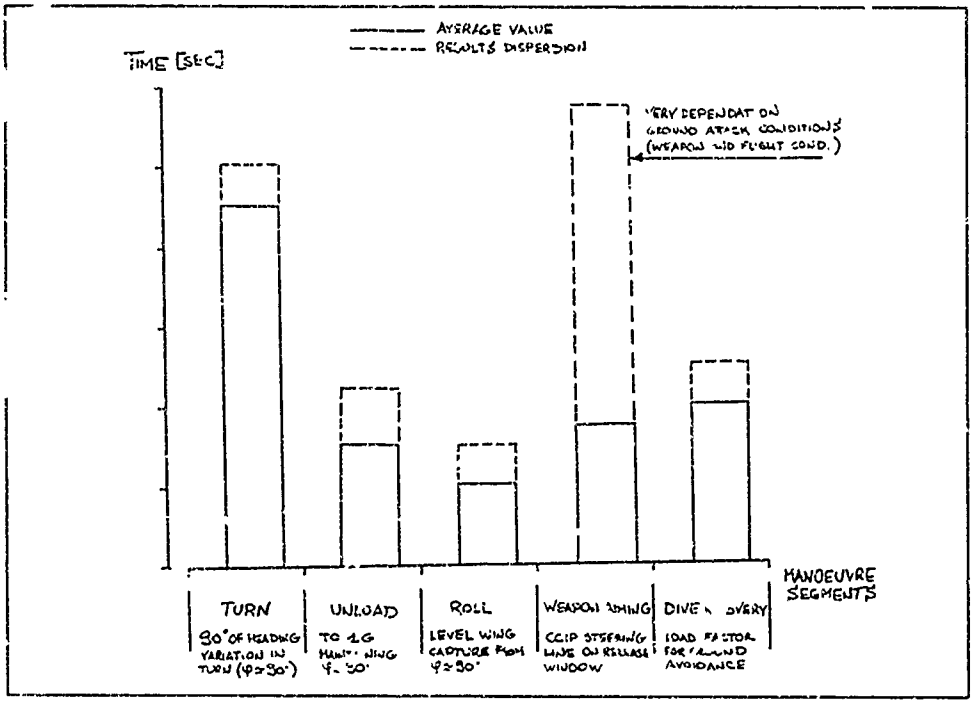

Fig.19 - Comparison of the Agility Time of Several Manoeuvre Segment

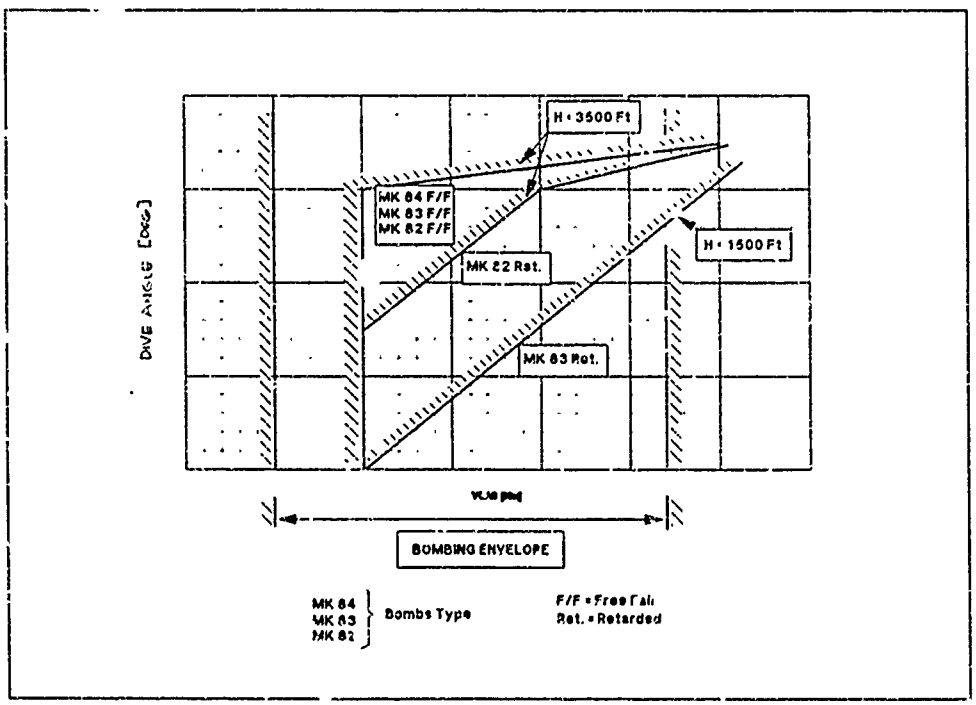

Fig.20 - Optimum Weapon Aiming Envelope

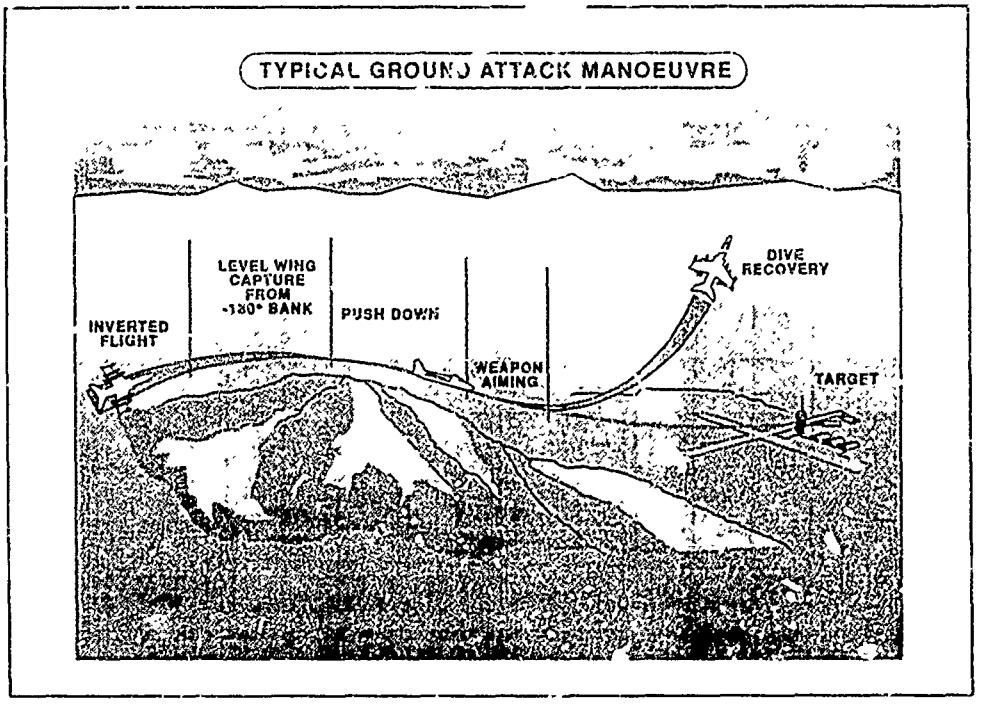

Fig.21 - Typical Ground Attack Manoeuvre

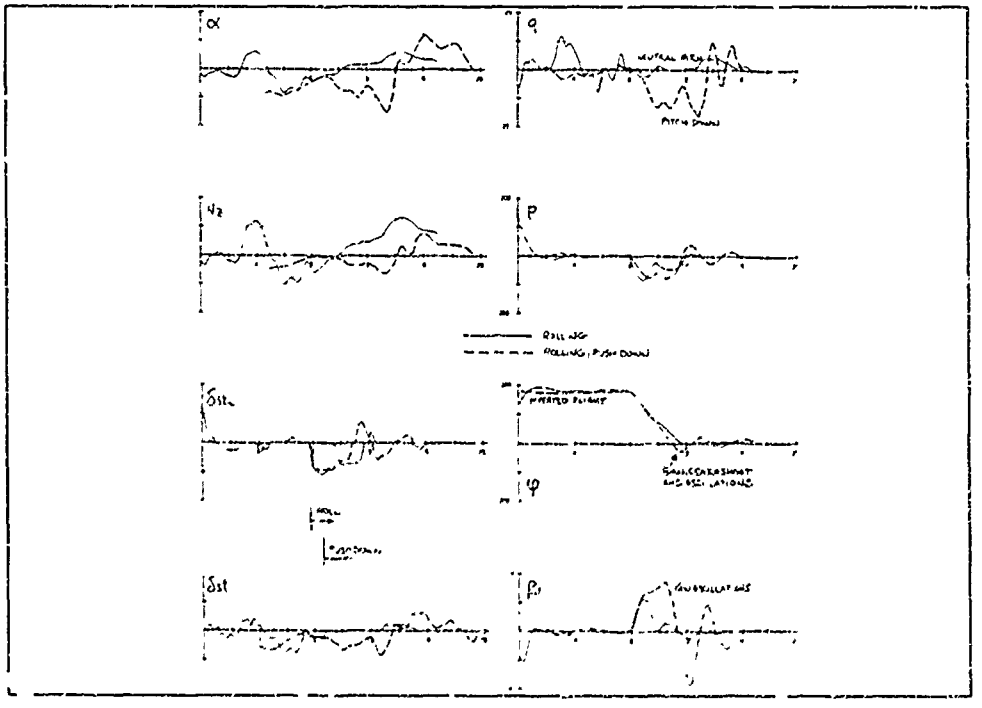

Fig.22 - Combined Rolling-Pitch Down Manoeuvre

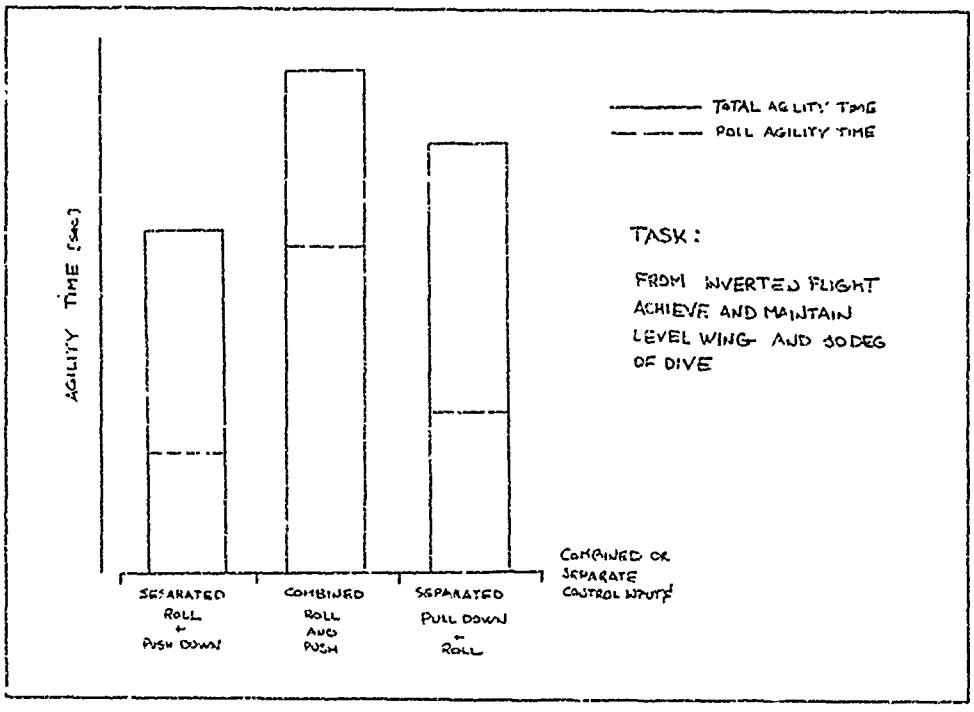

Fig.23 - Total Time Comparison of Several Combined Manoeuvre

Task	Agility Metric	
	Nose Pointing	Flight Path
Pitch Angle Capture	Time to capture $\Delta\theta$	
Bank Angle Capture		Time to capture $\Delta\Phi$
Load Factor Capture		Time to capture ΔNz
Level Yaw	Time to capture $\Delta\Psi$	

Tab. 4.1 - Single Axis Agility Tasks

EXPANDING THE PILOT'S ENVELOPE

Bruce E. Hamilton, PhD
Manager, RAH-66 Crew Station Design
MS Z102A
Sikorsky Aircraft
Stratford, CT 06601-1381
USA

1. SUMMARY

Advances in aircraft technology have allowed the construction of fighters which can easily exceed the pilot's capability to react and to sustain G forces. Advances in avionics have allowed these airframes to be fitted with sensors, weapons, and data processors to the point that the workload associated with mission accomplishment sometimes exceeds the pilot's capabilities. Consequently, some aircraft capabilities are rarely used due to lack of familiarity. These developments highlight the fact that the ability of the aircraft to fulfill its mission is dependent upon the pilot's utilizing its capabilities as an integrated weapon system. Pilots, like airframes, have operational envelopes and expanding the pilot's envelope allows fuller exploitation of the airframe's envelope and the avionics capabilities. The nature of the pilot's envelope is presented along with attributes of a pilot interface which support expansion of the pilot's envelope.

2. INTRODUCTION

Air-to-air combat began in World War I with men who flew in open cockpits. These earlier fighter pilots achieved their victories with air sense, sharp eyes, quick reflexes and gun sights. Victory in a first-generation fighter was often more a function of pilot skill and surprise rather than aircraft maneuverability. During World War II, high maneuverability was often achieved by reducing overall aircraft weight through reductions in armor protection. Ultimately, it proved easier to replace less maneuverable aircraft which returned their pilots than to replace the pilots of more maneuverable aircraft which were lost.

Avionics began influencing air-to-air combat during the Korean conflict and changed the maneuverability equation during the Vietnam conflict. It was thought that radar and missiles meant an end to dogfight style air-to-air combat. This thought was proven wrong and maneuverability without sacrificing pilot survivability became a major thrust. In the years since Vietnam, avionics have undergone revolutionary advances on a scale that rivals the advances in fighter maneuverability. Achieving a victory today requires the ability to use the electronic aids to gain better situation awareness while simultaneously exploiting a large maneuverability envelope.

While the technologies of air-to-air combat have advanced, today's pilot remains unchanged from the pilots who flew biplanes. As a result, today's fighter cockpit often demands more attention than many pilots can provide during time critical situations as evidenced by reports of high workload and task saturation. Pilot's, like an airframe, have an operational envelope. Like an airframe, demands which place the pilot outside of his envelope result in loss of performance. The next major advance in maneuverability needs to be in the pilot's ability to use tactically the capabilities provided; that is, to keep the pilot within his envelope. To do this, man-machine interface technology must be developed to enable the pilot t integrate flight maneuver and tactical avionics into situation awareness.

3. DEFINING THE PILOT'S ENVELOPE

Humans have amazing plasticity but they do have limits. These limits define the human envelope. Placing pilots outside of the human envelope may cause a degradation in performance similar to exceeding an operational flight envelope. Also, some excessive conditions may cause cessation of performance not unlike exceeding a structural flight envelope. One example of exceeding human limits is G (the force of gravity) induced loss of consciousness (GLOC). Sustained or excessive Gs will cause loss of consciousness.

This paper considers the pilot's envelope as having three primary components, physiological, environmental, and attentional demand. Categorization of the pilot's envelope into three components is a simplification of a complex topic which remains the subject of ongoing research. The lack of agreement as to how pilot physiology/ psychology and crew performance interact and influence each other makes quantitative statements about the pilot's envelope risky; however, qualitative statements about the envelope can be drawn and are quite useful to the engineering community. Each of the three primary components of the pilot's envelope is briefly defined in the following section.

3.1 Physiological Limits

Physiological limits are the best understood of the primary components of the human envelope. These limits are comprised of five factors, G, temperature, vibration, noise, and fatigue. The first four factors are imposed upon the pilot, the last, fatigue, is the product of the first four. In total, these five factors determine the pilot's physiological limit.

Presented at an AGARD Meeting on 'Technologies for Highly Manoeuvrable Aircraft', October 1993.

When the body is subjected to positive G forces over time, blood drains from the head to the chest. As blood flow reduces, brain functions diminish. The first noticeable symptom tends to be reduction in visual field, the so-called gray-out. If conditions continue, black-out occurs. G loss of consciousness (GLOC) tends to occur with rapid onset of 6 Gs but can occur at levels as low as 4 G if onset is unexpected. The US Air Force and US Navy have reported that as many as 12% of their aviators have experienced GLOC[1]. Besides strict black-outs, extended periods of functional incapacitation follow GLOC. Straining maneuvers, anti-G suits, and reclined seats are used typically to ameliorate the effects of G. Normative curves for G tolerance can be generated and these curves are relatively consistent in their response to other variables.

Extremes of temperature limit life and performance. At high or low temperatures the body is unable to cool or heat itself and unconsciousness occurs. The performance envelope temperature range is much more restricted than the pure survival temperature envelope. Deep body temperature increases of only 4°F can cause performance decrements after only 30 minutes[2]. Ambient effective temperatures of 85° - 90°F can drive the deep body temperature up by the .4°F needed for performance decrements. Severe environments up to 115°F cause more extensive decrements in shorter time periods. Normative curves for temperature tolerance can be generated and these curves are relatively insensitive to other variables. Most aircraft are built to specifications that control and limit the range of allowable temperatures; however, the impact of protective ensembles has not yet been adequately addressed.

Vibration reduces the pilot's ability to read displays and maps, to make fine motor movements (using hand controllers and pushing buttons), and to concentrate on secondary tasks. Fatigue is dramatically affected by prolonged vibration exposure. Most aircraft are built to specifications that limit the amount of vibration

Noise in the cockpit interferes with communications and can, over time, result in fatigue and general performance decrements. Most aircraft are built to specifications that limit the amount of noise in the cockpit. The focus in this area is now turning to the issue of speech intelligibility as opposed to that of noise level.

Perry[3] defined fatigue as "those changes that affect an individual consequent upon continued activity. The changes are typically a deterioration in the aviator's performance, or an increased cost or effort for a given level of performance, and characteristic subjective feelings that may include irritability, tenseness, mental sluggishness, tiredness and lack of energy. The exact pattern of effects will depend on whether the task is physical or mental and on the motivation of the aviator." He further states that "The main changes in performance due to skill fatigue can be summarized as:

(a) A deterioration in the accuracy of timing of the components of the skilled task with a consequent decrease in the level of skill.

(b) The pilot accepts lower standards of accuracy and performance on his own part without an appreciation that he is doing so.

(c) A disintegration of the perceptual field so that the readings from individual instruments are no longer integrated into an overall pattern.

(d) A narrowing of the pilot's range of attention so that some instruments or tasks (particularly the peripheral ones) are forgotten or ignored."

Fatigue is influenced by a variety of factors many of which are external to the aircraft. Aircraft related causes of fatigue are temperature, vibration and noise. Fatigue is variable and almost impossible to estimate. No accepted curves relate fatigue to performance because the measurement of fatigue is uncertain and performance is dependent upon the specifics of a single task. In aviation, the tasks are constantly changing but in general, higher fatigue levels lead to higher error rates and reduced concentration. Despite resistance to quantification, fatigue limits the pilot's ability to perform and must be considered.

3.2 Environmental Modifiers

The second primary component defining the pilot's envelope is environmental modifiers. This paper includes vision, controls and displays, and training as environmental modifiers. While these are arbitrary selections, they represent major drivers of performance.

The ability to see the world defines the amount of maneuverability the pilot is willing to use. Design standards specify the minimum out-the-window vision requirements. Airframe obstructions and/or reduced visual cues (night, night sensors, obscurants, or clouds) increase the effort and concentration required to control the aircraft through increased dependence upon instruments or stability augmentation (i.e. forcing the aircraft to be less maneuverable).

The controls and displays used in the cockpit influence the difficulty of maintaining flight control and using avionics. Displays which are not sunlight readable or are not compatible with night vision devices dramatically increase workload and timelines. Controls which are poorly placed, difficult to grasp or manipulate distract from situation awareness and flight control or can induce disorientation. Generally, the more difficult the interface the greater the impact upon performance, but the specific impact of an interface component is difficult to quantify

The degree and currency of training are major contributors to performance in complex tasks such as flying highly maneuverable aircraft. Training has long been recognized as a fundamental determinant of air-to-air combat outcome.

3.3 Attentional Demand

This paper uses the term attentional demand to describe generically the higher level cognitive functions involved in the concept of pilot intent. These are the elements that distinguish the pilot from a reflexive automaton. Elements of attentional demand include perception, situation awareness, decision making, and task execution.

Perception in this context is defined as, "What is happening around me?" It is more than noting objects and events that are happening around the pilot. The raw events must be formed into a model that correlates and describes current activities and forms the basis for predictions about future events. For example, noting a return moving on a radar display leads to the perception of the likely flight path of that aircraft. The traditional radar format displays the nose of the aircraft along the bottom of the display. Aircraft which will cross in front of ownship nose appear to be heading towards the center of the display while those on a collision course appear to be heading straight down the side of the display. The crew must cognitively re-map the viewed data in order to achieve a correct perception. In this context, perception is used to describe a process that is more than just sensing.

Determining what the perceived situation means to the pilot and his mission is often referred to as building situation awareness. In this sense, situation awareness is used to describe knowing what the perceived events mean or imply for future events. Seeing multiple radar blips in different places which time correlate with the expectation of movement leads to the perception of an aircraft on a certain flight path which, in turn, leads to the situation awareness that an attack opportunity may exist. Few metrics exist to measure situation awareness and no quantitative relationship between performance and situation awareness has been widely accepted.

Once the pilot believes that he understands what is happening around him (situation awareness), he must create alternative plans and select the plan that best supports mission goals and intents. Wrong decisions can lead to disastrous consequences. Decision making is heavily influenced by situation awareness, perception, and training. Some people are better decision makers than others. As is the case in situation awareness, no metrics exist to measure decision making and no quantitative relationship between performance and decision making has been accepted.

After deciding upon a plan of action, pilots have to implement the plan. In simple situations this may merely be flight control input. In more complex situations, the pilots may have to change avionics or weapon system mode settings. Often the processes of perception, situation awareness, and decision making may require additional information. This requires the pilots to get the information and return to the task of perceiving, building situation awareness, or decision making. In many cases, the decision may have serious affects on the pilot's environment which could include future survival. Employment of weapons or assessment of bad weather landing conditions are examples of decision which should be supported by unambiguous information but, in reality, often are not. Anytime pilots must execute a task, they must remember the trained procedure. The more difficult the task, the greater the memory and training burden. Usually the more difficult tasks take longer and are more disruptive to other demanding tasks. Once again, the human ability to cope with task execution is not quantifiable nor can specific guidelines be generated from generic knowledge.

4. EXPANDING THE PILOT'S ENVELOPE

The physiological limits for humans are well known and have been incorporated into specifications and technical data. Accommodation of the pilot's physiological envelope is, for the most part, a weight and cost trade-off and will not be discussed in this paper. The same is basically true of the environmental modifiers discussed above. The primary component of attentional demand, however, is not covered by a tidy body of knowledge that allows us to pick a performance level and derive how much is required. For instance, no design standard addresses the question of how much attentional demand a task is allowed. The advent of computerized, "glass cockpits" offers the opportunity to expand the pilot's envelope by employing a pilot-vehicle interface design that transfers some of the attentional demand tasks to automation and make task execution simpler. The climb/dive marker found in most HUDs is an example of automation expanding the pilot's perception envelope because it tells the pilot at a glance where the aircraft's flight path is in relation to the world rather than forcing the crew to monitor the flight path continuously. Providing aircraft location, flight path, and target data on a displayed map is an example of expanding the pilot's situation awareness by automating the development of a plan view of the mission. Hands on grip controls are examples of an expansion of the pilot's task execution envelope. However, merely adding sensors and information does not automatically expand the pilot's envelope; it may shrink the envelope through overload or confusion.

The key to expanding the pilot's envelope is to design an interface that reduces the amount of time and energy the pilot spends on acquiring information and executing decisions. This provides more time to think about the decisions being made. This kind of interface is the product of a design program that systematically explores the problems of perception, situation awareness, decision making, and task execution and develops an overt, conscious model of the pilot interface. This model can specify automation and specific control/display

implementations to achieve an expanded pilot's performance envelope.

Expanding the pilot's performance envelope is not generally recognized as a problem to be worked in the same sense as increased turn rate or load factor. Most programs allocate little resources specifically to the pilot-vehicle interface. Often this situation results from an inability to articulate what constitutes an envelope expanding interface and a failure to allocate direct responsibility for designing the interface. The result is a restriction of the pilot's performance envelope that limits or negates efforts to field a highly maneuverable aircraft. The following sections identify specific attributes that an interface must have to reduce the workload and increase situational awareness (i.e. expand the pilot's envelope.)

4.1 Information Display

Pilots form and maintain multiple views of their worlds. The most obvious one is the "ego" view which represents the world as seen through their own eyes. This view is used in conjunction with "air sense" to fly the aircraft and understand the external situation. Another common view is the plan or horizontal situation view. This view is used to understand where the pilot is in the world and where geographical locations are in relationship to current aircraft position. This view is commonly used for navigation and route planning. Another view is the "sensor" view. This is a view of the world as seen by one or more sensors such as radar or forward looking infra-red (FLIR). Pilots switch from view to view depending upon the current task. This switching of views is normal and the situation awareness generated in one view should be supported in other views. For instance, once the pilot switches to a plan view and decides where he wishes to fly next, he switches back to an ego view to fly the aircraft to that position. The location decided upon in the plan view should be represented in the ego view to connect and support the two types of situation awareness. This can be done by using a contact analog symbol in the ego view to pinpoint the location from the plan view.

Information needed to support decision making and situational awareness should be clustered together. Often information needed to form situational awareness is distributed across an interface, located in a menu structure dictated by the subsystems design. This forces the crew to spend significant time and energy navigating the menu structure and shopping for information. One-stop shopping can be achieved if all the data for situational awareness or decision making are brought to a centralized display location in a manner that is quickly interpreted relative to the mission, phase, segment, or task being performed.

Often displays provide data from which the crew must deduce or construct answers. Displays should provide information in an appropriate format compatible with the information demands of the crew. In simpler terms, if the question is how much fuel is remaining, then a good answer is provided by a digital display of pounds of fuel remaining; however, if the question is how long until flameout, then a better answer is X minutes (because displaying fuel remaining assumes that the pilot will divide by consumption rate to obtain time remaining.) Careful task analysis may reveal that data must be presented in a variety of formats to support all information demands.

4.2 Control of Options

More options do not always make for a happier pilot. As processing power on-board the aircraft increases, the ways in which sensors can be programmed and data viewed increases. Too many options result in pilots spending more time and energy setting up tasks than available. Multiple options also incur excessive training costs as pilots attempt to become proficient operating all of the various modes. Whenever possible, designers should limit the number of options to those essential to the mission requirements.

As with display attributes, controls should be clustered together to prevent the pilot from navigating the menu structure to find the on/off or adjustment options. All information required for tasks should be located together and all controls for those tasks also should be located together.

Pilots should not be required to set a series of switches in a particular position and sequence to perform a desired function. To set up a function, they should be provided with a switch that activates the system and the set up tasks should be automated. There should never be an error message to tell the pilot that something was not set correctly. As long as the function does not involve safety of flight, system safety, or a device which must by its nature have a direct interface with the pilot, then the interface should do the setup; not the pilot.

Incorrect switch choices (i.e. those whose order or setting does not apply) should not be presented. If an option does not apply then the control for it should not be presented. The pilot cannot throw the wrong switch if the switch is not available. If the function is normally provided, but is not available because of fault, then the switch should indicate non-functionality by "X'ing" through or striking over the label.

4.3 Organization of Information and Controls

Organization of information and controls needs to be planned carefully. A good menu structure and display format are not necessarily based upon subsystem functions. Previously mentioned attributes of clustering may require that subsystem boundaries be ignored. In fact, information or controls may need to appear in a variety of places to support decision making or execution in a timely manner. Good organization is based upon a human factors engineering task analysis. Optimum organization usually is not achieved on the first try. Therefore, design iterations, using man-in-the-loop simulation evaluations, are required to refine the organization.

The organization of display pages and the menu structure should be based on the concept of function. This concept states that a function is a set of activities that must be performed by the pilot to complete a portion of the mission segment. An example of a function might be Detect Target. This function might include tasks like pointing a sensor or changing the radar mode. Required information and controls for all of the displays and sensors needed to detect a target should be in close proximity in the menu structure. Obviously, all data cannot be provided all of the time. Data that are commonly used, are frequently cross-checked, or may be time critical should be readily available. However, other data may be used occasionally for decision making or situational awareness. These data should be nearby in the menu structure.

There is no reason why information, controls, and options cannot be segregated into groups that functionally represent maintenance, setup, normal operations, training, and tactical applications. These functions should be placed in distant corners of the menu structure. Single high-level mode selection should cause large segments of the menu structure to disappear from consideration. Selecting a "tactical" mode should enable the pilot to see and access only data and controls relevant to the tactical situation. This is one means of effectively "filtering" options and information for better organization

4.4 Menu Attributes

Consistency is the biggest ally of the pilot while surprise is the biggest enemy. The designer may be tempted to invent a new way to enter/display data or control a device. This might allow the absolute maximum efficiency of keystrokes and display usage, but it places a burden upon pilots if they must remember how to operate each method. Adding a few more keystrokes for consistency reduces pilot workload and increases pilot acceptance of the system. In time critical situations pilots will avoid systems that they do not know how to operate. Pilots will also avoid automation if it requires significant setup or option selection work.

Controls in a glass cockpit often take the form of bezel switches with displayed labels. A switch may turn something on or off, may select from a number of options, or may take the crew to another menu of options. The displayed labels should have a number of attributes. First, labels should indicate function. For example, the label "MODE" could be used to indicate that the switch is associated with control of a mode. Second, the current status of the function should be displayed. For example, the word "AUTO" may be displayed next to the label "MODE" so that the pilot knows that the current mode is automatic. Third, the menu result of selecting a switch should be indicated. For example, the MODE switch may toggle between manual and automatic or may call a submenu of selection options. Pilots should not be required to remember what each switch will do if they press it. In the example above, a "▷" symbol could be added to form the label "MODE AUTO▷" thus indicating transition to a lower level menu. If a simple toggle between automatic and manual were desired the label might look like "MODE AUTO ↔". Indicating to the pilots where he will go within the menu structure is analogous to putting up street signs at road intersections. In both cases a navigation task is made easier by transferring the mapping task from memory to reading. The labeling takes the guesswork out of the task and reduces the workload of the pilot.

The switch labels and status indicators should be in the language of the pilot, not the engineer who designed the system. The best situation is when pilots realize they need to do "X" and they look around and find a key labeled "X" They should not have to translate their view of the world into engineering language in order to work through a menu or to select correct options.

Data and tasks should be arranged so that the more detailed data and tasks are deeper in the menus. Pilots should not be forced to the bottom of a menu tree to find high-level data nor should basic controls be at the bottom of the menu. The first menu encountered should have most of the necessary quick glance data and controls.

4.5 System Attributes

In the world of pilots, many tasks are interrupted to do higher priority tasks. The system should be designed so that interrupting tasks can be entered easily and quickly Also, it should be simple to return to the interrupted tasks

Often subsystem capabilities are designed by a single vendor. It is easy to overlook the fact that other on-board subsystems may have data or processing capability which could be brought to bear upon system level problems. No one subsystem provides total situation awareness. By recognizing the strengths and weaknesses of the various subsystems and by allocating processing resources to integrate data from various subsystems, good situation awareness and low workload can be achieved.

5. AN EXPANDED ENVELOPE ENHANCES AIRCRAFT MANEUVERABILITY

The process of developing an expanded pilot's envelope is mature and the benefits are substantial. Generally speaking, the pilot-interface and the derived hardware requirements must be ready early in the development of an aircraft. This requires up-front investments, sometimes even prior to the development go-ahead. The question is, how do you justify this early investment? The answer is that aircraft are purpose built to satisfy specific mission requirements but pilots must be trained to use the aircraft If the pilots can use only a portion of the capabilities then the mission requirements will go unsatisfied and the effort expended upon the airframe and avionics will have limited return.

For example, if pilots do not realize that they should change their flight path or are so busy with avionics that they do not see the developing situation, then high maneuverability will not help the pilot survive and win. On the other hand, if pilots know that their current flight path ends with ground impact, they can alter their flight path immediately or they have the liberty to decide to continue until the final moment that the maneuver envelope allows escape. This kind of synergism between situation awareness and maneuver envelope allows maximum flexibility in an air combat environment. Likewise, if pilots understand the intent of a threat but have to change control settings in a complicated and time consuming manner, then they may not be able to take advantage of a position gained through high maneuverability. On the other hand, simple and direct means of changing configurations may allow tactical advantage without arduous maneuvering.

The pilot's problem is how to achieve and maintain tactical advantage. Achieving tactical advantage requires that pilots be aware of the total situation and be able to respond. One part of the answer is a highly maneuverable aircraft. Another part of the answer is a pilot-vehicle interface that allows fast assimilation of information and simple control procedures. The computer revolution and modern interface design methods provides the opportunity to achieve the required blend of man, airframe, weapons, and avionics.

6. REFERENCES

1. Johansen, D.C., Pheeny, H.T., Palmer, J.F., Mathews, R.A. "Inflight Loss of Consciousness: A First Look At the U.S. Navy Experience", Second GLC Conference, 2-3 April 1986. Norton AFB.

2. Perry, I.C., "Helicopter Aircrew Fatigue", AGARD Advisory Report No 69, May 1974.

3. Wing, J.F., "Upper Thermal Tolerance Limits for Unimpaired Mental Performance", Aerospace Medicine, October 1965, pp 960-964.

The Influence of Flying Qualities on Operational Agility

Gareth D. Padfield
Defence Research Agency
Building 109
DRA, Clapham
Bedford
UK MK416AE

John Hodgkinson
McDonnell Douglas Aerospace
3855 Lakewood Blvd. M/C 36-41
Long Beach, California, 90846
U.S.A.

1. SUMMARY

Flying Qualities standards are formally set to ensure safe flight and therefore to reflect minimum, rather than optimum, requirements. Agility is a flying quality but relates to operations at high, if not maximum, performance. While the quality metrics and test procedures for flying, as covered for example in MIL-STD-1797 or ADS33, may provide an adequate structure to encompass agility, they do not currently address flight at high performance. A current concern in both the fixed- and rotary-wing communities is the absence of substantiated agility criteria and the possible conflicts between flying qualities and high performance – i.e., more may not always be better. This Paper addresses these concerns and suggests an agility factor that quantifies performance margins in flying qualities terms. The attitude quickness, from the latest rotary-wing handling requirements, provides an ideal agility measure and links handling with agility. A new parameter, based on manoeuvre acceleration, is introduced as a potential candidate for defining upper limits to flying qualities. These concepts are introduced within a framework aimed at unifying flying qualities and performance requirements. Finally, a probabilistic analysis of pilot handling qualities ratings is presented that suggests a powerful relationship between inherent airframe flying qualities and operational agility.

2. INTRODUCTION

In current military requirements, good flying qualities are conferred to ensure that safe flight is guaranteed throughout the Operational Flight Envelope (OFE). Goodness, or quality, in flying can be measured on a scale spanning three Levels, as defined by Cooper and Harper.[1] Aircraft are normally required to be Level 1 throughout the operational flight envelope.[2,3] Level 2 is acceptable in failed and emergency situations. Level 3 is considered unacceptable. The achievement of Level 1 signifies that a minimum-required standard has been met or exceeded in design and can be expected to be achieved regularly in operational use, measured in terms of task performance and pilot workload

Compliance flight testing involves clinical measurements of flying qualities parameters for which good values are known from experience. It also involves the performance of pilot-in-the-loop mission task elements (MTE) along with the acquisition of subjective comments and pilot ratings. The emphasis on minimum requirements is important and is made to ensure that manufacturers are not unduly constrained when conducting their design trade studies.

Two issues arise out of this quality scale and assessment. First, the minimum requirements reflect and exercise only moderate levels of the dynamic operational flight envelope, rather than high or extreme levels. Second, the assessments are usually made in "clean" conditions, uncluttered by secondary tasks, degraded visual cues, or the stress of real combat. Beyond the minimum quality levels there remains the question of the value of good flying qualities to the overall mission effectiveness. For example, how much more effective is an aircraft that has, say, double the minimum required (Level 1) roll control power? More generally, how much more mission-effective is a Level 1 than a Level 2 aircraft when, for example, the pilot is stressed? A third question asks whether there are any upper limits to the flying qualities parameters, making quality boundaries closed contours. The answers to these questions cannot generally be found in flying qualities criteria like ADS33 (Ref. 2) or MIL-STD-1797 (Ref. 3). At higher performance levels, very little data are available on flying qualities and, consequently, there are very few defined upper limits on handling parameters.

Regular and safe, or carefree, use of high levels of transient performance has come to be synonymous with agility. The relationship between flying qualities and agility is important because it potentially quantifies the value of flying qualities to operational effectiveness.

This paper addresses those flying qualities that are important for agility, in both an enabling and limiting context, and considers how far existing flying qualities requirements go, or

Presented at an AGARD Meeting on 'Technologies for Highly Manoeuvrable Aircraft', October 1993.

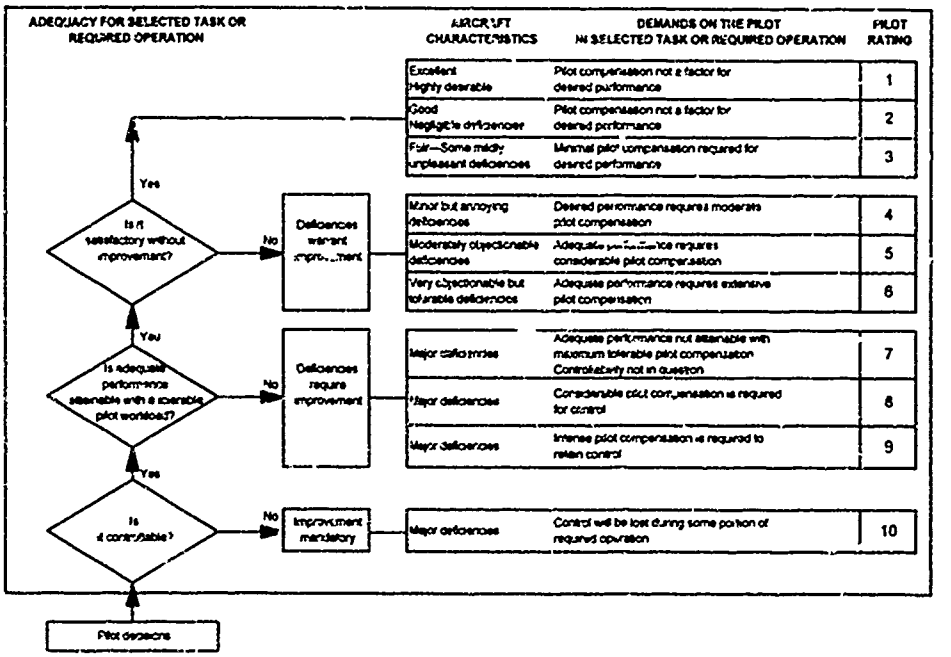

Figure 1. The Cooper-Harper Handling Qualities Rating Scale

can be extended, to embrace agility itself. The answers are developed within a framework of deterministic flying qualities criteria coupled with the probabilistic analysis of success and failure.

The definition of flying qualities by Cooper & Harper provides a convenient starting point:

> those qualities or characteristics of an aircraft that govern the ease and precision with which a pilot is able to perform the tasks required in support of an aircraft role.[1]

The pilot subjective rating scale and associated flying qualities Levels as introduced by Cooper & Harper (Figure 1) will be used in this paper in the familiar context of quality discernment and will be developed to make the link with agility and mission effectiveness.

Flying "Quality" can be further interpreted as the *synergy* between the *internal attributes* of the air vehicle and the *external environment* in which it operates (Figure 2). The internals consist typically of the air vehicle (airframe, powerplant and flight control system) response characteristics to pilot inputs (handling qualities) and disturbances (ride qualities) and the key elements at the pilot/vehicle interface, e.g., cockpit controls and displays. The key factors in the external environment which influence the flying qualities requirements are:

i) the mission, including individual mission task elements (MTE) and the required levels of task urgency and divided attention dictated by the circumstances governing individual situations, e.g., threat level, and

ii) the external natural environment, including the usable cue environment (UCE)[2] and level of atmospheric disturbance.

Flying qualities, as seen by the pilot who is ultimately the judge of quality, therefore change as the external world changes—with, for example, weather conditions, flight path constraints, and other task demands. Mission-oriented flying qualities requirements, like those for fixed-wing aircraft, MIL-STD-1797, but more particularly like those for helicopters, ADS33C, try to set quality standards by addressing the synergy of these internal attributes and external factors.

In a hierarchical manner, ADS33C defines the response types required to achieve Level 1 or 2 handling qualities for a wide variety of different mission task elements, in different usable cue environments for normal and degraded states, with full and divided pilot attention. At a deeper level, the response characteristics are broken down in terms of amplitude and

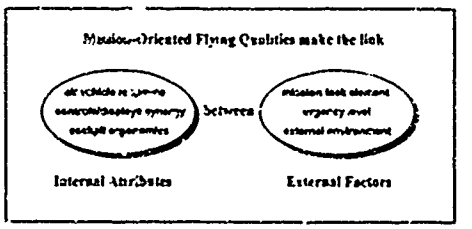

Figure 2. The Synergy of Flying Qualities

frequency range, from the small amplitude, higher-frequency requirements set by criteria like equivalent low order system response or bandwidth, to the large-amplitude manoeuvre requirements set by control power

MIL-STD-1797 takes a somewhat different perspective, with flight phases and aircraft categories, but the basic message is the same—how to establish flying quality. With these developments now mature, one would expect that any "special" flying characteristics, like agility, could be embraced by the flying qualities requirements, or at least that the flying qualities criteria should be an appropriate format and starting point for quantifying agility. A key question then arises as to whether there need be upper boundaries on handling parameters or whether more is always better. Furthermore, it may well be that the handling parameters and associated quality boundaries set for minimum safety standards are inappropriate for high performance levels and that new formats are required. These are primary concerns of this Paper.

The Paper considers both fixed- and rotary-wing aircraft in a unified approach. While speed and manoeuvre envelopes and associated limits for aeroplanes and helicopters are quite different, often paradoxically so, they share the essence of agility and operational effectiveness. Interestingly, agility requirements for the two vehicle types have traditionally stemmed from two quite different theatres: close combat of air-superiority fighters in the open skies, contrasting with stealth of anti-armour helicopters in the nap of the earth. While both still feature large in the two worlds, it is now recognised that there is a broad overlap in agility requirements, and there is relevance to a wider range of roles, including aircraft recovering to ships, transport refueling, support helicopters delivering loads into restricted areas, and, more recently, helicopters performing air-to-air combat.

AGARD Working Group 19 (in AGARD Advisory Report AR314) has considered operational agility in the broader context of the total weapon system, encompassing sensors, mission systems, pilot, airframe/engine, flight control system, and weapon. The concept is that the total system can only be as agile as the slowest element and that all elements need to work concurrently to be effective.

This Paper focuses on the vehicle and the pilot-centered agility requirements of the airframe, engine, and flight control system elements. The nature of operational agility is discussed, with an outline of some of the Working Group 19 background and motivation setting the scene for the later discussions of the relationship between flying qualities and agility. Three key innovations of this Paper are contained here. First, the agility factor is introduced and related to quantitative handling criteria. Second, the attitude quickness parameter[2] is interpreted as an agility parameter and extended to the acceleration response. Finally, the subjective quality scale (Cooper Harper) for pilot-perceived handling qualities is interpreted in a probabilistic fashion to indicate the likelihood of mission success or failure with a given level of flying qualities. Essentially, recognition is given to the fact that aircraft that are, say, Level 1 "on paper" will experience Level 2 and 3 situations in their operational life, e.g., through poor usable cue environments (UCE) and associated weather conditions, failed systems, or pilot fatigue. This novel interpretation of the handling quality ratings suggests a new approach for including flying qualities attributes in combat models, which are also discussed.

3. THE NATURE OF OPERATIONAL AGILITY

Operational agility is a key attribute for weapon system effectiveness. Within the broader context of the total weapon system, the Mission Task naturally extends to include the actions of the different co-operating (and non-co-operating) sub-systems, each having its own associated time delay.[4] We can imagine, for example, the sequence of actions for an air-to-air engagement: threat detection, engagement, combat, and disengagement. The pilot initiates the action and stays in command throughout, but a key to operational agility is to automate the integration of the subsystems—the sensors, mission systems, airframe/engine/control systems and weapon—to maximise the concurrency in the process.

Concurrency is one of the keys to Operational Agility. Another key relates to minimising the time delays of the subsystems to reach full operational capability and hence effectiveness in the MTE. Extensions to the MTE concept are required that encompass the functions and operations of the subsystems, providing an approach to assessing system operational agility. Working Group 19 has addressed these issues elsewhere. Minimising time delays is crucial for the airframe, but flying qualities can suffer if the accelerations are too high or the time constants too short, leading to jerky motion.

Later in this paper we examine how well existing flying qualities requirements address agility. To set the scene for this, we first consider one generalised definition of *agility* adopted by Working Group 19:

> the ability to adapt and respond rapidly and precisely with safety and with poise, to maximise mission effectiveness.

Agility requirements for both fixed and rotary-wing combat aircraft fall into four key mission phases:

a) stealthy flying—in particular, terrain—masked, to avoid detection,

b) threat avoidance once detected,

c) the primary mission engagement (e.g., threat engagement), and

d) recovery and launch from confined or otherwise demanding areas.

The key attributes of airframe agility, as contained in the above definition, are:

i) *rapid*—emphasizing speed of response, including both transient and steady-state phases in the manoeuvre change. The pilot is concerned to complete the manoeuvre change in the *shortest possible time*, what is possible will be bounded by a number of different aspects.

ii) *precise*—accuracy is the driver here, with the motivation that the greater the task precision—e.g., precision of pointing, achievability of flight path—the greater the chance of a successful outcome. (The combination of speed and precision emphasizes the special nature of agility, one would normally conduct a

process slowly to achieve precision, but agility requires both.)

iii) *safety*—this reflects the need to reduce piloting workload, making the flying easier and freeing the pilot from unnecessary concerns relating to safety of flight, e.g., respecting flight envelope limits.

iv) *poise*—this relates to the ability of the pilot to establish new steady-state conditions quickly and to be free to attend to the next task. It relates to precision in the last moments of the manoeuvre change but is also a key driver for ride qualities that enhance steadiness in the presence of disturbances. (Poise can be thought of as an efficiency factor, or measure of the unused potential energy, much like the agility factor itself).

v) *adapt*—the special emphasis here relates to the requirements on the pilot and aircraft systems to be continuously updating awareness of the operational situation. The possibility of rapid changes in the external factors discussed above (e.g., threats, UCE, wind shear/vortex wakes) or the internals, through failed or damaged systems, makes it important that agility is considered, not just in relation to set-piece manoeuvres and classical engagements, but also for initial conditions of low energy and/or high vulnerability or uncertainty.

Flying qualities requirements address some of the agility attributes implicitly—through the use of the handling qualities ratings (HQR's), that relate the pilot workload to task performance achieved—and explicitly—through criteria on response performance, e.g., control power, bandwidth, stability, etc. The relationship is more firmly established with the agility metric classification introduced by Reif in the AGARD AR 314 report, and reproduced below.

Transient—defined as a continuously varying property of the response

Experimental—defined as a compound property derived from an elemental manoeuvre

Operational—defined as a compound property derived from a complete mission-task-element

A transient metric would reflect the instantaneous values of the time and spatial variations of the aircraft's motion, e.g., roll rate, acceleration (agility vector), ... Experimental metrics are computed from the kinematics of a small manoeuvre slice, e.g., attitude quickness, power onset/loss rate, torsional metrics, ... The operational metrics reflect the agility of the aircraft in well defined mission task elements, e.g., time to complete air-to-air acquisition and tracking, helicopter re-positioning sidestep tasks, ... In the following section, where possible, this classification structure will be mapped onto flying qualities metrics.

4. FLYING QUALITIES—THE RELATIONSHIP WITH AGILITY

4.1. Fixed-Wing Perspectives

One of the fundamentals that Working Group 19 promoted is that flying qualities and airframe agility are outgrowths from the same attribute branch, but recent studies have identified a potential conflict. The original concern sprang from the notion that flying qualities specifications, as guardians of transient response, should embrace agility, since it too resides by definition in the transient domain. Initial thought on this theme appeared in References 5 and 6. Reference 5 indicated the interactions between agility, operational capability, and flying qualities, and listed some of the flying qualities requirements that, because of their treatment of the transient response, clearly crossed into the realm of agility.

At that time, it was hypothesized that simply increasing the available agility, in terms of accelerations, rates etc., would lead to diminishing operational returns, since an over-responsive vehicle would not be controllable. That point was considered worth making because some combat analyses were being performed using computer tools that approximated the transient response only in a gross fashion. These models resulted in aircraft which had unquestionably high performance but did not account for the interaction of the vehicle with the pilot. Also, due to the approximations made in the interests of computational tractability, the models did not obey the laws of motion in their transient responses. In Reference 6, the Control Anticipation Parameter (CAP), from the USAF Flying Qualities requirements,[3] was quoted as an example of a criterion defining over-responsiveness, since an upper limit is specified for it. Artificially high pitch agility could, according to CAP, correspond to excessive pitch acceleration relative to the normal load factor capability of the aircraft. Performance constraints are also suggested by the tentative upper limits set on pitch bandwidth in Reference 3. However, it is suspected that these limits reflect the adverse acceleration effects and control sensitivity problems associated with high bandwidth/control power combinations. This point will be revisited later.

At about the same time, Riley et al.[7,8,9] began a series of experiments on fighter agility. In Reference 7, they emphasized that the idea of an operationally useful vehicle with a rating worse than Level 2 was inconsistent with the definition of the categories in the Cooper-Harper pilot rating scale. And in Level 3, the operational effectiveness of the vehicle is compromised, so increasing performance would add little as the pilot could not use it safely. In References 7, 8, and 9, Riley and Drajeske describe a fixed-base simulation in which the maximum available roll rate and roll mode time constant were independently varied and the pilot's time to bank 90 degrees and stop was measured. Care was taken in the experiment to allow sufficient time for learning and to generate reasonably large numbers (10 to 15) of captures for analysis. The start of the manoeuvre was defined as when the stick deflection began, and the end was defined as when the roll rate was arrested to less than 5 degrees/second or 5% of the maximum rate used, whichever was greater. Therefore a realistic element of precision was introduced into the protocol.

The results from that experiment, in which the aircraft banked from -45 degrees to +45 degrees, are shown in Figure 3. The inner curved surface summarizes the calculated time responses for a step lateral input and shows the expected steady increase in agility, i.e., a decrease in the time to bank with increasing roll rate. The upper surface in the plot summarizes the bank-to-bank and stop data obtained in the piloted cases. The references to controllability on that surface are from the pilot ratings and comments that were collected. The time to complete the manoeuvre actually increases for the

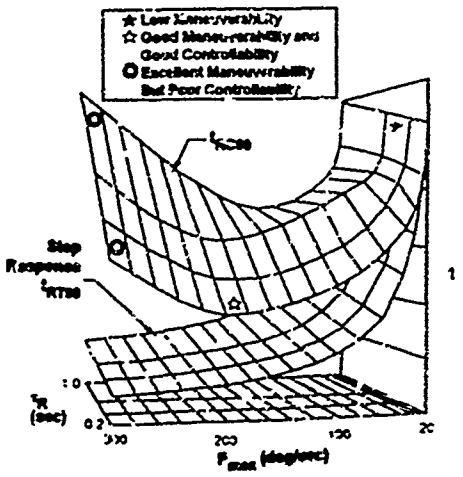

Figure 3. Agility in a Roll Manoeuvre (Ref. 7)

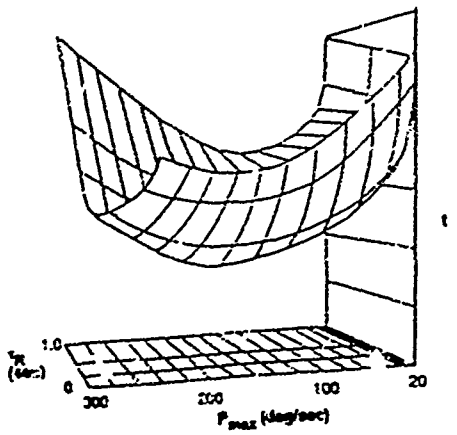

Figure 4. Effects of Motion on Agility

higher available roll rates, because the pilot could not adequately control the manoeuvre. The data therefore show that flying qualities considerations do limit agility. Though the data are from fixed-base simulation, we can speculate that in-flight results might show still more dramatic limitations. In Reference 9 the authors suggest that the effects of motion would in fact change the shape of Figure 3 to look like Figure 4

In MIL-STD-1797, upper limits on lateral flying qualities are almost exclusively set by tolerable levels of acceleration at the pilot station, in the form of lateral g per control power. The Level 1 boundary at about 2g for a typical fighter seems extraordinarily high, but Reference 3 does state that "in order to achieve the needed roll performance it may be necessary to accept some uncomfortable lateral accelerations." There is considerable discussion on lateral control sensitivity in Reference 3, but, as with helicopters, the criteria are strongly dependent on controller type and only guidance is given. Clearly there will always be upper limits to sensitivity and it should be an important goal to design the pilot/vehicle interface so that agility is not inhibited by this parameter.

4.2 Rotary-Wing Perspective and the Agility Factor

One of the most common causes of dispersion in pilot HQRs stems from a poor or imprecise definition of the performance requirements in a mission task element, leading to variations in interpretation and hence perception of achieved task performance and associated workload. In operational situations this translates into the variability and uncertainty of task drivers, commonly expressed in terms of precision, but the temporal demands are equally important. The effects of task time constraints on perceived handling have been well documented,[10,11,12] and represent one of the most important external factors that impact pilot workload. Flight results gathered on Puma and Lynx test aircraft at the Bedford Defense Research Agency[12,13] showed that a critical parameter was the ratio of the task performance achieved to the maximum available from the aircraft. This ratio gives an indirect measure of the spare capacity or performance margin and was consequently named the *agility factor*

The notion developed that if a pilot could use the full performance safely while achieving desired task precision requirements, then the aircraft could be described as agile. If not, then no matter how much performance margin was built into the helicopter, it could not be described as agile. The Bedford agility trials were conducted with Lynx and Puma operating at light weights to simulate the higher levels of performance margin expected in future types (e.g., up to 20–30% hover thrust margin). A convenient method of computing the agility factor was developed as the ratio of ideal task time to actual task time. The task was deemed to commence at the first pilot control input and to be complete when the aircraft motion decayed to within prescribed limits (e.g., position within a prescribed cube, rates < 5 deg/s) for re-positioning tasks or the when accuracy/time requirements were met for tracking or pursuit tasks. The ideal task time is calculated by assuming that the maximum acceleration is achieved instantaneously, in much the same way that some aircraft models work in combat games. So, for example, in a sidestep re-positioning manoeuvre, the ideal task time is derived with the assumption that the maximum *translational* acceleration (hence aircraft roll angle) is achieved instantaneously and sustained for half the manoeuvre, when it is reversed and sustained until the velocity is again zero

The ideal task time is then simply given by

$$T_i = \sqrt{4S/a_{max}} \qquad (1)$$

where S is the sidestep length and a_{max} is the maximum translational acceleration. With a 15% hover thrust margin, the corresponding maximum bank angle is about 30 deg, with a_{max} equal to 0.58g. For a 100-ft sidestep, T_i then equals 4.6 seconds. Factors that can increase the achieved task time beyond the ideal include:

i) delays in achieving the maximum acceleration (e.g., due to low roll attitude bandwidth/control power),

ii) pilot reluctance to use the maximum performance (e.g., no carefree handling capability, fear of hitting ground),

iii) inability to sustain the maximum acceleration due to drag effects and sideways velocity limits, and

iv) pilot errors of judgment leading to terminal re-positioning problems (e.g., caused by poor task cues, strong cross coupling).

To establish the kinds of agility factors that could be achieved in flight test, pilots were required to fly the Lynx and Puma with various levels of aggressiveness or manoeuvre "attack," defined by the maximum attitude angles and the rate of control application used. For the low speed, re-positioning Sidestep and Quickhop Mission Task Elements, data were gathered at roll and pitch angles of 10, 20, and 30 degrees, corresponding to low, moderate, and high levels of attack, respectively. Figure 5 illustrates the variation of pilot ratings with agility factor.

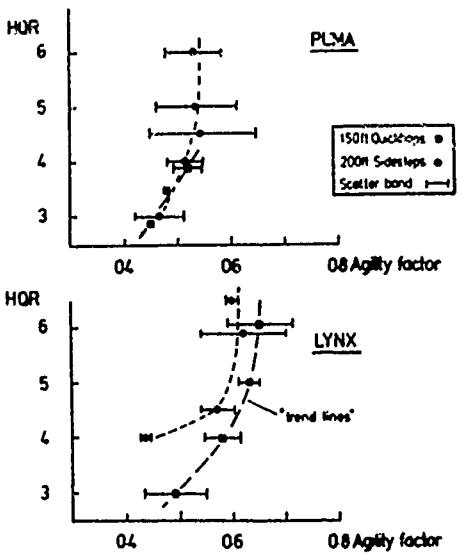

Figure 5. Variation of Cooper-Harper Rating with A_f Showing the Cliff-Edge of Handling Deficiencies

The higher agility factors achieved with Lynx are principally attributed to the hingeless rotor system and faster engine/governor response. Even so, maximum values of only 0.6 to 0.7 were recorded, compared with 0.5 to 0.6 for the Puma. For both aircraft, the highest agility factors were achieved at marginal Level 2/3 handling. In these conditions, the pilot is either working with little or no spare capacity or is not able to achieve the flight path precision requirements. According to Figure 5, the situation rapidly deteriorates from Level 1 to Level 3 as the pilot attempts to exploit the full performance, emphasizing the "cliff edge" nature of the effects of handling deficiencies. The Lynx and Puma are typical of current operational types with low authority stability and control augmentation; while they may be adequate for their current roles, flying qualities deficiencies emerge when simulating the higher performance required in future combat helicopters.

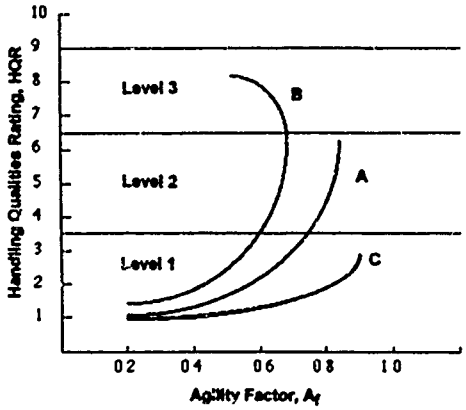

Figure 6. Variation of Cooper-Harper Rating with A_f for Different Notional Configurations

The different possibilities are illustrated in Figure 6. All three configurations are assumed to have the same performance margin and hence ideal task time. Configuration A can achieve the task performance requirements at high agility factors, but only at the expense of maximum pilot effort (poor level 2); the aircraft cannot be described as agile. Configuration B cannot achieve the task performance when the pilot increases his attack and Level 3 ratings are returned. In addition, the attempts to improve task performance by increasing manoeuvre attack have led to a decrease in agility factor, and hence to a waste of performance. This situation can arise when an aircraft is prone to pilot-induced oscillations, when an aircraft is difficult to re-trim, or when control or airframe limits are easily exceeded in the transient response. Configuration B is certainly not agile and the proverb "more haste, less speed" sums the situation up. With configuration C, the pilot is able to exploit the full performance at low workload; he has spare capacity for having situation awareness and being prepared for the unexpected. Configuration C can be described as truly agile.

The inclusion of such attributes as safety and poise within the concept of agility emphasizes its nature as a flying quality and suggests a correspondence with the quality Levels. These conceptual findings are significant because the flying qualities boundaries, which separate different quality levels, now become boundaries of available agility. Although good flying qualities are sometimes thought to be merely "nice-to-have," with this interpretation they can actually delineate a vehicle's achievable performance. This lends a much greater urgency to defining where those boundaries should be. Put simply, if high performance is dangerous to use, then most pilots will avoid using it.

In agility factor experiments the definition of the level of manoeuvre attack needs to be related to the key manoeuvre parameter, e.g., aircraft speed, attitude, turn rate, or target motion. By increasing attack in an experiment, we are trying to reduce the time constant of the task, or reduce the task bandwidth. It is adequate to define three levels—low,

moderate, and high, the lower corresponding to normal manoeuvring, the upper to emergency manoeuvres.

There are also potential misuses of the agility factor, Af, when comparing aircraft. The primary use of the Af is in measuring the characteristics of a particular aircraft performing different MTE's with different performance requirements. However, Af also compares different aircraft flying the same MTE. Clearly, a low performance aircraft will take longer to complete a task than a high performance one, all else being equal. The normalising ideal time will also be greater, and if the agility factors are compared, this will bias in favour of the poor performer. Further, the ratio of time in the steady-state to time in the transients may well be higher for the low performer.

To ensure that such potential anomalies are not encountered, when comparing aircraft us the agility factor it is important to use the same normalising factor—defined by the ideal time computed from a performance requirement. The agility factor concept, as an operational agility metric, was developed in the surge of rotary-wing handling qualities developments over the last ten years. It is equally applicable to fixed-wing aircraft, although the associated MTE database will need to be developed as a foundation.

Conferring operational agility on future fixed and rotary-wing aircraft, emulating configuration C above in Figure 6, requires significant improvements in handling, particularly for rotorcraft, but research into criteria at high performance levels and innovations in active control are needed to lead the way. There are two remaining links to be connected to assist in this process: first, between the agility factor and the operational agility or mission effectiveness, and second, between the agility factor and the flying qualities metrics themselves. If these links can be coherently established, then the way is open for combat analysts to incorporate prescribed flying qualities into their pseudo-physical models through a performance scaling effect using the agility factor. These links will now be developed.

5. THE OBJECTIVE MEASUREMENT OF QUALITY

Figure 7 provides a framework for discussing the influence of an aircraft's clinical flying qualities on agility The concept is that an aircraft's response characteristics can be described in terms of frequency and amplitude. The three lines refer to the minimum manoeuvre requirements, the normal operational flight envelope requirements, and some notional upper boundary reflecting a maximum capability. Response criteria are required for the different areas on this plane—from high frequency/small amplitude characterised by bandwidth, to low frequency/large amplitude motions characterised by control power. The region between is catered for by an ADS33 innovation, the Quickness parameter,[2] and is particularly germane to agility for both fixed- and rotary-wing aircraft. For a given manoeuvre amplitude change (e.g., bank angle, speed change), the pilot can exercise more of the aircraft's inherent agility by increasing the speed of the manoeuvre change, or "attack," and hence the frequency content of his control input and the manoeuvre quickness. Likewise, the pilot can increase the manoeuvre size for a given level of attack. Increasing the manoeuvre quickness will theoretically lead to an increase in agility factor. But the maximum manoeuvre quickness is a strong function of bandwidth and control power In ADS33C, the quickness parameter is only defined for attitude response (ϕ, θ, ψ) and is given by the ratio of peak attitude rate (p_{pk}, q_{pk}, r_{pk}) to attitude change,

$$p_{pk} / \Delta\phi, \quad q_{pk} / \Delta\theta, \quad r_{pk} / \Delta\psi.$$

As noted by Reif, there is scope for extending this experimental agility metric to other degrees of freedom, e.g., incidence. Figure 8 shows derived quickness parameters for a sidestep gathered on the DRA Lynx[13] and "Configuration T509" flown on the DRA Advanced Flight Simulator,[14] the latter designed to emulate the Lynx in terms of bandwidth and control power.

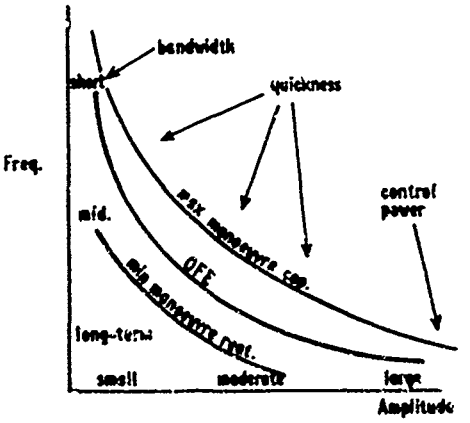

Figure 7. Response Characteristics on the Frequency-Amplitude Plane

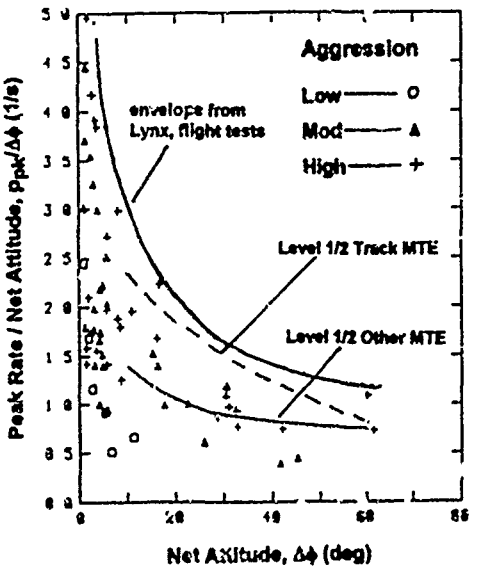

Figure 8. Roll Attitude Quickness from Sidestep Test Data In Flight (Lynx) and Ground-Based Simulation (AFS)

A quickness is calculated for every rate peak in the attitude time histories. The Lynx line on Figure 8 represents the upper boundary of all data gathered for a range of attack and sidestep sizes. The data include the cases plotted in Figure 5 showing that at the highest agility factors/quickness, poor Level 2 ratings were awarded, i.e., the performance degrades rather than improves. The Advanced Flight Simulator data correspond to a 150-ft sidestep flown at the three levels of attack shown. Although the roll bandwidth of configuration T509 was less than that of the Lynx (~3 rad/s for T509 compared with ~5 rad/s for the Lynx), the control power was similar (~100 deg/s), and the pilots achieved similar levels of quickness across the full amplitude range. Also shown on Figure 8 are the Level 1/2 boundaries for tracking and other mission task elements from ADS33C. There are several points worth making about these data that impact on agility:

1) The shape of the quickness boundaries reflects the shape of the response capability limits on Figure 7. The quickness has generic value and forms the link between the bandwidth and control power, but is not, in general, uniquely determined by them.

2) The result of increased attack is increased achieved quickness across the amplitude range

3) The cluster of quickness at small amplitude corresponds with the pilot applying closed-loop control in the terminal re-positioning phase and attitude corrections during the accel/decel phases.

4) At low amplitude, the maximum achievable quickness corresponds to the open-loop bandwidth except when a pure time delay is present (as with the Advanced Flight Simulator configuration), when the bandwidth is lower than the quickness.

5) The ADS33C quickness boundaries at high amplitude correspond to the minimum control power requirements of 50 deg/s.

From considerations of control power, quickness and bandwidth alone, Lynx and T509 are Level 1 aircraft. In practice, however, at the higher attack, when the highest quickness is recorded, both are Level 2. Some of this degradation can be accounted for by simulated visual cue deficiencies with T509 and by severe cross couplings with the unaugmented Lynx. The data in Figure 8 are a useful benchmark for the kind of quickness required in rotorcraft to achieve high agility factors in low speed MTE's, but it does not provide strong evidence for an upper boundary on quickness (or bandwidth and control power) Configuration T509 was implemented in the DRA's Conceptual Simulation Model[15] as a simple low-order equivalent system of the form

$$\frac{p}{\eta_{lc}} = K\frac{e^{-\tau s}}{\left(\frac{s}{\omega_m}+1\right)\left(\frac{s}{\omega_a}+1\right)} \qquad (2)$$

where p is the body axis roll rate (rad/s) and η_{lc} is the pilot's lateral cyclic stick displacement (±1). ω_m is the fundamental first-order break frequency or roll damping (rad/s) and ω_a is a pseudo-actuator break frequency (rad/s). K is the steady-state gain or control power (rad/s-unit η_{lc}) and τ is a pure time delay.

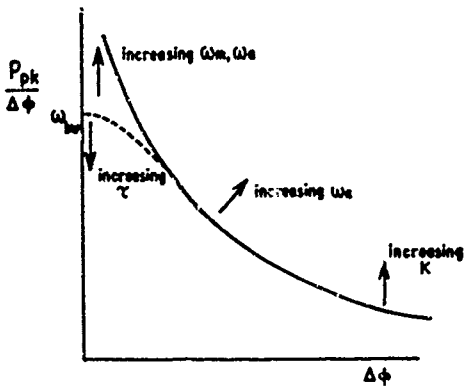

Figure 9. Effect of Conceptual Simulation Model Parameters on Roll Quickness

Figure 9 illustrates the effects of the various parameters in the Conceptual Simulation Model on the maximum achievable quickness. In particular, the actuator bandwidth has a powerful effect on quickness in the low to moderate amplitude range. Maximising the actuation bandwidth and minimising delays in the achievement of maximum acceleration are in accordance with maximising the agility factor. Moreover, while this configuration has been used for helicopter-related agility research, the results are equally applicable to fixed-wing aircraft.

The sensitivity of agility factor with the parameters of the Conceptual Simulation Model is relatively easy to establish. If we consider the same bank and stop task discussed in the fixed-wing context earlier in this paper, some useful insight can be gained. A pulse type control input will be assumed, although, in practice, pilots would adopt a more complex strategy to increase the agility factor. To illustrate the primary effect we consider the case where the "secondary" time delays are set to zero (i.e., $\tau = 0$, $\omega_a = 0$). For a roll angle change of $\Delta\phi$, the ideal time (assuming the time to achieve maximum rate is zero) is then given by

$$T_i = \Delta\phi / K = \Delta t \qquad (3)$$

where Δt is the control pulse duration.

The time to reduce the bank angle to within 5% of the peak value achieved is given by

$$T_s = \Delta t - \ln(0.05)/\omega_m \qquad (4)$$

The agility factor is then given by

$$A_f = T_i / T_s = \frac{\omega_m \Delta t}{\omega_m \Delta t - \ln(0.05)} \qquad (5)$$

Figure 10 illustrates the variation of A_f with $\omega_m \Delta t$. The bandwidth ω_m is the maximum achievable value of quickness for this simple case, and hence the function shows the sensitivity of A_f with both bandwidth and quickness. The normalised bandwidth is a useful parameter, as it represents

the ratio of aircraft to control input bandwidth, albeit rather crudely. For short, sharp control inputs, typical in tracking corrections, high aircraft bandwidths are required to achieve reasonable agility factors. For example, at the ADS33C minimum required value of 3.5 rad/s and with 1-second pulses, the pilot can expect to achieve agility factors of 0.5 using simple control strategies in the bank and stop manoeuvre. To achieve the same agility factor with a half-second pulse would require double the bandwidth. This is entirely consistent with the argument that the ADS33C boundaries are set for low to moderate levels of attack.

If values of agility factor up to 0.75 are to be achieved, Figure 10 suggests that bandwidths up to 8 rad/sec will be required; whether this is worth the 30% reduction in task time can only be judged in an overall operational context. Such high values of bandwidth are not uncommon in fixed-wing aircraft, of course, and Figure 10 serves to illustrate and underline the different operational requirements of the two vehicle classes.

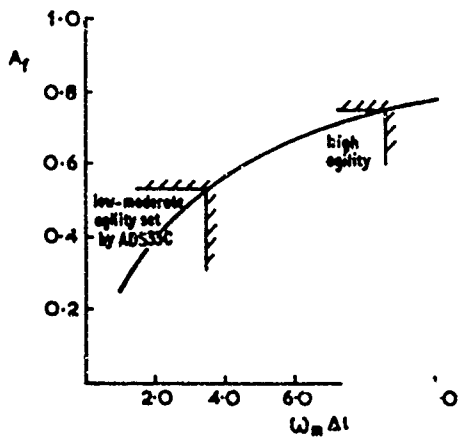

Figure 10. Notional Variation of A_f with Normalised Bandwidth

This simple example has many questionable assumptions but the underlying point, that increasing key flying qualities parameters above the ADS33C boundaries has a first order effect on task performance, still holds. However, it provides no clues to possible upper performance boundaries set by flying qualities considerations. As stated earlier, ADS33C does not address upper limits directly. Also, practically all the upper boundaries in MIL-STD-1797 are related to the acceleration capability of the aircraft. As noted earlier, there are tentative upper limits on pitch attitude bandwidth, but it is suspected that these are actually a reflection of the high control sensitivity required to maintain a defined level of control power, rather than the high values of bandwidth per se. Control sensitivity itself (rad/s^2-inch) is a fundamental flying qualities parameter and is closely related to the pilot's controller type. While some data exist for helicopter centre and side sticks, more research is required to establish the optimum characteristics including shaping functions. MIL-STD-1797 provides a comprehensive coverage of this topic for fixed-wing aircraft, rather more as guidance than firm requirements.

Another fruitful avenue appears to lie in the extension of the quickness parameter to the acceleration phase of a mission task element. The fixed-wing Control Anticipation Parameter already suggests this as the ratio of pitch acceleration to achieved normal "g" (effectively, pitch rate). The DRA Conceptual Simulation Model trials offers a good example to explore and develop this concept of rate quickness. Setting the pure delay term in the Conceptual Simulation Model to zero for this study, the magnitude and time constant of the peak roll acceleration, for a step control input, can be written in the form

$$\dot{p}_{pk} = \frac{K\omega_m}{\gamma} e^{-\omega_a t} \eta_{1c} \qquad (6)$$

$$\omega_a t = \frac{\log \gamma}{1-\gamma}, \qquad \gamma = \omega_m / \omega_a \qquad (7)$$

The rate quickness can then be written in the form,

$$\frac{\dot{p}_{pk}}{\Delta p} = \frac{\omega_m}{\gamma} e^{\frac{\log \gamma}{1-\gamma}} \qquad (8)$$

This is plotted in normalised form in Figure 11. During the Advanced Flight Simulator handling qualities trial described in Reference 14, the lag bandwidth ω_a was set at 20 rad/s to satisfy the pilot's criticism of jerky motion. This gave a g of about 0.5 at the highest bandwidth flown (T509) Corresponding values of rate quickness and time to peak acceleration were 0.5 and 0.7 respectively, both relative to the natural aircraft bandwidth, ω_m.

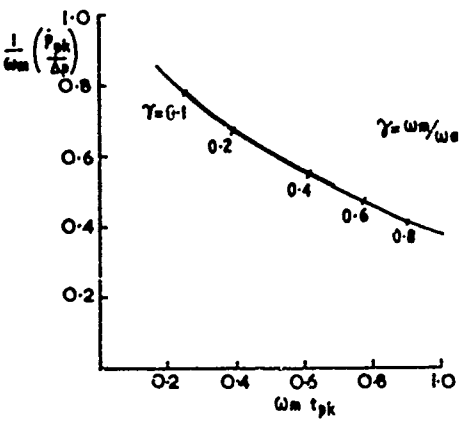

Figure 11. Variation of Rate Quickness with Acceleration Time Constant

Intuitively, there are likely to be upper and lower flying qualities bounds on both of these parameters. Hard and fast may be as unacceptable as soft and slow, both leading to low agility factors; the opposite extremes may be equally acceptable when referred to the maximum quickness. This suggests closed boundaries delineating the quality levels on the Figure 11 format. Clearly, more systematic research and data capture are required to test and develop this hypothesis further.

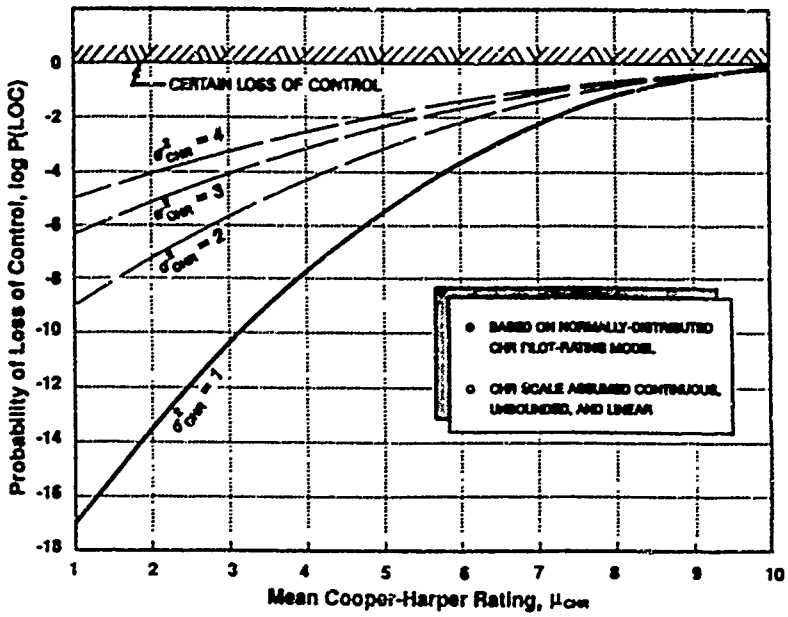

Figure 12. Relationship Between Mean CHR (Cooper-Harper Rating) and P(LOC)

The results of this objective quality analysis indicate that the flying qualities parameters are suitable for quantifying agility beyond the minimum levels set by the standards. The quickness, for example, is a natural measure of agility, increasing with manoeuvre attack, and spanning the low frequency/high amplitude to high frequency/low amplitude range of manoeuvre kinematics.

Upper limits on flying qualities may, however, be better expressed in terms of acceleration-based parameters, rather than the rate-based parameters more commonly found in the flying qualities standards. Upper limits for small amplitude motions appear to be well catered for by control sensitivity in the various axes. For larger motions, there is a significant gap; some of the ad hoc parameters in MIL-STD-1797, e.g., CAP, do point to a possible generic approach. ADS33C does not address upper limits at all. The quickness concept has been extended to the acceleration response with a view to bridging this gap.

6. THE SUBJECTIVE MEASUREMENT OF QUALITY

Flying quality is ultimately determined by pilot subjective opinion. The "measurement scale" and the understanding for this continue to stimulate vigorous debate but the Cooper-Harper handling qualities rating scale provides the most widely accepted standard.

The operational benefit of good flying qualities has never been properly quantified using the pilot rating approach, however. But the safety benefits have been addressed in References 16 and 17, using the Cooper-Harper pilot rating scale as a metric (Figure 1) These references consider the pilot as a vital system component who can fail (be stressed to failure) in an operational context. The authors point out that if a normal distribution of ratings is assumed, then the probability of control loss, P(LOC), can be calculated for various mean ratings and dispersions, as shown in Figure 12. P(LOC) is the probability of obtaining a rating greater/worse than 9.5, which in turn is simply proportional to the area under the distribution to the right of the 9.5 rating. Thus the probability of flight failure, due to flying qualities deficiencies can be estimated. For the case studied in Reference 16 and depicted in Figure 12, operating a barely Level 1 aircraft can reduce the probability of loss of control by an order of magnitude, compared to an aircraft in the better end of Level 2 This result immediately raises the question, what is the probability of mission success or failure, and can the same comparisons be made between aircraft with different mean flying qualities?

Figure 13 shows a notional distribution of ratings, with the regions of desired, adequate and inadequate performance clearly identified. The desired and adequate levels can be considered as reflecting varying degrees of mission (task element) success, while the inadequate level corresponds to mission (task element) failure. Effectively the mission is composed of a number of contiguous Mission Task Elements, each having a virtual Cooper-Harper rating assigned on the basis of performance and workload that the situation demands and allows, respectively. If a particular Mission Task Element were assigned a Level 3 rating, then the pilot would either have to try again or give up on the particular Mission Task Element.

Loss of control has obvious ramifications on mission success. The probability of obtaining a rating in one of the regions is proportional to the area under the distribution in that region.

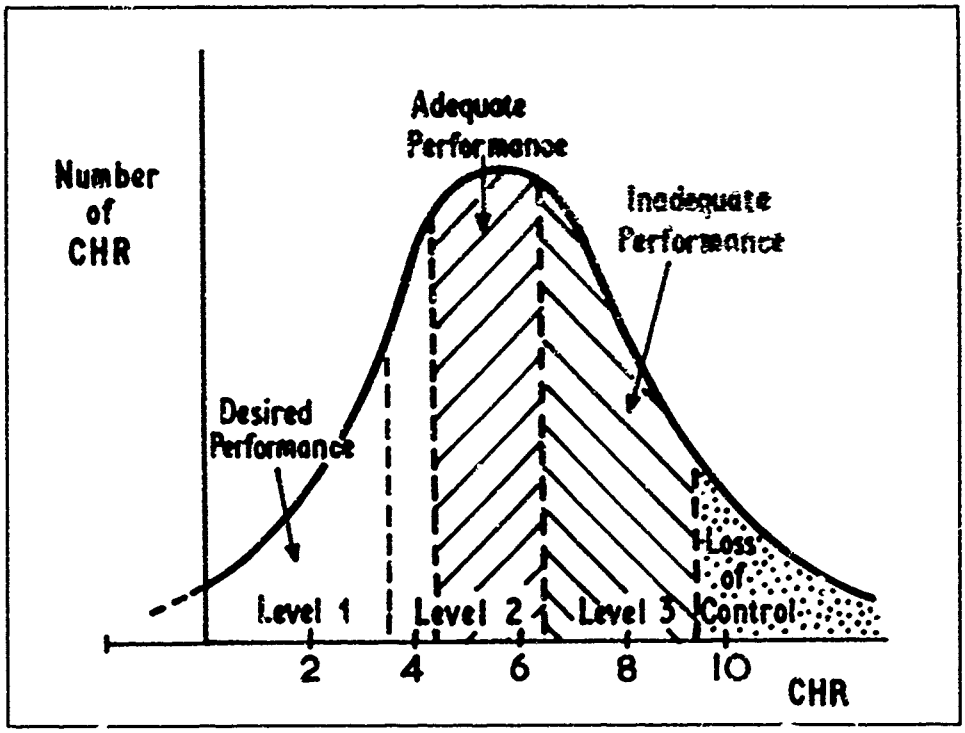

Figure 13. Notional Distribution of Pilot Handling Qualities Ratings for a Given Aircraft

Note that, as discussed in References 16 an 17, we include ratings greater than 10 and less than 1 in the analysis. The rationale is that there are especially good and bad aircraft or situations, whose qualities correspond to ratings like minus 2 or 13. However, the scale enforces recording them as 1 or 10.

Note too that the scatter produces, even with a good mean rating, a large probability of merely adequate performance and even a finite probability of total loss of control and crash. We have said in the Introduction to this Paper that flying qualities are determined by the synergy between internal attributes and external influences. It follows then that sources of scatter originate both internally and externally. Internal sources include divided attention, stress and fatigue, pilot skill and experience. External sources include atmospheric disturbances, changing operational requirements and timelines, threats, etc. The flying qualities community has done much to minimize scatter by careful attention to experimental protocol,[18] but in operational environments the effective pilot rating scatter is omnipresent.

Figure 14 shows the probability of obtaining ratings in the various regions when the standard deviation of the ratings is unity. This curve, which we have labeled as preliminary, has some interesting characteristics. First, the intersections of the lines occur at the ratings 4.5, 6.5, and 9.5, as expected. Also it turns out that for a mean rating of 7, the probability of achieving inadequate performance is, of course, high, and we can also see that the probability of achieving desired performance is about the same as that for loss of control—about one in a hundred. Improving that rating to 2, lowers the probability of loss to 10^{-13} (for our purposes zero) and ensures that performance is mostly at desired levels. Degrading the mean rating from 2 to 5 will increase the chances of mission failure by three orders of magnitude.

We describe these results as preliminary because we assume that there is a rational continuum between desired performance, adequate performance, and control loss. For example, desired and adequate performance may be represented by discrete touchdown zones/velocities on the back of a ship, and loss of control might be represented by, say, the edge of the ship or hanger door. On a smaller ship (or bigger helicopter, for example), the desired and adequate zones may be the same size as on the larger vessel, which puts the deck-edge closer to the adequate boundary, or may represent a similar fraction of the deck size, hence tightening up the whole continuum. This raises some fundamental questions about the underlying linearity of the scale. With the servo-model of piloting behaviour, for example, we can always define a desired level of flight path task performance so demanding that, whatever the aircraft attitude bandwidth, pilot induced oscillations will result, leading to level 3 ratings.

Though these questions remain, pilot rating and mission success or failure are powerfully related through the preliminary data in Figure 14. Flying qualities alone can determine whether operational agility is flawless or whether control is lost.

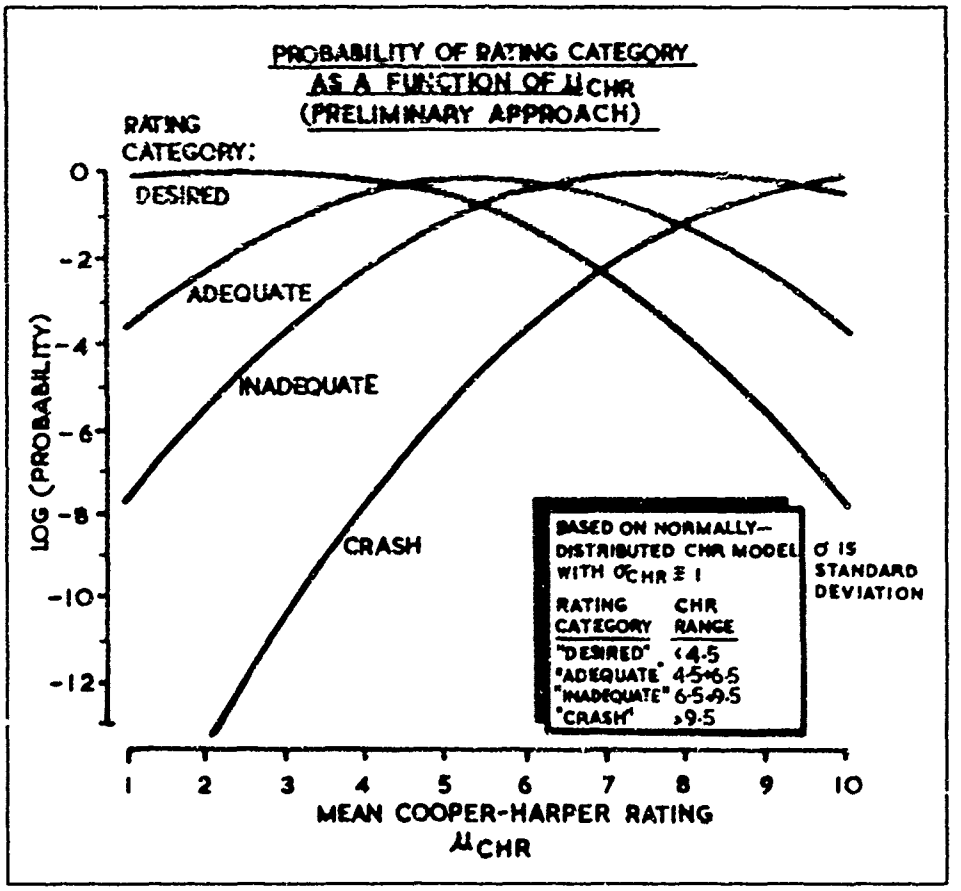

Figure 14. Relationship Between Mean CHR (Cooper-Harper rating) and Probability of Mission Success, Failure or Crash - Preliminary Results

7. INCLUDING FLYING QUALITIES EFFECTS IN COMBAT MODELS

The results highlighted in this paper suggest ways by which the effects of flying qualities can be incorporated into unmanned combat mission simulations. Such models are regularly used to establish the effectiveness of different weapon system attributes or tactics, but the human element is usually absent for obvious reasons. The aircraft are therefore assumed to have perfect flying qualities, and the models are often configured to ignore the transient responses, effectively assigning an agility factor of unity to each manoeuvre change or Mission Task Element. The impact of these assumptions is twofold: first, there is no way that flying qualities or their enabling technologies can be included in the trade studies conducted with such models. Second, the implied perfect flying qualities may give a false impression of the importance or the value of mission performance enhancements. The key steps to embodying the key flying qualities effects are suggested as follows:

1) Through objective design and assessment, establish the level of flying quality and hence the effective mean Cooper-Harper rating for a configuration.

2) Describe the mission in terms a series of contiguous Mission Task Elements, selectable in the same way that set-piece manoeuvres are in combat models.

3) Establish a Mission Task Element hazard weighting on the basis of threat, divided attention and other internal/external factors, that will define the effective virtual Cooper-Harper rating for the Mission Task Element. This will vary as the mission develops.

4) Establish a time scaling for each Mission Task Element, on the basis of the maximum achievable agility factor.

5) Overlay the time scaling on the mission profile, there will be an option for each Mission Task Element to fly at reduced agility factor with level 1 virtual Cooper-Harper rating or to fly at the higher agility factor at a poorer Cooper-Harper rating.

Improvements or degradations in flying qualities can then be explored through variations in the achievable agility factors, and mean Cooper-Harper rating for the aircraft and can be linked directly to the enabling control technologies. There

are, of course, some fundamental questions associated with this approach. How can we assign the mean rating and the standard deviation? How do we classify the hazards resulting from the various degrading influences? How are the maximum agility factors derived? These and others will need to be addressed if this approach is to be taken further; the benefits are potentially high however, both in terms of clarifying the value of active control to effectiveness and, conversely, establishing the cost of flying qualities limitations to operational agility.

8. CONCLUSIONS AND RECOMMENDATIONS

Operational agility is a key attribute of any weapon system and its subsystems from sensors, through the airframe elements and pilot, to the primary mission element, e.g., weapon. The total system can only be as agile as its slowest element, and maximising the concurrency within the subsystems is a key method for enhancing agility. The focus of this Paper is the airframe and its primary enabling attribute—its flying qualities. The adequacy of existing flying qualities criteria for providing agility is addressed along with the benefits to agility of good flying qualities and the penalties of poor flying qualities. The following principal conclusions can be drawn.

1) Existing flying qualities criteria provide an acceptable and necessary framework for describing and quantifying agility; the quickness parameter stands out as a useful agility metric and should be extended beyond the current rotary-wing attitude response requirements to flight-path variables and fixed-wing applications. However, the existing quality boundaries are only minimum standards and do not reflect or quantify the desirable characteristics at high performance levels. Indeed, there are very few boundaries defined that set upper limits on usable performance.

2) The agility factor provides a measure of usable performance and can be used to quantify the effects of flying qualities on agility. Rotary-wing research has shown that agility factors up to 0.7 can be achieved with current aircraft types operated with high performance margins, but handling deficiencies typically lead to Cooper-Harper ratings in the poor Level 2/Level 3 region. Moreover, the degradation from Level 1 to 3 is rapid. High agility factors achievable with Level 1 flying qualities should be a goal for future operational types.

3) Extensions of the ADS33C innovation, the quickness, into the acceleration response is suggested as a potentially useful parameter for setting flying qualities limits on performance. Flight and simulation data needs to be gathered and analysed systematically to test this hypothesis.

4) It is argued that even a Level 1 aircraft "on paper" will degrade to Level 2 and 3 in unfavourable situations. In this context, a probabilistic analysis can be used to highlight the benefits of improved flying qualities on operational agility and mission effectiveness. Operating a Level 2 aircraft is shown to increase the chances of mission failure by three orders of magnitude as compared to a Level 1 aircraft. The results are preliminary and dependent on a number of underlying assumptions, but indicate a powerful relationship. Experimental results are needed to substantiate the results. These could include learning runs and trials with varying degrees of external influences.

5) Considering the mission as a series of contiguous mission task elements enables the agility factor and probability of success/failure to be overlaid on non-piloted combat mission simulations. This should allow flying qualities to be included in such exercises and flight control technologies to be integrated into mission effectiveness trade studies.

6) The key to ensuring that future projects are not susceptible to performance shortcomings from flying quality deficiencies would appear to be in the development of a unified specification for flying qualities and performance, with a clear mission orientation in the style of the new flying qualities requirements.

9. ACKNOWLEDGMENT

The authors wish to thank Darrell Gillette of McDonnell Douglas Aerospace for his contributions to the technical content of this paper and also for his patience in creating the paper's layout.

10. REFERENCES

1. Cooper, G.E. and Harper, R.P., Jr., "The Use of Pilot Ratings in the Evaluation of Aircraft Handling Qualities," NASA TM D-5153, 1969.

2. AVSCOM, "Aeronautical Design Standard (ADS) 33C—Handling Qualities for Military Helicopters," US Army AVSCOM, 1989.

3. USAF, "MIL-STD-1797—Flying Qualities of Piloted Vehicles," USAF, 1987.

4. Skow, A.M., "Agility As a Contribution to Design Balance," AIAA 90-1305, 5th bi-annual Flight Test Conference, Ontario, Canada, May 1990.

5. Hodgkinson, J. and Hodgkinson, R.K., "Fighter Transient Agility and Flying Qualities," AIAA Conference on Atmospheric Flight Mechanics, Flying Qualities Workshop, Monterey, California, August 1987.

6. Hodgkinson, J., et al, "Relationships Between Flying Qualities, Transient Agility, and Operational Effectiveness of Fighter Aircraft," AIAA Paper 88-4329, AIAA Conference on Atmospheric Flight Mechanics, Minneapolis, Minn., August 1988.

7. Riley, D.R. and Drajeske, M.H., "An Experimental Investigation of Torsional Agility in Air-to-Air Combat," AIAA Paper 89-3388, Conference on Atmospheric Flight Mechanics, Boston, Massachusetts, August 1989.

8. Riley, D.R. and Drajeske, M.H., "Status of Agility Research at McDonnell Aircraft Company and Major Findings and Conclusions to Date," ICAS Paper 90-5.9.4, 1990.

9. Riley, D.R. and Drajeske, M.H., "Relationships Between Agility Metrics and Flying Qualities," Paper 901003, SAE Aerospace Atlantic, April 1990

10 Brotherhood, P. and Charlton, M.T., "An Assessment of Helicopter Turning Performance During NOE Flight," RAE TM FS(B) 534, January 1984

11 Heffley, R.E., "Study of Helicopter Roll Control Effectiveness," NASA CR 177404, April 1986

12 Padfield, G.D. and Charlton, M.T., "Aspects of RAE Flight Research into Helicopter Agility and Pilot Control Strategy," paper presented at a Handling Qualities (Mil Spec 8501) specialists meeting, NASA Ames, June 1986

13 Charlton, M.T., Padfield, G.D., and Horton, R.I., "Helicopter Agility in Low Speed Manoeuvres," Proceedings of the 13th European Rotorcraft Forum, Arles, France, September 1987 (also RAE TM FM 22, April 1989

14 Padfield, G.D., et al "Helicopter Flying Qualities in Critical Mission Task Elements," Paper F2, 18th European Rotorcraft Forum, Avignon, September 1992

15 Buckingham, S.L. and Padfield, G.D. "Piloted Simulations to Explore Helicopter Advanced Control Systems," RAE Tech Report 86022, April 1986

16 Hodgkinson, J., Page, M.A., Preston, J.D., and Gallette, D.E., "Continuous Flying Quality Improvement—the Measure and the Payoff," AIAA Paper 92-4527" 1992 Guidance, Navigation and Control Conference, Hilton Head Island, S. Carolina, August 1992

17 Page, M.A. Gallette, D.E. Hodgkinson, J. and Preston, J.D., "Quantifying the Pilot's Contribution to Flight Safety," International Air Safety Seminar, Flight Safety Foundation, Long Beach, California, MDC Paper 92K0377, November 1992

18 Wilson, D. and Riley, D. "Cooper-Harper Pilot Rating Variability," AIAA Paper 89-3358, Atmospheric Flight Mechanics Conference, Boston, Massachusetts, August 1989

AN AGILITY METRIC STRUCTURE

FOR OPERATIONAL AGILITY

Captain Andrew Reif, Flight Dynamics
Aerospace Engineering Test Establishment
CFB Cold Lake, Alberta, Canada, T0A 2M0

Summary

This paper summarizes how an agility metric organizational structure was developed by the Flight Mechanics Panel Working Group 19. The structure was developed from existing concepts and was generalized for application to both fixed and rotary wing aircraft. The approach was based on time domain analysis concepts focussing on the "time to complete" a specific operational task as the primary metric. From this metric a hierarchy of smaller time scale metrics were developed to emphasize the desired transient response dependent on the mission.

The metric structure was developed for organizing the concepts of airframe agility as these were the most mature. The metric scheme is comprised of transient, experimental, and operational metrics. The transient metrics were defined as those time dependent parameters that characterize instantaneous airframe state changes. Experimental metrics were defined by discrete small task elements with compound properties that were optimized for evaluation purposes but were not necessarily recognizable as a mission related maneuver. Operational metrics were defined as complete mission task elements including the total vehicle response in multiple degrees of freedom.

The structure was also found to be applicable to other aspects of agility through the evolving concept of operational agility. This entailed the limited study of possible systems, pilot/vehicle interface, and weapon system time based agility metrics. Finally, the working group identified areas which required further study.

Symbols and Abbreviations

a_x	Axial Acceleration
AQP	Attitude Quickness Parameter
CCT	Combat Cycle Time
DST	Dynamic Speed Turn
E-A	Energy-Agility
g	Acceleration due to Gravity
H	Altitude
HQR	Handling Qualities Rating
HQDT	Handling Qualities During Tracking
inst	instantaneous
LA	Lateral Agility
LAT	Large Amplitude Task
N_z	Body Axis Normal Load Factor
OA	Operational Agility
P	Roll Rate
PM	Pointing Margin
P_s	Specific Excess Power
PR	Power Rate
PN	Roll Rate Normal Load Factor Product
Q	Pitch Rate
R	Yaw Rate
RC90	Roll and Capture 90 degree Bank Angle
SAT	Small Amplitude Task
TA	Torsional Agility
TR	Turn Rate
U	axial velocity component

An Introduction to Operational Agility

Combat aircraft agility, in the sense of rapid transient maneuvering to gain a tactical advantage, has been the focus of roughly two decades of research. The emphasis was placed on the characterization of transient motions through the use of clear and unambiguous metrics. These metrics have been presented in a multitude of papers which by and large make up the literature on the subject of agility. Missing, though, is a framework with which to understand the broad implications of these metrics. This paper shall therefore focus on how to organize the agility metrics.

Formulating an agility metric structure is seen now to be an important step in the establishment of agility as a design objective because the operationally significant elements of agility need to be clarified and specifications developed. Agility concepts also need to be united with the well established concepts of performance, control, and stability. Without a usable structure and common language the goal of understanding agility and communicating its value has remained elusive.

Working Group 19 was assigned the task of making sense of the current agility state-of-the-art and providing clear direction for future efforts. The multi-disciplinary background of the Working Group facilitated discussion of the current knowledge. From this basis it was possible to focus on what agility means and how it influences combat aircraft design so as to perform the mission. The working group was comprised of design, evaluation, and operational experts from both the rotary and fixed wing aircraft community. The working group observed that much of the agility research focused on highly specialized aspects of the larger problem. That is, how to respond to a rapidly changing threat or hostile environment while at the same time successfully completing the mission. A concept that covers both design and operations yet still must be evaluated for cost effective specification compliance.

During the deliberations of Working Group 19 between 1991 and 1993, it became evident that the airframe elements of agility were in fact only part of what agility was in combat. A balanced total aircraft design was the key to the best chance for success in combat. The Operational Agility of this total aircraft system therefore became the new or evolved basis for agility.

Presented at an AGARD Meeting on 'Technologies for Highly Manoeuvrable Aircraft', October 1993.

Figure 1. Missile Engagement Task Time Components.

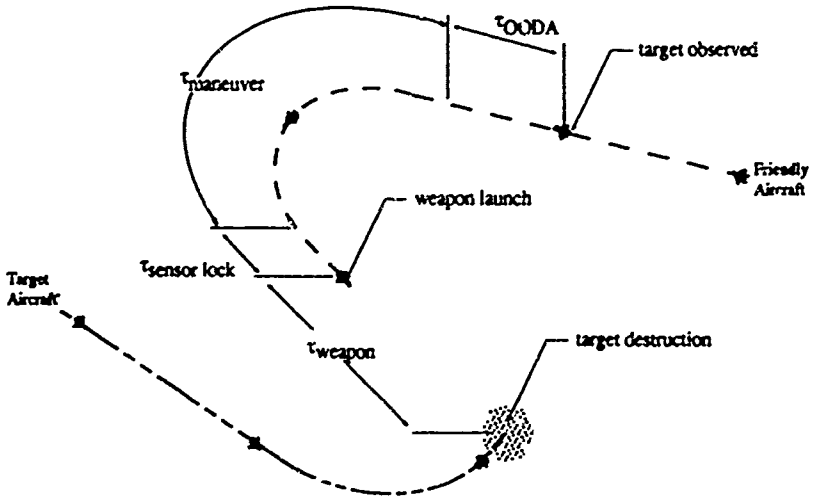

TOTAL TASK TIME = $\tau_{OODA} + \tau_{maneuver} + \tau_{sensor\ lock} + \tau_{weapon}$

Note: OODA is Object, Orientation, Decision, Action pilot loop.

How fast the total aircraft responded to a rapidly changing threat environment could naturally be measured with time, or more specifically, the time to perform a mission task. This concept was first proposed by Skow. (1) In Skow's paper the missile engagement task was used to illustrate how to characterize the overall time to complete a mission task. Each aircraft characteristic that influenced the task may be represented by a time delay, τ, as shown in Figure 1, that may be summed to determine the overall task time.

Overall, the relation of any one time delay to agility may be interpreted by its duration. That is maximizing the time delay increases the quickness and therefore agility. Multiple parallel actions and the ability to change, in minimum time, between actions can also be interpreted as improved agility. Lynch observed that over emphasizing one time delay, such as the airframe, could result in reaching a point of diminishing returns or, exposing a deficiency with another component of the aircraft by over extending its capabilities.(2)

An aircraft designed to minimize time delays overall, will be quicker at performing the mission task and therefore faster to engage and destroy a hostile aircraft or free to continue with the primary mission. Since the aircraft will be expected to perform many mission tasks quickly or in fact switch between several roles, Operational Agility will become a basic design objective. If on the other hand, the aircraft does not need to respond fast to a threat or changing battlefield then agility does not need to be a major design consideration. Agility is only one element of the aircraft's fighting qualities.

This paper will therefore develop a structure for the metrics that measure the operational agility characteristics of the total aircraft based on time domain techniques. The discussion begins with some OA terminology. Following that, previous metric structures shall be presented that have provided the foundation for the structure. With the benefit of this knowledge, the Working Group 19 structure or classification scheme will be developed and applied to all the elements of OA. The concepts will then be suggested as a means to develop specifications for agility. Finally, required future efforts will be outlined. For a more detail discussion of OA and the metrics themselves, the reader is referred to the Working Group 19 report.(2)

Terminology

A number of comprehensive terms were defined in order to describe the expanded scope of Operational Agility.(2) As the complete scope of Operational Agility is new to many readers, classical agility, that is aerodynamic, propulsion, control, and operator aspects of agility will be referred henceforth as airframe agility. In addition the working group identified the other major agility elements as systems (avionics) agility, and weapons agility. The working group defined these operational agility elements as:

1) Operational Agility - the ability to adapt and respond, rapidly and precisely, with safety and poise, to maximize mission effectiveness.

2) Airframe Agility - the physical properties of the aircraft which relate to its ability to change, rapidly and precisely, its flight path or pointing axis.

3) Systems Agility - the ability to rapidly change mission functions of the individual systems which provide the pilot with his tactical awareness and his ability to direct and launch weapons in response to and to alter the combat environment.

4) Weapons Agility - the ability to engage rapidly characteristics of the weapon and its associated onboard systems in response to hostile intent or counter-measures.

The aspect of the pilot/vehicle interface is closely tied to each of these elements and as such is a primary feature of the Operational Agility of the aircraft.

Classification Development

Most of the research has focussed on airframe agility and its metrics mainly for specific aircraft types, such as fighters and attack helicopters, but very little work has been done to establish an overall classification scheme. That is to say a classification scheme that enabled agility data to be structured for analysis or to permit a more detail statement within a specification other than "the aircraft shall be agile".

The first widely accepted agility metric classification scheme was developed by researchers at the USAF Air Force Flight Test Center (AFFTC) and attempted to classify metrics by initial response and long term response of a fighter aircraft.(3) This classification scheme separated the metrics into two groups: transient and functional metrics. The groups were originally defined as: (3)

1) Transient Metrics - metrics that characterized the acceleration or deceleration phase of a maneuver.

2) Functional Metrics - metrics that described the complete system including the pilot-vehicle interface, control mechanisms, aircraft performance, aircraft handling characteristics as the total system behaved in closed loop tasks.

In this context, the transient metrics were intended to provide agility information for designers to isolate the response and evaluators to compare data for specification compliance. Functional metrics provided information about the operational suitability of the airframe.

Recently, these same researchers at the AFFTC elected to modify the metric classification rules to more accurately represent the use of the agility metrics. This alteration was reported by Lawless (4) after gathering and analyzing data obtained from the X-29, F-15, F/A-18, F-16, F-4, and A-37 using airframe metrics proposed at the time. The revised classifications were:

1) Agility Design Parameters (ADP) - replaced transient metrics as a means to provide clearly defined design tools.

2) Evaluation Metrics - replaced functional metrics as a means of classifying the closed loop tasks. Within evaluation metrics, a further two categories:

   a) Flight Path Metrics characterized the pilot control of the lift vector comprised of load factor agility, torsional agility, and acceleration along the flight path.

   b) Attitude Metrics characterized the nose pointing capabilities of the aircraft including pitch and yaw pointing.

These revised groupings represented a fine tuning of the design aspect of airframe agility characterization. The operational suitability aspects were not emphasized. It is not clear at this time that the revised approach has received support.

Dorn presented a time-scale concept for interpreting agility using the state-change versus time plot shown in Figure 2.(5) This plot illustrates the state change capabilities of an aircraft. If defined in sufficient detail the state changes could permit comparison with other aircraft. Unfortunately, deriving the state change activity has been very difficult. Notwithstanding this limitation, the benefits of parallel task activity can be demonstrated. More state change, per unit time implies higher agility. Dorn proposed three time scales as a classification scheme to isolate the significant time realms for agile task activity. These were:(5)

1) Instantaneous Tasks(inst) - these tasks are characterized by instantaneous rates for 0-1 seconds.

2) Small Amplitude Tasks(SAT) - these tasks last 1-2 seconds or the time to perform a small task.

3) Large Amplitude Tasks(LAT) - these tasks last 10-20 seconds or time to perform a mission task element.

Dorn suggested that each of the time-scales was a building block for the next longer time scale. As the task time is increased, details become lost or hidden as the sequence of events or activities tend to a complex but more realistic scenario. LATs are therefore more operationally meaningful, but difficult to characterize. Conversely, as the task time is decreased, details become clear and simpler to characterize but the impact on the mission becomes vague. For this reason a third intermediate grouping becomes beneficial since it contains elements of design and mission task segments.

The working group found the three time realms to be very appropriate but discussed at length the quantitative time increments for each building block. The group felt that these time realms should not be articulated precisely as too many exceptions were possible which detracted from the strength of the concept.

Figure 2 Dorn's State Change versus Time Plot. (5)

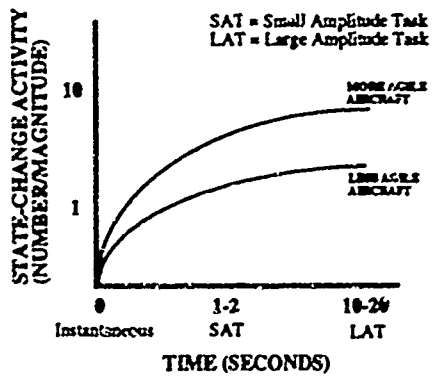

Fox supported Dorn's classification scheme and identified several existing agility metrics in use by the community for each time scale.(6) The instantaneous time scale includes the "analytical metrics that are mathematical manipulations of the governing EOM, the small amplitude tasks include such metrics as proposed by Skow (1), and finally the large amplitude tasks includes metrics proposed by Kalviste (7) and Tennant (8)."

One final structure related to the development of an agility metric structure, the mission task element (MTE). The use of operationally oriented mission tasks were suggested as a very powerful means of demonstrating in a clear and unambiguous way the operational suitability of the aircraft. Operationally oriented mission tasks for evaluation are nothing new. ADS-33C for rotary wing flying qualities(9), perhaps has gone the furthest to make use of them in a specification. ADS-33C proposed the MTE as a means for standardizing helicopter flying qualities evaluation during closed loop operational tasks.

Each of these metrics structures or classification schemes reflected the interests of the design, evaluation, and operational communities. The working group observed that:

1) Dom's three time scales portrayed the time dependence of agility facilitating a hierarchical structure.

2) The two AFFTC approaches presented a more detailed understanding of Dom's instantaneous and small amplitude task realms.

3) Fox classified some of the existing metrics within Dom's three tier approach indicating that the metrics could be logically united using time scales.

4) The ADS-33C MTE approach provided a more detailed method for characterizing the operational suitability aspect of ability.

A very logical structure emerged by combining all the previous structures.

Metric Classification Structure

The airframe agility metric classification concepts were combined to arrive with a scheme possessing three broad classes of metrics: transient, experimental, and operational. The transient metrics include Dom's Instantaneous class and the AFFTC transient metrics/ADPs. The Experimental class included Dom's Small Amplitude Task class, the AFFTC Evaluation metrics, and part of the AFFTC Functional metric class. The operational metric class includes Dom's Large Amplitude Task class, the MTE as defined within ADS-33C, and part of the AFFTC Functional metric class. Once grouped it became easier to define the metric levels within the structure.

The transient class may be considered to contain continuous characterizations of the instantaneous response of the aircraft. In other words, the continuous metrics include time dependent parameters such as the agility vector.(10)(11)(12)(13) The metrics can be calculated at any moment during a maneuver, and as such may not be the maximum possible. They lend themselves to optimization as suggested by NASA researchers. (14) From a time history of these parameters it will be more obvious when the agility capabilities of the aircraft are being exploited. Transient rate changes occur at the peak events suggesting the maneuver segments ideal for experimentation.

Certain characteristics can be formulated into "discrete" parameters to focus on the transient response to a particular set of control inputs. These are the experimental metrics. They are only calculated at specific moments immediately after the input is applied. The experimental metrics can be thought of as some of the basic building blocks of more recognizable operational maneuvers. As basic building blocks the maneuvers used would be short and easy to define, control, and repeat making these metrics ideal for test and evaluation.

Operational metrics are the final class and focus on the global agility concepts of quickness and precision as well as time to perform specific mission tasks. The mission task quickness metrics focus on the time to perform a task associated with a mission. Aggressiveness plays a significant role in weighting the time to perform the task. The mission task precision emphasizes the accuracy with which the task is controlled while being performed quickly.

The airframe agility metric scheme was then expanded to encompass the entire scope of Operational Agility. A metric hierarchy was constructed as shown in Figure 3. All the elements that contribute to the response time of the total aircraft system can now be represented with suitable metrics proposed for each element.

Figure 3. The Operational Agility Metric Hierarchy.

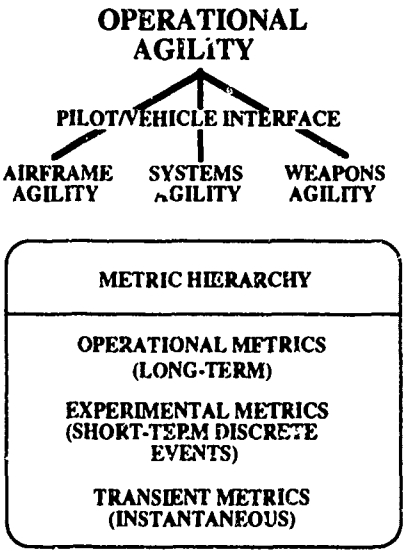

Although not intentional, the agility metric classes were analogous to existing handling qualities metric classes. The theoretical basis for continuous representation of the motions for handling qualities are the basic force and moment equations of motion. The aircraft static and dynamic stability characteristics are essentially obtained using an experimental approach. Precision task workload assessments using HQR/HQDT emphasize mission relation. This metric structure therefore facilitates incorporation of the agility metrics within existing handling qualities specifications and design concepts.

Airframe agility is perhaps the most mature element of OA, with many metrics proposed. Systems and weapons agility is not well understood but some basic concepts will be developed briefly. These subjects are clearly areas for future research.

The majority of the remainder of this paper will be devoted to classifying the existing airframe agility metrics within the metric hierarchy. A large number of metrics have been proposed. In order to understand the state-of-the-art within the classification scheme context a method was devised to assign attributes to each metric. These attributes provided a means of assigning the level of maturity and therefore need for research and are listed with each metric in Figures 5 to 12. The attribute definitions are:

A Easy to measure/fly/test with clearly defined success criteria for the task or task element.

B Supported by a substantiated database (1 - simulation, 2 - experimental flight test, 3 - operational flight test).

C Related to mission effectiveness.

D Related to design or design parameters.

Airframe Transient Metrics

The airframe transient metrics are those time dependent parameters that characterize airframe state changes. These metrics are continuously defined properties reflecting the instantaneous state of the airframe. Clearly, many suitable metrics already exist that can be used, eg Ps, turn rate. Some gaps exist that require more metrics to be defined. These gaps are: moderate and large amplitude maneuvers; a more complete set of acceptable maximum performance criteria for maneuvering; and the study of state change transitional events.

The transition events can be analyzed with the transient metrics. Theoretical developments for transient agility have been proposed. (10)(11)(12)(13) The agility vector components are the primary transient agility metrics.

Other metrics supplement these terms that when taken together provide unique insights into the large amplitude maneuvering trajectories as a function of time. These are: energy-maneuverability; maneuverability of the flight path (velocity vector components); and attitude maneuverability (body angular rates and euler angular rates), as suggested by Jouty.(2)

The presentation of the metric data is best achieved through time history plots during a maneuver with a well defined control input strategy. This presentation will reflect local maxima that determine when the state transition occurred and its characteristics.

The defining equations show how recognizable parameters may be related to the motion. These recognizable parameters may then be related to design parameters, such as was the intent with Lawless' Agility Design Parameters. Unfortunately, very little data are available in a format to illustrate these concepts.

The Flight Mechanics Panel Working Group 17 report, (15) discussed the lack of a formal recognition of moderate and large amplitude handling criteria. One manner in which to view this problem is with the amplitude versus frequency/time plot for a single degree of freedom as shown in Figure 4. Close inspection of this plot reveals where handling qualities research has emphasized small amplitude precision tasks. On this plane, the other areas that have not received wide recognition are more obvious. The central region provides insight into agility since this area represents moderate to large amplitude and moderate to high frequency (and greater) inputs, intuitively the realm of agility.

One area which requires further investigation is definition of the maximum performance limit or bound. A definition that will depend on handling qualities during aggressive maneuvering, structural, aerodynamic, and physiological limits. These issues have been addressed to some extent by (2) and (16) but more work is required.

Figure 4. Control Input Amplitude versus Frequency. (2)

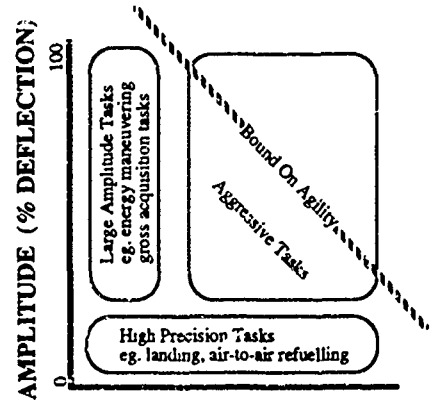

The continuous time history of the motions also provide a vehicle with which to prove compliance with specifications. Bise and Black argued that "by proper enumeration of the tasks (inputs) and desired responses (outputs), any maneuver including agile maneuvers may be described completely. Agile responses are then seen to be simply a subset of all possible responses".(17)

The range of possible maneuvers will be dependent on the aggressiveness of the pilot. In order to perform repeatable tests that provide useful data, the aggressiveness needs to be defined. Quantifying aggressiveness appears to be a current shortfall in handling qualities testing of agile maneuvers.

More research must be done to quantify aggressiveness. Instead of minimum performance specifications, in the design process, a spectrum of conceivable responses are now possible and it is up to the procurement agency to define unique performance criteria.

Airframe Experimental Metrics

Experimental metrics have been proposed to aid the evaluator in breaking down any maneuver into segments which are repeatable and controllable yet provide valuable information applicable to the overall mission. In other words, experimental metrics obtain engineering data from a maneuver segment. Some tactical maneuvers can become too complicated in terms of duration and number of aircraft axes of motion that they are not easy to model in a flight test environment. This class of metrics therefore places emphasis on "discrete" segments of a maneuver.

The transient metrics differ from experimental metrics in that they characterize continuously the transient flight mechanics regardless of the maneuver inputs. The experimental metrics characterize particular parts or building blocks of a recognized tactical maneuver and can be used to study transition events.

Most of the agility metrics proposed fall into this class of metric. Because many exist, further groupings within this class have been suggested. The groupings that have been used have been organized by the types of motions. The most popular have been:

1) pitch, lateral, axial (1)

2) flight path and nose pointing (3)

3) longitudinal,curvature, and torsional (10)

4) axial, pitch, turning, nose pointing, and roll (14)

Since the working group included rotary wing researchers, the observation was made that axial motion is only one of three translational components of motion possible. Therefore in order to be more general, a translational motion group would seem logical. Flight path bending, pitching, turning, and curvature groups fell logically into a nose pointing group. Finally roll, lateral and torsional groups all fell logically within one torsional group. The working group chose translational, nose pointing, and torsional as the primary groupings that served as a basis for common terminology.

Translational Metrics. The translational metrics include those metrics which focus on the transient changes in those parameters that are defined by pure linear motions of the center of gravity. These metrics are dominated by the performance of the aircraft. The following parameters characterize change: position, velocity components (forward/axial, sideways, vertical), accelerations, and jerk terms. Aggressive changes in translation state would be characterized by quick times, large changes in position and velocity, and maximum peak accelerations, and jerk terms.

For fighters the axial or longitudinal translations are important, but for helicopters and VSTOL aircraft vertical and sideways motions are also important. Translational metrics that have been proposed are illustrated in Figure 5 for vertical direction and Figure 6 for the axial direction. For obvious reasons motion in the axial direction have been emphasized. No sideways metrics could be found in the literature although similar presentations as the axial metrics are possible to characterize for example a helicopter sidestep maneuver. A complete set of metrics would consist of: capture times, rates, accelerations, and jerk terms for each axis.

Clearly, data obtained with these metrics would supplement existing performance data in the aircraft flight manual. Some metrics are suitable for specifications and indeed already exist in similar forms.

Figure 5 Vertical Translational Metrics.

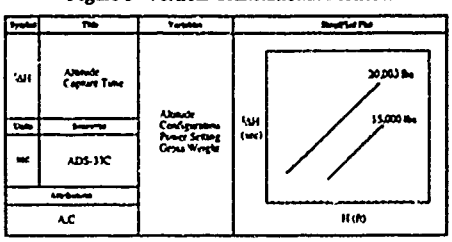

Figure 6. Axial Translational Metrics.

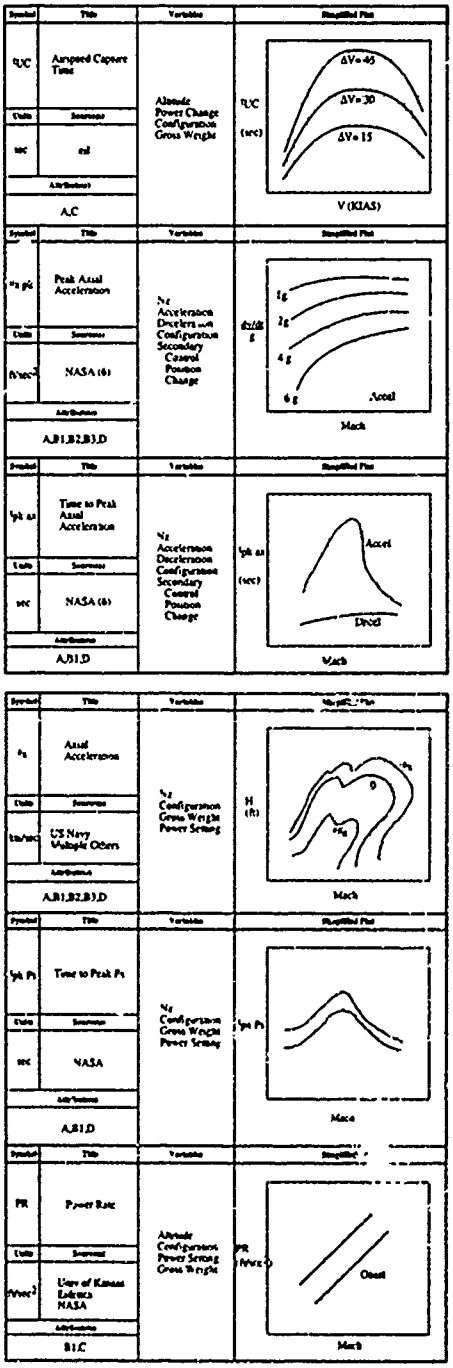

Nose Pointing Metrics. The nose pointing metrics include those metrics which focus on the transient change of the body x axis orientation with respect to the wind and earth or inertial reference frames. This assumes that the weapon boresight is fixed along this axis.

There has been great interest in the ability of an aircraft to point the nose at an opponent quickly. The behaviour of the flight path during a tactical engagement can be very complex, so for experimentation, special cases must be specified to simplify the motion. Three possible cases are:

1) Nose pointing while maintaining a linear flight path or disengaging the body axis from the velocity vector such as with the X-31A(10) in angle of attack or the Sikorsky S-76A Fantail Demonstrator (18) in sideslip. The body axis changes with respect to the wind axis reference frame. This maneuver would be the ultimate "angles" tactic capability.

2) Nose pointing while bending the flight path. The body axis changes with respect to the earth reference frame. This would be classical "energy" maneuvering.

3) Simultaneous changes of the body axis orientation with respect to both the wind and earth frames.

The third case is perhaps the most realistic for current generation fighters. NASA researchers observed that in pure pitch maneuvering, the longitudinal stick displacements in current fighters will behave differently at slow and fast regimes.(14) At high speeds the flight path displaces as per the nose pointing displacement as in the second case, but at slow speeds, the aircraft will exhibit no flight path response (purely wind axis motions as in the first case) or even opposite flight path displacements.(14)

Further simplifications can be made to isolate the effects of gravity. Motions can be grouped into pure vertical, pure horizontal, or any other discrete orientation with respect the local vertical. (14)

Nose pointing metrics proposed to focus on body axis changes with respect to the velocity vector are illustrated in Figure 7. The metrics result in a clear definition of the angles of attack and sideslip pointing envelopes. The weapons limits could then be superimposed illustrating mismatches. In all likelihood fighter type aircraft will emphasize the angle of attack envelope while helicopters emphasize sideslip pointing envelopes.

Nose pointing metrics proposed to focus on the flight path control in the body and inertial reference frames are listed in Figures 8 and 9. To be useful for operations analysis, the inertial reference frame permits direct geometrical angles assessments. The pitch attitude quickness parameter (AQP) was proposed within ADS-33C. This metric could become very useful for defining the "safe" agility envelope because data can be combined with handling qualities data to illustrate areas that are good for aggressive handling.

The nose pointing metrics logically group into: angular change capture times, peak angular rates, peak angular accelerations for angle of attack, sideslip, pitch angle and heading angle as well as load factor and Ps characteristics.

Figure 7. Wind Axis Nose Pointing Metrics.

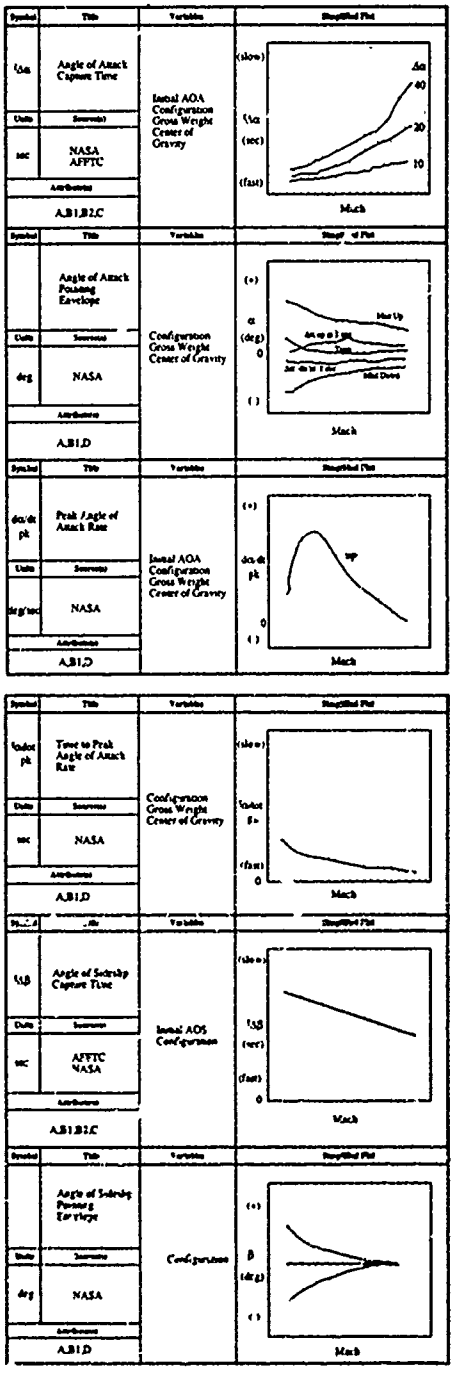

Figure 8. Nose Pointing Metrics.

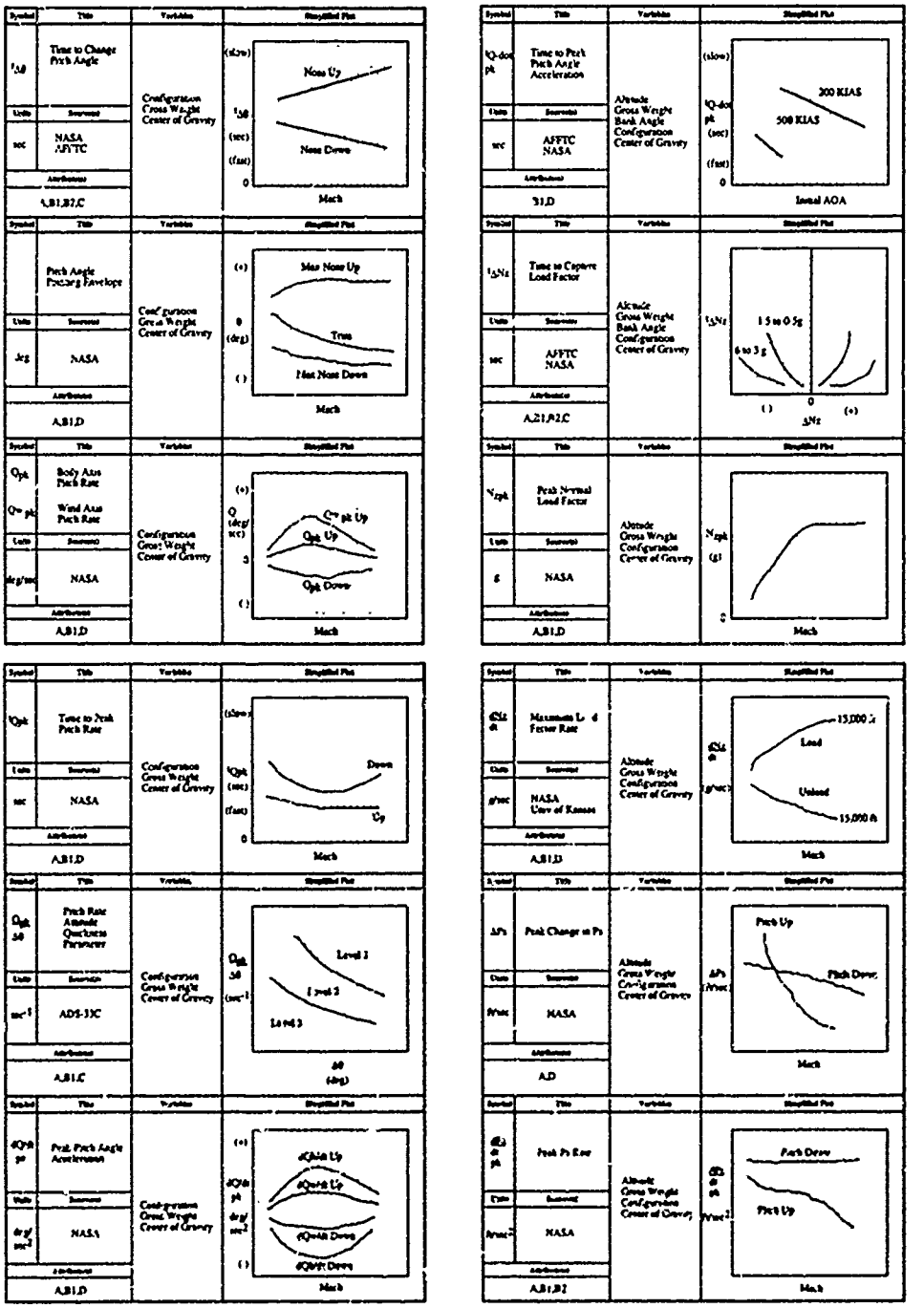

Figure 9. Continuation of Nose Pointing Metrics.

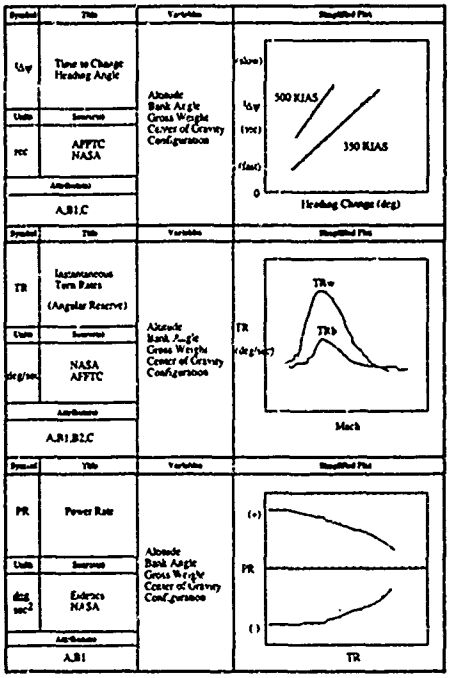

Figure 10. Torsional Metrics.

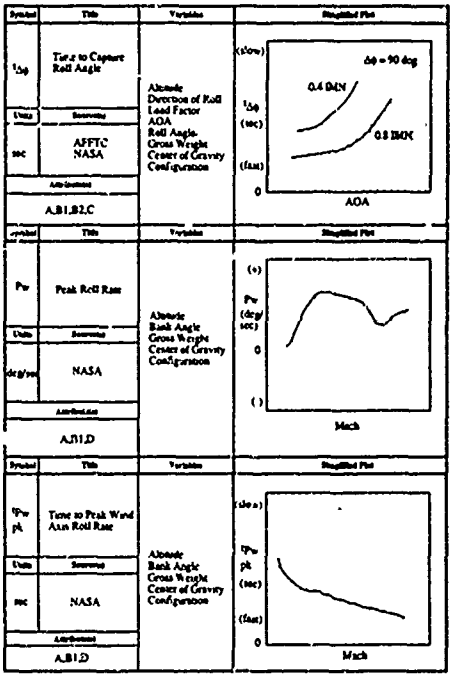

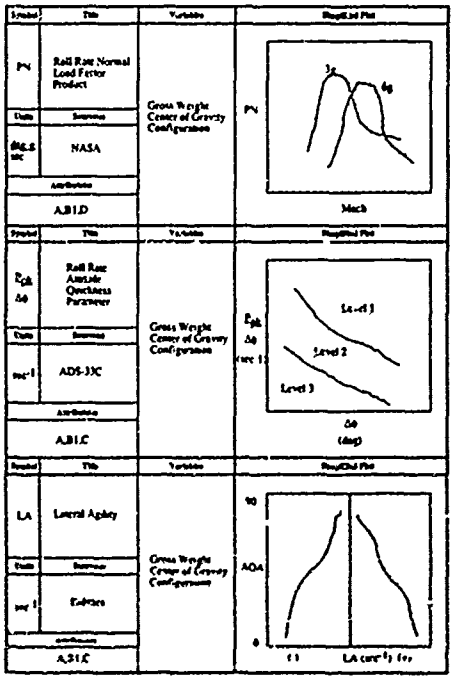

Torsional Metrics. Torsional metrics group those characteristics of the motion that involve rotation of the lift vector. Although not a direct capability to engage an opponent, torsional motions are necessary to re-orient the lift vector so as to nose point or to disengage.(1)

The torsional airframe metrics proposed are illustrated in Figures 10 and 11. The most notable of these are Skow's high AOA roll agility metrics: Torsional Agility (TA) and Lateral Agility (LA).(1) These metrics provides a means of combining limits imposed during nose pointing at elevated AOA and rolling maneuvers.

The roll AQP, like the pitch AQP was introduced in ADS-33C. This metric also provides a method to combine aggressive rolling and good handling qualities in order to bound agility.

The PN parameter might be better described as the peak PN or time to peak PN from a specified initial condition.

Rotations of the lift vector can be described by a rotation about the velocity vector in the wind axis system or with respect to an inertial frame, such as a change in roll angle. Body axis rolls at moderate or large angles of attack are not of great interest because of the risk of inertial coupling.

Like the nose pointing metrics, the torsional metrics can be logically grouped into angular change capture times, peak angular rates, peak angular accelerations for rolling maneuvers.

Figure 11. Continuation of Torsional Metrics.

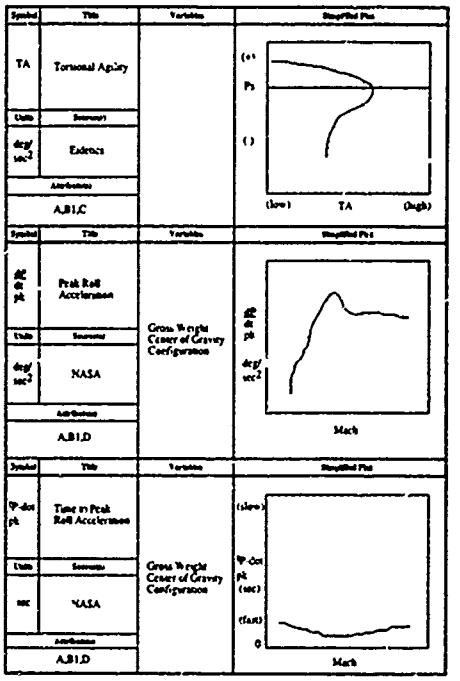

Airframe Operational Metrics

The airframe operational agility metrics consider the transient changes of state which occur in typical mission dependent maneuvers. The metrics characterize the behaviour of the aircraft in a more global sense looking at the performance, maneuvering, and man-machine interface aspects of airframe agility.

First and foremost, these metrics depend on the mission. This extends further than conventional flight mechanic principles and theory. The desired results obtained from the operational metrics would be detailed in a specification and may at this level be traded off to other more critical performance measures. For example, a trade-off between Within Visual Range (WVR) and Beyond Visual Range (BVR) requirements in the design process.

The operational metrics have two main aims: characterize the mission task quickness and mission task precision if a weapon/sensor is used. The mission task quickness is best characterized as a "time to perform a task". The mission task precision depends largely on the purpose of the task and is defined by a weapons system accuracy requirement for engagement.

Two groupings of metrics have been suggested: global metrics or mission specific.

Global OA Metrics. The global metrics characterize the overall airframe agility in a top-down sense for a mission task. These may be classified as offensive or defensive but other general classes are conceivable. The metrics that have also been proposed that fit into this group and are illustrated in figure 12.

Time to perform the overall task is the main metric, for example, time to engage and destroy a hostile aircraft under a certain set of conditions. Another good global metric that measures the cost of maneuvering is Dorn's energy-agility metric.(5) The accuracy of weapons aiming or flight condition tracking may be assessed at the global level. Finally, it is at the global level that aggressiveness could be characterized. Further study is required for many of these metrics.

Figure 12. Global Agility Metrics.

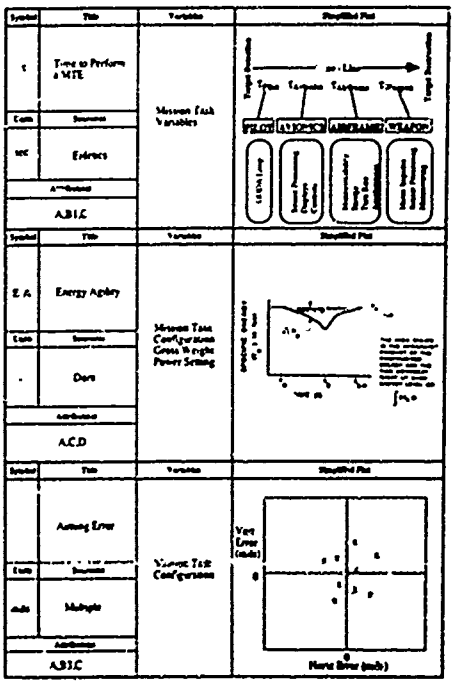

Mission Specific OA Metrics. Specific mission metrics are unique to a particular mission task, not necessarily an air vehicle type, that reflect realistic aircraft operations. The metrics are based on the Mission Task Element (MTE) as discussed previously. Defining MTEs provides a means of breaking down typical mission profiles into manageable components that are suitable to both designers and evaluators with the overall aim of being clearly identifiable to the operator. Any mission task may be broken into a sequence of series and parallel mission task elements, each of which possess a "time to perform" time delay.

Specific mission metrics are a large class of metrics because many missions are conceivable. The fighter mission has emphasized weapons engagement maneuvering and attack helicopter mission has emphasized nap-of-the-earth maneuvering for stealth and concealment. Aermacchi researchers believe that future aircraft that are designed to be agile will likely require trainers that are agile.(2) Other missions possibly making use of some aspect of agility are transports, utility helicopters, and perhaps for anti-submarine warfare aircraft. These may not necessarily be maneuverability issues rather tasks may need to be done fast using avionics for example but these will be discussed shortly. When breaking down these missions into possible profiles and then further into MTEs, some commonality will exist. In fact, ADS-33C lists several helicopter MTEs that are classic maneuvers to investigate handling qualities and agility. Building a library of typical MTEs will be of benefit and presents an opportunity for multi-national cooperation.

Specific Fighter Metrics

With reduced engagement times associated with modern air-to-air combat fighter aircraft are required to respond faster. Metrics were proposed that focussed specifically on the engagement phase of a maneuver. These metrics were:

1) Point and Shoot combat analysis (7),

2) Relative Energy State (8),

3) Combat Cycle Time (8),

4) Rolling Agility Metric (8),

5) Dynamic Speed Turn (15).

The metrics have enabled very complex sequences of maneuver elements to be evaluated in a complex mission scenario. Close inspection of the maneuver sequence reveals that these metrics are composed of numerous experimental metric defined previously. This characteristic makes analysis requirements more logical.

Specific Helicopter Metrics

An increased threat from other helicopters as well as hostile ground weapon systems has increased the need for helicopter concealment in the nap-of-the-earth environment. This has forced the time which the helicopter is exposed to a very short duration. This emphasis requires a good knowledge of how the helicopter performs aggressively in the NOE environment.

The discrete maneuver tasks, first proposed by Defence Research Agency Bedford, and incorporated into ADS-33C, were selected to represent realistic maneuvers.(19) These MTEs were:

1) bob-up/bob-down,

2) hurdle hopping,

3) slalom,

4) sidestep-unmask/remask,

5) dash/quick-stop,

6) scramble,

7) 90 degree bend turn,

8) 'S' turn,

9) triple bend,

10) teardrop turn,

11) pull-up/push-over,

12) rearward flight.

The Engagement Task

To illustrate how the metric classification scheme can be applied, a hypothetical missile engagement sequence for a fighter aircraft will be used as an example. For this situation it is assumed that the aircraft is cruising above corner velocity when it must engage one adversary and recover to be ready to engage another adversary. To employ its missile, the pilot is required to point the nose of the aircraft with a simultaneous change in heading and pitch angle. The time-line for the sequence is shown in Figure 13 and is based on the scenario shown in Figure 1 (up to the weapons launch).

The metric hierarchy facilitates a top-down analysis approach. The most important global agility metric is the time to complete the missile engagement. The more agile the aircraft, the quicker this task can be completed. A designer may look to reduce the engagement time so as to improve chances of survival and also enabling the aircraft to engage more threats.

The maneuver sequence provides a basis on which to break the task into MTEs. These include: roll-in, horizontal turn, missile launch, unload, and accelerate. At the MTE level, the designer can identify which mission task elements is/are the reasons for the excessive time delays if the time taken is too long. Other operational metrics specific to the fighter such as the combat cycle time(8) and pointing margin(7) parameter will provide guidance for comparison to threat knowledge of the response and launch times. The heading change, which for a current generation fighter typically bends its flight path, could be improved with technologies that permit rapid nose pointing, such as thrust vectoring.

The experimental metrics then provide a tool to investigate those airframe MTE times that are too long. The selection of which experimental metrics are appropriate would depend on the motion occurring. For example the roll-in could be characterised by the torsional metrics such as the LA, TA, Roll Quickness Parameter, or Power Rate. The rapid nose-pointing with thrust vectoring will result in a large drag increase, so the power rate metrics will assist in analyzing that transition event. These are the discrete characteristics of the MTE under investigation.

Throughout the sequence transient metrics identify when the peak state change events occur. At this point, the components of the agility vector as well as more traditional metrics such as Ps provide direct relation to recognizable elements controlled by the designer such as CLmax or T/W. This procedure occurs at the lowest level of detail. At this level, the instantaneous response of the aircraft can be analyzed. Another technique has been proposed by the AFFTC using what is referred to as onset and

Figure 13. Hypothetical Missile Engagement Task Implementing the Operational Agility Metric Structure.

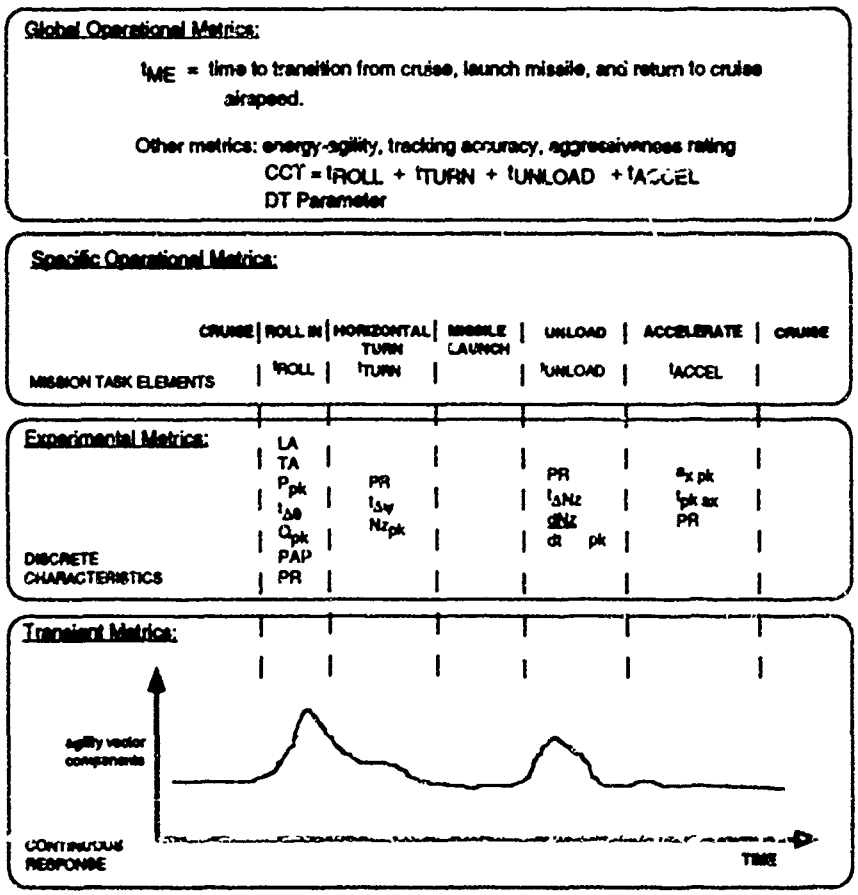

θ	pitch angle	PR	power rate
ψ	heading angle	PAP	pitch attitude quickness parameter
a	acceleration (x axial)	N_z	Normal load factor
A_A	agility vector axial component	t	time to perform a maneuver task
A_C	agility vector curvature component	pk	peak
A_T	agility vector tangential component		
CCT	combat cycle time		
LA	lateral agility		
P	roll rate		
Q	pitch rate		

capture transient analysis. (3)

This example was primarily dealing with the airframe contributions to OA, but clearly, the avionics and weapons also play a major role in determining how fast the hostile aircraft is defeated. The task of detecting, identifying the threat as hostile, and acquisition were not addressed.

Systems Agility Metrics

A system designed with Operational Agility concepts would be expected to be fast responding. This would apply to the user interface as well as the processing performed by the system. If the pilot is required to keep his head in the cockpit pushing numerous buttons and interpreting a complex display the response will not be agile. The agile system would therefore appear more "user friendly" and easier to train the operator.

Characterizing "user friendliness" with metrics has been very objective and must be defined clearly and precisely for OA design. Aircraft system operations can be characterized by functional task analysis. This approach fits well with the Operational Agility hierarchy presented in Figure 3.

Operational metrics will tend to be global and mission specific as were airframe metrics. In the mission specific group, the mission task elements could be organized as per functional goals proposed by Lappos(2): planning, reaction, observation, engagement, movement, communication, and vehicle management. These functions may transcend system boundaries requiring evaluation of the integrated avionic system.

The experimental metrics will tend to be system specific, eg radar or FLIR.

Defining transient metrics is somewhat more difficult as the concepts are not easily unified by a single theoretical basis as is possible for flight mechanics. Systems can be characterized by electromagnetic signal and information flows which could be used for the purpose of transient analysis. The concept can perhaps best be portrayed with an example.

Air-to-Air Radar System Agility. The OA of a radar is primarily a function of the antenna beam sweep characteristics, signal processing delay, and the operator interface.

Beal and Sweetman described the agility of the radar beam sweep by its ability to change in direction or transmitted signal waveform.(21) Signal processing delays are associated with: beam setup, transmit signal waveform setup and modulation, time of flight, demodulation, counter-counter measures processing, specific target analysis processing, and display presentation processing. Since radar designs have numerous tradeoff options, eg mechanically steered antenna or phased array antenna, these delays can be generalized as: time to setup beam and transmit desired signal, and time to process return and display data. An added delay could be added for sensor fusion prior to presentation to a pilot or pilot's associate. The magnitude of this time delay when compared with the cognitive processing traditionally performed by the pilot could in the overall OA time delay analysis, prove to be much shorter.

Transient metrics are well established for radar system analysis in the time and frequency domain.(22) Experimental metrics for the antenna could be: time to change beam boresight elevation and azimuth, and time to change beam pattern. Both the transient and experimental metric can be evaluated in a laboratory or anechoic chamber environment possibly with the radar broken into its component parts.

The operational metrics will be associated with the MTEs: time to acquire, identify, and lock-on to a target. These include all the characteristics of the antenna, signal processing, and display functions. These metrics should be evaluated in the real environment. The evaluator must define the specific mission scenario: radar-target geometry (elevation angle, azimuth angle, range) and target radar cross section. For valid results, further stipulations may be required such as a range less than maximum detection range for the particular target radar cross section.

Weapons Agility Metrics

A common observation made by the working group members was that a great deal of effort has been expended in developing the airframe so as to be highly agile which must be matched by the equivalent development of the weapons that are carried. In terms of safe separation, launch at high angles of attack must be considered concurrently in order to maximize effectiveness. Therefore, the nose pointing capabilities of the airframe may not be used to full advantage. Or as Skow stated "the agile airframe is only good for airshows".(1)

When viewed separately, the weapon itself, can be characterized by the airframe metrics and sensor metrics if the weapon is self-guided and autonomous after launch. The unique aspects of weapons agility that are interrelated with the aircraft then are those associated with the actions that occur: after detection of the hostile threat, launch, and weapon flyout if directed by the aircraft. The pilot vehicle interface for weapons agility is closely related to the system agility.

Applying the Metric Structure

The key activity when implementing the OA metric classification scheme is to clearly specify what are the critical time dependent mission tasks. By starting at the mission, the design balance can be performed sensibly.

A specification must be organized to ensure that the operator receives what is required. With designs now requiring years, numerous agencies involved, and specification compliance requirements, the mean mission requirements tend to be obscured. Mission testability could be achieved by breaking the mission into critical mission tasks which then serve to provide a tool for design and evaluation.

The operational agility metric structure discussed in this paper is one method of organizing the characteristics which define how aggressive the pilot can be in order to be quicker. Specifying values for the metrics in each of the classes places a "minimum performance" specification on the aircraft and its component parts.

By considering the total weapon system, the pilot and/or crew is at the center of the system. Rapid prototyping approaches used by several major avionic system integrators companies are directly applicable to operational agility. In fact, the working group observed that these rapid prototyping approaches are significant enabling technologies for operational agility. This is accomplished by customizing control functions, automation, and

tailoring controls/displays for the mission. The end result is the added benefit of potential time savings when the mission tasks are performed. With a cockpit prototyping environment, the inter-system interfaces (sensor fusion, data bus), pilot-vehicle interfaces, and inter-crew interfaces, can be optimized for mission tasks. For example: the Comanche crewstation design goals were to facilitate: "aggressive pilotage (move to survive in an NOE environment); mission management (to keep the mind on the mission); and tailor the avionics to the mission (that is fight the threat not the avionics)."(23) It is now common that well before the first flight the cockpit information flow and architecture has been analyzed indepth and the design matured.

This metric classification scheme, therefore provides a framework for:

1) an agility design database.

2) developing mission oriented specifications for agility.

3) to organize evaluations.

Future Study

One of the benefits of this metric classification structure is a clearer understanding of what agility subjects require future study.

First of all, much more agility data must be collected and organized within a logical framework. This is particularly true for transient and operational metrics. This situation has led to a poor understanding of the importance of many agility characteristics. Therefore, it will also be necessary to correlate design and operational data in order to provide guidance for future designs that is based on the mission.

It is evident that operational agility requires multi-disciplinary coordination and communication. The current trend towards increasingly complex integrated weapon systems is continuing. Weapons and systems agility are new concepts and will require many years of research. The most critical issue is that the weapons and avionics are integrated successfully with the pilot and airframe optimized for time critical demanding engagement scenarios.

Some newer technologies are placing increasing demand on the responsiveness of the total aircraft in unusual and disorienting attitudes. For example, thrust vectoring will place added demands on the weapons, avionics, and the pilot. The working group observed that researchers from the weapons, airframe, avionics, and PVI should study the impact of operational agility concepts.

For airframe agility, the limits or bounds on transient maneuvering need to be articulated more precisely. There is also a need to quantify aggressiveness and where a maneuver again falls in the spectrum (amplitude and frequency) of possible inputs.

A library of mission task elements should also be developed for standardized evaluations and comparisons. The USAF/USN Standard Test and Evaluation Maneuver Set for agility and the helicopter MTEs would form the bases of this library.

The metric organization structure also provides guidance for writing specifications that are clearly mission dependent. The concept of a "time budget" will likely be more prevalent in mission oriented design.

Acknowledgements

The author wishes to thank the agility researchers and contributions of the members of the Flight Mechanics Panel Working Group 19 who enabled this concept to be developed.

References

1. Show, A.M., "Agility as a Contribution to Design Balance", AIAA 90-1305, 22 May 90.

2. AGARD-AR-314 FMP Working Group 19 Report on Operational Agility, Fall 93.

3. Lawless, A., "Summary Report of the AFFTC Hosted Agility Metric/Flight Test Workshop", July 88.

4. Lawless, A., "Aircraft Agility Measurement Research and Development", AFFTC-TIM-91-01, June 91.

5. Dorn, M., "Aircraft Agility: The Science and the Opportunities", AIAA 89-2015, 2 Aug 89.

6. Fox, B.A., "Investigation of Advanced Aircraft Performance Measures of Merit including New Agility Metrics", AFIT/GAE/ENY/91S-3, Sep 91.

7. Kalviste, J. "Measures of Merit for Dynamic Aircraft Maneuvering", SAE 901005, April 90.

8. Tamrat, B.F., "Fighter Aircraft Agility Assessment Concepts and Their Implication of Future Agile Fighter Design", AIAA 88-4400, 7 Sep 88.

9. AVSCOM Aeronautical Design Standard-33C, "Handling Qualities Requirements for Military Rotorcraft", US Army AVSCOM, St Louis, August 89.

10. Herbst, W., et al, "Agility", MBB Report/X-31A A/R-29, October, 88.

11 Mazza, J., "Agility: A Rationale Development of Fundamental Metrics and their Relationship to Flying Qualities", AGARD-CP-508, Oct 89.

12. Myers, T.T, "Flying Qualities Analysis for Large Amplitude Maneuvers", AIAA-87-2904.

13 Cliff, E.M., and Thompson, B.G., "Aircraft Agility Manoeuvers", AIAA 92-4489.

14. Murphy, P., Bailey, M. and Ostroff,A. ,"Candidate Control Design Metrics for an Agile Fighter", NASA TM 4238, Mar 91.

15 AGARD-AR-279 FMP Working Group 17 Report, "Handling Qualities of Unstable Highly Augmented Aircraft", May 91.

16. Beck, J., and Detroit, M., "Agility and High Angle of Attack: An Air Force Research Perspective", SAE 912145, Sep 91.

17. Bree, M.E., and Black, G.T., "Is Agility Implicit in Flying Qualities", AIAA, 90.

18. Lappos, N., "Agility and Maneuverability Flight Tests of the Boeing Sikorsky Fantail Demonstrator", AIAA-7362, 91.

19. Padfield, G.D., Charlton, M.T., "Aspects of RAE Flight Research into Helicopter Agility and Pilot Control Strategy", Ames Research Center, 9 June 89.

20. Bunt, S. and Lawless, A., "Flight Testing for Aircraft Agility", AIAA 90-1308, May 90.

21. Boal, C. and Sweetman, B., "Fighter Radar in the 1990s", International Defence Review 8, 92.

22. Skolnik, M., "Introduction to Radar Systems", McGraw Hill Publishing, 1980.

23. Hamilton, B., "Comanche Configuration Design", AIAA Aerospace Design Conference, Feb 92.

APPLICATION OF CENTRIFUGE BASED DYNAMIC FLIGHT SIMULATION TO ENHANCED MANEUVERABILITY RDT&E

J. F. Calvert
Flight Dynamics and Controls Branch
Aero Analysis Division

D. A. Kiefer
Crew Systems Facilities Engineering Branch
Life Support Engineering Division

Air Vehicle and Crew Systems Technology Department
Naval Air Warfare Center, Aircraft Division, Warminster
Warminster, PA 18974-0591 USA

SUMMARY

This paper addresses the strengths of centrifuge simulation to provide the unfamiliar and severe motion environment associated with high angle of attack and post-stall maneuvering. The approach to development and testing of centrifuge motion control algorithms is outlined, including inherent modeling constraints such as 3 degrees-of-freedom, estimated human perceptual models, and the machine-associated mechanical/structural considerations. Difficulties of algorithm development are illustrated using the results of a recent flying qualities experiment initiated to study the effects of motion on pilot ratings for proposed nose-down control power guideline criteria. Use of off-line computer models to tune algorithm performance is also presented. Finally, current capabilities of centrifuge simulation and a discussion of future applications is outlined.

LIST OF SYMBOLS

A. Principal

A	- A-Gimbal Angle (+ Left/Inward)
A-A	- Air-to-Air
A-G	- Air-to-Ground
ANU	- Aircraft Nose-Up
AOA	- Angle of Attack
B	- B-Gimbal Angle (+ Up)
CCA	- Centrifuge Control Algorithm
CFS	- Centrifuge Flight Simulation
CFSAVT	- Centrifuge Flight Simulation Analysis and Validation Tool
C_m	- Pitching Moment Coefficient
DFS	- Dynamic Flight Simulator
DOF	- Degrees of Freedom
EM	- Enhanced Maneuverability
EOM	- Equations of Motion
FOV	- Field of View
G	- Instrument Measured Linear Acceleration (g's)
G-LOC	- G Induced Loss of Consciousness
GFAM	- Generic Fighter Aircraft Model - Modified
HANG	- HAOA Nose Down Control Power Guidelines
HAOA	- High Angle of Attack
KCAS	- Knots Calibrated Airspeed
LWC	- Light Weight Cockpit
msl	- Mean Sea Level
NASA	- National Aeronautics and Space Administration
NAWC	- Naval Air Warfare Center
N_i	- Instrument Measured Linear Acceleration (g's) Felt at the Cockpit Station Along The i-axis
P	- Roll Rate (+ Right Wing Down)
PSEM	- Pilot Sensory Estimate Model
PST	- Post-Stall Maneuvering
Q	- Pitch Rate (+ Nose Up)
R	- Yaw Rate (+ Nose Right)
R&D	- Research and Development
RDT&E	- Research, Development, Test and Evaluation
SA	- Situational Awareness
SAS	- Stability Augmentation System
SD	- Spatial Disorientation
T&E	- Test and Evaluation
TEU	- Trailing Edge Up
TV	- Thrust Vectoring

B. Greek

α	- Angle of Attack
β	- Angle of Sideslip (+ Nose Left)
δ	- Cockpit Control Position Reference; Aircraft Stabilator Position
ΔX	- Perturbation Variable X
ϕ	- Roll Attitude (+ Right Wing Down)
θ	- Pitch Attitude (+ Nose Up)
ψ	- Heading Attitude
ω	- DFS Rotation Rate (+ Nose Right, Clockwise)
$\widetilde{[X]}$	- Transformation Matrix

C. Subscripts

c	- Pertaining to DFS Command Parameters
o	- Pertaining to Initial Condition
stab	- Pertaining to Aircraft Stabilator
x	- Pertaining to x-axis (+ Forward)
y	- Pertaining to y-axis (+ Right)
z	- Pertaining to z-axis (+ Down; G_z + Up)

Presented at an AGARD Meeting on 'Technologies for Highly Manoeuvrable Aircraft', October 1993.

1. BACKGROUND

Within the last 5 years, technology advances in aircraft control are facilitating aircraft maneuvering up through 90 degrees angle of attack (AOA). More than ever, in this new flight regime pilots are experiencing unusual combinations of multi-axis rates and accelerations. This enhanced maneuverability (EM) flight environment, unfamiliar to the pilot, is leading to new engineering challenges in technologies related to situational awareness (SA), spatial disorientation (SD), and increased combat workload associated with high angle of attack (HAOA) energy management, multi-target tracking, and cockpit information fusion.

Current EM technology areas include flying qualities criteria development, human factors studies, heads-up display (HUD) and helmet mounted/off-axis display format development. In the total flight simulation environment, past experience has shown that conventional fixed-based and limited motion platform simulators can provide inappropriate motion cues for fighter and attack aircraft applications[1]. To adequately support EM technology development, improvements in high fidelity, safe, reliable, and inexpensive simulated motion environments for piloted flight simulation operations are needed. In addition, there is also a need for improved capability to simulate the effects of HAOA and post-stall (PST) maneuvering on pilot performance of air combat tasks.

The combat flight environment results in physical and cognitive stresses, both having a direct effect on pilot performance. In the HAOA flight regime, physical stresses include unusual combinations of high G-force, and high angular rates. Cognitive stresses include tactical decision making, weapons selections, target acquisition, basic flight operations, and combat communication. Cognitive stresses work to reduce attention, degrade rapid decision making, and induce time perception anomalies. The combined effect will lead to higher potential for reduced situational awareness and/or some degree of loss of spatial disorientation. At a minimum, the pilot will not be fully utilizing the technology benefits provided by advanced design EM aircraft without some improvement in pilot/aircraft interface. The design goal is to minimize SD and maximize SA through effective design of cockpit layouts, pilot aide systems, and advanced display technologies, all combining to provide optimum tactical information fusion. The modern design engineer realizes that flying qualities, human factors and performance can no longer be addressed as independent design disciplines. Similar to the concept of engine/airframe integration, there exists the concept of pilot/vehicle interface, an aircraft design must address the issue of tactical information fusion in order to maximize the utility of the highly augmented pilot/vehicle weapons system.

Although conventional, limited motion-base (up to 6 actuators) simulators have been successfully used for commercial aviation applications, they are significantly limited in providing the necessary motion cues associated with the highly dynamic motion environments of fighter and attack aircraft applications[1]. In addition, past studies have demonstrated that rate -augmented vehicles that exhibit good handling qualities in flight are much more difficult to control on ground-based simulators[2].

Today, a strong requirement exists for a simulator capable of providing a realistic biodynamic (motion) and cognitive stress environment for use in developing correct technologies including:

a. Situational Awareness and Spatial Disorientation R&D.
b. Displays and Information Fusion R&D.
c. A-A and A-G Operations Training (SD, SA, G-LOC).
d. Flying Qualities Criteria R&D (including HAOA, Departure, and Spin).
e. Simulator Concepts R&D.

Furthermore, a fundamental need remains for realistic simulation of high risk testing and training to support research, development, test, and evaluation (RDT&E).

2. OBJECTIVE

To address issues associated with the EM flight environment, we need a cost effective, repeatable, piloted simulation which places the pilot and the developing technology in the harsh operational environment. This includes subjecting the pilot to physical and cognitive stresses he must face and overcome during actual mission operations. Improved capability to simulate the effects of HAOA/PST tactical maneuvering on pilot performance of A-A and A-G mission tasks is needed. Although several concepts exist, one approach addressed to date has been to apply motion control algorithms with human centrifuge devices to create a closed-loop (pilot in control) simulator. The design objective in applied centrifuge flight simulation is to develop an additional flying qualities and human factors tool for research and evaluation of the effects of highly dynamic environments on pilot performance. This type of simulation would be used when sustained motion cues are essential in adequately evaluating closed-loop piloted tasks, including the tasks previously mentioned. The intent is to complement, not replace, current fixed and limited motion simulation by providing a cost effective, safe bridge between current ground simulation and flight test for closed-loop evaluations.

The concept of centrifuge flight simulation (CFS) continues to be explored at the Naval Air Warfare Center, Aircraft Division's Dynamic Flight Simulator (DFS) facility. The objective of this paper is to detail the utility and limitations of CFS as an EM simulation tool. The discussion includes examples of the cost-benefit design tradeoffs required to optimize a motion control algorithm. Examples are drawn for a developmental evaluation of the DFS conducted to modify the centrifuge control algorithm (CCA) to provide adequate motion fidelity to support a study of the effects of motion on proposed HAOA nose-down control power guidelines. Finally, an analysis of the effect of radius on motion artifacts, and insight on how to cope with Coriolis illusion during simulation operations is presented.

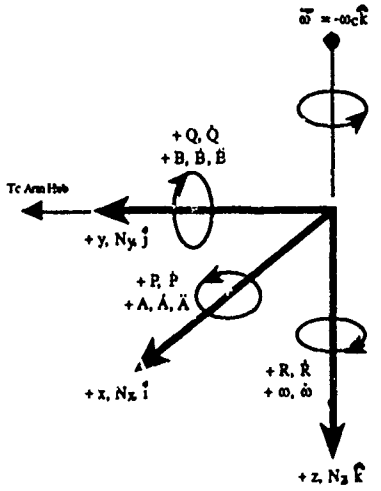

Figure 1 - Gondola Axis System Based On Physiological Axis (Reaction) Reference

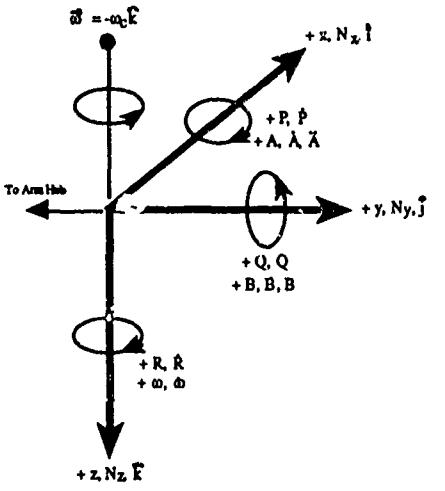

Figure 2 - Gondola Axis System Based On Standard Aircraft (Action) Axis Reference

3. SIGN CONVENTION

There are two fundamental axis systems used to reference DFS gondola parameters during closed-loop piloted operations. First, the Physiological system (Figure 1) defines positive parameters relative to the direction in which the inertial parameters react. Often, linear acceleration in this system is referred to as G_X, G_Y, and G_Z, which can also be referred to as N_X, N_Y, and N_Z. This system is often referred to as the reaction system.

Second, the standard aircraft axis system (Figure 2) defines positive parameters relative to the direction of positive net linear and angular acceleration of the body. This system is often referred to as the action system.

It is important to note that these axis systems share the same z-axis, and are equal and opposite relative to the x- and y-axes. Therefore, when a pilot executes a right hand climbing turn in the aircraft, both axis systems show positive linear and angular rate and acceleration parameters because relative to the net external forces acting on the system 1) the two axis systems are equal in magnitude and opposite in direction, except +z, and 2) the inertial force is equal in magnitude and opposite in sign. Therefore, as long as sign convention is maintained, the transformation matrices for both systems used to reference aircraft/gondola parameters may be applied.

4. DYNAMIC FLIGHT SIMULATOR (DFS)

The DFS uses a 16,000 horsepower electric motor to rotate a 50 ft cantilever arm which supports a gondola at the tip. The pilot begins flying the DFS by facing into the tangential velocity vector with his left shoulder aligned into the cantilever arm (which is the general radius of curvature). Rotation is to the pilots left, which corresponds to counter-clockwise when viewed from the top looking down.

The gondola is supported by two nested gimbal rings providing the ability to rotate the embedded cockpit about

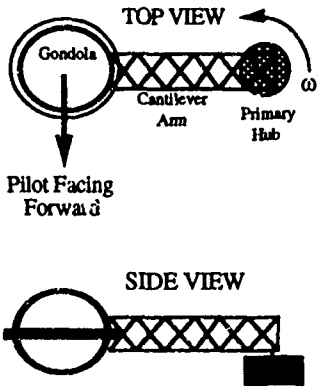

Figure 3 - Simplified DFS Setup

two fixed gimbal axes, roll and pitch, labeled A- and B-gimbal respectively. The inner most gimbal axis is oriented in pitch, and the outer gimbal is oriented in roll. The corresponding A- and B-gimbal angle motions are commanded using shafts driven by two hydraulic motors located at the primary hub. An illustration of the DFS setup is presented in Figure 3.

The A- and B- gimbal angles are similar to the Euler angles ϕ and θ, but with a different rotation scheme than normally used by the aircraft community. The standard aircraft Euler angle transformation between the earth to body axes occurs as

$$[\,]_e = [\phi \Rightarrow \theta \Rightarrow \psi][\,]_b = [\tilde{\psi}][\tilde{\theta}][\tilde{\phi}][\,]_b$$

$$[\,]_b = [\psi \Rightarrow \theta \Rightarrow \phi][\,]_e = [\tilde{\phi}]^{-1}[\tilde{\theta}]^{-1}[\tilde{\psi}]^{-1}[\,]_e$$

However, the transformation sequence for the DFS is assigned as,

$$[\,]_e = [B \Rightarrow A \Rightarrow \psi_c][\,]_b = [\tilde{\psi}_c]^{-1}[\tilde{A}]^{-1}[\tilde{B}]^{-1}[\,]_b$$

$$[\,]_b = [\psi_c \Rightarrow A \Rightarrow B][\,]_e = [\tilde{B}][\tilde{A}][\tilde{\psi}_c][\,]_e$$

where, $\psi_c = \int_0^t \omega_c \cdot dt$.

Since the Euler and DFS transformation schemes were different, the Euler transformation matrices were not valid for the DFS. The DFS was controlled by a CCA which used the aircraft states N_X, N_Y, N_Z, P, Q, and R as inputs to command arm rate (ω_C), and A- and B-gimbal position commands. ω_C, A, and B combine to develop a continuous realistic motion environment representative of the simulated aircraft state as perceived by the pilot in the gondola. The mechanical system constraints include position and rate limiters on the A- and B-gimbals, and angular arm rate and acceleration limiters.

5. CENTRIFUGE CONTROL ALGORITHM

A properly designed CCA is the key to producing good motion fidelity on centrifuge flight simulators. Without an adequate CCA the centrifuge recreates the aircraft G vector with very good accuracy, but angular motions are also created which produce unrealistic flight sensations termed as rate artifacts.

The goal of the CCA is to provide motion cues to the pilot in the gondola which represent an equivalent perceived motion environment characteristic of the current aircraft state. The CCA utilizes a vector transformation of aircraft body axes angular rates and linear accelerations, and equations of motion (EOM) to compute the necessary arm rate and gimbal positions required to provide the appropriate linear acceleration vector at the gondola station. The CCA then utilizes feed-forward gains and filters designed to induce a somatogravic illusion by application of translational accelerations which perceptively counter angular artifacts resulting from the reproduction of the G-vector. A flow diagram of this concept is presented in Figure 4. The CCA augments the physical 3-DOF centrifuge to provide a sustainable linear acceleration field which closely matches the aircraft. When combined with a washed out angular motion, the net effect is designed to provide an effective sustained full motion environment.

Utilizing the fixed CCA architecture, the design difficulty is in the determination of the proper gains and filter parameter values which produce adequate motion fidelity. The gains and filter coefficients used in the DFS CCA were designed while addressing three primary constraints: 1) satisfactory pilot perception of a 6-DOF sustained motion environment, 2) Rate and/or acceleration artifacts minimized to be within pilot tolerance, and 3) control gimbal and arm response characteristics to prevent gimbal backlash and/or excitation of the vertical arm oscillation mode associated with the cantilever beam arm.

The first constraint addresses the requirement to provide adequate motion response (magnitude, phase characteristics, and onset). The pilot must be able to feel the motion he is commanding, when he commands it, and in the proper direction. The second constraint addresses the necessity to minimize artifacts to preclude negative transferal of training, simulator sickness, motion cue mismatch, or general pilot discomfort. If the pilot is overwhelmed by artifacts, he will not believe that he is conducting flight operations thereby reducing the effectiveness of the simulator. The final constraint addresses the real-world mechanical characteristics of the centrifuge equipment including position and rate limiters, payload limits, and inertia and c.g. characteristics. The CCA must avoid exciting or exceeding mechanical and structural anomalies which could taint the motion fidelity.

The original architecture and gain schedules of the DFS CCA were based on The Pilot Sensory Estimation Model (PSEM). The PSEM was experimentally designed to estimate a human perception of a given orientation from rates and accelerations of the motion environment acting on a human. Crosbie[3,4] developed this model using data from Cohen[5] and estimated human perception of orientation for both the aircraft pilot and the centrifuge pilot. This served to provide a mathematical mapping of the linear and rotational 6 degrees-of-freedom (DOF) aircraft motion environment to the purely rotation 3 DOF environment of the DFS.

The limitations of this approach include the assumption that human orientation sensing mechanism can be modeled by two dynamic systems which add independently. An angular system responds to angular acceleration with high frequency sensitivity, but loses importance quickly. The linear system responds to linear acceleration with low frequency sensitivity, and provides an attitude reference to the vertical. Crosbie asserts that proper combinations of existing rates and accelerations of the 3-DOF system can be used to produce the illusion of rates or accelerations which are not present, or to remove the perception of an unwanted rate or acceleration artifact. Thus the motion provided by a 3-DOF motion environment can be summed to produce a 6-DOF perceived motion environment. For many applications, this assumption has been proven successful, however, for some applications and/or individual pilots it has been invalid. Further testing and development is necessary to determine the best applications of the current CCA, as well as to develop improvements to the current approach. The detailed philosophy and developmental testing of the baseline DFS CCA is presented in References 3, 4, 5, and 6.

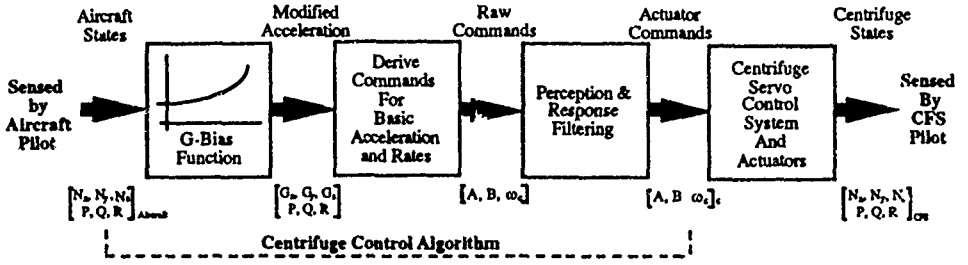

Figure 4 - CCA Flow Diagram

6. G-BIAS FUNCTION

A G-bias function is used in the CCA to provide a sense of acceleration unloading when the pilot commands less than 1g flight. To avoid extreme rate artifacts and harsh mechanical stresses, the current DFS CCA does not allow the development of negative N_Z. However the motion sensation of less than 1g flight is provided by reducing the gondola G_Z below the trim plateau. The trim plateau places the gondola above 1g when the aircraft is at 1g trimmed flight condition. Experimental operational data has shown that the pilot rapidly adjusts to the slightly elevated g environment (1.4 to 2.0g) and perceives a 1g flight environment during trimmed simulated flight operations. When the pilot commands less than 1g, the DFS unloads from the trim plateau G to a minimum of 1g (earth gravity) based upon the G-bias function. Although the sense of negative G cannot be easily duplicated using the current CCA, the unloading from trim plateau down to 1g combined with visual system cues provides a strong sensation of less than 1g flight operations. An example G-bias function is shown in Figure 5.

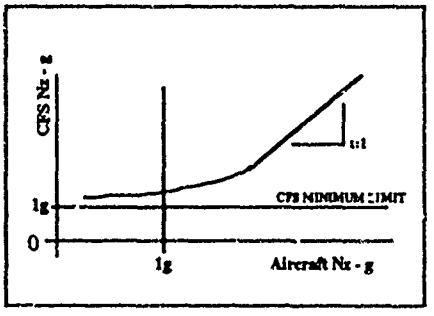

Figure 5 - Example G-bias Function Operating In The Aircraft N_Z Axis

Finally, the G-bias function also has the important effect of reducing the amount of gimbal axis rotation needed for radial and tangential G coordination. At the transition G, the function maps aircraft normal acceleration into centrifuge acceleration giving a 1:1 correspondence. Below the transition G, the DFS provides a skewed gondola cockpit N_Z with a magnitude greater than 1g and less than the transition G.

7. INHERENT LIMITATIONS

All ground-based flight simulators possess inherent motion and visual fidelity limitations in comparison with actual aircraft experience. The expanded simulation utility available with CFS devices also has inherent limitations. These limitations include 1) unrealistic angular velocity cross-coupling resulting in a motion artifact termed the Coriolis Illusion, 2) the fact that the earth's gravity field results in a continuous fixed direction and magnitude linear acceleration component; and 3) centrifuge payload weight and volume constraints.

The Coriolis illusion is the cross-coupling of angular velocities sensed by the semicircular canals due to either head motion or gimbal actuator motion in and out of the plane of arm angular velocity. Longer radius centrifuges need less angular velocity to generate required acceleration magnitudes and therefore exhibit less of this phenomenon. The DFS with a 50 foot arm requires approximately sixty percent of the angular velocity of a 20 foot centrifuge to provide a given normal acceleration. Large radius centrifuge designs have been proposed to minimize the Coriolis Illusion artifact. Unfortunately, the additional tangential acceleration generated on these devices results in a different undesirable artifact of the simulation. Estimated motion perceptual stimulation generated by these effects for various radii is shown in Figure 6.

The angular rotation inputs resulting in Coriolis Illusion most prominent at the initiation of arm rotation (start of the simulation). For some pilots, the effect can be overwhelming leading to simulator sickness or severe discomfort. However, experience has shown pilots rapidly develop tolerance to the Coriolis Illusion quickly after two or three 15 minute exposures. Some pilots can only adapt to the Coriolis Artifact by minimizing head movement, while other pilots adapt and ignore the effect altogether.

The cost/benefit trade-off of large radius vs. short radius centrifuge simulation is not well established. The

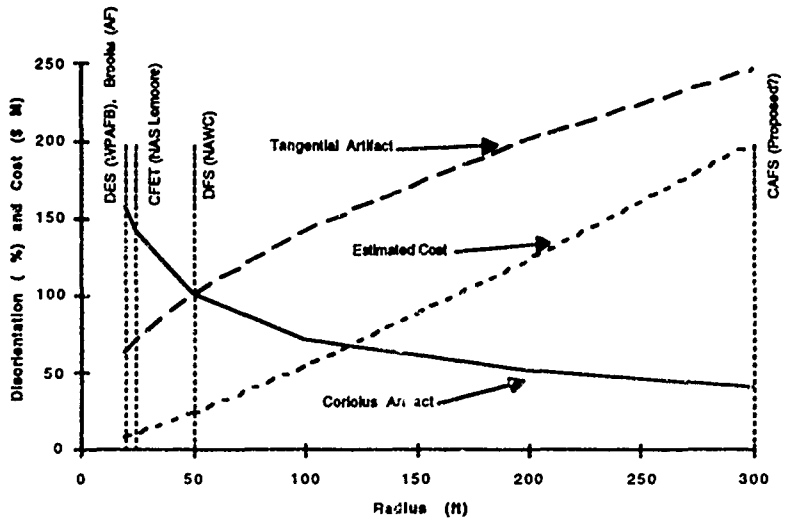

Figure 6 - CFS Motion Tradeoffs

primary benefit is advertised as a reduction in Coriolis Artifact. However, no research is available to determine what threshold the Coriolis Artifact must be below in order to be considered sufficiently diminished. Thus, no research is available to determine what the radius of the centrifuge should be for the minimum design threshold. Furthermore, with current PST aircraft providing 300 to 500 ft turn radius, the Coriolis Artifact will also be prevalent in the cockpit. Therefore, to provide adequate motion fidelity, some level of this effect may be required. Finally, even though the increased radius reduces Coriolis artifact, significant angular rate artifacts occur as a result of having to rapidly align the pilot into the G-vector.

With regard to the second noted limitation, the magnitude of acceleration in the DFS is always greater than 1g. As previously discussed, this is often compensated for by a G bias function which maps aircraft G_Z into centrifuge G_Z while providing capability to simulate less than 1g flight. Applying a G bias function to other than the z-axis may allow different directional compromises which may be appropriate for some applications.

Finally, the restricted weight and volume constraints of this type of simulation introduce a limitation in the type of simulation support equipment which may be used. The visual display system, for example, must be small, lightweight, and able to withstand the forces representative of actual flight. This results in secondary limitations such as limited field of view which are affected by the cost to design unique systems for this environment.

8. PHASE I EXPERIMENT: INVESTIGATION OF EFFECT OF MOTION ON THE PROPOSED NASA/NAVY HIGH ANGLE OF ATTACK NOSE DOWN GUIDELINE CRITERIA

8.1 General

In November, 1989, NASA commenced a program to investigate and establish quantitative high angle of attack (AOA) pitch recovery design guidelines and to develop flight test pitch recovery demonstration maneuvers/criteria. The research program was termed HANG[8,9], which referred to the high angle of attack nose-down guideline criteria which was to be the end product of the experiment. The effort entailed conducting piloted, fixed-based (no motion) simulation experiments which provided necessary data used to develop preliminary pitch axes control margin criteria.

The criteria accounted for two levels of flight operations, namely safety of flight and tactical utility. Based upon analysis and correlation, the two primary parameters of interest were decided to be pitch acceleration and pitch rate. These parameters were measured at the pinch point (see Figure 7). Based on the experimental data, NASA recommended criteria and corresponding magnitudes related to longitudinal control power requirements for HAOA flight operations.

HANG utilized a high fidelity, non-linear, 6 DOF F/A-18A manned simulation. The simulation was hosted on the NASA Langley Differential Maneuvering Simulator. Aerodynamic data and flight control laws were modified to ensure that test results would be representative of tactical aircraft. Additional information

regarding HANG is provided in References 1 and 3.

NAWC Patuxent River conducted flight tests to validate the overall research test results and methodology by comparing pilot comments, pilot ratings, and aircraft response characteristics gathered during in-flight recoveries from HAOA conditions to those gathered during the fixed base simulation sessions[1,3] Flight test results provided significant differences in pilot ratings than those obtained from the fixed base simulation results. The differences were explained as the result of several factors, of which the most noteworthy were the lack of motion cue effects, and differences in the actual aircraft control system and aerodynamics between the simulation and the test aircraft[9].

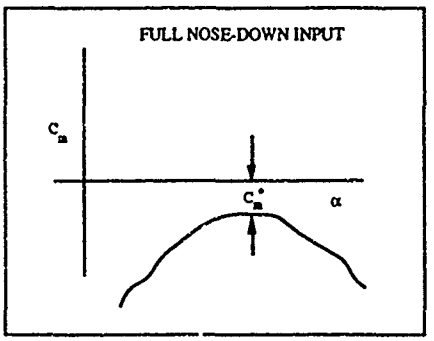

Figure 7 - Definition Of Pinch Point: Lowest Value Of Available Nose-Down C_m For Full Forward Stick Input As Depicted On The C_m Vs α Curve

The NAWC Flight Dynamics and Controls branch conducted preliminary analyses which indicated the proposed HANG criteria may require an additional parameter of N_Z and/or rate of change of N_Z. This is based on the following 3 DOF equation for high angle of attack flight operations:

$$\Delta\dot{\theta} = k\cdot\{\pm[a\cdot(\Delta N_{zb} - \Delta\theta \cos\theta_o)^2 + b\cdot(-(\Delta N_{zb} - \Delta\theta \sin\theta_o))^2]^{\frac{1}{2}}\}$$

$$a = [\sin^2\alpha_o + \Delta\alpha \sin 2\alpha_o + \Delta\alpha^2 \cos^2\alpha_o]$$

$$b = [\cos^2\alpha_o + \Delta\alpha \sin 2\alpha_o + \Delta\alpha^2 \sin^2\alpha_o]$$

$$k = \frac{-g}{(V_o + \Delta V)}$$

Clearly, the inability to apply small angle approximations significantly complicates the relationship between N_X, N_Z, q and α as compared with the familiar

$$\Delta\dot{\theta} = \frac{-g}{V_o}[\pm\Delta N_{zb}].$$

At high angle of attack, pitch rate is now

$$\Delta\dot{\theta} = f(V_o, \theta_o, \alpha_o, \Delta V, \Delta\theta, \Delta\alpha, \Delta N_x, \Delta N_z),$$

as opposed to

$$\Delta\dot{\theta} = f(V_o, \Delta N_z).$$

Humans sense-self motion cues via the vestibular system (located in the inner ear) which consists of the semicircular canals and otolith organs. Linear accelerations are perceived from visual cues, somatosensory information, and otolith stimulation. The otolith organs respond to force similar to linear accelerometers. Angular motion is primarily sensed from the semicircular canals which act similar to angular accelerometers at low frequency stimulus, and angular velocity transducers at high frequency stimulus.

The pilot's ability to detect pitch motion at high angle of attack is a complex combination of both linear, angular, and visual stimuli. The hypothesis is that during HAOA, low g pitching maneuvers, pilots cue on both the linear acceleration changes sensed through the otolith stimulus, as well as the angular motion sensed via the semicircular canals. Both are considered to be important in determining pitch motion response even at low g, low q conditions. Linear acceleration changes occur due to aircraft lift and the movement of the gravity vector with large pitch attitude changes. Therefore, adequate determination of HAOA control margin value may likely require pilots to sense motion physically as well as visually.

8.2 Approach

Since 1987, NAWC Warminster has been developing improvements to the Dynamic Flight Simulator's (DFS) hardware and Centrifuge Control Algorithm (CCA) in the development of a limited flying qualities and human factors simulation tool to be used when the sustained dynamic environment of actual flight is necessary in the RDT&E experiment. Recently, developmental evaluations at the DFS have demonstrated the potential to produce the fidelity required to conduct a pitch axis flying qualities experiment such as NASA's HANG investigation. The advantage of using the DFS over fixed base and conventional motion base simulation is the ability to provide a sustained motion environment.

Repeating the NAWC Patuxent River study in the DFS using a generic fighter aircraft would allow a direct evaluation of the effects of motion on pilot ratings and their correlation with the HANG-proposed criteria because the exact same aircraft model and cockpit will be used with and without motion. Therefore, the effect of motion on pilot ratings obtained during control power analyses tests could be assessed using the exact same aircraft control system and aerodynamic model.

The test program was designed as a two phase effort. First, developmental testing was conducted to adjust the CCA to provide the necessary motion fidelity for the HANG experiment to be conducted on the DFS. This included piloted developmental testing of the CCA to determine the necessary gain constants and G-bias function to provide adequate N_X, N_Z, and pitch response onset, perceptual magnitude, and phase while potentially sacrificing some lateral and directional axes motion fidelity.

Phase II will investigate the effects of motion on pilot evaluation of nose down control power using the proposed NASA guidelines. Any differences in pilot ratings of maneuvers performed with and without motion will be studied; and if necessary, proposed modifications to NASA's HANG requirements will be provided based upon experimental data obtained. The results of Phase I testing are covered in this paper. Phase II testing is pending.

8.3 Simulator Cockpit Description

Tests were conducted using the light weight cockpit (LWC) assembly incorporated into the DFS. The LWC had an F-16A throttle quadrant and side-stick controller. Thrust vectoring was controlled using the trigger switch on the side-stick controller. Speedbrakes were provided via a switch on the throttle. The seat base was the standard F-18 SJU-5A/6A.

The visual system was a three display/channel Paragon system providing 120 deg horizontal by 30 deg vertical field-of-view (FOV). The FOV was enhanced by a light dome grid superimposed onto the visual scene. The grid provided additional spatial orientation (including rate sensation) during large pitch attitude tasks. The visual database was representative of the northern Philadelphia area. The HUD was superimposed onto the center visual display. The HUD format is based upon the baseline F-18 format and modified with an AOA tape which indicated AOA up to 80 deg.

Data was collected using an embedded digital data collection system for post-flight analysis, and strip chart recorders for real time monitoring. The plot controlled digital data collection record numbers via the paddle switch on the stick grip.

8.4 Aircraft Simulation Model Description

The aircraft simulation model used for the experiment was the Generic Fighter Aircraft-Modified (GFAM). GFAM was a modified version of the Generic Fighter Aircraft[10] developed for real-time fixed base simulation at NAWC Warminster. The model utilized a modified F-18 aerodynamic database which incorporated an F-15 pitching moment curve (stable). Thrust was provided by a simplified F-110 engine simulation which approximated engine dynamics using first-order lags. Thrust-to-weight ratio initialized at 1.0 (Sea Level, static) and could be modified real-time, on-line during operations.

The generic control system included full state feedback for stability and control augmentation. In addition, the GFAM incorporated pitch and yaw thrust vectoring with departure resistance allowing controlled maneuvering up through 90 deg AOA. The flight envelope was approximately 200 KCAS to 1.0 M, Sea Level to 50000 ft. Thrust vectoring was blended with aerodynamic control, with full authority available at dynamic pressures below 100 psf.
The primary advantage of the GFAM is the ability to modify aircraft characteristics real-time. Results from qualitative evaluations indicate that the GFAM model had to have handling qualities at essentially between levels 1 and 2[11], and was therefore satisfactory for the purposes of the DFS/HANG Evaluation.
Control power was modified by changing thrust vector angle authority or the location of the pinch point. In addition, the characteristics of the C_m vs α curve were changed by adding a band-width about the pinch point. This is illustrated in figures 8 and 9.

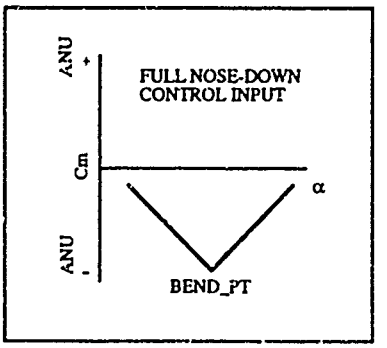

Figure 8 - Incorporation Of A Bend Point Into The Existing C_m Curve

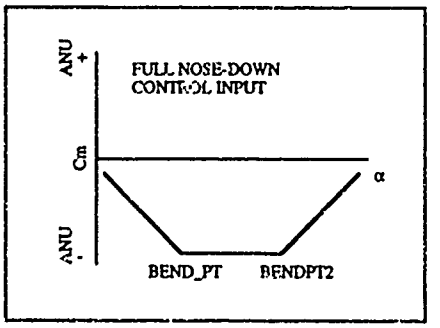

Figure 9 - Incorporation Of A Bend Point With A Bandwidth Into The Existing C_m Curve

9. RESULTS AND DISCUSSION

9.1 Initial Assessment

Three pilots were utilized to develop the appropriate gain and filter parameter values. The test pilots included both NASA and Navy pilots. In all cases the pilots were first introduced to the GFAM in the static mode to acquire familiarity with the flight characteristics. An immediate illustration of the effect of motion on a pilot's perception of flying qualities was obtained after the pilots flew the model in the full envelope (baseline CCA) DFS dynamic environment.

During static operations (no motion), the pilots conducted qualitative evaluations of the aircraft handling qualities. Each pilot noted that the aircraft stick sensitivity was too low, resulting in sluggish response characteristics in the longitudinal and lateral axis. During static test operations the GFAM model was modified on-line to

provide five times the longitudinal stick force to control surface ratio, six times the lateral stick force to control surface gearing ratio, and a roll SAS feedback three times the baseline value. Modifications were implemented in an effort to increase rate sensitivity based upon pilot comment. When flying the GFAM in this configuration the pilot felt that the rate sensitivity was indicative of current fighter aircraft characteristics.

During the first flight in the dynamic mode (full motion environment), each pilot was given the baseline GFAM model with no modifications (gain changes) embedded. After re-evaluation of the rate sensitivity characteristics, two pilots now stated that the rate sensitivity was too high, and the Navy pilot stated that it was satisfactory to slightly high.

The reason the pilots reversed their assessment of the rate sensitivity characteristics is readily explainable. In the static mode, the pilot's only motion feedback to command input was the visual system. However, in the dynamic mode, the motion feedback includes linear acceleration (N_x, N_y, N_z) and angular rates (P, Q, and R). The additional feedback to the human motion perceptual system improved the ability of the pilot to detect aircraft response and therefore changed his perception of the rate sensitivities. This simple example serves to demonstrate the effects of motion on a pilot's rating of closed loop handling qualities characteristics. Clearly motion will significantly effect pilot ratings of more complex tasks such as carrier operations, low level terrain following, A–A and A–G combat and aerial refueling.

9.2 CCA Modifications For Improved Pitch Response Characteristics

Approximately 5 hours of dynamic flight operations were conducted. After each pilot was familiar with the aircraft handling qualities and motion flight environment, CCA gain and parameter values were varied systematically in an attempt to provide increased motion perception of N_z, N_x, and pitch rate beyond that provided by the baseline full envelope CCA. The basis was that the lateral and directional motion fidelity, and full envelope capability could be sacrificed to provide a higher fidelity, limited envelope motion algorithm specifically designed for the DFS/HANG evaluation. At completion of this developmental testing, the pilots felt that several motion fidelity deficiencies required improvement. These deficiencies included low sensation of pitch rate and N_z unloading, delays in onset of N_z, roll rate artifacts felt during pushover, and motion perception conflict with the visual system during pushovers with rapid increases in airspeed.

Consequently, to better simulate the motion environment of a HAOA pushover maneuver, several modifications to the baseline CCA were required. These included increasing pitch rate response, minimizing onset of gondola N_y and roll response to g-onset, and providing a trim g plateau to allow for sufficient G-unloading concurrent with the pushover.

The following example test point illustrates the difficulty in providing precise motion fidelity required for a flying qualities investigation. Figures 10, 11, and 12 are the time history plots of a representative pushover maneuver used to assess control power response at HAOA. The trim g plateau was 2.0g, which represented the DFS state when the aircraft was at 1g, trimmed, level flight. The pilot initiates the pushover input at t = 12.4 sec from an initial flight condition of approximately 28,000 ft msl, 92 KCAS, and 30 deg AOA. The plots show the aircraft cockpit and gondola c.g.-referenced state conditions. The solid line is the GFAM, and the dashed line represents the DFS. The DFS traces are computed from a validated batch simulation model of the DFS driven using the GFAM data. Note that the pushover includes an inadvertent pilot commanded roll input.

In this case, the increased pitch sensitivity resulted in a force fight between the nose-up B-gimbal command (Figure 10) component required to provide an unloading sensation in N_z, and the nose-down B-gimbal command component required to provide the nose-down pitch rate sensation. When summed, the effect was to provide a fairly constant net B-gimbal command position over the initial response (< 2 sec) time interval of the commanded pushover maneuver. The constant B-gimbal position resulted in a reduced perception of N_z and Q magnitude. Some sensation in unloading was provided via N_x, and was later boosted in an attempt to provide better motion fidelity. However, each attempt to provide better pitch response resulted in more N_z response lag. The test pilots noted the limited magnitude and delayed pitch response, which was prevalent until the aircraft nose attitude dropped through the horizon. Consequently, the pilots rated the modified CCA as providing poor pitch response fidelity during HAOA pushover tasks.

9.3 Roll Characteristics

The effect of gimbal command fight was noted in the roll axis as well. During a simulated pure pushover maneuver, the CCA commands the gondola to roll right in order to reduce Nz in the gondola (see Figures 10, 11, and 12). If a pilot conducts a pure roll input at 1g, the CCA provides a roll sensation similar to the aircraft where left stick provides left roll in the gondola (see Figure 13). When a pilot combines a left roll with a pushover, the A-gimbal command increment for Nz is summed with the A-gimbal command increment for roll attitude change. The net command results in a positive gondola roll rate. Recalling the example pushover shown in Figure 12, note that the body axis roll rate of the gondola was to the right even though the aircraft simulation was rolling left. During rolling maneuvers the pilot never commented that he felt his roll rate was opposite to aircraft roll rate. The visual system provided a strong effect in convincing the pilot of his roll direction. However, if the pilot had been tasked to explicitly assess roll characteristics (thereby directing his attention to the roll axis), it is likely that he would have noticed this anomaly. In addition, the primary emphasis of the DFS/HANG program was to assess pitch response, which may have result in reduced awareness of lateral and directional axis artifacts.

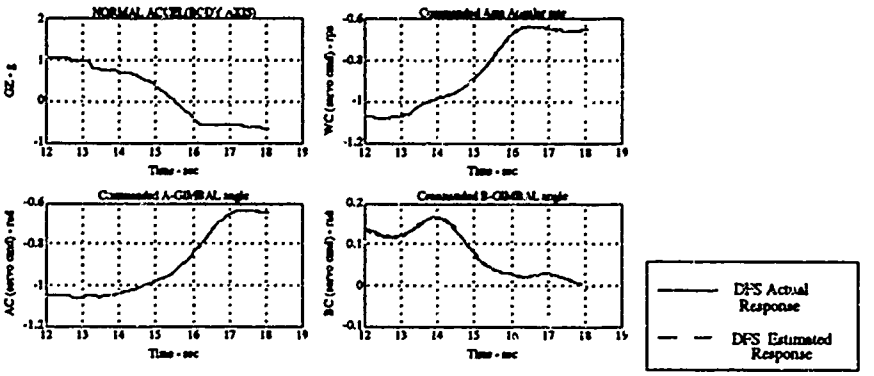

Figure 10 - ω_C, A_C, and B_C Time Histories During A 30 Deg Pushover

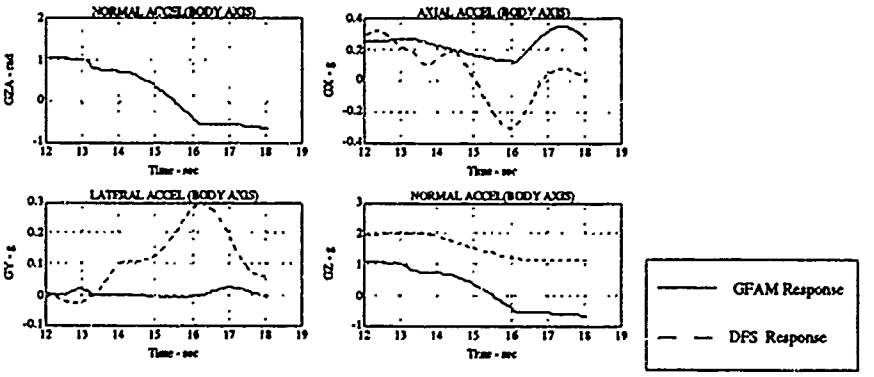

Figure 11 - N_X, N_Y, and N_Z Time Histories During A 30 Deg Pushover

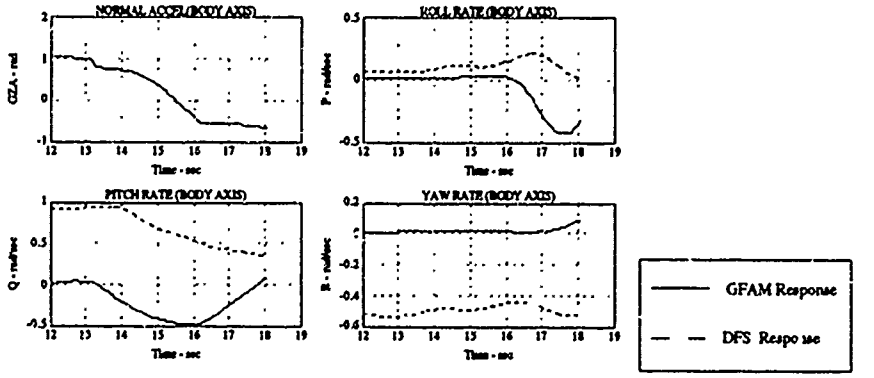

Figure 12 - P, Q, and R Time Histories During A 30 Deg Pushover

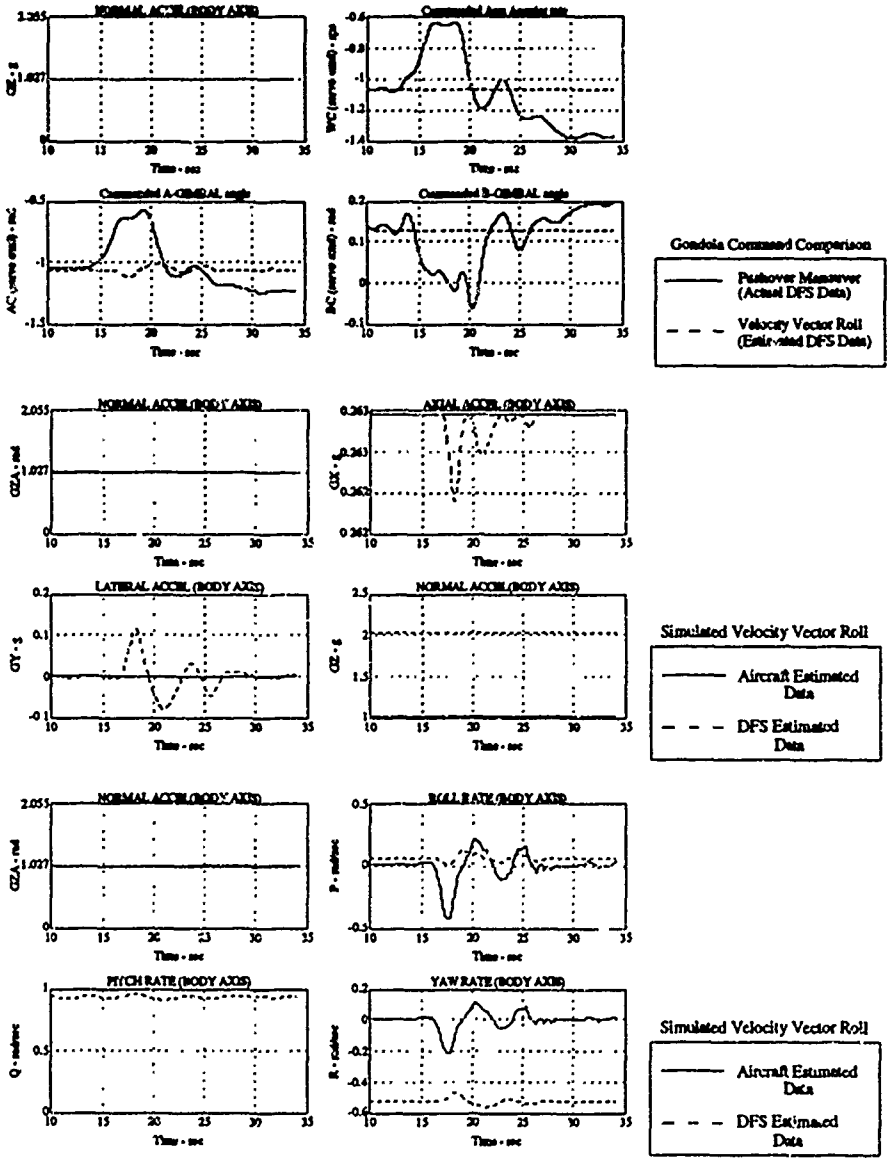

Figure 13 - Pure Velocity Vector Left Roll From a 30 Deg AOA Stabilized Flight Condition. Time History Data Computed Using GFAM State Data As Input To Drive A CCA Batch Simulation Model. Input Data Was The GFAM 30 Deg AOA Pushover (Figures 10, 11, and 12) Modified Off- line To Represent A Pure Velocity Vector Roll.

Keep in mind that for a single axis lateral input such as a left aileron roll, the CCA will command the gondola to roll left as expected. However, a command fight occurs when a left roll axis and a nose-down pitch axis input are combined, thereby leading to delays and/or reduced magnitude sensations of rolling. Avoiding command fights associated with multiple axis inputs requires establishment and incorporation of a command path hierarchy into the CCA. The hierarchy would provide precedence to designated control paths thereby minimizing the state delay and magnitude loss associated with the command fight. Until this is accomplished, motion artifacts such as pure delays, lags, phase reversals, and reduced magnitude commands will likely adversely affect motion fidelity.

9.4 Effect Of Visual System On Perception Of Motion

The visual system is paramount to the success of the CCA in the DFS. An earlier discussion pointed out the tremendous change in pilot perception of aircraft response when a full motion environment was added to augment the visual-only cues. In the same manner it must be emphasized that the visual system substantially facilitates human motion perception.

Several studies to date have provided qualitative data confirming that the visual system augments the sense of commanded motion felt by the pilot, and it attenuates many of the motion artifacts associated with centrifuge exposure. For example, during routine flight operations, the extraneous roll, pitch, and yaw motion cues associated with routine (benign) flight operations are not apparent to the pilot except via the visual system. On the other hand, as discussed previously, roll rates in the gondola which were opposite to the pilot command were not noticeable to the pilot. The visual system was successfully utilized to diminish the effect of the apparent motion artifact.

9.5 Transient And Long Term Response Motion Fidelity

During piloted operations, several HAOA pushover test points were conducted while varying CCA filter parameter and gain values. The results of these tests indicated that achieving adequate motion fidelity for short term flying qualities criteria development may require a close match in gondola and aircraft states during the initial ($t \leq 1$ to 2 sec) motion response.

During short duration HAOA pushover maneuvers unloading the aircraft approximately 0.5g, the DFS unloads from approximately 2.0 g to 1.5 g. Pilot comments indicated that to provide satisfactory initial onset motion fidelity, the DFS should provide the same relative initial response characteristics (pure delay, phase lag, magnitude ratio) as the actual aircraft. Furthermore, the pilots indicated that following initial onset of motion, the perceived motion environment improved. In general, during tasks where the motion effects were important beyond motion onset, the CCA provided better motion fidelity than for tasks which were short duration ($t \leq 1$ to 2 seconds) and primarily dependent on initial response fidelity.

It is difficult to determine the actual point where human perception to motion begins to be dominated by the sustained steady state motion cues relative to the transient initial response cues. Fortunately, it is not as difficult to classify most flight tasks as short duration or long term. For example, assessing the ability of a pilot to capture 30 deg AOA from a step input is a short duration task. However, studying pilot workload during A-A tracking, or approach to landing is a typical long term task. Based on these results, the utility of the current CCA and DFS setup is best suited for long term analyses such as pilot workload, advanced displays development, situational awareness and spatial disorientation studies, and cockpit information fusion RDT&E. Flying qualities criteria development is difficult to accomplish on the current configuration due to the problem in providing the short term response motion fidelity.

Consequently, if modifying the CCA for specific short term flying qualities programs, the gain and filter parameter values should be set to allow the onset of motion to closely represent the primary cues for the task. When studying pitch capture tasks, some fidelity can be sacrificed in the roll axis to allow better pitch response motion fidelity. However, care must be taken to prevent motion fidelity anomalies which cannot be ignored by the pilot, or which result in negative transfer of training.

Sacrificing motion fidelity in various flight regimes or axes is an inefficient approach to applying a motion control algorithm to a specific experiment. However, given the many constraints associated with development of a CCA for a particular centrifuge device, it offers one low cost, rapid approach. This is particularly true for a motion control algorithm with fixed architecture, gain, and filter parameter schedules. In the near future, the use of multi-variable optimum control schemes may provide better optimization performance and motion fidelity. Use of a neural network control scheme will likely be the best approach since the optimization problem is not clearly defined, and the current human motion perception models provide limited accuracy.

9.6 Effect Of Absolute Magnitude And Rate Of Change

Another important consideration related to near-term response is the relationship of absolute state magnitude to the magnitude of the state rate of change from a given datum. During aircraft 1g trimmed flight conditions, the DFS pilot is subjected to steady, non-zero roll rate, pitch rate, yaw rate, and elevated N_Z state conditions in the gondola. The non-zero rates and elevated N_Z state are computed by the CCA using the aircraft trim state inputs. Consider the case of a generic aircraft trimmed at 0.5 M, 15,000 ft msl. A comparison of the DFS and simulated aircraft state parameters is presented in Table I.

After approximately 30-45 seconds the pilot adjusts to the constant rotation thereby perceiving an aircraft 1g trimmed environment. The bias P, Q, R, and elevated

trim N_Z state associated with the constant turning of the DFS was washed out of the pilot's motion senses, and thus became the motion threshold point. The assumption was that during maneuvering flight, the pilot senses deviations in gondola states about the nominal DFS trim state as if the changes were in the actual aircraft states about the aircraft trim state.

During DFS/HANG pushover tasks, pilots noted that the sensation of negative pitch rate was minimal in magnitude and difficult to sense. A comparison of aircraft commanded pitch rate versus DFS pitch rate (see Figure 12) showed that a negative body-axis pitch rate never actually occurred. There is only a decrease in pitch rate from the nominal value representative of the steady state flight condition. This suggested that independent of the fact that the gondola is subjected to continuous arm rate, ω_c, it was very difficult to convince the pilot that a negative pitch rate was occurring because he was being continuously subjected to a large, positive pitch rate. Unfortunately, due to the large, inherent DFS yaw rate bias, there may also be difficulty in adequately simulating the yaw rate sensations associated with maneuvers such as HAOA stability axis rolls.

Table I
Comparison Of Trim States Between A Simulated Aircraft And The DFS Gondola C.G.

Parameter	Aircraft	DFS
δ_{stab} (deg)	-14.20 (TEU)	-
α_{trim} (deg)	4.04	-
A_c (deg)	-	-59.94
B_c (deg)	-	2.03
ω_c (deg/sec)	-	-60.44
N_X (g)	0.0706	0.0706
N_Y (g)	0.0000	0.0000
N_Z (g)	0.9975	1.9949
P (deg/sec)	0.00	1.07
Q (deg/sec)	0.00	52.3
R (deg/sec)	0.00	-30.3

9.7 Developing DFS/HANG CCA Performance Improvements Using Batch Simulation

A batch simulation model of the CCA and DFS primary mechanical characteristics was utilized to conduct off-line developmental testing for improvements to the DFS/HANG CCA. The batch simulation, designated Centrifuge Flight Simulation Analysis and Validation Tool (CFSAVT), can be driven using a 3-DOF generic fighter aircraft model, or by actual aircraft data files. CFSAVT allows both developmental analyses of the CCA and comparison of actual DFS data results with estimated (predicted) results. The model was validated using actual DFS and GFAM test data. The major benefit of CFSAVT is that it provides a low cost, rapid approach to experimenting with new parameter values and model architectures.

Using both pilot comments and quantitative data results, several combinations of CCA parameter values were tested off-line using CFSAVT. Selected modifications were implemented into the interim HANG CCA configuration developed during on-line developmental testing in Phase I of the HANG/DFS program. As with every optimization problem, several proposed CCA parameter value combinations provide the improved performance in N_Z and Q response, but also resulted in severe undesirable motion artifacts in N_X and N_Y.

The best results to date (Figure 14) show a significant (50%) reduction in the N_Z and Q onset delay with minimal change in artifacts. Unfortunately, adjustments in CCA gain and parameter values had only minimal effect on improving the response magnitude in N_Z and Q. If the reduction in onset delay combined with the current response magnitudes in N_Z and Q fail to provide sufficient motion fidelity, it is likely that CCA architecture modification will be required. This would also include the addition of control command hierarchy.

10. LESSONS LEARNED

Over the last two years, significant improvements have been accomplished on the baseline motion control algorithm of the DFS. Pilot comments and quantitative data from Phase I of DFS/HANG program are being used to design proposed corrections for Phase II of the project. Batch computer modeling is being utilized to facilitate this effort in a cost effective manner.

Following Phase I of the DFS/HANG investigation several lessons learned were noted with regard to motion control algorithm development. First, when using fixed-architecture, fixed-gain motion control algorithms, it may be required to optimize the algorithm to a specific portion of the flight envelope. This is done to provide satisfactory motion fidelity for conducting flying qualities and human factors RDT&E projects where the initial motion response characteristics are paramount to the success of the study. By limiting the flight envelope, motion fidelity on one axis can be reduced to improve the motion fidelity of the more important axis (as dictated by project requirements). Of course, this limits the utility and efficiency of the device, and should not be the end goal.

Developmental testing of CCA performance continues to be heavily required. Computer math modeling has reduced this effort; however, due to the wide perceptual response bandwidth of pilots, piloted developmental test is necessary for final adjustment and validation of the control algorithm and its related performance. This is particularly important since human models of perceptual response have significant limitations, including the inherent limited ability for validation.

Project experience indicates that maximum utility of centrifuge flight simulation will occur when combined with a team of CFS-rated pilots. These pilots would possess the ability to differentiate between motion, visual, and aircraft model simulation fidelities. Selected pilots should be test pilot school graduates to facilitate operations and better interface with engineers and test conductors. Finally, these pilots would have minimal

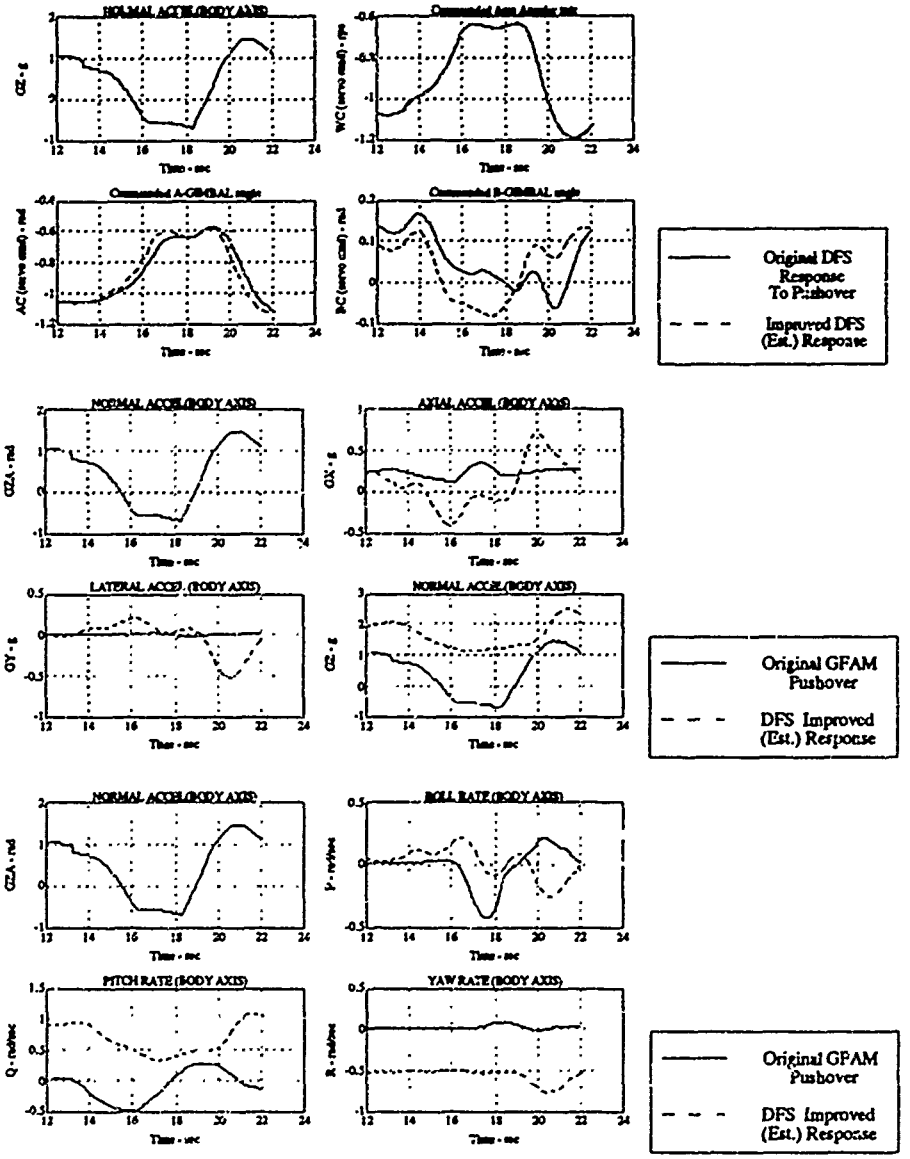

Figure 14 - Pushover Response Using Off-line Improved CCA

susceptibility to motion sickness, and the effects of the Coriolis artifact.

Dedicated development of motion control algorithm technology for sustained motion simulators is needed. To date, the primary research has been directed in a limited prototype approach to devise a motion control algorithm for centrifuge flight simulation. Research should now be directed toward the determination of methods to devise control architectures, gain schedules, and cost functions for optimal control of CFS. This includes addressing the utility of artificial intelligence and neural network schemes on non-linear, variable architecture and gain controllers. Furthermore, research must also address how to quantify the value of visual perception of motion response, and determine levels of human motion response threshold required to provide adequate motion fidelity for tactical aircraft simulations.

Finally, the design of a successful high fidelity, sustained motion flight simulator requires the interface and expertise of several technical communities. There is a need to develop improved sub-models, including human motion perception, optimal control cost functions, motion control algorithm architecture philosophy, and controller concepts. Since CFS devices subject a pilot to rate and acceleration magnitudes similar to tactical aircraft, development of a standard for accepted operational procedures and safety is required. Finally, there should be a standardization of symbology, nomenclature, and axes systems within the aircraft and physiological communities to minimize unnecessary work and confusion.

11. CONCLUSIONS

Centrifuge flight simulation is a tool which provides engineers the opportunity to challenge the man-machine weapon system under the harsh environmental conditions they must perform, but, in a safe, controlled, repeatable, cost effective, laboratory environment. There is a need for advanced piloted flight simulation to address flying qualities and human factors issues including criteria development, display technologies, and tactics/training. In addition, a strong need exists for improved motion control algorithm technologies, specifically for sustained motion simulators. All communities will benefit from this technology, and a successful design will require a combination of several technical skills including flying qualities, human factors and crew systems.

The development of a motion control algorithm is a multi-variable task. To obtain adequate short term response motion fidelity for flying qualities programs such as HANG/DFS, there is a strong possibility that the CCA will require variable architecture and control command hierarchy to preclude command force fights. This also applies to investigations requiring multi-axis fright maneuvers. Furthermore, when using CFS to study effects of initial or short term (< 2 sec) motion response on closed-loop piloted tasks, the initial (onset) motion response given by the CCA should closely match the aircraft motion onset response. This may require a design tradeoff to minimize gimbal command fights.
More sophisticated methods of development and optimization of motion control algorithms need to be developed. This includes 1) improvements in human motion perception response models, 2) development of adequate cost functions for control optimization, and 3) use of neural networks or artificial intelligence to deal with the inability to precisely model human motion perception.

Off-line CCA development using CFSAVT provides a cost-effective approach to developing and adapting the CCA to specific tasks. CFSAVT was successfully used to test several combination of gain and filter parameter values. Results of these analyses are being applied to the development of an improved CCA designed to minimize the pitch response delays identified during Phase I of the DFS/HANG test effort.

12. FUTURE EFFORTS

Future developmental efforts will be aimed at conducting limited flying qualities and human factors experiments which utilize the current and projected near-future capabilities of the DFS. A representative F-18 cockpit and simulation model is currently under design and certification for use within the DFS. Development of the control algorithm on and off-line will continue in support of maximizing the DFS's potential for an expanded role as a high fidelity, man-in-the-loop flight simulator.

CFSAVT will continue to be used in support of this effort. Human perceptual models[2] will be incorporated directly into the model to allow for improved methods of gain optimization. This includes the design and use of cost functions comparing human motion perceptual response estimates computed for a pilot in the aircraft and in the DFS during flight[12]. The ability to conduct off-line gain optimization ensures the highest potential for desired motion fidelity. Proposed CCA architecture and parameter value configurations designed off-line will be validated during piloted simulations.

13. REFERENCES

1. Smit, J., van Patten, R. E., "G-Tolerance and Spatial Disorientation: Can Simulation Help Us?", AGARD Flight Mechanics Panel Symposium on Piloted Simulation Effectiveness, AGARD-CP-513, Oct 91.

2. Mitchell, D. G., Hoh, R. H., Atencio, A, and Key, D. L., "The Use of Ground Based Simulation for Handling Qualities Research: A New Assessment", AGARD Conference Proceedings 513, Feb 92.

3. Crosbie, R.J., "Application of Experimentally Derived Pilot Perceptual Angular Response Transfer Functions", AIAA-83-1100-CP, AIAA Flight Simulation Technologies Conference and Technical Display, Jun 83.

4. Crosbie, R.J. and Kiefer, D.A., "Controlling the Human Centrifuge as a Force and Motion Platform for the Dynamic Flight Simulator", AIAA-85-1742, AIAA Flight Simulation Technologies Conference, Jul 85.

5. Cohen, M.M., "Human Performance During Exposure to Combined Linear and Angular Accelerations", NASA Contract MPRT-8477C.

6. Kiefer, D. A., Calvert, J. F., "Developmental Evaluation of a Centrifuge Flight Simulator As An Enhanced Maneuverability Flying Qualities Tool", AIAA-92-4157-CP, Flight Simulation Technologies Conference, Aug 92.

7. Ogburn, M. E., Foster, J. V., "Application of Piloted Simulation to High-Angle-of-Attack Flight-Dynamics Research for Fighter Aircraft", AGARD Conference Proceedings 513, Feb 92.

8. McNamara, W. G., et. al., "Navy High Angle of Attack Pitch Control Margin Requirements for Class IV Aircraft", NAWC Patuxent River Report No. TM 91-167 SA, 25 Jun 92.

9. Lackey, J., Hadfield, C., "Pitch Control Margin at High Angle of Attack - Quantitative Requirements (Flight Test Correlation With Simulation Predictions)", AIAA Flight Simulation Technologies Conference, Aug 92.

10. Anonymous, "Generic Fighter Aircraft FASTER Simulation Model Report", VEDA Report Number 33159-91U/P3551-005, Jan 91.

11. Anonymous, "Military Specification, Flying Qualities of Piloted Airplanes", MIL-F-8785C, Nov 80.

12. Bomar, J. B., et. al., "Engineering Design Analysis of a Large Radius Track Centrifuge", Biodynamic Research Corporation Report Number F41624-91-C-2002, Feb 93.

OPTIMAL TACTICS FOR AGILE AIRCRAFT TECHNOLOGY...A DIFFERENTIAL GAME METHODOLOGY

Urban H. D. Lynch
Eidetics International, Inc.
3415 Lomita Boulevard
Torrance, CA 90505. USA

SUMMARY

Historically, fighter aircraft tactics were not developed until a new aircraft reached operational use. In the past, this pilot/aircraft intensive process was affordable In the future, budgets and limited flying time will likely necessitate a more cost-effective way to develop tactics for innovative and unfamiliar aircraft technologies Such is the case for WVR technologies as high angle-of-attack (70°) supermaneuverability (X-31, F-18 HARV) and supermaneuverable missile (Archer-11, Aim-9X). The advent of very high, cost-effective computer power has made affordable optimal control techniques (that have been traditionally computationally prohibitive) and low-cost real-time piloted simulation of credible realism. Together, these two tools provide a cost-effective means to develop tactics for new technology prior to the new technology reaching the field in operational use. This paper presents the successful results of a first attempt to use Differential Games (the Eidetics AACDG) and the Eidetics low-cost ARENA Simulator to develop new tactics for new technology such as Extended Flight Maneuvering, (EFM). This work was sponsored by the 4-Power Senior National Representatives (SNR) through Aeronautical Systems Center at Wright-Patterson Air Force Base, Ohio, USA.

LIST OF SYMBOLS

AACDG	Air-to-Air Combat Differential Game
AOA	Angle-of-Attack
CIC	Close-in Combat
DG	Differential Game
DOF	Degree of Freedom
EFM	Extended Flight Maneuvering
HAOA	High Angle-of-Attack
IC	Initial Condition
IRCM	Infrared Countermeasure
IRM	IR missile
J	Differential Game payoff function
L/D	Lift/Drag ratio
Mach	Mach number
MGA	Mathematical Gaming Algorithm
MX	Missile
Ps	Specific power
SM	Supermaneuverability
T/W	Thrust/Weight ratio
TPBVP	Two-Point-Boundary-Value Problem
WVR	Within-Visual Range
YBR	Yellow Brick Road software

1.0 INTRODUCTION

The nature of air combat has changed dramatically over the years The collective impact of advances in weapons and airframe technologies has required changes in fighter tactics to ensure success especially when these same technologies are assumed in the threat Both Beyond Visual Range (BVR) combat and Within Visual Range (WVR) combat environments have become more lethal because of these improvements Although the pilot of a suitably equipped fighter is able to control the fight BVR and make only slashing engagements WVR, transition to sustained Close-In Combat (CIC) will be inevitable on occasions The transition between BVR and WVR combat has become an important tactical area with the need for precise timing and execution. Technology has greatly affected the pilot's choice of maneuvers and has compressed the time available for him to decide how best to react during many tactical situations

1.1 Tactics Versus Technology

It is a fact that there can be, and, indeed, in many cases must be, an interaction between fighter aircraft technologies and the tactics which are utilized to employ them. This concept is illustrated in Figure 1.0 where the "technology" that is shown is the combination of the controllable AOA range and the thrust-to-weight ratio of the fighter. An increase in the controllable AOA range can create an increase in the transient agility capability of the aircraft in all three axes. An increase in the installed thrust-to-weight ratio of the aircraft can significantly reduce the energy-bleed rate during aggressive maneuvering and can make energy addition during an unloaded acceleration much more rapid. Also shown in the figure is the tactical employment doctrine most appropriate to the technology.

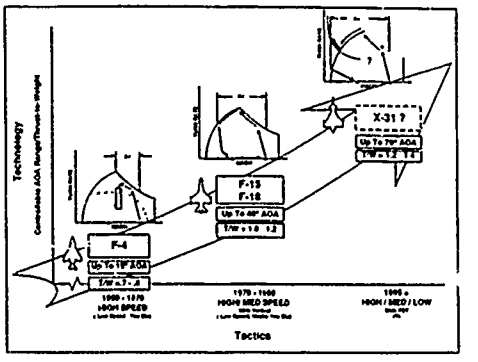

Figure 1.0 - Technology versus Tactics

F-4 Example

During the F-4 era, the controllable AOA range was less than 20° and aggressive agility usage near that angle-of-attack in the F-4 often resulted in departures and spins. Furthermore, due to the relatively low thrust-to-weight ratio of the F-4 (and due to the relatively high wing loading), maneuvering the aircraft at high AOA for very long resulted in a significant loss of airspeed and placed the pilot in an unfavorable position with limited options to enhance his survivability Hence, the tactics appropriate to this level of technology placed a premium on maintaining high airspeed Even in today's technological air combat environment, pilots continue to adhere to the air combat principle that "speed is life"

F-15 Example

After the F-15 was integrated into the USAF inventory, air-to-air tactics evolved to fit the technological advantage the aircraft offered. This aircraft has a controllable AOA range in excess of 35° and exhibits a combat thrust-to-weight ratio substantially higher than the F-4. With the F-15, the pilots can utilize its full transient agility potential very aggressively without concern for departure If the pilot maneuvers aggressively and decelerates to an airspeed below the corner speed, the high thrust and low wing loading of the Eagle give him multiple offensive and defensive options If the pilot of an F-15 flew his aircraft exactly as he flew the F-4, the combat value of the F-15 in a maneuvering engagement would be reduced from its maximum value. Hence, the tactics appropriate to the level of technology allow some relaxation of the "speed is life" doctrine when the conditions warrant more aggressive maneuvering Also, the F-15 can utilize vertical maneuvering to a much greater extent than the F-4.

X-31 Example

The technology differences between the F-4 and next generation aircraft like the F-16, F-15, F-18, F-14, etc. were significant, but not so different as to not allow a reasonable extrapolation of past tactics into the present. More importantly, in this time frame, has been the impact of missile technology enhancements on aircraft tactics. The realities of the all-aspect IR missile has greatly impacted WVR/CIC tactics whatever the airframe technology Similarly, the Archer / Aim-9X with helmet mounted sights will have a similar great impact on WVR CIC tactics

As an aircraft now, however, the EFM/HAOA capabilities of the X-31 are not a mere extrapolation from past aircraft. Angles-of-attack (AOA) of 70 degrees cause many tactical challenges to the pilot, of such magnitude, that past tactical experience offers minimal help in knowing how/when to apply the new technology to best advantage. Consider the following tactical challenges:

Presented at an AGARD Meeting on 'Technologies for Highly Manoeuvrable Aircraft', October 1993.

- A high AOA maneuver is accompanied with a rapid loss of airspeed and potential disorientation in situational awareness.
- Is the high AOA maneuver compatible with weapon constraints?
- How much AOA is realistic for tactical use?
- Should high AOA be used to rotate the velocity vector (at slow speed - Herbst maneuver) and unload to shoot, or to simply point-the-nose and get the first shot to threaten the adversary?
- What impact does higher thrust/weight (T/W) or lift/drag (L/D) have on the utility of EFM and appropriate tactics?
- What if the thr[illegible]ircraft has better performance in the conventional flight envelope than the EFM aircraft?
- Even with EFM capability, can the opponent negate most of its advantage by changing his tactic?

2.0 DIFFERENTIAL GAME AS A TACTICS GENERATION TOOL

Although there are several approaches to tactics-for-technology development, most are "brute-force" in nature and greatly depend on the intelligence of the analyst/user. Differential Games, on the other hand, (to be better defined later) is a branch of Optimal Control Theory that is a "near-perfect" mathematical gaming algorithm for WVR air-combat tactics development. Figure 2.0 portrays a definition of the DG. DGs is based on the Calculus of Variations to define the mathematical necessary conditions to optimize a payoff function. For example: Find the aircraft control schedule that minimizes the time-to-climb to a defined altitude. This problem is a simple single aircraft problem in Optimal Control Theory where "time" is the payoff and results in the classic Rutkowski climb paths. DGs is a bit more complex as there are now two players in which one player is attempting to minimize the payoff and the other player is attempting to maximize the payoff (i.e., a saddlepoint solution). For example: Find the aircraft (Pursuer) control schedule (tactic) that minimizes the time to closure while also finding the other aircraft (Evader) control schedule (tactic) that prevents/maximizes the time to closure. The resulting mathematical necessary conditions have two sets of differential equations:

- State equations (i.e., equations-of motion) defined initially (i.e., time = 0)
- Costate equations defined terminally (i.e., at the final time)

Figure 2.0 DIFFERENTIAL GAMES

A BRANCH OF OPTIMAL CONTROL THEORY THAT FINDS THE BEST CONTROL/TACTICS FOR THE SYSTEMS IN CONFLICT

AIR-TO-AIR COMBAT APPLICATION

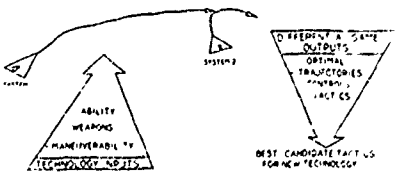

These two sets of differential equations form a two-point-boundary-value-problem (TPBVP) that can be solved by iterative numerical techniques (i.e., steepest descent gradient technique) on a high-speed computer. Figure 2.1 portrays features of the gradient technique. The outputs of the DG technique are the trajectories and control histories (tactics) to optimize a payoff function for the technologies characterizing the systems (i.e., equations-of-motion) in conflict. The power of the Differential Game is that it will find the "optimal tactic" for a new technology that you are not sure how to use to advantage. Furthermore, it will find the "optimal tactic" of the opponent that will best counter/negate the new technology.

The major "risk" in the DG approach is the development of an analytic payoff function that appropriately expresses what the adversaries are trying to accomplish. Fidelity in developing the Air-to-Air Combat Differential Game (AACDG) Model and a realistic air-combat payoff function that represents what fighter pilots are trying to achieve

GRADIENT APPROACH TO DIFFERENTIAL GAMES

Figure 2.1

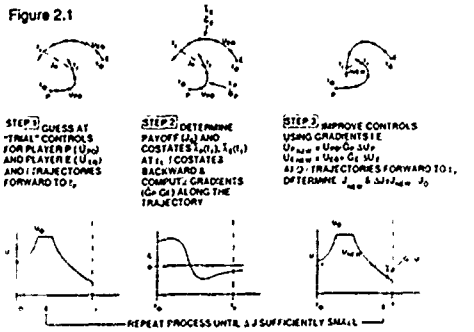

2.1 WVR Air Combat Payoff Function

Fighter pilots in reality fight weapon envelopes first and only indirectly fight aircraft in that the weapon envelope is attached to

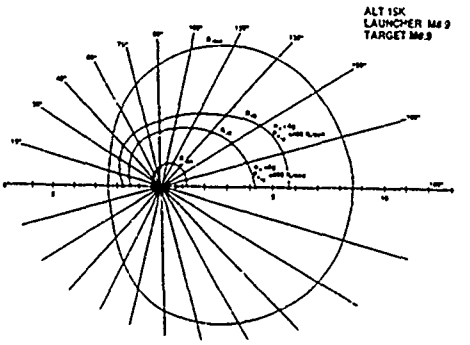

Figure 2.2 Missile Performance Envelope

the aircraft. Figure 2.2 shows the lead-collision guidance missile performance envelope of an Aim-9 like missile. Shown are the characteristic envelope performance parameters:

R_{MIN} - Minimum launch range (nm)
R_{MAX} - Maximum launch range (nm)
R_{NE} - No-escape range

Not shown in Figure 2.2 is the lead-collision launch angle, θ_Q, measured from the line-of-sight that is shown in Figure 2.3. The R_{MIN}/R_{MAX} magnitudes are a function of the launch altitude, missile characteristics, aircraft velocity vector magnitudes and orientations. The latter two parameters (i.e., velocity vector magnitude and orientation) for each aircraft are highly dynamic

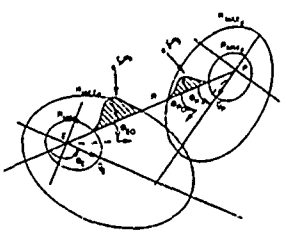

"TODAY'S TACTICS ARE DRIVEN BY THE ENVELOPES OF THE WEAPONS"

$$J = \left\{1 + e^{-\left[\frac{4R - 2(R_{min_P} + R_{max_E})}{R_{max_E} - R_{min_P}}\right]^2}\right\}^{-1} \sin^2\left(\frac{\theta_P - \theta_{Q_P}}{2}\right) \cdot \left\{1 + e^{-\left[\frac{4R - 2(R_{min_E} + R_{max_P})}{R_{max_P} - R_{min_E}}\right]^2}\right\}^{-1} \sin^2\left(\frac{\theta_E - \theta_{Q_E}}{2}\right)$$

Figure 2.3 - Generalized Air-to-Air Combat Payoff Function

variables in WVR air-combat that cause the missile performance envelope to also be highly dynamic. Any aircraft technology that rapidly influences aircraft velocity vector magnitude and orientation will highly couple into the missile performance envelope.

The realization that pilots primarily fight weapon envelopes and that these envelopes are highly dynamic in WVR air-combat, led to the quantitative generalized payoff function, J, shown in Figure 2 3. The subscripts P and E identify missile envelope parameters associated with the two aircraft in the 1v1 air combat. The payoff function, J, can be partitioned as follows:

$$J = f_P(R) \overset{*}{\div} f_P(\theta_P) + f_E(R) \overset{*}{\div} f_E(\theta_E)$$

where

$$f_P(R) = 1 - e^{\left[\frac{4R - 2(R_{MINP} + R_{MAXP})}{R_{MAXP} - R_{MINP}}\right]^2}$$

$$f_P(\theta_P) = \sin^2\left(\frac{\theta_P - \theta_{P_O}}{2}\right)$$

$$f_E(R) = 1 + e^{\left[\frac{4R - 2(R_{MINE} + R_{MAXE})}{R_{MAXE} - R_{MINE}}\right]^2}$$

$$f_E(\theta_E) = \sin^2\left(\frac{\theta_E + \theta_{E_O}}{2}\right)$$

The *, + options in the function allow the analyst to create a J function with different air-combat characteristics For illustrative purposes, consider the following J function option form

$$J = f_P(R) + f_P(\theta_P) + f_E(R) * f_E(\theta_E)$$

The following observations are noted about this payoff function J.

1 $e^{f(R)}$ is essentially zero (0) when $R_{max} < R < R_{min}$ and has it maximum value one (1) when $R = \frac{R_{min} + R_{max}}{2}$ i.e., the "heart" of the missile envelope

2. Min $[f_P(\theta_P) + f_E(\theta_E)]$ yields

θ_P, θ_E

$\theta_P = \theta_{P_O}$

$\theta_E = -\theta_{E_O}$

which is the "best" terminal orientation for P.

3. Max $[f_P(\theta_P) + f_E(\theta_E)]$ yields

θ_P, θ_E

$\theta_P = \theta_{P_O} + \pi$

$\theta_E = \pi - \theta_{E_O}$

which is the "best" terminal orientation for E.

4 Furthermore, J is structured such that

J_{min} ' best terminal position for P

J_{max} best terminal position for E

$\frac{J_{min} + J_{max}}{2}$ * neutral terminal positions for P and E.

5 The lowest value of J_{min} is zero (0) and the largest value of J_{max} is four (4)

The J function was not so much derived, as deduced based on Eidetics' experience It represents the best known analytic function that inherently contains the "best" that two air combatants can position themselves for terminal missile release through use of the minimum/maximum operation on the J function

The uses of the J function are potentially many, i e ,

- To formulate an air-to-air combat differential game and devise new tactics for new technology.
- A measure of air combat merit (i e , like summing shot opportunities) in a given engagement. The fraction of time J exceeds a given value (or is below a given value) is an example.
- A simulator cockpit cue to assess tactical advantage against any selected target

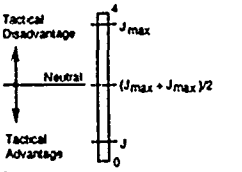

Note: J determines if the air combat situation is improving or getting worse.

The J function was key to development of the Eidetics Air-to-Air Combat Differential Game (AACDG) Model and proved to result in realistic tactics for innovative technology. In summary, it is worthy to note that J is a function of:

1. Altitude
2. Range to adversary
3. Aircraft velocity vector magnitudes
4 Aircraft velocity vector orientations
5 Missile characteristics

2.2 Capabilities of the Air-to-Air Combat Differential Game Model

Eidetics developed the Air-to-Air Combat Differential Game (AACDG) to have a capability to develop new tactics for innovative agility technologies Figure 2.4 shows the major forces acting on an airframe as modeled in the AACDG. Figure 2 5 lists the key

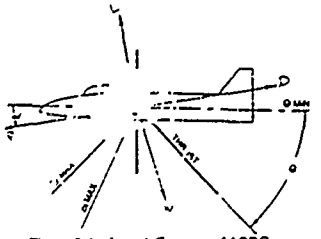

Figure 2 4 - Aircraft Forces in AACDG

EIDETICS AIR TO AIR COMBAT DIFFERENTIAL GAME CAPABILITIES Figure 2 5

PURPOSE: An engineering/operations analysis tool to understand to first order how to use (i.e tactics) new/innovative fighter technology to maximize WVR air combat effectiveness

FORTRAN CODE: 60 subroutines 4000 lines

MODEL CAPABILITIES

Environment - Flat Earth
- Standard atmosphere

Scenario - 1 v 1

Trajectory Mechanics - 5 DOF (no yaw)
- Quaternion coordinate transformation

Vehicles - Aircraft and/or Missiles

Sensors - RF/Radar, IR, Visual

Signature - Function of offnose angle

Body Forces - Weight $\dot{m}(h, m\theta, n)$
- Thrust . . $T(h, m\theta, n)$
- Lift ... Trimmed CL(α , $m\theta$) to poststall
  Thrust gimbaled Δ CL($m\theta$, n, Θ)
- Drag Trimmed CD(α , $m\theta$) to poststall
  Thrust gimbaled Δ CD($m\theta$, n, Θ)

Control/Transient Agility - AOA ... $\alpha_{min} < \alpha < \alpha_{poststall}$ $\leftarrow \dot{\alpha}(\alpha, Q)$

- Load Factor .. $n_{min} < n < n_{structure}$ $\leftarrow \dot{n}(\alpha)$
- Bank $\leftarrow \dot{\phi}(\alpha, Q)$
- Thrust Gimbal $0 < \Theta < \Theta_{max}$ $\leftarrow \dot{\Theta}(\Theta)$
- Engine Spool $n_{rev} < n < n_{AB}$ $\leftarrow \dot{n}(n)$

Missile Performance - Aircraft velocity vectors
- Propellant specific impulse
- Total weight
- Propellant fraction
- Guidance/fuse enable time
- Burntime
- Drag coefficient
- Diameter
- Minimum speed
- Lead pursuit guidance
  Roll and Pull
  Skid to Turn
- Boresight limit
- Rmax limited by sensor

aircraft performance, controllability, and weapons parameters that can be varied in the model as technology variations. Any or all of these parameters can have affect on the resulting "optimal" tactics As can be seen in Figure 2 5, the AACDG has ample capability to model a wide variety of EFM/agility technologies to include

- Conventional aircraft technology
- High AOA/EFM
- VIFF aircraft including circulation lift/drag influence
- Engine spool up/down
- Controllability effects at high AOA and low dynamic pressure
- Missile/gun characteristics

The basic AACDG is written in FORTRAN 7.0 and is compatible with a variety of computers. Eldetics currently runs the model on Apollo and Hewlett Packard workstation computers It is also hosted in a 386/33 MHz personal notebook computer.

The key outputs of the AACDG are time history files for computer plotting of a large variety of variables and to drive graphic software for real-time replay of tactics in God's eye view or from the cockpit

3.0 PROCESS TO DEVELOP TACTICS FOR NEW TECHNOLOGY

Figure 3 0 shows the key elements in a process whose end results are tactics that use innovative fighter aircraft technology to operational advantage The process begins with the DG (1) whose prime purpose is to find/suggest "optimal" candidate tactics to begin the process. These tactics are developed for a limited set of initial conditions (intended to span the key states of ranges, angle-off, airspeeds as tactical starting conditions a pilot is likely to encounter) Table 3 0 is an example set of starting conditions.

Table 3 0 - Initial Conditions (ICs)

	IC #	Mach # *	
		1	2
45° 500' Red (2) Tech (1)	11	9	.9
	12	.9	5
	13	5	9
500' Tech (1) 45° Red (2)	14	9	9
	15	9	5
	16	.5	9
3000' Tech (1) Red (2)	17	.5	5

* All aircraft in level 1-g flight at mil power.

	IC #	Mach # *	
Red (2) 1000' 500' Tech (1)	18	5	5
	19	5	.9
	20	9	5
Red (2) 3000' Tech (1)	21	5	5
Tech (1) Red (2)	22	5	5

Once the "candidate" optimal tactics are generated with the Differential Game (1), a pilot assessment/training phase (see elements 2 and 3 in Figure 3 0) begins on tactics that is a 4-phase process as shown in Table 3 1

Table 3 1 - Procedure Manned Tactics/Technology Evolvement

1. Prebrief
   - Aircraft/missile technology capability
   - Pilot review of each IC & plan/record trial tactic 1st pass, 2nd, etc.
2. ARENA Manned Simulator Trials
   - 1st trial per plan
   - Successive trials until satisfied have "best tactic" for Technology/IC
   - Record "best tactic" (Form) after each IC
3. Post Brief
   - Review "best tactics"
   - Identify candidate ICs for Diff-Game tactics rerun
4. ARENA Re-trials
   - Replay "best tactic"
   - Show Diff-Game "Yellow Brick Road"
   - Try Diff-Game tactics 1st pass
   - Evaluate Diff-Game tactic
   - Final questionnaire

Prebrief

The purpose of the daily prebriefing is to familiarize the pilots with the capabilities of the aircraft/weapon they are to fly that day, to review the set of initial conditions (ICs), and to give the pilots time to plan their initial maneuver for the first pass and general tactics plan for each IC Each pilot has a Pilot Notebook containing technology descriptions, IC figures, and forms for tactics planning and record keeping

ARENA Manned Simulator Trials

After prebriefing/planning come the real time piloted ARENA tactics experimentation whose purpose is to allow the pilots reasonable time to experience the new technology and to devise "best" tactics Pilots are allowed 5 - 10 ARENA trials with each technology/IC combination Although more simulator time is always desirable, the 5 - 10 trials are sufficient for pilots to devise a "best" maneuver in each technology/IC setup Pilots are given a couple hours in the simulator to get familiar with ARENA and its displays/switchology Pilots flying technology enhanced aircraft are given time to "feel-out" these aircraft prior to recorded tactics experimentation trials After pilots are ready, the recorded experimentation trials begin After each trial experimentation, pilots record notes in their Pilot Notebook and communicate (ARENA provides a pilot intercom system for real-time conversation) with one another so as to make the tactics trial experimentation efficient. The last trial in the experimentation trials of a given IC/technology is planned to be the "best" piloted tactic for that IC/technology combination Pilots identify and explain their "best" tactic on forms contained in their Pilot Notebook.

Postbrief

Once the real-time ARENA tactics experimentation trials are completed, a post briefing is held to discuss the pilot "best" tactics, examine major differences with Differential Game tactics decide on any ICs for further tactics experimentation the next day The pilot "best" tactics, both adversaries, are discussed one IC at a time using data recorded on the Pilots Notebook If a pilot "best" tactic and Differential Game optimal tactic are radically different, these differences are discussed to determine the merit of additional ARENA trials to examine the pros/cons of the optimal Differential Game tactic.

ARENA Retrials

The post briefing process usually uncovers one or more ICs for which the Differential Game "optimal" tactic is significantly different from the pilot "best" tactic. This results in ARENA re-trials for further tactics experimentation in the pros/cons of the Differential Game optimal tactic These re-trials are usually the first order of business on the following day. Re trials are flown by the pilots once the pilots are familiarized with the Differential Game optimal tactic through use of the Yellow Brick Road (YBR) ARENA cockpit replay software The YBR software presents to each pilot (in the 1v1 scenario) a cockpit oriented real-time replay of the Differential Game optimal tactic with visual cues to aid understanding of the optimal maneuver. The YBR software allows either pilot to stop/restart the real-time replay at his convenience repeatedly until the Differential Game optimal maneuver is understood This re trials are then done with the pilot flying the Differential Game optimal tactic and also the pilot "best" tactic to discern the pros/cons of each These re trial results are recorded in the Pilot Notebook

Figure 3 0

TACTICS DEVELOPMENT PROCESS

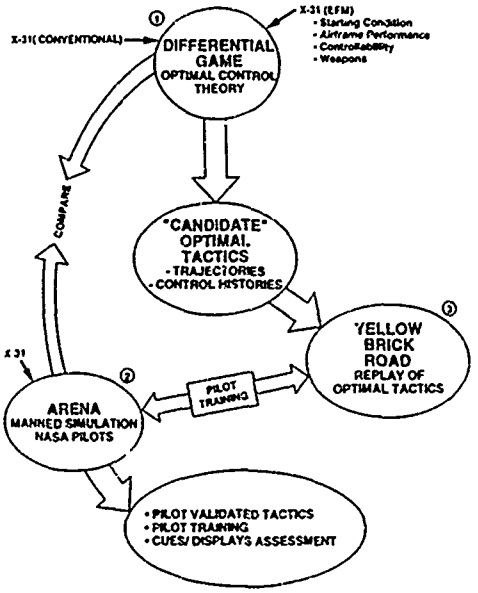

4.0 EXAMPLE DIFFERENTIAL GAME RESULTS

4.1 Technology Enhancements from a Baseline Aircraft

The 4-PWR Senior National Representatives group elected a "baseline" aircraft design that was named the NEW2 with the following basic aircraft parameters:

Weight	-	27250 lbs.
Thrust/Weight (Sea level)	-	1.40
Thrust/Wsight (10k ft)	-	1.03
Wing Area	-	537.9 ft
AOA stall	-	26 deg

The turn rate/Mach #/P_S performance of the NEW2 at 15K feet is shown in Figure 4 0. In some sense, the NEW2 is like the Rafale or a big-wing F-16 with improved thrust/weight. The NEW2 does not have supermaneuver capability, and exhibits a stall AOA (i e CL_{max}) around 26 degrees.

Figure 4 0 BASELINE CONFIGURATION
15000 FT MAX. POWER

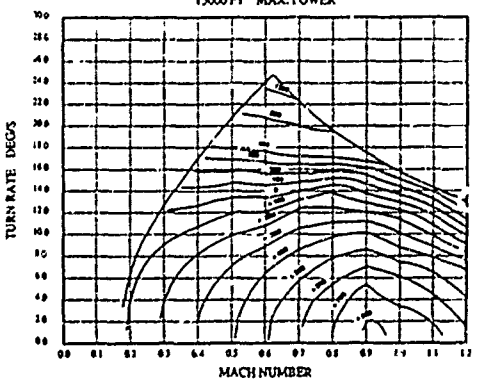

Table 4.0 lists and describes nine (9) major technologies variations in the total aircraft/ weapon system (6 aircraft variations and 3 IR missile variations). The variations are about the aircraft and missile baselines. The six (6) aircraft technology variations are technologies 2 (+30% T/W), 3 (+30% L/D), 4 (SM to 90° AOA to point velocity vector with a conventional IRM), 6 (enhanced roll agility), 7 (enhanced axial agility) and 8 (enhanced pitch agility) In order to create a high AOA (90°) version of the NEW2, F-XX high AOA coefficient of lift and drag data were appended to the basic NEW2 aero data. This was reasonable as the aero data at normal AOA was similar for the F-XX and NEW2. The supermaneuverable NEW2, however, exhibited CL_{max} at a higher AOA around 36 degrees. Turn rate/Mach #/Ps performance of the supermaneuverable NEW2 at 15K feet is shown in Figure 4 1.

Table 4 0 - SNR NEW2 Technology Excursions

#	Technology	A/C #	Technology Aircraft System	MX #	Parameters	Target Aircraft System
1	Baseline	1	NEW2 + IRM	1	Baseline pitch agility Baseline (good) roll agility 6 sec axial agility Less of control power < 250 kts	NEW2 + IRM
2	+30% T/W	2	NEW2 + IRM	1	Baseline + 30% thrust	same
3	+30% L/D	3	NEW2 + IRM	1	Baseline + 30% C_L	same
4	Longeudinal SM 90°	4	NEW2 SM + IRM Velocity Vector pointing	1	AOA max = 90° Best pitch agility Enhanced roll agility 6 sec axial transient No loss of control power	same
5	Longeudinal	4	NEW2 SM + IRM SM	2	Same as 4 except IRM/ can launch at 90° AOA	
6	Torsional Agility	5	NEW2 + IRM	1	Baseline + enhanced roll agility	same
7	Axial Agility	6	NEW2 + IRM	1	Baseline + 2 sec idle to A/B	same
8	Pitch Agility	7	NEW2 + IRM	1	Baseline + best pitch agility	same
9	Power Reduce	7	NEW2 + IRM fly;	3	IRM fuze time 50% reduced	same
10	70° Off Boresight	7	NEW2 + IRM 70	4	Baseline + 70° off-boresight for AIM 9L	same

Figure 4.1 SUPERMANEUVERABLE CONFIGURATION
15000 FT MAX POWER

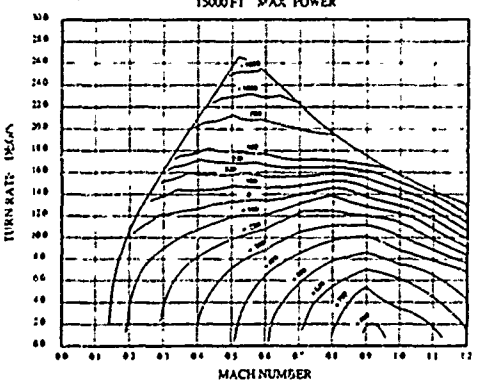

4.2 General Observations on Differential Game Optimal Tactics

The first Differential Game technology case run was NEW2 "baseline" vs. NEW2 "baseline" for the ICs. In these runs there was no technology advantage; only a tactical advantage as represented by the ICs of Table 3 0. These "baseline" tactics results are presented below up to first shot and show the following

1. Aircraft initially above the corner speed (M# .9) invariably use the vertical generally using a max load factor pitchback maneuver into a 1-circle fight ending up at stall AOA. Throttle is pulled back initially from mil power (5)° into the .3 range and terminally around .6 - .7.

2. Aircraft initially below the corner speed (M# .5) use a variety of maneuver planes, but generally prefer a slight pitchback to stall AOA (~ 5 0-ga) into the 1-circle fight. Throttle is pushed from mil power (5) to max A/B (1.0).

3. The terminal conditions are first shot (either aircraft) usually clustered around R_{MIN} and occur quickly (8 - 12 seconds).

4. IC 16 (i.e., technology aircraft-1 slow with adversary-2 fast, off right wing going to the rear) results in an unusual optimal tactic designed to minimize the affect of this poor tactical situation for the technology aircraft-1. The technology aircraft-1 does a 2g roll 360° (right) followed by a 300° roll (right) to a loft pitchback into the adversary ending up at 140 knots. This tactic is an "optimal" attempt to g, in energy in a low-g barrel roll down to exit a faster turn on a high speed adversary going to the rear and vertical. The adversary is attempting to take advantage of his opponents slow speed by forcing the fight up.

In an attempt to evaluate the "reasonableness" of these "baseline" optimal tactics, an experienced fighter pilot was asked what he would do in each of the "baseline" ICs. This pilot did the same as the Differential Game except he always used max A/B forminally and did not do the unusual acceleration tactic in 4 above.

All of the technologies run with the Differential Game exhibited these general tendences in their "optimal" tactics with variation in the use of the vertical and throttle depending on how the technology impacted loss of energy in a max load factor turn. Table 4.1 summarizes the technology/IC combinations that resulted in a noticeable change of "optimal" tactic (i.e., maneuver plane, load factor or throttle schedule) from the baseline. As can be seen, the improved L/D and SM technologies had the largest impact on the tactic perturbation from the baseline. In summary, it is also interesting to note that improved technology invariably resulted in improved (i.e., smaller) J results for the technology aircraft in every IC with few exceptions. These IC exceptions were found to be expected/rationale for the technology/IC combinations in which they rarely occurred. This gave much confidence in the capability of the Differential Game methodology to devise "optimal" tactics that took advantage of the technology change.

Table 4.1 - Optimal Tactic Differences from Baseline

Aircraft Technology \ IC		11	12	13	14	15	16	17
+30% T	1					•	•	
	2					•		
+30% L	1	•	•	•	•	•	•	•
	2		•			•	•	•
SM 90° VPoint	1	•	•	•		•	•	
	2	•		•	•		•	
SM 90° Nose Point	1	•	•	•	•	•	•	•
	2	•	•	•	•	•	•	•
Roll Enhanced	1							
	2							
Axial Enhanced	1	•			•	•	•	
	2							
Pitch Enhanced	1						•	
	2							
R_{MIN} Reduce	1			•			•	
	2			•			•	

4.3 Differential Game Ranking of Technology Operational Effectiveness

The impact of improved technology is directly reflected in the reduced value of J (i.e., negative change from baseline) in each IC. The average value of this negative J change over the fixed set of ICs results in a direct quantitative measure of the "goodness" of a technology change relative to the "baseline" NEW2 technology. These results are presented in Figure 4.2 and show the "optimal" ranking of the 8 technologies relative to the "baseline" NEW2. The SM aircraft with IRM-SM missile produces the largest improvement of the eight (8) technologies studied with the Differential Game. As will be seen in a later section, the IR missile off boresight technology also produces a great increase in operational effectiveness.

5.0 ARENA PILOTED SIMULATION RESULTS

The tactics technology entire process, beginning with the Differential Game and culminating with the piloted experimentation, revealed some WVR tactics "lessons learned" worthy of summary. Naturally, these lessons are related to the level of conventional performance of the baseline NEW2 that was purposely selected to be a current/near-term airframe design. In comparative terms, the baseline NEW2 is Rafale-like in character or like a big-wing F-16 with improved thrust-to-weight. The "lessons learned" are also influenced by the ICs (see Table 3.0) that were chosen to be a reasonable sample of WVR initial conditions likely to be encountered. These ICs were not designed to "exploit-the-nduct" of any technology. They were primarily designed to provide a WVR technology-tactic-rule-of-thumb to use should a pilot find himself in such a possible WVR tactical state. In this regard, the pilots often did not like an IC because they "could not employ the added technology to advantage". It must, however, be remembered that knowing where not to employ technology is equally important to knowing when to employ technology. Such was the reason for the set of ICs chosen. The lessons learned by the Differential Game and piloted ARENA runs are summarized by technology in paragraphs that follow.

5.1 Baseline Technology

The baseline cases really represent WVR air-combat between "similar" aircraft. In contrast, the other cases of technology really represent WVR air-combat between "dissimilar" aircraft. The baseline cases revealed the following lessons:

- If above the corner speed, use the vertical. If below the corner speed, use lift-vector-on.
- If slow and your adversary is fast with a high velocity vector angle-off, take time to accelerate before the turn. A tightly loaded slice may be the best accelerate tactic.
- If the threat aircraft is "similar" (i.e., in energy bleedrate), go for a 1-circle "inside" fight and IRCM the adversary at the merge if you engaged above corner speed. If you engage initially slow, you probably can't afford IRCM, especially if he is above corner speed initially.

5.2 +30% T/W and +30% L/D Technologies (2 &3)

These technology enhancements influenced the "dissimilar" WVR air-combat tactics in a similar way in that the common affect was to decrease bleedrate in a max performance turn. As such, the following lessons learned were common to both technologies:

- If I have a bleedrate advantage (i.e., less max bleedrate), use more of the vertical than the baseline case.
- When slow and the adversary is fast with a high velocity angle-off, acceleration first before the turn may not be needed.
- When at high velocity vector angle-off and he is at least as slow as I am, force a 1 circle fight to the "outside" to drive a longer initial merge to force him to bleed more energy to get his nose-on you.

5.3 Axial (6 - 2sec) Technology (7)

- With the faster spooling engine you can afford to leave the engine in A/B longer when employing IRCM techniques.

5.4 Torsional Agility Technology (6)

- Remember that the technology will allow you to roll when under max load factor.
- Be careful of the handling qualities under high load factor as you may likely over control in roll and defeat what the technology provides.
- The most likely tactical use is in quick maneuver defensive plane changes.

5.5 Supermaneuver (SM) to Point Velocity Vector Technology (4)

In examining the lessons learned here, it must be remembered that the basic philosophy is to get slow and use thrust/weight to turn the velocity vector. Supermaneuver to 90° provides angle induced drag to get slow provided there is time to do so. That time is related to how well your adversary performs conventionally. Assuming that you have time to get slow (and are willing to accept the tactical vulnerability of such an energy state), it is not good to do this unless your aircraft has enhanced thrust/weight (1.5-2.0) to turn the slow vector velocity and then to accelerate for missile

defense. Unfortunately, neither of these two requirements were met by the aircraft in this study. That is, the baseline adversary was very capable in conventional performance and the thrust/weight of the SM-NEW2 was only 1.05 at 10k altitude. As such, neither the Differential Game (DG) or piloted ARENA cases uncovered any real tactical advantage to SM to "bend" the velocity vector. The lessons learned are more related to aircraft design than tactics. With the weak SM design of the NEW2 and the ICs chosen, the pilots and DG fought more-or-less conventionally. If the SM aircraft was fortunate to survive the merge, the technology advantage was primarily in pointing the nose close-in to use the gun. Probably the most important lessons learned is the following one related to design:

- It is very unlikely that high AOA will aid an airframe of poor conventional performance. Said another way, "A diamond on a brass ring is no jewel!"
- Classic J-Turns and Herbst type maneuvers were not effective in these unbiased aircraft/tactical situations

5.6 Supermaneuver (SM) to Point Nose with a High AOA Missile Technology (5)

Prior to flying this technology, the pilots thought it would be unbeatable. However, the technology in this test offered little advantage over the conventional baseline for several reasons

- Although the technology provides 2-3 second, of missile shot time advantage, the early shots did not dissuade an agressive adversary from "gaming" the situation to effect a mutual kill
- Because of low thrust/weight, use of SM to get the early shot at high AOA always left you slow with no capability to recover speed quickly for missile maneuver defense, as compared to maneveling conventionally that achieved the same mutual kill results, but left you at higher speeds with some chance to evade an incoming missile

Perhaps there is more advantage to this technology in real WVR air-combat where "first-shot" causes the adversary to usually "sink of his skin" and MX defense rather than a mutual kill. However, high T/W recovery will still be needed in actual WVR air combat that is MVN in character.

5.7 R_{min} Reduction Technology (9)

- Improved R_{min} will allow closer shots, but one must be careful not to frag yourself

5.8 70° Off-Boresight Technology (10)

Interestingly, the pilots liked this technology best, even though it did not influence tactics in getting to a shot other than requiring them to "think-ahead" to be sure and shoot earlier. Their reasons for rating it best were the obvious: less turning (shorter time/higher velocity) to get the shot. IRCM, however, can greatly reduce the early shot advantage here.

5.9 Pilot Ranking of Technology Effectiveness

As a part of the debriefing and End of Day Questionnaire, pilots were asked to numerically rank a technology relative to the baseline NEW2. At this point, the pilots at the end of the day had definite opinions and seemed to find it easy to compare a technology just flown against the familiar baseline. At the end of the entire process, those pilots who flew multiple technologies were asked to rank the technologies they flew into a composite ranking 1-to-10. That pilot ranking is shown in Figure 5.0 as the "open" vertical bars. As can be seen, the top 5 technologies were (1) 70° off-boresight MX, (2) SM with SM MX, (3) SM velocity point, (4) + 30% L/D, (5) +30% T/W. Figure 5.0 also shows the Differential Game ranking of technologies (based on the average payoff reduction value in Figure 4.2) to be (2) SM with SM MX, (3) SM velocity point, (4) Pitch Agility, (5) +30% L/D. Except for the off-boresight MX (not run with the Differential Game) and the addition of Pitch Agility, the pilot and Differential Game rankings are very similar.

6.0 CONCLUSIONS

Each element of the tactics development process for technology (see Figure 3.0) was essential. There were situations where the Differential Game found a tactic of advantage that the pilots did not find, and there were tactics that the Differential Game suggested that were unrealistic and needed pilot input for tactical realism. It is clear that the combined process of Differential Game and piloted simulation mutually supported one another in a time efficient process to develop WVR tactics for new agility technologies. The software tools that cost-effectively brought the pilot into the technology process (i.e., the ARENA simulator and Yellow Brick Road replay software) were essential to forge a means of communication between the pilot and the engineer/technologist.

Figure 4.2 Δ (-) PAYOFF * DIFFERENTIAL GAME

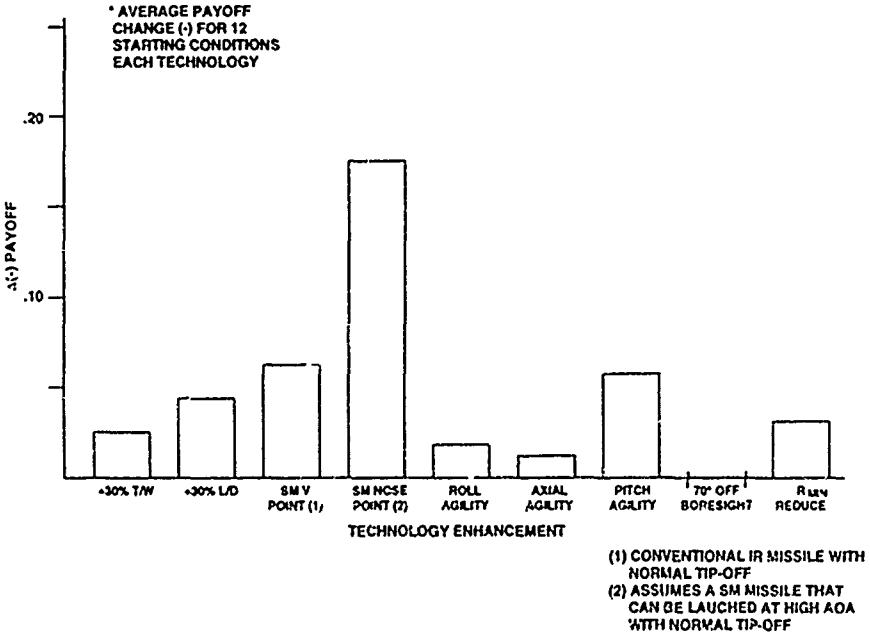

Figure 5.0

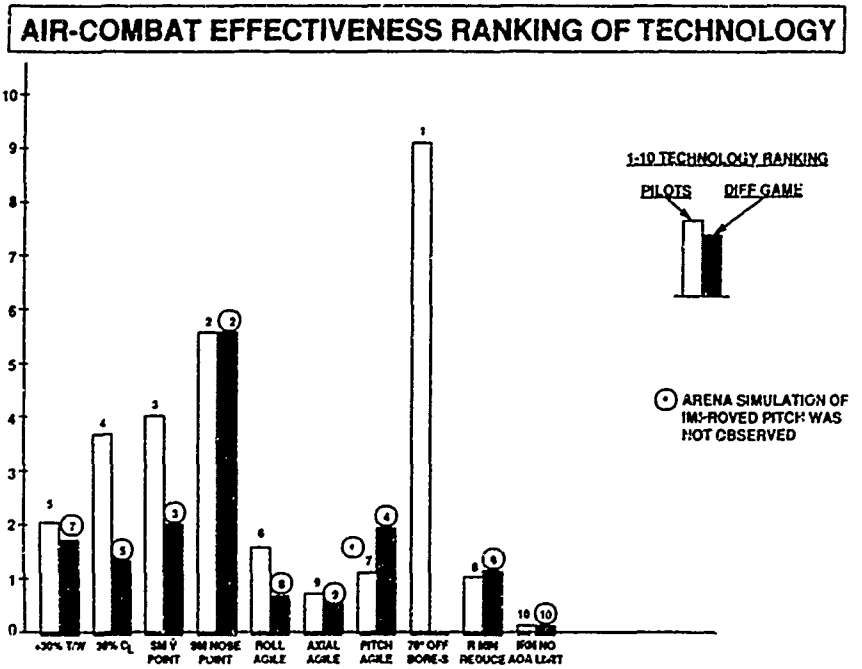
AIR-COMBAT EFFECTIVENESS RANKING OF TECHNOLOGY
1-10 TECHNOLOGY RANKING
PILOTS
DIFF GAME
ARENA SIMULATION OF IMPROVED PITCH WAS NOT OBSERVED
+30% T/W
30% C_L
SM Ÿ POINT
9M NOSE POINT
ROLL AGILE
AXIAL AGILE
PITCH AGILE
70° OFF BORE-S
R MIN REDUCE
IFDN NO AOA LIMIT

REPORT DOCUMENTATION PAGE			
1. Recipient's Reference	2. Originator's Reference AGARD-CP-548	3. Further Reference ISBN 92-835-0740-1	4. Security Classification of Document UNCLASSIFIED/ UNLIMITED

5. Originator	Advisory Group for Aerospace Research and Development North Atlantic Treaty Organization 7 rue Ancelle, 92200 Neuilly sur Seine, France
6. Title	TECHNOLOGIES FOR HIGHLY MANOEUVRABLE AIRCRAFT
7. Presented at	the Flight Mechanics Panel Symposium, held in Annapolis, Maryland, United States from 18th-21st October 1993.
8. Author(s)/Editor(s)	Various
9. Date	March 1994
10. Author(s)/Editor's Address	Various
11. Pages	350
12. Distribution Statement	There are no restrictions on the distribution of this document. Information about the availability of this and other AGARD unclassified publications is given on the back cover.

13. Keywords/Descriptors

High maneuverability	Flight test
Post stall control	Flying qualities
Agility	Integrated flight control
Supersonic maneuver	

14. Abstract

The new generation of combat aircraft, currently at demonstrator or development stage, incorporate significant advances in manoeuvre capability, especially in such areas as post-stall control and sustained supersonic manoeuvre. These technologies expand the operational capabilities, and are essential for survival in a sophisticated threat scenario, and also to obtain favourable exchange ratios against an opponent using the current generation of fighters. The aim of this Symposium was to review the various technologies, which combine to give this increased operational capability, and the techniques which are available or being developed, to overcome the design problems associated with the attainment of these goals.

The Symposium was divided into six sessions covering propulsion and integrated flight control, aerodynamics and control at high angles of attack, post-stall flight and control, flying qualities-applied criteria, agility and simulation. Examples of results from current demonstrator programmes were covered in appropriate sessions.

Two keynote papers presented an overview from an operational and acquisition viewpoint of the contribution of manoeuvrability to combat success.

For the first time in a Flight Mechanics Panel Symposium, the programme included a paper by a Russian author.

A Technical Evaluation Report on the Symposium is also included in this Conference Proceedings document.

AGARD Conference Proceedings 548
Advisory Group for Aerospace Research and Development, NATO
TECHNOLOGIES FOR HIGHLY MANOEUVRABLE AIRCRAFT
Published March 1994
350 pages

The new generation of combat aircraft, currently at demonstrator or development stage, incorporate significant advances in manoeuvre capability, especially in such areas as post-stall control and sustained supersonic manoeuvre. These technologies expand the operational capabilities, and are essential for survival in a sophisticated threat scenario, and also to obtain favourable exchange ratios against an opponent using the current generation of fighters. The aim of this Symposium was to review the

P.T.O.

AGARD-CP-548

High maneuverability
Post stall control
Agility
Supersonic maneuver
Flight test
Flying qualities
Integrated flight control

AGARD Conference Proceedings 548
Advisory Group for Aerospace Research and Development, NATO
TECHNOLOGIES FOR HIGHLY MANOEUVRABLE AIRCRAFT
Published March 1994
350 pages

The new generation of combat aircraft, currently at demonstrator or development stage, incorporate significant advances in manoeuvre capability, especially in such areas as post-stall control and sustained supersonic manoeuvre. These technologies expand the operational capabilities, and are essential for survival in a sophisticated threat scenario, and also to obtain favourable exchange ratios against an opponent using the current generation of fighters. The aim of this Symposium was to review the

P.T.O.

AGARD-CP-548

High maneuverability
Post stall control
Agility
Supersonic maneuver
Flight test
Flying qualities
Integrated flight control

AGARD Conference Proceedings 548
Advisory Group for Aerospace Research and Development, NATO
TECHNOLOGIES FOR HIGHLY MANOEUVRABLE AIRCRAFT
Published March 1994
350 pages

The new generation of combat aircraft, currently at demonstrator or development stage, incorporate significant advances in manoeuvre capability, especially in such areas as post-stall control and sustained supersonic manoeuvre. These technologies expand the operational capabilities, and are essential for survival in a sophisticated threat scenario, and also to obtain favourable exchange ratios against an opponent using the current generation of fighters. The aim of this Symposium was to review the

P.T.O.

AGARD-CP-548

High maneuverability
Post stall control
Agility
Supersonic maneuver
Flight test
Flying qualities
Integrated flight control

AGARD Conference Proceedings 548
Advisory Group for Aerospace Research and Development, NATO
TECHNOLOGIES FOR HIGHLY MANOEUVRABLE AIRCRAFT
Published March 1994
350 pages

The new generation of combat aircraft, currently at demonstrator or development stage, incorporate significant advances in manoeuvre capability, especially in such areas as post-stall control and sustained supersonic manoeuvre. These technologies expand the operational capabilities, and are essential for survival in a sophisticated threat scenario, and also to obtain favourable exchange ratios against an opponent using the current generation of fighters. The aim of this Symposium was to review the

P.T.O.

AGARD-CP-548

High maneuverability
Post stall control
Agility
Supersonic maneuver
Flight test
Flying qualities
Integrated flight control

various technologies, which combine to give this increased operational capability, and the techniques which are available or being developed, to overcome the design problems associated with the attainment of these goals.

The Symposium was divided into six sessions covering propulsion and integrated flight control, aerodynamics and control at high angles of attack, post-stall flight and control, flying qualities-applied criteria, agility and simulation. Examples of results from current demonstrator programmes were covered in appropriate sessions

Two keynote papers presented an overview from an operational and acquisition viewpoint of the contribution of manoeuvrability to combat success.

For the first time in a Flight Mechanics Panel Symposium, the programme included a paper by a Russian author.

A Technical Evaluation Report on the Symposium is also included in this Conference Proceedings document.

Copies of papers presented at the Flight Mechanics Panel Symposium held in Annapolis, Maryland, United States 18th-21st October 1993.

ISBN 92-835-0740-1

various technologies, which combine to give this increased operational capability, and the techniques which are available or being developed, to overcome the design problems associated with the attainment of these goals.

The Symposium was divided into six sessions covering propulsion and integrated flight control, aerodynamics and control at high angles of attack, post-stall flight and control, flying qualities-applied criteria, agility and simulation. Examples of results from current demonstrator programmes were covered in appropriate sessions.

Two keynote papers presented an overview from an operational and acquisition viewpoint of the contribution of manoeuvrability to combat success.

For the first time in a Flight Mechanics Panel Symposium, the programme included a paper by a Russian author.

A Technical Evaluation Report on the Symposium is also included in this Conference Proceedings document.

Copies of papers presented at the Flight Mechanics Panel Symposium held in Annapolis, Maryland, United States 18th-21st October 1993.

ISBN 92-835-0740-1

various technologies, which combine to give this increased operational capability, and the techniques which are available or being developed, to overcome the design problems associated with the attainment of these goals.

The Symposium was divided into six sessions covering propulsion and integrated flight control, aerodynamics and control at high angles of attack, post-stall flight and control, flying qualities-applied criteria, agility and simulation. Examples of results from current demonstrator programmes were covered in appropriate sessions.

Two keynote papers presented an overview from an operational and acquisition viewpoint of the contribution of manoeuvrability to combat success.

For the first time in a Flight Mechanics Panel Symposium, the programme included a paper by a Russian author.

A Technical Evaluation Report on the Symposium is also included in this Conference Proceedings document.

Copies of papers presented at the Flight Mechanics Panel Symposium held in Annapolis, Maryland, United States 18th-21st October 1993.

ISBN 92-835-0740-1

various technologies, which combine to give this increased operational capability, and the techniques which are available or being developed, to overcome the design problems associated with the attainment of these goals.

The Symposium was divided into six sessions covering propulsion and integrated flight control, aerodynamics and control at high angles of attack, post-stall flight and control, flying qualities-applied criteria, agility and simulation. Examples of results from current demonstrator programmes were covered in appropriate sessions.

Two keynote papers presented an overview from an operational and acquisition viewpoint of the contribution of manoeuvrability to combat success.

For the first time in a Flight Mechanics Panel Symposium, the programme included a paper by a Russian author

A Technical Evaluation Report on the Symposium is also included in this Conference Proceedings document.

Copies of papers presented at the Flight Mechanics Panel Symposium held in Annapolis, Maryland, United States 18th-21st October 1993.

ISBN 92-835-0740-1

AGARD
NATO OTAN
7 RUE ANCELLE · 92200 NEUILLY-SUR-SEINE
FRANCE
Télécopie (1)47.38.57.99 · Télex 610 176

DIFFUSION DES PUBLICATIONS
AGARD NON CLASSIFIEES

Aucun stock de publications n'a existé à AGARD. A partir de 1993, AGARD détiendra un stock limité des publications associées aux cycles de conférences et cours spéciaux ainsi que les AGARDographies et les rapports des groupes de travail, organisés et publiés à partir de 1993 inclus. Les demandes de renseignements doivent être adressées à AGARD par lettre ou par fax à l'adresse indiquée ci-dessus. *Veuillez ne pas téléphoner*. La diffusion initiale de toutes les publications de l'AGARD est effectuée auprès des pays membres de l'OTAN par l'intermédiaire des centres de distribution nationaux indiqués ci-dessous. Des exemplaires supplémentaires peuvent parfois être obtenus auprès de ces centres (à l'exception des Etats-Unis). Si vous souhaitez recevoir toutes les publications de l'AGARD, ou simplement celles qui concernent certains Panels, vous pouvez demander à être inclu sur la liste d'envoi de l'un de ces centres. Les publications de l'AGARD sont en vente auprès des agences indiquées ci-dessous, sous forme de photocopie ou de microfiche.

CENTRES DE DIFFUSION NATIONAUX

ALLEMAGNE
Fachinformationszentrum,
Karlsruhe
D-7514 Eggenstein-Leopoldshafen 2

BELGIQUE
Coordonnateur AGARD-VSL
Etat-Major de la Force Aérienne
Quartier Reine Elisabeth
Rue d'Evere, 1140 Bruxelles

CANADA
Directeur du Service des Renseignements Scientifiques
Ministère de la Défense Nationale
Ottawa, Ontario K1A 0K2

DANEMARK
Danish Defence Research Establishment
Ryvangs Allé 1
P.O. Box 2715
DK-2100 Copenhagen O

ESPAGNE
INTA (AGARD Publications)
Pintor Rosales 34
28008 Madrid

ETATS-UNIS
NASA Headquarters
Attention: CF 37, Distribution Center
300 E Street, S.W.
Washington, D.C. 20546

FRANCE
O.N.E.R.A. (Direction)
29, Avenue de la Division Leclerc
92322 Châtillon Cedex

GRECE
Hellenic Air Force
Air War College
Scientific and Technical Library
Dekelia Air Force Base
Dekelia, Athens TGA 1010

ISLANDE
Director of Aviation
c/o Flugrad
Reykjavik

ITALIE
Aeronautica Militare
Ufficio del Delegato Nazionale all'AGARD
Aeroporto Pratica di Mare
00040 Pomezia (Roma)

LUXEMBOURG
Voir Belgique

NORVEGE
Norwegian Defence Research Establishment
Attn: Biblioteket
P.O. Box 25
N-2007 Kjeller

PAYS-BAS
Netherlands Delegation to AGARD
National Aerospace Laboratory NLR
P.O. Box 90502
1006 BM Amsterdam

PORTUGAL
Força Aérea Portuguesa
Centro de Documentação e Informação
Alfragide
2700 Amadora

ROYAUME UNI
Defence Research Information Centre
Kentigern House
65 Brown Street
Glasgow G2 8EX

TURQUIE
Milli Savunma Başkanlığı (MSB)
ARGE Daire Başkanlığı (ARGE)
Ankara

Le centre de distribution national des Etats-Unis ne détient PAS de stocks des publications de l'AGARD.
D'éventuelles demandes de photocopies doivent être formulées directement auprès du NASA Center for Aerospace Information (CASI) à l'adresse suivante:

AGENCES DE VENTE

NASA Center for
Aerospace Information (CASI)
800 Elkridge Landing Road
Linthicum Heights, MD 21090-2934
United States

ESA/Information Retrieval Service
European Space Agency
10, rue Mario Nikis
75015 Paris
France

The British Library
Document Supply Division
Boston Spa, Wetherby
West Yorkshire LS23 7BQ
Royaume Uni

Les demandes de microfiches ou de photocopies de documents AGARD (y compris les demandes faites auprès du CASI) doivent comporter la dénomination AGARD, ainsi que le numéro de série d'AGARD (par exemple AGARD-AG 315). Des informations analogues, telles que le titre et la date de publication sont souhaitables. Veuiller noter qu'il y a lieu de spécifier AGARD-R-nnn et AGARD-AR-nnn lors de la commande des rapports AGARD et des rapports consultatifs AGARD respectivement. Des références bibliographiques complètes ainsi que des résumés des publications AGARD figurent dans les journaux suivants:

Scientifique and Technical Aerospace Reports (STAR)
publié par la NASA Scientific and Technical
Information Program
NASA Headquarters (JTT)
Washington D C. 20546
Etats-Unis

Government Reports Announcements and Index (GRA&I)
publié par le National Technical Information Service
Springfield
Virginia 22161
Etats-Unis

(accessible également en mode interactif dans la base de données bibliographiques en ligne du NTIS, et sur CD-ROM)

Imprimé par Specialised Printing Services Limited
40 Chigwell Lane, Loughton, Essex IG10 3TZ

AGARD
NATO OTAN
7 RUE ANCELLE · 92200 NEUILLY-SUR-SEINE
FRANCE
Telefax (1)47.38.57.99 · Telex 610 176

DISTRIBUTION OF UNCLASSIFIED AGARD PUBLICATIONS

AGARD holds limited quantities of the publications that accompanied Lecture Series and Special Courses held in 1993 or later, and of AGARDographs and Working Group reports published from 1993 onward. For details, write or send a telefax to the address given above. *Please do not telephone.*

AGARD does not hold stocks of publications that accompanied earlier Lecture Series or Courses or of any other publications. Initial distribution of all AGARD publications is made to NATO nations through the National Distribution Centres listed below. Further copies are sometimes available from these centres (except in the United States). If you have a need to receive all AGARD publications, or just those relating to one or more specific AGARD Panels, they may be willing to include you (or your organisation) on their distribution list. AGARD publications may be purchased from the Sales Agencies listed below, in photocopy or microfiche form.

NATIONAL DISTRIBUTION CENTRES

BELGIUM
Coordonnateur AGARD — VSL
Etat-Major de la Force Aérienne
Quartier Reine Elisabeth
Rue d'Evere, 1140 Bruxelles

CANADA
Director Scientific Information Services
Dept of National Defence
Ottawa, Ontario K1A 0K2

DENMARK
Danish Defence Research Establishment
Ryvangs Allé 1
P.O. Box 2715
DK-2100 Copenhagen Ø

FRANCE
O.N.E.R.A. (Direction)
29 Avenue de la Division Leclerc
92322 Châtillon Cedex

GERMANY
Fachinformationszentrum
Karlsruhe
D-7514 Eggenstein-Leopoldshafen 2

GREECE
Hellenic Air Force
Air War College
Scientific and Technical Library
Dekelia Air Force Base
Dekelia, Athens TGA 1010

ICELAND
Director of Aviation
c/o Flugrad
Reykjavik

ITALY
Aeronautica Militare
Ufficio del Delegato Nazionale all'AGARD
Aeroporto Pratica di Mare
00040 Pomezia (Roma)

LUXEMBOURG
See Belgium

NETHERLANDS
Netherlands Delegation to AGARD
National Aerospace Laboratory, NLR
P.O. Box 90502
1006 BM Amsterdam

NORWAY
Norwegian Defence Research Establishment
Attn: Biblioteket
P.O. Box 25
N-2007 Kjeller

PORTUGAL
Força Aérea Portuguesa
Centro de Documentação e Informação
Alfragide
2700 Amadora

SPAIN
INTA (AGARD Publications)
Pintor Rosales 34
28008 Madrid

TURKEY
Milli Savunma Başkanlığı (MSB)
ARGE Daire Başkanlığı (ARGE)
Ankara

UNITED KINGDOM
Defence Research Information Centre
Kentigern House
65 Brown Street
Glasgow G2 8EX

UNITED STATES
NASA Headquarters
Attendion: CF 37, Distribution Center
300 E Street, S.W.
Washington, D.C. 20546

The United States National Distribution Centre does NOT hold stocks of AGARD publications.
Applications for copies should be made direct to the NASA Center for Aerospace Information (CASI) at the address below.

SALES AGENCIES

NASA Center for
Aerospace Information (CASI)
800 Elkridge Landing Road
Linthicum Heights, MD 21090-2934
United States

ESA/Information Retrieval Service
European Space Agency
10, rue Mario Nikis
75015 Paris
France

The British Library
Document Supply Centre
Boston Spa, Wetherby
West Yorkshire LS23 7BQ
United Kingdom

Requests for microfiches or photocopies of AGARD documents (including requests to CASI) should include the word 'AGARD' and the AGARD serial number (for example AGARD-AG-315). Collateral information such as title and publication date is desirable. Note that AGARD Reports and Advisory Reports should be specified as AGARD-R-nnn and AGARD-AR-nnn, respectively. Full bibliographical references and abstracts of AGARD publications are given in the following journals:

Scientific and Technical Aerospace Reports (STAR)
published by NASA Scientific and Technical
Information Program
NASA Headquarters (JTT)
Washington D.C. 20546
United States

Government Reports Announcements and Index (GRA&I)
published by the National Technical Information Service
Springfield
Virginia 22161
United States
(also available online in the NTIS Bibliographic Database or on CD-ROM)

Printed by Specialised Printing Services Limited
40 Chigwell Lane, Loughton, Essex IG10 3TZ

ISBN 92-835-0740-1